

Jochen Vogt

Exam Survival Guide: Physical Chemistry

Exam Survival Guide: Physical Chemistry

Jochen Vogt

Exam Survival Guide: Physical Chemistry



Springer

Jochen Vogt
Chemisches Institut
der Universität Magdeburg
Magdeburg, Germany

ISBN 978-3-319-49808-9 ISBN 978-3-319-49810-2 (eBook)
DOI 10.1007/978-3-319-49810-2

Library of Congress Control Number: 2017933473

© Springer International Publishing AG 2017

This work is subject to copyright. All rights are reserved by the Publisher, whether the whole or part of the material is concerned, specifically the rights of translation, reprinting, reuse of illustrations, recitation, broadcasting, reproduction on microfilms or in any other physical way, and transmission or information storage and retrieval, electronic adaptation, computer software, or by similar or dissimilar methodology now known or hereafter developed.

The use of general descriptive names, registered names, trademarks, service marks, etc. in this publication does not imply, even in the absence of a specific statement, that such names are exempt from the relevant protective laws and regulations and therefore free for general use.

The publisher, the authors and the editors are safe to assume that the advice and information in this book are believed to be true and accurate at the date of publication. Neither the publisher nor the authors or the editors give a warranty, express or implied, with respect to the material contained herein or for any errors or omissions that may have been made. The publisher remains neutral with regard to jurisdictional claims in published maps and institutional affiliations.

Printed on acid-free paper

This Springer imprint is published by Springer Nature
The registered company is Springer International Publishing AG
The registered company address is: Gewerbestrasse 11, 6330 Cham, Switzerland

For Birgit

Preface

Novel concepts in teaching stress the active role of the student in the acquisition of competence. In this spirit, the *Exam Survival Guide: Physical Chemistry* was developed as a supplemental offer primarily to students, but also to teachers. The book presents more than 80 selected problems, some typical of physical chemistry examinations; others, owing to their relative complexity, suitable for seminars with the intention of reaching an in-depth understanding of the key topics in physical chemistry. The solutions to the problems are presented in a more extensive way compared with typical textbooks. Having worked out a solution independently, the student is invited to follow the solution offered in the text. Alternatively, the student can benefit from an solution, gain insight into solution strategies, methods of calculus, and additional information that draws attention to some remarkable points. The intention of the book is to encourage the reader to use paper, pencil, and computer to *cultivate* problem-solving in physical chemistry.

Each chapter deals with a key topic and starts with a short survey of the theory necessary to solve the problems. These basic concepts are not intended to replace the contents of tried-and-tested textbooks. Instead, they serve as starting points around which the topics of the exercises are developed. In addition, the book provides an extensive appendix of the essential mathematics typical of physical chemistry problems.

A first brief look through the chapters shows that the emphasis of this workbook is on the application of mathematical methods in physicochemical contexts. In fact, there are hardly any questions that can simply be answered by “yes” or “no.” The Chapter 1 deals with the aspects of this kind of quantitative problem-solving and provides a survey on the various topics, the level of difficulty, and hints on the manifold cross-links among certain problems.

Although I am aware of the varying curricula and examination formats, the different approaches that students develop during their career, the lively diversity among students - hard workers, sophisticated thinkers, pragmatists, optimists, and all the combinations in between - I hope this workbook is useful.

It is obvious that a book of this volume does not cover the entire field of physical chemistry. To maintain a clear and compact form, I have omitted topics

that some readers perhaps feel are lacking. If you have any comments, questions, or suggestions, or if you want to report errors, you are welcome to contact me under jochen.vogt@ovgu.de.

Magdeburg, Germany
September 2016

Jochen Vogt

Acknowledgements

I am grateful to Tobias Wassermann and the Springer Verlag for the production and publication of this book. Furthermore, the design of the periodic system of elements in the appendix of this book is based on a L^AT_EX template made available by Christoph Wölper.

Moreover, I am grateful to my sister Katrin Vogt, expert in the psychology of learning, for reading and improving the chapter on problem-solving in physical chemistry. This book would not have been possible without the motivation and support of my wife Birgit Vogt. As a physicist herself, she has helped to improve the text and the design of the illustrations. She has accompanied this project through almost all stages with patience and good spirit.

Contents

1 Quantitative Problem Solving in Physical Chemistry	1
1.1 A Concept for Problem-Solving in Physical Chemistry	1
1.2 Overview of Problems	4
References.....	8
2 Stoichiometry and Chemical Reactions	9
2.1 Basic Concepts	9
2.1.1 Chemical Reactions	9
2.1.2 Molar Mass and Molar Volume	11
2.2 Problems	12
Reference	16
3 Changes of State	17
3.1 Systems	17
3.2 Equation of State, Thermal State Variables	18
3.2.1 Problems.....	20
3.3 Caloric State Variables, Entropy	29
3.3.1 Internal Energy, Work, and Enthalpy	30
3.3.2 Reversible and Irreversible Changes of State, the Second Law and Entropy	32
3.3.3 Adiabatic Changes of State of a Perfect Gas	33
3.3.4 The Thermodynamic Potentials	34
3.3.5 Problems.....	35
3.4 Heterogeneous Systems and Phase Transitions	51
3.4.1 The Standard State	53
3.4.2 Real and Ideal Mixtures	53
3.4.3 Problems.....	54
References.....	69
4 Thermochemistry	71
4.1 Basic Concepts	71
4.1.1 Enthalpies of Formation	71

4.1.2	The Molar Reaction Enthalpy and the Molar Reaction Entropy	72
4.1.3	Kirchhoff's Law	73
4.1.4	Hess's Law	73
4.2	Problems	74
5	Chemical Equilibrium	83
5.1	Basic Concepts	83
5.1.1	The Law of Mass Action	85
5.1.2	Temperature Dependency of the Equilibrium Constant	86
5.1.3	Chemical Equilibrium in Dilute Solutions	86
5.2	Problems	87
6	Chemical Kinetics	119
6.1	Basic Concepts	119
6.1.1	Reaction Rate	119
6.1.2	Reaction Rate Laws	120
6.2	Problems	122
	Reference	145
7	Kinetic Theory	147
7.1	Basic Concepts	147
7.1.1	Maxwell-Boltzmann Velocity Distribution	147
7.1.2	Pressure	148
7.1.3	Collisions Between Particles	149
7.1.4	Collisions with Surfaces	150
7.2	Problems	151
8	Statistical Thermodynamics	175
8.1	Basic Concepts	175
8.1.1	Statistical Interpretation of Entropy	175
8.1.2	Boltzmann Distribution	176
8.1.3	Canonical Ensemble	176
8.2	Molecular Degrees of Freedom and Partition Functions	178
8.3	Problems	179
	References	211
9	Quantum Mechanics and Electronic Structure	213
9.1	Basic Concepts	213
9.1.1	Failure of Classical Mechanics: Key Experiments	214
9.1.2	Wave Mechanics	216
9.1.3	Atomic Structure	219
9.1.4	Atomic Units	220
9.2	Problems	221
	References	292

10 Spectroscopy	293
10.1 Basic Concepts	293
10.1.1 Fundamental Interaction Process Between Light and Matter	293
10.1.2 Rotational Spectroscopy: The Rigid Rotator	296
10.1.3 Vibrational Spectroscopy of Molecules	297
10.2 Problems	299
References	356
Appendix A	357
A.1 Physical Constants	357
A.2 Physical Units and Their Conversion	358
A.3 Compilation of Mathematical Formulas	358
A.3.1 Binomial Formulas	358
A.3.2 Quadratic Equation	359
A.3.3 Logarithms	359
A.3.4 Complex Numbers	359
A.3.5 Derivatives	360
A.3.6 Basic Integration Rules	362
A.3.7 Integral Table	363
A.3.8 Power Series Expansions	364
A.3.9 Factorials and the Stirling Formula	365
A.3.10 Normal Distribution	365
A.3.11 Spherical Coordinates	366
A.3.12 Cylindrical Coordinates	367
A.3.13 Harmonic Oscillator Wave Functions	367
A.3.14 Spherical Harmonics	368
A.3.15 Radial Wave Functions of the Hydrogen Problem	369
A.3.16 Matrices	369
A.3.17 Cramer's Rule for the Solution of a System of Linear Equations	370
A.3.18 Analytic Solution for a First-Order Inhomogeneous Differential Equation	371
A.3.19 Newton's Method of Solving a Nonlinear System of Equations	371
A.3.20 Bernoulli Differential Equation	372
A.3.21 Numerical Integration Schemes for the Initial Value Problem $y(t) = f(t, y)$	373
A.4 Periodic Table of Elements	374
A.5 List of Symbols	375
A.6 List of Acronyms	378
Index	379

Chapter 1

Quantitative Problem Solving in Physical Chemistry

Abstract This introductory chapter develops and discusses a concept of mathematically oriented problem-solving in physical chemistry. Based on a definition of the scientific discipline physical chemistry, the basic skills needed for successful problem-solving are identified. The concept of problem-solving is exemplified using a sample problem text. Finally, an overview of the problems in the various chapters is given, along with comments on the level of difficulty and thematic cross-links among the various topics.

1.1 A Concept for Problem-Solving in Physical Chemistry

Physical chemistry is a scientific discipline that explores chemical topics using physical theory and technique. This definition also explains the rather challenging nature of the subject physical chemistry taught as part of university curricula. It combines three basic skills that we must develop in the course of our studies. First, we should have enough of a chemical background to understand the problem. Second, we must know the fundamental laws of physics and we need to develop some sense of the significance of fundamental physical quantities in chemical contexts.¹ Third, we must be able to apply basic mathematical methods to work out quantitative results.² Finally, *experience* including the ability of *recognition* is a fourth necessary ingredient that considerably enhances our effectiveness in problem-solving. This is quite a lot. For the solution of a concrete, non-trivial problem of a certain complexity, all these skills need to be combined to work out a solution.

In this introductory chapter, a short guide to dealing with physical chemistry problems is offered to cultivate your problem-solving skills. It picks up on the typical difficulties experienced by students that I have noticed over a period of

¹ An example of such a fundamental physical quantity is *energy*. Indeed, it is worth reflecting on the significance of energy in conjunction with nearly all key topics, ranging from changes of state (Chap. 3) to quantum mechanics and spectroscopy (Chaps. 9 and 10).

² In fact, mathematics has been called the *language of physics* [1]. A mathematical formulation of a problem combines exactness with the complete refinement to the essential facts in a quantitative manner.

teaching of about 15 years at a faculty of engineering.³ The scheme assumes a problem of relatively high complexity that requires both logical linking of facts from one or more contexts, along with the setup and execution of a mathematical solution. The five different stages listed do not follow a strictly sequential scheme. Instead, these stages are merely simultaneous intellectual activities that work together to find the solution.

1. Read the problem text carefully.

- (a) Which quantities are given?
- (b) What is going to be calculated?
- (c) Analyze the problem text with regard to special key words.

2. Use your experience to identify the essential issues.

- (a) Relate the problem to a topic in physical chemistry.
- (b) Identify matches with contents from lectures, seminars, and laboratories.
- (c) Make a sketch that collects and illustrates the important facts.
- (d) Narrow the problem down as far as possible to identify the essential issues that are inevitable for the solution of the problem.

3. Assess the points you do not yet understand.

- (a) Think pragmatically! Distinguish those details you consider crucial from those that are merely decorative.
- (b) If crucial details are lacking, reflect again on the essential issues that might be missing.
- (c) If you think that essential quantities are undefined in the problem text, will these quantities be cancelled out at the stage of the mathematical solution?
- (d) Based on your experience, reflect on the expected results.
- (e) Be critical: are you convinced that you have found the correct approach?

4. Work out the solution—translate the problem into the language of mathematics

- (a) Write down the key equations on the basis of the essential issues identified.
- (b) Reflect on potential technical difficulties, e.g., those related to undefined quantities (see above).

5. Accomplish the solution

- (a) Think pragmatically! Possible technical difficulties may be resolved by the solution.
- (b) If you have obtained results, assess their plausibility.
- (c) Reflect again on the solution. Are you convinced that you have found the correct solution?

³An extensive analysis of such difficulties can be found in [2].

As an example of a concrete problem text, consider Problem 3.13 on page 64. The problem text is reproduced here and the quantities provided and sought, along with the key-words according to points 1.a, 1.b, and 1.c, are highlighted:

At 293 K, the vapor pressure of the solvent diethyl ether ($C_2H_5-O-C_2H_5$) is 586 hPa. After the addition of 20 g of an unknown non-volatile compound in 1 kg diethyl ether, the vapor pressure reduces to 583 hPa. Assume an ideal mixture of diethyl ether and the unknown compound, for which an elementary analysis yields mass fractions of 41.4% carbon, 5.5% hydrogen, 9.6% nitrogen, and 43.8% oxygen. Determine the molar mass and the molecular formula of the unknown compound.

Let us look at the various stages of this problem-solving scheme. Careful reading of the text is important. We must analyze the problem with regard to the quantities given and the quantities to be calculated. In preparation for stage 4, we should assign a unique symbol to each quantity. Note that in many cases it is crucial to distinguish between the initial value of a certain quantity and its value in the final state, or the values that the quantity takes during an ongoing process. In the concrete problem, we must distinguish between the vapor pressure of *pure* diethyl ether (a common symbol would be p^*), and its vapor pressure in the binary mixture (symbol p). Moreover, it is crucial to define all quantities in the same system of units, usually the SI system. Sometimes you need to convert some of the quantities (see Table A.2 in the appendix).

In the second stage, the *essential issues*, which are inevitable for the solution of the problem, are identified. A first assignment of the problem to a general topic is made based on the recognition of lecture content, seminar work, laboratory work, etc. Quite often, we find such essential issues coded in *key words* appearing in the problem text. In the concrete problem, such a key-word is the ideal mixture, implying the application of Raoult's law (Eq. (3.108) on page 54). Another essential issue is stoichiometry and the definition of the mole fraction and molar mass. A third ingredient is the fact that the solvent diethyl ether and the unknown compound constitute a *binary* mixture—a point that is not explicitly stated in the problem text. Sometimes, it is quite useful to make a sketch to collect and arrange such essential issues visually, and to identify the logical links between them. This is especially true for problems involving processes with an initial state and a final state.

Depending on your experience and the complexity of the problem, you will not immediately identify the correct approach. In this case, it is important to assess the points you do not yet understand (stage 3). Sometimes, it is good advice to think pragmatically. For example, do not become intimidated by problem texts filled with impressively long names of chemical compounds. Sometimes, you just need the

molecular formula to determine a molar mass; in other cases, they can be replaced altogether by shorter symbols. At the stage where you do not yet see through the solution pathway, an detail that is lacking, such as an undefined quantity may be canceled out in the calculation. However, it may also indicate that you have missed something. Be hopeful and at the same time critical with the setup of your solution.

The next step is to write down the equations resulting from the list of essential issues identified (stage 4). The more experience we have, the easier it is to transpose the solution concept into a set of mathematical equations. In fact, at a level of deeper understanding, the student's conceptual view based on essential issues and the mathematical formulation tend to merge. Also at this stage, we must be critical: the appearance of undefined quantities in the equations, but also too many redundant quantities, could indicate flaws in the approach and may force a reassessment. At the last stage, where the solution has been found, you should check the plausibility of your results. It is worth comparing the results with the initial estimations. An approximate agreement within the same order of magnitude strengthens the confidence with regard to the method of solution. Large differences, in contrast, require critical reflection on the entire method of solution. In this case, it is a good idea to consider possible technical errors first, e.g., arithmetic errors, such as confusion of signs or the addition of quantities with different physical units. Unexpected deviations in spite of a correct solution, in contrast, invite us to rethink a topic from a new perspective. In fact, in this case, a problem can prove to be highly useful to the individual student.

Note that not all problems collected in this book fit exactly into the scheme proposed above. For example, there are numerous problems where we prove a certain relationship before it is applied to a concrete case. Another popular category of problems involves a graphical solution or, in some cases, a numerical treatment using a computer.

1.2 Overview of Problems

In the following, the problems presented in the various chapters are listed.

Chapter 2: Stoichiometry and Chemical Reactions

Problem 2.1	Molar mass and molar volume	12
Problem 2.2	Stoichiometry of a combustion reaction	14
Problem 2.3	The limiting reactant	15

Chapter 3: Changes of State

Problem 3.1	Thermal state variables	20
Problem 3.2	Thermal expansion of condensed phases and gases	21
Problem 3.3	Perfect gas vs real gas	24

Problem 3.4	Van der Waals isotherms, Maxwell construction	26
Problem 3.5	Molar heat capacities of a van der Waals gas	35
Problem 3.6	Work and mechanical equilibrium	37
Problem 3.7	Adiabatic reversible expansion/compression	39
Problem 3.8	Entropy change and free expansion of a van der Waals gas	43
Problem 3.9	Reversible and irreversible adiabatic expansion	46
Problem 3.10	Vapor pressure of a pure substance	54
Problem 3.11	Molar Gibbs free energies of solids and gases, conversion of graphite to diamond	59
Problem 3.12	Ideal solutions	62
Problem 3.13	Vapor pressure reduction	64
Problem 3.14	Spontaneous freezing of supercooled water	66
Problem 3.15	Freezing of atmospheric water droplets to cubic or hexagonal ice	68

Chapter 4: Thermochemistry

Problem 4.1	Combustion enthalpies	74
Problem 4.2	Solvation enthalpy	77
Problem 4.3	Ellingham diagram	79

Chapter 5: Chemical Equilibrium

Problem 5.1	Br ₂ decay	87
Problem 5.2	Equilibrium in parallel reactions I	91
Problem 5.3	Equilibrium in parallel reactions II	93
Problem 5.4	Water-gas shift reaction	97
Problem 5.5	Dehydrogenation of methanol	100
Problem 5.6	Temperature dependence of equilibrium constants	103
Problem 5.7	Determination of reaction enthalpy and reaction entropy	106
Problem 5.8	A simple model of acid rain	109
Problem 5.9	CO ₂ dissolution in a closed bottle of water	111
Problem 5.10	Dissociation of trichloroacetic acid	115

Chapter 6: Chemical Kinetics

Problem 6.1	Reaction order and half-life	122
Problem 6.2	First order decay	125
Problem 6.3	Methane decay	127
Problem 6.4	Kinetic look at chemical equilibrium	130
Problem 6.5	Competing reactions	134
Problem 6.6	Oscillating chemical reactions I	138
Problem 6.7	Oscillating chemical reactions II	142

Chapter 7: Kinetic Theory

Problem 7.1	Maxwell-Boltzmann distribution I	151
Problem 7.2	Maxwell-Boltzmann distribution II	154
Problem 7.3	Relative velocity of two particles	159
Problem 7.4	Collision rates in a helium-xenon gas mixture	163
Problem 7.5	Gas effusion	166
Problem 7.6	Film growth	172

Chapter 8: Statistical Thermodynamics

Problem 8.1	Conformational entropy and protein structure	179
Problem 8.2	Mixing of gases	181
Problem 8.3	A simple model of diffusion	185
Problem 8.4	Surface diffusion	192
Problem 8.5	Derivation of Boltzmann distribution	195
Problem 8.6	Entropy of monatomic gases	199
Problem 8.7	Heat capacity of multilevel systems	202
Problem 8.8	Schottky anomaly	206

Chapter 9: Quantum Mechanics and Electronic Structure

Problem 9.1	Derivation of the average oscillator energy	221
Problem 9.2	The zero point energy	223
Problem 9.3	Electron impact heating	224
Problem 9.4	Photoelectric effect	226
Problem 9.5	Lithium atom and quantum defect	227
Problem 9.6	Schrödinger equation	231
Problem 9.7	Wave packets and uncertainty principle	234
Problem 9.8	Gaussian wave packet propagation	238
Problem 9.9	Conservation of the norm of the wave function	241
Problem 9.10	Operators I	244
Problem 9.11	Operators II	248
Problem 9.12	Quantization: the electron on a ring	253
Problem 9.13	Electronic excitation of the benzene molecule	255
Problem 9.14	Hydrogen first wave function	257
Problem 9.15	Hydrogen problem applied to semiconductor technology	260
Problem 9.16	Variational method	262
Problem 9.17	The quantum double well	272
Problem 9.18	The chemical bond	281

Chapter 10: Spectroscopy

Problem 10.1	Units of measurement in spectroscopy	299
Problem 10.2	Doppler broadening of spectral lines	302
Problem 10.3	UV absorption of proteins	307
Problem 10.4	HCN molecular structure	309
Problem 10.5	Asymmetric top rotation spectra	313
Problem 10.6	IR spectra of diatomics I	319
Problem 10.7	IR spectra of diatomics II	325
Problem 10.8	Vibrational modes of polyatomic molecules	334
Problem 10.9	Influence of nuclear spin statistics	340
Problem 10.10	LASER-I	345
Problem 10.11	LASER-II	352

The order of topics in this workbook roughly follows the way in which physical chemistry is presented in contemporary textbooks. Stoichiometry (Chap. 2) is the natural starting point of any quantitative treatment in general chemistry. Moreover, stoichiometry is a prerequisite for the understanding of fields such as chemical equilibrium (Chap. 5) and chemical kinetics (Chap. 6). The attentive reader will notice that certain concepts such as the extent of reaction introduced in Chap. 2, are systematically used in the subsequent chapters.⁴ In this sense, the arrangement of problems has an intrinsic order. But this should by no means prevent the reader from entering into the problems at an arbitrary point. In a few cases where the solution of a problem assumes that the reader has dealt with the preliminary contents of other problems, this is explicitly noted.

Concerning the complexity of the problems, the level of difficulty gradually increases from chapter to chapter, not only from a mathematical, but also from a conceptual point of view. Concerning mathematics and the methods of solution, the attentive reader will notice interesting parallels. A prime example is the set of problems dealing with *oscillating chemical reactions* (Problems 6.6 and 6.7) in the chapter on reaction kinetics on the one hand, and the set of problems dealing with *LASER* operation in Chap. 10 (spectroscopy) on the other.⁵ Seemingly an accidental mathematical conformity at first sight, these similarities reveal a *hidden* relationship with regard to interaction in complex systems that the reader might discover.⁶

⁴In my experience, many students are reserved in using the extent of reaction in concrete problems. Not appearing explicitly in any fundamental laws such as the law of mass action, it seems somehow dispensable. In fact, it is possible to work out a correct solution without using it explicitly. However, this requires an intellectual effort that unconsciously achieves the same purpose as the conscious use of this concept would do systematically.

⁵In fact, for the numerical solution of the laser equations in Problem 10.11, you can use the computer code of Problem 6.7, with only small modifications.

⁶The present book can, of course, only draw the reader's attention to such points without analyzing the relationships in full detail, as has been done by Hermann Haken [3].

In Chap. 9 dealing with quantum mechanics, problems highlighting some rather abstract aspects of quantum mechanics, such as operator algebra, were included, for several reasons. First, the interpretation of quantum mechanics raises interesting discussions in seminars. Second, operator algebra in quantum mechanics is a powerful method of producing results with sometimes surprisingly sparse efforts.⁷ Third, graduate students starting to listen to specialized conference talks, e.g., in spectroscopy, will experience the necessity of being familiar with these methods for their future scientific work.

References

1. Cullerne JP, Machacek A (2008) The language of physics—a foundation for university study. Oxford University Press, Oxford
2. Bodner GM, Herron JD (2003) Problem solving in chemistry. In: Gilbert JK, De Jong O, Justi R, Treagust DF, Van Driel JH (eds) Chemical education: towards research-based training. Springer, Berlin
3. Haken H (2004) Synergetics. Springer, Heidelberg

⁷An instructive example is the solution of the quantum double well problem (Problem 9.17) for which the energy levels can be calculated with arbitrary precision without solving one single integral explicitly.

Chapter 2

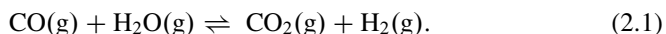
Stoichiometry and Chemical Reactions

Abstract Stoichiometry deals quantitatively with the conversion of substances in the course of a chemical reaction. In this short chapter, we make ourselves familiar with the definition of some important quantities concerning chemical reactions. We use them throughout this book, as stoichiometric considerations are applied in virtually all problems dealing with chemical reactions such as thermochemistry (Chap. 4) or chemical kinetics (Chap. 6). The problems presented in this chapter deal with elementary applications of stoichiometry.

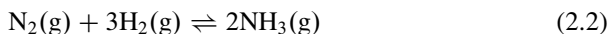
2.1 Basic Concepts

2.1.1 Chemical Reactions

One of the milestones in the development of chemistry is the discovery by John Dalton that during a chemical reaction the number of the elementary parts of an element, which he called atoms, is unchanged. Atoms are neither consumed nor created in a chemical reaction. Instead, a chemical reaction can be characterized by a *rearrangement* or *exchange* of atoms among various molecular entities. A concrete example is the water–gas shift reaction



As the number of molecules on the right and on the left is the same, the total number of molecules during this reaction is unchanged. Next, consider the ammonia synthesis reaction



Here, the number of molecules on the left is twice the number of molecules on the right. As a consequence, characteristic of a *synthesis* reaction, the total number of molecules in the reactor decreases as this reaction proceeds. Finally, consider the dissociation of $(\text{NO}_2)_2$ in the gas phase,



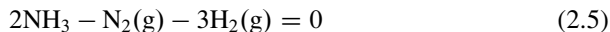
Here, the total number of molecules increases as the reaction proceeds, typical of a *dissociation* reaction. These examples show that the number of molecules is not necessarily constant in the course of a chemical reaction.

A substance on the left hand side is called an **educt** or **reactant**. The number of molecules of a reactant generally decreases in the course of a chemical reaction. In contrast, a substance on the right hand side, is called a **product**. The number of molecules of a product increases as the reaction proceeds.

The **most general formulation of a chemical reaction**, which we refer to throughout this book, is as follows:

$$\sum_J v_J X_J = 0 \quad (2.4)$$

The index J counts reactants and products denoted by the symbol X_J . The coefficients v_J are called **stoichiometric numbers**. Note that the stoichiometric numbers of the reactant are negative, whereas those of the products are positive. As an example, the ammonia synthesis reaction Eq. (2.2) can be rewritten as follows:



In order to quantify the number of molecules and its changes, the **SI unit mole** has been defined:

The SI unit mole is the amount of substance of a system containing as many elementary units as there are carbon atoms in exactly 0.012 kg of carbon-12. 1 mole of particles is $N_A = 6.02214129(27) \times 10^{23} \text{ mol}^{-1}$, the **Avogadro constant**.

It is essential to realize that in the course of a chemical reaction, the mole numbers of the various substances change in a specific manner. To describe this quantitatively, the **extent of reaction**, ξ , is introduced. This quantity enables the changes in the amounts of reactants and products to be expressed as a function of time:

$$n_J(t) = n_J^0 + v_J \xi(t) \quad (2.6)$$

Here, $n_J(t)$ is the amount of X_J at time t , and n_J^0 is its initial value. Note that because the definition of the stoichiometric numbers of the reactants is to be negative, the amount of reactant decreases, whereas the amount of product increases in a chemical reaction. Furthermore, as the number of moles of any substance is always positive, the reaction comes to an end, if one of the reactants $|v_J \xi|$ reaches n_J^0 . In general, all but one of the reactants is present in excess, and one reactant is the **limiting reactant**.

The definition of ξ does not refer to a specific substance: a differential change in the extent of reaction is given by

$$d\xi = \frac{dn_J(t)}{v_J} = \frac{dn_{J'}(t)}{v_{J'}} = \dots \quad (2.7)$$

Another important quantity that characterizes the composition of a system, is the **mole fraction** x_i :

$$x_i = \frac{n_i}{\sum_j n_j} \quad (2.8)$$

Note that the sum of all mole fractions in a system is 1. Similarly, the **concentration** c_i of a species is defined as

$$c_i = \frac{n_i}{V} \quad (2.9)$$

where V is the system volume.

2.1.2 Molar Mass and Molar Volume

In laboratory work, the determination of the amount of a chemical compound is often based on weighing, i.e., the determination of its mass. Characteristic of each element is its atomic mass, which is tabulated in the **periodic system of elements** (PSE, also called periodic table of elements, see appendix Sect. A.4). As the mass of a molecular compound is a very good approximation of the sum of the atomic masses constituting one molecular unit, the **molar mass** M of each compound can be deduced using the PSE. The number of moles of an arbitrary amount of a chemical compound with mass m is then

$$n = \frac{m}{M} \quad (2.10)$$

Because a pure material is characterized by a unique density ρ , the **molar volume** v of the material is given by

$$v = \frac{M}{\rho}. \quad (2.11)$$

The molar volumes of substances in the solid and in the liquid state are generally neglected in favor of the molar volumes of substances in the gaseous state. The relation among pressure p , volume V , and temperature T is established by the equation of state. For gases, the equation of state of the perfect gas,

$$p V = n R T, \quad (2.12)$$

is in many problems a reasonable approximation. $R = 8.314462 \text{ J K}^{-1} \text{ mol}^{-1}$ is the molar gas constant. At atmospheric pressure and a temperature of 298 K, the molar volume of a perfect gas is about 24.81.

2.2 Problems

An additional problem directly related to stoichiometry is Problem 3.13 on page 64.

Problem 2.1 (Molar Mass and Molar Volume) At a temperature of 293 K and atmospheric pressure, the density of sodium chloride is $\varrho = 2.165 \text{ g cm}^{-3}$. Use the periodic table of elements and determine the molar mass and the molar volume of NaCl. Calculate the nearest neighbor distance d in the rocksalt lattice (see Fig. 2.1).

Solution 2.1 The solution to this problem illustrates the amount of substance of a well-known material: sodium chloride. At first we shall determine its molar mass and its molar volume. From the periodic table of elements we take the atomic weights of sodium and chlorine, $M_{\text{Na}} = 22.990 \text{ g mol}^{-1}$ and $M_{\text{Cl}} = 35.453 \text{ g mol}^{-1}$, respectively. Thus, the molar mass of NaCl is the sum of these atomic weights: $M_{\text{NaCl}} = M_{\text{Na}} + M_{\text{Cl}} = 58.443 \text{ g mol}^{-1}$.

To determine the molar volume v of NaCl, we use the definition of the density as mass per volume (see Eq. (2.11)): $\varrho \stackrel{\text{def}}{=} \frac{m}{V} = \frac{M_{\text{NaCl}}}{v}$

Hence,

$$v = \frac{M_{\text{NaCl}}}{\varrho} = 26.994 \text{ cm}^3 \text{ mol}^{-1}. \quad (2.13)$$

Thus, according to our result, one mole of NaCl has the volume of a cube of about 3.0 cm in edge length.

Next, from our result on v , we shall determine the nearest neighbor distance of Na and Cl in the rocksalt lattice shown in Fig. 2.1. The crystal structure of NaCl

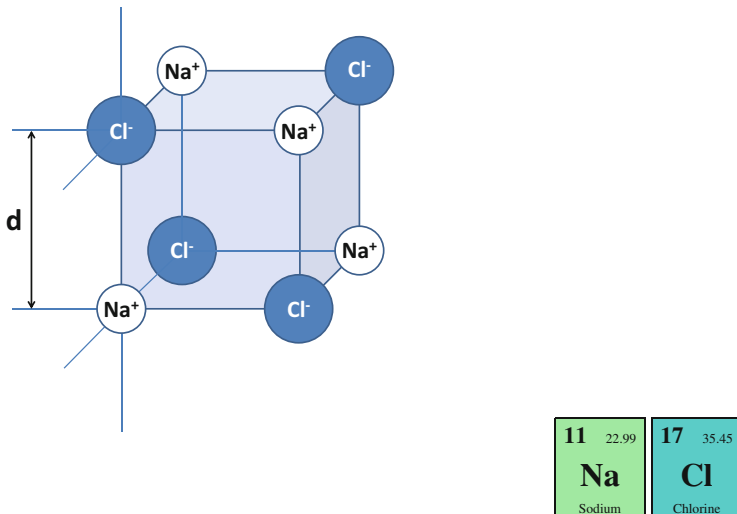


Fig. 2.1 *Left:* the NaCl crystal lattice. *Right:* cards with the atomic weights for the elements sodium and chlorine, taken from the periodic systems of the elements (see Sect. A.4)

is well-known from X-ray crystallography experiments, and the nearest-neighbor distance can be measured with great precision. However, just with our result of the molar volume of NaCl, we can determine d : one mole of NaCl corresponds to $N_A = 6.022 \times 10^{23}$ NaCl formula units. Hence, the volume occupied by one formula unit NaCl is

$$V_{\text{NaCl}} = \frac{v}{N_A} = 4.44825 \times 10^{-23} \text{ cm}^3 = 4.4825 \times 10^{-29} \text{ m}^3. \quad (2.14)$$

There are several possibilities for relating the volume per formula unit to the crystal structure shown in Fig. 2.1. The shaded cube has a volume $V_{\text{cube}} = d^3$. This cube has four chloride ions and four sodium ions at its corners. However, we must bear in mind that each ion is shared by eight neighboring cubes joining at the respective ionic site. Thus, each of the cubes contains $\frac{4}{8} = \frac{1}{2}$ sodium ions, and $\frac{4}{8} = \frac{1}{2}$ chloride ions, i.e., 0.5 NaCl formula units. Hence, $V_{\text{cube}} = d^3 = \frac{1}{2} V_{\text{NaCl}}$, and thus

$$d = \left(\frac{1}{2} V_{\text{NaCl}} \right)^{\frac{1}{3}} = 2.82 \times 10^{-10} \text{ m}. \quad (2.15)$$

This result is very close to the result obtained in X-ray diffraction experiments [1].

Problem 2.2 (Stoichiometry of a Combustion Reaction) After the combustion of 10.000 g of pure vanadium in an oxygen atmosphere, the reaction product has a mass of 17.852 g. Write down the reaction equation for the combustion of vanadium.

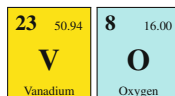


Fig. 2.2 Cards for the elements vanadium and oxygen in the periodic system of the elements (see Sect. A.4)

Solution 2.2 A simple experiment that does not require a complex setup is the determination of the stoichiometric composition of a metal oxide after it has been formed by combustion in an oxygen atmosphere. All that is needed is a laboratory weighing scale. In our problem, the mass of the reactant, pure vanadium, is $m_V = 10.000\text{ g}$. The mass of the reaction product, vanadium oxide, is $m_{\text{oxide}} = 17.852\text{ g}$. We determine its stoichiometric formula and the corresponding reaction. We start with the general reaction



and we need to determine x and y . First, we evaluate the amount of vanadium we have used. According to the PSE, the molar mass of vanadium is 50.942 g mol^{-1} . Thus, $n_V = \frac{m_V}{M_V} = 0.1963\text{ mol}$ (Fig. 2.2).

The reaction product has a higher mass than the reactant. The reason is the oxygen, which has been incorporated during the combustion. The mass of the oxygen is therefore merely the difference $m_{\text{oxide}} - m_V$. Hence, the amount of oxygen is

$$n_O = \frac{m_O}{M_O} = \frac{m_{\text{V}_x\text{O}_y} - m_V}{M_0} = \frac{7.852\text{ g}}{15.999 \frac{\text{g}}{\text{mol}}} = 0.4908\text{ mol}. \quad (2.17)$$

The ratio between oxygen and vanadium is thus $n_O:n_V = 0.4908:0.1963 = 5:2$. Therefore $x = 2$ and $y = 5$ and the reaction sought is



Problem 2.3 (The Limiting Reactant) At 1,000 K and a pressure of 5 MPa, a tank with 500 dm^3 containing $\text{TiCl}_4(\text{g})$ is connected to another tank with $1,000 \text{ dm}^3$ filled with $\text{CH}_4(\text{g})$. Given a complete stoichiometric conversion of these gases into solid $\text{TiC}(\text{s})$ and $\text{HCl}(\text{g})$, calculate the residual pressure after the reaction and the mass of TiC formed. Assume perfect gas behavior of all gaseous substances. Ignore the volume of the solid reaction product.

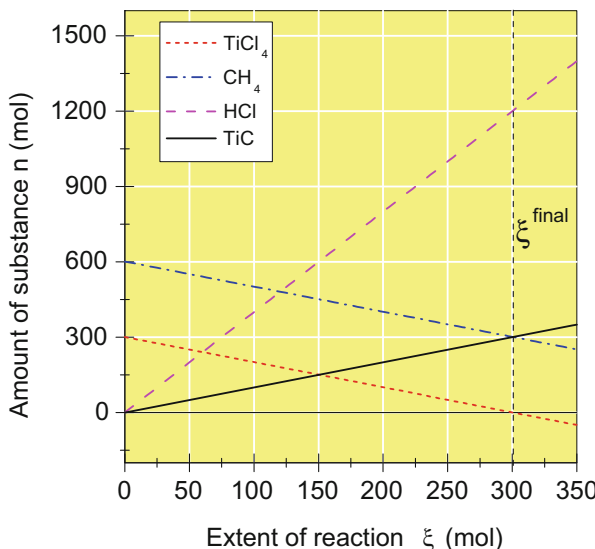
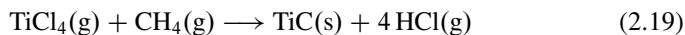


Fig. 2.3 Amounts of substances as a function of ξ for reaction Eq. (2.19). TiCl_4 limits the reaction at $\xi^{\text{final}} = 300.7 \text{ mol}$

Solution 2.3 This exercise deals with a chemical reaction that comes to an end when one of the educts is completely consumed. Initially, at a temperature $T = 1,000 \text{ K}$ and a pressure of $p^0 = 5 \text{ MPa}$, the tank with the volume $V_1 = 0.5 \text{ m}^3$ contains $\text{TiCl}_4(\text{g})$, the other tank with the volume $V_2 = 1 \text{ m}^3$ contains $\text{CH}_4(\text{g})$. We need to formulate the conversion reaction to $\text{TiC}(\text{s})$ and $\text{HCl}(\text{g})$:



Next, we calculate the initial mole numbers of these reactants assuming perfect gas behavior (Eq. (2.12)):

$$n_{\text{TiCl}_4}^0 = \frac{p^0 V_1}{RT} = 300.7 \text{ mol} \quad (2.20)$$

$$n_{\text{CH}_4}^0 = \frac{p^0 V_2}{RT} = 601.4 \text{ mol} \quad (2.21)$$

As there is an excess of methane, TiCl_4 limits the reaction. What does this mean? In our problem, the final extent of reaction according to Eq. (2.6) is $\xi^{\text{final}} = n_{\text{TiCl}_4}^0$ when all TiCl_4 is consumed. The situation is illustrated in Fig. 2.3. The amounts of CH_4 , HCl , and TiC can be obtained at ξ^{final} using Eq. (2.6): There will be $n_{\text{CH}_4}^{\text{final}} = n_{\text{CH}_4}^0 - \xi^{\text{final}} = 300.7 \text{ mol}$ of methane left in the reaction volume $V_1 + V_2$. Moreover, $n_{\text{HCl}}^{\text{final}} = 0 + 4\xi^{\text{final}} = 1,202.8 \text{ mol}$, and $n_{\text{TiC}}^{\text{final}} = 0 + \xi^{\text{final}} = 300.7 \text{ mol}$.

We calculate the final pressure

$$p^{\text{final}} = (n_{\text{HCl}}^{\text{final}} + n_{\text{CH}_4}^{\text{final}}) \frac{RT}{(V_1 + V_2)} = 8.3 \text{ MPa.} \quad (2.22)$$

The molar mass of TiC is $M_{\text{TiC}} = 59.9 \text{ g mol}^{-1}$. Hence, at the end of the reaction, the mass of the solid reaction product TiC is $m_{\text{TiC}}^{\text{final}} = M_{\text{TiC}} \times n_{\text{TiC}}^{\text{final}} = 18.0 \text{ kg}$.

Reference

1. Bragg WH, Bragg WL (1915) X rays and crystal structure. Bell, London

Chapter 3

Changes of State

Abstract Thermodynamics is introduced as a quantitative method of characterizing the changes of state of systems. The topic is subdivided in three categories. Problems dealing with *thermal state variables* and equations of state are found in Sect. 3.2, along with a compact summary of essential theory. Problems focusing on the *caloric state variables* are discussed in Sect. 3.3, again preceded by a summary of basic concepts. Finally, a set of problems dealing with heterogeneous systems, phase transitions, and mixtures is presented in Sect. 3.4.

This chapter deals with a field in physical chemistry that offers a direct approach from our every-day viewpoint: changes in state. A walk through a winter landscape may stir deep feelings in us about the beauty of nature in its entirety, but it may also be a good starting point for developing conceptions about processes in nature and their origin. If we look, for example, at a foggy lake in winter with ice cakes floating downstream, we see water in its different forms: water as a liquid, as vapor, or as ice. The melting of a snow-flake on a warm surface, or the vaporization of a rain drop are concrete examples of changes of state. But even a change in pressure, temperature, or volume is a change of state. Thermodynamics is the result of human reflection about such processes, and it provides the necessary concepts for understanding the general principles behind them, such as the phase diagram of a substance, which relates its states of aggregation to pressure and temperature (Fig. 3.1).

3.1 Systems

For the analysis of processes in nature, it is indispensable to subdivide the considered totality of interacting matter into parts. Typically, we are only interested in the evolution of a certain amount of matter, clearly distinguished by the environment, the surroundings. Usually, the properties of the surroundings are not well-known, but neglecting them completely would be too crude an approximation. Therefore, the concept of the system is introduced, which can be subdivided into subsystems, separated by well-defined boundaries. A system that exchanges neither matter nor heat with its surroundings is called an **isolated system**. A system that only

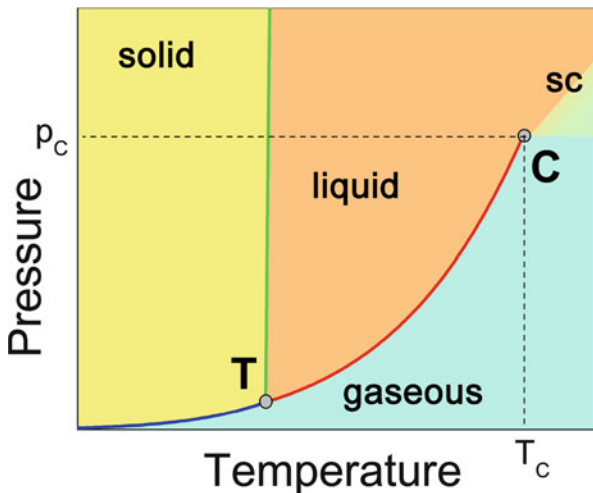


Fig. 3.1 Schematic phase diagram of a pure substance near the triple point (T) with coexistence lines of solid and liquid, gas and liquid, gas and solid. C is the critical point. SC marks the *supercritical phase*

exchanges heat with its surroundings is called a **closed system**. An open system exchanges both heat and matter with its surroundings. A chemical system usually contains a very large number of atoms or molecules, to the order of 10^{23} . On a macroscopic scale, one is primarily interested in only a few **state variables**, which result as the average of the movement of all the interacting atoms and molecules constituting the system. **Intensive** quantities characterizing a system do not depend on the size of the system, whereas **extensive** quantities do. Extensive properties of subsystems are additive. Note that for extensive quantities such as the volume V , capital letters are used in general. Lower case letters are reserved for the related (intensive) molar quantity, e.g., the molar volume v .

3.2 Equation of State, Thermal State Variables

The **thermal state variables** are the temperature T , the pressure p , and the volume V of the system consisting of a certain amount of substance n . There is always an **equation of state**

$$f(p, V, T, n) = 0 \quad (3.1)$$

that links these three thermal state variables. If the system under consideration is a **perfect gas**, the equation of state is

$$pV = nRT \quad (3.2)$$

with the molar gas constant $R = 8.3144621(75) \text{ J K}^{-1} \text{ mol}^{-1}$. The concept of the perfect gas assumes the particles to be point masses without extension, and the model neglects all intermolecular interactions.

Another well-known equation of state is the one proposed by **van der Waals**:

$$\left(p + \frac{an^2}{V^2} \right) (V - nb) = nRT \quad (3.3)$$

It contains two model parameters, a and b , which can be fitted for each substance to experimental p - V - T data. To some extent, the van der Waals model involves the existence of the *critical point* and a possible coexistence of condensed phase and gas phase, but it is of limited accuracy (see also Problem 3.4).

The **virial equation** for 1 mole of substance relates pressure p , temperature T , and the molar volume v in the following way:

$$\frac{p v}{RT} = 1 + \frac{B(T)}{v} + \frac{C(T)}{v^2} + \dots \quad (3.4)$$

It has the advantage of directly linking the p - V - T behavior of a substance to intermolecular interaction. The second virial coefficient B is a temperature-dependent quantity, which is related to pair interaction between molecules, the third virial coefficient C is related to interaction among three molecules, etc.

In the course of a change of state of the system, the thermal state variables are subject to changes. A change in volume, for example, results as a consequence of changes in pressure and temperature:

$$dV = \left(\frac{\partial V}{\partial T} \right)_p dT + \left(\frac{\partial V}{\partial p} \right)_T dp \quad (3.5)$$

Given a specific equation of state, the differential quotients themselves can be determined. Moreover, especially in the case of *condensed phases*, they can be expressed by important material properties such as the **isobaric thermal expansion**

coefficient,

$$\alpha = \frac{1}{V} \left(\frac{\partial V}{\partial T} \right)_p \quad (3.6)$$

or the **isothermal compressibility**

$$\kappa = \frac{1}{V} \left(\frac{\partial V}{\partial p} \right)_T \quad (3.7)$$

Thermodynamics is able to derive relations between material properties such as α and κ without assuming any microscopic theory of matter (see Problem 3.1). Note that a material property in general depends on the temperature or pressure.

3.2.1 Problems

Problem 3.1 (Thermal State Variables)

- a. For an arbitrary isochoric change of state, show that the following equation holds:

$$\left(\frac{\partial p}{\partial T} \right)_V = - \frac{(\partial V / \partial T)_p}{(\partial V / \partial p)_T} = \frac{\alpha}{\kappa} \quad (3.8)$$

- b. For an arbitrary change of state, show that the following relation holds

$$d(\ln V) = \alpha dT - \kappa dp \quad (3.9)$$

Solution 3.1 In this problem, we use the concept of the total differential to show some useful relations. It is worth mentioning that thermodynamics does not necessarily assume a microscopic theory of matter that would allow the prediction of material properties such as the compressibility of a substance or its expansion coefficient. Nevertheless, thermodynamics allows the formulation of relations between such material properties. One example is Eq. (3.8).

To show Eq. (3.8) in **subproblem (a)**, we consider the total differential of the volume, which is zero for an isochoric change of state:

$$\text{isochoric} \Leftrightarrow dV = \left(\frac{\partial V}{\partial T} \right)_p dT + \left(\frac{\partial V}{\partial p} \right)_T dp \stackrel{!}{=} 0 \quad (3.10)$$

$$\Leftrightarrow \left(\frac{\partial V}{\partial T} \right)_p dT = - \left(\frac{\partial V}{\partial p} \right)_T dp; \quad dV = 0 \quad (3.11)$$

$$\Leftrightarrow \left(\frac{dp}{dT} \right)_V = - \frac{\left(\frac{\partial V}{\partial T} \right)_p}{\left(\frac{\partial V}{\partial p} \right)_T} \quad (3.12)$$

As (see Sect. A.3.5.3 in the appendix)

$$\left(\frac{dp(T, V)}{dT} \right)_V = \left(\frac{\partial p(T, V)}{\partial T} \right)_V, \quad (3.13)$$

we have thus shown Eq. (3.8). For the proof of Eq. (3.9) in **subproblem (b)**, we start again with the total differential of the volume (Eq. (3.5)), and divide by V :

$$dV = \left(\frac{\partial V}{\partial T} \right)_p dT + \left(\frac{\partial V}{\partial p} \right)_T dp \quad (3.14)$$

$$\Leftrightarrow \frac{dV}{V} = \frac{1}{V} \left(\frac{\partial V}{\partial T} \right)_p dT + \frac{1}{V} \left(\frac{\partial V}{\partial p} \right)_T dp \quad (3.15)$$

With the definition of α (Eq. (3.6)) and κ (Eq. (3.7)), we have

$$\Leftrightarrow \frac{dV}{V} = \alpha dT - \kappa dp \quad (3.16)$$

$$\Leftrightarrow d(\ln V) = \alpha dT - \kappa dp \quad (3.17)$$

which is what was to be shown.

Problem 3.2 (Thermal Expansion of Condensed Phases and Gases) The thermal expansion coefficient of liquid water is $\alpha = 20.0 \times 10^{-5} \text{ K}^{-1}$, and its compressibility is $\kappa = 0.5 \times 10^{-9} \text{ Pa}^{-1}$.

Use Eqs. (3.8) and (3.9) to calculate

- The change in volume of 1 dm³ water being heated from 25 °C up to 50 °C at atmospheric pressure.
- The pressure exerted on the walls of a closed container of a volume of 1 dm³, which is heated to 50 °C after it was completely filled with water at 100,000 Pa and 25 °C.
- The thermal expansion coefficient α of a perfect gas at 25 °C, and the compressibility κ of a perfect gas at 100,000 Pa.

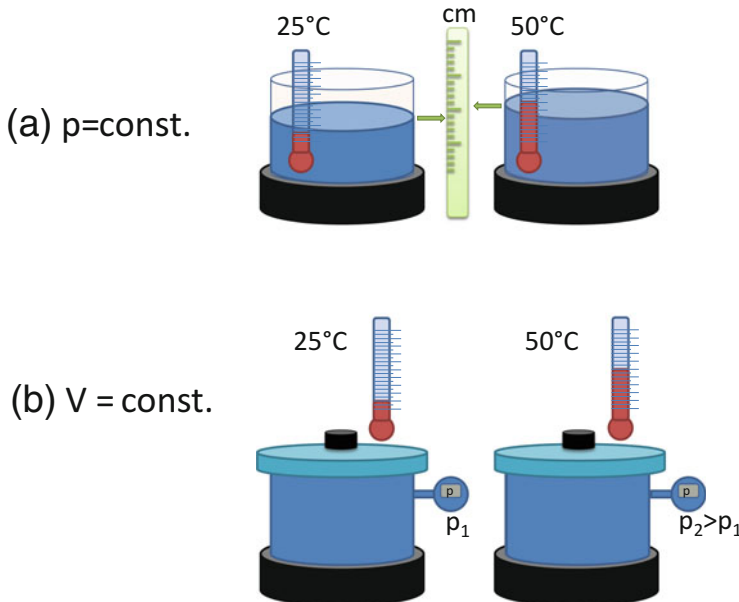


Fig. 3.2 (a) Thermal expansion of water at a constant pressure. (b) Heating of water at a constant volume causes an increase in pressure

Solution 3.2 Taking liquid water as an example of a condensed phase, we examine the effects of thermal expansion and compressibility in comparison with perfect gas behavior.

In **subproblem (a)** we calculate the change in volume of water, heated at an atmospheric pressure from $T_1 = 298.15$ to $T_2 = 323.15$ K. This is the situation in which we heat water in an open cooking pot, as shown in Fig. 3.2a. In our experience, the effect of thermal expansion is small. We adopt Eq. (3.9) for the case of constant pressure ($dp = 0$) and obtain

$$d(\ln V) = \alpha dT$$

What comes next is the necessary integration step

$$\int_{\ln V_1}^{\ln V_2} d \ln V = \alpha \int_{T_1}^{T_2} dT$$

Here, we assume that the material property α is independent of temperature within the range T_1 to T_2 . The rules for logarithms (see appendix Sect. A.3.3) allow

us to evaluate the integrals in the following way:

$$\ln V_2 - \ln V_1 = \ln \frac{V_2}{V_1} = \alpha (T_2 - T_1) \Leftrightarrow V_2 = V_1 \exp(\alpha(T_2 - T_1))$$

$$V_2 = V_1 \exp(\alpha(T_2 - T_1)) = 1 \text{ dm}^3 \exp(20.0 \times 10^{-5} \text{ K}^{-1} \times 25 \text{ K}) = 1.005 \text{ dm}^3$$

Hence, the sought change in volume upon heating is only $V_2 - V_1 = 0.005 \text{ dm}^3$.

Subproblem (b) deals with the case of heating liquid water at a constant volume (Fig. 3.2b). Although we have seen that the effect of thermal expansion is only small for condensed phases, heating the latter at a constant volume can involve enormous changes in pressure, as we will see. We start with Eq. (3.8)

$$\left(\frac{\partial p}{\partial T} \right)_V = \frac{\alpha}{\kappa} \Leftrightarrow dp = \frac{\alpha}{\kappa} dT; \quad V = \text{const.}$$

Integration within the limits $p_1 = 100,000 \text{ Pa}$ at $T_1 = 298.15 \text{ K}$ and p_2 —the sought pressure at $T_2 = 323.15 \text{ K}$ —yields

$$\int_{p_1}^{p_2} dp = \frac{\alpha}{\kappa} \int_{T_1}^{T_2} dT.$$

We obtain

$$p_2 = p_1 + \frac{\alpha}{\kappa} (T_2 - T_1) = 100,000 \text{ Pa} + \frac{20 \times 10^{-5} \text{ K}^{-1}}{0.5 \times 10^{-9} \text{ Pa}^{-1}} \times 25 \text{ K} = 10.1 \text{ MPa}$$

Hence, the pressure increases by a factor of 100. To avoid such drastic pressure changes, technical closed water circuits, such as domestic central heating systems, are equipped with an expansion tank.

Finally, we calculate α and κ for a perfect gas in **subproblem (c)**. From Eq. (3.2) we obtain by differentiation

$$\left(\frac{\partial V}{\partial T} \right)_p = \frac{nR}{p} \quad \left(\frac{\partial V}{\partial p} \right)_T = -\frac{nRT}{p^2}$$

We take these derivatives and obtain from Eqs. (3.6) and (3.7) after resubstitution of $V = \frac{nRT}{p}$

$$\alpha = \frac{1}{V} \left(\frac{\partial V}{\partial T} \right)_p = \frac{p}{nRT} \frac{nR}{p} = \frac{1}{T}$$

and

$$\kappa = -\frac{1}{V} \left(\frac{\partial V}{\partial p} \right)_T = -\frac{p}{nRT} (-1) \frac{nRT}{p^2} = \frac{1}{p}$$

Thus, for a perfect gas, the expansion coefficient is $\alpha = 3.35 \times 10^{-3} \text{ K}^{-1}$ at 298.15 K, and the compressibility is $\kappa = 1.0 \times 10^{-5} \text{ Pa}^{-1}$ at 100,000 Pa. Gases have a much larger thermal expansion coefficient than condensed phases, which, in addition, strongly depend on temperature. Gases also have a much higher compressibility than condensed phases: if you keep the outlet of a bicycle tire inflator shut, you can compress the air a small amount. However, human forces are not able to do the same with liquid water.

Problem 3.3 (Perfect Gas vs Real Gas) A high-pressure gas cell for laser spectroscopy experiments is filled with pure methane. At a temperature of 300 K, the pressure is 6 MPa.

- Determine the gas density in mol cm^{-3} , assuming perfect gas behavior of CH_4 .
- At 300 K, the second virial coefficient of methane is $-42.23 \text{ cm}^3 \text{ mol}^{-1}$. Determine the gas density in the cell. Judging from your results, is the real gas behavior of CH_4 under the given conditions dominated more by the repulsive or by the attractive part of the intermolecular interaction?
- To obtain accurate results, the third virial must generally be included in the calculation. For methane at 300 K, its value is $2,410 \text{ cm}^6 \text{ mol}^{-2}$. Use an iterative procedure or a cubic equation solver to determine the gas density in the cell.

Solution 3.3 This is a practical problem from the laboratory: the determination of the gas density from a simple measurement of pressure and temperature. For such applications, the model of the perfect gas gives only an approximate result, but it is easy to handle. For the solution of **subproblem (a)** we start with Eq. (3.2) and obtain the gas density in question

$$\frac{n}{V} = v^{-1} = \frac{p}{RT} = 2.405 \times 10^{-3} \text{ mol cm}^{-3}, \quad (3.18)$$

or 1.445×10^{21} particles per cm^3 . Note that the gas density is simply the inverse of the molar volume.

In **subproblem (b)** we use the virial equation Eq. (3.4), but we only consider the second virial coefficient, which is related to pair interactions between molecules.

Hence, we obtain

$$p = \frac{RT}{v} + \frac{RTB}{v^2}$$

This can be written as a quadratic equation

$$\frac{p}{RT}v^2 - v - B = 0,$$

with the two solutions

$$v_{1/2} = \frac{1 \pm \sqrt{1 + \frac{4pB}{RT}}}{\frac{2p}{RT}}$$

The solution with the negative sign yields a vanishing molar volume in the limit $B \rightarrow 0$. It is thus not meaningful in the sense of our problem. The solution with the positive sign yields a molar volume of $368.0 \text{ cm}^3 \text{ mol}^{-1}$. Hence, the gas density under consideration of the second virial coefficient is $2.717 \times 10^{-3} \text{ mol cm}^{-3}$ or $1.636 \times 10^{21} \text{ particles per cm}^3$.

To discover whether or not the repulsive or attractive nature of the intermolecular interaction is more important under the given conditions, we compare the molar volumes that we have calculated: if molecular interactions are neglected, i.e., in the approximation of the perfect gas, we obtain $v = 415.8 \text{ cm}^3 \text{ mol}^{-1}$ from Eq. (3.18). If we take molecular interactions into account by considering the second virial coefficient, we obtain a smaller value of $368.0 \text{ cm}^3 \text{ mol}^{-1}$. Imagine for a moment that we were able to switch the molecular interaction on and off. If we were to switch it off, a constant number of molecules would fill a larger volume. Then, if we were to switch it on again, the molar volume would shrink, i.e., the average distance between the molecules would be *smaller*. Thus, we conclude that under the chosen conditions, the molecular interaction among methane molecules is attractive, not repulsive. It is convenient to define the so-called **compression factor** $z = \frac{pv}{RT}$, which is less than 1 if attractive interactions are dominant, exactly 1 for vanishing interactions, and greater than 1 if repulsive interactions are dominant.

In **subproblem (c)** we include the third virial coefficient in the calculation:

$$p = \frac{RT}{v} \left(1 + \frac{B}{v} + \frac{C}{v^2} \right) \quad (3.19)$$

Note that the sum in the bracket is simply the compression factor z . Because an analytic solution is tedious, we determine the molar volume iteratively. Systematically, this could be done using Newton's method (see appendix Sect. A.3.19). But even a *trial and error* procedure starting from the best guess value $v = 368 \text{ cm}^3 \text{ mol}^{-1}$ yields the result with just five functional evaluations of Eq. (3.19), as demonstrated in Table 3.1.

Table 3.1 Iterative determination of the molar volume of methane based on the virial equation

v (cm 3 mol $^{-1}$)	z	p (MPa)	Deviation (MPa)
368	0.90304	6.121	+0.121
380	0.90556	5.944	-0.056
375	0.90452	6.017	+0.017
377	0.90490	5.987	-0.013
376	0.90473	6.002	+0.002

Hence, the molar volume of methane is 376 cm 3 mol $^{-1}$, determined with an accuracy of 1 cm 3 mol $^{-1}$. Our final result for the gas density is 2.660 \times 10 $^{-3}$ mol cm $^{-3}$. It is instructive to compare our results with experimental values for methane under these conditions. The true experimental molar volume of methane at 300 K and 0.6 MPa is 376.2 cm 3 mol $^{-1}$ [1], and the experimental compression factor is 0.90496. This shows that at a moderate pressure of 6 MPa, the inclusion of the third virial coefficient is sufficient for an accurate description of the p – V – T behavior of methane. Omission of the third virial coefficient, however, consistent with the neglect of three body interactions, gives a result that deviates by about 2% from the experimental value.

Problem 3.4 (Van der Waals Isotherms, Maxwell Construction) The critical temperature of nitrogen N₂ is 126.1 K, and the critical pressure is 35 bar.

- Plot the van der Waals isotherms of nitrogen at 100, 126, 150, and 300 K.
- Apply the Maxwell construction to the 100 K isotherm to obtain the vapor pressure of N₂ predicted by the van der Waals model.

Solution 3.4 This exercise deals with the van der Waals model of real gases, which to some extent is capable of explaining the coexistence of the gas phase with a condensed phase and the *critical point* (see Fig. 3.1). How good is the van der Waals model in predicting such properties in a concrete example? Before we move on to the solution, we recall the qualitative behavior of the pressure as a function of volume under isothermal conditions below the critical temperature where gas liquefaction is possible. Consider a gas in a sealed vessel (Fig. 3.3). By means of a moveable piston, the gas is more and more compressed, and the pressure increases. If the volume goes below a certain value, the gas is partially liquefied, and coexistence of the gas and the liquid is observed. Under these conditions, the pressure within the vessel is the vapor pressure p_v of the substance. If the gas is completely liquefied, the pressure increases considerably, because a condensed phase is barely compressible (see Problem 3.2).

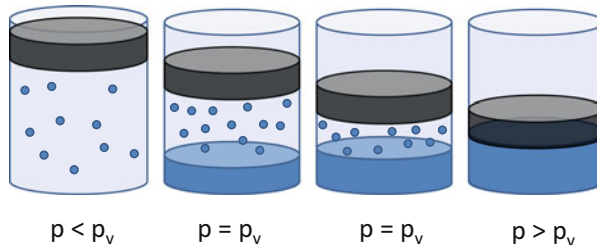


Fig. 3.3 The different stages of gas liquefaction at constant temperature

Moving on to the solution of the **subproblem (a)**, we use Eq. (3.3) to obtain the relation

$$p(v) = \frac{RT}{v-b} - \frac{a}{v^2} \quad (3.20)$$

for 1 mol of nitrogen, for which we shall plot isotherms at 100, 126, 150, and 300 K. At a constant temperature, Eq. (3.20) is the mathematical representation of a van der Waals isotherm. It has a pole for $v = b$, and thus involves a finite volume of the molecules. The two parameters a and b need to be determined from the critical data of nitrogen, the critical temperature $T_c = 126.1$ K, and the critical pressure provided $p_c = 3.5$ MPa (Fig. 3.1). Above the critical temperature, no coexistence of the gas phase and the liquid phase is possible, and a supercritical phase is formed. The relation between the critical data and the van der Waals parameters is obtained from the analysis of the *critical isotherm*, $p(v) = \frac{RT_c}{v-b} - \frac{a}{v^2}$. The textbook result is

$$T_c = \frac{8a}{27Rb} \quad (3.21)$$

$$p_c = \frac{a}{27b^2} \quad (3.22)$$

Division of these equations yields

$$b = \frac{RT_c}{8p_c} = 3.744 \times 10^{-5} \text{ m}^3 \text{ mol}^{-1}$$

and

$$a = \frac{27RT_c b}{8} = 0.133 \text{ Pa m}^6 \text{ mol}^{-2}.$$

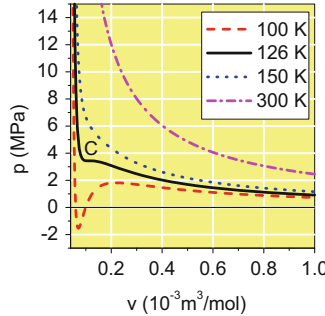


Fig. 3.4 Van der Waals isotherms of N_2 at various temperatures. C is the critical point

The van der Waals isotherms, computed with these values for the temperatures in question are shown in Fig. 3.4. The 126 K isotherm is the critical isotherm. It has the *critical point* as an inflection point.¹ The isotherms at 150 and 300 K show monotonic behavior. The 100 K isotherm has a minimum and a maximum, which does *not* reflect the real behavior of a gas described above.

To obtain a more realistic description within the van der Waals model, the **Maxwell construction** shall be applied in **subproblem (b)**. It is illustrated in Fig. 3.5, where the 100 K isotherm is again shown. The horizontal line intersecting the isotherm at the three points A , B , and C indicates a certain constant pressure \bar{p} , which within the model will be interpreted as the vapor pressure p_v at the given temperature, if the enclosed area between A and B has the same absolute value as the enclosed area between B and C . Mathematically, these areas are related to the integrals

$$W_{AB} = \int_{v_A}^{v_B} \left(\frac{RT}{v-b} - \frac{a}{v^2} - \bar{p} \right) dv \quad (3.23)$$

$$\stackrel{\text{Eq. (A.35), Eq. (A.37)}}{=} RT \ln \frac{v_B - b}{v_A - b} + \frac{a}{v_B} - \frac{a}{v_A} - \bar{p}(v_B - v_A)$$

and

$$W_{BC} = \int_{v_B}^{v_C} \left(\frac{RT}{v-b} - \frac{a}{v^2} - \bar{p} \right) dv = RT \ln \frac{v_C - b}{v_B - b} + \frac{a}{v_C} - \frac{a}{v_B} - \bar{p}(v_C - v_B) \quad (3.24)$$

The sum $W = W_{AB} + W_{BC}$ is the work done in a cycle starting at A along the van der Waals isotherm to the point C , and back on the constant pressure line $p(v) = \bar{p}$ to point A . For reasonable values of \bar{p} , W_{AB} takes negative values, whereas W_{BC} is

¹The condition of the inflection point to have vanishing first and second derivatives of the function $p(v)$ yields the relations between the van der Waals parameters a and b on the one hand, and the critical data p_c , T_c , and v_c on the other hand.

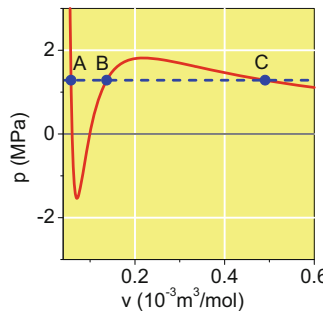


Fig. 3.5 Maxwell construction of the vapor pressure of nitrogen at 100 K. The *curved line* is the van der Waals isotherm at this temperature, the *horizontal dashed line* $p = \text{const.}$ marks the coexistence of liquid and gas, if the enclosed areas between the intersecting points A and B, and B and C take the same value

positive, and our task is to find \bar{p} , which is consistent with vanishing work done in this virtual thermodynamic cycle. The problem is complicated by the fact that the determination of the intersection points v_A , v_B , and v_C for a given value \bar{p} cannot be done analytically. Using an iterative procedure, we obtain $\bar{p} = 1.2843 \text{ MPa}$. The related intersection points are $v_A = 0.57509 \times 10^{-4} \text{ m}^3 \text{ mol}^{-1}$, $v_B = 0.13679 \times 10^{-3} \text{ m}^3 \text{ mol}^{-1}$, and $v_C = 0.49053 \times 10^{-3} \text{ m}^3 \text{ mol}^{-1}$. W_{AB} is $-0.1086 \times 10^3 \text{ J}$, and $W_{BC} = 0.1086 \times 10^3 \text{ J}$. Thus, for a temperature of 100 K, the van der Waals model predicts the vapor pressure of nitrogen to be $p_v = 1.28 \text{ MPa}$. It is instructive to compare this value with the experimental value taken from the literature [2], which is 0.76 MPa. We conclude that the van der Waals model only gives an approximate quantitative prediction of the vapor pressure of nitrogen.

3.3 Caloric State Variables, Entropy

In addition to the thermal state variables, the **caloric** state variables are of fundamental importance for the change of state of a system. According to the universal principle of potential energy minimization, any mechanical system left to itself tends to reduce its potential energy and thus its ability to do work. On the other hand, if the system is driven by external forces, work can be transferred to energy or to heat, or vice versa. There are, of course, many important technical applications for this, including heat engines, refrigerators, energy storage, and energy conversion.

There is a second universal principle based on the state variable entropy and the second law of thermodynamics, which predicts the direction of spontaneous processes.

3.3.1 Internal Energy, Work, and Enthalpy

The **internal energy** U corresponds to the sum of all kinetic and potential energy of the atoms and molecules of a system. Energy, defined as the ability of an object or a system to do work, changes, if work is done. By this, a *change* of a system's internal energy, dU , may be related to a certain amount of work δW done by it. Less obviously, there is also a change in internal energy, if an amount of heat δQ is transferred from or to the system:

$$dU = \delta Q + \delta W \quad (3.25)$$

This is the **First law of thermodynamics**. If a system undergoes a change of state without the transfer of heat to the surroundings, the process is called **adiabatic**. In contrast, if the temperature is constant during the change of state, it is called **isothermal**. If work is done during a change of state under isothermal conditions, there is usually a transfer of heat with the surroundings.

As a state variable, the value of the internal energy depends on other state variables, e.g., on T and V , but not on the way in which the system reached this state. This is expressed by the symbol dU for the total differential, in contrast to the infinitesimal changes in heat and work, which generally do depend on the way in which a change of state is performed.

Again, a change in the internal energy of a system depends on its material properties. If U is assumed as a function of temperature and volume,² $U = U(T, V)$, the total differential can be written:

$$dU = \left(\frac{\partial U}{\partial T} \right)_V dT + \left(\frac{\partial U}{\partial V} \right)_T dV \quad (3.26)$$

The derivative

$$C_V = \left(\frac{\partial U}{\partial T} \right)_V \quad (3.27)$$

is called the **constant volume heat capacity** of the system. The derivative

$$\Pi = \left(\frac{\partial U}{\partial V} \right)_T \quad (3.28)$$

²Because there is always an equation of state that relates p , T , and V , it does not make sense to assume U to be a function of all thermal state variables.

is called the **internal pressure**. As a result of the assumption of non-interacting point masses, the model of the perfect gas does not involve any dependence of the internal energy on system volume. Hence, its internal pressure is zero and internal energy depends only on temperature. In contrast, there is nonzero internal pressure in the model of van der Waals.

Based on the mechanical definition of work related to force F and distance s , $dW = Fds$, in addition to the definition of pressure $p = \frac{F}{A}$ as the quotient of force F acting on an area A , the work done on a system upon a change in volume from V_1 to V_2 is defined as

$$W = - \int_{V_1}^{V_2} p \, dV \quad (3.29)$$

If W is negative, work is done by the system at the expense of its internal energy or the transfer of heat according to Eq. (3.25). If W is positive, work is done to the system.

As the internal energy is the sum of all kinetic and potential energy among the atoms and molecules that constitute a system, the amount of energy needed to create this system at a certain temperature is U . If the system has a certain volume V , an additional amount of work pV is necessary to give it room by displacing the surroundings at an external pressure p . Hence, the work necessary to create a system and give it room is the **enthalpy**,

$$H = U + pV. \quad (3.30)$$

The differential

$$dH = dU + d(pV) = \delta Q - p \, dV + p \, dV + V \, dp = \delta Q + V \, dp$$

Shows the practical importance of the enthalpy: The heat δQ_p which is exchanged by a system with its surroundings at a constant pressure ($dp = 0$), directly corresponds to the change in enthalpy: $\delta Q_p = dH$. Similarly, the heat δQ_V exchanged under isochoric conditions ($dV = 0$) corresponds to the change in internal energy: $\delta Q_V = dU$. The two situations are illustrated in Fig. 3.6. Thus, the measurement of transferred heats in *calorimetric* experiments gives direct access to changes in U and H .

From the total differential of the enthalpy

$$dH = \left(\frac{\partial H}{\partial T} \right)_p \, dT + \left(\frac{\partial H}{\partial p} \right)_T \, dp, \quad (3.31)$$

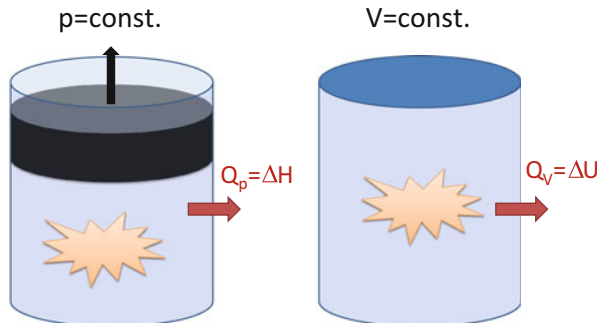


Fig. 3.6 Heat transfer of a system undergoing a change of state with its surroundings. Under isobaric conditions (*left*), the transferred heat corresponds to the change in enthalpy. Under isochoric conditions (*right*), the transferred heat corresponds to the change in internal energy

the **isobaric heat capacity**

$$C_p = \left(\frac{\partial H}{\partial T} \right)_p \quad (3.32)$$

is derived as a further material property.

3.3.2 Reversible and Irreversible Changes of State, the Second Law and Entropy

The first law of thermodynamics alone leaves a wealth of observations unexplained. One example is the transfer of heat. If two subsystems at different temperatures are brought into contact with each other, heat is always transferred from the subsystem at a higher temperature to the subsystem at a lower temperature, until the temperature of the two subsystems are equal. The reverse process is not observed spontaneously, although, using a cooling machine, for example, it is possible to transfer heat from a system at a lower temperature to a system at a higher temperature, at the expense of doing work. A spontaneous heat transfer from a hot object to a cold one is a typical example of an **irreversible process**. Another example is the spontaneous expansion of a gas. For example, consider a perfect gas: if its internal energy does not depend on volume, for what reason does it tend to expand freely into the whole accessible volume? Again, at the expense of doing work, the spontaneous free expansion of a perfect gas can be reversed by a process of compression.

It is the merit of Clausius to have figured out another state variable that can be used to predict the direction of a spontaneous change of state: the **entropy** S of a system. According to Clausius, entropy is defined by

$$dS = \frac{\delta Q_{\text{rev}}}{T} \quad (3.33)$$

where δQ_{rev} is the infinitesimal heat transferred reversibly to a system at a temperature T .

According to the **Second law of thermodynamics**, the entropy in an isolated system tends toward a maximum:

$$dS \geq 0 \quad (3.34)$$

In the limiting case of a reversible process, $\Delta S = 0$. At this point, it is worth noting that the calculation of ΔS in an irreversible process requires the consideration of a reversible equivalent thermodynamic process. For n moles of a perfect gas undergoing a change of state either from a temperature T_1 to T_2 , from a volume V_1 to V_2 , or from pressure p_1 to p_2 , the change in entropy is

$$\Delta S = n c_v \ln \frac{T_2}{T_1} + n R \ln \frac{V_2}{V_1} = n c_p \ln \frac{T_2}{T_1} - n R \ln \frac{p_2}{p_1} \quad (3.35)$$

where c_v is the constant volume molar heat capacity, and c_p is the isobaric molar heat capacity of the perfect gas. A similar equation also holds for a van der Waals gas (see Problem 3.8). The inspection of Eq. (3.35), although strictly only valid for a perfect gas, is the key to a general understanding of the direction of irreversible processes: the entropy of a gas increases, if $V_2 > V_1$, because in this case $\ln \frac{V_2}{V_1} > 0$. This is the explanation for the above-mentioned spontaneous free expansion of gases.

3.3.3 Adiabatic Changes of State of a Perfect Gas

If a perfect gas undergoes an adiabatic reversible change of state, pressure, temperature, and volume change according to Poisson's equations:

$$p_1 V_1^\gamma = p_2 V_2^\gamma \quad (3.36)$$

$$T_1 V_1^{\gamma-1} = T_2 V_2^{\gamma-1} \quad (3.37)$$

$$p_1^{1-\gamma} T_1^\gamma = p_2^{1-\gamma} T_2^\gamma \quad (3.38)$$

where $\gamma = \frac{c_p}{c_v}$ is the **heat capacity ratio**. Equation (3.37) will be derived in Problem 3.9.

3.3.4 The Thermodynamic Potentials

Apart from the internal energy and enthalpy, there are two further essential caloric quantities, the **Gibbs free energy**

$$G = H - TS, \quad (3.39)$$

and **Helmholtz free energy**

$$A = U - TS. \quad (3.40)$$

The definition of the free energies is that A and G are Minimized, either because of H and U being minimized or because of the entropy S being maximized. In that sense, the two above-mentioned principles energy minimization and entropy maximization are combined into one. It can be shown that there is another condition for the direction of a spontaneous change of a system: at constant pressure and temperature, the direction of spontaneous change of a system is such that G is minimized:

$$dG_{p,T} \leq 0 \quad (3.41)$$

At a constant volume and temperature, A is minimized:

$$dA_{V,T} \leq 0 \quad (3.42)$$

If a process is reversible, $dG_{p,T} = 0$ or $dA_{V,T} = 0$ respectively. These relations are not restricted to isolated systems, they hold for each subsystem separately. Further analysis shows that the Gibbs free energy G is the maximum non-expansion work that can be obtained from a closed system at a constant pressure and temperature. Similarly, A is the maximum work that can be done by a closed system.

Table 3.2 Compilation of thermodynamic potentials

Thermodynamic potential	Natural variables	Differential
Internal energy U	S, V	$dU = T dS - p dV$
Enthalpy $H = U + pV$	S, p	$dH = T dS + V dp$
Free energy $A = U - TS$	T, V	$dA = -S dT - p dV$
Free enthalpy $G = H - TS$	T, p	$dG = -S dT + V dp$

The thermodynamic potentials U, H, A , and G are summarized in Table 3.2 along with their natural variables.

The thermodynamic potentials, in combination with the Schwarz integrability condition for state functions, provide the extremely useful **Maxwell relations** among thermodynamic state functions:

$$\frac{\partial^2 U}{\partial S \partial V} = \frac{\partial^2 U}{\partial V \partial S} \Leftrightarrow \left(\frac{\partial T}{\partial V} \right)_S = - \left(\frac{\partial p}{\partial S} \right)_V \quad (3.43)$$

$$\frac{\partial^2 H}{\partial S \partial p} = \frac{\partial^2 H}{\partial p \partial S} \Leftrightarrow \left(\frac{\partial T}{\partial p} \right)_S = \left(\frac{\partial V}{\partial S} \right)_p \quad (3.44)$$

$$\frac{\partial^2 A}{\partial T \partial V} = \frac{\partial^2 A}{\partial V \partial T} \Leftrightarrow \left(\frac{\partial S}{\partial V} \right)_T = \left(\frac{\partial p}{\partial T} \right)_V \quad (3.45)$$

$$\frac{\partial^2 G}{\partial T \partial p} = \frac{\partial^2 G}{\partial p \partial T} \Leftrightarrow \left(\frac{\partial S}{\partial p} \right)_T = - \left(\frac{\partial V}{\partial T} \right)_p \quad (3.46)$$

3.3.5 Problems

Problem 3.5 (Molar Heat Capacities of a van der Waals Gas)

Derive an expression for $c_p - c_v$ for a van der Waals gas.

Solution 3.5 This exercise is an instructive example of how relations between material properties can be derived using the thermodynamic schemes of calculation. Before we start, we recall the textbook result for the difference in molar heat capacities c_p and c_v of a *perfect gas*:

$$c_p - c_v = R. \quad (3.47)$$

For a van der Waals gas, we expect a similar expression to hold that contains the two van der Waals parameters a and b . Moreover, we expect that the sought expression is identical to Eq.(3.47) in the limit $a \rightarrow 0$ and $b \rightarrow 0$. We start our derivation

considering the first law (Eq. (3.25)) for 1 mol of a substance, according to which $\delta q_p = du + p dv$ is the transferred heat at a constant pressure.³ Using the total differential for the molar internal energy (cf. Eq. (3.26)), this can be written as

$$\delta q_p = \left(\frac{\partial u}{\partial T} \right)_v dT + \left(\frac{\partial u}{\partial v} \right)_T dv + p dv$$

The first term on the right-hand side contains the constant volume heat capacity (see Eq. (3.27)). Hence,

$$\delta q_p = c_v dT + \left[\left(\frac{\partial u}{\partial v} \right)_T + p \right] \left(\frac{\partial v}{\partial T} \right)_p dT,$$

and thus, introducing the constant pressure heat capacity $c_p dT = \delta q_p$,

$$c_p = c_v + \left[\left(\frac{\partial u}{\partial v} \right)_T + p \right] \left(\frac{\partial v}{\partial T} \right)_p. \quad (3.48)$$

The expression in square brackets containing the internal pressure can be simplified by considering:

$$Td s = du + p dv = c_v dT + \left[\left(\frac{\partial u}{\partial v} \right)_T + p \right] dv. \quad (3.49)$$

Here, we have considered once more the total differential for the molar internal energy using the expression from Table 3.2 with the molar entropy s and the molar volume v as natural variables. Therefore,

$$\left[\left(\frac{\partial u}{\partial v} \right)_T + p \right] = T \left(\frac{\partial s}{\partial v} \right)_T \stackrel{\text{Eq. (3.45)}}{=} T \left(\frac{\partial p}{\partial T} \right)_v \quad (3.50)$$

follows, where we have made use of one of the Maxwell relations. Thus, Eq. (3.48) simplifies to

$$c_p = c_v + T \left(\frac{\partial p}{\partial T} \right)_v \left(\frac{\partial v}{\partial T} \right)_p \quad (3.51)$$

So far, our intermediate result (3.51) is general, as we have not yet specified an equation of state to replace the derivatives of the thermal state variables. Using Eq. (3.20), it is straightforward to get $\left(\frac{\partial p}{\partial T} \right)_v = \frac{R}{v-b}$. However, $\left(\frac{\partial v}{\partial T} \right)_p$ cannot be evaluated directly, as the van der Waals equation (3.20) cannot be solved for v . The

³For the use of lower letters for molar quantities, see Sect. 3.1.

trick is to consider the total differential dp , which is zero at a constant pressure: $dp \stackrel{!}{=} 0 = \left(\frac{\partial p}{\partial T}\right)_v dT + \left(\frac{\partial p}{\partial v}\right)_T dv$. Therefore,

$$\left(\frac{\partial v}{\partial T}\right)_p = -\frac{\left(\frac{\partial p}{\partial T}\right)_v}{\left(\frac{\partial p}{\partial v}\right)_T} \quad (3.52)$$

follows, and moreover

$$c_p - c_v \stackrel{\text{Eq. (3.51)}}{=} -T \frac{\left(\frac{\partial p}{\partial T}\right)_v^2}{\left(\frac{\partial p}{\partial v}\right)_T} = \frac{R}{1 - \frac{2a(v-b)^2}{RTv^3}} \quad (3.53)$$

As expected above, our result agrees with the expression for a perfect gas, if we set the van der Waals parameters at zero. Moreover, $c_p - c_v \rightarrow R$ for $v \rightarrow \infty$, i.e., for a dilute van der Waals gas, the difference $c_p - c_v$ is the same as for a perfect gas.

Problem 3.6 (Work and Mechanical Equilibrium) A gas cylinder with a total volume of $V = 1 \text{ dm}^3$ is divided initially by a movable piston into two equal volumes, V_{Ar}^0 and V_{Ne}^0 . V_{Ar}^0 contains argon at 1 bar, V_{Ne}^0 is filled with neon at 3 bar. Assume perfect gas behavior for both gases and isothermal conditions at $T = 298 \text{ K}$.

- Explain why the system is not in mechanical equilibrium and calculate the volume of both gases after the piston has reached its equilibrium position.
- For both gases, determine the expansion/compression work if the piston moves reversibly into its equilibrium position.

Solution 3.6 This problem deals with the case of an isothermal change of state of a system of two perfect gases, separated from each other. The initial situation is depicted in Fig. 3.7. In **subproblem (a)** we explain why the system is not in *mechanical equilibrium*. The latter is established, if the net force acting on the piston is zero. The force $\mathbf{F}_2 = -F_2 \mathbf{e}_z$ is directed downward (in a negative z -direction), $\mathbf{F}_1 = +F_1 \mathbf{e}_z$ points upward in a positive z -direction. Because the initial pressures are different, $p_{\text{Ar}}^0 \neq p_{\text{Ne}}^0$, we can prove that there is a net force acting on the piston with area A :

$$\mathbf{F} = \mathbf{F}_1 + \mathbf{F}_2 = p_{\text{Ar}}^0 A \mathbf{e}_z - p_{\text{Ne}}^0 A \mathbf{e}_z = (p_{\text{Ar}}^0 - p_{\text{Ne}}^0) A \mathbf{e}_z \neq 0 \quad (3.54)$$

Hence, mechanical equilibrium is not established, and the piston moves in the direction that increases the volume filled with neon, until the pressure in both

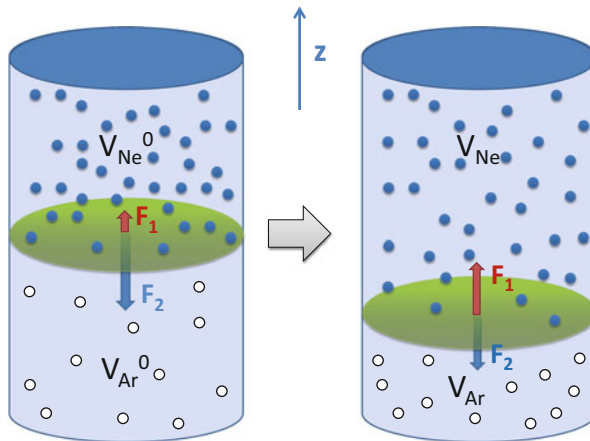


Fig. 3.7 Isothermal expansion of neon and compression of argon, separated by a piston that is free to move in a z direction. Mechanical equilibrium is established, if the forces acting on the piston balance each other

volumes is the same:

$$p_{Ne} \stackrel{!}{=} p_{Ar} \quad (3.55)$$

This is the condition for mechanical equilibrium that we use to calculate the final volumes of the two perfect gases:

$$\frac{n_{Ne}RT}{V_{Ne}} \stackrel{!}{=} \frac{n_{Ar}RT}{V_{Ar}}$$

We make use of the fact that the total volume $V = V_{Ar} + V_{Ne}$ of the gases is unchanged if the piston moves, and, moreover, $n_{Ne} = 3n_{Ar}$. Hence the condition for mechanical equilibrium is simplified to

$$\frac{3}{V - V_{Ar}} = \frac{1}{V_{Ar}}$$

which can be solved for V_{Ar} : the result is $V_{Ar} = \frac{V}{4} = 0.25 \text{ dm}^3$. Accordingly, $V_{Ne} = \frac{3V}{4} = 0.75 \text{ dm}^3$. We note that the equilibrium pressure on both sides of the piston is 2 bar, i.e., the average of the initial pressures.

In **subproblem (b)** we calculate the work done by the expansion of neon and the compression of argon. We make use of Eq. (3.29) and consider that the piston moves *reversibly*, i.e., at each of its positions, the pressure can be calculated by the

equation of state: $p_{\text{Ne}} = \frac{n_{\text{Ne}}RT}{V_{\text{Ne}}}$, and $p_{\text{Ar}} = \frac{n_{\text{Ar}}RT}{V_{\text{Ar}}}$:

$$W_{\text{Ne}} = -n_{\text{Ne}}RT \int_{V_{\text{Ne}}^0}^{V_{\text{Ne}}} \frac{dV}{V} = -p_{\text{Ne}}^0 V_{\text{Ne}}^0 \ln \frac{V_{\text{Ne}}}{V_{\text{Ne}}^0}$$

$$W_{\text{Ne}} = -3 \times 10^5 \text{ Pa} \times \frac{1}{2} \times 10^{-3} \text{ m}^3 \ln \frac{0.75}{0.5} = -60.8 \text{ J}$$

$$W_{\text{Ar}} = -n_{\text{Ar}}RT \int_{V_{\text{Ar}}^0}^{V_{\text{Ar}}} \frac{dV}{V} = -p_{\text{Ar}}^0 V_{\text{Ar}}^0 \ln \frac{V_{\text{Ar}}}{V_{\text{Ar}}^0}$$

$$W_{\text{Ar}} = -1 \times 10^5 \text{ Pa} \times \frac{1}{2} \times 10^{-3} \text{ m}^3 \ln \frac{0.25}{0.5} = +34.7 \text{ J}$$

Consistent with the compression of argon, the work done on argon, W_{Ar} , is positive. Accordingly, W_{Ne} is negative.

At the end of this problem it is worth reflecting on the significance of mechanical equilibrium in the context of thermodynamics. Although we are dealing with *changes* of state, we usually characterize these changes by an initial state, a final state, and perhaps intermediate states. Even if these states are not states of thermodynamic equilibrium, they may still be states of mechanical equilibrium in which the mechanical forces are balanced exactly. We deal with an example in Problem 3.7. Furthermore, mechanical equilibrium is a precondition for thermodynamic equilibrium.⁴ Therefore, states of mechanical equilibrium are, for example, important for the discussion of reversible and irreversible changes of state. An example is presented in Problem 3.9.

Problem 3.7 (Adiabatic Reversible Expansion/Compression)

A gas cylinder with a total volume of $V = 1 \text{ dm}^3$ is divided initially by a movable piston into two equal volumes, V_{Ar}^0 and V_{Ne}^0 . V_{Ar}^0 contains argon at 1 bar, V_{Ne}^0 is filled with neon at 3 bar. Assume perfect gas behavior for both gases. The initial temperature of the two gases is $T^0 = 298 \text{ K}$. Assume adiabatic conditions, i.e., that no heat is exchanged, neither between the gases, nor between the gases and the surroundings. For both gases, the constant volume heat capacity is $c_v = \frac{3}{2}R$

- Calculate the volume, the temperature, and the pressure of both gases, after the piston has moved reversibly into its equilibrium position.
- Calculate the work and the change in entropy for both gases.
- What is the temperature of the gases and the entropy change if the piston is suddenly removed?

⁴Thermodynamic equilibrium between two systems involves thermal, mechanical, and also chemical equilibrium.

Solution 3.7 This problem is an extension of Problem 3.6. Starting from the same initial conditions (see Fig. 3.7), we calculate the volume of the two gases, neon and argon, separated by a piston, if the latter moves reversibly and *adiabatically* instead of isothermally into its equilibrium position. What is different? If no heat exchange occurs, neon does expansion work at the expense of losing internal energy, and cools down. Conversely, argon, which is compressed, heats up. Hence, the final temperature of both gases is different. Furthermore, we cannot assume that the final equilibrium pressure on both sides of the piston will be the average of the initial values, as in Problem 3.6. Our solution is again based on the condition for mechanical equilibrium, Eq. (3.55), but we use Eq. (3.36) for reversible adiabatic changes of state:

$$p_{\text{Ne}}^0 V_{\text{Ne}}^{0,\gamma} = p_{\text{Ne}} V_{\text{Ne}}^\gamma \quad (3.56)$$

$$p_{\text{Ar}}^0 V_{\text{Ar}}^{0,\gamma} = p_{\text{Ar}} V_{\text{Ar}}^\gamma \quad (3.57)$$

$\gamma = \frac{c_p}{c_v} = \frac{5/2}{3/2} = \frac{5}{3}$ is the heat capacity ratio. Thus, by using Eq. (3.55), the condition is

$$\frac{p_{\text{Ne}}^0 V_{\text{Ne}}^{0,\gamma}}{V_{\text{Ne}}^\gamma} = \frac{p_{\text{Ar}}^0 V_{\text{Ar}}^{0,\gamma}}{V_{\text{Ar}}^\gamma}$$

Because $V_{\text{Ne}}^0 = V_{\text{Ar}}^0$, and $V = V_{\text{Ar}} + V_{\text{Ne}}$, we can eliminate V_{Ar} :

$$\frac{p_{\text{Ne}}^0}{V_{\text{Ne}}^\gamma} = \frac{p_{\text{Ar}}^0}{(V - V_{\text{Ne}})^\gamma}$$

This expression can be solved for V_{Ne} :

$$V_{\text{Ne}} = V \frac{\left(\frac{p_{\text{Ne}}^0}{p_{\text{Ar}}^0}\right)^{\frac{1}{\gamma}}}{1 + \left(\frac{p_{\text{Ne}}^0}{p_{\text{Ar}}^0}\right)^{\frac{1}{\gamma}}} = 1 \text{ dm}^3 \frac{3^{\frac{3}{5}}}{1 + 3^{\frac{3}{5}}} = 0.66 \text{ dm}^3$$

Thus, $V_{\text{Ar}} = V - V_{\text{Ne}} = 0.34 \text{ dm}^3$. Neon expands, but the final volume is smaller for adiabatic conditions than in the isothermal case treated in Problem 3.6a. The

equilibrium pressure on both sides of the piston is

$$p_{\text{Ar}} = p_{\text{Ar}}^0 \left(\frac{V_{\text{Ar}}^0}{V_{\text{Ar}}} \right)^\gamma = 1.8932 \text{ bar},$$

the same pressure is obtained for p_{Ne} . Note that the equilibrium pressure differs from our result for the isothermal case (Problem 3.6). Finally, we calculate the temperature of both gases using the equation of state for the perfect gas, and the initial temperature $T^0 = 298 \text{ K}$:

$$\begin{aligned} T_{\text{Ne}} &= \frac{p_{\text{Ne}} V_{\text{Ne}}}{n_{\text{Ne}} R} = \frac{p_{\text{Ne}} V_{\text{Ne}}}{\frac{p_{\text{Ne}}^0 V_{\text{Ne}}^0}{RT^0} R} = \frac{p_{\text{Ne}} V_{\text{Ne}}}{p_{\text{Ne}}^0 V_{\text{Ne}}^0} T^0 = 247.9 \text{ K} \\ T_{\text{Ar}} &= \frac{p_{\text{Ar}} V_{\text{Ar}}}{p_{\text{Ar}}^0 V_{\text{Ar}}^0} T^0 = 384.7 \text{ K} \end{aligned}$$

As expected, neon has cooled down after its expansion, and the compressed argon has heated up markedly.

In **subproblem (b)** we shall calculate the work and the change in entropy for both gases. For an adiabatic change of state, the work can be calculated from the first law (Eq. (3.25)) with the assumption $\delta Q = 0$. Therefore,

$$W_{\text{Ne}} = \Delta U_{\text{Ne}} = n_{\text{Ne}} c_v (T_{\text{Ne}} - T_{\text{Ne}}^0) = \frac{p_{\text{Ne}}^0 V_{\text{Ne}}^0}{RT_{\text{Ne}}^0} \frac{3R}{2} (T_{\text{Ne}} - T_{\text{Ne}}^0) = -37.8 \text{ J}$$

and

$$W_{\text{Ar}} = \Delta U_{\text{Ar}} = n_{\text{Ar}} c_v (T_{\text{Ar}} - T_{\text{Ar}}^0) = \frac{p_{\text{Ar}}^0 V_{\text{Ar}}^0}{RT_{\text{Ar}}^0} \frac{3R}{2} (T_{\text{Ar}} - T_{\text{Ar}}^0) = +21.8 \text{ J}$$

The total work done is therefore $W = W_{\text{Ne}} + W_{\text{Ar}} = 16 \text{ J}$, which will be further discussed below. The entropy change in the gases, undergoing an adiabatic reversible change of state, is zero: $\Delta S_{\text{Ne}} = 0$, $\Delta S_{\text{Ar}} = 0$.

In **subproblem (c)** the piston is suddenly removed from its equilibrium position, as indicated in Fig. 3.8. The gases spontaneously expand into the whole volume V , which is an irreversible process.⁵ In addition, there is an equilibration of temperature by a transfer of heat from argon at 384.7 K to neon at 247.9 K. We determine the final temperature of the gases after equilibration, and, in addition, the entropy changes involved with this irreversible process. In the first step, we calculate the final temperature T_f in two ways. The first method is to regard the determination of the final temperature as a problem of heat transfer: as no heat is exchanged with the

⁵For a rather elementary analysis of the mixing of gases based on statistics, see Problem 8.2.

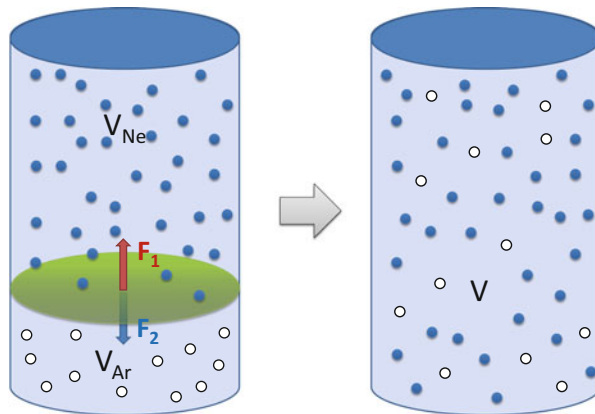


Fig. 3.8 Free expansion of neon and argon after removal of the piston

surroundings,

$$Q_{\text{Ne}} + Q_{\text{Ar}} = n_{\text{Ne}} c_v (T_f - T_{\text{Ne}}) + n_{\text{Ar}} c_v (T_f - T_{\text{Ar}}) = 0$$

We solve for T_f and obtain

$$T_f = \frac{n_{\text{Ne}} T_{\text{Ne}} + n_{\text{Ar}} T_{\text{Ar}}}{n_{\text{Ne}} + n_{\text{Ar}}} = \frac{3T_{\text{Ne}} + T_{\text{Ar}}}{4} = 282.1 \text{ K.} \quad (3.58)$$

We note that the number of moles of neon and argon can be calculated from the initial conditions, $n_{\text{Ar}} = \frac{p_{\text{Ar}}^0 V_{\text{Ar}}^0}{RT^0} = 0.02018 \text{ mol}$, and $n_{\text{Ne}} = 3n_{\text{Ar}}$, because $p_{\text{Ne}}^0 = 3p_{\text{Ar}}^0$. According to Eq.(3.58) T_f is 15.9 K smaller than T^0 , the initial temperature of the two gases, before the piston went into its position of mechanical equilibrium. Did we expect this? To check our result, we calculate T_f in a second way, using an argument of energy conservation. Between the initial state of the gases at temperature $T^0 = 298 \text{ K}$ and the final state at T_f , the above calculated work involved with the movement of the piston was $W = 16 \text{ J}$. No further was done, because, after the piston was removed, the expansion of the gases was a free expansion. As there was no heat transfer with the surroundings, we did indeed expect a cooling of the gases in the final state by

$$\Delta T = \frac{W}{(n_{\text{Ar}} + n_{\text{Ne}}) c_v} = \frac{16 \text{ J}}{0.08072 \text{ mol} \times 12.4718 \text{ JK}^{-1} \text{ mol}^{-1}} = 15.9 \text{ K,} \quad (3.59)$$

and thus $T_f = T^0 - \Delta T = 282.1\text{ K}$, i.e., the same result as above. Finally, we can calculate the entropy change in the gases using Eq. (3.35):

$$\Delta S_{\text{Ne}} = n_{\text{Ne}} c_v \ln \frac{T_f}{T_{\text{Ne}}} + n R \ln \frac{V}{V_{\text{Ne}}} = 0.308 \text{ J K}^{-1} \text{ mol}^{-1} \quad (3.60)$$

$$\Delta S_{\text{Ar}} = n_{\text{Ar}} c_v \ln \frac{T_f}{T_{\text{Ar}}} + n R \ln \frac{V}{V_{\text{Ar}}} = 0.103 \text{ J K}^{-1} \text{ mol}^{-1} \quad (3.61)$$

As expected, the mixing of the gases leads to an increase in their entropy, emphasizing the irreversible nature of this process.

Problem 3.8 (Entropy Change and Free Expansion of a van der Waals Gas)

Initially, at a temperature T_1 and a molar volume v_1 , a van der Waals gas undergoes a change of state to the final temperature T_2 and the molar volume v_2 . The van der Waals gas is characterized by the two parameters a and b (cf. Eq. (3.3)).

- a. Show that the change in molar entropy is

$$\Delta s = c_v \ln \frac{T_2}{T_1} + R \ln \frac{v_2 - b}{v_1 - b} \quad (3.62)$$

- b. A volume of 1 dm^3 is partitioned by a wall into two equal parts, one containing 1 mol xenon (van der Waals parameters $a = 4.250 \text{ dm}^6 \text{ bar mol}^{-2}$ and $b = 0.0511 \text{ dm}^3 \text{ mol}^{-1}$), the other part being evacuated. Calculate the change in the entropy of xenon after the wall is removed and the gas undergoes a free expansion under isothermal conditions ($T = 298.15\text{ K}$). Also, calculate the change in entropy of the surroundings.

Solution 3.8 Sometimes it is quite difficult to deal with entropy changes in the correct way. An instructive case is the *free expansion* of a perfect gas. The movement of individual gas particles is completely uncorrelated, and in a process of diffusion,⁶ the entirely accessible volume rapidly filled by the gas. This is an example of an irreversible process. From the atomistic point of view, the uncorrelated movement of non-interacting particles leaves a probability of finding all the particles back in the initial volume, which is so small, that it never happens in practice. Students frequently think that they have figured out a contradiction between the irreversible nature of the free expansion and the fact that there is no heat transfer with the surroundings. They argue that according to the Clausius equation, Eq. (3.33), the

⁶A simple model of diffusion is treated in Problem 8.3.

entropy change should then be zero, and thus the expansion should be reversible. Of course, they overlook the fact that the application of Eq. (3.33) assumes that the heat is exchanged in a *reversible* process, which is not the case. The reason for the zero heat transfer in the case of a free expansion of a perfect gas is the absence of intermolecular interaction, equivalent to the fact that the internal energy of a perfect gas is only a function of temperature, not of volume.

An even more puzzling case is the free expansion of a van der Waals gas, which we deal with in this problem. Here, we have to take molecular interaction into account, which, during expansion must be overcome. Thus, under isothermal conditions, if the gas is in thermal contact with the surroundings, there will be a small heat transfer; thus, there will also be a change in entropy of the surroundings.

In **subproblem (a)** we derive a general formula for the molar entropy change in a van der Waals gas undergoing a change of state. Equation (3.62) is analogous to Eq. (3.35), which is valid for a perfect gas. Our derivation starts with Eq. (3.26). If we consider 1 mol of substance,

$$du = c_v dT + \Pi dv, \quad (3.63)$$

where Π is the internal pressure. Equating the last expression to $du = T ds - p dv$, we obtain

$$ds = c_v \frac{dT}{T} + \frac{1}{T} (\Pi + p) dv. \quad (3.64)$$

Exploiting Eq. (3.50) in Problem 3.5 and the van der Waals equation of state Eq. (3.3), we can evaluate the bracket term and obtain

$$ds = c_v \frac{dT}{T} + \frac{R}{v-b} dv. \quad (3.65)$$

Finally, integration of the latter equation proves Eq. (3.62):

$$\Delta s = \int_{s_1}^{s_2} ds = c_v \int_{T_1}^{T_2} \frac{dT}{T} + R \int_{v_1}^{v_2} \frac{dv}{v-b} \quad (3.66)$$

$$= c_v \ln \frac{T_2}{T_1} + R \ln \frac{v_2-b}{v_1-b}. \quad (3.67)$$

This equation is very similar to the corresponding expression for a perfect gas (Eq. (3.35)). Interestingly, the change in molar entropy of a van der Waals gas does not depend on the van der Waals parameter a or on the internal pressure Π , which according to Eqs. (3.50) and (3.3), is given by

$$\Pi = T \left(\frac{\partial p}{\partial T} \right)_v - p = \frac{RT}{v-b} - \frac{RT}{v-b} + \frac{a}{v^2} = \frac{a}{v^2}. \quad (3.68)$$

Equation (3.66) can be generalized for arbitrary mole numbers:

$$\Delta S = n c_v \ln \frac{T_2}{T_1} + R \ln \frac{V_2 - nb}{V_1 - nb}. \quad (3.69)$$

In **subproblem (b)** we calculate the change in entropy ΔS for $n = 1$ mol xenon with $a = 4.250 \text{ dm}^6 \text{ bar mol}^{-2}$ and $b = 0.0511 \text{ dm}^3 \text{ mol}^{-1}$. The initial and final volume is $V_1 = 0.5 \text{ dm}^3$ and $V_2 = 1 \text{ dm}^3$ respectively. In SI units, $a = 0.4250 \text{ m}^6 \text{ Pa mol}^{-2}$ and $b = 5.11 \times 10^{-5} \text{ m}^3 \text{ mol}^{-1}$. Using Eq. (3.69), the entropy change in the gas due to the isothermal expansion is

$$\Delta S_{\text{gas}} = nR \ln \frac{V_2 - nb}{V_1 - nb} \quad (3.70)$$

$$= 1 \text{ mol} \times 8.3145 \text{ J K}^{-1} \text{ mol}^{-1} \ln \frac{10^{-3} - 5.11 \times 10^{-5}}{0.5 \times 10^{-3} - 5.11 \times 10^{-5}} \quad (3.71)$$

$$= +6.223 \text{ J K}^{-1}. \quad (3.72)$$

As expected, the entropy of the gas increases upon expansion, for a van der Waals gas as well. For comparison, the corresponding result for a perfect gas (Eq. (3.35)) would have been $+5.763 \text{ J K}^{-1}$. Now, we are interested in the entropy change in the surroundings associated with this process, ΔS_{surr} . As discussed above, there is a low heat transfer from the surroundings to the gas upon expansion, resulting in a negative ΔS_{surr} . However, is it correct to use the Clausius equation (3.33) and write

$$\Delta S_{\text{surr}} = \frac{\Delta Q_{\text{surr}}}{T} \quad (3.73)$$

at this point? Above, we have mentioned the significance of a heat transfer in a reversible process as a requirement for using the Clausius equation, but here, we assume the expansion of our van der Waals gas to be irreversible. Therefore, how can we justify Eq. (3.73)? Consider the surroundings as a system that is so large that the small heat transfer ΔQ_{surr} does not change the system temperature. The entropy change in the surroundings only depends on the amount of heat transferred. We could construct an alternative reversible thermodynamic process in a system in contact with the surroundings, leading to just the same heat transfer and thus to the same change in entropy of the surroundings. Hence, regarding the entropy change of the surroundings, it does not matter if the van der Waals gas undergoes a reversible or an irreversible change of state, as long as *only* the same heat is transferred. Next, we calculate $\Delta Q_{\text{surr}} = -\Delta Q_{\text{gas}}$ on the basis of the first law Eq. (3.25). Because in a free expansion, no work is done by the gas, ΔQ_{gas} corresponds to the change in its internal energy, $\Delta Q_{\text{gas}} = \Delta U_{\text{gas}}$. As $T = \text{const.}$,

$$dU_{\text{gas}} = \left(\frac{\partial U_{\text{gas}}}{\partial V} \right)_T dV = \Pi dV = \frac{an^2}{V^2} dV \quad (3.74)$$

After a step of integration, we obtain

$$\Delta U_{\text{gas}} = an^2 \left(\frac{1}{V_1} - \frac{1}{V_2} \right) \quad (3.75)$$

$$= 0.4250 \left(\frac{1}{0.5 \times 10^{-3}} - \frac{1}{10^{-3}} \right) \text{ J} \quad (3.76)$$

$$= +425 \text{ J.} \quad (3.77)$$

Thus, following our above argument,

$$\Delta S_{\text{surr}} = \frac{\Delta Q_{\text{surr}}}{T} = -\frac{-\Delta Q_{\text{gas}}}{T} = -\frac{425 \text{ J}}{298.15 \text{ K}} = -1.425 \text{ J K}^{-1}. \quad (3.78)$$

Hence, the total entropy change in the total system constituted by the surroundings and the van der Waals gas is $\Delta S = \Delta S_{\text{gas}} + \Delta S_{\text{surr}} = +4.798 \text{ J K}^{-1}$.

Problem 3.9 (Reversible and Irreversible Adiabatic Expansion)

A cylinder with a movable piston is filled with 2 mol of a perfect gas. The initial volume is 10 dm^3 , the initial temperature is $T_1 = 320 \text{ K}$. The constant volume molar heat capacity of the gas is $25 \text{ J K}^{-1} \text{ mol}^{-1}$. Then, the gas expands adiabatically against a constant external pressure of 10^5 Pa , until mechanical equilibrium is established.

- Calculate the final temperature and volume assuming an irreversible expansion of the gas.
- Calculate the final temperature and volume in the case of a reversible expansion.
- Calculate explicitly the entropy change in the gas, both for reversible and for irreversible expansion.

Solution 3.9 This exercise deals with adiabatic changes of state of a perfect gas and the differences between reversible and irreversible processes. Initially locked, a moveable piston limits the volume of the gas to $V_1 = 0.01 \text{ m}^3$. The perfect gas within the cylinder is thermally isolated from the surroundings, i.e., no heat transfer is possible. Using the equation of state (Eq.(3.2)), we can calculate the

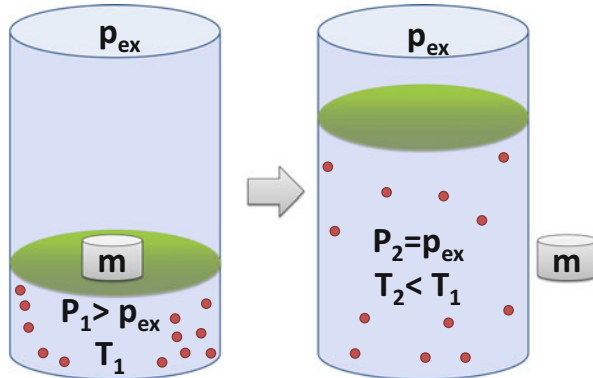


Fig. 3.9 Adiabatic irreversible expansion of a perfect gas, initiated by removing a mass from the piston. Upon expansion, the temperature of the gas is reduced

initial pressure within the cylinder,

$$p_1 = \frac{nRT_1}{V_1} \quad (3.79)$$

$$= \frac{2 \text{ mol} \times 8.3145 \text{ J K}^{-1} \text{ mol}^{-1} \times 320 \text{ K}}{0.01 \text{ m}^{-1}} \quad (3.80)$$

$$= 532,128 \text{ Pa} \quad (3.81)$$

As this initial pressure is larger than the external pressure of $p_{\text{ex}} = 10^5 \text{ Pa}$, the gas expands adiabatically as soon as the piston is unlocked. Hence, work is done upon expansion, and, according to the first law (Eq. (3.25)) and the adiabatic condition $\delta Q = 0$, the amount of work done by the gas is balanced by a reduction in its internal energy, which in turn is a function of temperature. Thus, we expect a *cooling* of the gas during expansion.

In **subproblem (a)** we assume an irreversible expansion. Experimentally, this could be realized by removing a single piece of mass from the top of the piston, for example, as illustrated in Fig. 3.9. The piston then expands immediately into its equilibrium position, which is characterized by a final pressure $p_2 = p_{\text{ex}}$. To calculate the final temperature T_2 and final volume V_2 of the gas, we use the first law⁷ (Eq. (3.25)) with the adiabatic condition $\delta Q = 0$:

$$dU = n c_v dT = -p_{\text{ex}} dV \quad (3.82)$$

⁷Note that we cannot use Poisson's equation here, because the latter assumes a *reversible* adiabatic change of state.

We assume that work is done by the piston moving against the constant external pressure. We discuss this below in more detail. After an integration step, we obtain

$$n c_v (T_2 - T_1) = -p_{\text{ex}} (V_2 - V_1)$$

This expression contains two unknowns, T_2 and V_2 . We can eliminate V_2 using the equation of state, $p_2 V_2 = nRT_2$. After solving for T_2 , we obtain the result

$$T_2 = \frac{p_2 V_1 + n c_v T_1}{n (c_v + R)} \quad (3.83)$$

$$= \frac{100,000 \text{ Pa} \times 0.01 \text{ m}^3 + 2 \text{ mol} \times 25 \text{ J K}^{-1} \text{ mol}^{-1} \times 320 \text{ K}}{2 \text{ mol} \times (25 \text{ J K}^{-1} \text{ mol}^{-1} + 8.3145 \text{ J K}^{-1} \text{ mol}^{-1})} \quad (3.84)$$

$$= 255.14 \text{ K} \quad (3.85)$$

The final volume is

$$V_2 = \frac{nRT_2}{p_2} = \frac{2 \text{ mol} \times 8.3145 \text{ J K}^{-1} \text{ mol}^{-1} \times 255.14 \text{ K}}{100,000 \text{ Pa}} = 0.0424 \text{ m}^3 \quad (3.86)$$

As expected, the gas has cooled down from 320 to about 255 K during expansion. The work is best calculated from this temperature difference,

$$W = n c_v (T_2 - T_1) = -3243 \text{ J.} \quad (3.87)$$

Before discussing these results, we move on to **subproblem (b)**, where reversible adiabatic expansion is assumed. How could we at least approximately realize this experimentally? We can obtain *quasi reversible* processing in a step-by-step procedure, by removing small pieces of mass one by one from the piston, as illustrated in Fig. 3.10. With the limit of arbitrarily small differential masses dm , we would obtain reversible expansion. We check this by recalling the difference between an irreversible and a reversible change of state: if a process is irreversible, then the initial state can only be re-established by doing work. If we look at Fig. 3.9, this corresponds to lifting the single mass upward back onto the piston by doing linear work. The piston then moves down until the initial state is reached. In contrast, as illustrated in Fig. 3.10, we could simply establish the initial state by putting the small mass pieces back on the piston one by one—without doing linear work. A second intuitive criterion of reversibility is time invariance. If we record a movie of the quasi-reversible expansion in Fig. 3.10 and run the movie in reverse, we could simply see a physically meaningful process: pieces of mass are taken back onto the piston, and the piston moves gradually down step by step, i.e., the reversible compression of the gas. In contrast, a movie of the process illustrated in Fig. 3.9 run backward would show a physically absurd scene: a gas does not spontaneously reduce its volume and heat up!

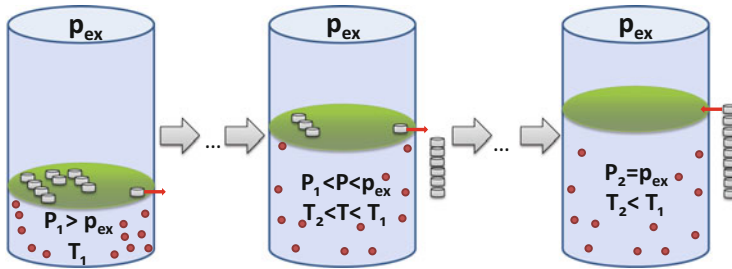


Fig. 3.10 Adiabatic quasi reversible expansion of a perfect gas by removing several small pieces of mass from the piston. In each of the intermediate steps, the gas takes different values of pressure and temperature

In the course of the reversible adiabatic expansion, the gas is permanently in a state of equilibrium, i.e., the thermal state variables are related to each other according to the equation of state: the more the piston moves up and the volume increases, the pressure is gradually reduced according to $p = \frac{nRT}{V}$. If we take this into account, the application of the first law gives

$$dU = n c_v dT = -\frac{n R T}{V} dV \Leftrightarrow c_v \frac{dT}{T} = -R \frac{dV}{V} \quad (3.88)$$

After integration,

$$c_v \int_{T_1}^{T_2} \frac{dT}{T} = -R \int_{V_1}^{V_2} \frac{dV}{V} \Leftrightarrow c_v \ln \frac{T_2}{T_1} = R \ln \frac{V_1}{V_2} \quad (3.89)$$

and consideration of Eq. (3.47), one of **Poisson's equations** follows:

$$\frac{T_2}{T_1} = \left(\frac{V_2}{V_1} \right)^{1-\gamma} \quad (3.90)$$

where $\gamma = \frac{c_p}{c_v}$. These equations need to be used to calculate the final volume and temperature after the reversible expansion:

$$V_2 = V_1 \left(\frac{p_{\text{ex}}}{p_1} \right)^{\frac{1}{\gamma}} = 0.01 \text{ m}^3 \left(\frac{100,000 \text{ Pa}}{532,128 \text{ Pa}} \right)^{0.75042} = 0.0351 \text{ m}^3 \quad (3.91)$$

$$T_2 = \frac{p_{\text{ex}} V_2}{n R} = \frac{100,000 \text{ Pa} \times 0.0351 \text{ m}^3}{2 \text{ mol} \times 8.3145 \text{ J K}^{-1} \text{ mol}^{-1}} = 210.84 \text{ K} \quad (3.92)$$

Finally, the work done by the gas is

$$W = n c_v (T_2 - T_1) = -5458 \text{ J} \quad (3.93)$$

In **subproblem (c)** we deal with entropies and calculate them explicitly. We expect $\Delta S_{\text{rev}} = 0$ for the case of the reversible adiabatic expansion, and $\Delta S_{\text{irrev}} > 0$ for the irreversible adiabatic expansion, consistent with the second law and Eq. (3.34). We bear in mind that the entropy of a gas increases upon expansion, but it decreases if its temperature is reduced. Thus, there are two competing effects that govern the total change in entropy. We start with Eq. (3.35), first dealing with the case of the irreversible adiabatic expansion, and use the results for V_2 and T_2 from subproblem (a):

$$\begin{aligned}\Delta S &= n c_v \ln \frac{T_2}{T_1} + n R \ln \frac{V_2}{V_1} \\ &= 2 \text{ mol} \times 25 \text{ J K}^{-1} \text{ mol}^{-1} \ln \frac{255.14 \text{ K}}{320 \text{ K}} \\ &\quad + 2 \text{ mol} \times 8.3145 \text{ J K}^{-1} \text{ mol}^{-1} \ln \frac{0.0424 \text{ m}^3}{0.01 \text{ m}^3} \\ &= -11.33 \text{ J K}^{-1} + 24.02 \text{ J K}^{-1} = +12.7 \text{ J K}^{-1}\end{aligned}\tag{3.94}$$

For the reversible adiabatic condition, we could proceed in the same way. However, starting with Eq. (3.35) and by using Eq. (3.37), we can generally prove that the entropy change in the gas is zero in the case of an adiabatic reversible expansion:

$$\begin{aligned}\Delta S &= n c_v \ln \frac{T_2}{T_1} + n R \ln \frac{V_2}{V_1} \\ &= n c_v \ln \left(\frac{V_2}{V_1} \right)^{1-\kappa} + n R \ln \frac{V_2}{V_1} \\ &= n (c_v (1 - \kappa) + R) \ln \frac{V_2}{V_1} \\ &= n (c_v - c_p + c_p - c_v) \ln \frac{V_2}{V_1} = 0\end{aligned}\tag{3.95}$$

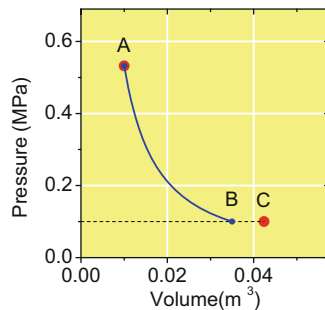
In the special case of an adiabatic reversible expansion, the entropy increase due to expansion is exactly balanced by the entropy decrease due to temperature reduction.

A summary of the results of this exercise can be found in Table 3.3 and Fig. 3.11.

Table 3.3 Comparison of reversible and irreversible expansion with regard to the final volume and gas temperature, expansion work, and entropy change

	Final temperature (K)	Final volume (m^3)	$W (\text{J})$	$\Delta S (\text{J K}^{-1})$
Reversible expansion	210.84	0.0351	-5458	0
Irreversible expansion	255.14	0.0424	-3243	+12.7

Fig. 3.11 p - V diagram of the adiabatic expansion. Point A is the initial state, B the final state of the reversible (isentropic) expansion, C is the final state of the irreversible case



In the isentropic, reversible adiabatic case more work is done upon expansion, consistent with stronger cooling of the gas and a smaller final volume. Thus, the final state variables of the gas do not coincide. This is also seen in the p - V diagram of the expansion in Fig. 3.11. The curve marks the reversible (isentropic) expansion, ending in the final state at point B. For each point between the initial and final volumes, the pressure of the gas is precisely defined according to the adiabatic line, which we could reconstruct by removing a series of infinitesimally small masses from the top of the piston, as outlined above. In contrast, the irreversible expansion lacks any intermediate states. In the p - V diagram, this case is only characterized by the two points A and C of the initial and final state.

3.4 Heterogeneous Systems and Phase Transitions

Heterogeneous systems are formed by substances in two or more different states of aggregation. To describe changes in such systems, the thermodynamic potentials in Table 3.2 are augmented by the dependency on the amount of substance of each species, and thus on the *composition of the system*:

$$dU = T dS - p dV + \sum_j \mu_j dn_j \quad (3.96)$$

$$dH = T dS + V dp + \sum_j \mu_j dn_j \quad (3.97)$$

$$dA = -S dT - p dV + \sum_j \mu_j dn_j \quad (3.98)$$

$$dG = -S dT + V dp + \sum_j \mu_j dn_j \quad (3.99)$$

The **chemical potential** μ_j of a substance in a special phase is the amount of Gibbs free energy the system gains, if dn_j mol of substance are added at constant

pressure and temperature:

$$\mu_j = \left(\frac{\partial G}{\partial n_j} \right)_{p,T,\{n_i\}} \quad (3.100)$$

Moreover, using the **Euler equation** $U = TS - pV + \sum_j \mu_j n_j$ it can be shown that

$$G = \sum_j \mu_j n_j, \quad (3.101)$$

i.e., the Gibbs free energy of a system is the sum of the chemical potentials of all substances in their various phases, weighted with their respective amounts of substance. The conditions for the direction of a spontaneous change, Eqs. (3.41) and (3.42), in addition to the above equations, are the basis for the description of heterogeneous systems, including *phase diagrams* and, moreover, the phenomena related to the mixing of substances, the *colligative properties*: osmotic pressure, vapor pressure reduction, the increase in the boiling point, and the lowering of the freezing point.

The *coexistence lines* in a phase diagram (see Fig. 3.1) are characterized by a reversible exchange of atoms or molecules between two different phases, e.g., the liquid phase and the gas phase. Because $\Delta G = \Delta H - T\Delta S = 0$ in this case, the molar entropy change involved with such a phase transition on a point of the coexistence line is

$$\Delta s_{\text{tr}} = \frac{\Delta h_{\text{tr}}}{T}, \quad (3.102)$$

where Δh_{tr} is the respective molar transition enthalpy, e.g., the molar heat of vaporization. On the coexistence lines, the chemical potentials in two phases are equal. This condition is sufficient to deduce the coexistence lines in the phase diagram of a pure substance (Fig. 3.1). The **Clapeyron equation**

$$\frac{dp}{dT} = \frac{\Delta s_{\text{tr}}}{\Delta v_{\text{tr}}} \quad (3.103)$$

provides the gradient of a coexistence line on the p - T diagram, where Δv_{tr} is the change in the molar volume involved with the phase transition. For the special cases of a gas-liquid or a gas-solid phase transition, two approximations are frequently made: (1) The gas-phase is described by the equation of state for a perfect gas

(Eq. (3.2)). (2) The molar volume of the condensed phase is neglected over the molar volume of the gas phase. In this case, Eq. (3.103) together with Eq. (3.102) can be used to derive the **Clausius-Clapeyron equation** (see Problem 3.10a)

$$\frac{d \ln p}{dT} = \frac{\Delta h_{\text{tr}}}{RT^2} \quad (3.104)$$

3.4.1 The Standard State

As material properties, transition enthalpies and entropies are quantities that depend on both temperature and pressure. For their tabulation it is convenient to *define* a suitable **standard state** of a substance:

The standard state of a substance is the state in which it is stable at a pressure of $p^\ominus = 10^5 \text{ Pa}$.

The value of a material property at standard pressure is indicated by the superscript \ominus . Note that this standard state is not the only standard state used in physical chemistry. Moreover, a reference temperature of $T = 298.15 \text{ K}$ is usually chosen to tabulate these material properties.

3.4.2 Real and Ideal Mixtures

A heterogeneous system may contain more than one component, e.g., *mixtures* constituting a liquid phase, or a gas phase. If two substances A and B constitute a binary mixture, their chemical potentials change relative to the respective standard chemical potentials. In the gas phase assuming perfect gas behavior,

$$\mu_A = \mu_A^\ominus + RT \ln \frac{p_A}{p^\ominus}. \quad (3.105)$$

An idea of how this relation can be derived gives the solution to Problem 3.11b. In the liquid phase, the respective expression is

$$\mu_A = \mu_A^* + RT \ln a_A \quad (3.106)$$

where the a_A is the **activity** of substance A in solution, and μ_A^* is the chemical potential of the pure substance A. The symbol $*$ now refers to a *new standard state* of a pure substance, which is also called *Raoult's law standard state*. The activity of A is defined via its partial pressure p_A over the solution, related to the vapor pressure

of the pure substance, p_A^* :

$$a_A = \frac{p_A}{p_A^*} \quad (3.107)$$

It is important to understand that the activity is a property of the solution, but it is determined indirectly by the partial pressure in the gas phase above the solution in chemical equilibrium, where the chemical potential in the solution and in the gas phase are equal. For a real solution, the activity may depend on the composition of the solution in a complicated way. In the limiting case of an *ideal solution*, the activity corresponds to the mole fraction: $a_A = x_A$, and the partial pressure of A can be calculated using **Raoult's law**:

$$p_A = x_A p_A^* \quad (3.108)$$

In general, the relation between activity and mole fraction is

$$a_A = x_A \gamma_A, \quad (3.109)$$

where γ_A is the activity coefficient of A.

3.4.3 Problems

Problem 3.10 (Vapor Pressure of a Pure Substance)

The vapor pressure of ethylamine ($\text{CH}_3\text{--CH}_2\text{--NH}_2$) was measured as a function of temperature:

T (K)	250.25	259.25	267.55	278.95
p (kPa)	14.83	24.40	37.57	64.17

- Derive the Clausius–Clapeyron equation Eq. (3.104) from the condition of equal chemical potentials in the liquid and the gas phase.
- Determine the molar heat of vaporization, the molar entropy of vaporization, and the standard boiling point of ethylamine, assuming ideal behavior in the gas phase.

(continued)

Problem 3.10 (continued)

- c. Two identical vessels with a volume of 1 dm^3 are filled with 5 and 10 g of ethylamine respectively. Then, the vessels are sealed and heated to 333 K. Calculate the internal pressure of the two vessels.

Solution 3.10 If a liquid is held in a closed vessel, it forms a gas phase above its surface, even if the vessel was initially evacuated. We have dealt with this coexistence of liquid and gas phase already in Problem 3.4, where we investigated the use of the van der Waals equation of state to estimate the vapor pressure of a gas at a given temperature. Now, we will deal with the phenomenon of vapor pressure from a different point of view: energetics. A molecule in a liquid is exerted to a much stronger intermolecular attractive interaction than in the gas phase. Thus, why does it leave the liquid phase at all, if it takes heat to bring it into the gas phase? From the viewpoint of thermodynamics, the answer is entropy. The entropy of a substance in the gaseous state is generally higher than in a condensed phase, implying a positive entropy of vaporization, ΔS_{vap} . The gain in entropy favors the transition into the gaseous state, and with increasing temperature, this effect becomes increasingly important, consistent with a lowering of the Gibbs free energy of vaporization, $\Delta G_{\text{vap}} = \Delta H_{\text{vap}} - T \Delta S_{\text{vap}}$. If at constant pressure and temperature there is an equilibrium between molecules leaving the gas phase and those entering the gas phase, the phase transition is reversible, consistent with a change in the system's Gibbs free energy being zero (see Eq. (3.41)). Hence, using Eq. (3.99),

$$dG = \mu_{\text{gas}} dn_{\text{gas}} + \mu_{\text{liq}} dn_{\text{liq}} = 0 \quad (3.110)$$

As $dn_{\text{gas}} = -dn_{\text{liq}}$, the condition of reversibility requires equal chemical potentials in the gas phase and the liquid phase:

$$dG = (\mu_{\text{gas}} - \mu_{\text{liq}}) dn_{\text{gas}} \stackrel{!}{=} 0 \quad \Leftrightarrow \quad \mu_{\text{gas}} \stackrel{!}{=} \mu_{\text{liq}} \quad (3.111)$$

Based on the equality of the chemical potentials, we derive the coexistence line between vapor and liquid in **subproblem (a)**. Starting with a point on the coexistence line at a given pressure and temperature, p and T , we consider the chemical potentials of the vapor and the liquid at $p + dp$ and $T + dT$, still on the coexistence line:

$$\mu_{\text{gas}}(p + dp, T + dT) = \mu_{\text{liq}}(p + dp, T + dT) \quad (3.112)$$

We can expand these chemical potentials into a power series and consider only the linear terms,

$$\mu_i(p + dp, T + dT) = \mu_i(p, T) + \left(\frac{\partial \mu_i}{\partial p} \right)_T dp + \left(\frac{\partial \mu_i}{\partial T} \right)_p dT + \dots \quad (3.113)$$

Using the definition of the chemical potential Eq.(3.100) and the relations $(\frac{\partial G}{\partial T})_p = -S$ and $(\frac{\partial G}{\partial p})_T = V$, the differential quotients $(\frac{\partial \mu_i}{\partial p})_T$ and $(\frac{\partial \mu_i}{\partial T})_p$ are identified as the negative (partial) molar entropy s_i and the (partial) molar volume v_i of the substance in phase i respectively. Thus,

$$\mu_i(p + dp, T + dT) = \mu_i(p, T) + v_i dp - s_i dT + \dots ,$$

and as we may consider the chemical potentials of the vapor and the liquid phase to be equal at $p + dp$ and $T + dT$ as well,

$$\mu_{\text{gas}}(p, T) + v_{\text{gas}} dp - s_{\text{gas}} dT = \mu_{\text{liq}}(p, T) + v_{\text{liq}} dp - s_{\text{liq}} dT$$

and thus, because $\mu_{\text{gas}}(p, T) = \mu_{\text{liq}}(p, T)$,

$$\frac{dp}{dT} = \frac{s_{\text{gas}} - s_{\text{liq}}}{v_{\text{gas}} - v_{\text{liq}}} = \frac{\Delta s_{\text{vap}}}{\Delta v_{\text{vap}}} \stackrel{\text{Eq. (3.102)}}{=} \frac{\Delta h_{\text{vap}}}{T \Delta v_{\text{vap}}} \quad (3.114)$$

We have now derived the Clapeyron equation. Next, we make the approximation $\Delta v_{\text{vap}} \approx v_{\text{gas}}$, i.e., we neglect the molar volume of the liquid over the molar volume of the gas phase, which is reasonable at moderate pressures. Moreover, assuming perfect gas behavior, we can express $v_{\text{gas}} = \frac{RT}{p}$ by the equation of state. Inserting this into the Clausius equation, we obtain:

$$\frac{dp}{dT} = \frac{p \Delta h_{\text{vap}}}{RT^2} \quad \Leftrightarrow \quad \frac{dp}{p} = \frac{\Delta h_{\text{vap}} dT}{RT^2}$$

Here, we have arrived at the Clausius-Clapeyron equation because $\frac{dp}{p} = d \ln p$.

We go one step further and integrate the last expression, assuming that the molar heat of vaporization is independent of temperature and takes the value of the standard molar heat of vaporization, $\Delta h_{\text{vap}}^\ominus$. We obtain

$$\ln \frac{p}{p^\ominus} = -\frac{\Delta h_{\text{vap}}^\ominus}{R} \left(T^{-1} - T_b^{\ominus -1} \right) \quad (3.115)$$

As a consequence, if the molar heat of vaporization is known and one point on the coexistence line, e.g., the standard boiling point, the vapor pressure at any given temperature can be determined. Moreover, because the standard molar entropy of vaporization is $\Delta s_{\text{vap}}^\ominus = \frac{\Delta h_{\text{vap}}^\ominus}{T_b^\ominus}$ as a special case of Eq. (3.102), we obtain

$$\ln \frac{p}{p^\ominus} = -\frac{\Delta h_{\text{vap}}^\ominus}{R} T^{-1} + \frac{\Delta s_{\text{vap}}^\ominus}{R} \quad (3.116)$$

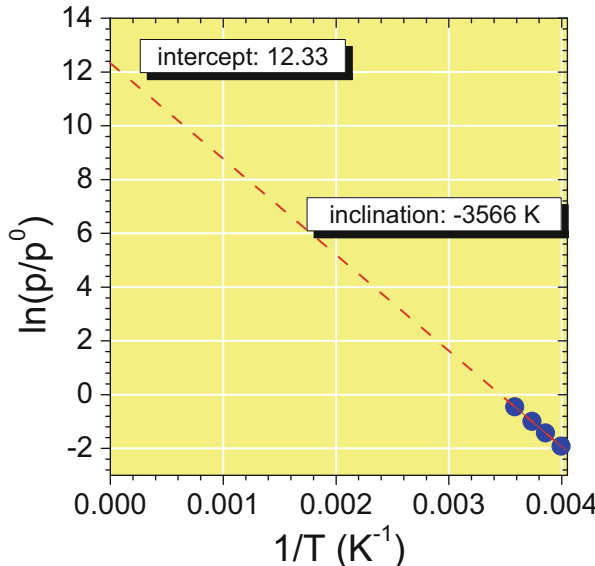


Fig. 3.12 Graphical determination of the enthalpy and entropy of vaporization from vapor pressure variation with temperature according to Eq. (3.116)

We can use this relation to determine $\Delta h_{\text{vap}}^{\ominus}$ and $\Delta s_{\text{vap}}^{\ominus}$ and the standard boiling point of ethylamine, as we do in **subproblem (b)**. Therefore, we plot $\ln \frac{p(T)}{p^{\ominus}}$ against the reciprocal temperature, as shown in Fig. 3.12. If $\Delta h_{\text{vap}}^{\ominus}$ and $\Delta s_{\text{vap}}^{\ominus}$ are constant over the temperature range of tabulated data, then a linear behavior can be expected. Inspection of the diagram shows that this seems to be the case. A linear regression provides the axis intercept and the inclination of the best-fit line:

$$\begin{aligned}\frac{\Delta s_{\text{vap}}^{\ominus}}{R} &= 12.33 \quad \Leftrightarrow \quad \Delta s_{\text{vap}}^{\ominus} = 102.5 \text{ J K}^{-1} \text{ mol}^{-1} \\ \frac{\Delta h_{\text{vap}}^{\ominus}}{R} &= -3566 \text{ K} \quad \Leftrightarrow \quad \Delta h_{\text{vap}}^{\ominus} = 29.7 \text{ kJ mol}^{-1}\end{aligned}$$

Note that in general, Δh_{vap} and Δs_{vap} will depend markedly on temperature, if the examined temperature interval is sufficiently large. The standard boiling point can be determined in two different ways. The simplest way is based on Eq. (3.102) and yields

$$T_b^{\ominus} = \frac{\Delta h_{\text{vap}}^{\ominus}}{\Delta s_{\text{vap}}^{\ominus}} = 289.3 \text{ K.} \quad (3.117)$$

The alternative way is based on the analysis of Fig. 3.12. Because at T_b^\ominus the vapor pressure is only p^\ominus , the best-fit line intersects the line $\ln \frac{p}{p^\ominus} = 0$ at $(T_b^\ominus)^{-1} = 0.003458 \text{ K}^{-1}$. We therefore obtain $T_b^\ominus = 289.2 \text{ K}$. The discrepancy of 0.1 K can be explained by the statistical and systematic uncertainties in the experimental vapor pressure data. In **subproblem (c)** we calculate the pressure within two identical vessels, which at $T = 333 \text{ K}$ contain 5 and 10 g of ethylamine respectively. This question challenges the student's ability to assess whether under given conditions a system is a *homogeneous* system or a *heterogeneous* system. The molar mass of ethylamine is $M = 45 \text{ g mol}^{-1}$. Thus, the first vessel contains an amount of

$$n_1 = \frac{5 \text{ g}}{45 \text{ g mol}^{-1}} = 0.\bar{1} \text{ mol.} \quad (3.118)$$

The second vessel is filled with 10 g of ethylamine, which corresponds to $n_2 = 0.\bar{2} \text{ mol}$. Next, we calculate the vapor pressure of ethylamine at $T = 333 \text{ K}$ using our results from subproblem (a). Apparently, the vapor pressure is

$$p_{\text{vap}}(T) = p^\ominus \exp \left(-\frac{\Delta h_v^\ominus}{R} \left(\frac{1}{T} - \frac{1}{T_b^\ominus} \right) \right) \quad (3.119)$$

$$= 100,000 \text{ Pa} \times \exp \left(-3566 \left(\frac{1}{333} - \frac{1}{289.3} \right) \right) \quad (3.120)$$

$$= 504,000 \text{ Pa} \quad (3.121)$$

If ethylamine in the vessel is present as a liquid phase coexisting with a gas phase, i.e., as a heterogeneous system, then the inner pressure of the vessel will be this vapor pressure of about 5 bar. Here, however, we have also take the possibility into account that the amount of ethylamine might be insufficient to establish the coexistence of liquid and vapor. If we assume that gaseous ethylamine is a perfect gas, then the nominal gas phase pressure at a given amount of substance and temperature according to the equation of state is

$$p_1 = \frac{n_1 RT}{V} = \frac{0.\bar{1} \text{ mol} \times 8.3145 \text{ J K}^{-1} \text{ mol}^{-1} \times 333 \text{ K}}{10^{-3} \text{ m}^3} = 308,000 \text{ Pa} < p_{\text{vap}}(T). \quad (3.122)$$

As a consequence, the 5 g of ethylamine in the first vessel is present in the gaseous state. This is also illustrated in Fig. 3.13, where the coexistence line between vapor and liquid is shown in a p - T diagram. The point p_1 resides in the area below the coexistence line, i.e., in the area of gaseous ethylamine. The pressure within the vessel is thus $p_1 = 3.08 \text{ bar}$

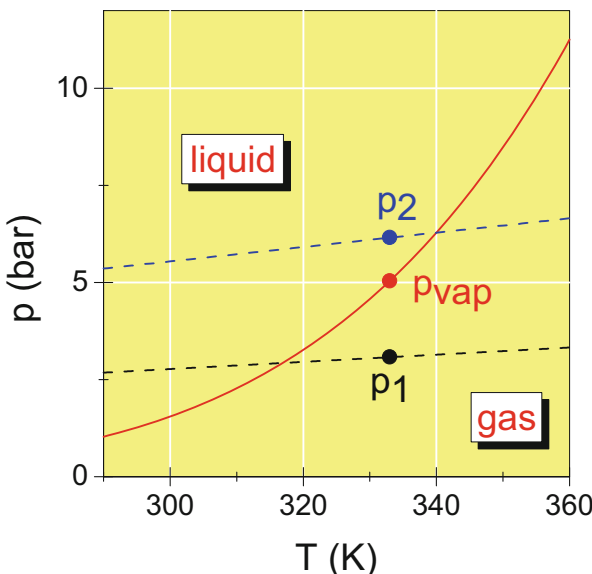


Fig. 3.13 Coexistence line $p_{\text{vap}}(T)$ of gaseous and liquid ethylamine (solid line) according to Eq. (3.119). The dashed lines indicate the nominal gas pressure of 5 g (p_1) and 10 g (p_2) ethylamine in the vessel according to the perfect gas equation of state. At $T = 333 \text{ K}$, $p_2 > p_{\text{vap}} > p_1$

In contrast, a vessel containing 10 g of ethylamine would have a nominal gas pressure

$$p_2 = \frac{n_1 RT}{V} = \frac{0.2 \text{ mol} \times 8.3145 \text{ J K}^{-1} \text{ mol}^{-1} \times 333 \text{ K}}{10^{-3} \text{ m}^3} = 616,000 \text{ Pa} > p_{\text{vap}}(T), \quad (3.123)$$

as also shown in Fig. 3.13. Therefore, a fraction of ethylamine condenses and forms a liquid phase coexisting with gaseous ethylamine. In this case, the pressure within the vessel is thus the vapor pressure $p_{\text{vap}} = 5.04 \text{ bar}$.

Problem 3.11 (Molar Gibbs Free Energies of Solids and Gases, Conversion of Graphite to Diamond)

At 298 K the molar standard Gibbs free energy of graphite is zero, whereas the corresponding value for diamond is $+2.9 \text{ kJ mol}^{-1}$. The densities of graphite and diamond are 2.3 and 3.5 g cm^{-3} respectively.

(continued)

Problem 3.11 (continued)

- For both forms of carbon, calculate the molar Gibbs free energy of formation at a pressure of 10 bar and 298 K. Assume that diamond and graphite are incompressible solids.
- At 298 K, the molar standard Gibbs free energy of gaseous CO₂ is $-394.4 \text{ kJ mol}^{-1}$. Assume perfect gas behavior and calculate the molar Gibbs free energy of formation of CO₂(g) at a pressure of 10 bar. What do you conclude concerning the pressure dependence of the free Gibbs energy of gaseous and condensed phases?
- Calculate the minimum pressure, at which diamond is the stable form of carbon.

Solution 3.11 In this exercise, we deal with the relative stability of two forms of carbon, diamond and graphite. We deal with the relationship between the Gibbs free energy of a substance as a function of pressure, its structure, and the phase diagram.

Graphite is the stable form of carbon under normal atmospheric pressure. As an element in its standard state, by definition, its *standard* molar Gibbs free energy of formation is zero.⁸ Diamond, however, can be formed if a high pressure is exerted on carbon. Its crystal structure is more compact and thus its density is higher than that of graphite.

In **subproblem (a)**, we seek the function $g(p)$ of diamond and graphite and we treat them as incompressible solids. From Eq. (3.99),

$$\left(\frac{\partial g}{\partial p} \right)_T = v \quad (3.124)$$

where v is the molar volume, which is related to the density ρ and the molar mass M : $\rho = \frac{M}{v}$. Integration yields

$$g(p) = g(p^\ominus) + v \int_{p^\ominus}^p dp = g(p^\ominus) + v(p - p^\ominus) = g(p^\ominus) + \frac{M}{\rho}(p - p^\ominus) \quad (3.125)$$

For graphite with $g(p^\ominus) = 0$ and $\rho = 2300 \text{ kg m}^{-3}$, the molar free Gibbs energy takes a value of

$$g(10^6 \text{ Pa}) = 0 + \frac{12 \times 10^{-3} \text{ kg mol}^{-1}}{2300 \text{ kg m}^{-3}} (10^6 - 10^5) \text{ Pa} = +4.7 \text{ J mol}^{-1}. \quad (3.126)$$

For diamond with $g(p^\ominus) = 2900 \text{ J mol}^{-1}$, we obtain a value of 2903.1 J mol⁻¹.

⁸See the definition of the enthalpy of formation in Sect. 4.1.1 at page 71.

Table 3.4 Molar Gibbs free energies of graphite, diamond, and CO₂ at standard pressure and at $p = 10^6$ Pa

Substance	State	$g(p^\ominus)$	$g(10^6 \text{ Pa})$	Δg
C (Graphite)	Solid	0	$+4.7 \times 10^{-3}$	$+4.7 \times 10^{-3}$
C (Diamond)	Solid	+2.9000	+2.9031	$+3.1 \times 10^{-3}$
CO ₂	Gaseous	-394.4	-388.7	+5.7

All values are given in kJ mol⁻¹

In **subproblem (b)** we consider the function $g(p)$ for CO₂ treated as a perfect gas:

$$g(p) = g(p^\ominus) + \int_{p^\ominus}^p v(p) dp \quad (3.127)$$

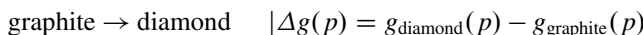
Using the equation of state, $v(p) = \frac{RT}{p}$.

$$g(p) = g(p^\ominus) + RT \int_{p^\ominus}^p \frac{dp}{p} = g(p^\ominus) + RT \ln \frac{p}{p^\ominus} \quad (3.128)$$

For CO₂ with $g^\ominus = -394.4 \text{ kJ mol}^{-1}$, we obtain a value of $g(10^6 \text{ Pa}) = -388.7 \text{ kJ mol}^{-1}$. In Table 3.4, all results are summarized:

Although the molar Gibbs free energy of solids changes only weakly to the order of a few J mol⁻¹ under a moderate change in pressure, the Gibbs free energy of a perfect gas changes markedly to the order of several kJ mol⁻¹. This general trend allows a different treatment of gases and condensed phases in the thermodynamic characterization of the chemical equilibrium in Chap. 4.

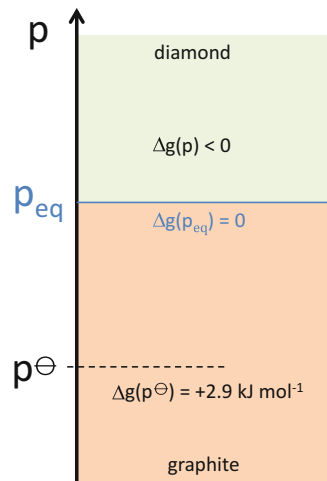
In **subproblem (c)** we calculate the pressure at which diamond becomes the stable form of carbon. Looking at our tabulated results, we recognize that the molar Gibbs free energy of diamond increases slightly more weakly than that of graphite, if the pressure is increased. Thus, at a certain pressure p_{eq} , the molar Gibbs free energies of diamond and graphite are equal. For $p > p_{\text{eq}}$, diamond becomes the stable form of carbon, indicated by the lower value of $g(p)$. The situation is illustrated in the schematic phase diagram in Fig. 3.14. To evaluate p_{eq} , we use our above results and consider the transition



with the change in molar Gibbs free energy

$$\Delta g(p) = g_{\text{diamond}}^\ominus - g_{\text{graphite}}^\ominus + \Delta v (p - p^\ominus), \quad (3.129)$$

Fig. 3.14 Schematic phase diagram of carbon with the phase boundary between graphite and diamond



and the change in molar volume $\Delta v = v_{\text{diamond}} - v_{\text{graphite}}$. With the different densities of diamond and carbon given, we obtain

$$\begin{aligned}\Delta v &= \frac{M}{\rho_{\text{diamond}}} - \frac{M}{\rho_{\text{graphite}}} \\ &= 12 \times 10^{-3} \text{ kg mol}^{-1} \left(\frac{1}{3500} - \frac{1}{2300} \right) \text{ m}^3 \text{ kg}^{-1} \\ &= -1.79 \times 10^{-6} \text{ m}^3 \text{ mol}^{-1}\end{aligned}$$

On the coexistence line between diamond and graphite, i.e., at $p = p_{\text{eq}}$, the transition between the two carbon phases is reversible. Therefore, the molar Gibbs free energy of the phase transition is zero: $\Delta g \stackrel{!}{=} 0$. In this special case, Eq. (3.129) yields

$$p_{\text{eq}} = \frac{p^\Theta \Delta v - \Delta g^\Theta}{\Delta v} = \frac{10^5 \text{ Pa} \times (-1.79 \times 10^{-6} \text{ m}^3 \text{ mol}^{-1}) - 2900 \text{ J mol}^{-1}}{(-1.79 \times 10^{-6} \text{ m}^3 \text{ mol}^{-1})}$$

and our result for p_{eq} is 1.62 GPa. Experimentally, the transition from graphite to diamond is observed at pressures above 2 GPa.

Problem 3.12 (Ideal Solutions)

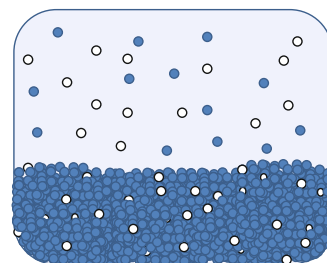
The main components of liquid petroleum gas (LPG) are propane and butane in seasonally varying compositions. Assuming that propane and butane constitute an ideal mixture, calculate the maximum acceptable mole fraction

(continued)

Problem 3.12 (continued)

of propane, for which at a temperature of 50 °C the internal pressure of a tank containing LPG does not exceed a value of 12 bar. The molar standard heats of vaporization of pure propane and butane are 19.0 and 22.4 kJ mol⁻¹ respectively. The standard boiling points of propane and butane are 231.1 and 272.7 K respectively.

Fig. 3.15 A tank containing a binary solution of a more volatile substance indicated by *white balls*, and a less volatile species (*blue balls*), which is in excess. In the gas phase, the more volatile component is enriched



Solution 3.12 In middle Europe, the summer composition of LPG fuels is about 40 mass-% propane and 60 mass-% n-butane, and vice versa in winter. At the filling station, a compressor has to work against the tank internal pressure. Hence, to guarantee successful filling, the internal pressure should not exceed the maximum pressure of the compressor, $p_{\max} = 12$ bar in this problem. In summer, the temperature of a car tank may easily reach 50 °C. At this temperature, the vapor pressure of *pure* butane and propane is calculated using the Clausius Clapeyron law (Eq. (3.115)). For butane, with $\Delta h_{\text{vap, butane}}^{\ominus} = 22.4 \text{ kJ mol}^{-1}$ and $T_{b, \text{butane}}^{\ominus} = 272.7 \text{ K}$

$$p_B^* = p^{\ominus} \exp \left(-\frac{\Delta h_{\text{vap, butane}}^{\ominus}}{R} \left(\frac{1}{T} - \frac{1}{T_{b, \text{butane}}^{\ominus}} \right) \right) = 4.74 \text{ bar.}$$

For propane with $\Delta h_{\text{vap, butane}}^{\ominus} = 19.0 \text{ kJ mol}^{-1}$ and $T_{b, \text{butane}}^{\ominus} = 231.1 \text{ K}$, a value of 16.94 bar results. Consistent with the higher enthalpy of vaporization and the lower standard boiling temperature, propane is more volatile than butane. The situation is illustrated in Fig. 3.15. Propane (C_3H_8) and n-butane (C_4H_{10}) are hydrocarbons with similar chemical properties. The assumption of an ideal mixture is thus reasonable and justifies the application of Raoult's law (Eq. (3.108)), by which we calculate the total pressure in the gas phase

$$p = x_B p_B^* + x_P p_P^* \quad (3.130)$$

For $p = p_{\text{max}}$ and $x_B = 1 - x_P$, we obtain an expression for the maximum acceptable mole fraction of propane:

$$x_P = \frac{p_{\text{max}} - p_B^*}{p_P^* - p_B^*} = \frac{12 - 4.74}{16.94 - 4.74} = 0.595$$

Hence, at least in summer, the fraction of propane should not exceed 60%. From this result, and the molar masses of propane and butane (44.1 and 58.1 g mol⁻¹), the maximum acceptable mass fraction of propane is 53%.

Problem 3.13 (Vapor Pressure Reduction)

At 293 K, the vapor pressure of the solvent diethyl ether ($\text{C}_2\text{H}_5-\text{O}-\text{C}_2\text{H}_5$) is 586 hPa. After the addition of 20 g of an unknown nonvolatile compound in 1 kg of diethyl ether, the vapor pressure is reduced to 583 hPa. Assume an ideal mixture of diethyl ether and the unknown compound, for which an elementary analysis yields mass fractions of 41.4% carbon, 5.5% hydrogen, 9.6% nitrogen, and 43.8% oxygen. Determine the molar mass and the molecular formula of the unknown compound.

Solution 3.13 The lowering of the vapor pressure of a solvent in the mixture with another substance is one of four **colligative properties**.⁹ These are used in analytics to determine the molar mass of a solute. Combined with results from an elementary analysis providing the relative abundances of chemical elements, the molecular formula of an unknown compound can be determined. In this problem, we consider $m_X = 20$ g of an unknown compound (denoted X), which is dissolved in $m_D = 1000$ g diethyl ether. This causes a lowering of the vapor pressure of diethyl ether from $p_D^* = 586$ hPa to $p_D = 583$ hPa. Moreover, elementary analysis of X yields mass fractions $f_C = 0.414$ for carbon, $f_H = 0.055$ for hydrogen, $f_N = 0.096$ for nitrogen, and $f_O = 0.438$ for oxygen. We determine the molar mass and the molecular formula. As stated in the text of the problem, the unknown substance X and the solvent are assumed to constitute an ideal binary mixture. We can thus use Raoult's law Eq. (3.108) to obtain the mole fraction of diethyl ether:

$$x_D = \frac{p_D}{p_D^*} = \frac{583 \text{ hPa}}{586 \text{ hPa}} = 0.99488 \quad (3.131)$$

The mole fraction for X results from the condition

$$x_D + x_X = 1. \quad (3.132)$$

⁹The other colligative properties are the elevation of the boiling point, the depression of the freezing point, and osmotic pressure.

Thus,

$$x_X = 1 - x_D = 5.12 \times 10^{-3}. \quad (3.133)$$

Using the definition of the mole fraction in Eq. (2.8) at page 11 we obtain

$$x_X = \frac{n_X}{n_X + n_D} \quad (3.134)$$

where n_X and n_D are the amounts of X and diethyl ether respectively. We can solve this equation for the value of X:

$$n_X = \frac{x_X}{1 - x_X} n_D = \frac{x_X}{x_D} \frac{m_D}{M_D} \quad (3.135)$$

Here, we have expressed n_D using the given mass of the solvent and its molar mass, $M_D = 74 \text{ g mol}^{-1}$, determined from the given molecular formula of diethyl ether. If we combine

$$n_D = \frac{m_X}{M_X} \quad (3.136)$$

with Eq. (3.135), we obtain an expression for the molar mass of X:

$$M_X = m_X \frac{x_D}{x_X} \frac{M_D}{m_D} = \frac{20 \text{ g}}{1000 \text{ g}} \frac{0.99488}{5.12 \times 10^{-3}} \times 74 \text{ g mol}^{-1} = 288 \text{ g mol}^{-1}. \quad (3.137)$$

The given mass fractions of the elements can now be exploited to determine the molecular formula of the unknown substance: if Z_C is the number of carbon atoms in X and $M_C = 12 \text{ g mol}^{-1}$ is the elemental atomic weight of carbon, the following relation holds:

$$Z_C M_C = f_C M_X. \quad (3.138)$$

As a consequence, the number of carbons is

$$Z_C = f_C \frac{M_X}{M_C} = 0.414 \frac{288}{12} = 9.9 \approx 10. \quad (3.139)$$

In the same way, we obtain

$$Z_H = f_H \frac{M_X}{M_H} = 0.055 \frac{288}{1} = 15.8 \approx 16, \quad (3.140)$$

$$Z_N = f_N \frac{M_X}{M_N} = 0.096 \frac{288}{14} = 1.97 \approx 2, \quad (3.141)$$

$$Z_0 = f_0 \frac{M_X}{M_O} = 0.438 \frac{288}{16} = 7.9 \approx 8. \quad (3.142)$$

We therefore conclude that the molecular formula of the unknown compound is $C_{10}H_{16}N_2O_8$.

Problem 3.14 (Spontaneous Freezing of Supercooled Water)

Using the second law of thermodynamics, show that the freezing of 1 mol of liquid water at a temperature of 250 K is a spontaneous change of state. The standard molar heat of fusion is $6.008 \text{ kJ mol}^{-1}$, and the constant pressure molar heat capacities of liquid water and ice are 75.3 and $37.7 \text{ J K}^{-1} \text{ mol}^{-1}$.

Solution 3.14 According to the second law, a change of state in an isolated system is spontaneous, if the total entropy change is positive. To apply the second law, we calculate the entropy change involved with the freezing of supercooled water and thereby show that this process is indeed spontaneous. This can be quite tedious, because upon the process of freezing, the supercooled water exchanges heat with the surroundings. Our analysis of entropy changes thus has to include not only the entropy change of the water, but also the entropy change of the surroundings:

$$\Delta S = \Delta S_{\text{water}} + \Delta S_{\text{surroundings}} \quad (3.143)$$

Moreover, the application of the Clausius formula Eq. (3.33) requires reversible heat transfers: for the calculation of ΔS , we therefore have to replace the direct freezing at 250 K by (a) the heating of the supercooled water to the standard temperature of fusion T_f^\ominus , (b) the reversible freezing of the water at T_f^\ominus , and (c) the cooling of the frozen ice from T_f^\ominus to 250 K, as outlined in Fig. 3.16. The property of entropy to be a state function guarantees that the sum of entropy changes in the steps (a), (b), and (c) in Fig. 3.16 corresponds to the entropy change of the entire irreversible process, indicated as the dashed line in Fig. 3.16. For $n = 1 \text{ mol}$, the entropy change of water is

$$\Delta S_{\text{water}} = \int_{250 \text{ K}}^{T_f^\ominus} \frac{n c_p(\text{liq.}) dT}{T} - \frac{n \Delta h_f^\ominus}{T_f^\ominus} + \int_{T_f^\ominus}^{250 \text{ K}} \frac{n c_p(\text{ice}) dT}{T}. \quad (3.144)$$

The first integral corresponds to the virtual entropy change of heating the water from the temperature $T_1 = 250 \text{ K}$ to T_f^\ominus . The second term is the entropy change involved with the reversible freezing of water at T_f^\ominus , according to Eq. (3.102). The negative sign takes into account that the latent heat of freezing is the negative of the given molar heat of fusion, $\Delta h_f^\ominus = 6008 \text{ J mol}^{-1}$. The third term, finally, gives the entropy change of cooling the frozen ice from T_f^\ominus to 250 K. After the evaluation of

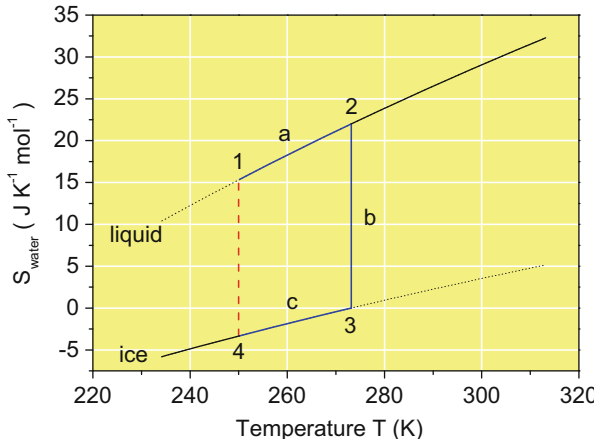


Fig. 3.16 Temperature dependence of the entropy of liquid water and ice as a function of temperature (schematic). The entropy change involved with the freezing of supercooled water at 250 K (dashed line) is the same as the alternative route (solid line) consisting of heating of liquid water to the standard temperature of fusion at 273.15 K (a), reversible freezing (b), and cooling the ice down to 250 K (c)

the integrals,

$$\Delta S_{\text{water}} = n c_p(\text{liq.}) \ln \frac{T_f^\ominus}{T_1} - \frac{n \Delta h_f^\ominus}{T_f^\ominus} + n c_p(\text{ice}) \ln \frac{T_1}{T_f^\ominus} \quad (3.145)$$

$$= +6.669 \text{ J K}^{-1} - 21.995 \text{ J K}^{-1} - 3.339 \text{ J K}^{-1}. \quad (3.146)$$

As expected from the diagram in Fig. 3.16, ΔS_{water} corresponding to the difference in S_{water} between point 4 and point 1 is negative. Next, we focus on the entropy changes in the surroundings involved with steps a, b, and c respectively. We presume that the surroundings constitute a huge heat reservoir, so that arbitrary amounts of heat can be exchanged with the surroundings without a change in its temperature, which is $T_1 = 250 \text{ K}$. Then, we can calculate the entropy changes of the surroundings, as we have done in Problem 3.8 (Eq. (3.73)) and obtain

$$\Delta S_{\text{surroundings}} = -\frac{n c_p(\text{liq.})(T_f^\ominus - T_1)}{T_1} + \frac{n \Delta h_f^\ominus}{T_1} - \frac{n c_p(\text{ice})(T_1 - T_f^\ominus)}{T_1} \quad (3.147)$$

$$= -6.973 \text{ J K}^{-1} + 24.032 \text{ J K}^{-1} + 3.491 \text{ J K}^{-1} \quad (3.148)$$

The first term corresponds to the entropy change of the surroundings, if the heat $n c_p(\text{liq.})(T_f^\ominus - T_1)$ necessary to heat the liquid water to T_f^\ominus is transferred from the surroundings to the water in step (a). The second term is the gain of entropy if the latent heat released by the water upon freezing is transferred to the surroundings in

step (b). The third term, finally, is the gain of entropy of the surroundings due to the heat released by the frozen ice when it is cooled back to the lower temperature T_1 . Thus, summing up all entropy changes using Eq. (3.143), we obtain an increase in total entropy of $\Delta S = +1.885 \text{ J K}^{-1}$. Using the second law, we conclude that the cooling of supercooled water at 250 K is a spontaneous process.

Problem 3.15 (Freezing of Atmospheric Water Droplets to Cubic or Hexagonal Ice)

The molar Gibbs free energy of a substance with a surface area A is

$$g = h - Ts + \gamma A \quad (3.149)$$

where h and s are the molar enthalpy and entropy respectively, and γ is the surface tension or surface energy. Consider small water droplets of supercooled atmospheric water at a temperature of 200 K. Calculate the range of droplet radii for which freezing to cubic ice is thermodynamically favorable over freezing to hexagonal ice. For both forms of ice, assume a density of 0.93 g cm^{-3} , and $h_{\text{cubic}} - h_{\text{hexagonal}} = 35 \text{ J mol}^{-1}$. The surface energies are $\gamma_{\text{cubic}} = 22 \text{ mJ m}^{-2}$ and $\gamma_{\text{hexagonal}} = 31 \text{ mJ m}^{-2}$ respectively. Assume equal molar entropies of cubic and hexagonal ice. (Literature reference: G. P. Johari, J. Chem. Phys. **122**, 194504 (2005).)

Solution 3.15 Multi-phase systems necessarily have phase boundaries: surfaces. As the chemical environment at an interface is generally different, the molecules experience a different bonding at the interface compared with the bulk. As a consequence, the total energy of a finite piece of matter also depends on its surface area. The dependency of the thermodynamic potentials on the surface area is considered via the surface energy γ per unit area, equivalent to a *surface tension*. For larger systems, surface effects on the thermodynamic properties can often be neglected. However, for objects on the *nano* scale, such as the very small atmospheric water droplets considered in this problem, the surface energy may influence, among other things, the ice crystallization properties of such droplets. From the viewpoint of thermodynamics, water crystallizes in the form that under given conditions has the lower Gibbs free energy of formation. Presuming the same molar entropy of cubic and hexagonal ice, water crystallizes as hexagonal ice if we neglect the influence of the interface, because, as stated in the text of the problem, its molar enthalpy is 35 J mol^{-1} smaller than that of cubic ice. Let us consider a water droplet with a radius of r , a volume $V(r) = \frac{4\pi}{3}r^3$, a surface area $A(r) = 4\pi r^2$, and mole number $n(r) = \frac{\rho}{M}V(r)$. $M = 18 \text{ g mol}^{-1}$ is the molar mass of water, and $\rho = 0.93 \text{ g cm}^{-3}$ is the density. The Gibbs free energy of a droplet of hexagonal

ice is

$$G_{\text{hexagonal}}(r) = n(r) h_{\text{hexagonal}} - n(r) T s_{\text{hexagonal}} + \gamma_{\text{hexagonal}} A(r) \quad (3.150)$$

For a droplet of cubic ice of the same radius,

$$G_{\text{cubic}}(r) = n(r) h_{\text{cubic}} - n(r) T s_{\text{cubic}} + \gamma_{\text{cubic}} A(r) \quad (3.151)$$

If the entropies of cubic and hexagonal ice are the same as stated above,

$$G_{\text{cubic}} - G_{\text{hexagonal}} = n(r) (h_{\text{cubic}} - h_{\text{hexagonal}}) + (\gamma_{\text{cubic}} - \gamma_{\text{hexagonal}}) A(r) \quad (3.152)$$

$$= \frac{4\pi\rho}{3M} r^3 (h_{\text{cubic}} - h_{\text{hexagonal}}) + 4\pi r^2 (\gamma_{\text{cubic}} - \gamma_{\text{hexagonal}}) \quad (3.153)$$

We use this expression to determine the *critical radius* at which cubic and hexagonal water droplets of the same radius have the same Gibbs free energy ($G_{\text{cubic}}(r_{\text{crit.}}) - G_{\text{hexagonal}}(r_{\text{crit.}}) = 0$):

$$r_{\text{crit.}} = -\frac{3M}{\rho} \frac{(\gamma_{\text{cubic}} - \gamma_{\text{hexagonal}})}{(h_{\text{cubic}} - h_{\text{hexagonal}})} \quad (3.154)$$

$$= -\frac{3 \times 18 \times 10^{-3} \text{ kg mol}^{-1}}{930 \text{ kg m}^{-3}} \frac{(22 - 31) \times 10^{-3} \text{ J m}^{-2}}{35 \text{ J mol}^{-1}} \quad (3.155)$$

$$= 14.9 \times 10^{-9} \text{ m} \quad (3.156)$$

The critical radius for a water droplet is only about 15 nm. If $r > r_{\text{crit.}}$, the Gibbs free energy of hexagonal ice is lower than that of cubic ice, and the droplet crystallizes in the hexagonal crystal structure. For $r < r_{\text{crit.}}$, thermodynamics supports crystallization in the cubic form of ice.

References

1. Frenkel M, Marsh KN (eds) (2003) Virial coefficients of pure gases and mixtures. Landolt-Börnstein, New Series, Group IV, vol 21. Springer, Heidelberg
2. Friedman AS, White D (1950) J Am Chem Soc 72:3931–3932

Chapter 4

Thermochemistry

Abstract Thermochemistry deals with the heat transferred or released by a system during a change of its state or a chemical reaction. Calorimetry is an experimental method for measuring such heat transfers. The reaction enthalpy, the reaction entropy, and the Gibbs free energy of reaction are defined and related to the molar standard enthalpies of formation and molar standard entropies of reactants and products. The selection of problems in this chapter deals with key aspects of thermochemistry, such as the determination of molar heat of formation. Problem 4.3 exemplifies the use of the Gibbs free energy of reaction as a criterion for the occurrence of chemical processes.

4.1 Basic Concepts

It is assumed that the reader is familiar with stoichiometry and thermodynamics, especially the use of caloric state variables, which were introduced in Chap. 3.

4.1.1 Enthalpies of Formation

To predict the enthalpy change of a system in the course of a chemical reaction, textbooks introduce the molar enthalpy of formation h_f of a substance in a suitable standard state.¹

The molar standard enthalpy of formation Δh_f^\ominus of a substance is the reaction enthalpy by which it is formed from its elements under standard state conditions.

Note that this definition implies that the standard enthalpy of the formation of elements in their standard state is zero. In the same way, the standard molar Gibbs free energy of formation of substances are defined and tabulated at a reference

¹For the definition of the standard state see Sect. 3.4.1.

temperature of 298.15 K. Tabulated standard molar entropies, however, are absolute values.²

4.1.2 The Molar Reaction Enthalpy and the Molar Reaction Entropy

Consider a chemical system before and after a reaction $\sum_J v_J X_J = 0$. The enthalpy change in the system H_r is the difference in its enthalpy before and after the reaction took place. Using the familiar concept of the extent of reaction ξ introduced in Chap. 2, the enthalpy change $H_r(\xi)$ is

$$H_r(\xi) = \sum_J (n_J^0 + v_J \xi) \Delta h_f(J) - \sum_J n_J^0 \Delta h_f(J) = \sum_J v_J \xi \Delta h_f(J) \quad (4.1)$$

The **molar reaction enthalpy** is the change of H_r with ξ :

$$\Delta h_r = \frac{\partial}{\partial \xi} H_r(\xi) = \sum_J v_J \Delta h_f(J) \quad (4.2)$$

Note that unlike H_r , the molar reaction enthalpy Δh_r is an intensive property (see Sect. 3.1). Tabulated heats of formation refer to the standard state at the reference temperature 298.15 K. The standard molar reaction enthalpy is thus

$$\Delta h_r^\ominus = \sum_J v_J \Delta h_f^\ominus(J) \quad (4.3)$$

A process or chemical reaction characterized by $\Delta h_r > 0$ is called **endothermic**. In contrast, a process or reaction characterized by $\Delta h_r < 0$ is called **exothermic**. Similarly, the **molar standard reaction entropy** of this reaction is calculated from the molar standard entropies of the reactants:

$$\Delta s_r^\ominus = \sum_J v_J \Delta s_f^\ominus(J) \quad (4.4)$$

The **molar standard Gibbs free energy of reaction** is calculated from the standard free enthalpies of formation of the reactants or the values of Δh_r^\ominus and Δs_r^\ominus at the reference temperature T_r :

²For the calculation of the absolute entropy of monatomic gases based on statistical thermodynamics, see Problem 8.6.

$$\Delta g_r^\ominus(T) = \sum_J v_J \Delta g_f^\ominus(J) = \Delta h_r^\ominus - T \Delta s_r^\ominus \quad (4.5)$$

A process or chemical reaction characterized by $\Delta g_r > 0$ is called **endergonic**. In contrast, a process or reaction characterized by $\Delta g_r < 0$ is called **exergonic**.

4.1.3 Kirchhoff's Law

In practice, chemical reactions take place under different conditions concerning pressure and temperature. Based on Eq.(3.32) **Kirchhoff's law** can be derived, which allows the calculation of a reaction enthalpy at arbitrary temperature T from the respective value at a reference temperature T_r :

$$\Delta h_r(T) = \Delta h_r(T_r) + \int_{T_r}^T \sum_J v_J c_{p,J}(T') dT'. \quad (4.6)$$

Similarly, using the relation $dS = \frac{c_p dT}{T}$, the reaction entropy at T is

$$\Delta s_r(T) = \Delta s_r(T_r) + \int_{T_r}^T \sum_J v_J \frac{c_{p,J}(T')}{T'} dT'. \quad (4.7)$$

Note that these equations assume that no phase transition occurs in the temperature range under consideration between the reference temperatures T_r and T . In Problem 3.14 we dealt with the entropy change in a case in which a phase transition occurs.

4.1.4 Hess's Law

As enthalpy is a state function, the change in enthalpy between an initial state and a final state does not depend on the reaction pathway. This is the origin of **Hess's law**:

The total reaction enthalpy of a given chemical reaction does not depend on the route taken. If a chemical reaction can be separated into several reaction steps, the total reaction enthalpy is the *sum* of the reaction enthalpies of the reaction steps.

Hess's law is useful to indirectly determine reaction enthalpies of reactions that are otherwise not accessible by an experiment.

4.2 Problems

Additional problems related to thermochemistry can be found in Chap. 5 (chemical equilibrium).

Problem 4.1 (Combustion Enthalpies) Isopropanol is produced by the hydration of propene,



The following data are given: at 298.15 K, the molar standard heats of combustion of propene and isopropanol are 2,040 and 2,006 kJ mol⁻¹ respectively. The constant pressure molar heat capacities of propene, isopropanol, and water are 64, 86, and 34 J K⁻¹ mol⁻¹ respectively.

- Calculate the molar standard heat of reaction Eq. (4.8) at the reference temperature 298.15 K.
- Calculate Δh_x^\ominus at 550 K.

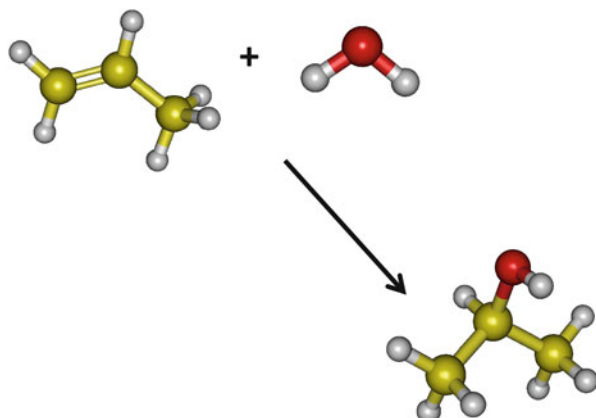
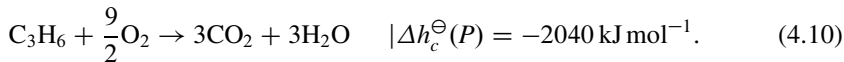


Fig. 4.1 Hydration of propene to isopropanol (2-propanol)

Solution 4.1 Combustion calorimetry offers the possibility of determining reaction enthalpies indirectly using Hess's law. In **subproblem (a)** we determine the molar standard reaction enthalpy Δh_x^\ominus for the hydration of propene (Eq. (4.8), Fig. 4.1) from the given molar heats of combustion of the hydrocarbons propene and isopropanol. Technically, this reaction is conducted in a reactor containing a suitable catalyst. A direct determination of Δh_x^\ominus is hampered by the fact that parallel reactions occur, e.g., the reaction to 1-propanol. Using Eq. (4.3) we write down an expression for Δh_x^\ominus ,

$$\Delta h_x^\ominus = \Delta h_f^\ominus(C_3H_8O) - \Delta h_f^\ominus(C_3H_6) - \Delta h_f^\ominus(H_2O) \quad (4.9)$$

Next, we express the unknown molar enthalpies of formation occurring on the right side using the given heats of combustion. Combustion means the complete reaction of a substance with oxygen (see Problem 2.2 in Chap. 2). If the reactant is a hydrocarbon, the combustion products are CO₂ and H₂O. To exploit the heats of combustion provided for propene and isopropanol (2-propanol), we must formulate the equation for their combustion. In the case of propene, we have



For isopropanol, we have



Be aware that combustion reactions are exothermic (Δh_c^\ominus negative), and the heat *released* to the surroundings is thus positive. Using Eq. (4.3), we can set up two equations that relate the molar combustion enthalpies of these substances to their formation enthalpies. Note that gaseous O₂ is an element in its standard state. Its enthalpy of formation is thus zero.

$$\Delta h_c^\ominus(P) = 3\Delta h_f^\ominus(H_2O) + 3\Delta h_f^\ominus(CO_2) - \Delta h_f^\ominus(C_3H_6) \quad (4.12)$$

$$\Delta h_c^\ominus(I) = 4\Delta h_f^\ominus(H_2O) + 3\Delta h_f^\ominus(CO_2) - \Delta h_f^\ominus(C_3H_8O) \quad (4.13)$$

If we now subtract Eq. (4.13) from Eq. (4.12), we obtain

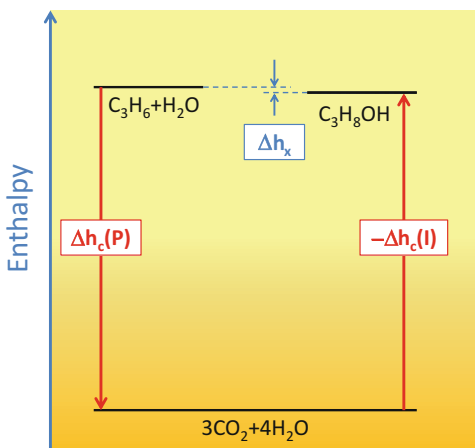
$$\Delta h_c^\ominus(P) - \Delta h_c^\ominus(I) = \Delta h_f^\ominus(C_3H_8O) - \Delta h_f^\ominus(C_3H_6) - \Delta h_f^\ominus(H_2O) \quad (4.14)$$

By comparing this expression with Eq. (4.9), we see that the reaction enthalpy sought is simply the difference in the combustion enthalpies:

$$\Delta h_x^\ominus = \Delta h_c^\ominus(P) - \Delta h_c^\ominus(I) = (-2040 + 2006) \text{ kJ mol}^{-1} = -34 \text{ kJ mol}^{-1} \quad (4.15)$$

An alternative solution is based on the graphical representation of the reactions Eqs. (4.8), (4.10), and (4.11) in a Born Haber cycle diagram, as illustrated in Fig. 4.2. It is obvious that the reaction of propene and water can be realized by the exothermic combustion of propene followed by the endothermic synthesis of three CO_2 and four H_2O molecules to form isopropanol. According to Hess's law (see Sect. 4.1.4) the total molar reaction enthalpy Δh_x is the sum of the molar reaction enthalpies in the sequence of reaction steps, i.e., $\Delta h_c(P)$ and $-\Delta h_c(I)$, as indicated in the figure.

Fig. 4.2 Born Haber cycle diagram for the hydration of propene (schematic). The reaction of propene (C_3H_6) and water to isopropanol ($\text{C}_3\text{H}_8\text{OH}$) is realized by the combustion of propene followed by the synthesis of the combustion products to form isopropanol



Moreover, the inspection of the Born Haber cycle in Fig. 4.2 reveals a typical difficulty of experimental calorimetry: accuracy. To obtain the standard molar heat of reaction Δh_x^\ominus sought, we must subtract comparatively large combustion enthalpies and the result Δh_x^\ominus is smaller orders of magnitude. A precise measurement of heats of combustion is thus the key to obtaining useful results. The goal is to achieve *chemical accuracy*, which means that a heat of formation is determined with a maximum uncertainty of 1 kcal mol⁻¹.

The value for Δh_x^\ominus is valid for the reference temperature $T_r = 298.15 \text{ K}$. In practice, the hydration of propene is conducted at a higher temperature. In **subproblem (b)** we determine Δh_x^\ominus at $T_2 = 550 \text{ K}$. This is an application of Kirchhoff's law (see Sect. 4.1.3). Moreover, this task is simplified by the fact that the constant pressure molar heat capacities given are assumed to be constant over the temperature range specified.³ Using Eq. (4.6) under special consideration of reaction

³A problem with temperature-dependent heat capacities can be found in Chap. 5 (Problem 5.6).

Eq. (4.8), the reaction enthalpy sought is

$$\begin{aligned}\Delta h_x^\ominus(550 \text{ K}) &= \Delta h_x^\ominus(298.15 \text{ K}) + \int_{T_r}^{T_2} (c_p(\text{C}_3\text{H}_8\text{O}) - c_p(\text{C}_3\text{H}_6) - c_p(\text{H}_2\text{O})) \, dT \\ &= -34,000 \text{ J mol}^{-1} + (86 - 64 - 34) \text{ J K}^{-1} \text{ mol}^{-1} (550 - 298.15) \text{ K} \\ &= -37 \text{ kJ mol}^{-1}\end{aligned}\quad (4.16)$$

Problem 4.2 (Solvation Enthalpy)

- Under standard conditions, 1 g of LiCl powder is dissolved in 50 ml of water (Fig. 4.3). As the solution is stirred, the temperature increases from 298 to 302.2 K. The constant pressure molar heat capacity of water is $75.3 \text{ J K}^{-1} \text{ mol}^{-1}$. Estimate the molar standard heat of solvation of LiCl. You may ignore the contribution of the dissolved LiCl to the heat capacity of the solution. The density of water is 1 g ml^{-1} .
- In another experiment, 1 g KCl(s) is dissolved in the same amount of water under the same conditions. A temperature reduction of 1.1 K was measured. Determine the molar standard heat of solvation of KCl and calculate the standard heat of formation of $\text{K}^+(\text{aq})$ relative to the value of Li^+ , if the standard heats of formation for KCl and LiCl are -436.7 and $-408.7 \text{ kJ mol}^{-1}$ respectively.

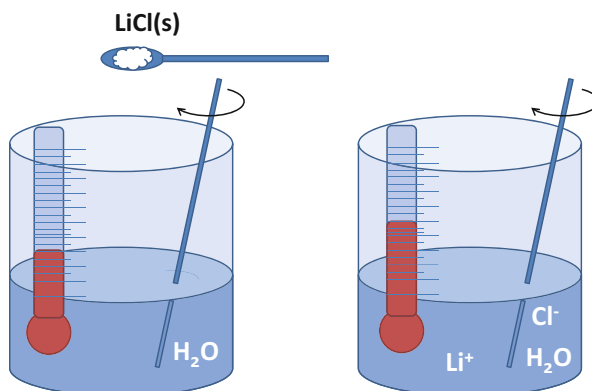
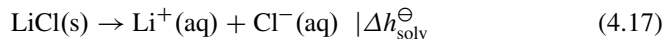


Fig. 4.3 A simple form of calorimetry to measure the heat of solvation of a salt

Solution 4.2 This problem deals with a very simple case of calorimetry. LiCl is an ionic crystal and completely dissolves in water according to



In **subproblem (a)** we determine the standard molar heat of solvation $\Delta h_{\text{solv}}^{\ominus}$ of this reaction. We exploit the temperature change $\Delta T = +4.2 \text{ K}$ of the solution and the molar heat capacity of the solvent water given. We notice that the increase in temperature indicates that the dissolution of LiCl is an exothermic process. Apparently, we ignore any heat transfer to the environment, i.e., the amount of heat

$$Q = C_p \Delta T \quad (4.18)$$

involved with the temperature jump in the solution is directly related to the heat of reaction. The heat capacity C_p of the solution is approximately given by the heat capacity of water. The amount of water is determined using the density ρ and the molar mass $M_{\text{H}_2\text{O}}$ which is 18 g mol^{-1} :

$$C_p = n_{\text{H}_2\text{O}} c_{p,\text{H}_2\text{O}} = \frac{m_{\text{H}_2\text{O}}}{M_{\text{H}_2\text{O}}} c_{p,\text{H}_2\text{O}} = \frac{\rho V}{M_{\text{H}_2\text{O}}} c_{p,\text{H}_2\text{O}} = 209.17 \text{ J K}^{-1} \quad (4.19)$$

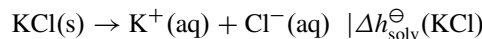
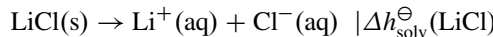
As a consequence, the heat released by the reaction was

$$Q = 209.17 \text{ J K}^{-1} \times 4.2 \text{ K} = 878.5 \text{ J.} \quad (4.20)$$

To determine the molar heat of solvation, we need to know the amount of 1 g LiCl. From the periodic system, we take the atomic weights of Li and Cl and obtain the molar mass $M_{\text{LiCl}} = 42.39 \text{ g mol}^{-1}$. Hence, the amount of 1 g LiCl is $n_{\text{LiCl}} = \frac{1 \text{ g}}{42.39 \text{ g mol}^{-1}} = 0.0236 \text{ mol}$. The molar standard heat of solvation is thus $\Delta h_{\text{solv}}^{\ominus} = \frac{-Q}{n_{\text{LiCl}}} = -37.2 \text{ kJ mol}^{-1}$.

In the same way, we can proceed in **subproblem (b)**, where the same experiment leads to a temperature reduction of 1.1 K for the salt KCl, indicating an endothermic reaction. The molar mass of KCl is $M_{\text{KCl}} = 74.55 \text{ g mol}^{-1}$ and 1 g of KCl thus corresponds to an amount of $n_{\text{KCl}} = 0.0134 \text{ mol}$. A temperature reduction of 1.1 K is consistent with a heat loss of $Q = -230.0 \text{ J}$. The molar heat of solvation for KCl is thus $\Delta h_{\text{solv}}^{\ominus} = \frac{-Q}{n_{\text{KCl}}} = +17.2 \text{ kJ mol}^{-1}$.

The second part of the subproblem deals with the determination of heats of formation from the calorimetric results obtained so far. Although it is principally not possible to determine the absolute heat of formation of an ion in aqueous solution by performing an experiment,⁴ we can use Hess' law and eliminate the unknown heat of formation of chlorine, which is the anionic species occurring in both reactions:



⁴Electrolyte solutions are electrically neutral, requiring at least two different kinds of charged species in a calorimetric experiment.

Using Eq. (4.3), we write

$$\Delta h_{\text{solv}}^{\ominus}(\text{LiCl}) = \Delta h_f^{\ominus}(\text{Li}^+) + \Delta h_f^{\ominus}(\text{Cl}^-) - \Delta h_f^{\ominus}(\text{LiCl}) \quad (4.21)$$

$$\Delta h_{\text{solv}}^{\ominus}(\text{KCl}) = \Delta h_f^{\ominus}(\text{K}^+) + \Delta h_f^{\ominus}(\text{Cl}^-) - \Delta h_f^{\ominus}(\text{KCl}) \quad (4.22)$$

Subtraction of both equations yields

$$\begin{aligned} \Delta h_f^{\ominus}(\text{K}^+) - \Delta h_f^{\ominus}(\text{Li}^+) &= \Delta h_{\text{solv}}^{\ominus}(\text{KCl}) - \Delta h_{\text{solv}}^{\ominus}(\text{LiCl}) + \Delta h_f^{\ominus}(\text{KCl}) - \Delta h_f^{\ominus}(\text{LiCl}) \\ &= (17.2 + 37.2 - 436.7 + 408.7) \text{ kJ mol}^{-1} = 26.4 \text{ kJ mol}^{-1} \end{aligned}$$

This is just the heat of formation sought *relative* to the value for Li^+ ions.

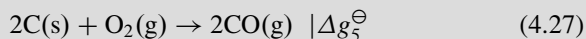
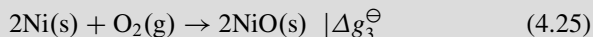
Problem 4.3 (Ellingham Diagram) Consider a sealed reaction vessel containing graphite (C(s)), nickel oxide (NiO(s)), and noble gas. The vessel may be heated to a high temperature.

- a. Use the thermochemical data in Table 4.1 to determine the temperature above which nickel oxide is reduced to nickel according to the following reactions:



You may assume that reaction enthalpies and entropies are constant over the whole temperature range.

- b. Plot the Gibbs free energy of reaction as a function of temperature for each of the following reactions:



Interpret this Ellingham diagram and use it to determine the temperature above which nickel oxide is reduced by carbon.

Solution 4.3 According to thermodynamics, the stability of a compound against reaction with other reactants is governed by the Gibbs free energy of reaction, which depends on temperature (Eq. (4.5)). If Δg_r^{\ominus} is positive, the compound is stable. A negative sign, in contrast, favors its reaction. In metallurgy, a practical

Table 4.1 Thermochemical standard data for selected substances, valid for the reference temperature 298.15 K

Substance	Δh_f^\ominus (kJ mol ⁻¹)	s^\ominus (J K ⁻¹ mol ⁻¹)
Ni(s)	0	29.9
NiO(s)	-239.7	38.0
C(s)	0	5.74
CO(g)	-110.5	197.7
CO ₂ (g)	-393.5	216.8
O ₂ (g)	0	205.2

tool to estimate the stability of metals and their oxides against reaction with carbon is the **Ellingham diagram**. Here, we take the example of the reduction of nickel oxide to become acquainted with this method. The nickel oxide in the vessel may be reduced by carbon in two ways, with carbon monoxide or carbon dioxide as a gaseous reaction product.

In **subproblem (a)**, we use the thermochemical data provided in Table 4.1 to calculate the molar standard reaction enthalpies (Eq. (4.3)) and the molar standard reaction entropies (Eq. (4.4)) for the reactions Eqs. (4.23) and (4.24). For reaction Eq. (4.23), we obtain

$$\Delta h_1^\ominus = \Delta h_f^\ominus(\text{CO}_2) - 2\Delta h_f^\ominus(\text{NiO}) = 85.9 \text{ kJ mol}^{-1} \quad (4.28)$$

where we have already taken into account that the molar standard heat of formation of Ni(s) and C(s) is zero. Moreover, the molar standard reaction entropy for this reaction is

$$\Delta s_1^\ominus = s^\ominus(\text{CO}_2) + 2s^\ominus(\text{Ni}) - 2s^\ominus(\text{NiO}) - s^\ominus(\text{C}) = +194.9 \text{ J K}^{-1} \text{ mol}^{-1} \quad (4.29)$$

Thus, at the reference temperature 298.15 K, the molar Gibbs free energy of reaction is endergonic,

$$\Delta g_1^\ominus(298.15 \text{ K}) = +27.8 \text{ kJ mol}^{-1}$$

and thus, not favored by thermodynamics. If we now assume that these values for the reaction entropy and the reaction enthalpy are constant, in good approximation even for higher temperatures, we can look for the temperature where Δg_1^\ominus changes its sign, i.e. the temperature above which the reaction is exergonic:

$$\Delta g_1^\ominus(T_1) = \Delta h_1^\ominus - T_1 \Delta s_1^\ominus \stackrel{!}{=} 0 \Leftrightarrow T_1 = \frac{\Delta h_1^\ominus}{\Delta s_1^\ominus} = \frac{85,900 \text{ J mol}^{-1}}{194.9 \text{ J K}^{-1} \text{ mol}^{-1}} = 440.7 \text{ K.} \quad (4.30)$$

In the same way in which we determine the molar reaction enthalpy and entropy for the reaction Eq. (4.24), where NiO is reduced and carbon monoxide is formed, we obtain:

$$\Delta h_2^\ominus = \Delta h_f^\ominus(\text{CO}) - \Delta h_f^\ominus(\text{NiO}) = 129.2 \text{ kJ mol}^{-1} \quad (4.31)$$

and

$$\Delta s_2^\ominus = s^\ominus(\text{CO}) + s^\ominus(\text{Ni}) - s^\ominus(\text{NiO}) - s^\ominus(\text{C}) = +183.9 \text{ J K}^{-1} \text{ mol}^{-1} \quad (4.32)$$

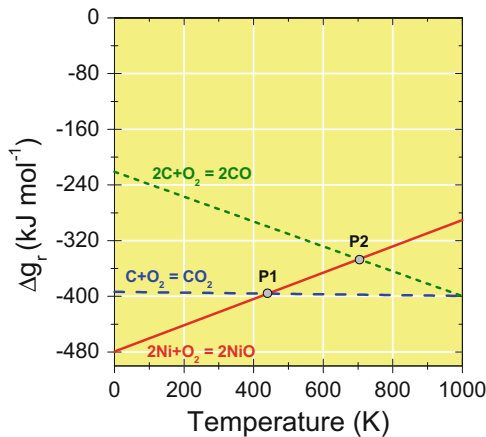
This reaction is also endergonic at the reference temperature 298.15 K ($\Delta g_2^\ominus = +74.4 \text{ kJ mol}^{-1}$) and becomes exergonic above

$$T_2 = \frac{\Delta h_2^\ominus}{\Delta s_2^\ominus} = \frac{129,200 \text{ J mol}^{-1}}{183.9 \text{ J K}^{-1} \text{ mol}^{-1}} = 702.6 \text{ K.} \quad (4.33)$$

To conclude, thermodynamics predicts that nickel oxide may be reduced by carbon above $T_1 = 441 \text{ K}$ under the formation of CO_2 , and above $T_2 = 703 \text{ K}$ under the production of CO.

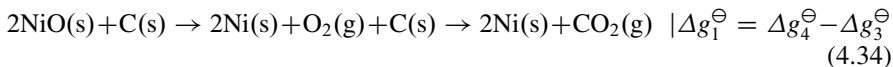
In **subproblem (b)**, we follow a second method to obtain the same result. We consider the three oxidation reactions, namely the oxidation of nickel (Eq. (4.25)), the oxidation of carbon to CO_2 (Eq. (4.26)), and to CO (Eq. (4.27)). For each of these reactions, we can again use the data in Table 4.1 to determine the molar Gibbs free energy of reaction as a function of temperature. These plots are straight lines, owing to the functional form $\Delta g_r^\ominus(T) = \Delta h_r^\ominus - T \Delta s_r^\ominus$. They are shown in Fig. 4.4.

Fig. 4.4 Ellingham diagram for oxidation reactions Eqs. (4.25), (4.26), and (4.27). The intersection points $P1$ and $P2$ of the lines are at the temperatures T_1 and T_2 obtained in subproblem (a)

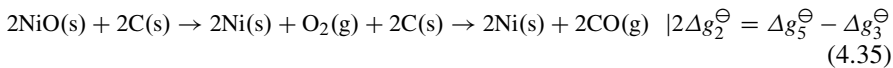


It is striking that the three lines have quite different slopes owing to the very different reaction entropies. Gaseous species have a much higher standard entropy than the solid elements and compounds, as can be seen in Table 4.1. Moreover, the entropies of the three gaseous species are similar. In a reaction that does not change the number of gaseous species, the reaction entropy is thus small. This is the case for the dashed line in Fig. 4.4, representing the oxidation of carbon to carbon dioxide. The oxidation of carbon to carbon monoxide increases the number of gaseous species; therefore, the reaction entropy is positive and the standard Gibbs free energy of reaction has a negative slope (short dashed line). The oxidation of nickel, on the

other hand, reduces the number of gaseous species; $\Delta g_r^\ominus(T)$ has a positive slope (solid line). The three lines have intersection points with each other. Two of them are indicated as $P1$ and $P2$. The temperatures of the intersection points, 441 and 703 K, match the temperatures T_1 and T_2 we have determined in subproblem (a). How can this be explained? The idea behind the Ellingham diagram is to compare the Gibbs free energies of reaction of oxidation reactions. If the oxidation of a substance has a higher Δg_r^\ominus than the oxidation reaction of another species, the former is reduced rather than oxidized. In this sense, we can set up a sequence of reactions in which NiO is reduced and carbon is oxidized:



and



The first reaction is reaction Eq. (4.23); the second is reaction Eq. (4.24) with the stoichiometric numbers multiplied by two. It is obvious that the conditions $\Delta g_1^\ominus = 0$ and $\Delta g_2^\ominus = 0$ are identical to the condition for the intersection points, i.e., $\Delta g_4^\ominus = \Delta g_3^\ominus$ for the reduction of nickel and production of CO_2 , and $\Delta g_5^\ominus = \Delta g_3^\ominus$ for the reduction of nickel and production of CO. The sense of the Ellingham diagram becomes apparent if the Gibbs free energies of reaction of a larger number of oxidation reactions are plotted on the same diagram. A look at such a diagram then provides quick information if oxidation or reduction is favored in the presence of another element or its oxides. The weak temperature dependence of the reaction enthalpy and the reaction entropy can be included in the diagram, in addition to phase transitions that lead to a characteristic bending of the lines. However, such diagrams only reflect the thermodynamics of these reactions, not the kinetics.

Chapter 5

Chemical Equilibrium

Abstract Chemical reactions are irreversible processes that reach a state of equilibrium. Under well-defined conditions, this state of chemical equilibrium of a system is characterized by a unique composition, defined by the law of mass action.

Problems dealing with chemical equilibrium and the law of mass action are among those topics that students consider to be difficult. A general method based on the equilibrium extent of reaction is presented to tackle such problems in a systematic way. The selection of problems highlights different aspects of chemical equilibrium, such as equilibrium in parallel reactions, equilibrium in open and closed systems, or equilibrium in dilute solutions.

5.1 Basic Concepts

Under the condition of chemical equilibrium, the amounts of substances in a reaction mixture are constant with time. Note that this does not imply that the elementary reaction processes come to an end, but that a state is reached where the reaction rates of the forward and backward reaction are in balance. Problem 6.4 in Chap. 6 deals with this kinetic aspect of chemical equilibrium in detail. To characterize chemical equilibrium, the *extent of reaction* ξ introduced in Chap. 2 is a key quantity. In the state of chemical equilibrium, the reaction

$$\sum_j v_j X_j = 0 \quad (5.1)$$

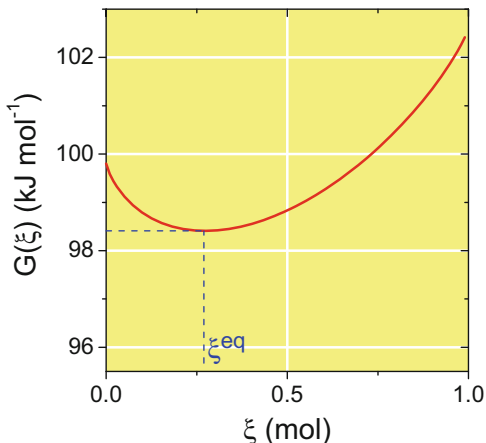
reaches a special value ξ^{eq} . The equilibrium amount of substance n_j^{eq} of each species X_j participating in the reaction is given by (see also Eq. (2.6))

$$n_j^{\text{eq}} = n_j^0 + v_j \xi^{\text{eq}} \quad j = 1, 2, \dots \quad (5.2)$$

where n_j^0 is the initial amount of substance X_j . Once ξ^{eq} is known, *all* the amounts of substances can be determined by the set of equations Eq. (5.2). Four things are worth mentioning here. The determination of $n_j^{\text{eq}}, j = 1, 2, \dots$ is not a multidimensional

Fig. 5.1 Gibbs free energy as a function of extent of reaction in a concrete case of a chemical system.

Equilibrium is reached as $G(\xi)$ reaches its minimum at ξ^{eq}



problem, as the quantities n_j do not vary independently. As already outlined in Chap. 2, the particle numbers strictly follow the reaction Eq. (5.1). Thus, the seeming complexity of typical textbook problems in chemical equilibrium is reduced in most cases to the determination of only one number, namely ξ^{eq} . Second, important for the correct identification of ξ^{eq} in many problems is the following inequality:

$$0 \leq \xi^{\text{eq}} \leq \min \left\{ \frac{n_j^0}{|\nu_j|} \right\}_{\text{educts}} \quad (5.3)$$

It is based on the fact that the extent of reaction is by definition a positive mole number, and, as all n_j^{eq} are positive, ξ^{eq} cannot become larger than the smallest fraction $\frac{n_j^0}{|\nu_j|}$, formed by the initial amounts of all reactants and their stoichiometric numbers.¹ Problem 5.7 presents an application of Eq. (5.3). The third point to remember is that under well-defined conditions (e.g., constant pressure and temperature) the set $n_j^{\text{eq}}, j = 1, 2, \dots$ is unique and does not change unless the external conditions are changed. The third point is that not only the particle numbers reach a constant value, the state of chemical equilibrium is also characterized by constant values of caloric state variables, in particular, the Gibbs free energy of the system, $G(\xi^{\text{eq}})$. As shown for a concrete case in Fig. 5.1, this value is the minimum of the function $G(\xi^{\text{eq}})$. Searching this minimum is equivalent to the formulation of the law of mass action.

¹See also the discussion of the *limiting reactant* in Problem 2.3.

5.1.1 The Law of Mass Action

The derivation of the **law of mass action** is found in the textbooks. In the absence of chemical equilibrium, a reaction is an irreversible process. Under the conditions of constant pressure and temperature, the system develops towards the minimum of its Gibbs free energy (see Eqs. (3.101) and (3.41)):

$$G = \sum_j \mu_j n_j, \quad (5.4)$$

$$dG_{p,T} \leq 0 \quad (5.5)$$

Here, μ_j is the *chemical potential*² of species X_j . Depending on the nature of the chemical system considered in a problem, the chemical potential is best expressed in terms of partial pressure (Eq. (3.105)) in the case of perfect gases participating in a reaction, in terms of *activity* (3.106) in the case of real solutions, or in terms of concentrations, or mole fractions. Then, insertion into Eq. (5.4) and application of the minimum condition $\left(\frac{\partial G}{\partial \xi}\right)_{p,T} \stackrel{!}{=} 0$ following from Eq. (5.5) leads to the law of mass action. Three common forms of the law of mass action are given in the following equations.

$$\prod_j a_j^{v_j} = K = \exp\left(-\frac{\Delta g_r^0}{RT}\right) \quad (5.6)$$

$$\prod_j \left(\frac{p_j}{p^\ominus}\right)^{v_j} = K = \exp\left(-\frac{\Delta g_r^\ominus}{RT}\right) \quad (5.7)$$

$$\prod_j c_j^{v_j} = K_c \quad (5.8)$$

In these equations a_j , p_j , and c_j denote activity, partial pressure, and concentration in the state of chemical equilibrium; v_j is the stoichiometric coefficient of substance X_j . K is an **equilibrium constant** deduced from the value of the **standard molar Gibbs free energy of reaction** Δg_r^0 . The standard state to which Δg_r^0 refers is indicated by the superscript 0. This nomenclature takes into account that, especially for reactions in the liquid phase, other standard states than that defined in Sect. 4.1.1

²For the definition of the chemical potential see Eq. (3.100) at page 52.

might be used. For gas phase reactions, the standard state is related to standard pressure p^\ominus . The equilibrium constant K_c is not directly related to fundamental thermodynamic data. In problems dealing with gas phase reactions of perfect gases, the concentrations are easily expressed by the partial pressure, temperature, and the equation of state, $c_j = \frac{p_j}{RT}$. Thus, it is no difficult task to get the value of K_c from the general equilibrium constant K .

5.1.2 Temperature Dependency of the Equilibrium Constant

In many problems, the equilibrium constant is calculated based on thermochemical data tabulated at the reference temperature $T_1 = 298.15\text{ K}$. In concrete applications, however, the equilibrium constant needs to be calculated for a different temperature T_2 . It can be rigorously shown that the following relation holds:

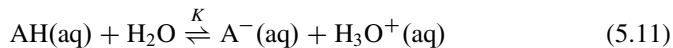
$$\left(\frac{\partial \ln K}{\partial T} \right)_p = \frac{\Delta h_r^\ominus(T)}{RT^2} \quad (5.9)$$

Textbook and examination problems almost always assume that the standard molar heat of reaction is constant with temperature. This is an approximation. Integration of Eq. (5.9) then yields the simple relation called **Van't Hoff reaction isobar**:

$$\ln K(T_2) = \ln K(T_1) - \frac{\Delta h_r^\ominus}{R} \left(\frac{1}{T_2} - \frac{1}{T_1} \right) \quad (5.10)$$

5.1.3 Chemical Equilibrium in Dilute Solutions

Equilibrium of chemical reactions of acids and bases in dilute solutions is a frequently occurring topic. For a given reaction



it is common to write the law of mass action in the following way:

$$K_{\text{CH}_2\text{O}} = K_a = \frac{c_{\text{A}^-} \cdot c_{\text{H}_3\text{O}^+}}{c_{\text{AH}}} \quad (5.12)$$

Here, AH is an acid, A^- its acetate ion, and it is assumed that the concentration of water (55.55 mol dm^{-3}) is much higher than the concentrations of all other

substances. In this case, $c_{\text{H}_2\text{O}}$ can be considered constant. By convention, the equilibrium constant and $c_{\text{H}_2\text{O}}$ are then combined and their product is the *dissociation constant*³ K_a . Moreover, it is common to write

$$\text{pH} = \text{p}K_a + \log_{10} \frac{c_{\text{A}^-}}{c_{\text{AH}}} \quad (5.13)$$

Here,

$$\text{pH} = -\log_{10} \frac{c_{\text{H}_3\text{O}^+}}{1 \text{ mol dm}^{-3}} \quad (5.14)$$

is the pH value of the solution,⁴

$$\text{p}K_a = -\log_{10} \frac{K_a}{1 \text{ mol dm}^{-3}}. \quad (5.15)$$

Equation (5.13) is also called **Henderson-Hasselbalch equation**.

5.2 Problems

Problem 5.1 (Br₂ Decay) A reaction vessel is operated at a constant pressure of 10 mbar and a constant temperature of 1,500 K. The vessel initially contains Br₂(g). Then the chemical equilibrium is established.

- a. Write down the law of mass action for the reaction



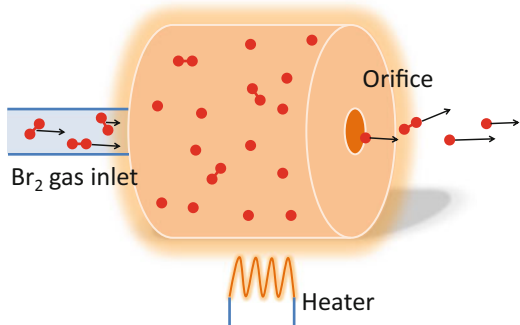
- b. The standard molar heats of formation of Br(g) and Br₂(g) are 111.9 and 30.9 kJ mol⁻¹ respectively. The standard molar Gibbs free energy of formation of Br(g) and Br₂(g) is 82.4 and 3.1 kJ mol⁻¹ respectively. Calculate the equilibrium constants at 298 and 1500 K. You may assume

(continued)

³Whether the dissociation constant or the equilibrium constant is given in a concrete problem can be decided by a consideration of its physical dimension: although K in Eq. (5.11) is dimensionless, K_a in Eq. (5.12) has the dimension of a concentration.

⁴Strictly speaking, the definition of the pH value is based on activities rather than on concentrations.

Fig. 5.2 Scheme of a Br atom beam source operating at constant pressure and high temperature



Problem 5.1 (continued)

- that the standard molar heat of reaction is constant within the range 298 to 1,500 K.
- Calculate the mole fractions and the partial pressure of Br(g) and Br₂(g) at 150 K. *Hint: express the partial pressure by the mole fraction and total pressure.*
 - To further increase the mole fraction of Br, would you increase or decrease the temperature? Would it be better to increase or to decrease the total pressure?

Solution 5.1 This problem deals with the dissociation of molecular bromine, which is in fact an endothermic reaction, as atomization of diatomic molecules requires energy for the breaking of its chemical bond. An application of this problem could be the construction of an atomic beam source for bromine atoms, as illustrated in Fig. 5.2. In **subproblem (a)**, we write down the law of mass action for the dissociation reaction of bromine, Eq. (5.16). Although bromine is a liquid under standard conditions, we only consider the gas phase reaction. Therefore, we use the representation with partial pressure (see Eq. (5.7)):

$$K = \exp\left(-\frac{\Delta g_r^\ominus}{RT}\right) = \frac{\left(\frac{p_{\text{Br}}}{p^\ominus}\right)^2}{\frac{p_{\text{Br}_2}}{p^\ominus}} = \frac{p_{\text{Br}}^2}{p_{\text{Br}_2} p^\ominus} \quad (5.17)$$

K is the equilibrium constant and Δg_r^\ominus the molar Gibbs free energy of reaction. In **subproblem (b)** we calculate K for two different temperatures: for the reference temperature $T_1 = 298\text{ K}$, where thermochemical data are given, and, for later application, for a higher temperature $T_2 = 1500\text{ K}$. At the reference temperature,

the standard molar heat of reaction is

$$\Delta h_r^\ominus = 2\Delta h_f^\ominus(\text{Br}) - \Delta h_f^\ominus(\text{Br}_2) = (2 \times 111.9 - 30.9) \text{ kJ mol}^{-1} = 192.9 \text{ kJ mol}^{-1}. \quad (5.18)$$

This high positive value confirms our above thoughts on the endothermic nature of this reaction. The molar Gibbs free energy of reaction at the reference temperature is

$$\Delta g_r^\ominus = 2\Delta g_f^\ominus(\text{Br}) - \Delta g_f^\ominus(\text{Br}_2) = (2 \times 82.4 - 3.1) \text{ kJ mol}^{-1} = 161.7 \text{ kJ mol}^{-1}. \quad (5.19)$$

Thus, at T_1 , the reaction is not only endothermic, but also largely endergonic. We therefore expect a very small equilibrium constant:

$$K_1 = \exp\left(-\frac{\Delta g_r^\ominus(T_1)}{RT_1}\right) = 4.435 \times 10^{-29} \quad (5.20)$$

This is consistent with the notion that at room temperature almost no Br_2 molecule will decay spontaneously. If the temperature is raised to the much higher temperature T_2 , we can expect that the vibrational degrees of freedom of the diatomic will be excited, involving an increased probability of dissociation. We therefore expect a higher equilibrium constant at T_2 . We may assume that the molar heat of reaction is constant between T_1 and T_2 . Therefore, we can use the *Van't Hoff reaction isobar* (Eq. (5.10)) and obtain

$$\ln K_2 = \ln K_1 - \frac{\Delta h_r^\ominus}{R} \left(\frac{1}{T_2} - \frac{1}{T_1} \right) \quad (5.21)$$

$$\ln K_2 = -65.2854 - \frac{192,900 \text{ J mol}^{-1}}{8,3145 \text{ JK}^{-1} \text{ mol}^{-1}} \left(\frac{1}{1500 \text{ K}} - \frac{1}{298 \text{ K}} \right) = -2.8986 \quad (5.22)$$

Therefore, the equilibrium constant at 1,500 K is $K_2 = 0.0551$ and is thus many orders of magnitude greater than the room temperature value. A note here about calculus: an error often seen in examinations is the addition or division of terms with incompatible physical units. In this case, we need to pay attention to the correct insertion⁵ of the heat of reaction $\Delta h_r^\ominus = 192.9 \text{ kJ mol}^{-1}$, which is $192,900 \text{ J mol}^{-1}$. Having obtained the equilibrium constant at 1500 K, we predict the mole fractions of bromine atoms and bromine molecules at this temperature in **subproblem (c)**. The total pressure is fixed at $p = 10 \text{ mbar}$. Taking this into account, we can introduce

⁵A frequently occurring error of novices is to add quantities with different units or, as in this case, to misapply the factor 10^3 hidden in the unit *kilojoule* (kJ).

the mole fractions x_{Br_2} and x_{Br} and write

$$p_{\text{Br}_2} = x_{\text{Br}_2} p; \quad p_{\text{Br}} = x_{\text{Br}} p \quad (5.23)$$

Insertion of these relations into the law of mass action (Eq. (5.17)) yields

$$K_2 = \frac{x_{\text{Br}}^2}{x_{\text{Br}_2}} \frac{p}{p^\ominus}, \quad (5.24)$$

which contains the two unknown mole fractions. To determine the latter, we need additional equations. The strategy is, as outlined in Sect. 5.1, to determine the equilibrium extent of reaction ξ^{eq} and then to re-express the mole fractions sought by ξ^{eq} . We have (see Eq. (5.2))

$$n_{\text{Br}_2} = n_{\text{Br}_2}^0 - \xi^{\text{eq}}, \quad n_{\text{Br}} = 0 + 2\xi^{\text{eq}} \quad (5.25)$$

where we exploit the information that initially only molecular bromine is present in the vessel with an amount $n_{\text{Br}_2}^0$. Using the definition of the mole fraction in Eq. (2.8) we can write

$$x_{\text{Br}} = \frac{n_{\text{Br}}}{n_{\text{Br}} + n_{\text{Br}_2}} = \frac{2\xi^{\text{eq}}}{n_{\text{Br}_2}^0 + \xi^{\text{eq}}}; \quad x_{\text{Br}_2} = \frac{n_{\text{Br}_2}^0 - \xi^{\text{eq}}}{n_{\text{Br}_2}^0 + \xi^{\text{eq}}} \quad (5.26)$$

If we insert these expressions in Eq. (5.24), we obtain

$$K_2 = \frac{4\xi^{\text{eq}2}}{(n_{\text{Br}_2}^0 + \xi^{\text{eq}})^2} \frac{n_{\text{Br}_2}^0 + \xi^{\text{eq}}}{n_{\text{Br}_2}^0 - \xi^{\text{eq}}} \frac{p}{p^\ominus} \quad (5.27)$$

The latter equation can be simplified using the third binomial formula (Eq. (A.3)):

$$K_2 = \frac{4\xi^{\text{eq}2}}{n_{\text{Br}_2}^{0^2} - \xi^{\text{eq}2}} \frac{p}{p^\ominus} \quad (5.28)$$

This is an equation with only one unknown, ξ^{eq} . We can solve for ξ^{eq} and obtain

$$\xi^{\text{eq}} = n_{\text{Br}_2}^0 \sqrt{\frac{1}{\frac{4p}{K_2 p^\ominus} + 1}} = 0.7612 \times n_{\text{Br}_2}^0 \quad (5.29)$$

With the value of K_2 from subproblem (b) and $p^\ominus = 100,000 \text{ Pa}$ the root takes the value 0.7612. If we finally reinsert this result into the above expressions for the mole fractions Eq. (5.26), we obtain

$$x_{\text{Br}} = \frac{2 \times 0.7612}{1 + 0.7612} = 0.8644; \quad x_{\text{Br}_2} = \frac{1 - 0.7612}{1 + 0.7612} = 0.1356 \quad (5.30)$$

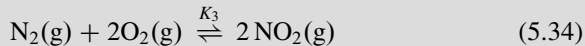
The partial pressure of atomic bromine is thus $p_{\text{Br}} = x_{\text{Br}} p = 8.6 \text{ mbar}$, and the partial pressure of Br_2 is 1.4 mbar, accordingly. Hence, 86% of the particles in the vessel are atomic bromine, whereas only 14% of the particles are Br_2 molecules.

Subproblem (d) deals with the question how the mole fraction of atomic bromine can be further increased. Concerning temperature, our results of subproblem (b) provide a clear answer: if we further increase the temperature, the equilibrium constant further increases because of the endothermic nature of the dissociation reaction, and hence the fraction of bromine atoms then increases further. But what about total pressure? Let us check the results of subproblem (c): the fraction of bromine is increased if the equilibrium extent of reaction ξ^{eq} is increased. We therefore analyze Eq. (5.29):

$$\lim_{p \rightarrow 0} \xi^{\text{eq}} = n_{\text{Br}_2}^0 \lim_{p \rightarrow 0} \sqrt{\frac{1}{\frac{4p}{K_2 p^\ominus} + 1}} = n_{\text{Br}_2}^0 \quad (5.31)$$

At the limit of vanishing total pressure *all* bromine molecules dissociate. Reduction of total pressure thus increases the fraction of bromine atoms. As a consequence, we should operate the effusion source for atomic bromine at a high temperature and low total pressure.

Problem 5.2 (Equilibrium in Parallel Reactions I) Oxides of nitrogen are trace gases in the atmosphere with anthropogenic and natural sources. Consider the chemical equilibrium between NO , NO_2 with the main components of clean air:



- Show that $K_3 = K_1 \times K_2$.
- Clean air normally contains 78% N_2 and 21% O_2 . Calculate the mole fraction and the concentration of NO and NO_2 in clean air (total pressure 100,000 Pa, 298.15 K), assuming conditions of chemical equilibrium and $K_1 = 1.69 \times 10^{12}$, $K_2 = 4.2 \times 10^{-32}$.

Solution 5.2 This problem deals with nitrogen oxide, NO_x . These molecules occur as trace gases in the atmosphere. Although atmospheric processes, strictly speaking, never reach a state of equilibrium, we may ask if the observed abundance of these trace gases is roughly in accordance with the prediction from the law of mass action. For simplicity, only the molecules NO and NO_2 are considered. The reaction laws

Eqs. (5.33) and (5.34) describe the formation of these oxides from the elements N₂ and O₂ in their standard states. Equation (5.32) describes the conversion of NO into NO₂ and vice versa. If we consider the chemical equilibrium for each of these parallel reactions, there must be relations among the equilibrium constants. In **subproblem (a)** we show that $K_3 = K_1 \times K_2$. We write down the law of mass action for each of these reactions and assume perfect gas behavior:

$$K_1 = \frac{\left(\frac{p_{\text{NO}_2}}{p^\ominus}\right)^2}{\left(\frac{p_{\text{NO}}}{p^\ominus}\right)^2 \frac{p_{\text{O}_2}}{p^\ominus}}; \quad K_2 = \frac{\left(\frac{p_{\text{NO}}}{p^\ominus}\right)^2}{\frac{p_{\text{N}_2}}{p^\ominus} \frac{p_{\text{O}_2}}{p^\ominus}}; \quad K_3 = \frac{\left(\frac{p_{\text{NO}_2}}{p^\ominus}\right)^2}{\frac{p_{\text{N}_2}}{p^\ominus} \left(\frac{p_{\text{O}_2}}{p^\ominus}\right)^2} \quad (5.35)$$

Therefore,

$$K_1 \times K_2 = \frac{\left(\frac{p_{\text{NO}_2}}{p^\ominus}\right)^2}{\left(\frac{p_{\text{NO}}}{p^\ominus}\right)^2 \frac{p_{\text{O}_2}}{p^\ominus}} \times \frac{\left(\frac{p_{\text{NO}}}{p^\ominus}\right)^2}{\frac{p_{\text{N}_2}}{p^\ominus} \frac{p_{\text{O}_2}}{p^\ominus}} = \frac{\left(\frac{p_{\text{NO}_2}}{p^\ominus}\right)^2}{\frac{p_{\text{N}_2}}{p^\ominus} \left(\frac{p_{\text{O}_2}}{p^\ominus}\right)^2} = K_3. \quad (5.36)$$

In **subproblem (b)**, we consider clean air with mole fractions $x_{\text{N}_2} = 0.78$ and $x_{\text{O}_2} = 0.21$. We determine the mole fractions and concentrations of NO and NO₂. We introduce the mole fractions using its definition in Chap. 2, Eq. (2.8), and the fact that under standard conditions the total pressure of air is simply the standard pressure:

$$x_i \stackrel{\text{Eq. (2.8)}}{=} \frac{n_i}{n_{\text{total}}} = \frac{p_i}{p_{\text{total}}} \stackrel{p_{\text{total}} = p^\ominus}{=} \frac{p_i}{p^\ominus} \quad (5.37)$$

Hence, the laws of mass action can be expressed in terms of mole fractions:

$$K_1 = \frac{x_{\text{NO}_2}^2}{x_{\text{NO}}^2 \cdot x_{\text{O}_2}}; \quad K_2 = \frac{x_{\text{NO}}^2}{x_{\text{N}_2} \cdot x_{\text{O}_2}}; \quad K_3 = \frac{x_{\text{NO}_2}^2}{x_{\text{N}_2} \cdot x_{\text{O}_2}^2} \quad (5.38)$$

In the next step, we notice a considerable simplification of the problem if we recognize that there is excess nitrogen and oxygen. Hence, their mole fractions can thus be assumed to be constant. Therefore, x_{NO_2} and x_{NO} are best calculated using K_2 and K_3 :

$$x_{\text{NO}} = \sqrt{K_2 x_{\text{N}_2} x_{\text{O}_2}} = \sqrt{4.2 \times 10^{-32} \times 0.78 \times 0.21} = 8.3 \times 10^{-17} \quad (5.39)$$

and

$$x_{\text{NO}_2} = \sqrt{K_3 x_{\text{N}_2} x_{\text{O}_2}^2} = \sqrt{7.1 \times 10^{-20} \times 0.78 \times 0.21^2} = 4.9 \times 10^{-11}. \quad (5.40)$$

Here, we have used the relation $K_3 = K_1 \times K_2$ shown in subproblem (a). Finally, we calculate concentrations. Using the equation of state for a perfect gas

(Eq. (2.12)), the definition of concentration (Eq. (2.9)), and Eq. (5.37), we obtain

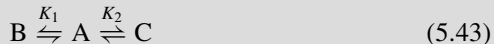
$$c_{\text{NO}} = \frac{p^\ominus}{RT} x_{\text{NO}} = 3.3 \times 10^{-15} \text{ mol m}^{-3} \quad (5.41)$$

and

$$c_{\text{NO}_2} = \frac{p^\ominus}{RT} x_{\text{NO}_2} = 2.0 \times 10^{-9} \text{ mol m}^{-3} \quad (5.42)$$

The long-term concentration of NO_2 in the USA at the beginning of the twenty-first century⁶ is about 50 ppb, ($1 \text{ ppb} = 10^{-9}$). Hence, our result for nitrogen dioxide underestimates the real concentration by a factor of 25.

Problem 5.3 (Equilibrium in Parallel Reactions II) Consider the chemical equilibrium of a molecule that occurs in three different conformers, A, B, and C:



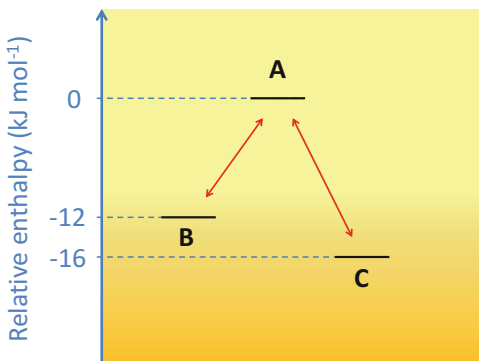
The molar heats of reaction of $\text{A} \rightarrow \text{B}$ and $\text{A} \rightarrow \text{C}$ are -12 , and -16 kJ mol^{-1} respectively (see Fig. 5.3). For simplicity, assume that entropy differences between the conformers are negligible. Ignore all possible intermolecular interactions.

- Write down the laws of mass action for both reactions and calculate the equilibrium constants both for room temperature (T_1) and for $T_2 = 700 \text{ K}$.
- Derive expressions for the mole fractions of each the three conformers in chemical equilibrium. Calculate x_A , x_B , and x_C for both temperatures T_1 and T_2 . Under which condition is the abundance of the intermediate conformer A insignificantly small?

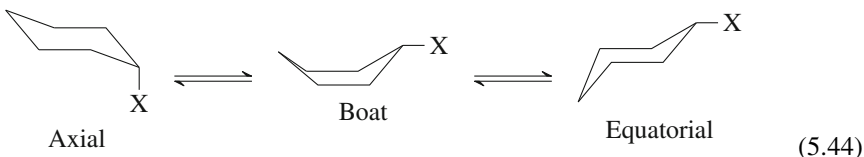
Solution 5.3 In Problem 5.2 we have dealt with a set of parallel reactions, in which equilibrium abundances of all substances could be easily calculated because there were excess amounts of several reactants. This led to a decoupling of the problem. But how do we proceed in the general case of coupled parallel reactions? In this

⁶According to the United States Environmental Protection Agency (<http://www.epa.gov>).

Fig. 5.3 Relative enthalpies of the three different conformers A, B, and C



problem, we shall consider three conformers A, B, and C of one substance in chemical equilibrium. An example could be a monosubstituted cyclohexane:



The molecule has two different stable chair conformations. In the axial conformation, the substituent group X is oriented perpendicularly with regard to the *seat* of the chair, whereas in the equatorial conformation, X is within this plane. Both geometries have a slightly different total energy. A transition from the axial into the equatorial conformation is caused by an internal *flipping* of the molecule into its energetically less favorable boat configuration. This brings the group X into the equatorial position. Then, by a second flipping at the opposite end, the molecule comes back into the equatorial chair position.

In **subproblem (a)**, we write down the laws of mass action and calculate equilibrium constants for both reactions. We use the amounts of substances n_A , n_B , and n_C to characterize the equilibrium:

$$K_1 = \frac{n_B}{n_A}; \quad K_2 = \frac{n_C}{n_A} \quad (5.45)$$

If the molar entropies of A, B, and C are equal, the molar reaction entropy is zero and thus the molar Gibbs free energies of reaction are $\Delta g_1 = \Delta h_1 = -12 \text{ kJ mol}^{-1}$ and $\Delta g_2 = \Delta h_2 = -16 \text{ kJ mol}^{-1}$ respectively. The room temperature equilibrium constants are thus:

$$K_1(T_1) = \exp\left(-\frac{\Delta g_1}{RT_1}\right) = 126.56 \quad (5.46)$$

and

$$K_2(T_1) = \exp\left(-\frac{\Delta g_2}{RT_1}\right) = 635.43. \quad (5.47)$$

Equilibrium constants at $T_2 = 700\text{ K}$ are calculated using Eq. (5.10). We obtain

$$\ln K_1(T_2) = \ln K_1(T_1) - \frac{\Delta h_1}{R} \left(\frac{1}{T_2} - \frac{1}{T_1} \right) = 4.841 - 2.779 = 2.062 \quad (5.48)$$

and thus $K_1(T_2) = 7.86$. In the same way, we obtain $K_2(T_2) = 15.63$.

In **subproblem (b)**, we seek formulas predicting the abundances of the three conformers in chemical equilibrium. We assume that initially, all molecules are present in the conformer A with an amount n_A^0 . Because A undergoes two different types of chemical reactions, we generalize Eq. (5.2) by introducing two different numbers, ξ_1 and ξ_2 , representing the extent of reaction in these two reaction channels. Hence, in chemical equilibrium, the amounts of the conformers are:

$$n_A = n_A^0 - \xi_1^{\text{eq}} - \xi_2^{\text{eq}}; \quad n_B = \xi_1^{\text{eq}}; \quad n_C = \xi_2^{\text{eq}} \quad (5.49)$$

Insertion of these expressions in Eq. (5.45) yields

$$K_1 = \frac{\xi_1^{\text{eq}}}{n_A^0 - \xi_1^{\text{eq}} - \xi_2^{\text{eq}}}; \quad K_2 = \frac{\xi_2^{\text{eq}}}{n_A^0 - \xi_1^{\text{eq}} - \xi_2^{\text{eq}}} \quad (5.50)$$

These two equations can be rearranged in a system of equation $\mathbf{A} \boldsymbol{\xi} = \mathbf{y}$ with \mathbf{A} being a 2×2 matrix:

$$\begin{pmatrix} K_1 + 1 & K_1 \\ K_2 & K_2 + 1 \end{pmatrix} \begin{pmatrix} \xi_1^{\text{eq}} \\ \xi_2^{\text{eq}} \end{pmatrix} = \begin{pmatrix} K_1 n_A^0 \\ K_2 n_A^0 \end{pmatrix} \quad (5.51)$$

We use Cramer's rule (see Appendix Sect. A.3.17) to solve this system. By evaluating the determinant of the coefficient matrix \mathbf{A} and the determinants of \mathbf{A}_1 and \mathbf{A}_2 with the first and second columns replaced by the 'vector' \mathbf{y} ,

$$\det \mathbf{A} = \begin{vmatrix} K_1 + 1 & K_1 \\ K_2 & K_2 + 1 \end{vmatrix} = K_1 + K_2 + 1 \quad (5.52)$$

$$\det \mathbf{A}_1 = \begin{vmatrix} K_1 n_A^0 & K_1 \\ K_2 n_A^0 & K_2 + 1 \end{vmatrix} = K_1 n_A^0 \quad (5.53)$$

$$\det \mathbf{A}_2 = \begin{vmatrix} K_1 + 1 & K_1 n_A^0 \\ K_2 & K_2 n_A^0 \end{vmatrix} = K_2 n_A^0 \quad (5.54)$$

we obtain the solutions

$$\xi_1^{\text{eq}} = \frac{\det \mathbf{A}_1}{\det \mathbf{A}} = \frac{K_1}{K_1 + K_2 + 1} n_A^0 \quad (5.55)$$

and

$$\xi_2^{\text{eq}} = \frac{\det \mathbf{A}_2}{\det \mathbf{A}} = \frac{K_2}{K_1 + K_2 + 1} n_A^0 \quad (5.56)$$

Insertion of these results into Eq. (5.50) yields the amounts of the three conformers. Recognizing that the total amount of the substance is always n_A^0 , we can compute the mole fractions sought:

$$x_A = \frac{n_A}{n_A^0} = \frac{1}{K_1 + K_2 + 1} \quad (5.57)$$

$$x_B = \frac{n_B}{n_A^0} = \frac{K_1}{K_1 + K_2 + 1} \quad (5.58)$$

$$x_C = \frac{n_C}{n_A^0} = \frac{K_2}{K_1 + K_2 + 1} \quad (5.59)$$

Using these formulae and the above calculated values for the equilibrium constants K_1 and K_2 , the mole fractions for both temperatures can be determined. These are given in Table 5.1.

At 298 K only about one in a thousand molecules has the A conformation, and 83% of the molecules are B conformers. If the temperature is raised to 700 K, however, even conformer A, with the highest Gibbs free energy, has a notable abundance. Asked about the criterion when the abundance of this conformer is insignificantly small we refer to Eqs. (5.57)–(5.59): x_A becomes negligible over x_B and x_C if in the denominator $K_1 + K_2 \gg 1$. In this case, conformer A serves only as a *transition state* between the energetically more favorable conformers B and C. The problem then simplifies and can be treated as an equilibrium problem of the type $B \rightleftharpoons C$. Note also that the condition $K_1 + K_2 \gg 1$ is better met at room temperature than at T_2 .

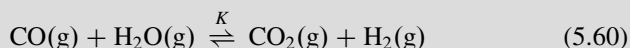
Table 5.1 Mole fractions of the three conformers A, B, and C in chemical equilibrium at 298 and at 700 K

Temperature (K)	x_A	x_B	x_C
298	0.0013	0.1659	0.8328
700	0.0408	0.3209	0.6382

Table 5.2 Standard molar heats of formation and standard Gibbs free energy of formation of some compounds at 298.15 K

Molecule	Δh_f^\ominus (kJ mol ⁻¹)	Δg_f^\ominus (kJ mol ⁻¹)
CO(g)	-110.5	-137.2
CO ₂ (g)	-393.5	-394.4
H ₂ (g)	0	0
H ₂ O(g)	-241.8	-228.6

Problem 5.4 (Water-Gas Shift Reaction) The water-gas shift reaction



is widely used to reduce the content of carbon monoxide in hydrogen gas.

- Write down the law of mass action for the given reaction. From thermochemical data found in Table 5.2, calculate the equilibrium constants at 298.15 and at 400 K. Does a catalyst influence the chemical equilibrium?
- A reactor contains a mixture of CO and H₂ with an initial proportion $n_{\text{CO}}^0:n_{\text{H}_2}^0 = 0.1:0.9$. Then, H₂O(g) is added at a temperature of 400 K and the chemical equilibrium is established. Calculate the initial proportion $n_{\text{H}_2\text{O}}^0:n_{\text{H}_2}^0$ necessary to reduce the equilibrium proportion $n_{\text{CO}}^{\text{eq}}:n_{\text{H}_2}^{\text{eq}}$ to 0.01:0.99.

Solution 5.4 Some examination problems for chemical equilibrium require the consideration of *extra* constraints apart from the law of mass action and the set of equations given in Eq. (5.2). Such an extra constraint may be the request for a special composition of the system in the state of equilibrium. In this case, the obvious task is to determine the initial composition of the system. This problem offers an example in which we deal with the water gas shift reaction Eq. (5.60), which is used in industrial scale production of high purity syngas⁷. In **subproblem (a)** we write down the law of mass action using partial pressures:

$$K = \exp\left(-\frac{\Delta g_r^\ominus}{RT}\right) = \frac{\frac{p_{\text{CO}_2}}{p^\ominus} \frac{p_{\text{H}_2}}{p^\ominus}}{\frac{p_{\text{CO}}}{p^\ominus} \frac{p_{\text{H}_2\text{O}}}{p^\ominus}} = \frac{p_{\text{CO}_2} p_{\text{H}_2}}{p_{\text{CO}} p_{\text{H}_2\text{O}}} \quad (5.61)$$

⁷Syngas or synthesis gas is a mixture of hydrogen and carbon monoxide.

Now, we determine the equilibrium constant from the thermochemical data in Table 5.2. The standard molar heat of reaction is:

$$\begin{aligned}\Delta h_r^\ominus &= \sum_i v_i \Delta h_f^\ominus(i) = \Delta h_f^\ominus(\text{CO}_2) + \Delta h_f^\ominus(\text{H}_2) - \Delta h_f^\ominus(\text{CO}) - \Delta h_f^\ominus(\text{H}_2\text{O}) \\ &= -41.2 \text{ kJ mol}^{-1}\end{aligned}\quad (5.62)$$

The standard molar Gibbs free energy of reaction is:

$$\begin{aligned}\Delta g_r^\ominus &= \sum_i v_i \Delta g_f^\ominus(i) = \Delta g_f^\ominus(\text{CO}_2) + \Delta g_f^\ominus(\text{H}_2) - \Delta g_f^\ominus(\text{CO}) - \Delta g_f^\ominus(\text{H}_2\text{O}) \\ &= -28.6 \text{ kJ mol}^{-1}\end{aligned}\quad (5.63)$$

Hence, the equilibrium constant at the reference temperature $T_1 = 298.15 \text{ K}$ is

$$K(T_1) = \exp\left(-\frac{\Delta g_r^\ominus}{RT}\right) = 102,443. \quad (5.64)$$

The equilibrium constant at $T_2 = 400 \text{ K}$ is calculated using Van't Hoff's reaction isobar (Eq. (5.10)):

$$\ln K(T_2) = \ln K(T_1) - \frac{\Delta h_r^\ominus}{R} \left(\frac{1}{T_2} - \frac{1}{T_1} \right) = 7.3053 \quad (5.65)$$

Hence, at 400 K the equilibrium constant is $K(T_2) = 1,488$ and thus considerably smaller compared with the room temperature value. This is consistent with the fact that the water gas shift reaction is exothermic. Like many reactions of high technical relevance, the water gas shift reaction is conducted on the surface of a catalyst. We answer the question, does a catalyst influence the equilibrium, with a no. The Gibbs free energy of reaction, from which the equilibrium constant is calculated, does not depend on the reaction pathway. The presence and the nature of the catalyst only influence reaction rates, and not the composition of the system in chemical equilibrium.

In **subproblem (b)**, we determine how much water vapor needs to be added to a 0.1:0.9 mixture of CO and H₂ to achieve a reduction of the CO content to 1% as the equilibrium is established. We first define the initial ratio

$$R_0 = \frac{n_{\text{CO}}^0}{n_{\text{H}_2}^0} = \frac{1}{9} \quad (5.66)$$

expressed by unknown initial amounts n_{CO}^0 and $n_{\text{H}_2}^0$, which are not given. Do we need to know them? No, because, with regard to the composition, it should not matter if we are dealing with 1 mol or with 100 t of gas mixture. In the same way, we define

the equilibrium ratio

$$R_{\text{eq}} = \frac{n_{\text{CO}}^{\text{eq}}}{n_{\text{H}_2}^{\text{eq}}} = \frac{1}{99} \quad (5.67)$$

Finally, we define a third ratio

$$R_x = \frac{n_{\text{H}_2\text{O}}^0}{n_{\text{H}_2}^0} \quad (5.68)$$

It is the initial ratio of water vapor and hydrogen sought. Now, we introduce the equilibrium extent of reaction ξ^{eq} . Using Eq. (5.2) and recognizing that initially there is no carbon dioxide present in the vessel, we write

$$n_{\text{H}_2}^{\text{eq}} = n_{\text{H}_2}^0 + \xi^{\text{eq}}; \quad n_{\text{CO}_2}^{\text{eq}} = \xi^{\text{eq}}; \quad n_{\text{H}_2\text{O}}^{\text{eq}} = n_{\text{H}_2\text{O}}^0 - \xi^{\text{eq}}; \quad n_{\text{CO}}^{\text{eq}} = n_{\text{CO}}^0 - \xi^{\text{eq}} \quad (5.69)$$

We insert these relations into Eq. (5.67) and obtain

$$R_{\text{eq}} = \frac{n_{\text{CO}}^0 - \xi^{\text{eq}}}{n_{\text{H}_2}^0 + \xi^{\text{eq}}} = \frac{R_0 n_{\text{H}_2}^0 - \xi^{\text{eq}}}{n_{\text{H}_2}^0 + \xi^{\text{eq}}} \quad (5.70)$$

Solving for ξ , we obtain, after some rearrangements:

$$\xi^{\text{eq}} = \frac{R_0 - R_{\text{eq}}}{R_{\text{eq}} + 1} n_{\text{H}_2}^0 \stackrel{\text{def}}{=} B n_{\text{H}_2}^0 = 0.1 \times n_{\text{H}_2}^0. \quad (5.71)$$

This equation relates the extent of the reaction to the quantities given and the unknown $n_{\text{H}_2}^0$. The next step is to exploit the law of mass action. We assume perfect gas behavior and therefore a proportionality of the partial pressure and amount of the substance. As a consequence,

$$K(T_2) = \frac{n_{\text{H}_2}^{\text{eq}} n_{\text{CO}_2}^{\text{eq}}}{n_{\text{H}_2\text{O}}^{\text{eq}} n_{\text{CO}}^{\text{eq}}} = \frac{\xi^{\text{eq}} (n_{\text{H}_2}^0 + \xi^{\text{eq}})}{(n_{\text{CO}}^0 - \xi^{\text{eq}}) (n_{\text{H}_2\text{O}}^0 - \xi^{\text{eq}})} = \frac{B n_{\text{H}_2}^0 (n_{\text{H}_2}^0 + B n_{\text{H}_2}^0)}{(n_{\text{CO}}^0 - B n_{\text{H}_2}^0) (n_{\text{H}_2\text{O}}^0 - B n_{\text{H}_2}^0)} \quad (5.72)$$

We recognize that we can factor out $n_{\text{H}_2}^0$ in numerator and denominator and obtain:

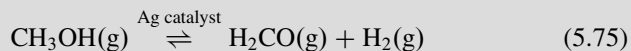
$$K(T_2) = \frac{B(1+B)}{(R_0 - B)(R_x - B)} \quad (5.73)$$

Apart from the sought ratio R_x , this equation only contains known quantities. Solving for R_x we obtain:

$$R_x = \frac{B(1+B)}{K(T_2)(R_0 - B)} + B = \frac{0.1 \times 1.1}{1488 \times (\frac{1}{9} - 0.1)} + 0.1 = 0.107 \quad (5.74)$$

About more than 10% water vapor has to be added to the gas mixture and nearly all the water is converted to hydrogen gas, whereas carbon monoxide is oxidized. Further analysis would show that greater purification, e.g., CO:H₂ = 1:999, would require a disproportionate addition of water ($B = 0.11$, $R_x = 0.18$) and subsequent removal of the excess water.

Problem 5.5 (Dehydrogenation of Methanol) Formaldehyde is produced on an industrial scale via the dehydrogenation of methanol on silver catalysts:



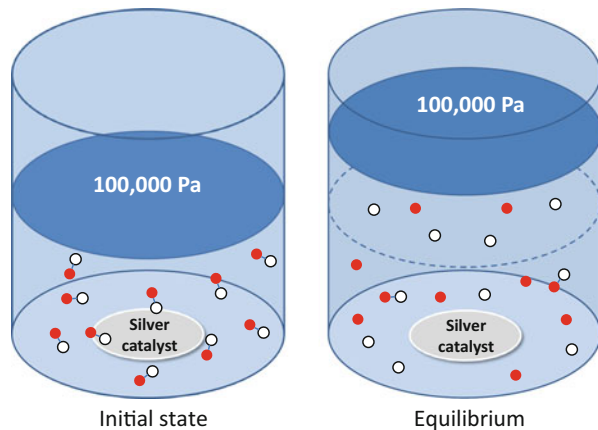
- Write down the law of mass action for the given reaction. Calculate the equilibrium constants at 298.15 and 920 K from the thermochemical data given in Table 5.3.
- At a temperature of 920 K, a reactor with a movable piston contains a silver catalyst and is filled at standard pressure with methanol. The initial volume of the reactor is 1 dm³. Then, the chemical equilibrium is established. Assume perfect gas behavior of reactants and products. Calculate the partial pressures of all gases in the state of chemical equilibrium and determine the work done by the piston. Is this process reversible?

Solution 5.5 Here, we have another problem of chemical equilibrium that requires the consideration of additional conditions. In this problem, the total pressure is constant, whereas the volume may change as the reaction proceeds. As we are dealing with a dissociation reaction where the number of molecules increases, we expect that the volume increases by an upward movement of the piston (see Fig. 5.4).

Table 5.3 Standard molar heats of formation and standard molar entropies of some compounds at 298.15 K

Molecule	Δh_f^\ominus (kJ mol ⁻¹)	s^\ominus (JK ⁻¹ mol ⁻¹)
CH ₃ OH(g)	-201.0	+239.9
H ₂ CO(g)	-108.6	+218.8
H ₂ (g)	0	+130.7

Fig. 5.4 Dissociation reaction at constant pressure



Thus, work is done during this process. The goal of **subproblem (a)** is to calculate the equilibrium constants from thermochemical data in Table 5.3. Here, standard heats of formation and standard entropies of the reactants and products are given. At the reference temperature $T_1 = 298.15\text{ K}$ the standard molar reaction enthalpy is:

$$\begin{aligned}\Delta h_r^\ominus &= \Delta h_f^\ominus(\text{H}_2\text{CO}) + \Delta h_f^\ominus(\text{H}_2) - \Delta h_f^\ominus(\text{CH}_3\text{OH}) \\ &= (-108.6 + 0 + 201.0)\text{ kJ mol}^{-1} = +92.4\text{ kJ mol}^{-1}\end{aligned}\quad (5.76)$$

The standard molar reaction enthalpy is:

$$\begin{aligned}\Delta s_r^\ominus &= s^\ominus(\text{H}_2\text{CO}) + s^\ominus(\text{H}_2) - s^\ominus(\text{CH}_3\text{OH}) \\ &= (+218.8 + 130.7 - 239.9)\text{ J K}^{-1}\text{ mol}^{-1} = +109.6\text{ J K}^{-1}\text{ mol}^{-1}\end{aligned}\quad (5.77)$$

The standard molar Gibbs free energy of reaction at this temperature is thus:

$$\Delta g_r^\ominus = \Delta h_r^\ominus - T_1 \Delta s_r^\ominus = +59.7\text{ kJ mol}^{-1}\quad (5.78)$$

Therefore, the reaction is endothermic, and also endergonic at this temperature, consistent with a very small equilibrium constant, which is:

$$K(T_1) = \exp\left(-\frac{\Delta g_r^\ominus}{RT_1}\right) = \exp(-24.11) = 3.38 \times 10^{-11}. \quad (5.79)$$

The equilibrium constant at the higher temperature $T_2 = 920\text{ K}$ is calculated using Eq. (5.10) under the assumption that Δh_r^\ominus is constant between T_1 and T_2 :

$$\ln K(T_2) = \ln K(T_1) - \frac{\Delta h_r^\ominus}{R} \left(\frac{1}{T_2} - \frac{1}{T_1} \right) = -24.11 + 25.21 = 1.10 \quad (5.80)$$

Hence, the equilibrium constant at 920 K is $K(T_2) = 3.01$ and the reaction is exergonic. For the calculation of the partial pressures in **subproblem (b)** we thus expect that most of the methanol is dissociated in the state of chemical equilibrium, whereas the volume of the reaction vessel is essentially filled with hydrogen and formaldehyde in equal amounts (see Fig. 5.4). Introducing the partial pressures p_F , p_H , p_M of formaldehyde, hydrogen, and methanol respectively, we write down the law of mass action for the reaction:

$$K(T_2) = \frac{\frac{p_F}{p^\ominus} \frac{p_H}{p^\ominus}}{\frac{p_M}{p^\ominus}} = \frac{n_F n_H}{n_M} \frac{RT_2}{p^\ominus} \quad (5.81)$$

Here, we have expressed partial pressures by the respective amounts of substances using the perfect gas equation of state. Following the basic procedure outlined above in Sect. 5.1, we write down the set of equations describing the change of the amounts of reactants and products (Eq. (5.2)). We take into account that at first only methanol, with an initial amount of n_M^0 , is present in the reactor, whereas the amounts of the products formaldehyde and hydrogen are zero:

$$n_M^{\text{eq}} = n_M^0 + \xi^{\text{eq}} \quad n_F^{\text{eq}} = \xi^{\text{eq}} \quad n_H^{\text{eq}} = \xi^{\text{eq}} \quad (5.82)$$

We calculate n_M^0 from the initial volume V^0 and pressure p^\ominus using the state of equation of a perfect gas:

$$n_M^0 = \frac{p^\ominus V^0}{RT_2} = 0.013 \text{ mol} \quad (5.83)$$

We recognize that not only the amounts of methanol, formaldehyde, and hydrogen depend on the extent of reaction, but also the volumes: because of Dalton's law of additivity of the partial pressures we can write:

$$p^\ominus = p_M + p_F + p_H = \frac{RT_2}{V} (n_M + n_F + n_H). \quad (5.84)$$

Solving for V we obtain:

$$V = \frac{RT_2}{p^\ominus} (n_M + n_F + n_H) \stackrel{\text{Eq. (5.82)}}{=} \frac{RT_2}{p^\ominus} (n_M^0 + \xi^{\text{eq}}). \quad (5.85)$$

Now, we insert the last equation and Eq.(5.82) into the law of mass action (Eq.(5.81)) and obtain:

$$K(T_2) = \frac{\xi^{\text{eq}2}}{(n_M^0 + \xi^{\text{eq}})(n_M^0 - \xi^{\text{eq}})} \stackrel{\text{Eq.(A.3)}}{=} \frac{\xi^{\text{eq}2}}{n_M^0{}^2 - \xi^{\text{eq}2}} \quad (5.86)$$

We can solve this equation for the extent of reaction:

$$\xi^{\text{eq}} = n_M^0 \sqrt{\frac{K(T_2)}{1 + K(T_2)}} = 0.011 \text{ mol} \quad (5.87)$$

Using Eq.(5.85) we calculate the volume in the state of equilibrium and obtain $V = 1.87 \times 10^{-3} \text{ m}^3$. At constant pressure the work is thus:

$$W = p^\ominus (V - V^0) = -87 \text{ J} \quad (5.88)$$

The partial pressure of hydrogen and formaldehyde is computed using the equation of state and the equilibrium amounts of these substances:

$$p_F = p_H \stackrel{\text{Eq.(5.82)}}{=} \xi^{\text{eq}} \frac{RT_2}{V} = 46,422 \text{ Pa.} \quad (5.89)$$

Methanol has an equilibrium partial pressure of:

$$p_M = (n_M^0 + \xi^{\text{eq}}) \frac{RT_2}{V} = 7157 \text{ Pa} \quad (5.90)$$

We can check our result by summing the partial pressures. Our results confirm our expectation that most of the methanol is converted to formaldehyde and hydrogen. Discussing the results in a seminar group, one of the students was astonished about the fact that work is done in this reaction, even though it is endothermic. Is this really a contradiction? What would you have answered? The last question of the problem is about reversibility. The process is irreversible. If a state of chemical equilibrium is reached, it cannot be reversed without changing the external conditions.

Problem 5.6 (Temperature Dependence of Equilibrium Constants) The often-made assumption of a constant heat of reaction leading to Van't Hoff's reaction isobar in the form of Eq.(5.10) is an approximation.

- Use Kirchhoff's law on the heat of reaction and derive an expression for the equilibrium constant at a temperature of T_2 if the equilibrium constant

(continued)

Table 5.4 Polynomial representation of constant pressure molar heat capacities of various gases, valid in the temperature range between 298 and 800 K

Molecule	a_0 (J K $^{-1}$ mol $^{-1}$)	a_1 (J K $^{-2}$ mol $^{-1}$)	a_2 (J K $^{-3}$ mol $^{-1}$)	a_3 (J K $^{-4}$ mol $^{-1}$)
CO(g)	31.08	-1.452×10^{-2}	3.1415×10^{-5}	-1.4973×10^{-8}
CO ₂ (g)	18.86	7.937×10^{-2}	-6.7834×10^{-5}	2.4426×10^{-8}
H ₂ (g)	22.66	4.381×10^{-2}	-1.0835×10^{-4}	1.1710×10^{-7}
H ₂ O(g)	33.80	-0.795×10^{-2}	2.8228×10^{-5}	-1.3115×10^{-8}

Problem 5.6 (continued)

- at a temperature of T_1 is given. Assume the constant pressure heat capacity in the form $c_p(T) = \sum_{k=0}^{\infty} a_k T^k$, valid in the interval between T_1 and T_2 .
- b. Consider the water-gas shift reaction (Eq. (5.60)). Use information from Problem 5.4 and the data given in Table 5.4 to calculate the equilibrium constant at various points in the temperature range between $T_1 = 298.15$ and 500 K. Compare with approximative results using Van't Hoff's reaction isobar Eq. (5.10) and thereby check the validity of the results in Problem 5.4.

Solution 5.6 As stated in Sect. 5.1.2, the assumption of a constant reaction enthalpy can be a crude approximation if larger temperature intervals are considered. In the concrete case of the water-gas shift reaction, we check the difference between an approximative and the more precise treatment. In **subproblem (a)**, the goal is the generalized form of the Van't Hoff reaction isobar with a temperature-dependent heat of reaction, $\Delta h_r(T)$. Integration of Eq. (5.9) yields:

$$\int_{K(T_1)}^{K(T_2)} d \ln K = \int_{T_1}^{T_2} \frac{\Delta h_r(T) dT}{RT^2}. \quad (5.91)$$

According to Kirchhoff's law (see Eq. (4.6), on page 73),

$$\Delta h_r(T) = \Delta h_r(T_1) + \int_{T_1}^T \Delta c_p(\tau) d\tau \quad (5.92)$$

where $\Delta h_r(T)$ is the value of the heat of reaction at the reference temperature T_1 , and $\Delta c_p(\tau) = \sum_i v_i c_{p,i}(\tau)$. The left side of Eq. (5.91) is easily integrated. Inserting Kirchhoff's law (Eq. (5.92)), we obtain:

$$\ln K(T_2) = \ln K(T_1) + \int_{T_1}^{T_2} \frac{\Delta h_r(T_1)}{RT^2} dT + \int_{T_1}^{T_2} \frac{1}{RT^2} \int_{T_1}^T \Delta c_p(\tau) d\tau dT \quad (5.93)$$

Using a polynomial representation of the molar heat $\Delta c_p(\tau) = \sum_k \Delta a_k \tau^k$ with $\Delta a_k = \sum_i \nu_i a_{k;i}$, we can write:

$$\ln K(T_2) = \ln K(T_1) + \frac{\Delta h_r(T_1)}{R} \int_{T_1}^{T_2} \frac{dT}{T^2} + \int_{T_1}^{T_2} \frac{dT}{RT^2} \sum_{k=0} \frac{\Delta a_k}{k+1} (T^{k+1} - T_1^{k+1}) \quad (5.94)$$

Sorting the terms with regard to the dependence on T , we obtain:

$$\begin{aligned} \ln K(T_2) &= \ln K(T_1) + \frac{[\Delta h_r(T_1) - \sum_{k=0} \frac{\Delta a_k}{k+1} T_1^{k+1}]}{R} \int_{T_1}^{T_2} \frac{dT}{T^2} \\ &\quad + \frac{\Delta a_0}{R} \int_{T_1}^{T_2} \frac{dT}{T} + \sum_{k=1} \frac{\Delta a_k}{(k+1)R} \int_{T_1}^{T_2} T^{k-1} dT \end{aligned} \quad (5.95)$$

The integrals are now evaluated using the integral table in the appendix (Sect. A.3.7):

$$\begin{aligned} \ln K(T_2) &= \ln K(T_1) - \frac{[\Delta h_r(T_1) - \sum_{k=0} \frac{\Delta a_k}{k+1} T_1^{k+1}]}{R} \left(\frac{1}{T_2} - \frac{1}{T_1} \right) \\ &\quad + \frac{\Delta a_0}{R} \ln \frac{T_2}{T_1} + \sum_{k=1} \frac{\Delta a_k}{k(k+1)R} (T_2^k - T_1^k) \end{aligned} \quad (5.96)$$

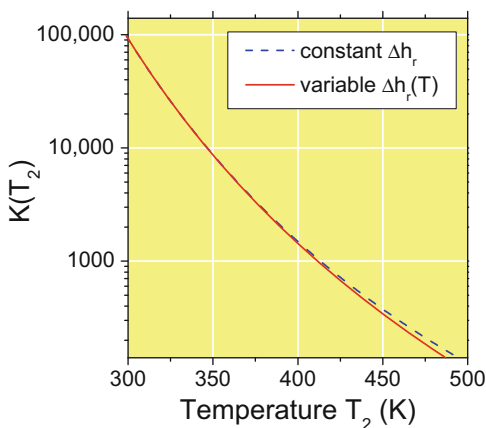
This is our generalized form for evaluating the equilibrium constant at a temperature of T_2 .

In **subproblem (b)**, we apply this equation to the water gas shift reaction already studied in Problem 5.4. At the reference temperature $T_1 = 298.15\text{ K}$, the equilibrium constant, obtained from thermochemical data, is $K(T_1) = 102,443$. The standard molar reaction enthalpy is $\Delta h_r(T_1) = -41.2\text{ kJ mol}^{-1}$. From the coefficients given in Table 5.4, we determine the quantities Δa_i , $i = 0, \dots, 3$, for the reaction $\text{CO} + \text{H}_2\text{O} \longrightarrow \text{CO}_2 + \text{H}_2$. We obtain

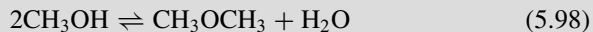
$$\Delta a_0 = (18.86 + 22.66 - 31.08 - 33.80)\text{ J K}^{-1}\text{ mol}^{-1} = -23.36\text{ J K}^{-1}\text{ mol}^{-1} \quad (5.97)$$

and, in the same way, $\Delta a_1 = 0.14565\text{ J K}^{-2}\text{ mol}^{-1}$, $\Delta a_2 = -2.35827 \times 10^{-4}\text{ J K}^{-3}\text{ mol}^{-1}$, and $\Delta a_3 = 1.69614 \times 10^{-7}\text{ J K}^{-4}\text{ mol}^{-1}$. Using Eq. (5.96), we can now calculate for arbitrary T_2 . The results are depicted in Fig. 5.5 (*solid line*). For comparison, the *dashed line* represents the value of the equilibrium constant according to Eq. (5.10). In particular, the corrected value of the equilibrium constant at 400 K is 1,433. The uncorrected value, used in Problem 5.4, is 1,488. Therefore, the systematic error in this case is about 4%. If the temperature intervals become larger, of course, the deviations become more significant.

Fig. 5.5 Equilibrium constant for the water gas shift reaction as a function of temperature. Note the logarithmic scaling



Problem 5.7 (Determination of Reaction Enthalpy and Reaction Entropy) Dimethyl ether ($\text{CH}_3\text{O-CH}_3$) is a possible replacement for diesel fuel. Dimethyl ether is produced from methanol using a suitable catalyst:



- a. Measurements of the equilibrium K constant as a function of temperature yield the following empirical law:

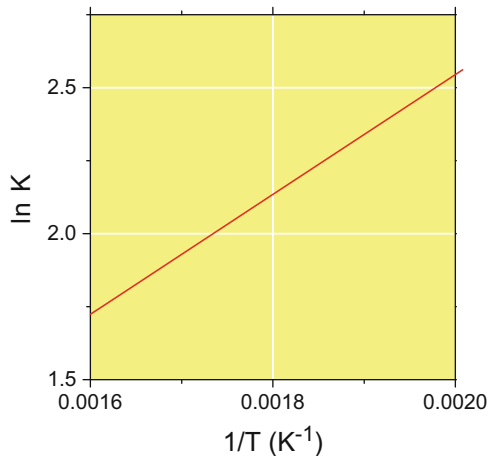
$$\ln K(T) = \frac{2051.7}{\frac{T}{\text{K}}} - 1.5587 \quad (5.99)$$

Determine the molar heat of reaction Δh_r and the reaction enthalpy Δs_r of the reaction. You may assume that both Δh_r and Δs_r are constant within the temperature range 498 to 623 K.

- b. 2 g methanol are filled in a vessel with a volume of 1 dm³. The vessel, containing a catalyst, is sealed and heated to 250°C and the chemical equilibrium is established according to Eq. (5.99). Calculate the equilibrium partial pressures of the gases assuming ideal behavior.

Solution 5.7 The measurement of equilibrium constants as a function of temperature is one way of determining reaction enthalpies and reaction entropies. The procedure is quite similar to the evaluation of the heat of vaporization and the entropy of vaporization discussed in Problem 3.10. In **subproblem (a)** we deal with the synthesis of dimethyl ether from methanol. Equation (5.99) is the empirical relationship between the equilibrium constant and temperature, fitted to experimental data. Usually, the logarithm of the measured equilibrium constant

Fig. 5.6 Graphical representation of Eq. (5.99) in the temperature range between 625 and 500 K



plotted against the reciprocal temperature exhibits a linear behavior, which is shown in Fig. 5.6, where we have plotted the function Eq. (5.99) in this way. The relation to Δh_r and Δs_r is established, taking into account the law of mass action Eq. (5.7),

$$K = \exp\left(-\frac{\Delta g_r}{RT}\right) \quad (5.100)$$

and, moreover, the relation:

$$\Delta g_r(T) = \Delta h_r - T\Delta s_r. \quad (5.101)$$

Hence,

$$\ln K = -\frac{\Delta h_r}{R} \frac{1}{T} + \frac{\Delta s_r}{R} \quad (5.102)$$

Comparison with Eq. (5.99) reveals

$$\Delta h_r = -R \times 2015.7 \text{ K} = -16.8 \text{ kJ mol}^{-1} \quad (5.103)$$

and

$$\Delta s_r = R \times (-1.5587) = +13.0 \text{ J K}^{-1} \text{ mol}^{-1} \quad (5.104)$$

In **subproblem (b)**, we shall calculate the partial pressures of dimethyl ether, water, and methanol in the state of chemical equilibrium at 523.15 K. Using Eq. (5.99), we calculate the equilibrium constant for this temperature and obtain $K(523.15 \text{ K}) = 10.624$. The following procedure is similar to our solution of Problem 5.5b. If p_D , p_W , and p_M are the equilibrium partial pressures of dimethyl ether, water, and

methanol respectively, the law of mass action is

$$K \stackrel{\text{Eq.(5.7)}}{=} \frac{p_D p_W}{p_M^2} = \frac{n_D n_W}{n_M^2}, \quad (5.105)$$

where n_D , n_W , and n_M are the amounts of substances. Introducing the equilibrium extent of reaction, ξ (we omit the superscript 'eq'), we can write:

$$n_M = n_M^0 - 2\xi; \quad n_D = n_W = \xi \quad (5.106)$$

where n_M^0 is the initial amount of methanol in the vessel. The molar mass of methanol is $M_M = 31.05 \text{ g mol}^{-1}$ and its initial mass is $m = 2 \text{ g}$. Thus, the initial amount is $n_M^0 = \frac{m}{M_M} = 0.0624 \text{ mol}$. We insert Eq. (5.106) into Eq. (5.105) and obtain the conditional equation for ξ :

$$K = \frac{\xi^2}{(n_M^0 - 2\xi)^2} = \frac{\xi^2}{n_M^{0\ 2} - 4n_M^0 \xi + 4\xi^2} \quad (5.107)$$

Solving for ξ we obtain a quadratic equation:

$$(4K - 1)\xi^2 - 4n_M^0 K \xi + K n_M^{0\ 2} = 0 \quad (5.108)$$

with the two solutions

$$\xi_{1,2} = \frac{4n_M^0 K \pm \sqrt{16n_M^{0\ 2} K^2 - 4(4K - 1)K n_M^{0\ 2}}}{2(4K - 1)} = n_M^0 \frac{2K \pm \sqrt{K}}{4K - 1} \quad (5.109)$$

The two solutions are $\xi_1 = 0.5906 \times n_M^0$ and $\xi_2 = 0.4335 \times n_M^0$. Here, we have to decide which of the two solutions is the correct one according to the problem. The decision is possible using Eq. (5.3), which poses the requirement that ξ leads to positive values for all reactants. Applied to our problem, where we have only one reactant,

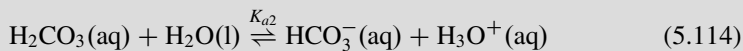
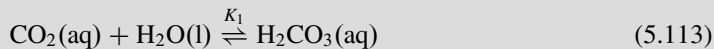
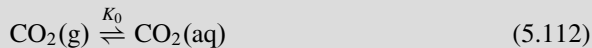
$$0 \leq \xi \leq \frac{n_M^0}{2} \quad (5.110)$$

Hence the first solution, ξ_1 , is rejected, and thus $\xi = 0.4335 \times n_M^0 = 0.0271 \text{ mol}$. With this result and Eq. (5.106), we obtain the equilibrium mole numbers of all substances $n_M = 0.0083 \text{ mol}$, $n_W = n_D = 0.02705 \text{ mol}$. With the equation of state and the given volume $V = 10^{-3} \text{ m}^{-3}$ the equilibrium partial pressures are

$$p_M = \frac{RT}{V} n_M = 36,103 \text{ Pa}; \quad p_W = p_D = 117,660 \text{ Pa} \quad (5.111)$$

It is advisable to insert these partial pressures again in Eq. (5.105) to test if our results are correct. The fraction $\frac{p_{\text{DPW}}}{p_{\text{M}}^2}$ is 10.621, in very good agreement with the equilibrium constant $K = 10.624$ on which our calculation was based. The small deviation is a contaminant from round-off errors during the calculation.

Problem 5.8 (A Simple Model of Acid Rain) A simple model of the acidity of rain water is based on the solution of atmospheric carbon dioxide in water:



Given that $K_0 = 1$, $K_1 = 3.0 \times 10^{-5} \text{ mol}^{-1}$, $K_{a2} = 2.5 \times 10^{-4} \text{ mol}^{-1}$, and a CO_2 concentration of $14.6 \mu\text{mol l}^{-1}$ in clean air, calculate the pH value of raindrops. Hint: autoprotolysis of water and the deprotonation of HCO_3^- can be ignored.

Solution 5.8 This simple application of the law of mass action deals with the acidity of rain water. Even in clean air—free from atmospheric trace gases such as SO_2 or NO_x —carbon dioxide is present and is thus dissolved in rain water forming carbonic acid (see Fig. 5.7). The equilibrium between gaseous CO_2 and dissolved CO_2 is described by the so-called Ostwald solubility coefficient, which we assume

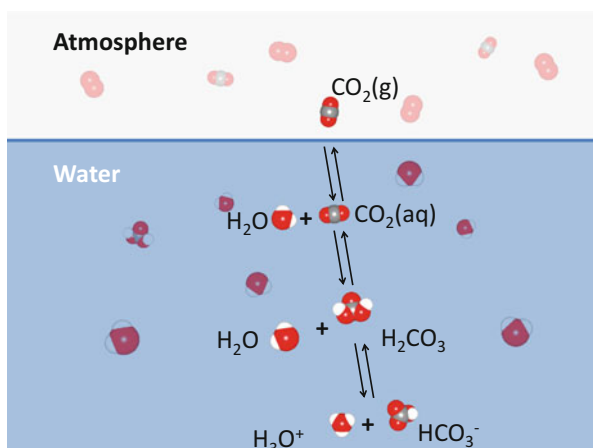


Fig. 5.7 Dissolution and dissociation of atmospheric CO_2 in water (schematic)

to be $K_0 = 1$. A fraction of the dissolved CO_2 reacts to carbonic acid, H_2CO_3 . After deprotonation HCO_3^- is formed (Eq. (5.112)), which causes the production of hydronium ions and thus a decrease in the pH value. For simplicity, we ignore the autoprotolysis of the solvent water and, moreover, the fact that additional H_3O^+ ions are formed by the reaction $\text{HCO}_3^-(\text{aq}) + \text{H}_2\text{O}(\text{l}) \rightleftharpoons \text{CO}_3^{2-}(\text{aq}) + \text{H}_3\text{O}^+(\text{aq})$. This is because the equilibrium constant for this reaction is orders of magnitude smaller than K_2 . We write down the law of mass action for the first reaction:

$$K_0 = \frac{c_{\text{CO}_2}^{\text{aq}}}{c_{\text{CO}_2}^g} \quad (5.115)$$

Here, $c_{\text{CO}_2}^g = 14.6 \mu\text{mol l}^{-1}$ is the given concentration of atmospheric CO_2 , and $c_{\text{CO}_2}^{\text{aq}}$ is the concentration of physically dissolved CO_2 in water. The law of mass action for the second equilibrium reaction is

$$K_1 = \frac{c_{\text{H}_2\text{CO}_3}}{c_{\text{CO}_2}^{\text{aq}} \cdot c_{\text{H}_2\text{O}}} \quad (5.116)$$

The dissociation of carbonic acid is characterized by the dissociation constant K_{a2} , which is defined above in Eq. (5.12) and is more commonly used to describe the dissociation of acids in dilute solutions:

$$K_{a2} = \frac{c_{\text{HCO}_3^-} \cdot c_{\text{H}_3\text{O}^+}}{c_{\text{H}_2\text{CO}_3}} \quad (5.117)$$

If we solve Eq. (5.115) for $c_{\text{CO}_2}^{\text{aq}}$ and insert this concentration into Eq. (5.116), we obtain

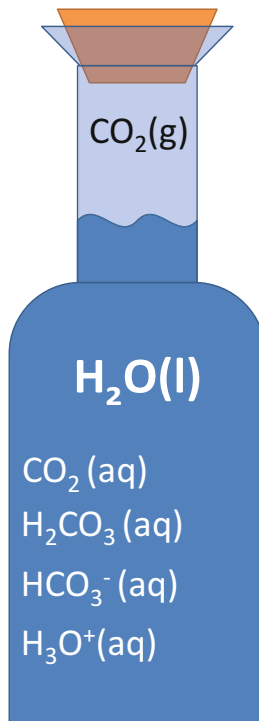
$$c_{\text{H}_2\text{CO}_3} = K_1 c_{\text{CO}_2}^{\text{aq}} c_{\text{H}_2\text{O}} = K_0 K_1 c_{\text{CO}_2}^g c_{\text{H}_2\text{O}} \quad (5.118)$$

Because no other acids are present (perfectly clean water) and autoprotolysis is ignored, $c_{\text{HCO}_3^-} = c_{\text{H}_3\text{O}^+}$. The concentration of the solvent water, which is largely in excess, is $c_{\text{H}_2\text{O}} = 55.555 \text{ mol l}^{-1}$. Therefore, insertion of Eq. (5.118) into Eq. (5.117) yields:

$$c_{\text{H}_3\text{O}^+} = \sqrt{K_0 K_1 K_{a2} c_{\text{CO}_2}^g c_{\text{H}_2\text{O}}} = 2.47 \times 10^{-6} \text{ mol l}^{-1} \quad (5.119)$$

With the definition of the pH value (Eq. (5.14)), we obtain $\text{pH} = 5.6$ for clean air rain water. Hence, because of the presence of atmospheric natural CO_2 , rain water is already acid. Recapitulating our method of solving this problem it is worth mentioning the following: in this problem the abundance of atmospheric CO_2 takes a constant value regardless of how much CO_2 is dissolved in water. Thus, the initial concentration and the equilibrium concentration of carbon dioxide are identical. The same is true for the concentration of water. Therefore, the calculation of $c_{\text{H}_3\text{O}^+}$ can

Fig. 5.8 Chemical equilibrium between gaseous and dissolved CO_2 in a sealed bottle of water



be carried out in a straightforward way. When deciding whether we have to balance floating concentrations using the concept of the extent of reaction (Eq.(5.2)) or whether it is justified to assume constant concentrations, the following question may also be helpful: is the system under consideration an *open system* or a *closed system*? In the present problem concerning atmospheric CO_2 we have an open system—the carbon dioxide of the entire atmosphere is in equilibrium with the dissolved carbon dioxide in a small rain drop. Now, consider the more complicated case of a sealed bottle of mineral water where the gas phase in the small volume between the water surface and the crown seal is in equilibrium with the dissolved gas (see Fig. 5.8). In this more complicated case, we have a closed system and we must distinguish between initial concentration and equilibrium concentration.

Problem 5.9 (CO_2 Dissolution in a Closed Bottle of Water) A sealed bottle with a total volume of 1 l contains 0.95 l of clean water (see Fig. 5.8). Initially, the gas phase between the water surface and the sealing contains carbon dioxide at a total pressure of 2 bar at room temperature. Then the chemical equilibrium according to Eq. (5.112) is established. Use the

(continued)

Problem 5.9 (continued)

values for the equilibrium constants given in Problem 5.8 and determine the concentrations of dissolved CO₂, H₂CO₃, and HCO₃⁻ along with the pH value of the water under the conditions of chemical equilibrium. Assume a density of water of 1 g cm⁻³ and the ideal behavior of gaseous carbon dioxide. *Hints:* You may ignore the autoprotolysis of the solvent water. It is assumed that you have already dealt with Problem 5.8.

Solution 5.9 This problem again picks up on the problem of carbon dioxide solvation in water (see Fig. 5.7). As stated in the discussion of the solution to Problem 5.8, the solvation of a finite amount of CO₂ in a closed system requires a treatment using floating concentrations, which is the method we must follow now. Moreover, it is a good idea to use a representation of the laws of mass action (Eqs. (5.115)–(5.117)) involving amounts of substances. With the volumes of the gas phase and the water, $v_g = 0.05\text{ l}$ and $v_l = 0.95\text{ l}$, we can introduce new equilibrium constants κ_0 , κ_1 , and κ_3 , and write:

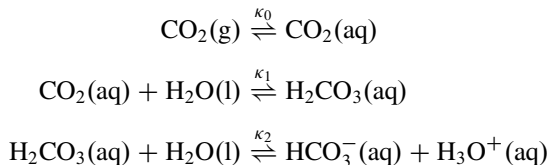
$$\kappa_0 = K_0 \frac{v_l}{v_g} = \frac{n_{\text{CO}_2}^{\text{aq}}}{n_{\text{CO}_2}^g}, \quad (5.120)$$

$$\kappa_1 = K_1 c_{\text{H}_2\text{O}} = \frac{n_{\text{H}_2\text{CO}_3}^{\text{aq}}}{n_{\text{CO}_2}^g}, \quad (5.121)$$

and

$$\kappa_2 = v_l K_{a2} = \frac{n_{\text{HCO}_3} n_{\text{H}_3\text{O}}}{n_{\text{H}_2\text{CO}_3}}, \quad (5.122)$$

where $\kappa_0 = K_0 \frac{0.95}{0.05} = 19$, $\kappa_1 = K_1 c_{\text{H}_2\text{O}} = 3.0 \times 10^{-5}\text{ mol}^{-1} \times 55.555\text{ mol l}^{-1} = 1.667 \times 10^{-3}$, and $\kappa_2 = v_l K_{a2} = 0.95 \times 2.5 \times 10^{-4}\text{ mol l}^{-1} = 2.375 \times 10^{-4}\text{ mol}$. The mole numbers in Eqs. (5.120)–(5.122) are understood to be equilibrium mole numbers. These depend on the equilibrium extents of reaction for



which simultaneously reach chemical equilibrium. Therefore, we introduce the equilibrium extents of reaction ξ_0 , ξ_1 , and ξ_2 associated with the equilibrium constants κ_0 , κ_1 , and κ_2 respectively. According to Eq. (5.2), we set up the equations

for the mole numbers as follows:

$$n_{\text{CO}_2}^g = n_{\text{CO}_2}^0 - \xi_0 \quad (5.123)$$

$$n_{\text{CO}_2}^{\text{aq}} = \xi_0 - \xi_1 \quad (5.124)$$

$$n_{\text{H}_2\text{CO}_3} = \xi_1 - \xi_2 \quad (5.125)$$

$$n_{\text{H}_3\text{O}} = n_{\text{HCO}_3} = \xi_2 \quad (5.126)$$

Here, $n_{\text{CO}_2}^0$ is the initial mole number of gaseous CO_2 , and we take into account the fact that all other substances have initial mole numbers of zero. Treating CO_2 as a perfect gas,

$$n_{\text{CO}_2}^0 = \frac{p^0 V_g}{RT} = \frac{2 \times 10^5 \text{ Pa} \times 0.05 \times 10^{-3} \text{ m}^3}{8.3145 \text{ J K}^{-1} \text{ mol}^{-1} \times 298 \text{ K}} = 4.034 \times 10^{-3} \text{ mol.} \quad (5.127)$$

In the next step, we insert Eqs. (5.123)–(5.126) into Eqs. (5.120)–(5.122) and obtain the following set of three equations for the three unknowns ξ_0 , ξ_1 , and ξ_2 :

$$\kappa_0 = \frac{\xi_0 - \xi_1}{n_{\text{CO}_2}^0 - \xi_0}; \quad \kappa_1 = \frac{\xi_1 - \xi_2}{\xi_0 - \xi_1}; \quad \kappa_2 = \frac{\xi_2^2}{\xi_1 - \xi_2} \quad (5.128)$$

The strategy is to eliminate two of the unknowns and obtain an equation for one extent of reaction. Therefore, we take the first equation and solve for ξ_0 :

$$\xi_0 = \frac{\kappa_0 n_{\text{CO}_2}^0 + \xi_1}{\kappa_0 + 1} \quad (5.129)$$

Insertion into the middle expression of Eq. (5.128) yields

$$\kappa_1 = \frac{\xi_1 - \xi_2}{\frac{\kappa_0 n_{\text{CO}_2}^0}{\kappa_0 + 1} + \left(\frac{1}{\kappa_0 + 1} - 1\right)\xi_1} = \frac{1}{A} \frac{\xi_1 - \xi_2}{n_{\text{CO}_2}^0 - \xi_1} \quad (5.130)$$

where we have defined $A = \frac{\kappa_0}{\kappa_0 + 1} = \frac{19}{20}$. We can solve Eq. (5.130) for ξ_1 and insert this into the third expression of Eq. (5.128):

$$\xi_1 = \frac{A \kappa_1 n_{\text{CO}_2}^0 + \xi_2}{1 + A \kappa_1} \quad (5.131)$$

$$\kappa_2 = \frac{\xi_2^2}{\frac{A \kappa_1 n_{\text{CO}_2}^0 + \xi_2}{1 + A \kappa_1} - \xi_2} \quad (5.132)$$

This expression can be written as a quadratic equation for ξ_2 ,

$$\xi_2^2 + C\xi_2 - Cn_{\text{CO}_2}^0 = 0; \quad C = \frac{A\kappa_1\kappa_2}{1 + A\kappa_1} = \frac{\kappa_0\kappa_1\kappa_2}{1 + \kappa_0(\kappa_1 + 1)} \quad (5.133)$$

We obtain the roots of the quadratic equation using Eq. (A.4) and obtain

$$\xi_{2;1,2} = \frac{-C \pm \sqrt{C^2 + 4Cn_{\text{CO}_2}^0}}{2} \quad (5.134)$$

As $C = 3.75447 \times 10^{-7}$ mol is positive, we can exclude the solution with the minus sign in front of the root. Hence,

$$\xi_2 = \frac{\sqrt{C^2 + 4Cn_{\text{CO}_2}^0} - C}{2} = 3.8730 \times 10^{-5} \text{ mol} \quad (5.135)$$

Having obtained this result, we use Eq. (5.131) and obtain $\xi_1 = 4.50471 \times 10^{-5}$ mol. Insertion of this result into Eq. (5.129) then yields $\xi_0 = 3.83455 \times 10^{-3}$ mol. Using Eqs. (5.123)–(5.126), we can now calculate all mole numbers:

$$n_{\text{CO}_2}^g = n_{\text{CO}_2}^0 - \xi_0 = 1.9945 \times 10^{-4} \text{ mol}$$

$$n_{\text{CO}_2}^{\text{aq}} = \xi_0 - \xi_1 = 3.789503 \times 10^{-3} \text{ mol}$$

$$n_{\text{H}_2\text{CO}_3} = \xi_1 - \xi_2 = 6.3171 \times 10^{-6} \text{ mol}$$

$$n_{\text{H}_3\text{O}} = n_{\text{HCO}_3} = \xi_2 = 3.7930 \times 10^{-5} \text{ mol}$$

As a consistency test we can add up all equilibrium mole numbers of CO₂ containing species and obtain $n_{\text{CO}_2}^g + n_{\text{CO}_2}^{\text{aq}} + n_{\text{H}_2\text{CO}_3} + n_{\text{HCO}_3} = 4.0340001 \times 10^{-3}$ mol, which, according to Eq. (5.127), is just the initial amount of gas phase CO₂. In addition, these mole numbers satisfy the three laws of mass action Eqs. (5.120), (5.121), and (5.122). If we inspect these data, we see that the dominant amount of CO₂ is physically dissolved as CO₂(aq), whereas only about 2×10^{-4} mol remain in the gas phase, which corresponds to an equilibrium pressure of only $p = \frac{n_{\text{CO}_2}^g RT}{V_g} = 9883 \text{ Pa}$ and a concentration of $c_{\text{CO}_2}^g = 3.99 \times 10^{-3} \text{ mol l}^{-1}$. The concentrations of the dissolved species are $c_{\text{CO}_2}^{\text{aq}} = 3.99 \times 10^{-3} \text{ mol l}^{-1}$, $c_{\text{H}_2\text{CO}_3} = 6.65 \times 10^{-6} \text{ mol l}^{-1}$, and $c_{\text{HCO}_3^-} = c_{\text{H}_3\text{O}^+} = 4.08 \times 10^{-5} \text{ mol l}^{-1}$. Hence, the pH value of the water under equilibrium conditions is 4.4.

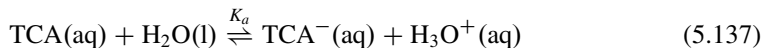
Problem 5.10 (Dissociation of Trichloroacetic Acid) Under normal conditions, trichloroacetic acid (TCA) forms crystals with a sharp odor. 5 g of TCA are dissolved in 1 dm³ perfectly clean water, and the dissociation equilibrium is established:



- The dissociation constant of the reaction is $K_a = 0.30$. Determine the equilibrium concentrations of dissociated and undissociated TCA, the pH value of the solution, and the degree of dissociation defined as $\alpha = \frac{c_{\text{TCA}^-}}{c_{\text{TCA}}^0}$, where c_{TCA^-} is the equilibrium concentration of dissociated TCA, and c_{TCA}^0 is the initial concentration of undissociated TCA.
- Show that the degree of dissociation reaches a value of 1 in the limit $c_{\text{TCA}}^0 \rightarrow 0$.

Hint: You may ignore the autoprotolysis of the solvent water.

Solution 5.10 This problem is a typical application of chemical equilibrium in dilute solutions (compare Sect. 5.1.3). Although strong acids such as HCl dissociate completely, a weak acid such as acetic acid (CH_3COOH) is only partially dissociated. In TCA, the hydrogens of the methyl group are replaced by the more electronegative chlorine, which affects the bonding in the carboxyl group. As a consequence, TCA has a higher dissociation constant than acetic acid. Given $K_a = 0.3$, we determine the equilibrium concentrations and the degree of dissociation of TCA in **subproblem (a)** according to the reaction:



Analogous to Eq. (5.12), we can write

$$K_a = \frac{c_{\text{TCA}^-} \cdot c_{\text{H}_3\text{O}^+}}{c_{\text{TCA}}} \quad (5.138)$$

We can assume that initially no H_3O^+ and TCA^- ions are present in the solution. Hence, $c_{\text{H}_3\text{O}^+}^0 = c_{\text{TCA}^-}^0 = 0$. To determine the initial concentration of TCA we have to consider its molar mass, $M_{\text{TCA}} = 163.38 \text{ g mol}^{-1}$. If $m = 5 \text{ g}$ of TCA are dissolved in 1 dm³ water, then $c_{\text{TCA}}^0 = \frac{5 \text{ g}}{163.38 \text{ g mol}^{-1} \cdot 1 \text{ dm}^3} = 0.0306 \text{ mol dm}^{-3}$. In the next step we have to set up the equations for the equilibrium concentrations

analogous to Eq. (5.2):

$$c_{\text{TCA}} = c_{\text{TCA}}^0 - \tilde{\xi} \quad (5.139)$$

$$c_{\text{TCA}^-} = c_{\text{H}_3\text{O}^+} = \tilde{\xi} \quad (5.140)$$

Note that the concentration of the solvent water is taken as a constant contained in the dissociation constant K_a . The concentration $\tilde{\xi} = \frac{\xi^{\text{eq}}}{1 \text{ dm}^3}$ is related to the equilibrium extent of reaction. Insertion of these equations into Eq. (5.138) yields

$$K_a = \frac{\tilde{\xi}^2}{c_{\text{TCA}}^0 - \tilde{\xi}} \quad (5.141)$$

If we solve for $\tilde{\xi}$ we obtain the quadratic equation

$$\tilde{\xi}^2 + K_a \tilde{\xi} - K_a c_{\text{TCA}}^0 = 0 \quad (5.142)$$

with the roots

$$\tilde{\xi}_{1,2} = \frac{\pm \sqrt{K_a^2 + 4K_a c_{\text{TCA}}^0} - K_a}{2} \quad (5.143)$$

The meaningful mathematical solution is the one that yields a positive concentration. Hence, we can exclude the solution with the negative sign in front of the square root and obtain

$$\tilde{\xi} = \frac{\sqrt{K_a^2 + 4K_a c_{\text{TCA}}^0} - K_a}{2} = 0.0280 \text{ mol dm}^{-3} \quad (5.144)$$

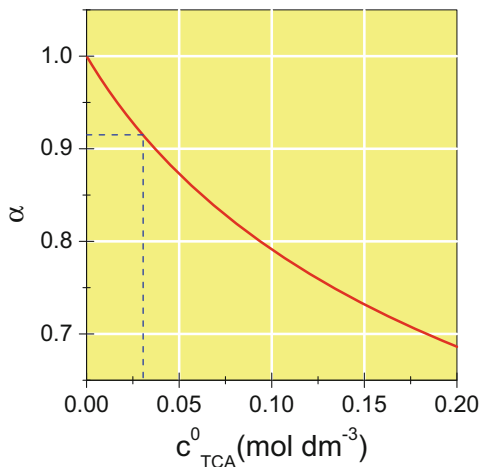
Reinserting this result into Eqs. (5.139) and (5.138) yields $c_{\text{TCA}^-} = c_{\text{H}_3\text{O}^+} = 0.028 \text{ mol dm}^{-3}$ and $c_{\text{TCA}} = 2.61 \times 10^{-3} \text{ mol dm}^{-3}$. Hence, the pH value of the solution is $\text{pH} = -\log_{10} c_{\text{H}_3\text{O}^+} = 1.6$. The degree of dissociation is

$$\alpha = \frac{c_{\text{TCA}^-}}{c_{\text{TCA}}^0} = \frac{0.0280}{0.0306} = 0.915. \quad (5.145)$$

Thus, more than 90% of the TCA is dissociated.

Moving to **subproblem (b)** we deal with the question of how the degree of dissociation is affected by the initial concentration of TCA; more precisely, we study the case $\alpha(c_{\text{TCA}}^0)$ as $c_{\text{TCA}}^0 \rightarrow 0$. We have already dealt with the analogous problem for a gas phase reaction in Problem 5.1. A superficial inspection of Eq. (5.144) shows that $\tilde{\xi} \rightarrow 0$ and thus $c_{\text{TCA}^-} \rightarrow 0$ in the limit $c_{\text{TCA}}^0 \rightarrow 0$. However, this

Fig. 5.9 Degree of dissociation of trichloroacetic acid as a function of initial concentration. The *dashed lines* indicate the situation treated in subproblem (a)



does not mean that the degree of dissociation reaches zero. We have to consider the

$$\lim_{c^0_{\text{TCA}} \rightarrow 0} \alpha = \lim_{c^0_{\text{TCA}} \rightarrow 0} \frac{\tilde{\xi}}{c^0_{\text{TCA}}} = \lim_{c^0_{\text{TCA}} \rightarrow 0} \frac{K_a}{2c^0_{\text{TCA}}} \left(\sqrt{1 + \frac{4c^0_{\text{TCA}}}{K_a}} - 1 \right) \quad (5.146)$$

Using the power series expansion of $\sqrt{1+x} = 1 + \frac{1}{2}x - \dots$ (see Eq. (A.59)), we obtain

$$\lim_{c^0_{\text{TCA}} \rightarrow 0} \alpha = \lim_{c^0_{\text{TCA}} \rightarrow 0} \frac{K_a}{2c^0_{\text{TCA}}} \left(1 + \frac{2c^0_{\text{TCA}}}{K_a} - 1 \right) = 1 \quad (5.147)$$

Thus, at the limit of infinite dilution of the acid, the degree of dissociation reaches a value of 1, which means that *all* TCA molecules are deprotonated. The limiting behavior of $\alpha(c^0_{\text{TCA}})$ is illustrated in Fig. 5.9.

Chapter 6

Chemical Kinetics

Abstract Reaction kinetics deals with the question how fast a chemical reaction proceeds. From a mathematical point of view, problems in reaction kinetics are formulated as rate equations, i.e., differential equations in time. In the limit $t \rightarrow \infty$ the results of reaction kinetics and thermodynamics (chemical equilibrium) must coincide. We consider this in detail in Problem 6.4. At the end of the chapter we deal with the fascinating field of autocatalysis and oscillating chemical reactions.

6.1 Basic Concepts

In the following it is assumed that the reader is familiar with stoichiometry (Chap. 2), especially the concept of the extent of reaction.

6.1.1 Reaction Rate

There is an obvious phenomenological definition of the reaction rate r based on the *change of extent of reaction with time*,

$$r = \frac{1}{V} \frac{d\xi}{dt} = \frac{1}{v_J} \frac{d[J]}{dt} \quad (6.1)$$

where $[J] = \frac{n_J}{V}$ is the concentration of species J in a given volume V . Hence, a reaction rate can be measured, for example, by observing the *decay* of the concentration of an educt. But how does the reaction rate depend on the conditions under which a reaction proceeds?

6.1.2 Reaction Rate Laws

Obviously, the reaction rate r depend on the educt concentrations. To classify chemical kinetics, it is common to consider a **rate law** and to introduce **reaction orders**¹:

$$r = k [J_1]^{\alpha_1} [J_2]^{\alpha_2} \dots \quad (6.2)$$

Here, k is the **rate constant**, and α_i is the order of the reaction with regard to educt J_i , the latter being present with the concentration $[J_i]$. The sum of the specific orders α_i is the **integral order** or simply the **order** of the reaction. It is important to realize that the coefficients α_i are *not* the stoichiometric numbers of the reaction. Only in the special case of an *elementary reaction* can the order be deduced by a simple inspection of the reaction. The determination of the reaction orders, either experimentally, or by deduction from a suitable *reaction mechanism*, is a frequent task of reaction kinetics.

If we combine the rate law Eq.(6.2) with Eq.(6.1) for one of the educts or products, we obtain a differential equation for the concentration of this species as a function of time, which may be solved by integration observing the initial conditions.

6.1.2.1 Elementary Reaction

In general, a chemical reaction has to be taken as a *net* reaction as the result of an underlying reaction mechanism. The latter can be further characterized by introducing the concept of elementary reaction. A reaction is called an elementary reaction if it occurs in a single step, i.e., it cannot be subdivided into further reaction steps.

6.1.2.2 Molecularity

What kinds of elementary reactions are possible? Fortunately, there are only three relevant types, differing in the number of educt molecules participating in the elementary reaction step. This number is called the molecularity of the reaction. Molecularity one is an **unimolecular reaction** $A \rightarrow \text{Products}$, which is a **decay reaction**. Molecularity two is called a **bimolecular reaction**, either of type $2A \rightarrow \text{Products}$, or the somewhat more complicated type $A + B \rightarrow \text{Products}$. Molecularity three is called a **termolecular reaction**, in its most general case

¹Note that there are cases where the most general form $r = kf([J_1], [J_2], \dots)$ is more appropriate.

$A + B + C \longrightarrow \text{Products}$. It is obvious that the probability of a simultaneous impact of three molecules is much smaller in comparison with a collision of only two molecules. However, depending on the number of product molecules, the laws of energy and momentum conservation sometimes require the presence of a third collision element. An elementary reaction of molecularity four, however, is so unlikely that we do not even have to consider it. Thus, a net chemical reaction may be mapped to only these few relevant types of elementary steps, and, of course, their variations.

6.1.2.3 Determination of the Reaction Order

Combining Eqs. (6.1) and (6.2), we obtain a differential equation, which can be integrated to determine the concentration of a certain educt or product as a function of time. By comparison with experimental data, a certain reaction order can be verified or falsified.

Another technique is the *analysis of initial reaction rate*, r_0 , as a function of the initial concentrations, $[J]_0$. From Eq. (6.1) we obtain:

$$\ln r_0 = \ln k + \alpha_1 \ln [J_1]_0 + \alpha_2 \ln [J_2]_0 + \dots \quad (6.3)$$

A plot of $\ln r_0$ against $\ln [J_1]_0$ should give a straight line with a slope α_1 . Thus, by means of systematic variation of the initial concentration of all educts, all reaction orders can be determined.

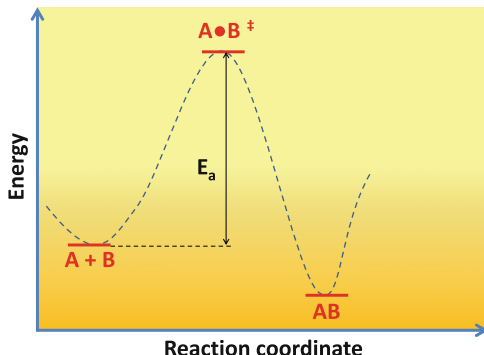
6.1.2.4 Temperature Dependence of the Rate Constant

The reaction rate typically increases with temperature, although sometimes, the opposite is observed. Phenomenologically, this temperature dependence is described by means of the temperature-dependent **rate constant** k (see Eq. (6.2)). The simplest approach is described by the **Arrhenius** equation,

$$k(T) = A \exp\left(-\frac{E_a}{RT}\right). \quad (6.4)$$

E_a is called the **energy of activation**, A is the **pre-exponential factor**. A frequent task is to determine the activation energy and the pre-exponential factor from experimental data. The determination of an activation energy within a reaction mechanism provides information about the *energy barrier* that has to be overcome for a certain reaction to occur. In theoretical terms, the energy barrier depends on the reaction path on the *potential energy surface* characterizing a reaction (see Fig. 6.1).

Fig. 6.1 Schematic illustration of a potential energy surface in one dimension for a hypothetical reaction $A + B \rightarrow AB$. E_a is the activation energy as the height of the energy barrier relative to the educts A and B. The maximum energy characterizes the *transition state* AB^\ddagger leading to bond formation



More general models consider an additional weak temperature dependence in the pre-exponential factor:

$$k(T) = AT^\beta \exp\left(-\frac{E_a}{RT}\right). \quad (6.5)$$

For example, a consideration of the number of collisions in a gas of two different species based on the kinetic theory of gases would predict² $\beta = \frac{1}{2}$ in Eq. (6.5).

6.2 Problems

Problem 6.1 (Reaction Order and Half Life)

- a. Consider the reaction $A \xrightarrow{k} P$ with the rate constant k . The initial concentration of the educt A is $c_A(0)$. If $\alpha > 1$ is the order of the reaction, show that the half-life is

$$t_{\frac{1}{2}} = \frac{2^{\alpha-1} - 1}{\alpha - 1} \frac{1}{k c_A(0)^{\alpha-1}} \quad (6.6)$$

- b. At an initial concentration of 1 mol dm^{-3} the half-life of the educt A was 200 s. When the initial concentration was doubled, the half-life reduced to 141 s. Determine the reaction order and the rate constant of the reaction.

²According to kinetic theory (Eq. (7.3)), the collision rate between N_A particles of a species A and N_B particles of species B at temperature T is $N_A N_B \sigma_{AB} \left(\frac{8k_B T}{\mu}\right)^{\frac{1}{2}}$ where σ_{AB} is the collision cross section and μ is the effective mass.

Solution 6.1 The half-life of an educt is the time after which its concentration decays to half of its initial value:

$$c_A(t_{\frac{1}{2}}) = \frac{1}{2}c_A(0) \quad (6.7)$$

In **subproblem (a)**, we shall prove the relationship between $t_{\frac{1}{2}}$, the rate constant, and the initial concentration $c_A(0)$ given by Eq. (6.6). This relation is valid if the order of the reaction α is greater than 1. The rate law (Eq. (6.2)) for this reaction is:

$$r = k c_A(t)^\alpha,$$

which, on the other hand, can be expressed by the change of c_A with time (Eq. (6.1)):

$$r = -\frac{dc_A(t)}{dt}$$

Thus, the differential equation describing the change in c_A is

$$-\frac{dc_A(t)}{dt} = k c_A(t)^\alpha \quad (6.8)$$

The separation of variables

$$\frac{dc_A}{c_A^\alpha} = -k dt$$

is followed by an integration step:

$$\int_{c_A(0)}^{c_A(t)} \frac{dc_A}{c_A^\alpha} = -k \int_0^t dt.$$

Using the integral table (Eq. (A.35)), we obtain:

$$\frac{1}{1-\alpha} [c_A^{1-\alpha}]_{c_A(0)}^{c_A(t)} = -k t$$

and thus

$$\frac{1}{\alpha - 1} \left(\frac{1}{c_A(t)^{\alpha-1}} - \frac{1}{c_A(0)^{\alpha-1}} \right) = k t.$$

Note that we could solve now for $c_A(t)$ and obtain the explicit expression for the concentration of the educt as a function of time, always provided that $\alpha > 1$, as stated above. In the next step, we use the definition of the half-life (Eq. (6.7)): after the time $t_{\frac{1}{2}}$, the concentration c_A has decayed to half of its initial value. Inserting this in the last expression, we obtain:

$$t_{\frac{1}{2}} = \frac{1}{k(\alpha - 1)} \left(\frac{1}{\frac{1}{2^{\alpha-1}} c_A(0)^{\alpha-1}} - \frac{1}{c_A(0)^{\alpha-1}} \right) = \frac{2^{\alpha-1} - 1}{k(\alpha - 1) c_A(0)^{\alpha-1}}$$

which is simply the maintained equation.

In **subproblem (b)**, we apply this equation to determine the reaction order α and also to rate constant k from the measurements of the half-life at two different initial concentrations. For $c_A(0) = 1 \text{ mol dm}^{-3}$ we have $t_{\frac{1}{2}} = 200 \text{ s}$. If the initial concentration is increased to $\tilde{c}_A(0) = 2 \text{ mol dm}^{-3}$, the reaction proceeds faster and $\tilde{t}_{\frac{1}{2}} = 141 \text{ s}$. The data pairs given are sufficient to determine α and k . However, the structure of Eq. (6.6) does not allow us to solve for α . The trick is to form the ratio of half-lives, which eliminates the unknown k :

$$\frac{t_{\frac{1}{2}}}{\tilde{t}_{\frac{1}{2}}} \stackrel{\text{Eq. (6.6)}}{=} \left(\frac{\tilde{c}_A(0)}{c_A(0)} \right)^{\alpha-1} = 2^{\alpha-1}$$

By considering the natural logarithm and the rules for logarithms (see appendix Sect. A.3.3), we can solve for α :

$$\alpha = 1 + \frac{\ln(t_{\frac{1}{2}}/\tilde{t}_{\frac{1}{2}})}{\ln 2} = 1 + \frac{\ln(200/141)}{\ln 2} = 1.504 \quad (6.9)$$

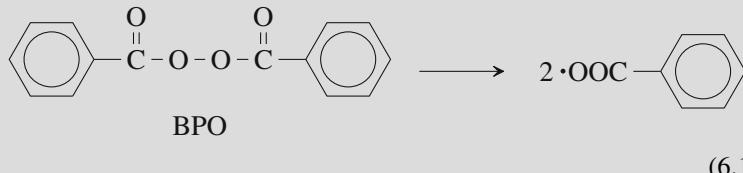
Hence, the sought reaction order is about $\frac{3}{2}$. Inserting this result into Eq. (6.7) together with one data pair enables us to solve for the rate constant k :

$$k = \frac{2^{\alpha-1} - 1}{t_{\frac{1}{2}}(\alpha - 1)c_A(0)^{\alpha-1}} = \frac{2^{\frac{1}{2}} - 1}{200 \text{ s} \times 1 \left(\text{mol dm}^{-3} \right)^{\frac{1}{2}}} \frac{1}{\left(\text{mol dm}^{-3} \right)^{\frac{1}{2}}}$$

Thus, the rate constant is $k = 4.13 \times 10^{-3} \text{ dm}^{\frac{3}{2}} \text{ mol}^{-\frac{1}{2}} \text{ s}^{-1}$. It is worth mentioning that the physical dimension of k always depends on the reaction order.

Problem 6.2 (First Order Decay)

Benzoyl peroxide (BPO) is an active pharmaceutical agent against acne. Its medical efficacy is based on the decay and the formation of benzyloxy radicals, which shall be assumed to follow first-order kinetics:



- a. In microcalorimetric experiments the rate constant of the above reaction was determined as a function of temperature (F. Zaman et al., Int. J. Pharm. **277**, 133 (2001).):

T ($^\circ\text{C}$)	20	25	30	35	40	45
k (10^{-9} s^{-1})	1.16	4.33	6.85	20.0	58.4	107.0

Determine the energy of activation and the pre-exponential factor assuming an Arrhenius law for the temperature dependence of the rate constant.

- b. A salve containing 10% by weight BPO was stored at a temperature of 25°C . Determine the mass fraction after a storage period of 60 days.
 c. A portion of 0.02 g of the salve is applied to the skin. If a temperature of the skin of 35°C is assumed, how many benzyloxy radicals are formed within a residence time of 2 h?

Solution 6.2 As temperature has an enormous impact on reaction rates (and other degradation processes), the room-temperature storage of pharmaceuticals may be an important issue. Here, we consider the stability of a typical radical former assuming first-order kinetics.

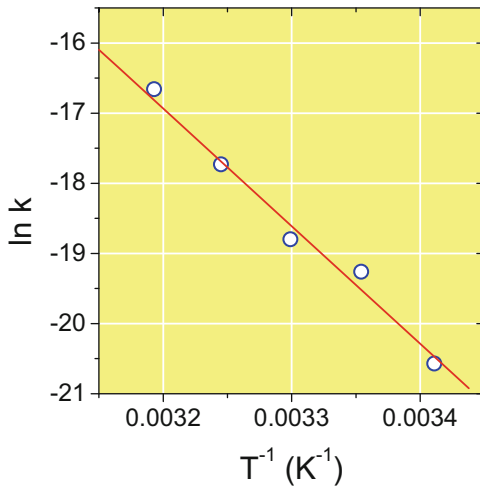
In **subproblem (a)**, we determine the energy of activation and the pre-exponential factor from a suitable plot of rate constants measured at different temperatures. Starting from the Arrhenius law Eq. (6.4), we interpret

$$\ln k = -\frac{E_a}{R} \frac{1}{T} + \ln A$$

Table 6.1 Kinetic data qualified to determine the energy of activation and the pre-exponential factor using an Arrhenius-type plot (see Fig. 6.2)

$T^{-1} (10^{-3} \text{ K}^{-1})$	3.411	3.354	3.299	3.245	3.193	3.143
$\ln k$	-20.57	-19.26	-18.80	-17.73	-16.66	-16.05

Fig. 6.2 Arrhenius type plot of the kinetic data given in Table 6.1. A linear regression of the data yields a slope of $-16770 \pm 860 \text{ K}$, and an axis intercept of 37 ± 3



as a linear equation. A plot of $\ln k$ against the reciprocal temperature should be a line with a slope $-\frac{E_a}{R}$, and the axis intercept $\ln A$. There is one point to consider, which often leads to errors: the latter expression requires an absolute temperature, whereas the original data in the above table are given in degrees Celsius. The kinetic data in the form qualified to determine the energy of activation E_a and the pre-exponential factor A are given in Table 6.1. The Arrhenius plot is shown in Fig. 6.2.

A linear regression of the data yields a slope of $s = -16,770 \text{ K}$. Because of the scattering in the experimental raw data, there is an uncertainty of 860 K. Hence, the sought energy of activation is $E_a = -Rs = 8.3145 \text{ J K}^{-1} \text{ mol}^{-1} \times 16,770 \text{ K} = 139.4 \text{ kJ mol}^{-1}$. From the evaluated intercept of $c = 37 \pm 3$, the pre-exponential factor $A = e^c = 1.2 \times 10^{16} \text{ s}^{-1}$ follows. This value is quite high. Typical values for A in a first-order reaction are within the range 10^{13} s^{-1} , which is the range of molecular vibrational frequencies.³ From the statistical error, however, an uncertainty of one order of magnitude can be deduced from these data.

In subproblem (b), we investigate how much of the BPO has reacted after a room-temperature storage period of 60 days. As we can assume first-order kinetics, the combination of Eqs. (6.1), (6.2), and (6.10) yields the following differential

³See Problem 10.1.

equation for the concentration of BPO:

$$-\frac{d [\text{BPO}]}{dt} = k [\text{BPO}]$$

The integration in the manner demonstrated in Problem 6.1 is straightforward. The result is the well-known exponential decay of the concentration:

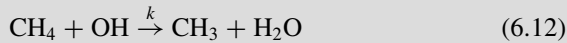
$$[\text{BPO}](t) = [\text{BPO}](0) \exp(-kt) = 0.978 \times [\text{BPO}](0) \quad (6.11)$$

Here we have taken the room-temperature value for the rate constant, $k = 4.33 \times 10^{-9} \text{ s}^{-1}$, and we have inserted $t = 60 \times 24 \times 3600 \text{ s}$. We can assume a direct proportionality between the concentration of BPO and its mass fraction in the salve. Thus, starting with an initial mass fraction of 10% BPO in the salve, a 60-day period of storage reduces the mass fraction to 9.78%. Apparently, there is no significant loss of efficacy during this time.

In **subproblem (c)**, we finally assess the number of benzyloxy radicals freed within 2 h by a portion of 0.02 g salve at a skin temperature of 35 °C. At this temperature, the rate constant is $k = 20.0 \times 10^{-9} \text{ s}^{-1}$. Assuming a mass fraction of 10% BPO, the initial mass of the BPO molecules in 0.02 g salve is 0.002 g. From Eq. (6.10) we can extract information about the molar mass of BPO, M_{BPO} . Its sum formula is C₁₄H₁₀O₄. Therefore, $M_{\text{BPO}} = 242 \text{ g mol}^{-1}$. Hence, the sample initially contains $n_{\text{BPO}}(0) = \frac{0.002 \text{ g}}{242 \text{ g mol}^{-1}} = 8.26 \times 10^{-6} \text{ mol}$ BPO molecules. After 2 h the number of BPO molecules is reduced by a factor $\exp(-kt) = \exp(-20.0 \times 10^{-9} \text{ s}^{-1} \times 7200 \text{ s}) = 0.99986$. As a consequence, a fraction of 1.4×10^{-4} of the BPO molecules reacts, each molecule producing two benzyloxy radicals (see Eq. (6.10)). Thus, the number of radicals produced is:

$$Z = 2 \times 1.4 \times 10^{-4} \times 8.26 \times 10^{-6} \text{ mol} \times N_A = 1.4 \times 10^{15}.$$

Problem 6.3 (Methane Decay) An important decay channel of the atmospheric trace gas methane (CH₄) is via the reaction with hydroxyl radicals:



- Write down the rate law of this reaction assuming that reaction Eq. (6.12) is an elementary reaction.
- If the initial concentrations of methane and hydroxyl radicals are $1 \times 10^{-9} \text{ mol m}^{-3}$ and $4 \times 10^{-12} \text{ mol m}^{-3}$, what is the half-life of OH? Assume a rate constant of $k = 4.75 \times 10^3 \text{ m}^3 \text{ mol}^{-1} \text{ s}^{-1}$.

Solution 6.3 This problem deals with the decay of methane and hydroxyl in a bimolecular reaction according to Eq.(6.12). The exercise is instructive as it demonstrates two different views of a classical problem in chemical kinetics.

In **subproblem (a)**, we write down the rate law for this elementary reaction of type $A + P \rightarrow \text{Products}$, which is the first order for methane, and also first order for OH. Thus, the reaction rate is:

$$r = k[\text{CH}_4][\text{OH}]. \quad (6.13)$$

In **subproblem (b)**, we shall determine the time t_{50} , after which the concentration of hydroxyl decays to 50% of its initial value $[\text{OH}]^0 = 4 \times 10^{-12} \text{ mol m}^{-3}$. As mentioned above, there are two different ways to solve this problem. This is possible because there is an excess of the other reactant, methane: $[\text{CH}_4]^0 = 1 \times 10^{-9} \text{ mol m}^{-3}$. Note that after a complete decay of OH, the concentration of methane is still $9.96 \times 10^{-10} \text{ mol m}^{-3} \approx [\text{CH}_4]^0$. Under these conditions, we may treat the problem as a first-order decay of OH with an effective rate constant:

$$k_{\text{eff}} = k[\text{CH}_4]^0 = 4.75 \times 10^3 \times 1 \times 10^{-9} \text{ s}^{-1} = 4.75 \times 10^{-6} \text{ s}^{-1} \quad (6.14)$$

$$-\frac{d[\text{OH}]}{dt} = k_{\text{eff}}[\text{OH}]. \quad (6.15)$$

The well-known textbook result for the half-life is

$$t_{50} = \frac{\ln 2}{k_{\text{eff}}} = \frac{0.69315}{4.75 \times 10^{-6} \text{ s}^{-1}} = 145,926 \text{ s} \approx 41 \text{ h}. \quad (6.16)$$

The second view of the problem is the exact treatment of the second order reaction. Ready to use analytical expressions can be found in textbooks, but it is instructive to recapitulate the details. If more than one reactant is present, then the integration of the rate law is more complicated than in the cases we have already dealt with in Problem 6.1. Focusing on the extent of reaction ξ we can write

$$r = \frac{1}{V} \frac{d\xi}{dt} = k \frac{n_{\text{CH}_4}}{V} \frac{n_{\text{OH}}}{V}, \quad (6.17)$$

where V is the volume. The amounts of methane and hydroxyl are (see Eq.(2.6))

$$n_{\text{CH}_4} = n_{\text{CH}_4}^0 - \xi \quad (6.18)$$

and

$$n_{\text{OH}} = n_{\text{OH}}^0 - \xi. \quad (6.19)$$

Insertion of these two expressions into Eq.(6.17) yields after separation of the

variables and integration

$$\int_0^{\xi(t)} \frac{d\xi'}{(n_{\text{CH}_4}^0 - \xi') (n_{\text{OH}}^0 - \xi')} = \frac{k}{V} \int_0^t d\tau. \quad (6.20)$$

Integration using Eq. (A.38) in the appendix yields

$$\frac{1}{n_{\text{CH}_4}^0 - n_{\text{OH}}^0} \ln \left(\frac{n_{\text{CH}_4}^0 - \xi}{n_{\text{OH}}^0 - \xi} \right) \Big|_0^{\xi(t)} = \frac{k}{V} t. \quad (6.21)$$

Further evaluation by insertion of the integration limits under special consideration of Eqs. (6.18) and (6.19) yields

$$\frac{1}{n_{\text{CH}_4}^0 - n_{\text{OH}}^0} \ln \left(\frac{\frac{n_{\text{CH}_4}(t)}{n_{\text{CH}_4}^0}}{\frac{n_{\text{OH}}(t)}{n_{\text{OH}}^0}} \right) = \frac{k}{V} t \quad (6.22)$$

or, again in terms of concentration,

$$\frac{1}{[\text{CH}_4]^0 - [\text{OH}]^0} \ln \left(\frac{\frac{[\text{CH}_4](t)}{[\text{CH}_4]^0}}{\frac{[\text{OH}](t)}{[\text{OH}]^0}} \right) = kt. \quad (6.23)$$

This equation is the basis for the determination of the half-life of the hydroxyl radicals. After the time t_{50} , the concentrations of the reactants are

$$[\text{OH}](t_{50}) = \frac{1}{2} [\text{OH}]^0 \quad (6.24)$$

and⁴

$$[\text{CH}_4](t_{50}) = [\text{CH}_4]^0 - \frac{1}{2} [\text{OH}]^0. \quad (6.25)$$

Insertion of these expressions into Eq. (6.23) yields

$$\begin{aligned} t_{50} &= \frac{1}{k} \frac{1}{[\text{CH}_4]^0 - [\text{OH}]^0} \ln \frac{\frac{[\text{CH}_4]^0 - \frac{1}{2} [\text{OH}]^0}{[\text{CH}_4]^0}}{\frac{\frac{1}{2} [\text{OH}]^0}{[\text{CH}_4]^0}} \\ &= \frac{1}{k} \frac{1}{[\text{CH}_4]^0 - [\text{OH}]^0} \ln 2 \left(1 - \frac{1}{2} \frac{[\text{OH}]^0}{[\text{CH}_4]^0} \right) \\ &= 146,089 \text{ s} \end{aligned} \quad (6.26)$$

⁴According to Eq. (6.19), the extent of reaction at time t_{50} is $\xi_{50} = \frac{1}{2} [\text{OH}]^0$.

which is fairly close to the above approximate result. This is obvious because in the second line in Eq. (6.26) the neglect of $[\text{OH}]^0$ transforms this expression just into Eq. (6.16). The example teaches us that it may be quite useful to look at the initial conditions. If there is an excess of one reactant, its concentration is approximately constant, and this can mean a considerable simplification. Experiments for the determination of the kinetics of a reaction with several reactants are often designed in such a way that there is an excess of all but one of the educts. In this way, the reaction order with regard to a certain reactant can be determined.

Problem 6.4 (Kinetic Look on Chemical Equilibrium) Consider the coupled reactions



and assume that both forward and backward reactions follow a first-order kinetics with the rate constants k_1 and k_2 respectively.

- a. Show that the equilibrium constant of this reaction is given by $K = \frac{k_1}{k_2}$.
- b. If n_A^0 and n_B^0 are the initial amounts of A and B in a state far from chemical equilibrium, show that the extent of reaction is given by

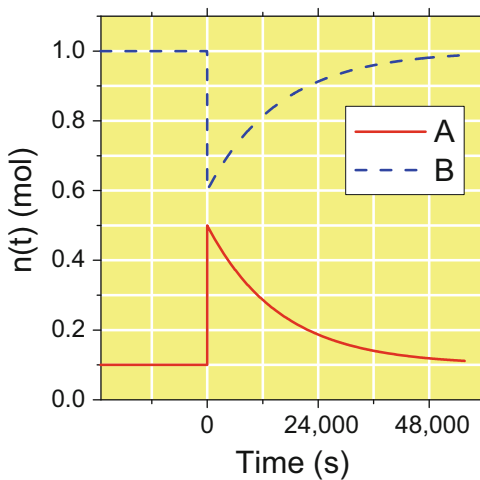
$$\xi(t) = \frac{k_1 n_A^0 - k_2 n_B^0}{k_1 + k_2} \left(1 - e^{-(k_1+k_2)t} \right) \quad (6.28)$$

- c. Two molecular conformers A and B are in chemical equilibrium with different amounts of A and B. At $t = 0$ s, a short heat pulse effects a momentary increase in temperature in the system, which cause the amounts of both conformers to change rapidly, as indicated in Fig. 6.3. Then, the system relaxes back into equilibrium. Extract the necessary information from Fig. 6.3 to estimate the equilibrium constant and the first-order rate constants of the forward and backward reactions.

Solution 6.4 In this problem, we investigate in detail how a chemical reaction comes to equilibrium. The problem sheds light on an important technique for determining rate constants: *relaxation methods*. The thermodynamic description of the equilibrium by means of the equilibrium constant $K(T)$ must be identical to the kinetic description in the limit $t \rightarrow \infty$. Hence, there must be a relationship between the rate constants and K , which we find in **subproblem (a)**. In the first step, we set up the differential equations for the concentrations of both species. We consider the forward and the backward reaction of Eq. (6.27), in addition to Eqs. (6.1) and (6.2):

$$\frac{d [\text{A}]}{dt} = -k_1 [\text{A}] + k_2 [\text{B}] \quad (6.29)$$

Fig. 6.3 Distortion and relaxation back into chemical equilibrium of two coexisting molecular conformers A and B



$$\frac{d[B]}{dt} = k_1 [A] - k_2 [B] \quad (6.30)$$

These equations consider that A decays in a first-order kinetics with a rate constant k_1 , and it builds up in a first-order kinetics with rate constant k_2 . Conversely, B is formed in a first-order reaction with rate constant k_1 , and it decays in a first-order reaction with rate constant k_2 . In the second step, we assume additional conditions in the special case of chemical equilibrium. Under the stationary conditions of chemical equilibrium, the forward and backward reactions balance, so that the net changes in concentrations are exactly zero:

$$0 \stackrel{!}{=} -k_1 [A]_{\text{eq}} + k_2 [B]_{\text{eq}} \Leftrightarrow \frac{k_1}{k_2} = \frac{[B]_{\text{eq}}}{[A]_{\text{eq}}} \quad (6.31)$$

Here, $[A]_{\text{eq}}$ and $[B]_{\text{eq}}$ are the equilibrium concentrations of A and B. On the other hand, the latter are related by the law of mass action to the equilibrium constant:

$$K = \frac{[B]_{\text{eq}}}{[A]_{\text{eq}}} \quad (6.32)$$

Comparison of the last two equations thus establishes the important relation sought:

$$K = \frac{k_1}{k_2} \quad (6.33)$$

Similar relations between the rate constants of the forward and backward reactions and K could also be derived for the general case where the reaction orders differ from unity.

In **subproblem (b)**, we shall investigate in detail how the system comes to equilibrium. The goal is to integrate the coupled differential equations Eq. (6.29) and (6.30). We are advised to introduce the extent of reaction ξ and to prove Eq. (6.28). In doing so, we learn how to use the extent of reaction to solve more complicated examples of chemical kinetics problems. Using Eq. (2.6) we can express the amount of substances of A and B as a function of time:

$$n_A(t) = n_A^0 - \xi(t) \quad (6.34)$$

$$n_B(t) = n_B^0 + \xi(t) \quad (6.35)$$

Within a constant volume we can set up a differential equation for n_A based on Eq. (6.29),

$$\frac{dn_A}{dt} = -k_1 n_A + k_2 n_B, \quad (6.36)$$

in which we insert the last two expressions. Because $\frac{dn_A}{dt} = -\frac{d\xi}{dt}$, we obtain

$$-\frac{d\xi}{dt} = -k_1(n_A^0 - \xi) + k_2(n_B^0 + \xi) = (k_1 + k_2)\xi - k_1 n_A^0 + k_2 n_B^0 \quad (6.37)$$

We separate the variables and integrate with the proper boundaries $t = 0$, $\xi(0) = 0$, and $\xi(t)$ at an arbitrary time t :

$$\int_0^{\xi(t)} \frac{d\xi}{(k_1 + k_2)\xi - k_1 n_A^0 + k_2 n_B^0} = - \int_0^t d\tau \quad (6.38)$$

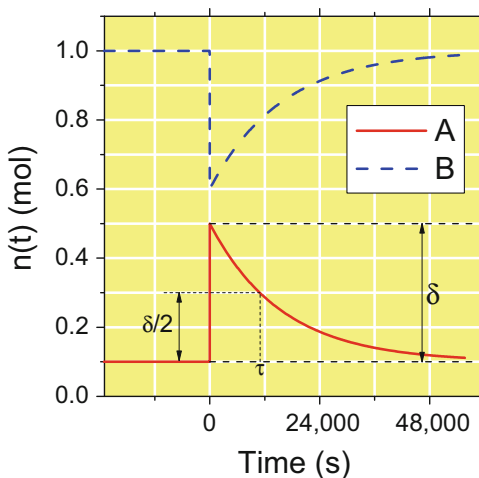
Using the integral Table in the appendix (Eq. (A.37)) we can solve the left integral. After insertion of the integration boundaries and application of Eq. (A.6) we obtain:

$$\ln \frac{(k_1 + k_2)\xi(t) + k_2 n_B^0 - k_1 n_A^0}{k_2 n_B^0 - k_1 n_A^0} = -(k_1 + k_2)t \quad (6.39)$$

If this equation is solved for the extent of reaction $\xi(t)$,

$$\xi(t) = \frac{k_1 n_A^0 - k_2 n_B^0}{k_1 + k_2} \left(1 - e^{-(k_1 + k_2)t} \right) \quad (6.40)$$

Fig. 6.4 Determination of the rate constants k_1 and k_2 for the forward and reverse reactions from the relaxation dynamics back to chemical equilibrium. The excess amount of conformer A due to perturbation is δ ; the characteristic relaxation time is τ



is obtained, which was demonstrated. Together with Eqs. (6.34) and (6.35), this equation is the basis for calculating the amounts of both species A and B at an arbitrary time starting from $t = 0$, and the respective initial values n_A^0 and n_B^0 .

It is worth inspecting this expression in more detail. It is striking that chemical equilibrium is established with an *effective rate constant* $k_1 + k_2$. In those cases, however, where equilibrium largely favors either A or B, one of the two rate constants can be ignored. Moreover, we briefly consider the special case where n_A^0 and n_B^0 are already the equilibrium amounts of A and B respectively. Because of $n_B^0 = K n_A^0$ and $k_2 = \frac{k_1}{K}$, the prefactor in Eq. (6.28) is zero in this case and therefore $\xi = 0$.

In subproblem (c), we consider a simple example that demonstrates how the observation of chemical relaxation is used to determine rate constants of the forward and backward reactions. Figure 6.3 is reproduced in Fig. 6.4 with additional annotations. As can be deduced from the constant levels at $t < 0$, the two conformers A and B are in chemical equilibrium with $n_A^{\text{eq}} = 0.1 \text{ mol}$ and $n_B^{\text{eq}} = 1.0 \text{ mol}$. Hence, the equilibrium constant at this temperature is:

$$K = \frac{n_B^{\text{eq}}}{n_A^{\text{eq}}} = 10$$

Because of the heat pulse at $t = 0$, the system is temporarily perturbed, causing a momentary increase in the amount of conformer A to $n_A^{\text{eq}} + \delta$, i.e., to 0.5 mol. After the heat pulse, the system reaches its original temperature, and n_A and n_B change toward their initial values, n_A^{eq} , and n_B^{eq} respectively. We expect this relaxation to be described by Eqs. (6.34), (6.35), and (6.28). Therefore, for $t > 0$ the amount of

conformer A is given by:

$$n_A(t) = (n_A^{\text{eq}} + \delta) - \delta \left(1 - e^{-(k_1+k_2)t}\right) = n_A^{\text{eq}} + \delta e^{-\frac{t}{\tau}}$$

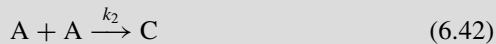
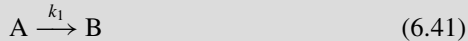
where τ is the relaxation time defined as the time after which half of the excess amount δ is decayed. From the figure, we estimate a relaxation time of 11,000 s. This is consistent with an effective rate constant

$$k_1 + k_2 = \frac{\ln 2}{\tau} = \frac{\ln 2}{11,000 \text{ s}} = 6.3 \times 10^{-5} \text{ s}^{-1}$$

Using Eq. (6.33), we can substitute k_2 and obtain $k_1 = 5.7 \times 10^{-5} \text{ s}^{-1}$ for the forward reaction. The rate constant of the backward reaction is thus:

$$k_2 = \frac{k_1}{K} = 5.7 \times 10^{-6} \text{ s}^{-1}.$$

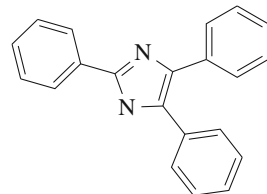
Problem 6.5 (Competing Reactions) Consider the following scheme of elementary chemical reactions:



- Set up the differential equation describing the decay of substance A.
 - If $[A]_0$ is the initial concentration of A, show that the following relation holds:
- $$\frac{1}{[\text{A}](t)} = \left(\frac{2k_2}{k_1} + \frac{1}{[\text{A}]_0} \right) e^{k_1 t} - \frac{2k_2}{k_1}. \quad (6.43)$$
- Based on Eq. (6.43), derive a relation for the reaction half-life. Test your relation by considering the limits $k_1 \gg 2k_2[\text{A}]_0$ and $2k_2[\text{A}]_0 \gg k_1$ for which the half-life should take the forms of first-order and second-order reactions respectively.
 - Given $k_1 = 6 \times 10^{-4} \text{ s}^{-1}$, $k_2 = 10 \text{ dm}^3 \text{ mol}^{-1} \text{ s}^{-1}$, and $[\text{A}]_0 = 1.2 \times 10^{-4} \text{ mol dm}^{-3}$, calculate the reaction half-life.

Solution 6.5 Sometimes, there are different possible reaction channels for a substance to decay. For example, the triphenylimidazolyl radical (TPI, see Fig. 6.5) can react with the solvent chloroform in a pseudo first-order reaction via hydrogen

Fig. 6.5 The triphenylimidazolyl (TPI) radical



capture [1]



However, TPI can also undergo a dimerization in a second-order reaction:



We thus have the reaction scheme outlined in Eqs. (6.41) and (6.42). The objective is of course to find an analytic solution for the concentration of the reactants as a function of time. The first step is to set up the rate equations, which we do in **subproblem (a)**. If we add up the reaction rates for the first-order decay according to Eq. (6.41) on the one hand, and the second-order reaction (6.42) on the other hand, we obtain

$$\frac{d[\text{A}]}{dt} = -k_1[\text{A}] - 2k_2[\text{A}]^2. \quad (6.46)$$

The rate equation has a nonlinear term. At first sight, an analytic solution seems to be tedious. In **subproblem (b)**, we simply prove that such an expression exists. Equation (6.43) contains the *reciprocal* concentration. Intuitively, it may thus be a good starting point to check whether the introduction of the reciprocal concentration might simplify the problem:

$$\frac{d\frac{1}{[\text{A}]}}{dt} \stackrel{\text{Eq. (A.17)}}{=} -\frac{1}{[\text{A}]^2} \frac{d[\text{A}]}{dt} \stackrel{\text{Eq. (6.46)}}{=} k_1 \frac{1}{[\text{A}]} + 2k_2$$

Indeed, it does! The problem is reduced to a first-order linear heterogeneous differential equation, for which an analytic solution exists. If we define $f = \frac{1}{[\text{A}]}$, we obtain

$$\frac{df(t)}{dt} - k_1 f(t) = 2k_2. \quad (6.47)$$

In mathematical terms, our problem is a special case of the *Bernoulli differential equation* (see Sect. A.3.20). For $t = 0$, $f(t) = \frac{1}{[\text{A}]_0}$. Expressions for the solution of this differential equation are given in the appendix Sect. A.3.18. If we introduce the

integrating factor

$$M(\tau) = e^{-\int k_1 d\tau} = e^{-k_1 \tau}$$

the solution of Eq. (6.47) is:

$$f(t) = e^{k_1 t} \left[-\frac{2k_2}{k_1} e^{-k_1 \tau} \Big|_0^t + C \right] = -\frac{2k_2}{k_1} + e^{k_1 t} \frac{2k_2}{k_1} + Ce^{k_1 t}$$

where C is an integration constant that is determined by the initial condition, $[A](t = 0) = [A]_0$. As a consequence, $C = \frac{1}{[A]_0}$, and therefore

$$f(t) = \left(\frac{2k_2}{k_1} + \frac{1}{[A]_0} \right) e^{k_1 t} - \frac{2k_2}{k_1}. \quad (6.48)$$

This result is simply Eq. (6.43). If the rate constants and $[A]_0$ had been given, we would be able to calculate the concentration.

In **subproblem (c)**, however, we deal with the reaction half-life $t_{\frac{1}{2}}$ resulting from Eq. (6.43). We proceed in the same way as in Problem 6.1. Following the definition for the half-life given there (Eq. (6.7)), we can write

$$[A](t_{\frac{1}{2}}) \stackrel{!}{=} \frac{1}{2}[A]_0.$$

Hence,

$$\begin{aligned} \left(\frac{2k_2}{k_1} + \frac{1}{[A]_0} \right) e^{k_1 t_{\frac{1}{2}}} - \frac{2k_2}{k_1} &= \frac{2}{[A]_0} \\ \frac{\frac{2}{[A]_0} + \frac{2k_2}{k_1}}{\frac{2k_2}{k_1} + \frac{1}{[A]_0}} &= e^{k_1 t_{\frac{1}{2}}} \end{aligned}$$

We solve for the half-life by taking the logarithm:

$$t_{\frac{1}{2}} = \frac{1}{k_1} \ln \frac{\frac{2}{[A]_0} + \frac{2k_2}{k_1}}{\frac{2k_2}{k_1} + \frac{1}{[A]_0}}$$

This can be written in a nicer way:

$$t_{\frac{1}{2}} = \frac{1}{k_1} \ln \left(1 + \frac{1}{1 + \frac{2k_2[A]_0}{k_1}} \right) \quad (6.49)$$

We check whether this expression is correct by testing the limiting cases of $k_1 \gg 2k_2[A]_0$ and $2k_2[A]_0 \gg k_1$. In the first case, the fraction $\frac{2k_2[A]_0}{k_1}$ becomes a very small number and thus:

$$t_{\frac{1}{2}} \approx \frac{1}{k_1} \ln \left(1 + \frac{1}{1+0} \right) = \frac{\ln 2}{k_1}.$$

This is simply the expression for the half-life of a first-order reaction. In the second case, $2k_2[A]_0 \gg k_1$, the fraction $\frac{2k_2[A]_0}{k_1}$ becomes a very large number, much greater than 1. Therefore, we can write:

$$t_{\frac{1}{2}} = \frac{1}{k_1} \ln \left(1 + \frac{1}{1 + \frac{2k_2[A]_0}{k_1}} \right) \approx \frac{1}{k_1} \ln \left(1 + \frac{k_1}{2k_2[A]_0} \right).$$

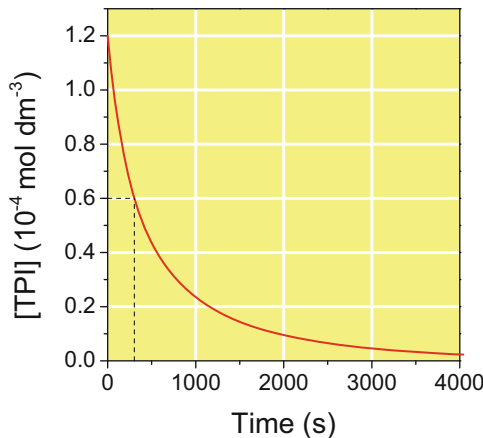
As $\frac{k_1}{2k_2[A]_0}$ is a very small number in this case, we can use a power series expansion (see Eq. (A.56) in the appendix). If we ignore the higher terms, $\ln(1+x) \approx x + \dots$, thus we obtain

$$t_{\frac{1}{2}} = \frac{1}{k_1} \ln \left(1 + \frac{k_1}{2k_2[A]_0} \right) \approx \frac{1}{k_1} \frac{k_1}{2k_2[A]_0} = \frac{1}{2k_2[A]_0}.$$

This is simply the expression for a pure second-order reaction, as can be seen from Eq. (6.6) for $\alpha = 2$.

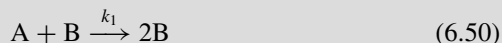
In **subproblem (d)**, finally, we calculate the reaction half-life in a concrete case. It is the example of the above-mentioned TPI radical. In Fig. 6.6 the concentration of TPI, based on Eq. (6.43) and the parameters k_1 , k_2 , and $[A]_0$, is shown. The dashed lines indicate the moment when the concentration has decayed to 50% of its initial value $[A]_0$. If we insert these parameters into Eq. (6.49), we obtain a reaction half-

Fig. 6.6 Mixed first- and second-order decay of TPI radical according to Eq. (6.43)



life of $t_{\frac{1}{2}} = 304\text{ s}$. For comparison, a first-order decay with $k_1 = 6 \times 10^{-4}\text{ s}^{-1}$ would have a considerably longer reaction half-life of $1,155\text{ s}$. In the initial stages of the reaction, when the reactant concentration is comparatively large, the second-order dimerization (Eq. (6.45)) is more effective, as the rate is proportional to $[\text{TPI}]^2$. Therefore, the reaction proceeds much faster in the initial stages than a first-order reaction. Then, as $[\text{TPI}]$ becomes smaller, the pseudo first-order reaction (Eq. (6.44)) becomes more effective. As a consequence, the evolution of the TPI concentration resembles the prediction of neither first-order nor second-order kinetics. There are certainly situations in which experimental data can be fitted to first-order kinetics and second-order kinetics with only moderate agreement. In this case, the assumption of two different reaction channels, as discussed in this problem, might be reasonable. However, one should always take into account the fact that a model with three parameters generally always fits better than one with only two parameters.

Problem 6.6 (Oscillating Chemical Reactions I) Consider the following scheme of chemical reactions:



The reactant A is either continuously supplied to the system, or is in excess; thus, a constant concentration $[\text{A}]_0$ can be assumed: $[\text{A}]_0 = 1\text{ mol dm}^{-3}$, $k_1 = 2.8\text{ dm}^3\text{ mol}^{-1}\text{ s}^{-1}$, $k_2 = 142\text{ dm}^3\text{ mol}^{-1}\text{ s}^{-1}$, and $k_3 = 3.9 \times 10^{-3}\text{ s}^{-1}$.

- Reactions of the type Eqs. (6.50) and (6.51) are called *autocatalytic* reactions. Can you comment on this?
- Write down the rate equations for the reactants B and C. Assuming a stationary state for the concentrations of reactants B and C, calculate the stationary concentrations $[\text{B}]_s$ and $[\text{C}]_s$ of the latter as a function of the rate constants and $[\text{A}]_0$.
- Assume small variations of concentrations of B and C around the respective stationary state concentrations, i.e., $[\text{B}](t) = [\text{B}]_s + \beta(t)$ and $[\text{C}](t) = [\text{C}]_s + \gamma(t)$. Based on the rate equations from subproblem (b), show that the differential equations for β and γ are:

$$\frac{d\beta}{dt} = -k_3\gamma \quad (6.53)$$

$$\frac{d\gamma}{dt} = k_1 [\text{A}]_0 \beta \quad (6.54)$$

(continued)

Problem 6.6 (continued)

- d. Show that $\beta(t) = \beta_0 \cos(\omega t)$ is a solution of this linearized problem with an amplitude β_0 . Derive an expression for the oscillation frequency and calculate it. Furthermore, write down the associated expression for $\gamma(t)$ and discuss the phase shift between $\beta(t)$ and $\gamma(t)$.
- e. At $t = 0$, the concentration of species B is 3.75×10^{-5} mol dm⁻³. Based on the preceding results, plot the intermediate concentrations [B] and [C] as a function of time. Also, plot [C] against [B]. What would happen if the concentration of one intermediate became zero?

Solution 6.6 Chemical reactions during which the concentration of some reactants oscillate with time are a fascinating phenomenon. Under special conditions, such a reaction, in principle, does not reach chemical equilibrium. Instead, the concentrations oscillate around their steady-state value. In this exercise, we investigate these oscillations in detail. The reaction mechanism defined by Eqs. (6.50)–(6.52) is the well-known *Lotka-Volterra* kinetic model.

In **subproblem (a)**, we comment on the term *autocatalytic* reaction used, e.g., for Eq. (6.50). A reaction is called autocatalytic if at least one reactant is also a product. This is the case for Eq. (6.50), where species B in a bimolecular reaction with reactant A is *reproduced*. As a consequence, the number of B molecules would increase continuously if species A were held constant. Moreover, Eq. (6.51) falls under the category autocatalytic reaction, in which species C is reproduced.

The formulation of the rate equations is our first task in **subproblem (b)**. We have to consider that the concentration of B increases with rate constant k_1 in reaction Eq. (6.50), and decreases with rate constant k_2 in reaction Eq. (6.51). Application of Eqs. (6.1) and (6.2) for the special case of a bimolecular reaction gives us:

$$\frac{d[B]}{dt} = k_1 [A]_0 [B] - k_2 [B] [C] \quad (6.55)$$

In a similar way, we obtain:

$$\frac{d[C]}{dt} = k_2 [B] [C] - k_3 [C] \quad (6.56)$$

where we consider the first-order decay of species C with rate constant k_3 and its production in reaction Eq. (6.51) with rate constant k_2 . We note that the concentration of product D continuously increases if the system is fed with A. In that sense, a steady state, which we consider, is a *dynamic equilibrium* characterized by constant concentrations of the intermediates, $[B]_s$ and $[C]_s$ respectively. We find

these steady-state concentrations assuming zero reaction rates for B and C in Eqs. (6.55) and (6.56). Thus,

$$0 = k_1 [A]_0 [B]_s - k_2 [B]_s [C]_s$$

and

$$0 = k_2 [B]_s [C]_s - k_3 [C]_s$$

Therefore, the nonzero steady-state concentrations of the intermediates are

$$[B]_s = \frac{k_3}{k_2} \quad (6.57)$$

and

$$[C]_s = \frac{k_1}{k_2} [A]_0 \quad (6.58)$$

Inserting the given values for the rate constants and $[A]_0$, we obtain $[B]_s = 2.75 \times 10^{-5} \text{ mol dm}^{-3}$ and $[C]_s = 0.02 \text{ mol dm}^{-3}$ as the stationary concentrations of the reaction intermediates. It is worth mentioning that a second steady state exists: $[B]_s = [C]_s = 0$. As soon as $[B](t)$ becomes zero, there is no further production of species C and the latter decays to zero according to Eq. (6.52).

We continue with **subproblem (c)**, where we seek to find nonstationary solutions for our system. Analytic solutions, however, are difficult, because the coupled equations contain nonlinear terms. Therefore, we restrict our analysis to small perturbations $\beta(t)$ and $\gamma(t)$ of the nonzero stationary state values. In this case, terms containing the product $\beta \gamma$ can be ignored and the differential equations become linearized. To derive these equations we insert $[B](t) = [B]_s + \beta$ and $[C](t) = [C]_s + \gamma$ in Eq. (6.55) and obtain:

$$\begin{aligned} \frac{d\beta}{dt} &= k_1 [A]_0 ([B]_s + \beta) - k_2 ([B]_s + \beta) ([C]_s + \gamma) \\ &\approx k_1 [A]_0 [B]_s - k_2 [B]_s [C]_s + k_1 [A]_0 \beta - k_2 [C]_s \beta - k_2 [B]_s \gamma \end{aligned}$$

Insertion of Eqs. (6.57) and (6.58) proves that all but the last term on the right-hand side cancel each other out. This proves Eq. (6.53). In a similar manner, we proceed with Eq. (6.53), where we obtain:

$$\begin{aligned} \frac{d\gamma}{dt} &= k_2 ([B]_s + \beta) ([C]_s + \gamma) - k_3 ([C]_s + \gamma) \\ &\approx k_2 [B]_s [C]_s - k_3 [C]_s + k_2 [B]_s \gamma - k_3 \gamma + k_2 [C]_s \beta \end{aligned}$$

Where, again, all but the last term cancel each other out, which proves Eq. (6.54).

In **subproblem (d)** we deal with nonzero solutions of Eqs. (6.53) and (6.54), which constitute a coupled linear system with constant coefficients. The rigorous mathematical treatment of such a system is sketched in the appendix or described in mathematics textbooks. Here, we take a more direct way and take the derivative of Eq. (6.53)

$$\frac{d^2 \beta}{dt^2} = -k_3 \frac{d \gamma}{dt} \stackrel{\text{Eq. (6.54)}}{=} -k_3 k_1 [A]_0 \beta$$

and obtain the harmonic oscillator equation

$$\frac{d^2 \beta}{dt^2} + \omega^2 \beta = 0 \quad (6.59)$$

with the angular frequency

$$\omega = \sqrt{k_3 k_1 [A]_0} = 0.104 \text{ s}^{-1} \quad (6.60)$$

Equation (6.59) has harmonic solutions of the form $\beta(t) = \beta_0 \cos(\omega t)$, which is easily shown by insertion. Because the derivative of $\cos(\omega t)$ is $-\omega \sin(\omega t)$, we obtain the related harmonic expression for γ from Eq. (6.53):

$$\gamma(t) = \frac{\omega}{k_3} \beta_0 \sin(\omega t) \quad (6.61)$$

Hence, the concentrations of the reaction intermediates oscillate harmonically around their nonzero steady-state values. One period takes $\frac{2\pi}{\omega} \approx 60 \text{ s}$. There is a phase shift of 90° between the perturbations β and γ . The oscillations and the phase shift are consequences of the coupling between the concentrations of the two intermediates. According to Eq. (6.54) γ grows if the concentration of species B is above its steady-state value. However, as the concentration of species C exceeds its average value and thus γ reaches a positive level, β starts to decay again and the concentration of species B thus diminishes.

In **subproblem (e)**, we plot the oscillating concentrations of the reaction intermediates. At $t = 0$, $[B] = 3.75 \times 10^{-5} \text{ mol dm}^{-3}$, i.e., the amplitude β_0 of the oscillation around the stationary state value $[B]_s$ is $10^{-5} \text{ mol dm}^{-3}$. A plot of the intermediate concentrations can be found in the left-hand diagram of Fig. 6.7. In the right-hand diagram $[C]$ is plotted against $[B]$. The shape of the closed trajectory is elliptic, and its center is the stationary point. Let us discuss what would happen if the amplitude β_0 became larger so that the trajectory would cross the line $[B] = 0$. In this case, there would be no further production of species C according to the autocatalytic reaction Eq. (6.51) and $[C]$, from that time on, would decay exponentially with the rate constant k_3 . On the other hand, $[C]$ would reach a value of zero, and $[B]$ would grow from that time on.

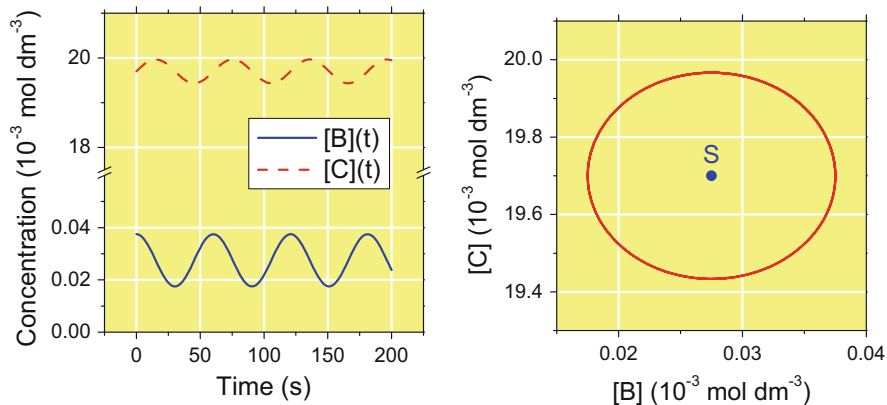
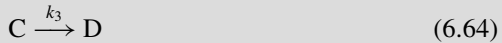
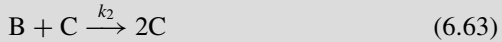


Fig. 6.7 Concentration of the reaction intermediates B and C oscillating around their stationary state values in harmonic approximation. Note the break and the different scaling of the ordinate axis. *Left:* Concentrations as a function of time. *Right:* Elliptic trajectory around the stationary state point S

Problem 6.7 (Oscillating Chemical Reactions II) Hint: It is assumed that you have dealt before with Problem 6.6. Consider the following scheme of chemical reactions:



The reactant A is either continuously supplied to the system, or is in excess; thus, a constant concentration $[A]_0$ can be assumed: $[A]_0 = 1 \text{ mol dm}^{-3}$, $k_1 = 2.8 \text{ dm}^3 \text{ mol}^{-1} \text{ s}^{-1}$, $k_2 = 142 \text{ dm}^3 \text{ mol}^{-1} \text{ s}^{-1}$, and $k_3 = 3.9 \times 10^{-3} \text{ s}^{-1}$.

- The rate equations and the stationary state of the given reaction mechanism have been discussed already in Problem 6.6 (Eqs. (6.55)–(6.58)). Show that the dynamics of the system conserves the quantity

$$V = k_2 ([B] + [C]) - k_3 \ln[B] - k_1 [A]_0 \ln[C] \quad (6.65)$$

- Use numeric methods to solve the rate Eqs. (6.55) and (6.56). Assume $[B](t = 0) = 3.75 \times 10^{-5} \text{ mol dm}^{-3}$ and for $[C]$ the steady-state concentration. Plot the resulting concentrations of the reaction intermediates

(continued)

Problem 6.7 (continued)

- [B] and [C] as a function of time. Also, make a plot [C] against [B] and compare these results with the curves obtained in Problem 6.6d. Determine the quantity $V(t)$ defined in subproblem (a) to test the numerical stability of your calculation.
- c. Repeat your calculation for $[B](t = 0) = 4 \times 10^{-4} \text{ mol dm}^{-3}$ and interpret the variation of the intermediate concentrations with time.

Solution 6.7 This problem assumes that you have already dealt with the Problem 6.6, where the reaction mechanism of the *Lotka-Volterra* reaction has been treated in a linearized approximation. This is valid if the variations of the concentrations of the reaction intermediates from the corresponding steady-state values are small. Now, we further investigate this model system of autocatalysis.

In **subproblem (a)**, we pick up the rate Eqs. (6.55) and (6.56) and consider the quantity V defined in Eq. (6.65). The task is to prove that V is conserved by the model, i.e., we must show that:

$$\frac{dV}{dt} = 0$$

Using Eqs. (6.65), (6.55)–(6.56), and the basic differentiation rule Eq. (A.23), we obtain

$$\begin{aligned}\frac{dV}{dt} &= k_2 \frac{d[B]}{dt} + k_2 \frac{d[C]}{dt} - \frac{k_3}{[B]} \frac{d[B]}{dt} - \frac{k_1[A]_0}{[C]} \frac{d[C]}{dt} \\ &= k_2 k_1 [A]_0 [B] - k_2^2 [C][B] + k_2^2 [C][B] - k_2 k_3 [C] - k_3 k_1 [A]_0 + k_3 k_2 [C] \\ &\quad - k_1 [A]_0 k_2 [B] + k_1 [A]_0 k_3 \\ &= 0\end{aligned}$$

All terms on the right-hand side cancel each other out. Thus, V is constant over time.

In **subproblem (b)**, we seek numerical solutions for the rate equations

$$\frac{d[B]}{dt} = k_1 [A]_0 [B] - k_2 [B][C] \tag{6.66}$$

$$\frac{d[C]}{dt} = k_2 [B][C] - k_3 [C], \tag{6.67}$$

starting with the same initial concentrations as in Problem 6.6d. This gives us the possibility of checking the validity of the harmonic approximation assumed in that exercise. In mathematical terms, this is an *initial value problem*. Nowadays, there are a number of mathematical software packages available to students that tackle

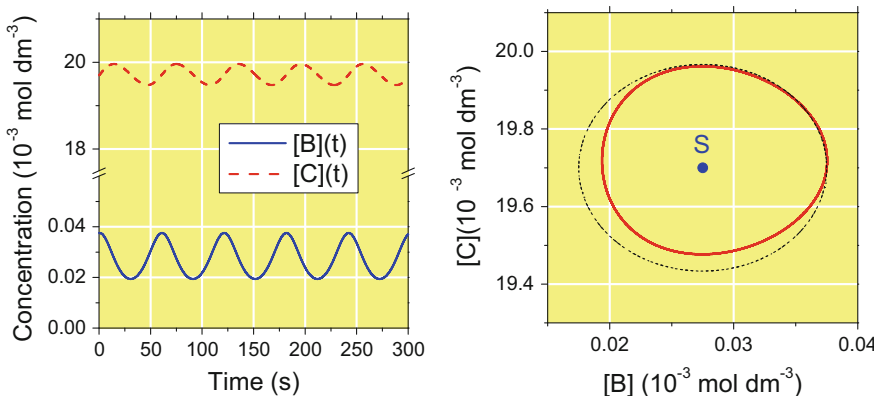


Fig. 6.8 Concentration of the reaction intermediates B and C oscillating around their stationary state values. Note the break and the different scaling of the ordinate axis. *Left:* Concentrations as a function of time. *Right:* Egg-shaped trajectory around the stationary state point S. The *dashed line* indicates the approximative trajectory from Problem 6.6d

the numerical solution of initial value problems. A minimum amount of coding is necessary to obtain numerical solutions. Other students who are eager to gain a deeper insight in the technical details of numerics use a programming language and code the problem on their own. Following the latter case, we have to choose a suitable numerical scheme and an adequate step length $h = t_{n+1} - t_n$ ($n = 1, 2, \dots$) to calculate the concentrations $[B](t_{n+1})$ and $[C](t_{n+1})$ from $[B](t_n)$ and $[C](t_n)$, starting from the initial concentrations, $[B](t_0 = 0)$ and $[C](t_0 = 0)$. Some popular methods with different accuracies can be found in the appendix (Sect. A.3.21). The fourth order Runge-Kutta method, with a time interval $h = 10^{-3} \text{ s}$, yields the results shown in Fig. 6.8.

The oscillations of the intermediate concentrations around their stationary state values shown in the diagram on the left appear to be quite similar to those in Fig. 6.7. In the diagram on the right of Fig. 6.8, the nature of the resulting egg-shaped trajectory is directly compared with the elliptic trajectory predicted by the harmonic approximation (dashed line), which we have taken from the diagram on the right of Fig. 6.7. A closer inspection of the maxima and minima gives a time-period of 60.4 s for the oscillations, which is quite close to the harmonic value of 60 s obtained in Problem 6.6. Looking at the right-hand diagram, we notice that the numerical solution yields slightly smaller deviations from the stationary state point S, and the trajectory is egg-shaped, indicating a certain degree of anharmonicity. To check the integrity of our trajectory, we calculate the quantity V according to Eq. (6.65). Within a simulation time of 300 s, the numerically determined value of V is constantly 13.838545. From this, we deduce that the simulation provides meaningful results and we are able to investigate solutions to the problem for other initial conditions, which are beyond the limits of validity of harmonic approximation.

In **subproblem (c)**, we repeat the simulation with a much larger initial concentration $[B](t = 0) = 4 \times 10^{-4} \text{ mol dm}^{-3}$, whereas $[C](t)$ starts again with

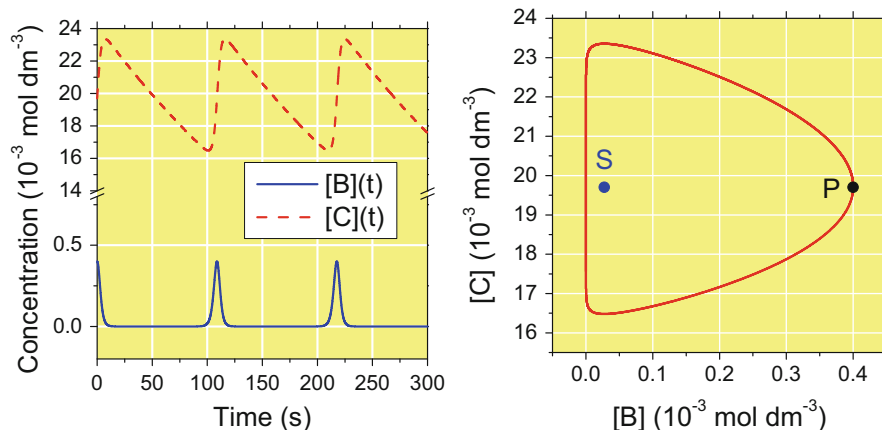


Fig. 6.9 Concentration of the reaction intermediates B and C oscillating around their stationary state values. Note the break and the different scaling of the ordinate axis. *Left:* Concentrations as a function of time. *Right:* Trajectory around the stationary state point S. Point P indicates the starting point of the simulation

its stationary state value. The results are shown in Fig. 6.9. The concentrations still show oscillatory behavior, but the curves are now largely anharmonic: $[C](t)$ has the shape of a saw tooth, whereas $[B](t)$ can be characterized by short pulses repeated periodically within about 110 s. The anharmonic behavior is apparent in the right diagram showing the trajectory. The point P marks the starting point of the trajectory, which is run anti-clockwise. Due to the high initial value of intermediate B, there is rapid production of C according to reaction Eq. (6.63), and also a rapid decay of B. The lack of B drastically reduces the production of C, which then decays exponentially with the rate constant k_3 . This decay of C is continued until its concentration goes below the stationary state concentration. Intermediate B is then rapidly recovered according to Eq. (6.63) and again reaches the starting point P.

Looking back on our solution, we have used numerical methods to solve the rate equations for a reaction mechanism featuring oscillatory behavior. It is worth mentioning that in Chap. 10 we deal with the LASER⁵ in Problems 10.10 and 10.11 in a similar manner. As it turns out, the mathematical description of a *lasing* system, consisting of an electromagnetic field within a resonator and an active medium in a dynamic equilibrium, is similar to the description of the kinetic model of the Lotka-Volterra type.

Reference

1. Lavabre D, Pemienta V, Levy G, Micheau JC (1993) J Phys Chem 97:5321

⁵LASER is the abbreviation for light amplification by stimulated emission of radiation.

Chapter 7

Kinetic Theory

Abstract Kinetic theory provides the basis for macroscopic state variables, such as pressure and temperature, by developing a microscopic picture of particles with kinetic energy, momentum, and, moreover, internal degrees of freedom. Thus, it follows an atomistic model. To treat a system of typically 10^{23} particles, kinetic theory introduces the concept of probability and statistics into science. (The probability concept is, moreover, key to the description of quantum mechanics. However, we must clearly distinguish between *thermodynamic* probability introduced by Ludwig Boltzmann and *quantum mechanical* probability resulting from Max Born's interpretation of the wave function (see Sect. 9.1.2 on page 216).) Among the probability density functions, the Maxwell-Boltzmann distribution for the particle velocity is the most prominent, and we deal with it in several problems. The characteristics of a molecular beam leaving an effusion cell, in addition to film growth, are further examples that demonstrate the practical use of kinetic theory.

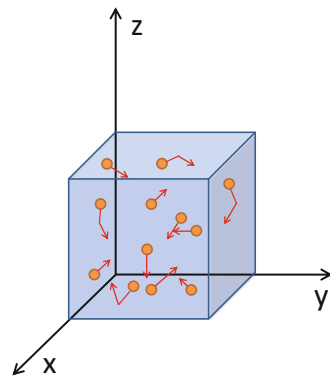
7.1 Basic Concepts

In the following, it is assumed that the reader is familiar with the basic principles of classical mechanics.

7.1.1 Maxwell-Boltzmann Velocity Distribution

Strictly speaking, thermodynamics can be formulated without a fundamental concept of the nature of matter. The atomistic concept worked out by John Dalton and Amedeo Avogadro, however, is fundamental to chemistry. Textbooks demonstrate how pressure and the equation of state of a perfect gas can be traced back to the statistical movement of microscopic particles making elastic collisions with system walls (see Fig. 7.1). The **Maxwell-Boltzmann** velocity distribution can be chosen

Fig. 7.1 Microscopic model of a gas within a box



as a basis. It states that at a temperature T the fraction $\frac{dN(\mathbf{v})}{N_{\text{tot}}}$ of particles of mass m with a velocity between \mathbf{v} and $\mathbf{v} + d\mathbf{v}$ is

$$\frac{dN(\mathbf{v})}{N_{\text{tot}}} = \left(\frac{m}{2\pi k_B T} \right)^{\frac{3}{2}} \exp \left(-\frac{mv^2}{2k_B T} \right) d\mathbf{v}, \quad (7.1)$$

where N_{tot} is the total number of particles, and $k_B = 1.3806488 \times 10^{-23} \text{ J K}^{-1}$ is the Boltzmann constant (see Sect. A.1). This distribution follows from very general assumptions, such as the homogeneity and the isotropy of the system. Note that the Maxwell-Boltzmann distribution assumes thermal equilibrium, which in many situations may not be established.

7.1.2 Pressure

The microscopic picture (Fig. 7.1) gives the relationship between the velocity of the particles and pressure p . The assumption of elastic collisions of particles with the system walls and momentum conservation yields:

$$p = \frac{1}{3} \mathcal{N} m \langle v^2 \rangle \quad (7.2)$$

where \mathcal{N} is the number of particles per volume, m is their mass, and $\langle v^2 \rangle$ their mean square velocity resulting from Eq. (7.1).

7.1.3 Collisions Between Particles

The total collision frequency Z_{AB} between N_A particles of types A and N_B particles of type B depends on the **cross-section** σ_{AB} , their masses m_A and m_B , and temperature:

$$Z_{AB} = N_A N_B \sigma_{AB} \left(\frac{8k_B T}{\mu} \right)^{\frac{1}{2}}, \quad (7.3)$$

where

$$\mu = \frac{m_A m_B}{m_A + m_B} \quad (7.4)$$

is the **effective mass**. In the simplest case of elastic collisions of rigid spherical particles with diameters d_A and d_B , the cross-sectional area is that of a disk of *radius* $d_{AB} = \frac{1}{2}(d_A + d_B)$ (see Fig. 7.2):

$$\sigma_{AB} = \pi d_{AB}^2 \quad (7.5)$$

Equation (7.3) is based on the summation of the z_{AB} individual collisions of N_A particles of type A with type B. To calculate z_{AB} , it is tentatively assumed that all particles are at rest, except for one of type A sweeping through the gas with the mean velocity $\langle v_A \rangle$. A collision with a particle of type B occurs if it is passed by the moving particle at a distance less than or equal to d_{AB} (see Fig. 7.2), i.e., within the cross-sectional area σ_{AB} . The latter defines the basal plane of the cylindrical volume $\sigma_{AB} \langle v_A \rangle$, which the moving particle passes per unit of time.

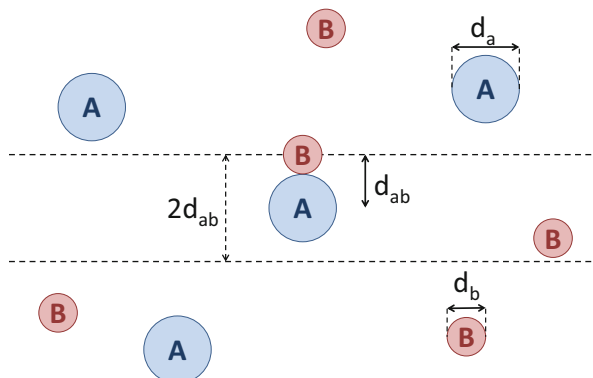


Fig. 7.2 Collisions between particles in a mixture of perfect gases of types A and B, treated within the *hard sphere model*. Collisions of the particle in the center occur with all particles within a cylindrical volume with a cross-sectional area πd_{AB}^2

Given the particle density \mathcal{N}_B of type B particles, the moving particle collides with $\sigma_{AB}\langle v_A \rangle \mathcal{N}_B$ particles of type B. The picture, however, is incorrect because all particles are in permanent movement. Therefore, the mean velocity of particle A is replaced by the mean *relative* velocity $\langle v_{AB} \rangle$ of the particles. Therefore, the collision frequency of one particle of type A with particles of type B is

$$z_{AB} = \sigma_{AB} \langle v_{AB} \rangle \mathcal{N}_B \quad (7.6)$$

The somewhat tedious calculation of $\langle v_{AB} \rangle$ is treated in Problem 7.3. The result is

$$\langle v_{AB} \rangle = \left(\frac{8k_B T}{\pi \mu} \right)^{\frac{1}{2}}. \quad (7.7)$$

From the collision frequency of a particle of type A, its **mean free path** λ_A between two collisions results:

$$\lambda_A = \frac{\langle v_A \rangle}{z} \quad (7.8)$$

Here z is the number of collisions the particle experiences per unit of time.

7.1.4 Collisions with Surfaces

The rate at which particles collide with a surface is key for gas surface interactions, such as scattering, adsorption, and film growth processes. Moreover, the number of particles that strike a certain surface area per second is also an important quantity for dealing with gas effusion through a small orifice. A rigorous calculation found in many textbooks shows that the impingement rate I , i.e., the number of particles striking a surface element dA in the time dt is related to the mean velocity at a given temperature:

$$I = \frac{N}{dA dt} = \frac{1}{4} \mathcal{N} \langle v \rangle \quad (7.9)$$

Very often, the impingement rate is expressed in terms of pressure, which can be related to \mathcal{N} via the equation of state: $p = \mathcal{N} k_B T$. Moreover, as shown in Problem 7.1 (Eq. (7.16)), the assumption of a Maxwell-Boltzmann distribution of the gas particles with mass m leads to $\langle v \rangle = \left(\frac{8k_B T}{\pi m} \right)^{\frac{1}{2}}$. Thus,

$$I = \frac{p}{\sqrt{2\pi m k_B T}} \quad (7.10)$$

7.2 Problems

Problem 7.1 (Maxwell-Boltzmann Distribution I)

- Write down explicit expressions of the Maxwell-Boltzmann distribution in Cartesian coordinates, polar coordinates, and cylindrical coordinates (*Hint: useful information on polar and cylindrical coordinates can be found in the appendix in Sects. A.3.11 and A.3.12*).
- Prove that the Maxwell-Boltzmann distribution (Eq. (7.1)) is normalized, i.e.,

$$\int_{\text{all molecules}} \frac{dN(\mathbf{v})}{N_{\text{tot}}} = 1 \quad (7.11)$$

- Provide expressions for the average speed $\langle v \rangle$, the mean square speed $\langle v^2 \rangle$, and the velocity at which the distribution takes its maximum value. Give explicit values of these quantities for helium gas at 300 K and at 1,000 K.

Solution 7.1 In this problem, we familiarize ourselves with the Maxwell-Boltzmann distribution function for the velocity of particles in a gas. The velocity of a single particle is a vector. In the absence of conditions that would define a preferred direction, however, the gas is an isotropic system. This must also be reflected in the various forms of the Maxwell-Boltzmann distribution using different sets of coordinates.

In **subproblem (a)**, we give expressions for the distribution using different choices of coordinates. In **Cartesian coordinates**, the velocity squared is $v^2 = v_x^2 + v_y^2 + v_z^2$, where v_x , v_y , and v_z are the velocity in x -, y -, and z -direction respectively. Hence,

$$\frac{dN(v_x, v_y, v_z)}{N_{\text{tot}}} = \left(\frac{m}{2\pi k_B T} \right)^{\frac{3}{2}} \exp \left(-\frac{m}{2k_B T} (v_x^2 + v_y^2 + v_z^2) \right) dv_x dv_y dv_z \quad (7.12)$$

Apparently, the distribution function is separable, i.e.,

$$\frac{dN(v_x, v_y, v_z)}{N_{\text{tot}}} = f(v_x) f(v_y) f(v_z) dv_x dv_y dv_z$$

and for each Cartesian component, the same symmetric Gaussian distribution function holds:

$$f(v_x) = \left(\frac{m}{2\pi k_B T} \right)^{\frac{1}{2}} \exp \left(-\frac{m}{2k_B T} v_x^2 \right) \quad (7.13)$$

In many problems, however, **spherical coordinates** (see Sect. A.3.11) are the suitable choice. The velocity vector is characterized by its scalar value v , and the direction expressed by a polar angle θ and the azimuthal angle ϕ . We obtain:

$$\frac{dN(v, \theta, \phi)}{N_{\text{tot}}} = \left(\frac{m}{2\pi k_B T} \right)^{\frac{3}{2}} \exp \left(-\frac{mv^2}{2k_B T} \right) v^2 \sin \theta \, dv \, d\theta \, d\phi \quad (7.14)$$

In some cases, **cylindrical coordinates** (see Sect. A.3.12) are appropriate. Apart from a velocity component v_z in the z direction, a velocity component v_r perpendicular to the z axis and an azimuthal angle ϕ is considered. We obtain:

$$\frac{dN(v_z, v_r, \phi)}{N_{\text{tot}}} = \left(\frac{m}{2\pi k_B T} \right)^{\frac{3}{2}} \exp \left(-\frac{m}{2k_B T} (v_z^2 + v_r^2) \right) v_r \, dv_z \, dv_r \, d\phi \quad (7.15)$$

In **subproblem (b)**, we check the normalization of the Maxwell-Boltzmann distribution by integrating over the entire velocity space. We are free to choose one of the coordinate systems and select spherical coordinates (Eq. (7.14)). The integral in Eq. (7.11) can be separated in a product of three integrals. Using the integrals given in Sect. A.3.7 in the appendix, we obtain:

$$\begin{aligned} \int_{\text{all molecules}} \frac{dN(\mathbf{v})}{N_{\text{tot}}} &= \left(\frac{m}{2\pi k_B T} \right)^{\frac{3}{2}} \underbrace{\int_0^\infty v^2 \exp \left(-\frac{mv^2}{2k_B T} \right) dv}_{= \frac{\sqrt{\pi}}{4} \left(\frac{m}{2k_B T} \right)^{\frac{3}{2}} (\text{see Eq. (A.47)})} \underbrace{\int_0^\pi \sin \theta \, d\theta}_{= 2(\text{see Eq. (A.39)})} \underbrace{\int_0^{2\pi} d\phi}_{= 2\pi} \\ &= 1 \end{aligned}$$

Hence, the distribution is normalized and we can use it to calculate expectation values of relevant quantities, such as the average speed $\langle v \rangle$ of the particles, as we do in **subproblem (c)**. In Fig. 7.3 the velocity distribution of helium is shown for two temperatures, 300 K and 1,000 K respectively. We notice the asymmetry of the curves. The high velocity tail is wider than at low velocities.

$$\langle v \rangle = \int_{\text{all molecules}} v \frac{dN(v, \theta, \phi)}{N_{\text{tot}}} = 4\pi \left(\frac{m}{2\pi k_B T} \right)^{\frac{3}{2}} \int_0^\infty v^3 \exp \left(-\frac{mv^2}{2k_B T} \right) dv$$

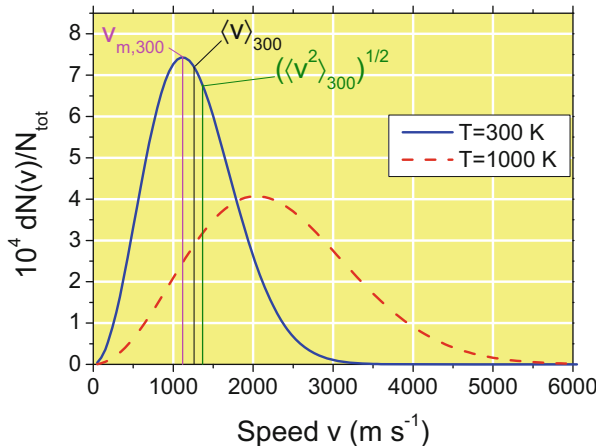


Fig. 7.3 Maxwell-Boltzmann velocity distribution for helium near room temperature (*solid line*) and at 1,000 K (*dashed line*). As shown for $T = 300$ K, the maximum of the distribution v_m , the average speed $\langle v \rangle$, and the root mean square velocity $\sqrt{\langle v^2 \rangle}$ take different values because the distribution is asymmetric

The integral is evaluated using the integral table in the appendix (Eq. (A.48)). We obtain:

$$\langle v \rangle = 4\pi \left(\frac{m}{2\pi k_B T} \right)^{\frac{3}{2}} \frac{2k_B^2 T^2}{m^2} = \left(\frac{8k_B T}{\pi m} \right)^{\frac{1}{2}} \quad (7.16)$$

The noble gas helium has an atomic mass $4m_u = 6.64 \times 10^{-27}$ kg. At a temperature of 300 K, its average speed is thus 1260 m s^{-1} . At a temperature of 1,000 K, $\langle v \rangle$ is 2300 m s^{-1} . For the mean square speed $\langle v^2 \rangle$, we obtain:

$$\langle v^2 \rangle = \int_{\text{all molecules}} v^2 \frac{dN(v, \theta, \phi)}{N_{\text{tot}}} = 4\pi \left(\frac{m}{2\pi k_B T} \right)^{\frac{3}{2}} \int_0^\infty v^4 \exp \left(-\frac{mv^2}{2k_B T} \right) dv$$

Using the integral table (Eq. (A.49)), we obtain:

$$\langle v^2 \rangle = 4\pi \left(\frac{m}{2\pi k_B T} \right)^{\frac{3}{2}} \frac{3\sqrt{\pi}}{8} \left(\frac{2k_B T}{m} \right)^{\frac{5}{2}} = \frac{3k_B T}{m} \quad (7.17)$$

At a temperature of 300 K, the mean square velocity of helium is thus $1.87 \times 10^6 \text{ m}^2 \text{ s}^{-2}$; the root mean square velocity $\sqrt{\langle v^2 \rangle}$ is 1368 m s^{-1} . At a temperature of 1,000 K, $\langle v^2 \rangle$ reaches $6.24 \times 10^6 \text{ m}^2 \text{ s}^{-2}$, and $\sqrt{\langle v^2 \rangle}$ is 2497 m s^{-1} . Equation (7.17)

is an important result by which the **average kinetic energy** is obtained:

$$\langle E_{\text{kin}} \rangle = \frac{1}{2}m\langle v^2 \rangle = \frac{3}{2}k_B T \quad (7.18)$$

This expression is related to the internal energy of a monatomic perfect gas with its three translational degrees of freedom. Moreover, the result for $\langle v^2 \rangle$ inserted into Eq. (7.2) yields the equation of state of the perfect gas: $pV = N_{\text{tot}}k_B T$. Finally, we seek the most probable velocity, i.e., the maximum of the Maxwell-Boltzmann distribution. The necessary condition for the maximum is:

$$\frac{1}{N_{\text{tot}}} \frac{dN(v)}{dv} \stackrel{!}{=} 0.$$

Insertion of Eq. (7.14) yields

$$4\pi \left(\frac{m}{2\pi k_B T} \right)^{\frac{3}{2}} \left[2v \exp\left(-\frac{mv^2}{2k_B T}\right) - \frac{mv^3}{k_B T} \exp\left(-\frac{mv^2}{2k_B T}\right) \right] \stackrel{!}{=} 0.$$

For arbitrary T and m , this requires

$$2v - \frac{mv^3}{k_B T} \stackrel{!}{=} 0$$

Therefore, the velocity distribution function is a maximum of:

$$v_m = \sqrt{\frac{2k_B T}{m}}. \quad (7.19)$$

At 300 K, the maximum value of helium is $1,117 \text{ m s}^{-1}$; at 1,000 K $v_m = 2,039 \text{ m s}^{-1}$ is obtained. Our results for v_m , $\langle v \rangle$, and $\sqrt{\langle v^2 \rangle}$ are different for a given temperature, which is also illustrated in Fig. 7.3 for $T = 300 \text{ K}$. This is caused by the asymmetry of the distribution functions.

Problem 7.2 (Maxwell-Boltzmann Distribution II)

- a. Prove that the Maxwell-Boltzmann velocity distribution Eq. (7.1) leads to a probability density distribution for the kinetic energy that does only depend on temperature and physical constants. Prove that the latter can be mapped to:

$$\frac{dN(\epsilon)}{N_{\text{tot}}} = \frac{2}{\sqrt{\pi}} e^{-\epsilon} \sqrt{\epsilon} d\epsilon \quad (7.20)$$

(continued)

Problem 7.2 (continued)

where $\epsilon = \frac{E}{k_B T}$.

- b. Plot Eq. (7.20), give an interpretation of the shape of the distribution function, and determine its maximum.
- c. Cumulative probabilities: show that the probability of a particle having a kinetic energy less than or equal to a certain threshold energy ϵ^* is:

$$W_c(0, \epsilon^*) = \int_{\epsilon < \epsilon^*} \frac{dN(\epsilon)}{N_{\text{tot}}} = \frac{4}{\sqrt{\pi}} \epsilon^{*\frac{3}{2}} \sum_{n=0}^{\infty} \frac{(-1)^n}{n!} \frac{1}{2n+3} \epsilon^{*n} \quad (7.21)$$

- d. Use Eq. (7.21) to calculate the probability that the energy of a particle exceeds the thermal energy by a factor of 2, 3, 4, 5, and 10. Alternatively, you can use the following identity with $\text{erfc}(x)$ being the *complementary error function*:

$$W_c(\epsilon^*, \infty) = \int_{\epsilon > \epsilon^*} \frac{dN(\epsilon)}{N_{\text{tot}}} = \frac{2}{\sqrt{\pi}} \sqrt{\epsilon^*} e^{-\epsilon^*} + \text{erfc}(\sqrt{\epsilon^*}) \quad (7.22)$$

Solution 7.2 In this exercise, we deal with the kinetic energy distribution of a gas. Classical mechanics relates the kinetic energy of a particle of mass m to its velocity v by means of:

$$E = \frac{1}{2}mv^2. \quad (7.23)$$

The derivation of the probability density distribution of the particles having a kinetic energy between E and $E + dE$ should thus be straightforward. In **subproblem (a)**, we start from the Maxwell-Boltzmann velocity distribution

$$\frac{dN(v)}{N_{\text{tot}}} = 4\pi \left(\frac{m}{2\pi k_B T} \right)^{\frac{3}{2}} v^2 \exp\left(-\frac{mv^2}{2k_B T}\right) dv \quad (7.24)$$

We make a substitution in the exponent according to Eq. (7.23). Moreover, we consider $dE = mv dv = p dv$ and the relation $p = \sqrt{2mE}$ between momentum p

and kinetic energy E . We obtain:

$$\begin{aligned}\frac{dN(E)}{N_{\text{tot}}} &= 4\pi \left(\frac{m}{2\pi k_B T} \right)^{\frac{3}{2}} \underbrace{\frac{2}{m} \frac{mv^2}{2}_E}_{\frac{dE}{\sqrt{2mE}}} \exp \left(-\frac{E}{k_B T} \right) \underbrace{\frac{dv}{\sqrt{2mE}}}_{\frac{dE}{\sqrt{2mE}}} \\ &= 2\pi \left(\frac{2}{m} \right)^{\frac{3}{2}} \left(\frac{m}{2\pi k_B T} \right)^{\frac{3}{2}} \exp \left(-\frac{E}{k_B T} \right) \sqrt{E} dE\end{aligned}$$

Therefore,

$$\frac{dN(E)}{N_{\text{tot}}} = 2\pi \left(\frac{1}{\pi k_B T} \right)^{\frac{3}{2}} \exp \left(-\frac{E}{k_B T} \right) \sqrt{E} dE \quad (7.25)$$

The last equation shows that the energy distribution is independent of the particle mass and only depends on temperature, as expected for a perfect gas (compare also Eq. (7.18) in Problem 7.1). The exponent suggests a special scaling of energy in units of the thermal energy $k_B T$ at an arbitrary given temperature. Thus, we define the dimensionless quantity $\epsilon = \frac{E}{k_B T}$. Accordingly, we use $dE = k_B T d\epsilon$ and obtain:

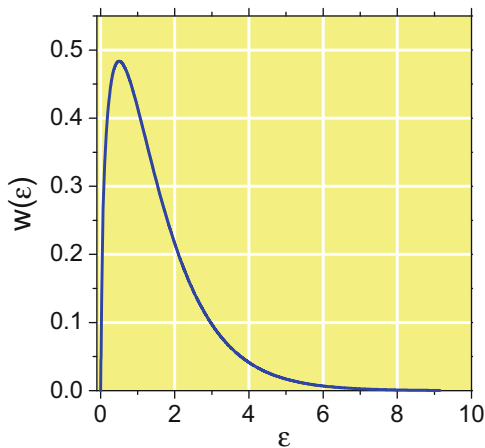
$$\begin{aligned}\frac{dN(\epsilon)}{N_{\text{tot}}} &= 2\pi \left(\frac{1}{\pi k_B T} \right)^{\frac{3}{2}} \exp(-\epsilon) \underbrace{\sqrt{\frac{E}{k_B T}}}_{\sqrt{\epsilon}} \underbrace{\sqrt{k_B T}}_{k_B T d\epsilon} \underbrace{\frac{dE}{k_B T d\epsilon}}_{\sqrt{\epsilon}} \\ &= \frac{2}{\sqrt{\pi}} e^{-\epsilon} \sqrt{\epsilon} d\epsilon\end{aligned}$$

The last line proves Eq.(7.20). The resulting probability density function

$$w(\epsilon) = \frac{2}{\sqrt{\pi}} e^{-\epsilon} \sqrt{\epsilon}, \quad (7.26)$$

to be plotted in **subproblem (b)** is shown in Fig. 7.4. The distribution is clearly asymmetric with a steeply rising probability density in the low-energy tail. Gas particles with low kinetic energy are apparently very rare in the situation of thermal equilibrium, where collisions among particles rapidly distribute the energy. A particle at rest is rapidly *kicked* by some other molecule. On the other hand, inspection of Fig. 7.4 leads to the qualitative conclusion that the number of molecules with an energy above the thermal energy ($\epsilon > 1$) is quite high and

Fig. 7.4 Probability density function for the kinetic energy ϵ of a perfect gas scaled to the thermal energy according to Eq. (7.26)



we seek quantitative results in our next steps. At first, it is easy to determine the maximum of $w(\epsilon)$ by taking the necessary condition for a maximum, i.e., the first derivative of $w(\epsilon)$ must be zero:

$$\frac{d w(\epsilon)}{d \epsilon} \stackrel{\text{Eq. (A.15)}}{=} \frac{2}{\sqrt{\pi}} \left[\frac{1}{2\sqrt{\epsilon}} - \sqrt{\epsilon} \right] e^{-\epsilon} \stackrel{!}{=} 0$$

This requires the bracket to vanish, which happens for $\epsilon_{\max} = \frac{1}{2}$, where $w(\epsilon_{\max}) = 0.48$.

Next, we deal with the calculation of *cumulative probabilities* in **subproblem (c)**, i.e., the probability that the energy of a particle falls within a certain range. For example, cumulative probabilities of particles, whose kinetic energy is higher than a specific activation energy, influence the reaction rate if one assumes that the activation of a particle is mediated by collisions. To calculate such probabilities, we have to integrate Eq. (7.26) with arbitrary integration limits, but for this purpose we must find the primitive of $w(\epsilon)$. We use a power series ansatz to calculate cumulative probabilities and start with:

$$W_c(0, \epsilon^*) = \int_{\epsilon < \epsilon^*} \frac{dN(\epsilon)}{N_{\text{tot}}} = \int_0^{\epsilon^*} w(\epsilon) d\epsilon = \int_0^{\epsilon^*} \frac{2}{\sqrt{\pi}} e^{-\epsilon} \sqrt{\epsilon} d\epsilon, \quad (7.27)$$

which gives the fraction of molecules with an energy between zero and ϵ^* . We write the exponential function as a power series (see appendix Eq. (A.55)) and obtain:

$$W_c(0, \epsilon^*) = \frac{2}{\sqrt{\pi}} \int_0^{\epsilon^*} \epsilon^{\frac{1}{2}} \sum_{n=0}^{\infty} \frac{(-1)^n \epsilon^n}{n!} d\epsilon,$$

Then, the strategy is to make the integration piecewise for every member of the sum:

$$W_c(0, \epsilon^*) = \frac{2}{\sqrt{\pi}} \sum_{n=0}^{\infty} \frac{(-1)^n}{n!} \int_0^{\epsilon^*} \epsilon^{n+\frac{1}{2}} d\epsilon, = \frac{2}{\sqrt{\pi}} \sum_{n=0}^{\infty} \frac{(-1)^n}{n!} \frac{1}{n + \frac{3}{2}} \Big|_0^{\epsilon^*}$$

We thus obtain:

$$W_c(0, \epsilon^*) = \int_{\epsilon < \epsilon^*} \frac{dN(\epsilon)}{N_{\text{tot}}} = \frac{4}{\sqrt{\pi}} \epsilon^{*\frac{3}{2}} \sum_{n=0}^{\infty} \frac{(-1)^n}{n!} \frac{1}{2n+3} \epsilon^{*n} \quad (7.28)$$

which proves Eq.(7.21). Is this equation applicable? This depends on the convergence of the series.

In **subproblem (d)**, we check this by experience. We set up a simple computer routine that, starting from the first term for $n = 0$, repeatedly calculates the next member of the series and adds it to the sum, until a certain convergence limit κ is reached. For a given index n with $a_n = \frac{(-1)^n}{n!} \frac{1}{2n+3} \epsilon^{*n}$, the next member of the sequence is easily calculated using the following method: $a_{n+1} = -\frac{a_n \epsilon^*}{(n+1)(2n+5)}$. Proceeding in this way avoids the repeated expensive calculation of factorials $n!$. If we were to choose a convergence criterion of $\kappa = 10^{-9}$, convergence would be reached after the summation up to $n = 12$ for $\epsilon^* = 1$. For larger values of ϵ^* more terms would have to be added. For $\epsilon^* = 10$ we would need to add 40 terms to reach convergence.

For values of ϵ^* up to 10, the results obtained with Eq.(7.28) are depicted in Fig. 7.5 (red curve). Starting from zero, the $W_c(0, \epsilon^*)$ raises and reaches a saturation value of 1, corresponding to the expected normalization of the probability density distribution $w(\epsilon)$. The solid curve in Fig. 7.5 illustrates the

Fig. 7.5 Cumulative probability for particles with a kinetic energy below a threshold value ϵ^* ($W_c(0, \epsilon^*)$, dashed curve), or above ϵ^* ($W_c(\epsilon^*, \infty)$, solid curve)

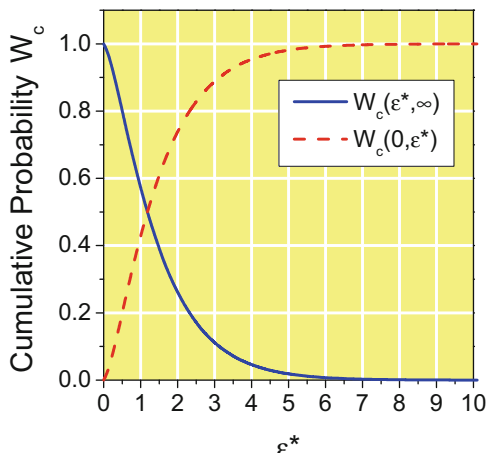


Table 7.1 Cumulative probability $W_c(\epsilon^*, \infty)$ of particles with energies above several multiples of the thermal energy, ϵ^*

ϵ^*	2	3	4	5	10
$W_c(\epsilon^*, \infty)$	0.261	0.112	0.046	0.019	1.7×10^{-4}

See also the solid curve in Fig. 7.5

reversed cumulative probability of finding a particle with kinetic energy above the threshold value, $W_c(\epsilon^*, \infty) = 1 - W_c(0, \epsilon^*)$. It is unity for $\epsilon^* = 0$ and reaches a saturation value of zero. It can be shown that $W_c(\epsilon^*, \infty)$ is obtained using Eq.(7.22). The complimentary error function $\text{erfc}(x) = 1 - \text{erf}(x)$ used in this equation is implemented by standard mathematical software packages. It is calculated numerically by a power series (see Eq.(A.60) in the appendix). Using the function $W_c(\epsilon^*, \infty)$, we can determine the sought probabilities of particles having energies above numerous threshold values. These probabilities are summarized in Table 7.1. More than 26% of the particles in a perfect gas have a kinetic energy that is twice the thermal energy at equilibrium. The energy of nearly 2% of the particles exceeds the thermal energy fivefold.

Problem 7.3 (Relative Velocity of Two Particles) In classical mechanics the kinetic energy of a particle of mass m moving at velocity v is $E = \frac{mv^2}{2}$.

- a. Prove that the total kinetic energy of two particles A and B moving with the velocities v_A and v_B can be written

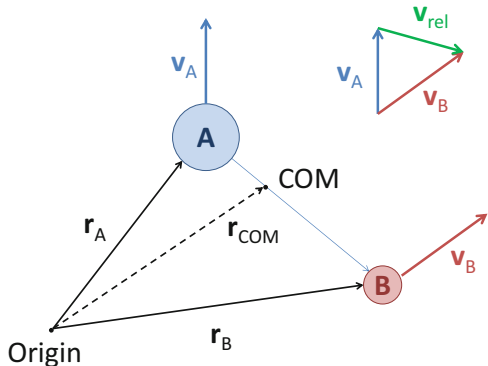
$$E_{\text{tot}} = \frac{Mv_{\text{COM}}^2}{2} + \frac{\mu v_{\text{rel}}^2}{2} \quad (7.29)$$

M is the total mass of the two particles, \mathbf{v}_{COM} is the velocity vector of their center of mass, $\mathbf{v}_{\text{rel}} = \mathbf{v}_B - \mathbf{v}_A$ is the relative velocity vector, and μ is the effective mass (Eq.(7.4)).

- b. Based on Eq.(7.29) and the Maxwell-Boltzmann velocity distribution for both types of particles, determine the mean relative velocity $\langle v_{AB} \rangle$.

Solution 7.3 This problem is related to interatomic or intermolecular collision rates (Sect. 7.1.3, Eqs. (7.3) and (7.6) respectively). In **subproblem (a)**, we use classical mechanics and vector calculus to prove that the kinetic energy of two particles A and B moving with the velocity vectors \mathbf{v}_A and \mathbf{v}_B can be written as the sum of the

Fig. 7.6 Center of mass (COM) and relative velocity of two particles A and B located at $\mathbf{r}_A(t)$ and $\mathbf{r}_B(t)$ moving with velocities \mathbf{v}_A and \mathbf{v}_B



kinetic energy of their center of mass (COM),

$$\mathbf{r}_{\text{COM}}(t) = \frac{m_A \mathbf{r}_A(t) + m_B \mathbf{r}_B(t)}{m_A + m_B}, \quad (7.30)$$

and a second kinetic energy term containing the relative velocity squared of the two particles and an effective mass μ . The situation is illustrated in Fig. 7.6. The center of mass is located between the two particles. Its velocity vector is obtained by differentiation of Eq. (7.30):

$$\mathbf{v}_{\text{COM}} = \frac{d \mathbf{r}_{\text{COM}}(t)}{dt} = \frac{m_A \mathbf{v}_A(t) + m_B \mathbf{v}_B(t)}{M}, \quad (7.31)$$

The total kinetic energy of the two particles, on the one hand, is the sum of the individual kinetic energies of the particles, i.e.,

$$E_{\text{tot}} = \frac{m_A v_A^2}{2} + \frac{m_B v_B^2}{2} \quad (7.32)$$

We could start from this last expression by ingeniously expanding both fractions, but it seems easier to start from the right-hand side of Eq. (7.29):

$$\begin{aligned} \frac{M v_{\text{COM}}^2}{2} + \frac{\mu v_{\text{rel}}^2}{2} &\stackrel{\text{Eq. (7.31)}}{=} \frac{M}{2} \left(\frac{m_A}{M} \mathbf{v}_A + \frac{m_B}{M} \mathbf{v}_B \right)^2 + \frac{1}{2} \frac{m_A m_B}{M} (\mathbf{v}_B - \mathbf{v}_A)^2 \\ &= \frac{M}{2} \left(\frac{m_A^2}{M^2} v_A^2 + \frac{m_B^2}{M^2} v_B^2 + \frac{2 m_A m_B}{M^2} \mathbf{v}_A \mathbf{v}_B \right) \\ &\quad + \frac{m_A m_B}{2M} (v_A^2 + v_B^2 - 2 \mathbf{v}_A \mathbf{v}_B) \end{aligned}$$

The two terms containing the scalar product $\mathbf{v}_A \mathbf{v}_B$ cancel each other out. We obtain:

$$\begin{aligned}
\frac{M v_{\text{COM}}^2}{2} + \frac{\mu v_{\text{rel}}^2}{2} &= \frac{1}{2} \left(\frac{m_A^2}{M} v_A^2 + \frac{m_B^2}{M} v_B^2 + \frac{m_A m_B}{M} v_A^2 + \frac{m_A m_B}{M} v_B^2 \right) \\
&= \frac{1}{2} \left(\frac{m_A^2}{M} + \frac{m_A m_B}{M} \right) v_A^2 + \frac{1}{2} \left(\frac{m_B^2}{M} + \frac{m_A m_B}{M} \right) v_B^2 \\
&= \frac{m_A}{2} \left(\frac{m_A + m_B}{M} \right) v_A^2 + \frac{m_B}{2} \left(\frac{m_A + m_B}{M} \right) v_B^2 \\
&= \frac{m_A v_A^2}{2} + \frac{m_B v_B^2}{2} \\
&\stackrel{\text{Eq. (7.32)}}{=} E_{\text{tot}}
\end{aligned}$$

It is worth mentioning that Eq. (7.29), which we have just proven, is used extensively in the treatment of two-body problems.¹ Usually, the origin in Fig. 7.6 in the center of mass is chosen and thus a separation from the kinetic energy of the center of mass from the energy of the *internal* degrees of freedom.

In **subproblem (b)** the mean relative velocity $\langle v_{AB} \rangle$ is computed under the assumption of the Maxwell-Boltzmann velocity distribution Eq. (7.1) for both types of particles. The relative velocity is:

$$v_{AB} = |\mathbf{v}_B - \mathbf{v}_A| = \sqrt{(v_{B,x} - v_{A,x})^2 + (v_{B,y} - v_{A,y})^2 + (v_{B,z} - v_{A,z})^2}. \quad (7.33)$$

The expectation value is thus obtained:

$$\begin{aligned}
\langle v_{AB} \rangle &= \left(\frac{m_A}{2\pi k_B T} \right)^{\frac{3}{2}} \left(\frac{m_B}{2\pi k_B T} \right)^{\frac{3}{2}} \iiint_A \iiint_B dv_{A,x} dv_{A,y} dv_{A,z} dv_{B,x} dv_{B,y} dv_{B,z} \\
&\quad \sqrt{(v_{B,x} - v_{A,x})^2 + (v_{B,y} - v_{A,y})^2 + (v_{B,z} - v_{A,z})^2} \\
&\quad e^{\left[-\frac{m_A(v_{A,x}^2 + v_{A,y}^2 + v_{A,z}^2)}{2k_B T} \right]} e^{\left[-\frac{m_B(v_{B,x}^2 + v_{B,y}^2 + v_{B,z}^2)}{2k_B T} \right]}
\end{aligned} \quad (7.34)$$

where the triple integral over all Cartesian velocity components of the particles A and B is from $-\infty$ to $+\infty$ respectively. In the next step, we make a transformation from the six Cartesian velocity components of particle A and particle B to the three velocity components of the center of mass, $v_{\text{COM},x}$, $v_{\text{COM},y}$, $v_{\text{COM},z}$, and the three

¹Text book examples of two-body problems are, for example, the hydrogen problem or the rigid rotator.

relative velocity components $v_{\text{rel},x}$, $v_{\text{rel},y}$, and $v_{\text{rel},z}$:

$$v_{\text{COM},i} = \frac{m_A v_{\text{A},i} + m_B v_{\text{B},i}}{m_A + m_B} \quad i = x, y, z \quad (7.35)$$

$$v_{\text{AB},i} = v_{\text{B},i} - v_{\text{A},i} \quad i = x, y, z \quad (7.36)$$

The apparent advantage is that the root in Eq. (7.34) only contains the three relative velocity components. Based on the results of subproblem (a), the Boltzmann factors can be transformed in:

$$\begin{aligned} & \exp \left[-\frac{m_A (v_{\text{A},x}^2 + v_{\text{A},y}^2 + v_{\text{A},z}^2)}{2k_B T} \right] \exp \left[-\frac{m_B (v_{\text{B},x}^2 + v_{\text{B},y}^2 + v_{\text{B},z}^2)}{2k_B T} \right] \\ &= \exp \left[-\frac{M (v_{\text{COM},x}^2 + v_{\text{COM},y}^2 + v_{\text{COM},z}^2)}{2k_B T} \right] \exp \left[-\frac{\mu (v_{\text{AB},x}^2 + v_{\text{AB},y}^2 + v_{\text{AB},z}^2)}{2k_B T} \right] \end{aligned} \quad (7.37)$$

Finally, we must consider the differentials. Evaluation of the *Jacobian* (see appendix Sect. A.3.6.1) yields the result that:

$$dv_{\text{A},x} dv_{\text{A},y} dv_{\text{A},z} dv_{\text{B},x} dv_{\text{B},y} dv_{\text{B},z} = dv_{\text{COM},x} dv_{\text{COM},y} dv_{\text{COM},z} dv_{\text{AB},x} dv_{\text{AB},y} dv_{\text{AB},z}$$

To prove this, we consider, for example, the x components $v_{\text{COM},x}$ and $v_{\text{AB},x}$. With Eqs. (7.35) and (7.36) we obtain:

$$\frac{\partial (v_{\text{COM},x}, v_{\text{AB},x})}{\partial (v_{\text{A},x}, v_{\text{B},x})} = \begin{vmatrix} \frac{\partial v_{\text{COM},x}}{\partial v_{\text{A},x}} & \frac{\partial v_{\text{AB},x}}{\partial v_{\text{A},x}} \\ \frac{\partial v_{\text{COM},x}}{\partial v_{\text{B},x}} & \frac{\partial v_{\text{AB},x}}{\partial v_{\text{B},x}} \end{vmatrix} = \begin{vmatrix} \frac{m_A}{m_A + m_B} & -1 \\ \frac{m_B}{m_A + m_B} & +1 \end{vmatrix} = \frac{m_A + m_B}{m_A + m_B} = 1 \quad (7.38)$$

For the other components, we obtain the same results and thus the entire Jacobian is unity. Therefore, we can separate the triple integral for the center of mass velocity components and obtain:

$$\begin{aligned} \langle v_{\text{AB}} \rangle &= \frac{(m_A m_B)^{\frac{3}{2}}}{(2\pi k_B T)^3} \iiint_{\text{COM}} e^{-\frac{M(v_{\text{COM},x}^2 + v_{\text{COM},y}^2 + v_{\text{COM},z}^2)}{2k_B T}} dv_{\text{COM},x} dv_{\text{COM},y} dv_{\text{COM},z} \\ &\quad \iiint_{\text{AB}} \sqrt{v_{\text{AB},x}^2 + v_{\text{AB},y}^2 + v_{\text{AB},z}^2} e^{-\frac{\mu(v_{\text{AB},x}^2 + v_{\text{AB},y}^2 + v_{\text{AB},z}^2)}{2k_B T}} dv_{\text{AB},x} dv_{\text{AB},y} dv_{\text{AB},z} \end{aligned} \quad (7.39)$$

The boundaries of the triple integrals are again $-\infty$ and ∞ for each component. The first triple integral for the center of mass components can be further separated into Gaussian integrals (see appendix Sect. A.3.7) for the Cartesian

components:

$$\int_{-\infty}^{\infty} e^{-\frac{M}{2k_B T} v_{\text{COM},i}^2} dv_{\text{COM},i} \stackrel{\text{Eq. (A.46)}}{=} \frac{\sqrt{\pi}}{\sqrt{\frac{M}{2k_B T}}} = \sqrt{\frac{2\pi k_B T}{M}} \quad i = x, y, z$$

Thus, we obtain

$$\langle v_{AB} \rangle = \frac{(m_A m_B)^{\frac{3}{2}}}{(2\pi k_B T)^3} \left(\frac{2\pi k_B T}{M} \right)^{\frac{3}{2}} \iiint_{AB} \sqrt{v_{AB,x}^2 + v_{AB,y}^2 + v_{AB,z}^2} e^{-\frac{\mu(v_{AB,x}^2 + v_{AB,y}^2 + v_{AB,z}^2)}{2k_B T}} dv_{AB,x} dv_{AB,y} dv_{AB,z} \quad (7.40)$$

The triple integral for the relative velocity components can be separated if we transform from Cartesian to spherical coordinates v_{AB} , θ , and ϕ . Because $\sqrt{v_{AB,x}^2 + v_{AB,y}^2 + v_{AB,z}^2} = v_{AB}$ and $dv_{AB,x} dv_{AB,y} dv_{AB,z} = v_{AB}^2 dv_{AB} d\theta d\phi$

$$\begin{aligned} \langle v_{AB} \rangle &= \left(\frac{\mu}{2\pi k_B T} \right)^{\frac{3}{2}} \int_0^\infty v_{AB}^3 e^{-\frac{\mu}{2k_B T} v_{AB}^2} dv_{AB} \underbrace{\int_0^\pi \sin \theta d\theta}_{2} \underbrace{\int_0^{2\pi} d\phi}_{2\pi} \\ &= 4\pi \left(\frac{\mu}{2\pi k_B T} \right)^{\frac{3}{2}} \int_0^\infty v_{AB}^3 e^{-\frac{\mu}{2k_B T} v_{AB}^2} dv_{AB} \end{aligned}$$

The remaining integral for the radial velocity component can be evaluated with Eq. (A.48) from the appendix:

$$\int_0^\infty v_{AB}^3 e^{-\frac{\mu}{2k_B T} v_{AB}^2} dv_{AB} = 2 \left(\frac{k_B T}{\mu} \right)^2$$

Hence, the expression for the mean relative velocity is

$$\langle v_{AB} \rangle = 4\pi \left(\frac{\mu}{2\pi k_B T} \right)^{\frac{3}{2}} 2 \left(\frac{k_B T}{\mu} \right)^2 = \left(\frac{8k_B T}{\pi\mu} \right)^{\frac{1}{2}} \quad (7.41)$$

which is identical to Eq. (7.7).

Problem 7.4 (Collision Rates in a Helium-Xenon Gas Mixture)

Assume the perfect gas behavior of helium and xenon and calculate both the individual collision rates and the mean free path of both species for a 50:50 mixture at room temperature with a total pressure of 1×10^{-8} , 0.1, and 10^5 Pa. The van der Waals radii of helium and xenon are 140 pm and 216 pm respectively.

Solution 7.4 Picking up the example of a gas mixture of helium and xenon, this exercise gives us an idea of the collision rates occurring in a gas at different pressures, and, moreover, the mean free paths. Such quantities are of importance, for example, for the characterization of transport processes in the gas, which depend significantly on pressure. If we assume perfect gas behavior for both species, we can relate the particle density to the total pressure by means of:

$$\mathcal{N}_{\text{He}} = \mathcal{N}_{\text{Xe}} = \frac{P_{\text{tot}}}{2k_B T}.$$

Note that both species are equally abundant and that their partial pressures are thus half the total pressure. At $P_{\text{tot}} = 1 \times 10^{-8}$ Pa we have the conditions of *ultrahigh vacuum* (UHV). We obtain $\mathcal{N}_{\text{He}} = \mathcal{N}_{\text{Xe}} = \mathcal{N} = 1.22 \times 10^{12} \text{ m}^{-3}$. For $P_{\text{tot}} 0.1$ Pa, we have the conditions of *medium vacuum*, where the particle densities take a value of $1.22 \times 10^{19} \text{ m}^{-3}$. Under the conditions of atmospheric pressure, we have $\mathcal{N} = 1.22 \times 10^{25} \text{ m}^{-3}$.

Equations for the collision rates and the mean free path were provided in Sect. 7.1.3. Collisions may occur between helium and helium, xenon and xenon, and helium and xenon. The cross-sections for these collisions can be estimated using the *hard sphere* model (Fig. 7.2) and the given van der Waals radii. If d_{AB} is the sum of the radii of two collision partners A and B, then the hard sphere collision cross-section is $\sigma_{AB} = \pi d_{AB}^2$. Thus,

$$\sigma_{\text{He Xe}} = \pi (r_{\text{He}} + r_{\text{Xe}})^2 = 3.982 \times 10^{-19} \text{ m}^2.$$

In the same way, we obtain $\sigma_{\text{He He}} = 2.463 \times 10^{-19} \text{ m}^2$ and $\sigma_{\text{Xe Xe}} = 5.863 \times 10^{-19} \text{ m}^2$.

In the next step, we need to calculate the effective masses needed in turn for the evaluation of the mean relative velocities (Eq. (7.7)). From the periodic system of the elements we take the atomic weights 4.00 amu for helium, and 131.29 amu for xenon. Thus, we have $\mu_{\text{He Xe}} = \frac{m_{\text{He}} m_{\text{Xe}}}{m_{\text{He}} + m_{\text{Xe}}} = 3.88$ amu, $\mu_{\text{He He}} = 2$ amu, and $\mu_{\text{Xe Xe}} = 65.65$ amu respectively. From the appendix Sect. A.1, we take the value of one atomic mass unit, 1 amu = $1.660538921(73) \times 10^{-27}$ kg. For room temperature (298 K) we obtain the mean relative velocity for helium:

$$\langle v_{\text{He He}} \rangle = \left(\frac{8k_B T}{\pi \mu_{\text{He He}}} \right)^{\frac{1}{2}} = \left(\frac{8 \times 1.38065 \times 10^{-23} \text{ J K}^{-1} \times 298 \text{ K}}{\pi \times 2 \times 1.66054 \times 10^{-27} \text{ kg}} \right)^{\frac{1}{2}} = 1776 \text{ m s}^{-1}.$$

In the same way, we obtain $\langle v_{\text{Xe Xe}} \rangle = 310 \text{ m s}^{-1}$, and $\langle v_{\text{He Xe}} \rangle = 1275 \text{ m s}^{-1}$. The individual collision rates z_{AB} can be evaluated using Eq. (7.6):

$$z_{\text{AB}} = \sigma_{\text{AB}} \langle v_{\text{AB}} \rangle \mathcal{N}$$

where \mathcal{N} is the particle density of the collision partner. Inserting the cross-sections, mean relative velocities and particle densities, we obtain $z_{\text{He He}} = 5.33 \times 10^{-4} \text{ s}^{-1}$ under ultrahigh vacuum conditions, $5.33 \times 10^3 \text{ s}^{-1}$ under medium vacuum, and $5.33 \times 10^9 \text{ s}^{-1}$ at atmospheric pressure. Similarly, for collisions among xenon atoms, we have $z_{\text{Xe Xe}} = 2.22 \times 10^{-4} \text{ s}^{-1}$, $2.22 \times 10^3 \text{ s}^{-1}$, and $2.22 \times 10^9 \text{ s}^{-1}$ for UHV, medium vacuum, and atmospheric pressure respectively. For collisions of helium and xenon we obtain $z_{\text{He Xe}} = 6.19 \times 10^{-4} \text{ s}^{-1}$, $6.19 \times 10^3 \text{ s}^{-1}$, and $6.19 \times 10^9 \text{ s}^{-1}$ for UHV, medium vacuum, and atmospheric pressure respectively.

Having obtained these collision rates, we can determine the mean free path for both species under the various conditions according to Eq. (7.8):

$$\lambda_{\text{He}} = \frac{\langle v_{\text{He}} \rangle}{z_{\text{He He}} + z_{\text{He Xe}}} \quad (7.42)$$

$$\lambda_{\text{Xe}} = \frac{\langle v_{\text{Xe}} \rangle}{z_{\text{Xe Xe}} + z_{\text{He Xe}}} \quad (7.43)$$

The mean velocities of helium and xenon are calculated using Eq. (7.16) and the respective atomic masses: $\langle v_{\text{He}} \rangle = 1256 \text{ m s}^{-1}$, $\langle v_{\text{Xe}} \rangle = 219 \text{ m s}^{-1}$. The resulting values for λ_{He} and λ_{Xe} at various pressures can be found in Table 7.2.

Under all pressure conditions, helium has a fourfold larger mean free path than xenon. Under ultrahigh vacuum conditions (10^{-8} Pa), the mean free paths are very large, much larger than the extension of every vacuum recipient. At 10^{-1} Pa , however, the mean free paths have values that are comparable with the tube diameters of vacuum equipment. It is worth mentioning that in fluid mechanics, the so-called *Knudsen number*

$$\text{Kn} = \frac{\lambda}{l} \quad (7.44)$$

is used to characterize the flow within vacuum components of extension l by comparison with the mean free path. Under ambient pressure conditions (10^5 Pa), the mean free path is within the submicrometer range. Under such conditions, collisions between particles markedly influence spectroscopic line profiles (coll-

Table 7.2 Mean free path of helium and xenon in a 50:50 mixture at room temperature and various pressure conditions

Pressure (Pa)	$\lambda_{\text{He}} (\text{m})$	$\lambda_{\text{Xe}} (\text{m})$
10^{-8}	1.09×10^6	2.6×10^5
10^{-1}	1.09×10^{-1}	2.6×10^{-2}
10^5	1.09×10^{-7}	2.6×10^{-8}

sional broadening). Another application is related to the above-mentioned transport processes, e.g., heat conduction. To be efficient, heat conduction requires many collisions between gas particles. In an ultrahigh vacuum where the mean free path exceeds the typical extensions of vacuum equipment by orders of magnitude, heat conduction mediated by particle collisions is thus largely suppressed. Under these conditions, heat transfer based on radiation is the only effective process. In Problem 9.3 this situation is considered in more detail.

Problem 7.5 (Gas Effusion) Consider a perfect gas in equilibrium at a temperature of T . Through a small sharp-edged orifice of area A gas effuses from the compartment into a vacuum if a shutter is opened (see Fig. 7.7). The particle density is so low that the mean free path is large compared with the orifice diameter. A particle detector is situated at a distance d in axial alignment with the orifice.

- Starting from the Maxwell-Boltzmann distribution function (Eq. (7.1)), show that the velocity distribution function of the effusing molecular beam is

$$\frac{dN(v)}{N} = \frac{m^2}{2k_B^2 T^2} \exp\left(-\frac{mv^2}{2k_B T}\right) v^3 dv \quad (7.45)$$

- N is the number of particles in the beam, and $dN(v)$ is the number of particles with velocity between v and $v + dv$.
- Based on Eq. (7.45) derive a distribution function for the kinetic energy in the beam (see Problem 7.2). What is the mean kinetic energy in the molecular beam leaving the cell? Why are these distribution functions different from the Maxwell-Boltzmann functions?
 - Based on Eq. (7.45) derive an expression for the time-of-flight (TOF) distribution function of particles arriving at the detector at a time t after the shutter was opened for a very short time, negligible compared with the TOF. Assume neon at a temperature of 400 K and calculate the arrival of the TOF peak at $d = 0.5, 1.0$, and 1.5 m. Also, calculate the vertical shift of the beam due to gravitation.

Solution 7.5 In this exercise, we work out the principle of a simple method of molecular beam formation: effusion. The so-called **Knudsen effusion cells** are widely used in molecular beam epitaxy to grow thin films on surfaces or to investigate molecular beam reactive scattering in surface catalysis.

In **subproblem (a)**, our aim is to establish the velocity distribution of the particles emitted through the orifice. Equation (7.45) is not identical to the Maxwell-Boltzmann velocity distribution, as would perhaps be expected at first sight. To see

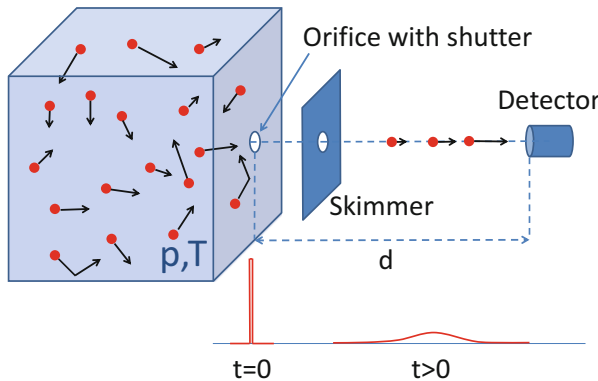


Fig. 7.7 Sketch of an effusion cell experiment with an axially aligned particle detector analyzing the molecular beam. The skimmer selects only particles moving in an axial direction

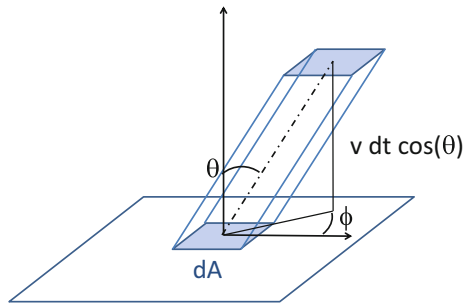
this, we have to recapitulate the derivation of the total impingement rate on a surface area element dA , which is part of the orifice area. All particles impinging on this area leave the compartment if the shutter is opened. Because the mean free path is larger than the orifice extension, we can assume that there will be no collisions among the particles. Hence, a particle with velocity between v and $v + dv$ coming from a direction characterized by a polar angle between θ and $\theta + d\theta$ and an azimuthal angle between ϕ and $\phi + d\phi$ leaves the orifice with only these values. Using results from Problem 7.1, we use the Maxwell-Boltzmann distribution in spherical coordinates:

$$\frac{dN(v, \theta, \phi)}{N_{\text{tot}}} = \left(\frac{m}{2\pi k_B T} \right)^{\frac{3}{2}} \exp \left(-\frac{mv^2}{2k_B T} \right) v^2 \sin \theta \, dv \, d\theta \, d\phi \quad (7.46)$$

This gives us the effective number of particles with only this particular velocity and direction. If we put the origin in the center of the surface element dA as illustrated in Fig. 7.8, we can narrow down the number of particles that hit the surface element within the time dt . First, the polar angle θ must take values between 0 (perpendicular impingement) and $\frac{\pi}{2}$ (extreme grazing incidence). Second, dependent on its velocity, the distance a particle moves within a time interval between t and $t + dt$ is $v dt$. Hence, a particle with this speed only hits the surface element if it is within the prism volume shown in Fig. 7.8. Its volume is $dV = v \cos(\theta) dt dA$. The number of particles with speed v and direction within this prism is therefore:

$$dN(v, \theta, \phi) = \frac{N_{\text{tot}}}{V} \left(\frac{m}{2\pi k_B T} \right)^{\frac{3}{2}} \exp \left(-\frac{mv^2}{2k_B T} \right) v^2 \sin \theta \, dv \, d\theta \, d\phi \underbrace{v dt dA \cos \theta}_{dV}, \quad (7.47)$$

Fig. 7.8 Derivation of the number of particles with velocity between v and $v + dv$ impinging on a surface area element dA within the time interval between t and $t + dt$ from a polar angle between θ and $\theta + d\theta$ and an azimuthal angle between ϕ and $\phi + d\phi$



where V is the compartment volume and $\frac{N_{\text{tot}}}{V}$; thus, the number density \mathcal{N} . If we integrate this expression, we obtain the total impingement rate:

$$\begin{aligned} \frac{N}{dA dt} &= \int_0^\infty dv \int_0^{2\pi} d\phi \int_0^{\frac{\pi}{2}} d\theta \mathcal{N} \left(\frac{m}{2\pi k_B T} \right)^{\frac{3}{2}} e^{-\frac{mv^2}{2k_B T}} v^3 \sin \theta \cos \theta \\ &= \mathcal{N} \left(\frac{m}{2\pi k_B T} \right)^{\frac{3}{2}} \underbrace{\int_0^\infty e^{-\frac{mv^2}{2k_B T}} v^3 dv}_{\substack{\text{Eq. (A.48)} \\ = 2\left(\frac{k_B T}{m}\right)^{\frac{1}{2}}}} \underbrace{\int_0^{2\pi} d\phi \int_0^{\frac{\pi}{2}} \sin \theta \cos \theta d\theta}_{= 2\pi} \underbrace{\frac{1}{2}}_{\substack{\text{Eq. (A.41)}}} \\ &= \mathcal{N} \left(\frac{k_B T}{2\pi m} \right)^{\frac{1}{2}} \end{aligned}$$

which is in accordance with Eq. (7.9). If we omit in the last step the integration over the velocity, we obtain the impingement rate of all particles with velocities between v and $v + dv$:

$$\frac{dN(v)}{dA dt} = \pi \mathcal{N} \left(\frac{m}{2\pi k_B T} \right)^{\frac{3}{2}} e^{-\frac{mv^2}{2k_B T}} v^3 dv \quad (7.48)$$

If we divide $\frac{dN(v)}{dA dt}$ by the total impingement rate obtained above, we obtain an expression for the velocity distribution:

$$\frac{dN(v)}{N} = \pi \frac{\left(\frac{m}{2\pi k_B T} \right)^{\frac{3}{2}}}{\left(\frac{k_B T}{2\pi m} \right)^{\frac{1}{2}}} e^{-\frac{mv^2}{2k_B T}} v^3 dv = \frac{m^2}{2k_B^2 T^2} e^{-\frac{mv^2}{2k_B T}} v^3 dv \quad (7.49)$$

which is simply Eq.(7.45). The distribution function is normalized, which is easily seen if we integrate it over the entire velocity range using Eq.(A.48) from the integral table. The essential difference between this velocity distribution and the Maxwell-Boltzmann distribution Eq.(7.46) is the cubic factor for velocity. Therefore, compared with the Maxwell-Boltzmann distribution valid for the gas

particles within the effusion cell volume, more particles with higher velocity reach the orifice and are emitted if the shutter is opened. Thus, the velocity distribution of the particles leaving the cell through the orifice is non-Maxwellian.

In **subproblem (b)**, we find the kinetic energy distribution compatible with Eq. (7.45), similar to what we have done for the Maxwell-Boltzmann distribution in problem 7.2. If $E = \frac{1}{2}mv^2$ is the kinetic energy and $p = mv$ the momentum of a particle, $dE = p\,dv$. Therefore, Eq. (7.45) can be written in the following way:

$$\begin{aligned}\frac{dN(v)}{N} &= \frac{m}{k_B T} \frac{mv^2}{2k_B T v^2} e^{-\frac{mv^2}{2k_B T}} v^3 \underbrace{\frac{dv}{\frac{dE}{p}}}_{\frac{dp}{m}} \\ &= \frac{m}{k_B T} \frac{E}{k_B T} \underbrace{\frac{v}{\frac{p}{m}}}_{\frac{v}{m}} \frac{dE}{p}.\end{aligned}$$

Thus,

$$\frac{dN(E)}{N} = \frac{1}{k_B T} \frac{E}{k_B T} e^{-\frac{E}{k_B T}} dE. \quad (7.50)$$

We now scale the energy to the thermal energy introducing $\epsilon = \frac{E}{k_B T}$. With $dE = k_B T d\epsilon$ we obtain the simple expression

$$\frac{dN(\epsilon)}{N} = w(\epsilon) = \exp(-\epsilon) \epsilon d\epsilon. \quad (7.51)$$

Apparently, the kinetic energy distribution of molecular beam effusing through the orifice only depends on the temperature, and not on the particle mass. It is instructive to compare $w(\epsilon)$ with the corresponding function from the Maxwell-Boltzmann distribution (Eq. (7.20)) from Problem 7.2, i.e., with the kinetic energy distribution within the compartment.

Both functions are shown in Fig. 7.9. Already a qualitative inspection shows that the molecular beam leaving the compartment has a higher mean kinetic energy. This is consistent with our above interpretation of the velocity distribution function. We obtain the most probable kinetic energy ϵ_{\max} by setting the first derivative of $w(\epsilon)$ to zero:

$$\left. \frac{dw(\epsilon)}{d\epsilon} \right|_{\epsilon=\epsilon_{\max}} = \exp(-\epsilon_{\max}) (1 - \epsilon_{\max}^2) \stackrel{!}{=} 0$$

Thus, $\epsilon_{\max} = 1$. In Problem 7.2 we found $\epsilon_{\max} = \frac{1}{2}$ for the Maxwell-Boltzmann distribution. Thus, the most probable kinetic energy of the particles leaving the orifice, the peak of $w(\epsilon)$ in Fig. 7.9 is twice the peak value of the kinetic energy in the compartment. Furthermore, we calculate the mean kinetic energy $\langle \epsilon \rangle$ of the

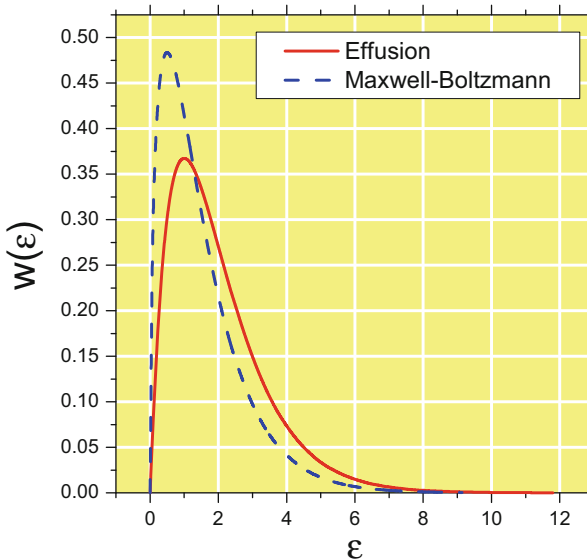


Fig. 7.9 Comparison between the kinetic energy distribution function of a molecular beam leaving the effusion cell (solid line) and the kinetic energy distribution within the compartment (dashed line, see Problem 7.2)

particles in the molecular beam. This is:

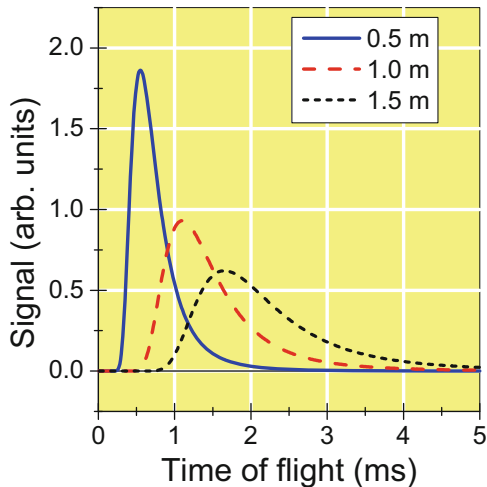
$$\langle \epsilon \rangle = \int_0^\infty \epsilon w(\epsilon) d\epsilon = \int_0^\infty \epsilon^2 e^{-\epsilon} d\epsilon$$

$$\stackrel{\text{Eq. (A.44)}}{=} e^{-\epsilon} (-\epsilon^2 + 2\epsilon - 2) \Big|_0^\infty = 2$$

Hence, the mean kinetic energy of the particles in the molecular beam at a given temperature is $2k_B T$. Again, this value is larger than the mean kinetic energy of the particles in the compartment of $\frac{3}{2}k_B T$ (see Eq. (7.18) in Problem 7.1).

In **subproblem (c)** we deal with the TOF of a pulse of particles leaving the compartment if the shutter is opened instantaneously for a very short period at time $t = 0$. The situation is shown in Fig. 7.7. We can assume that the particle beam at $t = 0$ is a *delta* peak, i.e., an arbitrarily sharp peak. Because faster particles need a shorter time to cover the distance between the orifice and the detector than slower ones, the pulse expands and thus changes its profile. To determine the TOF profile, we must transform the velocity distribution into a TOF distribution. If d is the distance covered by a particle arriving between time t and $t + dt$, its velocity is $v = \frac{d}{t}$ and thus $dv = -\frac{d}{t^2} dt$. Therefore, we can rewrite

Fig. 7.10 Time of flight distribution of a group of particles at different distances from the detector



Eq. (7.45):

$$\frac{dN(v(t))}{N} = -\frac{m^2}{2k_B^2 T^2} \exp\left[-\frac{m}{2k_B T} \left(\frac{d}{t}\right)^2\right] \left(\frac{d}{t}\right)^3 \frac{d}{t^2} dt \quad (7.52)$$

The negative sign compensates for the fact that an increase in velocity by a positive dv involves a negative dt . Defining a parameter $\alpha = \sqrt{\frac{m}{2k_B T}}$, we use the last expression to obtain the rate at which particles arrive at the detector at a given time t :

$$\frac{dN(t)}{dt} = -\frac{2Nd^4}{\alpha^4 t^5} \exp\left(-\frac{d^2}{\alpha^2 t^2}\right) \quad (7.53)$$

The detector counts the incoming particles per period of time; thus, we assume that the detector signal is proportional to this rate.² Thus, the detector signal, $S(t)$, is:

$$S(t) = c \frac{d^4}{\alpha^4 t^5} \exp\left(-\frac{d^2}{\alpha^2 t^2}\right), \quad (7.54)$$

where c is a constant. $S(t)$ is plotted in Fig. 7.10 for the case of neon (atomic mass $m = 20.18$ amu), a temperature of 400 K, and three different distances. With increasing distance, the TOF profile becomes broader and its maximum moves, as expected, to longer arrival times. We could look up the respective peak values or obtain an expression for the position t_{\max} of the TOF peak at which the first

²In practice, the detector sensitivity is a function of the velocity, with the tendency to decrease as v increases.

derivative of $S(t)$ becomes zero:

$$S(t_{\max}) = c \frac{d^4}{\alpha^4 t_{\max}^5} \exp\left(-\frac{d^2}{\alpha^2 t_{\max}^2}\right) \left[\frac{2d^2}{\alpha^2 t_{\max}^8} - \frac{5}{t_{\max}^6} \right] \stackrel{!}{=} 0 \quad (7.55)$$

We thus obtain:

$$t_{\max} = \sqrt{\frac{2}{5}} \frac{d}{\alpha} \quad (7.56)$$

With $\alpha = 574.12$ for the given conditions, we thus locate the TOF peaks at 0.55 ms for $d = 0.5$ m, 1.10 ms for $d = 1.0$ m, and 1.65 ms for $d = 1.5$ m, corresponding to a velocity of 909 m s^{-1} . Finally, it is instructive to check whether gravitational effects have a significant influence on the trajectories of the particles between shutter and detector. Given the gravity acceleration of $g = 9.81 \text{ m s}^{-2}$, the vertical shift after the time t is given by $y = \frac{1}{2}gt^2$. If we insert the above values for the TOF, we obtain a vertical shift of 1.5×10^{-6} m at distance of 0.5 m, 5.9×10^{-6} m at $d = 1$ m, and 1.3×10^{-5} m at $d = 1.5$ m. Gravitational effects are therefore negligible under these conditions.

Problem 7.6 (Film Growth) Water vapor (partial pressure of 1×10^{-5} Pa, gas temperature 300 K) condenses on a cold surface and freezes as amorphous ice (density $\rho = 0.94 \text{ g cm}^{-3}$). If each molecule impinging on the surface sticks to it, how long does it take to grow an ice film 1 μm thick?

Solution 7.6 In this exercise, we deal with the growth of an amorphous ice film on a cold surface. Within kinetic theory, it is possible to include time in considerations of changes of state—a point that is excluded in an analysis based on thermodynamics in Chap. 3. The goal is to calculate the time t to grow an ice film 1 μm thick on a cold surface, given the gas phase partial pressure p and temperature T . The problem is a simple application of the relation of the impingement rate Eq. (7.10), which gives the relation between the number of particles impinging on a surface per second and per m^2 , and the gas temperature and partial pressure of the particles. We may assume that each particle that hits the surface sticks to it—an assumption that in the case of ice is valid at cryogenic temperature below 100 K. Under these conditions H_2O freezes as amorphous ice (see Fig. 7.11). At first, we calculate the number of H_2O molecules forming a $d = 1 \mu\text{m}$ thick ice film with an area of, say, $A = 1 \text{ m}^2$. Because the density is

$$\rho = \frac{m}{V} = \frac{m}{A d}, \quad (7.57)$$

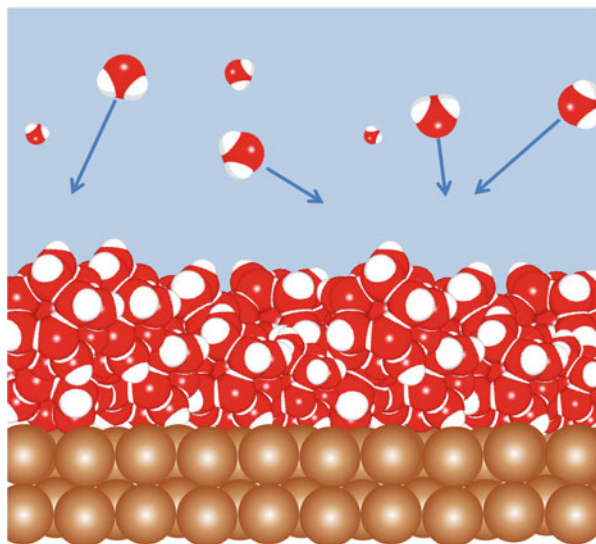


Fig. 7.11 Water molecules impinging on a surface form a film of amorphous ice

this film has the mass $m = \rho A d$, corresponding to an amount

$$n = \frac{m}{M_{\text{H}_2\text{O}}} = \frac{\rho A d}{M_{\text{H}_2\text{O}}} \quad (7.58)$$

and thus a particle number of

$$N = \frac{N_A \rho A d}{M_{\text{H}_2\text{O}}} \quad (7.59)$$

where $M_{\text{H}_2\text{O}} = 18 \text{ g mol}^{-1}$ is the molar mass of water and N_A is the Avogadro constant. Given an impingement rate

$$I = \frac{p}{\sqrt{2\pi m_{\text{H}_2\text{O}} k_B T}} = \frac{N}{A t}, \quad (7.60)$$

the time sought is

$$t = \frac{N_A \rho d}{M_{\text{H}_2\text{O}}} \frac{\sqrt{2\pi m_{\text{H}_2\text{O}} k_B T}}{p} \quad (7.61)$$

With a mass $m_{\text{H}_2\text{O}} = 2.989 \times 10^{-26} \text{ kg}$ of the water molecule and $\rho = 940 \text{ kg m}^{-3}$ we obtain the result $t = 87,712 \text{ s}$, i.e., under the given conditions a film thickness of $1 \mu\text{m}$ is reached after more than 24 h.

Chapter 8

Statistical Thermodynamics

Abstract Using the concept of statistics and probability, statistical thermodynamics relates the state variables of macroscopic systems to the properties of its microscopic constituents. The state variables can be attributed to one single quantity: the partition function of the system.

The selection of problems in this chapter focuses primarily on the basic principles of probability calculus, as it is the prerequisite for a deeper understanding of statistical thermodynamics. The correct treatment of factorials (see Sect. A.3.9 in the appendix) is a frequently occurring technical issue that is addressed, for example, in Problem 8.3. Using the probability calculus, we see how the Boltzmann distribution can be motivated and how the phenomenon of diffusion can be understood. A second focus is on problems dealing with concrete cases of partition functions and their relation to thermodynamic quantities such as entropy or molar heat capacities.

8.1 Basic Concepts

In the following, it is assumed that the reader is familiar with basic stochastic calculus. Moreover, statistical thermodynamics makes use of the correct description of atoms and molecules within quantum mechanics (see Chap. 9).

8.1.1 Statistical Interpretation of Entropy

The statistical interpretation of entropy introduced by L. Boltzmann follows the notion that a system composed of many particles can take a very large number of states characterized by the individual positions and velocities and all other kinds of degrees of freedom of the molecular entities. These states of the system are called **microstates**. However, the system can in practice only be characterized by its total energy E or other macroscopic state variables. These constitute the spectrum of possible **macrostates**. For example, there is generally a large number of different microstates leading to the same total energy. If under certain conditions these microstates occur with equal probability, it is obvious that the macrostate comprising the highest number of different microstates is most likely to occur in

reality, which means that the dynamics of the system have a tendency to reach this state. Such considerations led to the statistical definition of **entropy** S

$$S = k_B \ln W \quad (8.1)$$

where

$$W = \frac{N!}{\prod_i N_i!} \quad (8.2)$$

called **statistical weight** is the number of ways in which a macrostate can be realized, N is the number of particles, and N_i is the number of particles in the i th range of possible position and momentum.

8.1.2 Boltzmann Distribution

Consider a system of fixed composition at a fixed temperature T . A certain state i of the system has the energy ϵ_i . The probability of the state i is:

$$p_i = \frac{e^{-\beta \epsilon_i}}{Q}; \quad \beta = \frac{1}{k_B T} \quad (8.3)$$

with the partition function

$$Q = \sum_i e^{-\beta \epsilon_i}; \quad \beta = \frac{1}{k_B T}. \quad (8.4)$$

The goal is to determine macroscopic state variables such as internal energy U , the heat capacity C_V , or its entropy S from the system partition function Q .

8.1.3 Canonical Ensemble

For the statistical treatment of the system the **ensemble** concept is key, which was introduced by J.W. Gibbs. An ensemble is a collection of \mathcal{N} identical copies of the system. The ensemble concept allows the treatment of systems comprising only a few molecules, or in an extreme case, only one single molecule. Moreover, by

Fig. 8.1 Illustration of a canonical ensemble of $\mathcal{N} = 16$ copies of a system at a constant N, T, V . The walls of the systems are rigid and diathermic

N,V,T	N,V,T	N,V,T	N,V,T
N,V,T	N,V,T	N,V,T	N,V,T
N,V,T	N,V,T	N,V,T	N,V,T
N,V,T	N,V,T	N,V,T	N,V,T

choosing a large number \mathcal{N} of copies, the application of Stirling's approximation to handle factorials is justified. If temperature T , volume V , and particle number N are constant in each of these copies, then the ensemble is called a **canonical ensemble**, and the partition function is called **canonical partition function**. Such a canonical ensemble is illustrated in Fig. 8.1 for small \mathcal{N} . The diathermic walls in the ensemble guarantee constant temperature in all copies of the system, but the energy fluctuates around the most probable energy value. At very large \mathcal{N} the probability distribution has a very sharp peak. If q is the partition function of one copy of the system, then the partition function Q is obtained as a product over all \mathcal{N} copies. Depending on whether or not these copies are distinguishable, the partition function is

$$Q = q^{\mathcal{N}} \quad \text{distinguishable} \quad (8.5)$$

$$Q = \frac{1}{\mathcal{N}!} q^{\mathcal{N}} \quad \text{indistinguishable} \quad (8.6)$$

The classification into distinguishable and indistinguishable units is frequently based on quantum mechanics in which the indistinguishability of identical particles is established. It has been pointed out, however, that in his early analysis of the Gibbs paradox, Gibbs argued on the basis of *operational distinguishability* on purely classical grounds [1]. It can be shown that the internal energy of the system, expressed using the canonical partition function, is

$$U = - \left(\frac{\partial \ln Q}{\partial \beta} \right)_{T,V} = k_B T^2 \left(\frac{\partial \ln Q}{\partial T} \right)_{T,V}; \quad \beta = \frac{1}{k_B T}. \quad (8.7)$$

The entropy is

$$S = \left(\frac{d}{dT} (k_B T \ln Q) \right)_{V,T} \quad (8.8)$$

8.2 Molecular Degrees of Freedom and Partition Functions

Using the ensemble concept, the system partition function Q can be written as a product of molecular partition functions q (cf. Eqs. (8.5) and (8.6)). Using quantum mechanics, the molecular partition function can be separated into a product of partition functions associated with the various degrees of freedom, translation, rotation, vibrations, and electronic excitation¹:

$$q_{\text{molecule}} = q_{\text{trans.}} q_{\text{rot.}} q_{\text{vib.}} q_{\text{el.}} \quad (8.9)$$

This assumes that the energy levels of the molecule can be written as the sum

$$E_{\text{molecule}} = E_{\text{trans.}} + E_{\text{rot.}} + E_{\text{vib.}} + E_{\text{el.}} \quad (8.10)$$

For the calculation of the partition function associated with a special degree of freedom, the possibility of a g_i -fold **degeneracy** of an energy level ϵ_i has to be taken into account:

$$q = \sum_i g_i e^{-\beta \epsilon_i}; \quad \beta = \frac{1}{k_B T} \quad (8.11)$$

The quantum mechanical result for the translational part of the partition function obtained from the particle in a box model is, as textbooks show,

$$q_{\text{trans.}} = \frac{V}{\Lambda^3} = \frac{(2\pi m k_B T)^{\frac{3}{2}}}{h^3} V \quad (8.12)$$

¹Strictly speaking, rotational and vibrational degrees of freedom are coupled in a molecule. In many cases, however, the treatment of a molecule as a rigid rotator with entirely harmonic vibrational modes is a useful approximation. It allows a separation of rotation and vibrational degrees of freedom.

where h is the Planck constant (see Sect. A.1), Λ is a *thermal wavelength*, and V is the system volume.

The rotational partition function of a heteronuclear diatomic is

$$q_{\text{rot}} = \sum_J (2J + 1) e^{-\beta hcBJ(J+1)}; \quad \beta = \frac{1}{k_B T} \quad (8.13)$$

where J is the rotational quantum number and B is the rotational constant (see Sect. 10.1.2). Based on the harmonic oscillator model (see Sect. 10.1.3), the vibrational partition function of the diatomic takes a compact form:

$$q_{\text{vib.}} = \frac{e^{-\beta \frac{\hbar\nu}{2}}}{1 - e^{-\beta \hbar\nu}} \quad (8.14)$$

Here, ν is the vibrational frequency of the stretch vibration. In the case of polyatomic molecules, or in all cases beyond the harmonic oscillator model, the expressions are more complicated. Moreover, in symmetric molecules like H_2 or CO_2 , nuclear spin statistics must also be considered when the molecular partition function is determined.

8.3 Problems

A further problem related to statistical thermodynamics is Problem 9.1 at page 221.

Problem 8.1 (Conformational Entropy and Protein Structure) Myoglobin (see Fig. 8.2) is a protein structure made of 150 amino acids. Assume that each of these subunits can take six different orientations, which in principle leads to a huge number of different conformer structures. Can you calculate this number? However, within the cellular environment, the protein has a well-defined structure. Assume that the latter is characterized by only one single conformation. Use Boltzmann's statistical definition of entropy (Eq. (8.1)) to calculate the protein's conformational entropy.

Solution 8.1 This problem is a simple application of Boltzmann's entropy formula. However, it illustrates the astonishing aspects of life on the molecular scale, and shows us an extreme example of thermodynamic stability. Myoglobin (Fig. 8.2) has a very complex structure and thus a huge number of internal degrees of freedom. In the cellular environment, the covalent bonds of the molecule can be considered

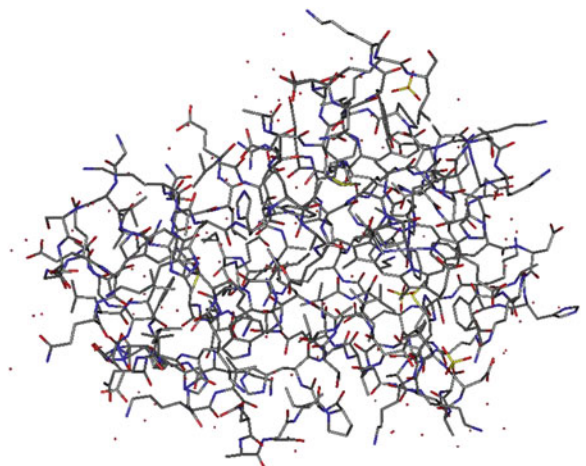


Fig. 8.2 Myoglobin protein structure

stable. If we leave the vibrational degrees of freedom aside, the conformations² of the molecule's substructure, the amino acids, are most important. For simplicity, we assume that each amino acid has six possible conformations. For two amino acids, there is a total of $6 \times 6 = 36$ different conformations; for 150 amino acids, we have

$$N = 6^{150} \quad (8.15)$$

different structures. A conventional pocket calculator cannot display this number in the usual way. What we can do is to rewrite this number as follows:

$$N = 6^{150} = 10^x \Leftrightarrow x = \frac{150 \ln 6}{\ln 10} = 116.7226878$$

Thus,

$$N = 10^{116.7226878} = 10^{116} 10^{0.7226878} = 5.280655064 \times 10^{116}. \quad (8.16)$$

An astonishing fact about the molecule is that under cellular conditions the molecule only occurs in a few well-defined conformational structures characterized by a few special sequences out of 6^{150} . For simplicity, we assume that there is only one such functional form of the molecule. If the molecule had to find this unique structure in a random-walk process where each conformational change takes only a few picoseconds, this process would take a very long time. In contrast, real folding times are less than 1 s [2]. This discrepancy is called *Levinthal paradox*.

²The switching of a molecule between different conformations has been treated in Problem 5.3.

Moreover, if the folding process were driven by the minimization of the Gibbs free energy $\Delta G = \Delta H - T\Delta S$ of the molecule, then this unique functional form would have to be characterized by a steep minimum in enthalpy that balances the large entropic contribution $-T\Delta S$ to ΔG , where ΔS is the conformational entropy. It is our task to calculate this entropy using Boltzmann's statistical approach to entropy. We assume two macrostates: (1) the functional state, which is realized by $W_1 = 1$ configuration of the molecule, and (2) the dysfunctional state, realized by all remaining $W_2 = N-1$ conformational sequences. As N is so large, we can safely assume $W_2 = N$. Thus,

$$\Delta S = S_{\text{functional}} - S_{\text{dysfunctional}} = N_A k_B \ln W_1 - N_A k_B \ln W_2 \quad (8.17)$$

Using $N_A k_B = R = 8.3145 \text{ J K}^{-1} \text{ mol}^{-1}$ and $\ln W_1 = \ln 1 = 0$, we obtain

$$\Delta S = -2235 \text{ J K}^{-1} \text{ mol}^{-1}.$$

To compensate for this decrease in entropy during the folding process, therefore, the room temperature enthalpy change must be at least below $\Delta H = 298K \times \Delta S = -666 \text{ kJ mol}^{-1}$.

Problem 8.2 (Mixing of Gases) Consider the arrangement of two compartments I and II with the same volume V , as shown in Fig. 8.3. Initially, the compartments are separated by a baffle and contain an equal number of particles of two different species, which may be treated as a perfect gas. If the baffle is removed the gas particles may change the compartment. Assume $N = 4$ particles of each species, as shown in the figure.

- Calculate the probability that all particles of whatever species are located in compartment I.
- What is the probability of finding all particles of species B (dark balls) in compartment I, and all particles of the other species G (white balls) in compartment II?
- Draw a probability distribution of finding n particles of species B ($n = 0, \dots, 4$) in compartment I. Draw a probability distribution of finding n particles of whatever species ($n = 0, \dots, 2N$) in compartment A.

Solution 8.2 This exercise gives a rather elementary demonstration of the mixing of gases and how it is related to the basic principles of probability.³ The initially separated gases in the two compartments I and II comprise only four particles. This enables us to write down all possibilities regarding how the particles can be

³We have dealt with a thermodynamical description of gas mixing in Chap. 3, Problem 3.7.

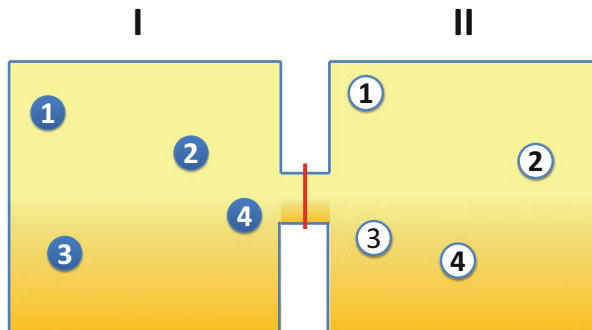


Fig. 8.3 Two compartments filled with different gases, separated by a baffle

distributed in the compartments after the baffle is removed. In our solution, we use the following notation to indicate a special configuration of particles: we use the number 1 to indicate when a particle is found in compartment I, and the number 0 if it is in compartment II. The initial configuration as shown in Fig. 8.3 is:

$$1111, 0000$$

i.e., the first four numbers indicate the positions of the species B (the dark balls) with label 1, 2, 3, and 4. The next four numbers give the positions of the particles 1, 2, 3, and 4 of species G (white balls).

In **subproblem (a)**, we give the probability that all particles, no matter whether they belong to species G or species B, are found in compartment I. This is the configuration:

$$1111, 1111.$$

In a perfect gas, the particles do not interact; thus, their movements are independent, and the probability of finding one special particle, say B1 (dark ball with label 1), is $p = \frac{1}{2}$. Either it is found in compartment I, or, with the same probability $\frac{1}{2}$, it is found in compartment II. As the particles move independently, the presence of particles in the compartment does not influence the probability of finding the other particles in the compartment. All particles have the same probability $\frac{1}{2}$, and the joint probability for this configuration is thus:

$$p(1111, 1111) = \left(\frac{1}{2}\right)^{2N} = \left(\frac{1}{2}\right)^8 = 3.9 \times 10^{-3}. \quad (8.18)$$

The probability is small, but not too small. Statistically, 1 in 256 measurements would yield this configuration. However, if the total number of particles were increased to $2N = 100$, the probability of finding all the particles in compartment

I would be within the range 10^{-30} . For realistic particle numbers $N \approx 10^{23}$, the probability of this event is *de facto* zero.

In **subproblem (b)**, we give the probability of finding all particles of species B in compartment I and all particles of species G in compartment II. This event is in fact the initial configuration. It has the same probability as any of the possible $2^{2N} = 256$ configurations. The probability is, therefore:

$$p(1111, 0000) = \left(\frac{1}{2}\right)^8 = 3.9 \times 10^{-3}. \quad (8.19)$$

Thus, the event of a perfect separation of the gases is rare; when limited to realistic particle numbers, it is unimaginably small.

In **subproblem (c)**, we generate a probability distribution of finding n particles of species B in compartment 1, where n is 0, 1, 2, 3, or 4. These events represent in general several possible configurations. We can write them down explicitly:

$$0000\} n = 0$$

$$\begin{matrix} 1000 \\ 0100 \\ 0010 \\ 0001 \end{matrix} \left. \right\} n = 1$$

$$\begin{matrix} 1100 \\ 1010 \\ 1001 \\ 0110 \\ 0101 \\ 0011 \end{matrix} \left. \right\} n = 2$$

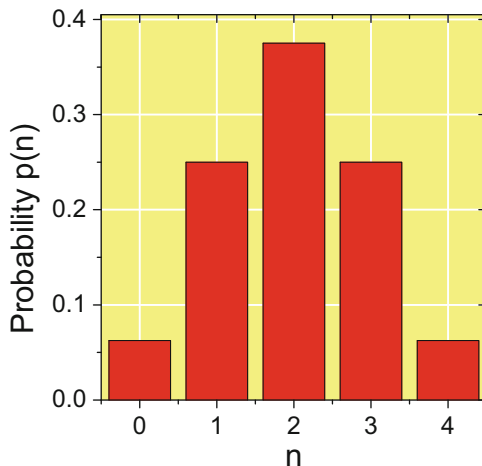
$$\begin{matrix} 1110 \\ 1101 \\ 1011 \\ 0111 \end{matrix} \left. \right\} n = 3$$

$$1111\} n = 4$$

If we define the statistical weight as the number of configurations for an event, $W(n)$, then we have $W(0) = W(4) = 1$, $W(1) = W(3) = 4$, and $W(2) = 6$. Because all the $Z = 2^N = 2^4 = 16$ configurations are assumed to appear with the same probability, the joint probability for the event n particles in compartment I is

$$p(n) = \frac{W(n)}{Z}. \quad (8.20)$$

Fig. 8.4 Probability distribution for the event of finding n particles of species B in compartment I



The resulting probabilities are depicted in Fig. 8.4. Two particles of species B being found in compartment I is the most probable event, which shows that there is a tendency that half of the particles are found in compartment I, the other half in compartment II. In terms of thermodynamics, the gas undergoes a free expansion into the total accessible volume after the baffle is removed. Limited to realistically large particle numbers, the event $n = \frac{N}{2}$ is dominant. If we want to show this⁴, we need an equation for the statistical weight $W(n)$ for arbitrary N . Our elementary analysis for $N = 4$ above shows that $W(n)$ is just the number of possible permutations of a sequence of numbers. In our case $W(n)$ is given by (see Eq. (8.2))

$$W(n) = \frac{N!}{n!(N-n)!}. \quad (8.21)$$

With this relation, it is straightforward to generate the second probability distribution of finding n particles of whatever species in compartment I. With the total number of $2N = 8$ particles, the probabilities are:

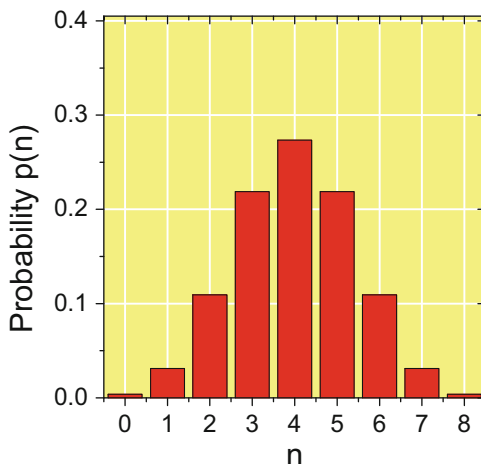
$$p(n) = \frac{(2N)!}{2^{2N}n!(2N-n)!} = \frac{8!}{2^8n!(8-n)!} \quad (8.22)$$

The resulting distribution is shown in Fig. 8.5.

The distribution has a maximum, as expected, at $n = 4$. Note that in the limiting case of identical species B and G, nothing happens from the macroscopic point of view if the baffle is removed. This is the origin of the Gibbs paradox, which

⁴The dominant event $n = \frac{N}{2}$ would have the probability $p\left(\frac{N}{2}\right) = \frac{N!}{2^N\left(\frac{N}{2}\right)!\left(\frac{N}{2}\right)!}$. Consideration of $\ln p\left(\frac{N}{2}\right)$ and Stirling's formula Eq. (A.62) yields $\ln p\left(\frac{N}{2}\right) = 0$ and thus $p\left(\frac{N}{2}\right) = 1$.

Fig. 8.5 Probability distribution for the event of finding n particles of whatever species in compartment I



deals with the entropy of mixing of identical species. Straightforward application of Eq. (3.35) would yield a positive entropy of mixing, even in the case of identical species, although no macroscopic change of state occurs. Based on our simple model of gas mixing we cannot analyze this in more detail; in particular, the calculation of entropy changes of the gases must be based on Eq. (8.8). In summary, we have seen in a very simplified case how statistics governs the distribution of independently moving gas particles.

Problem 8.3 (A Simple Model of Diffusion) Being initially located at $x = 0$, a molecule takes discrete steps in one dimension with a step length a . With the same probability, it takes a step to the right (R) or to the left (L). For example, a possible hopping sequence with eight steps is LRRLLLRL, leaving the molecule at the position $x = -2a$.

- a. Show that probability of finding the molecule after N steps at position m is

$$P_N(m) = \left(\frac{1}{2}\right)^N \frac{N!}{\left(\frac{N+m}{2}\right)! \left(\frac{N-m}{2}\right)!} \quad (8.23)$$

- b. Plot $P_N(m)$ for $N = 4, 5, 8$.
c. Show that for large N the probability of finding the molecule at position m is

$$P_N(m) = \frac{2}{\sqrt{2\pi N}} \exp\left(-\frac{m^2}{2N}\right) \quad (8.24)$$

(continued)

Problem 8.3 (continued)

and give an interpretation of this result. Hint: Use Stirling's approximation $\ln n! = (n + \frac{1}{2}) \ln n - n + \ln \sqrt{2\pi}$ (see Eq. (A.63)) and the Taylor expansion Eq. (A.56).

Solution 8.3 In this problem, we apply the principles of probability and statistics to a simple model of molecular diffusion processes in one dimension. **Diffusion** is a prime example of an irreversible process. How does irreversibility occur in a process that is a sequence of individual reversible steps? In **subproblem (a)**, we work out the expression for the probability that a molecule is found at a certain position m after N steps on a discrete lattice in one dimension. The situation is illustrated in Fig. 8.6 for the special path sequence given in the problem formulation, LRRLLLRL. As every step to the right or to the left occurs with the same probability, $\frac{1}{2}$, the joint probability for this special 8-step sequence is $(\frac{1}{2})^8$. For a special N -step sequence, the joint probability is $(\frac{1}{2})^N$. This special sequence puts the molecule in its final position at $x = -2a$. However, this is not the only sequence that produces this result. For example, the sequence RLRLLLRL would also put the molecule in this final position. Clearly, the total number of steps to the right (R) and steps to the left (L) is decisive with regard to the final position. If there are n steps to the right, then we have $N - n$ moves to the left. Among the 2^N different sequences with N steps, there are

$$Z_N(n) = \frac{N!}{n!(N-n)!} \quad (8.25)$$

sequences with n steps to the right. We have to add up the probabilities of each sequence among this subset and obtain the probability that the molecules move n steps to the right:

$$P_N(n) = \sum_i Z_N(n) \left(\frac{1}{2}\right)^N = \left(\frac{1}{2}\right)^N \frac{N!}{n!(N-n)!} \quad (8.26)$$

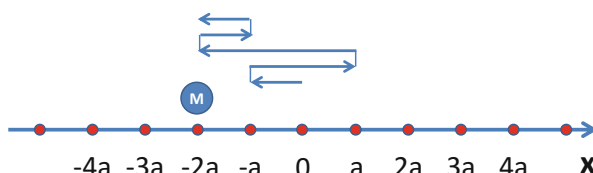


Fig. 8.6 Discrete movement of a molecule "M" in one dimension. After an eight-step hopping sequence, LRRLLLRL, the molecule is situated at $x = -2a$ with a being the step length

In the next step, we have to analyze at which position the molecule is placed after a N -step sequence with n steps to the right and $N - n$ steps to the left. Each step to the right increases the position index m by one, while m is reduced by one in a step to the left. As a consequence, after N steps, the position index is

$$m = (n - (N - n)) = 2n - N. \quad (8.27)$$

Hence, the number of steps to the right leading to the special position index m is:

$$n = \frac{N + m}{2}. \quad (8.28)$$

If we insert this result into Eq. (8.26) we obtain:

$$P_N(m) = \left(\frac{1}{2}\right)^N \frac{N!}{\left(\frac{N+m}{2}\right)! \left(N - \frac{N+m}{2}\right)!} = \left(\frac{1}{2}\right)^N \frac{N!}{\left(\frac{N+m}{2}\right)! \left(\frac{N-m}{2}\right)!} \quad (8.29)$$

which is simply the expression Eq. (8.23). It is worth inspecting Eq. (8.27) again: if we have an even total number of steps ($N = 2K$, $K = 0, 1, 2, \dots$), then $m = 2n - 2K = 2(n - K)$ will also be even. Therefore, an even total number of steps places the molecule at an even position, $m = 0, \pm 2, \pm 4, \dots$. Conversely, if the total number of steps is odd, then m will also be odd and the molecule reaches $m = \pm 1, \pm 3, \dots$. This notion is important for the correct interpretation of the results in subproblem (c), but also for the plotting of the probabilities in **subproblem (b)** for $N = 4, 5, 8$. For $N = 4$, the possible end points are $m = \pm 2, \pm 4$. Evaluation of the associated probabilities using Eq. (8.23) yields:

$$P_4(\pm 2) = \left(\frac{1}{2}\right)^4 \frac{4!}{3! 1!} = 0.25 \quad P_4(\pm 4) = \left(\frac{1}{2}\right)^4 \frac{4!}{4! 0!} = 0.0625$$

Moreover, we have:

$$P_4(\pm 0) = \left(\frac{1}{2}\right)^4 \frac{4!}{2! 2!} = 0.375$$

We can check if P_4 is normalized by adding all probabilities and obtain:

$$\sum_m P_4(m) = 0.0625 + 0.25 + 0.375 + 0.25 + 0.0625 = 1$$

As expected, this discrete probability distribution is normalized. In the same way, we can calculate the possible values for the requested distributions P_5 and P_8 . The results are illustrated in Fig. 8.7. Inspection of the plots reveals that the probability of finding the molecule in the center (low values of m) is highest, whereas high absolute values of m have decreasing probability. Moreover, the bell-shaped profile of the

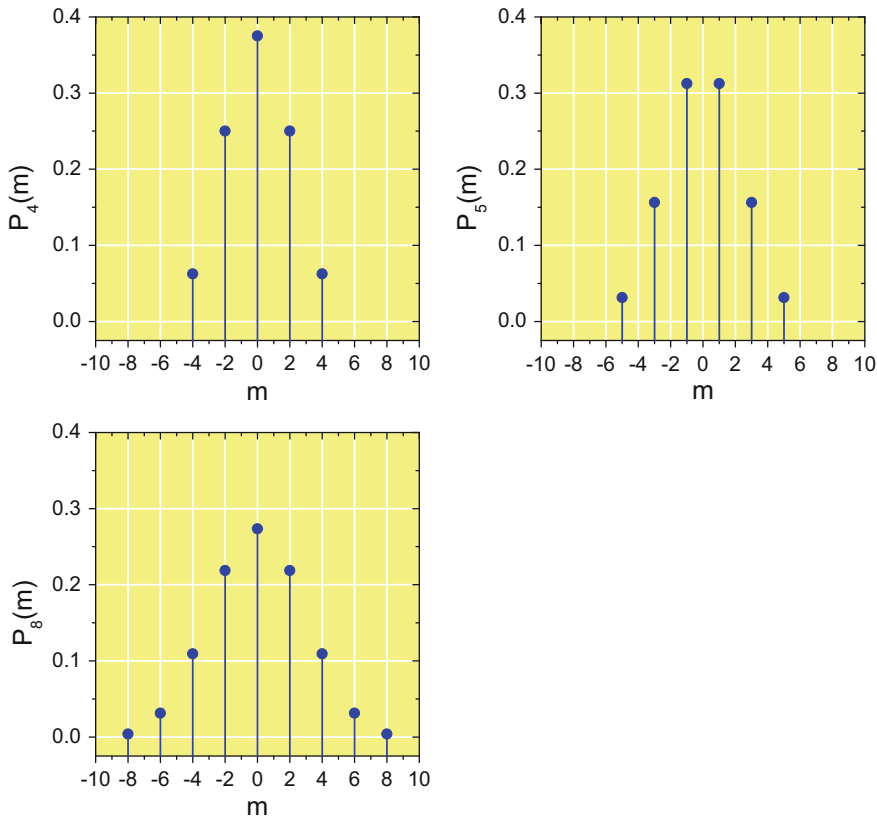


Fig. 8.7 Probability distributions $P_N(m)$ for $N = 4, 5, 8$

distribution is especially apparent in the case of P_8 . This suggests that for a large total number of steps, the distribution could take the Gaussian shape of a normal distribution as illustrated in the appendix in Fig. A.2. This limiting case is examined in **subproblem (c)**. We prove that Eq. (8.23) is identical to Eq. (8.24) when limited to high N . This task is instructive because we learn how to cope with factorials using *Stirling's approximation*. This sort of calculus is typical for problems occurring in statistical thermodynamics. For large N , the factorial $N!$ is⁵

$$N! \approx \left(\frac{N}{e}\right)^N \sqrt{2\pi N} \quad (8.30)$$

and thus

⁵Note that in some textbooks you might find a less precise version of Stirling's formula: $\ln N! \approx N \ln N - N$ which, in the present problem would not yield the correct prefactor containing $\sqrt{2\pi N}$.

$$\ln N! \approx \left(N + \frac{1}{2} \right) \ln N - N + \frac{1}{2} \ln \sqrt{2\pi} \quad (8.31)$$

Using Eq. (8.31) and the rules for logarithms in the appendix (Sect. A.3.3), we write

$$\begin{aligned} \ln P_N(m) &= N \ln \frac{1}{2} + \ln N! - \ln \left(\frac{N+m}{2} \right)! - \ln \left(\frac{N-m}{2} \right)! \\ &= N \ln \frac{1}{2} + \left(N + \frac{1}{2} \right) \ln N - N + \ln \sqrt{2\pi} \\ &\quad - \left(\frac{N+m}{2} + \frac{1}{2} \right) \ln \frac{N+m}{2} + \frac{N+m}{2} - \ln \sqrt{2\pi} \\ &\quad - \left(\frac{N-m}{2} + \frac{1}{2} \right) \ln \frac{N-m}{2} + \frac{N-m}{2} - \ln \sqrt{2\pi} \end{aligned}$$

The three highlighted terms cancel each other out. Further evaluation yields:

$$\begin{aligned} \ln P_N(m) &= N \ln \frac{1}{2} + \left(N + \frac{1}{2} \right) \ln N - \ln \sqrt{2\pi} \\ &\quad - \left(\frac{N+m+1}{2} \right) \left[\ln(N+m) + \ln \frac{1}{2} \right] \\ &\quad - \left(\frac{N-m+1}{2} \right) \left[\ln(N-m) + \ln \frac{1}{2} \right] \\ &= N \ln \frac{1}{2} + \left(N + \frac{1}{2} \right) \ln N - \ln \sqrt{2\pi} \\ &\quad - \frac{N}{2} \ln \frac{1}{2} - \frac{m}{2} \ln \frac{1}{2} - \frac{1}{2} \ln \frac{1}{2} - \frac{N}{2} \ln \frac{1}{2} + \frac{m}{2} \ln \frac{1}{2} - \frac{1}{2} \ln \frac{1}{2} \\ &\quad - \left(\frac{N+m+1}{2} \right) \ln N \left(1 + \frac{m}{N} \right) - \left(\frac{N-m+1}{2} \right) \ln N \left(1 - \frac{m}{N} \right) \end{aligned}$$

Again, the highlighted terms cancel each other out.

$$\begin{aligned} \ln P_N(m) &= \left(N + \frac{1}{2} \right) \ln N - \ln \sqrt{2\pi} - \ln \frac{1}{2} \\ &\quad - \left(\frac{N+m+1}{2} \right) \ln N - \left(\frac{N-m+1}{2} \right) \ln N \\ &\quad - \left(\frac{N+m+1}{2} \right) \ln \left(1 + \frac{m}{N} \right) - \left(\frac{N-m+1}{2} \right) \ln \left(1 - \frac{m}{N} \right) \end{aligned}$$

$$\begin{aligned}
&= N \ln N + \frac{1}{2} \ln N - \ln \sqrt{2\pi} - \ln \frac{1}{2} \\
&\quad - \frac{N}{2} \ln N - \frac{m}{2} \ln N - \frac{1}{2} \ln N - \frac{N}{2} \ln N + \frac{m}{2} \ln N - \frac{1}{2} \ln N \\
&\quad - \left(\frac{N+m+1}{2} \right) \ln \left(1 + \frac{m}{N} \right) - \left(\frac{N-m+1}{2} \right) \ln \left(1 - \frac{m}{N} \right)
\end{aligned}$$

Highlighted terms cancel each other out. Further simplification using the rules for logarithms is not possible. However, the terms $\ln(1 \pm \frac{m}{N})$ can be expanded in a power series according to Eq. (A.56) in the appendix:

$$\ln \left(1 \pm \frac{m}{N} \right) = \pm \frac{m}{N} - \frac{m^2}{2N^2} + \dots \quad (8.32)$$

For large N , the power series can be truncated. However, at this point it is important to collect *all* terms up to the second order. If we were to truncate the expansion after the first term, then we would lose some quadratic terms in m . Therefore, we insert the expansion truncated after the second term and obtain:

$$\begin{aligned}
\ln P_N(m) &= -\frac{1}{2} \ln N - \ln \sqrt{2\pi} - \ln \frac{1}{2} \\
&\quad - \left(\frac{N+m+1}{2} \right) \left(\frac{m}{N} - \frac{m^2}{2N^2} \right) - \left(\frac{N-m+1}{2} \right) \left(-\frac{m}{N} - \frac{m^2}{2N^2} \right) \\
&= -\frac{1}{2} \ln N - \ln \sqrt{2\pi} - \ln \frac{1}{2} \\
&\quad - \frac{N m}{2 N} - \frac{m^2}{2N} - \frac{m}{2N} + \frac{m^2}{4N} + \frac{m^3}{4N^2} + \frac{m^2}{4N^2} \\
&\quad + \frac{N m}{2 N} - \frac{m^2}{2N} + \frac{m}{2N} + \frac{m^2}{4N} - \frac{m^3}{4N^2} + \frac{m^2}{4N^2} \\
&= -\frac{1}{2} \ln N - \ln \sqrt{2\pi} - \ln \frac{1}{2} - \frac{m^2}{2N} + \frac{m^2}{2N^2}
\end{aligned}$$

For large N , the last term becomes small and can be ignored. Rearranging then yields

$$\ln \left(P_N(m) \sqrt{2\pi N} \frac{1}{2} \right) = -\frac{m^2}{2N} \quad (8.33)$$

and thus

$$P_N(m) = \frac{2}{\sqrt{2\pi N}} \exp\left(-\frac{m^2}{2N}\right) \quad (8.34)$$

which is simply the expression that was to be proven.

This distribution function has a Gaussian shape, suggesting a normal distribution function⁶ for the probability density $W(x)$ limited to large N and small a . With this limitation, the discrete lattice of locations $x = ma$ becomes continuous. Moreover, we can associate the total step number with time if we let $t = N\tau$, where τ is the hopping time of the molecule. The hopping interval is $\Delta x = 2a$, as discussed above in subproblem (a) (see also Fig. 8.7). Now, as $W(x, t) dx$ is the probability of finding the molecule between x and $x + dx$ at time t ,

$$W(x, t) = \frac{P_N(m)}{2a} = \frac{1}{\sqrt{2\pi Na^2}} \exp\left(-\frac{m^2}{2N}\right) = \frac{1}{\sqrt{2\pi a^2 \frac{t}{\tau}}} \exp\left(-\frac{x^2}{2a^2 \frac{t}{\tau}}\right) \quad (8.35)$$

which is in fact a normal distribution. Note that the continuum limit requires that $a \rightarrow 0$ and $\tau \rightarrow 0$ in a way that $\frac{a^2}{\tau}$ is constant. Then, the variance of the distribution function,

$$\sigma^2 = \frac{a^2 t}{\tau}, \quad (8.36)$$

increases with time, consistent with an irreversible *diffusion process* of the molecule. It is common to introduce the *diffusion constant* D :

$$\sigma^2 = 2Dt. \quad (8.37)$$

Hence the probability density function takes the form:

$$W(x, t) = \frac{1}{\sqrt{4\pi D t}} \exp\left(-\frac{x^2}{4Dt}\right) \quad (8.38)$$

This probability density function is a solution of Fick's second law:

$$\frac{\partial W(x, t)}{\partial t} = D \frac{\partial^2 W(x, t)}{\partial x^2} \quad (8.39)$$

A generalization of the diffusion of the molecule in three dimensions is straightforward. The random walk approach to diffusion we have worked out in this problem

⁶See Eq. (A.64).

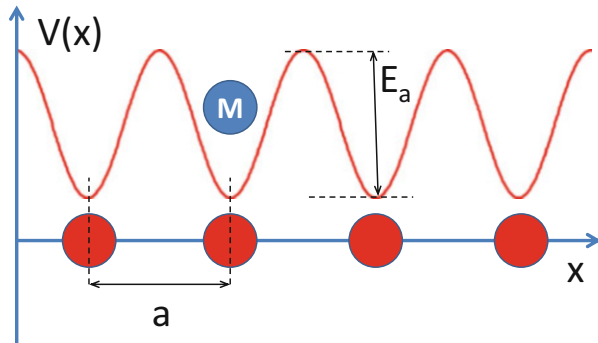


Fig. 8.8 Simplified one-dimensional model of a molecule M adsorbed on a surface. E_a is the activation energy for surface diffusion in the periodic potential $V(x)$, a the lattice parameter of the surface

is instructive in conjunction with the origin of irreversibility: even though each elementary step of the molecule is in principle a reversible operation, a sequence of such steps statistically introduces irreversibility.

Problem 8.4 (Surface Diffusion) Hint: This problem presumes that you have dealt with Problem 8.3.

At a temperature of 80 K, a molecule is adsorbed on a strictly periodic surface (see Fig. 8.8). The lattice constant of the surface is $a = 6 \times 10^{-10}$ m. The activation energy for surface diffusion is $E_a = 8.5 \text{ kJ mol}^{-1}$, the attempt frequency (= frequency of frustrated lateral translations) is 1 THz.

- Use Eqs. (8.35)–(8.37) and give an expression for the diffusion coefficient of the molecule as a function of temperature in one dimension.
- Calculate the expectation values $\langle x \rangle$ and $\langle x^2 \rangle$ for the distance and the square of the distance of the molecule from its original adsorption site after 1 min.
- What is the probability of finding the molecule after 60 s between $x = -\frac{a}{2}$ and $x = +\frac{a}{2}$, i.e., within the adsorption site from which the random walk starts?

Solution 8.4 Here, we deal with a concrete example of the random walk approach to diffusion on surfaces. On the atomic scale, single crystals have a periodic structure. At the interface, the periodicity is canceled in the dimension perpendicular to the surface, but the periodicity in the other two lateral dimensions is often maintained on mesoscopic length scales. This is demonstrated, for example, in atomic resolution scanning tunneling spectroscopy (STM) experiments, or, in the case of insulating materials, in scanning force microscopy (SFM) experiments.

Nowadays, these *surface science* techniques have reached a resolution that detects single molecules and maps their movements from scan to scan [3]. Molecules can be bound to a surface, either by *chemisorption* (covalent bonding, binding energies $> 50 \text{ kJ mol}^{-1}$), or by *physisorption* (weak van der Waals forces, binding energies $< 50 \text{ kJ mol}^{-1}$). Decisive for the molecule's mobility - quite often the prerequisite for surface chemical reactions to occur - is the depth of the lateral potential the molecule faces. For simplicity, we identify the well depth of the lateral potential with the activation energy for diffusion, $E_a = 8.5 \text{ kJ mol}^{-1}$. Attempts of the molecule to move to a neighboring adsorption site are lateral frustrated translations with a restoring force that is mediated by the lateral potential. In our example, the frequency of this degree of freedom is $\nu_0 = 1 \text{ THz}$.

In **subproblem (a)**, we derive an expression for the diffusion coefficient D introduced in the discussion of Problem 8.3(c). According to Eqs. (8.36) and (8.37), the diffusion constant is given by

$$D = \frac{a^2}{2\tau} \quad (8.40)$$

where τ is the time for one elementary step of the molecule. It is obvious that the hopping of the molecule from one site to the next site is itself a statistical process and τ has the nature of an average time that is influenced by temperature. If the number of hopping attempts is ν_0 , this frequency has to be multiplied with a Boltzmann factor $\exp\left(-\frac{E_a}{RT}\right)$ to obtain the number of successful attempts:

$$\nu = \frac{1}{\tau} = \nu_0 \exp\left(-\frac{E_a}{RT}\right). \quad (8.41)$$

As a consequence, our expression for the diffusion constant as a function of temperature is:

$$D = \frac{a^2 \nu_0}{2} \exp\left(-\frac{E_a}{RT}\right) \quad (8.42)$$

At a temperature of 80 K, we obtain

$$D = \frac{(6.0 \times 10^{-10} \text{ m})^2 \times 10^{12} \text{ s}^{-1}}{2} \times \exp\left(-\frac{8500 \text{ J mol}^{-1}}{8.3145 \text{ JK}^{-1} \text{ mol}^{-1} \times 80 \text{ K}}\right) \\ = 5.08 \times 10^{-13} \text{ m}^2 \text{ s}^{-1}.$$

In **subproblem (b)**, we answer how far the molecule will come statistically after a 1 min random walk, assuming the continuum approximation Eq. (8.35). It has been stressed in the solution of Problem 8.3 that the probability density distribution

$$W(x, t) = \frac{1}{\sqrt{4\pi D t}} \exp\left(-\frac{x^2}{4Dt}\right) \quad (8.43)$$

is normalized, i.e.,

$$\int_{-\infty}^{+\infty} W(x, t) dx = 1. \quad (8.44)$$

The expectation value $\langle x \rangle$, also called the *first moment* of W is:

$$\langle x \rangle = \int_{-\infty}^{+\infty} x W(x, t) dx = 0. \quad (8.45)$$

This is because $W(x, t)$ is symmetrical with regard to the variable x : $W(x, t) = W(-x, t)$, while at the same time the integral $xW(x, t)$ is asymmetrical. Therefore, we must look at the *second moment* of the distribution, $\langle x^2 \rangle$. As $W(x, t)$ is symmetrical:

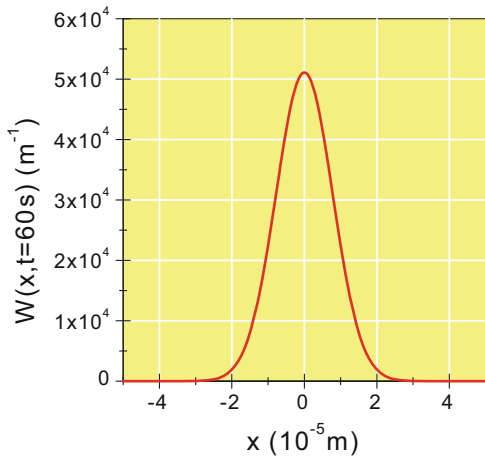
$$\begin{aligned} \langle x^2 \rangle &= \int_{-\infty}^{+\infty} x^2 W(x, t) dx \\ &= 2 \int_0^{+\infty} x^2 W(x, t) dx \\ &= 2 \int_0^{+\infty} x^2 \frac{1}{\sqrt{4\pi Dt}} \exp\left(-\frac{x^2}{4Dt}\right) dx \\ &\stackrel{\text{Eq. (A.47)}}{=} \frac{2\sqrt{\pi}(4Dt)^{\frac{3}{2}}}{4\sqrt{4\pi Dt}} = 2Dt = 2 \times 5.08 \times 10^{-13} \text{ m}^2 \text{ s}^{-1} \times 60 \text{ s} \\ &= 6.1 \times 10^{-11} \text{ m}^2 \end{aligned}$$

Thus, $\langle x^2 \rangle$ is the spatial variance σ^2 of $W(x, t)$ at time t (see Eq. (8.36)), and its standard deviation is $\sigma = \sqrt{\langle x^2 \rangle} = 7.8 \times 10^{-6} \text{ m}$. This corresponds to 13,000 unit cells. Hence, even at 80 K, the molecule is quite mobile on the surface. The corresponding profile of the probability of finding the molecule between location x and $x + dx$ after this time is illustrated in Fig. 8.9.

In **subproblem (c)**, we determine the probability of finding the molecule after 1 min at its original site, i.e., between $x = -\frac{a}{2}$ and $x = \frac{a}{2}$. Note that $x = 0$, the center of the distribution, has the highest probability density. The probability sought is a *cumulative* probability, similar to what we discussed in Problem 7.2 or in Problem 9.14c in connection with quantum mechanical probability. The cumulative probability is the definite integral:

$$\begin{aligned} p(t) &= \int_{-\frac{a}{2}}^{+\frac{a}{2}} W(x, t) dx \\ &= \int_{-\frac{a}{2}}^{+\frac{a}{2}} \frac{1}{\sqrt{4\pi Dt}} \exp\left(-\frac{x^2}{4Dt}\right) dx \end{aligned}$$

Fig. 8.9 Probability density function $W(x, t)$ of a molecule after a 60 s random walk



Again, we can use the fact that $W(x, t)$ is symmetrical with regard to x . Therefore,

$$p(t) = \frac{2}{\sqrt{4\pi Dt}} \int_0^{+\frac{a}{2}} \exp\left(-\frac{x^2}{4Dt}\right) dx$$

The substitution $u = \frac{x}{\sqrt{4Dt}}$ transforms⁷ the integral into a form that can be related to the *error function* $\text{erf}(u)$:

$$p(t) = \frac{2}{\sqrt{\pi}} \int_0^{+\frac{a}{2\sqrt{4Dt}}} \exp(-u^2) du \stackrel{\text{Eq. (A.50)}}{=} \text{erf}\left(\frac{a}{4\sqrt{Dt}}\right) \quad (8.46)$$

The function $p(t)$ is shown in Fig. 8.10 for arbitrary time t between 0 and 60 s, calculated with the given value of $a = 6 \times 10^{-10}$ m and the diffusion constant obtained above: $D = 5.08 \times 10^{-13}$ m² s⁻¹. As expected, $p(0)$ equals 1 and reaches within 1 s a value of 2×10^{-4} . After 60 s the probability is $p(60\text{ s}) = 3.1 \times 10^{-5}$. This means that statistically only 1 in 30,000 experiments would detect the molecule at its initial site.

Problem 8.5 (Derivation of Boltzmann Distribution) Consider two identical systems A and B with diathermic walls in equilibrium at constant temperature (see Fig. 8.11). The probability of measuring the energy E_A in

(continued)

⁷The differential dx is thus $dx = \sqrt{4Dt} du$.

Fig. 8.10 Probability as a function of time to find the molecule at its initial adsorption site. Note the logarithmic scaling

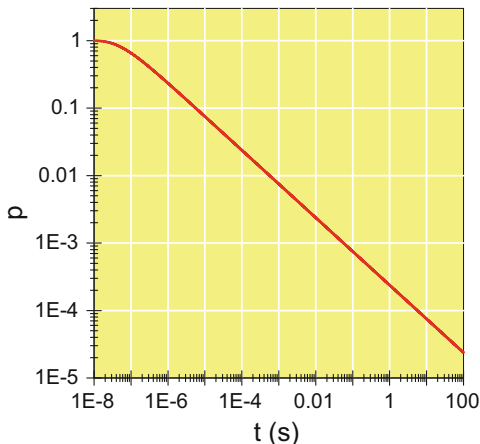
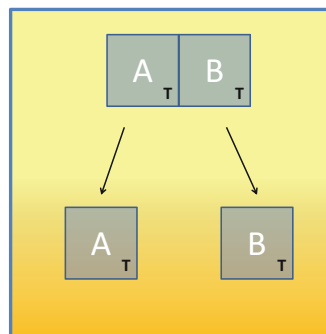


Fig. 8.11 Two systems A and B initially in contact at temperature T stay in equilibrium after their separation, where they can be considered decoupled



Problem 8.5 (continued)

system A is $p_A(E_A)$, the respective probability of measuring the energy E_B in system B is $p_B(E_B)$.

- If the systems are separated from each other so that they can be considered decoupled, are they still in equilibrium and maintaining their initial temperature?
- Write down an expression for the total energy E of both systems. If the systems are decoupled from each other, which condition follows for the probability $p(E)$ of measuring the total energy E ?
- Show that $p(E)$ is the Boltzmann distribution Eq. (8.3). Hint: Set up a differential equation for the probability distribution.

Solution 8.5 In this exercise, it is our goal to derive the Boltzmann distribution Eq. (8.3) for a system composed of two identical subsystems from very general

assumptions. Among the various derivations found in textbooks, this one is quite compact; thus, it can be reproduced in oral examinations. The two systems are initially in contact with each other and in equilibrium. The temperature in both subsystems is constant, but the energies E_A and E_B in the systems fluctuate around a mean value.

In **subproblem (a)**, we answer the question whether both systems stay in equilibrium if they are separated from each other. This is in fact the case. If two systems at different temperature are brought into contact, they equalize their temperature until equilibrium is established. If they are then decoupled, they maintain this temperature, at least if adhesion effects can be ignored. This idea, first introduced by J.W. Gibbs, guarantees the equilibrium of two perfectly decoupled systems at a constant temperature.

In **subproblem (b)**, we focus on the consequences of this situation: the total energy E is *additive*, i.e.,

$$E = E_A + E_B. \quad (8.47)$$

If the probability of finding an energy E_A in system A is $p_A(E_A)$, and the probability of measuring E_B in system B is $p_B(E_B)$, then we can set up a joint probability for the total system to measure the energy E . Because the systems are now independent of each other, the joint probability is obtained by multiplication of the probability distributions p_A and p_B :

$$p(E) = p_A(E_A) p_B(E_B) \quad (8.48)$$

In **subproblem (c)**, we show that $p(E)$ is the Boltzmann distribution Eq. (8.3). In fact, the additivity of the energies in the subsystems (Eq. (8.47)) and their mutual independence (Eq. (8.48)) unambiguously determine the mathematical form of the probability distribution. But how can we show this? The first step may be the notion that the condition Eq. (8.48) is special, and that it is satisfied by the exponential function:

$$e^{cE_a} \times e^{cE_b} = e^{c(E_a+E_b)} = e^{cE}; \quad c = \text{const.}$$

A second thought may be related to the property of a probability distribution function to be normalized. This requires $p_A(E_A) \rightarrow 0$ as $E_A \rightarrow \infty$ and thus the gradient of $p_A(E_A)$ to be negative. A good idea is to set up a differential equation for p_A . The starting point consists of the derivatives

$$\frac{\partial}{\partial E_A} p(E) = \frac{\partial}{\partial E_A} p_A(E_A) p_B(E_B) = p_B(E_B) \frac{\partial p_A(E_A)}{\partial E_A} \quad (8.49)$$

$$\frac{\partial}{\partial E_B} p(E) = \frac{\partial}{\partial E_B} p_A(E_A) p_B(E_B) = p_A(E_A) \frac{\partial p_B(E_B)}{\partial E_B} \quad (8.50)$$

on the one hand, and on the other hand

$$\frac{\partial}{\partial E_A} p(E) = \frac{\partial p(E)}{\partial E} \underbrace{\frac{\partial E}{\partial E_A}}_{=1} = \frac{\partial p(E)}{\partial E} \quad (8.51)$$

$$\frac{\partial}{\partial E_B} p(E) = \frac{\partial p(E)}{\partial E} \underbrace{\frac{\partial E}{\partial E_B}}_{=1} = \frac{\partial p(E)}{\partial E} \quad (8.52)$$

Division by $p(E)$ shows that these derivatives yield:

$$\frac{1}{p(E)} \frac{\partial p(E)}{\partial E} = \frac{1}{p_A(E_A)} \frac{\partial p_A(E_A)}{\partial E_A} = \frac{1}{p_B(E_B)} \frac{\partial p_B(E_B)}{\partial E_B} \quad (8.53)$$

Note that this condition holds for arbitrary E_A and E_B . As a consequence, these expressions must be constant. Because p_A , p_B and p are probability densities, they must be positive. Their gradients, as mentioned above, should be negative. Therefore, the constant must be a negative number:

$$\frac{1}{p(E)} \frac{\partial p(E)}{\partial E} = \frac{1}{p_A(E_A)} \frac{\partial p_A(E_A)}{\partial E_A} = \frac{1}{p_B(E_B)} \frac{\partial p_B(E_B)}{\partial E_B} = -\beta; \quad \beta > 0 \quad (8.54)$$

The differential equation, e.g., for p_A is obtained by rearrangement of this expression:

$$\frac{\partial p(E)}{\partial E} + \beta p_A(E_A) = 0 \quad (8.55)$$

Its solution is:

$$p_A(E_A) = C e^{-\beta E_A} \quad (8.56)$$

which is the Boltzmann distribution. The constant C must follow from the normalization of the distribution function. Its determination would require further assumptions about the nature of the system, e.g. if the spectrum of possible energy values is continuous or if it is discrete. C is closely related to the partition function. The assignment of β to the temperature of the system is achieved by comparison with a concrete case, e.g., the Maxwell-Boltzmann velocity distribution of a monatomic perfect gas. In this case, the average energy is $\frac{3}{2}k_B T$ (see Eq. (7.18) in Problem 7.1). By comparison, it can be shown that $\beta = \frac{1}{k_B T}$.

Problem 8.6 (Entropy of Monatomic Gases)

- a. Prove that the molar entropy of a monatomic perfect gas with mass m and volume V is:

$$s = R \ln \left[\frac{(2\pi mk_B T)^{\frac{3}{2}}}{h^3} \frac{V}{N_A} \right] + \frac{5}{2}R \quad (8.57)$$

- b. Calculate the standard molar entropies of gaseous neon, gaseous zinc, and gaseous lithium at $T = 298.15\text{ K}$. Compare the results with experimental values $s^\ominus(\text{Ne(g)}) = 146.3\text{ J mol}^{-1}\text{ K}^{-1}$, $s^\ominus(\text{Zn(g)}) = 161.0\text{ J mol}^{-1}\text{ K}^{-1}$, and $s^\ominus(\text{Li(g)}) = 138.8\text{ J mol}^{-1}\text{ K}^{-1}$.

Solution 8.6 Is statistical thermodynamics able to correctly predict the molar entropy of a monatomic gas? In this exercise, we analyze this in more detail. In **subproblem (a)**, we show that the molar entropy of a monatomic perfect gas is given by Eq. (8.57), which is called a *Sackur-Tetrode* equation in the literature. It is obvious that our starting point for calculating the entropy is Eq. (8.8)

$$S = \left(\frac{d}{dT} (k_B T \ln Q) \right)_{V,T}$$

which traces back the entropy to the system partition function, Q . The partition function in turn can be written as a product of the N single particle partition functions, where N is the number of particles, q . In our case $N = N_A$. The proper form of the latter is that of *indistinguishable particles* (see Eq. (8.6)); thus, the expression for the molar entropy becomes

$$s = \frac{d}{dT} \left(k_B T \ln \frac{1}{N_A!} q^{N_A} \right) = \frac{d}{dT} (N_A k_B T \ln q - k_B T \ln N_A!) \quad (8.58)$$

Next, we apply Stirling's approximation for the factorial $N_A! = N_A \ln N_A - N_A$ (see Eq. (A.62)) and we use the product rule Eq. (A.15) to form the derivative with regard to temperature:

$$s = N_A k_B \ln q + N_A k_B T \frac{d \ln q}{dT} - N_A k_B \ln N_A + N_A k_B \quad (8.59)$$

By means of Eq. (A.23) and $N_A k_B = R$, this can be transformed to

$$s = R \ln \frac{q}{N_A} + RT \frac{1}{q} \frac{dq}{dT} + R \quad (8.60)$$

Now, we must make an explicit assumption about the single particle partition function: a monatomic particle has only three translational degrees of freedom. Its partition function is given in Eq. (8.12). In particular, we have:

$$q = q_{\text{trans.}} = \frac{(2\pi mk_B T)^{\frac{3}{2}}}{h^3} V \quad (8.61)$$

and

$$\frac{1}{q} \frac{dq}{dT} = \frac{h^3}{(2\pi mk_B)^{\frac{3}{2}} VT^{\frac{3}{2}}} \frac{(2\pi mk_B)^{\frac{3}{2}} V^{\frac{3}{2}} T^{\frac{1}{2}}}{h^3} = \frac{3}{2T} \quad (8.62)$$

Insertion of these results into Eq. (8.60) yields the expression

$$s = R \ln \left[\frac{(2\pi mk_B)^{\frac{3}{2}}}{h^3} T^{\frac{3}{2}} \frac{V}{N_A} \right] + \frac{5}{2} R \quad (8.63)$$

which is equivalent to Eq. (8.57). A remarkable point is the occurrence of the Planck constant in the expression. This suggests that a quantum mechanical treatment of the gas might be necessary for the correct determination of the entropy.⁸ Another remarkable point is that the only element-specific quantity in Eq. (8.57) is the particle mass. It is thus interesting to see how entropies calculated using the Sackur-Tetrode formula compare with experimental values for the standard molar entropies of monatomic gases.

In **subproblem (b)** we consider two examples, the rare gas neon, Ne(g), and zinc vapor, Zn(g). The atomic weights are $m_{\text{Ne}} = 20.18 m_u$ and $m_{\text{Zn}} = 65.41 m_u$ respectively. Assuming standard conditions and room temperature, the gas volume is:

$$V = 1 \text{ mol} \times \frac{RT}{p^\ominus} = 2.479 \times 10^{-2} \text{ m}^3. \quad (8.64)$$

By taking the values h , k_B , N_A , and m_u from the appendix (Sect. A.1), we obtain the values shown in Table 8.1.

For neon and zinc, the agreement between calculated and experimental standard entropies is excellent. In the case of lithium, however, a deviation of more than $5 \text{ J K}^{-1} \text{ mol}^{-1}$ is recognized. Can we understand and correct this discrepancy in detail? It is related to the internal degrees of freedom of the gas particles. The Sackur-Tetrode equation only takes into account the *translational* entropy of the gas, as we considered only the translational part of the partition function. Thus, we have overlooked one or more degrees of freedom, which are present in lithium,

⁸The calculation of the internal energy of the perfect gas based on Eq. (8.7) and the partition function Eq. (8.61) would in fact reproduce the classical result $U = \frac{3}{2}RT$.

Table 8.1 Standard molar entropies of monatomic gases at $T = 298.15\text{ K}$, calculated using the Sackur-Tetrode equation (8.57) in comparison with experimental values. All values in $\text{J K}^{-1}\text{ mol}^{-1}$

Element	$s_{\text{calc}}^{\ominus}$	s_{exp}^{\ominus}
Ne(g)	146.329	146.3
Zn(g)	160.995	161.0
Li(g)	133.017	138.8

but apparently not in zinc or in xenon: we need to consider the electronic structure of these particles. Lithium (atomic number $Z = 3$) has the electron configuration $1s^2 2s^1$. Its electronic ground state is characterized by the term symbol ${}^2S_{\frac{1}{2}}$. The superscript "2" is the *multiplicity* of the electronic state.⁹ The electronic partition function is obtained from Eq. (8.11), where the degeneracy g_i of the i th electronic state is given by its multiplicity $2S_i + 1$ with S_i being the total electronic spin in this state:

$$q_{\text{el.}} = \sum_i (2S_i + 1) e^{-\frac{E_i}{k_B T}} \quad (8.65)$$

The first excited electronic states of lithium have the term symbols ${}^2P_{\frac{1}{2}}$ and ${}^2P_{\frac{3}{2}}$. Their energy measured relative to the ground state energy is 178.5 kJ mol^{-1} . As a consequence, these states are not occupied under room temperature conditions. They are thus negligible for the calculation of $q_{\text{el.}}$. By taking $E_0 = 0$,

$$q_{\text{el.}} = 2S_0 + 1 = 2, \quad (8.66)$$

and thus

$$q = q_{\text{trans.}} q_{\text{el.}} = 2 \frac{(2\pi m k_B T)^{\frac{3}{2}}}{h^3} V. \quad (8.67)$$

This modification leads to a contribution to the entropy of $R \ln 2 = 5.763\text{ J K}^{-1}\text{ mol}^{-1}$. The corrected value for the standard room temperature entropy of lithium is thus $138.780\text{ J K}^{-1}\text{ mol}^{-1}$, in good agreement with the experimental value in Table 8.1. The ground states of atomic zinc and neon both have the term symbols 1S_0 . There is thus no significant contribution of the electronic degrees of freedom to their room temperature entropy. Note that contributions resulting from the nuclear spin multiplicity and mixing of different isotopes are not included in the experimental value of the standard molar entropy. This is consistent with the third law of thermodynamics, i.e., the statement that $s^{\ominus}(T = 0\text{ K})$ of an element in

⁹The multiplicity $2S + 1$ of an electronic state is related to the total electronic spin S , which is determined in the case of the ground state by the single electron in the $2s$ atomic orbital. The electronic structure of lithium is treated in more detail in Problem 9.5.

the state of ideal crystallization is zero [4]. In summary, we see that statistical thermodynamics is able to predict the molar entropies of monatomic gases with remarkably good agreement. We have also seen how internal degrees of freedom of the gas particles contribute to the entropy.

Problem 8.7 (Heat Capacity of Multilevel Systems) Consider a system with the energy levels E_i and degeneracies g_i , $i = 1, \dots, L$.

- a. Prove that the constant volume molar heat capacity of the system can be written:

$$c_V(T) = R \frac{\sum_i^L \sum_j^L g_i g_j \frac{E_i^2 - E_i E_j}{k_B T^2} e^{-\frac{E_i + E_j}{k_B T}}}{\sum_i^L \sum_j^L g_i g_j e^{-\frac{E_i + E_j}{k_B T}}} \quad (8.68)$$

- b. Apply Eq. (8.68) to the rotational contribution to the heat capacity of molecular hydrogen, $\text{H}_2(\text{g})$. The energy levels are given by (see Eq. (10.11) in Chap. 10):

$$E_J = \frac{\hbar^2}{8\pi^2 I} J(J+1) \quad (8.69)$$

where J is the rotational quantum number and $I = 4.6 \times 10^{-48} \text{ kg m}^2$ is the molecule's moment of inertia. If nuclear spin symmetry is ignored, J can take even and odd values $J = 0, 1, 2, \dots$ and a given rotational state is $(2J+1)$ -fold degenerate. Plot $c_V(T)$ in the range between 0 and 500 K. Use at least ten rotational levels for your calculation. Interpret the behavior of $c_V(T)$ in the limit $T \rightarrow 0$ and $T \rightarrow \infty$. Can you explain the *overshooting* of the heat capacity in the temperature range between 50 and 100 K?

- c. Molecular hydrogen is a mixture of ortho- H_2 and para- H_2 . The ortho species is characterized by a total nuclear spin of $I = 1$ (multiplicity 3) and allows only odd rotational states, i.e., $J = 1, 3, 5, \dots$. The para species combines a total nuclear spin of $I = 0$ (multiplicity 1) with even rotational states $J = 0, 2, 4, \dots$. Plot the rotational contribution to the molar heat capacity of ortho and para hydrogen in the range between 0 and 500 K and comment on the differences.

Solution 8.7 In this problem, we deal with the rotational degrees of freedom of the diatomic molecule H_2 and how they contribute to its molar heat capacity. Historically, the correct interpretation of the low temperature molar heat capacity of molecular hydrogen was a problem that stimulated the development of early quantum mechanics [5]. The evaluation of the rotational contribution to the constant

volume molar heat capacity is based on the rotational partition function, q_{rot} . For the latter, however, no closed expression can be given, as in the case of the translational partition function or the harmonic oscillator vibrational partition function. Thus, we must fall back on Eq. (8.11).

In **subproblem (a)**, we show that Eq. (8.68) is the correct expression for the molar heat capacity of a system with L discrete energy levels E_i with a degree of degeneracy g_i respectively. We assume N indistinguishable subunits. Using Eq. (8.6), we have:

$$Q = \frac{1}{N!} q^N \quad (8.70)$$

where q is the partition function of an ensemble subunit, e.g., a single molecule. The internal energy is obtained from Eq. (8.7), i.e.,

$$U = - \left(\frac{\partial \ln Q}{\partial \beta} \right)_{T,V} = - \frac{\partial}{\partial \beta} \left(\ln \frac{q^N}{N!} \right) \quad (8.71)$$

where $\beta = \frac{1}{k_B T}$. Using Stirling's formula Eq. (A.62), we obtain:

$$U = - \frac{\partial}{\partial \beta} \left[N \ln \left(\sum_i^L g_i e^{-\beta E_i} \right) - N \ln N + N \right]. \quad (8.72)$$

Then, application of the chain rule (Eq. (A.17)) yields

$$U = N \frac{\sum_i^L g_i E_i e^{-\beta E_i}}{\sum_i^L g_i e^{-\beta E_i}} \quad (8.73)$$

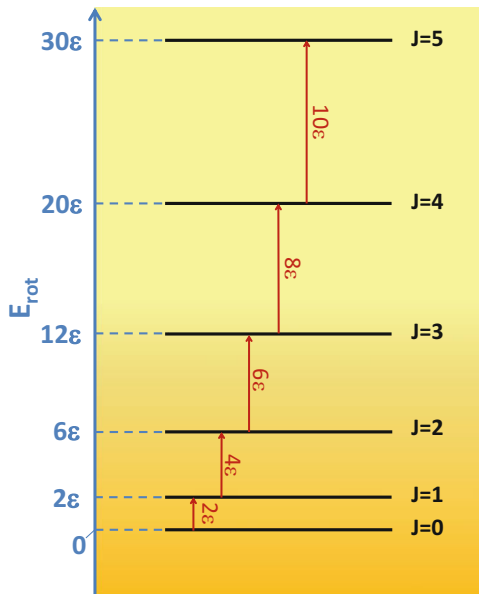
as the proper expression for the internal energy. The constant volume heat capacity for N particles is the derivative with regard to temperature:

$$C_V(T) = \left(\frac{\partial U}{\partial T} \right) = N \frac{\partial}{\partial T} \left(\frac{\sum_i^L g_i E_i e^{-\frac{E_i}{k_B T}}}{\sum_i^L g_i e^{-\frac{E_i}{k_B T}}} \right) \quad (8.74)$$

We must apply the product rule for differentiation in combination with the chain rule to obtain:

$$C_V(T) = N \left(\frac{\sum_i^L g_i E_i e^{-\frac{E_i}{k_B T}} \left(\frac{E_i}{k_B T^2} \right)}{\sum_i^L g_i e^{-\frac{E_i}{k_B T}}} - \frac{\sum_i^L g_i E_i e^{-\frac{E_i}{k_B T}} \sum_j^L g_j e^{-\frac{E_j}{k_B T}} \left(\frac{E_j}{k_B T^2} \right)}{\left(\sum_i^L g_i e^{-\frac{E_i}{k_B T}} \right)^2} \right) \quad (8.75)$$

Fig. 8.12 Rotational energy levels of the H₂ molecule in the model of the rigid rotator (schematic). Rotational energies are multiples of $\epsilon = \frac{\hbar^2}{8\pi^2 I}$, where I is the molecule's moment of inertia



In fact, we can write this in a more symmetrical way by reducing the terms to a common denominator, but we have to pay attention to the correct indexing:

$$C_V(T) = N \frac{\sum_i^L \sum_j^L g_i g_j E_i \left(\frac{E_i}{k_B T^2} \right) e^{-\frac{E_i+E_j}{k_B T}} - \sum_i^L \sum_j^L E_i \left(\frac{E_i}{k_B T^2} \right) e^{-\frac{E_i+E_j}{k_B T}}}{\sum_i^L \sum_j^L g_i g_j e^{-\frac{E_i+E_j}{k_B T}}} \quad (8.76)$$

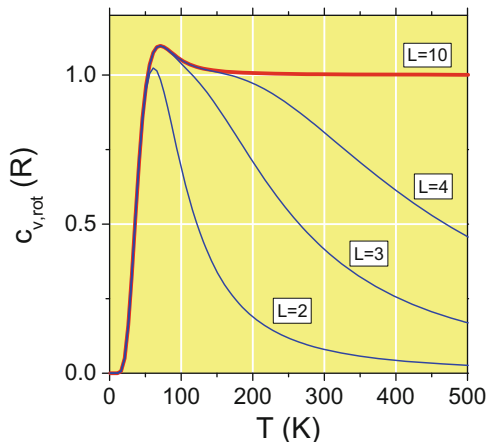
If we now factor out k_B from the numerator and assume that the particle number is Avogadro's number N_A , we obtain the molar heat capacity

$$c_v(T) = \underbrace{N_A k_B}_R \frac{\sum_i^L \sum_j^L g_i g_j \left(\frac{E_i^2 - E_i E_j}{k_B^2 T^2} \right) e^{-\frac{E_i+E_j}{k_B T}}}{\sum_i^L \sum_j^L g_i g_j e^{-\frac{E_i+E_j}{k_B T}}} \quad (8.77)$$

which is identical to the expression Eq. (8.68).

In **subproblem (b)**, we apply this to the concrete case of a rotating diatomic molecule H₂ if the effects of nuclear spin symmetry on the molecular rotation are ignored. The quantum mechanical model of molecular rotation is the rigid rotator, which is described in detail in Sect. 10.1.2. The rotational energy levels depend on the molecule's moment of inertia I and on the rotational quantum number J . According to Eq. (8.69), the energy levels are not equidistant, as can be seen in Fig. 8.12.

Fig. 8.13 Rotational contribution to the low temperature heat capacity of H₂ by ignoring nuclear spin symmetry, based on Eq. (8.68), with consideration of different numbers of rotational levels L . $c_{V,\text{rot}}$ is plotted in units of the gas constant R

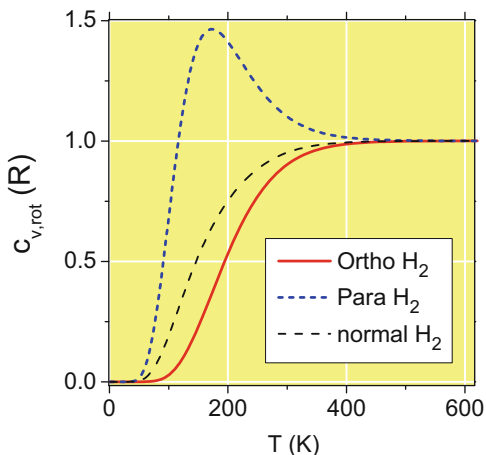


If we define $\epsilon = \frac{\hbar^2}{8\pi^2 I} = 1.21 \times 10^{-21}$ J, then the energy levels and the distance between neighboring energy levels are multiples of ϵ . These distances become greater with increasing J (we refer to this point below). In addition, the rigid rotator energies have a degree of degeneracy of $g_i = (2J + 1)$. With this information, we can calculate the rotational contribution to the low temperature heat capacity using Eq. (8.68) and mathematical software. The result is shown in Fig. 8.13.

If at least $L = 10$ levels are considered, the heat capacity follows the bold line. At $T = 0$ K, the heat capacity is zero. Then, between 20 and 50 K it increases steeply and reaches a maximum at about 70 K. Above this temperature, the molar heat capacity decreases gradually toward a saturation value of $1R$. This high temperature limit is the classical value for two rotational degrees of freedom of the molecule contributing $\frac{1}{2}R$ to c_V . The fact that $c_{V,\text{rot}} \rightarrow 0$ for $T \rightarrow 0$ shows that the rotational degrees of freedom are frozen at a very low temperature, where only the rotational level $J = 0$ is occupied. It is instructive to analyze the *overshooting* of the molar heat capacity exceeding the classical value of $1R$ by about 10% at about 70 K. The characteristics of $c_{V,\text{rot}}$ in the case of a two-level system ($L = 2$) is also shown in Fig. 8.13. The steep increase above 20 K is caused by the population of the $J = 1$ level. Because the population of this excited state reaches a state of saturation at a higher temperature, the system can no longer absorb further energy; thus, the heat capacity decreases. If three levels are considered ($L = 3$), the peak in the heat capacity curve is well reproduced. The overshooting is thus caused by the population of the levels $J = 1$ and $J = 2$. The decrease in the heat capacity appears to be a consequence of the fact that the level $J = 3$ has too much in energy to be reached below 100 K.

Although a similar trend in the rotational molar heat capacity is observed in deuterated hydrogen (HD), ordinary H₂ shows a different behavior. As proposed for the first time in 1929 by Bonhoeffer and Harteck [6], H₂ has two spin-isomers, ortho-H₂ with a total nuclear spin of $I = 1$ (multiplicity 3) and para-H₂ with a total nuclear spin of $I = 0$ (multiplicity 1). Nuclear spin symmetry and the Pauli principle

Fig. 8.14 Rotational contribution to the low temperature heat capacity of ortho H₂ (solid) and para H₂ (short dashed) based on Eq. (8.68). Also shown (dashed) is the curve for normal H₂, i.e., a mixture of ortho and para H₂ 3:1. $c_{V,\text{rot}}$ is plotted in units of the gas constant R



state that ortho-H₂ can only occupy the rotational states with odd J , whereas para-H₂ populates only states with even J .

In **subproblem (c)** we determine $c_{V,\text{rot}}(T)$ in the region between 0 and 500 K for these two species. It is worth mentioning that a direct transition between these two species is forbidden. With

$$g_J^{\text{ortho}} = 3(2J + 1) \quad g_J^{\text{para}} = 2J + 1 \quad (8.78)$$

and the restriction concerning the possible occupation of rotational states, the curves shown in Fig. 8.14 are obtained. The molar heat capacity of the para species increases considerably at temperatures above 50 K and overshoots the classical value $1R$ by nearly 50%. Above 170 K it decreases and approaches the classical limit. The function for ortho species, in contrast, continuously increases at temperatures above 100 K and approaches the classical limit. Normal H₂, i.e., a mixture of ortho and para hydrogen with the composition 3:1 also does not exhibit a heat capacity maximum. Looking back on our results, we have worked out the relation between the partition function and the molar heat capacity of a system of indistinguishable particles with a finite number of discrete energy levels. We have applied the method to the rotational contribution to the molar heat capacity of molecular hydrogen.

Problem 8.8 (Schottky Anomaly) Two-level systems exhibit a peak-shaped contribution to the molar heat capacity, known as Schottky anomaly.

- a. Use Eq. (8.68) in Problem 8.7 and show that the contribution to the molar heat capacity of a two-level system is

(continued)

Problem 8.8 (continued)

$$c_{\text{Schottky}}(T) = R \left(\frac{\Delta}{k_B T} \right)^2 \frac{e^{\frac{\Delta}{k_B T}}}{\left(1 + e^{\frac{\Delta}{k_B T}} \right)^2} \quad (8.79)$$

where Δ is the energy difference between the two levels without degeneracy.

- b. Show that $c_{\text{Schottky}}(T)$ has a peak value near

$$T_{\text{Peak}} \approx \frac{\Delta}{2.4 k_B}. \quad (8.80)$$

Lithium doped potassium chloride, Li:KCl, exhibits a Schottky anomaly with a peak value near 0.4 K. Determine the energy difference Δ . Can you give an interpretation of the peak in the heat capacity vs temperature curve?

Solution 8.8 The appearance of a peak in the heat capacity vs temperature curves of materials is associated with the term Schottky anomaly. It appears, for example, in paramagnetic materials, but also in crystals of the alkali halide KCl, which are doped with the smaller lithium ion. The multilevel nature of this system is discussed in detail in Problem 9.17. In **subproblem (a)**, we lead back to Eq. (8.79), describing the heat capacity of a two-level system for the more general expressions for multilevel systems found in Problem 8.7. For $L = 2$ and $g_i = 1$, $i = 1, 2$ we can write:

$$c_{\text{Schottky}}(T) = R \frac{\frac{E_1^2 - E_1 E_2}{k_B^2 T^2} e^{-\frac{E_1 + E_2}{k_B T}} + \frac{E_2^2 - E_1 E_2}{k_B^2 T^2} e^{-\frac{E_2 + E_1}{k_B T}}}{e^{-\frac{2E_1}{k_B T}} + 2e^{-\frac{E_1 + E_2}{k_B T}} + e^{-\frac{2E_2}{k_B T}}} \quad (8.81)$$

Introducing the energy difference Δ between the two levels, we can make the substitution $E_2 = E_1 + \Delta$ and obtain

$$\begin{aligned} c_{\text{Schottky}}(T) &= R \frac{\frac{-E_1 \Delta}{k_B^2 T^2} e^{-\frac{2E_1 + \Delta}{k_B T}} + \frac{\Delta^2 + E_1 \Delta}{k_B^2 T^2} e^{-\frac{\Delta + 2E_1}{k_B T}}}{e^{-\frac{2E_1}{k_B T}} + 2e^{-\frac{\Delta + 2E_1}{k_B T}} + e^{-\frac{2E_1 + 2\Delta}{k_B T}}} \\ &= R \frac{\frac{\Delta^2}{k_B^2 T^2} e^{-\frac{\Delta}{k_B T}} e^{-\frac{2E_1}{k_B T}}}{e^{-\frac{2E_1}{k_B T}} + 2e^{-\frac{\Delta}{k_B T}} e^{-\frac{2E_1}{k_B T}} + e^{-\frac{2\Delta}{k_B T}} e^{-\frac{2E_1}{k_B T}}} \\ &= R \frac{\frac{\Delta^2}{k_B^2 T^2} e^{-\frac{\Delta}{k_B T}}}{1 + 2e^{-\frac{\Delta}{k_B T}} + e^{-\frac{2\Delta}{k_B T}}} \end{aligned} \quad (8.82)$$

If we expand numerator and denominator by a factor $e^{\frac{2\Delta}{k_B T}}$ and apply the first binomial formula (Eq. (A.1)) to the denominator, we obtain the sought Eq. (8.79).

In **subproblem (b)**, we are interested in the position of the peak in the heat capacity vs temperature curve. We show that the peak temperature, T_{Peak} , is related to the splitting between the two levels according to Eq. (8.80). The trick is to introduce the dimensionless parameter $\alpha = \frac{\Delta}{k_B T}$. The heat capacity of the two-level system can be written as a function of α only:

$$c_{\text{Schottky}}(\alpha) = R \frac{\alpha^2 e^\alpha}{(1 + e^\alpha)^2} \quad (8.83)$$

Extrema of the heat capacity will thus be characterized by a special value of α_m . The necessary condition for the maximum in the heat capacity vs temperature curve is:

$$\frac{d}{d\alpha} c_{\text{Schottky}}(\alpha) = \frac{d}{d\alpha} \frac{R\alpha^2 e^\alpha}{(1 + e^\alpha)^2} \stackrel{!}{=} 0; \quad \alpha = \alpha_m \quad (8.84)$$

Application of the product rule for differentiation (Eq. (A.15)) yields:

$$\frac{2\alpha e^\alpha + \alpha^2 e^\alpha}{(1 + e^\alpha)^2} - \frac{2\alpha^2 e^{2\alpha}}{(1 + e^\alpha)^3} = 0; \quad \alpha = \alpha_m \quad (8.85)$$

Additional simplifications yield a transcendental equation:

$$e^{\alpha_m} = \frac{2 + \alpha_m}{\alpha_m - 2} \quad (8.86)$$

or

$$\alpha_m = \ln \frac{2 + \alpha_m}{\alpha_m - 2} \quad (8.87)$$

which cannot be further simplified. A graphical solution of the last equation is shown in Fig. 8.15, according to which the extremum is characterized by $\alpha_m = 2.3994 \approx 2.4$. We have thus justified Eq. (8.80). In **subproblem (c)**, we deal with the example of lithium doped KCl. Low-temperature measurements of the heat capacity show that this material exhibits a Schottky anomaly with a peak temperature of only $T_{\text{Peak}} \approx 0.4$ K. This corresponds to a small energy splitting of:

$$\Delta = 2.4 k_B T_{\text{Peak}} = 1.3 \times 10^{-23} \text{ J} = 8.3 \times 10^{-5} \text{ eV}. \quad (8.88)$$

Below, in Problem 9.17, we deal with a simplified model of the Li:KCl system using quantum mechanics.

Fig. 8.15 Graphical solution of the transcendental equation (8.87). Function $f_1(\alpha) = \alpha$ is a line through the origin, function $f_2(\alpha) = \ln \frac{2+\alpha}{\alpha-2}$. The intersection of f_1 and f_2 is at $\alpha_m = 2.3994$

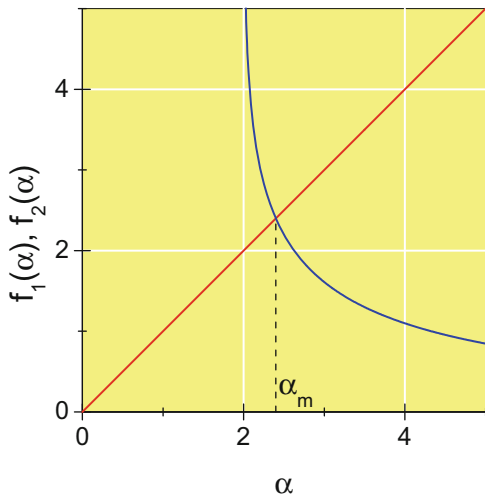
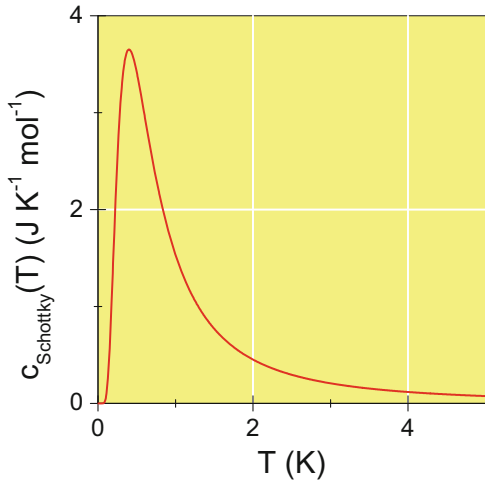


Fig. 8.16 Schottky anomaly in the system Li:KCl according to Eq. (8.79)



The heat capacity vs temperature curve of the Schottky anomaly in Li:KCl is shown in Fig. 8.16. Can we associate the peak temperature with a special condition of the two-level system? To analyze this, we consider the occupation probabilities of the two levels. Using the Boltzmann statistics Eq. (8.3), the latter can be expressed in terms of the parameter α :

$$p_1 = \frac{e^{-\frac{E_1}{k_B T}}}{e^{-\frac{E_1}{k_B T}} + e^{-\frac{E_2}{k_B T}}} = \frac{1}{1 + e^{-\frac{\Delta}{k_B T}}} = \frac{1}{1 + e^{-\alpha}} \quad (8.89)$$

$$p_2 = 1 - p_1 = \frac{e^{-\alpha}}{1 + e^{-\alpha}} \quad (8.90)$$

Let us consider the *change* in the occupation probability of the ground state:

$$\frac{\partial p_1}{\partial T} = \frac{\partial p_1}{\partial \alpha} \frac{\partial \alpha}{\partial T} = \frac{e^{-\alpha}}{(1 + e^{-\alpha})^2} \left(-\frac{\Delta}{k_B T^2} \right) = -\frac{\Delta}{k_B T^2} \frac{e^{-\frac{\Delta}{k_B T}}}{(1 + e^{-\frac{\Delta}{k_B T}})^2} \quad (8.91)$$

From Eq. (8.83) we obtain:

$$c_{\text{Schottky}}(T) = N_A k_B \frac{\Delta^2}{k_B^2 T^2} \frac{e^{-\frac{\Delta}{k_B T}}}{(1 + e^{-\frac{\Delta}{k_B T}})^2} \quad (8.92)$$

As a consequence, the change in occupation probability of the ground state is proportional to $c_{\text{Schottky}}(T)$:

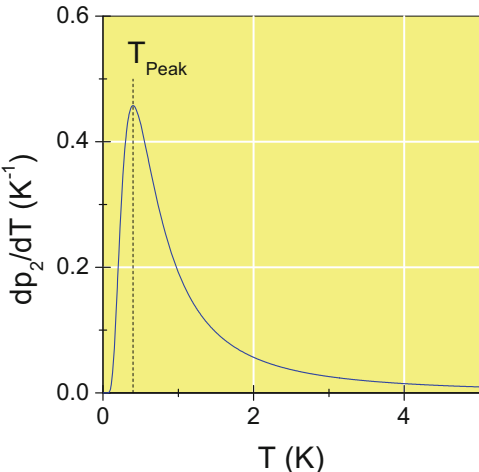
$$\frac{\partial p_1}{\partial T} = -\frac{1}{N_A \Delta} c_{\text{Schottky}}(T) \quad (8.93)$$

Therefore, the peak in the heat capacity can be associated with the maximum decrease in occupation probability of the ground state. Obviously, because of Eq. (8.90) and thus

$$\frac{\partial p_2}{\partial T} = -\frac{\partial p_1}{\partial T}, \quad (8.94)$$

the population gain of level 2 also reaches a maximum at the peak temperature T_{Peak} . The change in occupation probability of the excited state as a function of temperature is also shown in Fig. 8.17.

Fig. 8.17 Population change of the excited state in the two-level system related to the Schottky anomaly in Li:KCl. The maximum gain of p_2 is found at the peak temperature T_{Peak} (Eq. (8.80))



References

1. Jaynes ET (1992) The Gibbs paradox. In: Smith CR, Erickson GJ, Neudorfer PO (eds) Maximum entropy and Bayesian methods. Kluwer, Dordrecht, pp 1–22
2. Levinthal C (1969) How to fold graciously. In: Debrunner P, Tsibris J, Münck E (eds) Mössbauer spectroscopy in biological systems. University of Illinois Press, Urbana (IL), p 22
3. Davies, PR, Roberts MW (2008) Atom resolved surface reactions. RSC Publishing, Cambridge
4. Pitzer KS (1995) Thermodynamics. McGraw-Hill, New York
5. Gearhart CA (2010) "Astonishing Successes" and "Bitter Disappointment": the specific heat of hydrogen in quantum theory. Arch Hist Exact Sci 64:113
6. Bonhoeffer KF, Harteck P (1929) Z Phys Chem 4B:113

Chapter 9

Quantum Mechanics and Electronic Structure

Abstract Quantum mechanics provides the basis for the description of matter on the atomic scale. Developed in conjunction with progress in spectroscopy, it explains phenomena such as the photoelectric effect, molecular spectra, electronic structure, and the chemical bond. Challenging and at the same time fascinating, the predictions of quantum mechanics are beyond direct everyday perception. (To some extent this is in contrast to thermodynamics and changes of state (Chap. 3) where experience from everyday perception is a reasonable criterion for assessing the soundness of predictions.) The basic concepts introduce the postulates of quantum mechanics. Aside from problems dealing with black body radiation, wave-packet propagation, and the hydrogen atom, applications of operator calculus and the variational principle are highlights that show perspectives with regard to tackling advanced problems in this field.

9.1 Basic Concepts

John Dalton's atomic model of matter is successful in the quantitative description of chemical reactions outlined in Chap. 2. From the beginning of the twentieth century, however, material science made tremendous progress in obtaining increasing insight into the structure of matter. Joseph John Thomson discovered the negatively charged *cathode rays* and deduced from his discovery the existence of the electron as an elementary particle. He developed a more precise atomic model, based on positive and negative charge being distributed in the atom. Ernest Rutherford deduced from scattering experiments that the entire positive charge and nearly the complete mass of the atom is concentrated in the nucleus. At the beginning of the twentieth century, thermodynamics and electrodynamics were fully developed theories, but they failed to explain the structure and stability of the atom. Moreover, they could not explain the structure of emission and absorption spectra of atoms investigated by Joseph Fraunhofer and others. At this time, Pieter Zeeman had already observed the splitting of characteristic spectral lines of sodium in an external magnetic field. These discoveries, however, revealed the necessity of a new description of the properties of matter in terms of quantum mechanics. It is thus obvious that the development of quantum mechanics is closely related to discoveries in the field of spectroscopy.

Quantum mechanics makes use of complex numbers (see Sect. A.3.4). In the following, it is thus assumed that the reader is familiar with the basic rules for complex number calculus.

9.1.1 Failure of Classical Mechanics: Key Experiments

9.1.1.1 Photoelectric Effect

If a cathode material is irradiated in a vacuum with light of wavelength λ , electrons are emitted if the wavelength is below a certain threshold wavelength λ_0 characteristic for the material. The kinetic energy of the electrons can be determined by applying a negative stopping potential between the irradiated material and an anode material. This necessary stopping potential U , which results in zero photo current, depends linearly on the light frequency $\nu = \frac{c}{\lambda}$:

$$U(\nu) = \frac{h}{e} (\nu - \nu_0) \quad (9.1)$$

From the slope of the function $U(\nu)$, the fundamental constant h can be determined, which is called **Planck's constant**.

If the frequency of the light irradiating the cathode is below the threshold frequency ν_0 , no electrons are detected, no matter how high the light intensity. The interpretation of the photoelectric effect given by Albert Einstein is that the energy of light is mediated in discrete portions, *quanta*, with the energy

$$E = h\nu \quad (9.2)$$

The associated particle with zero mass called *photon* moves at the speed of light c , and has the momentum

$$p = \frac{h}{\lambda}. \quad (9.3)$$

The resulting wave-particle duality was extended by Louis-Victor de Broglie to electrons and other massive particles. In this context, Eq. (9.3) is called the de Broglie equation and λ **de Broglie wavelength**.

9.1.1.2 Black Body Radiation

If a piece of matter is heated to a high temperature, it starts to glow. This phenomenon was intensively studied at the end of the nineteenth century, and it was found that classical thermodynamics and the theory of electrodynamics could not fully explain the emission characteristics. *Black body* absorbs all electromagnetic radiation in the complete frequency spectrum. If it is in thermal equilibrium with its surroundings, it also emits electromagnetic radiation, and the spectral energy density depends only on temperature. The radiation emitted through a small hole of a cavity is in very good approximation with black body radiation, as all radiation impinging on the hole from the surroundings is absorbed by the atoms of the cavity walls, which are in equilibrium with the radiation field. Electromagnetic theory predicts the **spectral energy density** of such a black body to be:

$$u(\nu, T) = \frac{8\pi\nu^2}{c^3} \langle E_{\text{osc}} \rangle \quad (9.4)$$

Here, $\langle E_{\text{osc}} \rangle$ is the *average oscillator energy* of an atomic oscillator with a frequency ν . The classical equipartition theorem predicts $\langle E_{\text{osc}} \rangle = k_B T$. Thus, the spectral energy would diverge to infinity if $\nu \rightarrow \infty$. Max Planck has corrected the expression for $\langle E_{\text{osc}} \rangle$ based on his hypothesis of the quantization of the oscillator energy:

$$E = n h\nu \quad n = 0, 1, 2, \dots \quad (9.5)$$

In Problem 9.1, we show that Planck's assumption leads to the correct expression for the energy density of a black body:

$$u(\nu, T) = \frac{8\pi h\nu^3}{c^3} \frac{1}{e^{\frac{h\nu}{k_B T}} - 1} \quad (9.6)$$

The power P emitted by a black body with a total area A depends only on its temperature and is given by the **Stefan-Boltzmann law**:

$$P = \sigma A T^4 \quad (9.7)$$

Here,

$$\sigma = \frac{2\pi^5 k_B^4}{15h^3 c^2} = 5.670373 \times 10^{-8} \text{ W m}^{-2} \text{ K}^{-4} \quad (9.8)$$

is the Stefan-Boltzmann constant.

9.1.2 Wave Mechanics

9.1.2.1 Postulates of Quantum Mechanics

Quantum mechanics, as it appears adequate for providing a description of systems on the atomic and molecular scale, can be summarized by a few postulates¹:

Postulate 1: To every state of a system there is a complex function ψ ascribed to and defining the state.

Comments: (1) For one particle this function is $\psi(x, t)$. (2) According to Max Born, $|\psi(x, t)|^2 dx$ is the (quantum mechanical) probability of finding the particle in a region between x and $x + dx$. (3) Dirac's abstract generalization of the wave function is a **ket-vector** $|\psi\rangle$.

Postulate 2: The wave functions form a complex vector space. If ψ_1 and ψ_2 are two possible wave functions, then $\psi = \alpha\psi_1 + \beta\psi_2$ (where α and β are complex numbers) is also a possible wave function.

Comment: This is the **superposition principle**.

Postulate 3: The *scalar product* of two wave functions ψ_1 and ψ_2 is:

$$\langle \psi_1 | \psi_2 \rangle = \int_{-\infty}^{+\infty} \psi_1^*(x, t) \psi_2(x, t) dx \quad (9.9)$$

Specifically,

$$\langle \psi | \psi \rangle = \int_{-\infty}^{+\infty} |\psi(x, t)|^2 dx \quad (9.10)$$

is called the *norm* of the wave function.

Comment: Dirac's notation calls $\langle \psi |$ a **bra-vector**

Postulate 4: A **Hermitian operator** \hat{A} is one for which

$$\langle \hat{A}\psi_1 | \psi_2 \rangle = \langle \psi_1 | \hat{A}\psi_2 \rangle; \quad (9.11)$$

Observables, i.e., measurable quantities with real eigenvalues, are represented by Hermitian operators. Comment: If \hat{A} is an arbitrary operator, then \hat{A}^+ is called its **adjoint operator**, and

$$\langle \hat{A}^+ \psi_1 | \psi_2 \rangle = \langle \psi_1 | \hat{A} \psi_2 \rangle; \quad (9.12)$$

As a consequence, a Hermitian operator is called **self adjoint operator**: $\hat{A}^+ = \hat{A}$.

¹The number of postulates differs from textbook to textbook, although they cover the same content.

Postulate 5: If \hat{A} is an arbitrary operator, then $|\psi_n\rangle$ is called eigenfunction or eigenstate of \hat{A} , and λ_n eigenvalue, if the following equation holds:

$$\hat{A}|\psi_n\rangle = \lambda_n|\psi_n\rangle \quad (9.13)$$

If there are several possible eigenstates, then the eigenstates are orthonormal²:

$$\langle\psi_m|\psi_n\rangle = \delta_{mn} \quad (9.14)$$

Comment: This requires the eigenstates to be normalized. The spectrum of possible eigenstates constitutes a complete basis, and an arbitrary state function can be written:

$$|\phi\rangle = \sum_n c_n |\psi_n\rangle.$$

Since

$$\langle\psi_m|\phi\rangle = \sum_n c_n \langle\psi_m|\psi_n\rangle = \sum_n c_n \delta_{nm} = c_m$$

Postulate 6: If the state $|\phi\rangle$ of a system is not an eigenstate of an operator \hat{A} , a measurement of its observable provides one of the possible eigenvalues λ_n . The quantum mechanical **expectation value** for this observable is:

$$\langle\hat{A}\rangle = \frac{\langle\phi|\hat{A}|\phi\rangle}{\langle\phi|\phi\rangle} \quad (9.15)$$

Comment: The probability that the result of the measurement provides the eigenvalue λ_n is: $|c_n|^2$ where $c_n = \langle\psi_n|\phi\rangle$. This follows from:

$$\langle\hat{A}\rangle = \langle\phi|\hat{A}|\phi\rangle = \sum_m \sum_n c_m^* c_n \langle\psi_m|\hat{A}|\psi_n\rangle = \sum_m \sum_n c_m^* c_n \lambda_n \underbrace{\langle\psi_m|\psi_n\rangle}_{\delta_{mn}} = \sum_n |c_n|^2 \lambda_n$$

Postulate 7: The state function of a system follows from the solution of the time-dependent **Schrödinger equation**:

$$i\hbar \frac{\partial}{\partial t} |\psi(t)\rangle = \hat{H} |\psi(t)\rangle \quad (9.16)$$

²The Kronecker delta δ_{mn} is defined as follows: $\delta_{mn} = 1$ if $m = n$, and $\delta_{mn} = 0$ if $m \neq n$.

Comment: The operator \hat{H} is the Hamiltonian whose eigenvalue is the total energy (see Problem 9.6).

9.1.2.2 Commutators

Application of quantum mechanics to special systems and their discussion frequently makes use of the concept of a commutator between two operators \hat{A} and \hat{B} :

$$[\hat{A}, \hat{B}] \stackrel{\text{def}}{=} \hat{A}\hat{B} - \hat{B}\hat{A} \quad (9.17)$$

If $[\hat{A}, \hat{B}] = 0$ then the two operators commute with each other. In this case, the order of these operators does not influence the result. An important consequence is that commuting operators share a common orthonormal system of eigenfunctions.

9.1.2.3 Harmonic Oscillator

The harmonic oscillator problem is defined by the Schrödinger equation of a particle of mass m moving in a harmonic potential that is characterized by the force constant k :

$$-\frac{\hbar^2}{2m} \frac{d^2}{dx^2} \psi_n(x) + \frac{1}{2} kx^2 \psi_n(x) = E_n \psi_n(x) \quad (9.18)$$

The problem can be treated exactly and the solutions can be found in textbooks. The energy eigenvalues are:

$$E_n = \hbar\omega \left(n + \frac{1}{2} \right); \quad n = 0, 1, 2, \dots \quad (9.19)$$

where the angular frequency ω of the motion is related to the force constant k

$$\omega = \sqrt{\frac{k}{m}}. \quad (9.20)$$

Even in the ground state $n = 0$, the particle has a zero-point vibrational energy $E_0 = \frac{\hbar\omega}{2}$ (see also Problem 9.2). The first energy levels of the harmonic oscillator and the wave functions are shown in Fig. 9.1. The ground state wave function of the harmonic oscillator is a Gaussian function, excited state wave functions contain Hermite polynomials (see Appendix Sect. A.3.13). The harmonic oscillator problem is the basis for the description of molecular vibrations (see Sect. 10.1.3).

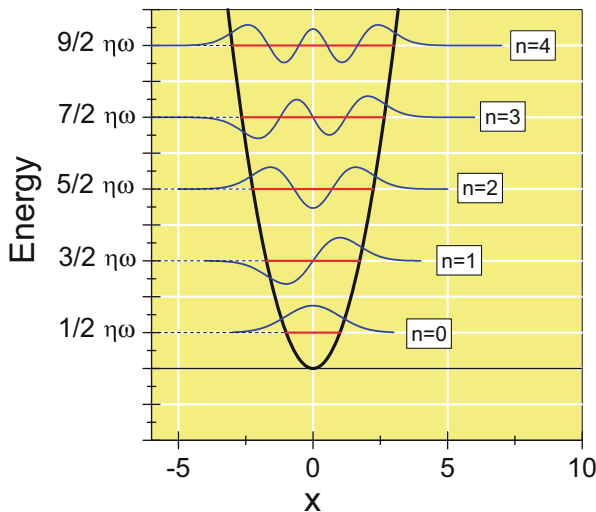


Fig. 9.1 Energy levels and wave functions of the harmonic oscillator. The amplitude of the wave functions was scaled by a factor of 0.5

9.1.3 Atomic Structure

Exact descriptions of the electronic structure of atoms can only be given for the neutral hydrogen atom along with other one-electron systems, such as He^+ , Li^{2+} . The textbook results for the energy levels in these systems are:

$$E_{nl} = -\frac{Z^2 \mu e^4}{8\epsilon_0^2 h^2} \frac{1}{n^2} \quad n = 1, 2, \dots \quad (9.21)$$

where μ is the effective mass of the two-body system.³ The number n is the principal quantum number and $l = 0, 1, \dots, n - 1$ is the quantum number for the orbital angular momentum. The quantity

$$\text{Ry} = \frac{m_e e^4}{8\epsilon_0^2 h^2} = 13.605693 \text{ eV} \quad (9.22)$$

is the Rydberg energy. As can be seen in Eq. (9.21), there is a *degeneracy* of the energy levels with regard to different values of l . In the absence of external fields a further degeneracy with regard to the magnetic quantum number m occurs, which takes integer values between $-l$ and $+l$. The wave functions for the hydrogen

³If $M \gg m_e$ is the mass of the nucleus, the effective mass $\mu = \frac{M m_e}{M + m_e}$ is close to m_e . In the case of positronium consisting of an electron and a positron of the same mass, however, $\mu = \frac{m_e}{2}$.

problem are a solution of the Schrödinger equation

$$\left(-\frac{\hbar^2}{2\mu} \Delta - \frac{Ze^2}{4\pi\epsilon_0 r} \right) \psi_{nlm}(r, \theta, \phi) = E_{nlm} \psi_{nlm}(r, \theta, \phi) \quad (9.23)$$

where the Laplacian operator Δ is best expressed in spherical coordinates r , θ and ϕ (see Eq. (A.68) in Sect. A.3.11). The wave function separates into two parts:⁴ a radial function $R_{nl}(r)$ and a spherical harmonic $Y_{lm}(\theta, \phi)$:

$$\psi_{nlm}(r, \theta, \phi) = R_{nl}(r) Y_{lm}(\theta, \phi) \quad (9.24)$$

The eigenvalue equation for the angular part is:

$$\hat{L}^2 Y_{lm}(\theta, \phi) = l(l+1)\hbar^2 Y_{lm}(\theta, \phi); \quad l = 0, 1, 2, \dots; m = -l, -l+1, \dots, 0, \dots, l-1, l \quad (9.25)$$

with \hat{L}^2 being the operator of the angular momentum squared, and l is the angular momentum quantum number. A state with $l = 0$ is called an s-state, $l = 1$ is called a p-state, and $l = 2$ a d-state. Explicit expressions for the first spherical harmonics are given in the Appendix in Sect. A.3.14. The eigenvalue equation of the radial function is:

$$\left[-\frac{\hbar^2}{2\mu} \left(\frac{\partial^2}{\partial r^2} + \frac{2}{r} \frac{\partial}{\partial r} \right) + \frac{\hbar^2 l(l+1)}{2\mu r^2} - \frac{Ze^2}{4\pi\epsilon_0 r} \right] R_{nl}(r) = E_{nl} R_{nl}(r). \quad (9.26)$$

Its solutions are tabulated in the Appendix Sect. A.3.15 for hydrogen ($Z = 1$).

The spatial shape of some orbital wave functions is shown in Fig. 9.2.

9.1.4 Atomic Units

In atomic and molecular structure theory, it is common to introduce *atomic units* (a.u.). This involves setting:

$$\hbar = e = m_e = 4\pi\epsilon_0 = 1. \quad (9.27)$$

As a result, the atomic energy unit is 1 E_h (Hartree)=27.211386eV, which is twice the Rydberg energy. The atomic unit of length is $1a_0 = 0.52917721092(17) \times 10^{-10}$ m, i.e., 1 bohr radius.

⁴For explicit expressions of $R_{nl}(r)$ and $Y_{lm}(\theta, \phi)$ see Sects. A.3.14 and A.3.15.

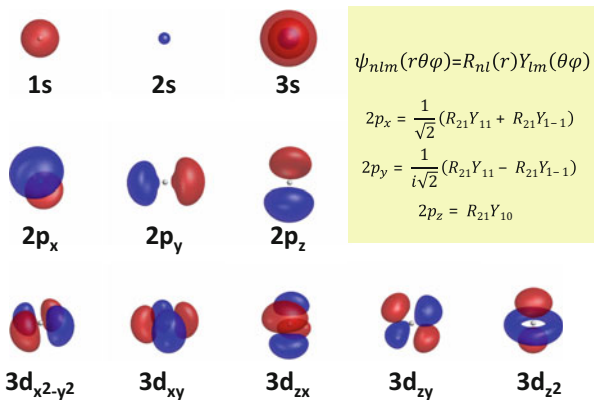


Fig. 9.2 Spacial geometry of some orbitals of the hydrogen atom. The surface of the constant contour value ± 0.05 of the orbital wave functions is shown. The *inset* demonstrates the construction of (real) $2p_x$, $2p_y$ and $2p_z$ functions from radial functions and (complex) spherical harmonics

9.2 Problems

Problem 9.1 (Derivation of the Average Oscillator Energy) Given the possible energy values of an oscillator,

$$E_n = E_0 + nh\nu, \quad n = 0, 1, \dots, \quad (9.28)$$

and a Boltzmann distribution for the average occupation number,

$$\langle n \rangle = \sum_n n \exp(-\alpha n), \quad \alpha = \frac{h\nu}{k_B T}, \quad (9.29)$$

derive Planck's equation for the average oscillator energy

$$\langle E_{\text{osc}} \rangle = E_0 + \frac{h\nu}{\exp\left(\frac{h\nu}{k_B T}\right) - 1}. \quad (9.30)$$

E_0 is an arbitrary constant energy that is determined in Problem 9.2.

Solution 9.1 In this exercise, we deal with the average oscillator energy introduced in Sect. 9.1.1.2. Doing so, we understand an essential part of Planck's law for the radiation density of a black body. Before entering the calculation, it is useful

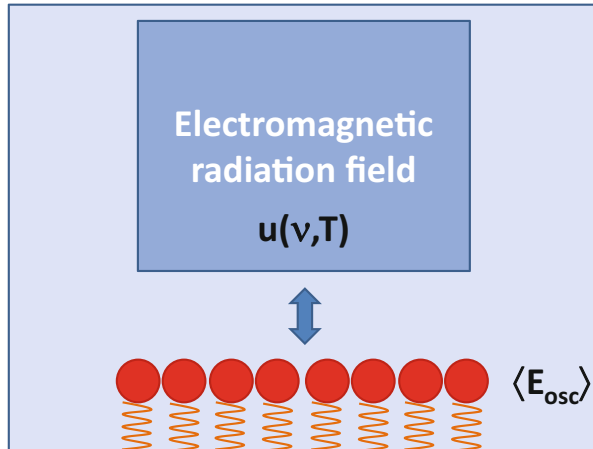


Fig. 9.3 Thermal equilibrium between the electromagnetic radiation field within a cavity coupled with absorption and emission to atomic oscillators at the cavity walls (schematic)

to reflect on the nature of the oscillators for which we calculate the average energy. Following Planck, we can assume a thermal equilibrium between the electromagnetic radiation field within a cavity and the atoms at the cavity walls. The equilibrium is established by absorption and emission processes of quanta of energy $h\nu$. The scenario is sketched schematically in Fig. 9.3. Experimentally, it has been found that the spectral energy density of a black body is independent of its composition, chemical nature, and structure. The simple model representing the atoms of the cavity wall is thus an ensemble of so-called *Lorentz-oscillators*, spring mass systems vibrating at a frequency ν . We have seen how such an ensemble of oscillators can be treated by means of statistical thermodynamics in Sect. 8.1.2.

According to Planck's assumption, the energy values of an oscillator of frequency ν is:

$$E_n = E_0 + n h\nu \quad n = 0, 1, 2, \dots \quad (9.31)$$

Here, n counts the number of quanta by which the oscillator is excited. Next, the concept of probability and statistics is introduced: we express the expectation value of the oscillator energy, $\langle E_{\text{osc}} \rangle$, by the average number of quanta, $\langle n \rangle$:

$$\langle E_{\text{osc}} \rangle = \langle n \rangle h\nu \quad (9.32)$$

For $\langle n \rangle$ we use a *Boltzmann-Ansatz*:

$$\langle n \rangle = \frac{\sum_n^\infty n \exp\left(-\frac{E_n}{k_B T}\right)}{\sum_n^\infty \exp\left(-\frac{E_n}{k_B T}\right)} = \frac{\sum_n^\infty n \exp(-\alpha n)}{\sum_n^\infty \exp(-\alpha n)}; \quad \alpha = \frac{h\nu}{k_B T} \quad (9.33)$$

Note that the factor α compares the quantum energy of the oscillator with the thermal energy at a given temperature T . The rest is clever mathematics. The sums in the last equation can be expressed by a geometrical series (see Eq. (A.57) in the Appendix):

$$\sum_n^{\infty} e^{-\alpha n} = \frac{1}{1 - e^{-\alpha}}, \quad (9.34)$$

and

$$\sum_n^{\infty} n e^{-\alpha n} = -\frac{\partial}{\partial \alpha} \sum_n^{\infty} e^{-\alpha n} = -\frac{\partial}{\partial \alpha} \frac{1}{1 - e^{-\alpha}} = \frac{e^{-\alpha}}{(1 - e^{-\alpha})^2}. \quad (9.35)$$

Putting the last three equations together, we obtain:

$$\langle n \rangle = \frac{e^{-\alpha} (1 - e^{-\alpha})}{(1 - e^{-\alpha})^2} = \frac{1}{e^{\alpha} - 1} \quad (9.36)$$

Hence, by resubstitution, the average energy of a harmonic oscillator at a temperature of T is

$$\langle E_{\text{osc}} \rangle = E_0 + \frac{h\nu}{\exp\left(\frac{h\nu}{k_B T} - 1\right)} \quad (9.37)$$

leading to the correct expression for the spectral energy density of black body radiation, Eq. (9.6). Interestingly, Max Planck went a slightly different route, focusing on the average oscillator entropy [1].

Problem 9.2 (The Zero Point Energy) Hint: It is assumed that you have dealt with Problem 9.1. The constant E_0 in Problem 9.1 is the quantum mechanical zero point energy. From the condition $h\nu \ll k_B T$ and the average oscillator energy given in Problem 9.1, prove that $E_0 = \frac{h\nu}{2}$.

Solution 9.2 Although the zero point energy of an oscillator would follow from a rigorous quantum mechanical treatment of the harmonic oscillator based on the Schrödinger equation, the same result has already been obtained from consideration of the so-called *correspondence principle*, proposed by Niels Bohr [2]: Each quantum system should behave like a classical system in the limit where classical mechanics applies. Classically, one expects an ensemble of oscillators at a finite temperature to have an average oscillator energy of $k_B T$. This value should be reproduced by the quantum mechanical treatment; if high quantum numbers n are occupied, i.e., if the average energy of the oscillator consists of so many energy

portions $h\nu$ that the discrete nature of the excitation spectrum becomes negligible: this is the limit $h\nu \ll k_B T$. Therefore, we start with the oscillator energy in Eq.(9.30) and make use of the power series expansion Eq.(A.58) found in the Appendix,

$$\frac{\alpha}{e^\alpha - 1} = 1 - \frac{\alpha}{2} + B_1 \frac{\alpha^2}{2!} - B_2 \frac{\alpha^4}{4!} + \dots$$

where $B_1 = \frac{1}{6}$ and $B_2 = \frac{1}{30}$ are the first Bernoulli numbers. With $\alpha = \frac{h\nu}{k_B T}$ we write

$$\begin{aligned}\langle E_{\text{osc}} \rangle &= E_0 + k_B T \frac{\alpha}{e^\alpha - 1} = E_0 + k_B T \left(1 - \frac{\alpha}{2} + B_1 \frac{\alpha^2}{2!} - B_2 \frac{\alpha^4}{4!} + \dots \right) \\ \langle E_{\text{osc}} \rangle &= E_0 + k_B T - \frac{h\nu}{2} + \frac{1}{12} k_B T \left(\frac{h\nu}{k_B T} \right)^2 - \frac{1}{720} k_B T \left(\frac{h\nu}{k_B T} \right)^4 + \dots\end{aligned}$$

In the limit $h\nu \ll k_B T$, the terms containing powers of $\frac{h\nu}{k_B T}$ can be ignored and thus the correspondence principle requires

$$\lim_{h\nu \ll k_B T} \langle E_{\text{osc}} \rangle = E_0 + k_B T - \frac{h\nu}{2} \stackrel{!}{=} k_B T,$$

from which the zero point energy

$$E_0 = \frac{h\nu}{2} = \frac{\hbar\omega}{2} \quad (9.38)$$

follows.

Problem 9.3 (Electron Impact Heating, see Fig. 9.4) In the ultrahigh vacuum technique, electron impact heating is often used to heat a sample to high temperature. Consider a thin sample with a cross-sectional area of 1 cm^2 grounded to earth potential. Its initial temperature of 300 K is that of the surroundings. A tungsten wire emits electrons with an emission current of 1.5 mA . Under the assumption that the sample is a black body and that radiation is the only heat transfer mechanism, calculate the potential between the tungsten wire and the sample to achieve a sample temperature of $1,200 \text{ K}$.

Solution 9.3 Cathode rays discovered by J.J. Thomson have practical applications in science and technology. The impact of electrons is a very effective way of heating

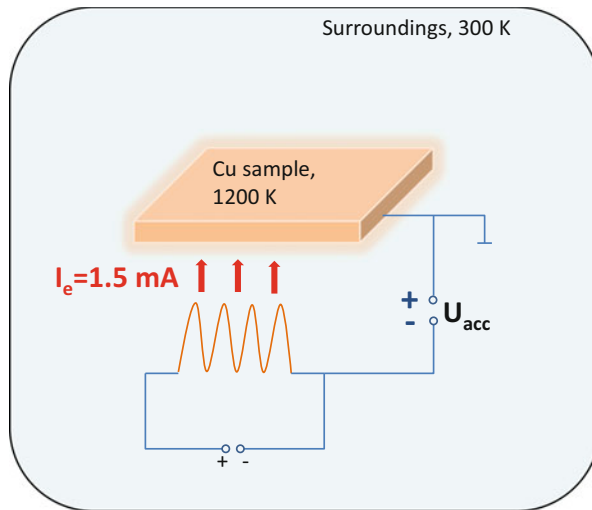


Fig. 9.4 Principle of electron impact heating. U_{acc} is the high voltage, by which emitted electrons are accelerated toward the copper sample

a sample to a high temperature.⁵ Under ultrahigh vacuum conditions at a pressure below 10^{-5} Pa , heat transfer from the sample to the surroundings is predominantly radiative; if heat losses across the sample mounting can be ignored.⁶ Assuming the copper sample to be a black body, the total radiation power emitted can be estimated using the Stefan Boltzmann law (Eq. (9.7)). If we additionally account for the temperature of the surroundings $T_{\text{surr.}}$, the net thermal power emitted by the sample at a given temperature T_{sample} is

$$P_{\text{thermal}} = A\sigma \left(T_{\text{sample}}^4 - T_{\text{surr.}}^4 \right)$$

where A is the total area of the copper sample, i.e., twice the cross-sectional area. To determine the necessary acceleration voltage, we equate this thermal power with the electrical power as the product of U_{acc} and the electron current I_e impinging on the sample. Hence,

$$P_{\text{el.}} = U_{\text{acc}}I_e \quad (9.39)$$

⁵Sample heating to high temperature, also called tempering, is, for example, needed to obtain well-defined, clean and crystalline materials.

⁶In Problem 7.4 we have seen that heat conduction mediated by particle collisions is largely suppressed under ultrahigh vacuum conditions.

and solving for U_{acc} we obtain

$$\begin{aligned} U_{\text{acc}} &= \frac{A\sigma}{I_e} \left(T_{\text{sample}}^4 - T_{\text{surr.}}^4 \right) \\ &= \frac{2 \times 10^{-4} \text{ m}^2 \times 5.670373 \times 10^{-8} \text{ W m}^{-2} \text{ K}^{-4}}{0.0015 \text{ A}} \left((1200 \text{ K})^4 - (300 \text{ K})^4 \right) \\ &= 15,616 \text{ V}. \end{aligned}$$

We thus need high-voltage acceleration to reach the requested sample temperature. In this context, it is worth mentioning another practical application: generation of X-rays. Electrons impinging on the sample surface with an energy in the keV range produce a certain amount of X-ray radiation.⁷

Problem 9.4 (Photoelectric Effect) Different cathode materials are irradiated with LASER light at a wavelength of $\lambda = 633 \text{ nm}$:

Cathode material	Al	Ba	Ba on WO_3	Cd	Cs	K
Work function (eV)	4.30	2.52	0.30	4.04	1.94	2.22

- Which of the cathode materials show the photoelectric effect?
- The intensity of the LASER radiation is continuously increased. Does this alter the number of cathode materials showing the photoelectric effect?

Solution 9.4 The photoelectric effect is the basis of several important experimental methods such as X-ray and ultraviolet photoelectron spectroscopy (XPS, UPS, ESCA⁸). On the other hand, a simple setup (Fig. 9.5) to demonstrate the photoelectric effect is possible so that the experiment can be regularly performed on high-school physics courses. A cathode on ground potential is irradiated with monochromatic LASER light of wavelength λ . In our case, it is a helium neon LASER with $\lambda = 633 \text{ nm}$. The associated quantum energy is:

$$\begin{aligned} E = h\nu &= \frac{hc}{\lambda} = \frac{6.626 \times 10^{-34} \text{ J s} \times 2.99792 \times 10^8 \text{ m s}^{-1}}{633 \times 10^{-9} \text{ m}} \\ &= 3.14 \times 10^{-19} \text{ J} = 1.96 \text{ eV}. \end{aligned} \tag{9.40}$$

⁷See Problem 10.1 and Table 10.1 at page 300.

⁸XPS X-ray photoelectron spectroscopy, UPS ultraviolet photoelectron spectroscopy, ESCA electron spectroscopy for chemical analysis.

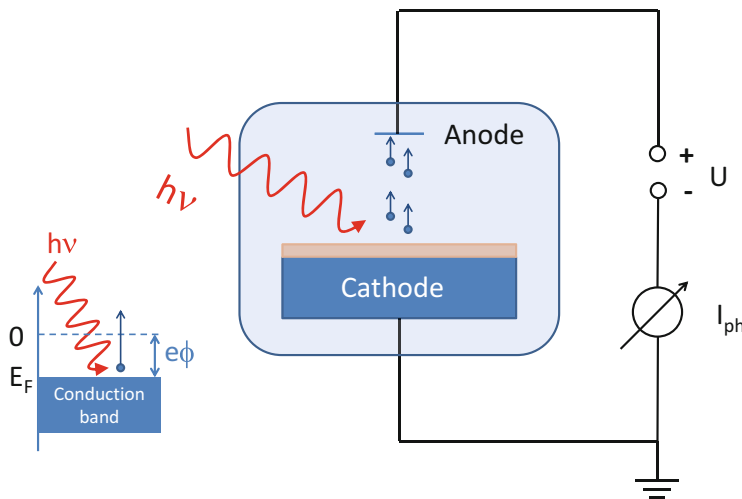


Fig. 9.5 Experimental setup to measure the photoelectric effect from cathode materials. The *inset* on the *left* illustrates the photo effect in the energy band model of a metal. The work function $e\phi$ is the difference in energy of the Fermi energy E_F and the vacuum potential level

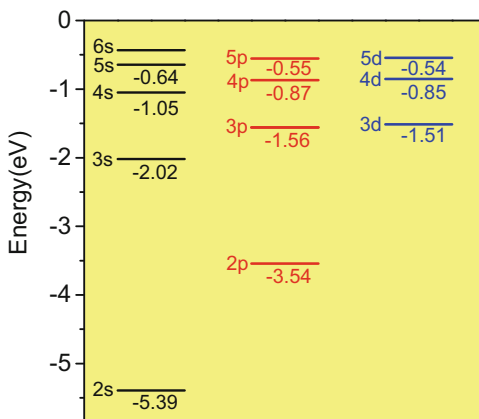
If the quantum energy exceeds the work function $e\phi$ of the cathode material, a photo electron excited from the *Fermi level* may escape into the vacuum and be extracted to the anode, the latter being on a positive potential level. Thus, only if the LASER light generates photoelectrons is a photocurrent I_{ph} measured. Our task in **subproblem (a)** is to check which of the cathode materials have a work function energy smaller than or equal to the quantum energy of our LASER. This is the case for barium on tungsten oxide ($\text{Ba on } \text{WO}_3$) and for cesium (Cs). In the latter case the quantum energy exceeds the work function only by 0.02 eV. In all other cases, the quantum energy of the LASER is not sufficient to generate photo electrons. In **subproblem (b)**, we are asked if an increase of LASER intensity could induce a photoelectric effect in the other cathode materials, too. This is not the case. The excitation of a photoelectron appears to be an elementary process requiring an energy of at least $e\phi$. The number of light quanta, i.e., the intensity of the LASER beam, is not decisive for the photoelectric effect to occur.

Problem 9.5 (Lithium Atom and Quantum Defect)

- The ionization energy of Lithium ($Z = 3$) is 5.39 eV. Assume that the model of the hydrogen atom can be applied to lithium and calculate the effective charge Z_{eff} of the nucleus as a result of the shielding by the $1s$ electrons.

(continued)

Fig. 9.6 Atomic energy levels of the element lithium



Problem 9.5 (continued)

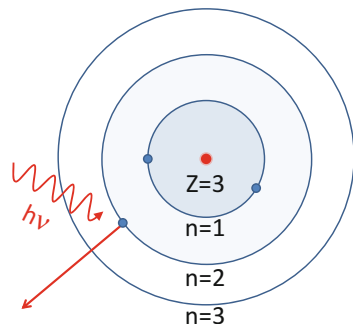
- b. Figure 9.6 shows the energy levels of the Li atom (L.J. Radziemski et al., Phys. Rev. A **52** (1995), 4462). Use the result of subproblem (a) to calculate the energy levels of the lithium atom. Compare the result with the experimental data and describe the differences.
- c. An improved approximative model for hydrogen-like atoms makes use of the so-called quantum defects δ_l ($l = s, p, \dots$), which modify the formula for the energy levels according to:

$$E_{n,l} = -\frac{\text{Ry}}{(n - \delta_l)^2}. \quad (9.41)$$

Use the data in Fig. 9.6 and determine the parameters δ_l for lithium.

Solution 9.5 Although the quantum mechanical models give a very concise picture for atoms and ions with one single electron, systems with more than one electron can only be treated in an approximate fashion. Here, we shall consider the lithium atom with three electrons and the ground state configuration $1s^2 2s^1$. If the atom undergoes a process of ionization, the $2s$ electron is removed. The situation is shown in Fig. 9.7. In the simple picture of the Bohr model, the two $1s$ electrons lead to a shielding of nuclear charge. If the shielding were complete, the $2s$ electron would see an effective charge of $+e$. For all transitions in which only the $2s$ electron is involved, an approximative treatment on the basis of an adapted model for the hydrogen atom can be applied.

Fig. 9.7 Simple picture of the lithium atom within the Bohr model. The charge of the nucleus is partially shielded by the 1s electrons



In **subproblem (a)**, we apply the simplest adaption and consider an effective nuclear charge $Z_{\text{eff}}e$ replacing the charge Ze of the "naked" nucleus:

$$\Delta E = E_f - E_i = Z_{\text{eff}}^2 \frac{m_e e^4}{8\epsilon_0^2 h^2} \left(\frac{1}{n_i^2} - \frac{1}{n_f^2} \right) \quad (9.42)$$

If the model is reasonable, we expect Z_{eff} close to 1. In the ionization process ($n_i = 2$ and $n_f \rightarrow \infty$), the last equation yields:

$$E_{\text{ion}} = Z_{\text{eff}}^2 \text{Ry} \left(\frac{1}{4} - 0 \right)$$

and thus

$$Z_{\text{eff}} = \sqrt{\frac{4E_{\text{ion}}}{\text{Ry}}} = 1.26$$

The result is in fact close to 1, but it also indicates that the shielding of the nuclear charge by the 1s electrons is not complete.

Further, in **subproblem (b)**, we deal with the lithium atom and refine the treatment of its electronic structure to some extent. Alkali metals (Li, Na, K, ...) have a single valence electron and the electronic excitations of the atom are governed by transitions of this valence electron in excited states. The energy levels of such states are given in Fig. 9.6. At first, we investigate how well the effective nuclear charge $Z_{\text{eff}} = 1.26$ can reproduce this term diagram. The energy levels depend only on the quantum number n and are calculated using:

$$E_n = \frac{Z_{\text{eff}}^2 \text{Ry}}{n^2} \quad (9.43)$$

We obtain $E_2 = -4.28 \text{ eV}$, $E_3 = -1.90 \text{ eV}$, $E_4 = -1.07 \text{ eV}$, and $E_5 = -0.69 \text{ eV}$. We notice that the lithium energy levels E_{nl} depend markedly on the angular

momentum quantum number l , which is not reproduced by our simple formula. Our result for E_2 lies between the 2s level (-5.39 eV), and the 2p level (-3.54 eV). Similarly, our result for E_3 falls between 3s (-2.02 eV) and 3d (-1.51 eV). Our value E_4 is fairly close to the energy of the 4s state (-1.05 eV), the same is true for E_5 , which is close to the energy of the 5s state (-0.64 eV). In summary, we can conclude that the higher the principal quantum number n , the better the prediction based on the effective nuclear charge. For $n = 2$, the agreement is worse and the model cannot explain the observed splitting between 2s and 2p, for example. Is an improved treatment possible?

In **subproblem (c)**, we follow an alternative treatment that goes back to the work of Rydberg and Schrödinger [3], who introduced the quantum defect δ_l . We use Eq. (9.41) and determine δ_l from the energy levels in Fig. 9.6. We could carry out a trial and error procedure or nonlinear fitting to determine δ_s from the values for 2s, 3s, 4s, and 5s. Alternatively, we solve for δ_l and obtain:

$$\delta_l = n - \sqrt{-\frac{\text{Ry}}{E_{n,l}}} \quad (9.44)$$

We obtain $\delta_s = 0.412$ (2s), 0.405 (3s), 0.401 (4s), and 0.390 (5s). All values are close to each other. We take the average value of 0.402 δ_s and obtain the energy levels shown in Table 9.1. With the same method, we obtain $\delta_p = 0.040$ and $\delta_d = 0.000$. The agreement between experimental and calculated energies is good.

Because of its simplicity the quantum defect model has been popular and is still used to describe highly excited atoms, the so-called Rydberg atoms.

Table 9.1 Comparison of energy levels in the lithium atom (see Fig. 9.6) and calculated energies based on the quantum defect approximation with Eq. (9.41)

State	2s	3s	4s	5s
Experiment	-5.39	-2.02	-1.05	-0.64
Calculated ($\delta_s = 0.402$)	-5.33	-2.01	-1.05	-0.64
State	2p	3p	4p	5p
Experiment	-3.54	-1.56	-0.87	-0.55
Calculated ($\delta_p = 0.040$)	-3.54	-1.55	-0.87	-0.55
State	3d	4d	5d	
Experiment	-1.51	-0.85	-0.54	
Calculated ($\delta_d = 0.000$)	-1.51	-0.85	-0.54	

Problem 9.6 (Schrödinger Equation)

- What is the classical relation between the kinetic energy E_{kin} of a particle of mass m and its momentum p ? What is the *Hamilton function*? Give the classical trajectory of the particle.
- Consider a particle moving in x direction in a constant potential V . For a quantum mechanical description, use a plane wave:

$$\psi(x, t) = \psi_0 e^{\frac{i}{\hbar}(px - Ht)} \quad (9.45)$$

where H is the total energy of the particle, and p its momentum. Apply the following operators to the free particle wave function:

$$i\hbar \frac{\partial}{\partial t} \quad \frac{\hbar}{i} \frac{\partial}{\partial x} \quad - \frac{\hbar^2}{2m} \frac{\partial^2}{\partial x^2}$$

Use the classical relationship from subproblem (a) and identify the differential equation, which is satisfied by the plane wave description of the free particle.

Solution 9.6 In this problem, we familiarize ourselves with the foundations of quantum mechanics by considering the simple problem of a single particle moving without forces in space. The laws of quantum mechanics as a theory describing matter on the atomic scale cannot be derived in a strict way. Instead, even the interpretation of the wave function must be based on the comparison with experimental results. As a result of this comparison, the laws of quantum mechanics are formulated as *postulates*⁹ (see Sect. 9.1.2). According to the famous *correspondence principle*, the predictions of quantum mechanics must meet the prediction of classical mechanics within the macroscopic limit, or, otherwise, within the fictive limit $\hbar \rightarrow 0$, i.e., if Planck's constant were zero, and thus no quantization would occur. In **subproblem (a)**, we first look at the classical mechanics of a free particle of mass m and momentum p . Its kinetic energy is given by:

$$E_{\text{kin}} = \frac{1}{2}mv^2 = \frac{p^2}{2m}. \quad (9.46)$$

In theoretical mechanics there are two functions on which the equations of motion of a classical mechanical system are based: one is the *Hamilton function*, or the Hamiltonian H , which is the total kinetic energy plus the total potential energy of

⁹An extensive discussion can be found in the book by David Bohm [4].

the system¹⁰:

$$H = E_{\text{kin}} + V \quad (9.47)$$

In the case of a single particle moving freely, the potential V takes a constant value. In general, however, V may vary with the location of the particle. If V also depended on time, we would be dealing with a nonconservative system. If the Hamiltonian of a system is known, the equations of motion follow from:

$$\dot{x}_i = \frac{\partial H}{\partial p_i} \quad (9.48)$$

$$\dot{p}_i = -\frac{\partial H}{\partial x_i} \quad (9.49)$$

Here, p_i is the momentum of the i th particle and x_i is its position. In our case of a one-particle system, the equations of motion are thus:

$$\dot{x} = \frac{p}{m} \quad (9.50)$$

and

$$\dot{p} = 0 \quad (9.51)$$

The momentum of the particle is constant, and its position is obtained by integration. If $x(0)$ is the position at $t = 0$, then:

$$\int_{x(0)}^{x(t)} dx = \int_0^t \frac{p}{m} dt \Leftrightarrow x(t) = x(0) + vt \quad (9.52)$$

where $v = \frac{p}{m}$ is the constant velocity of the particle. Thus, the classical trajectory is well-defined by classical mechanics.

In **subproblem (b)**, we switch to a quantum mechanical description using the one-particle wave function Eq. (9.45). This choice is not mandatory, but note that – provided that the superposition principle holds in quantum mechanics – any arbitrary complex wave function can be represented by a superposition of plane waves. Another strong argument is the analogy with optics and electromagnetic wave theory, which in a vacuum makes use of a plane wave representation of the electric and the magnetic field vector, which is a solution of the wave equation. What sort of wave equation does Eq. (9.45) satisfy? We check this by taking the

¹⁰The other function is the Lagrangian $L = E_{\text{kin}} - V$

partial derivative in time:

$$i\hbar \frac{\partial}{\partial t} \psi(x, t) = i\hbar \frac{\partial}{\partial t} \psi_0 e^{\frac{i}{\hbar}(px-Ht)} = H\psi_0 e^{\frac{i}{\hbar}(px-Ht)} = H\psi(x, t) \quad (9.53)$$

Thus, the special operator $i\hbar \frac{\partial}{\partial t}$ applied to the wave function reproduces the latter, and multiplies it with the total energy. In mathematical terms, Eq.(9.53) is an *eigenvalue problem*. The plane wave is an eigenfunction of the special operator $i\hbar \frac{\partial}{\partial t}$. We call this operator the *Hamiltonian operator* \hat{H} , as its eigenvalue is simply the total energy (see subproblem (a)). The same arithmetic can be performed using the other operators. For the partial derivative in x , we obtain:

$$\frac{\hbar}{i} \frac{\partial}{\partial x} \psi(x, t) = \frac{\hbar}{i} \frac{\partial}{\partial x} \psi_0 e^{\frac{i}{\hbar}(px-Ht)} = p\psi_0 e^{\frac{i}{\hbar}(px-Ht)} = p\psi(x, t) \quad (9.54)$$

Thus, we identify the special operator $\hat{p} = \frac{\hbar}{i} \frac{\partial}{\partial x}$ as the momentum operator (in x -direction), and the wave function also proves to be an eigenfunction of \hat{p} , and p is its eigenvalue. It is straightforward now to seek an *operator of the kinetic energy*, $\frac{\hat{p}^2}{2m}$, which is the third operator we apply. We obtain:

$$-\frac{\hbar^2}{2m} \frac{\partial^2}{\partial x^2} \psi(x, t) = -\frac{\hbar^2}{2m} \frac{\partial^2}{\partial x^2} \psi_0 e^{\frac{i}{\hbar}(px-Ht)} = \frac{p^2}{2m} \psi_0 e^{\frac{i}{\hbar}(px-Ht)} = E_{\text{kin}} \psi(x, t) \quad (9.55)$$

Moreover, we recognize that there is a second way of expressing the Hamiltonian operator as the sum of the operator of the kinetic energy and the constant potential:

$$\hat{H}\psi(x, t) = \left[-\frac{\hbar^2}{2m} \frac{\partial^2}{\partial x^2} + V \right] \psi(x, t) = \left(\frac{p^2}{2m} + V \right) \psi(x, t) = H\psi(x, t) \quad (9.56)$$

Thus, if we combine Eq. (9.53) with Eq. (9.56), we obtain the wave equation sought, which is satisfied by the plane wave:

$$i\hbar \frac{\partial}{\partial t} \psi(x, t) = \left[-\frac{\hbar^2}{2m} \frac{\partial^2}{\partial x^2} + V \right] \psi(x, t) \quad (9.57)$$

This is the Schrödinger equation of a massive particle for the special case of a constant potential. Note that derivatives in space (second order) and in time (first order) differ, whereas the wave equation describing electromagnetic waves in a vacuum contains second-order derivatives in space and time, as the textbooks show. In summary, using the plane wave description of a particle moving in a constant potential, we have identified the wave equation describing the motion of the particle. Moreover, we have seen that the physical observables total energy H , kinetic energy E_{kin} , and momentum p are associated with special operators. This concept can be generalized to an arbitrary observable O and its associated operator \hat{O} .

Problem 9.7 (Wave Packets and Uncertainty Principle)

The wave function of a localized particle can be described as a superposition of plane waves with different momentum:

$$\psi(x) = \int_{-\infty}^{+\infty} B(p) \exp\left(\frac{i}{\hbar}px\right) dp \quad (9.58)$$

where $B(p)$ is the distribution function for the momentum. Consider the special distribution function:

$$B(p) = \begin{cases} 0 & p < (p_0 - \Delta p) \\ A & (p_0 - \Delta p) \leq p \leq (p_0 + \Delta p) \\ 0 & p > (p_0 + \Delta p) \end{cases}$$

- Give the expression for the probability density $w(x) = |\psi(x)|^2$ to find the particle within x and $x + dx$. Note that A follows from the normalization of the wave function. Sketch the probability density for an electron with average kinetic energy $E_0 = 100 \text{ eV}$ and $\Delta p = 2.5 \times 10^{-3} p_0$.
- Express the uncertainty Δx defined as the distance x from the center of $w(x)$, where the probability density has fallen to half of its maximum value. Calculate the product $\Delta p \Delta x$ and give an interpretation of the result.

Solution 9.7 According to the superposition principle in quantum mechanics (see Sect. 9.1.2), an arbitrary function can be written as a superposition of plane waves. Although a single plane wave has a well-defined momentum and energy, a wave packet constructed by the superposition of many plane waves is characterized by a momentum distribution, thus involving the statistical aspect of the wave function. Quantum mechanics assumes that the wave function $\psi(x, t)$ contains all the information about the particle, and $|\psi(x)|^2 = \psi^*(x)\psi(x) dx$ is the probability of finding the particle between x and $x + dx$. Note that the rules dealing with complex numbers are summarized in the Appendix, Sect. A.3.4.

In **subproblem (a)**, we calculate the probability density $w(x) = |\psi(x)|^2$ for the wave packet Eq. (9.58). In the first step, we seek the spatial representation of the wave function:

$$\psi(x) = \int_{-\infty}^{+\infty} B(p) \exp\left(\frac{i}{\hbar}px\right) dp = A \int_{p_0-\Delta p}^{p_0+\Delta p} \exp\left(\frac{i}{\hbar}px\right) dp \quad (9.59)$$

Here, we have inserted the special momentum distribution function $B(p)$ which states that within a certain interval $2\Delta p$ around the average momentum p_0 , all values of p have the same weight characterized by the quantity A , which we will determine

later. The integral can be solved using the integral table in the Appendix. We obtain:

$$\psi(x) = A \left[\frac{e^{\frac{i}{\hbar} px}}{\frac{i}{\hbar} x} \right]_{p_0 - \Delta p}^{p_0 + \Delta p} = A \frac{\hbar}{i} e^{\frac{i}{\hbar} p_0 x} \frac{e^{\frac{i}{\hbar} \Delta px} - e^{-\frac{i}{\hbar} \Delta px}}{x} \quad (9.60)$$

If we use Euler's formula $e^{i\phi} = \cos \phi + i \sin \phi$ (see Eq. (A.11)), we can further simplify and obtain:

$$\psi(x) = A \frac{\hbar}{i} \frac{2i \sin\left(\frac{\Delta px}{\hbar}\right)}{x} e^{\frac{i}{\hbar} p_0 x} = 2A\hbar \frac{\sin\left(\frac{\Delta px}{\hbar}\right)}{x} e^{\frac{i}{\hbar} p_0 x} \quad (9.61)$$

The wave function has a complex phase factor $e^{\frac{i}{\hbar} p_0 x}$ which is enveloped by an amplitude function describing spatial variations depending on Δp . The spatial probability density function is the square of the wave function:

$$w(x) = \psi^*(x)\psi(x) = 4A^2\hbar^2 \frac{\sin^2\left(\frac{\Delta px}{\hbar}\right)}{x^2} \quad (9.62)$$

We determine A from the normalization of $w(x)$:

$$\int_{\infty}^{+\infty} w(x) dx \stackrel{!}{=} 1 = 4A^2\hbar^2 \int_{\infty}^{+\infty} \frac{\sin^2\left(\frac{\Delta px}{\hbar}\right)}{x^2} dx \stackrel{\text{Eq. (A.51)}}{=} 4A^2\hbar^2 \pi \frac{\Delta p}{\hbar} \quad (9.63)$$

Solving for A , we get

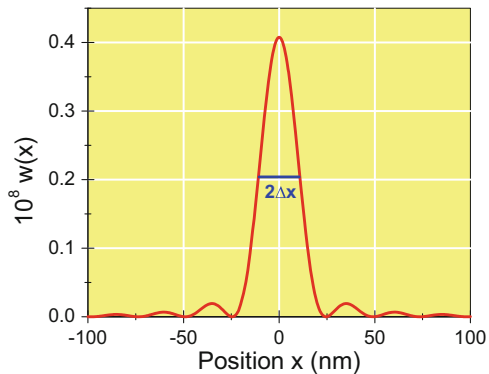
$$A = \sqrt{\frac{1}{4\pi\Delta p\hbar}} \quad (9.64)$$

and thus the probability density function is

$$w(x) = |\psi(x)|^2 = \frac{\hbar}{\pi\Delta p} \frac{\sin^2\left(\frac{\Delta px}{\hbar}\right)}{x^2} \quad (9.65)$$

Note that the point $x = 0$ requires special treatment because of the pole. Using the rule of l'Hôpital, we verify that $w(0) = \frac{\Delta p}{\pi\hbar}$. Next, we consider the concrete example of an electron with an energy of 100 eV. This is a typical energy measurement of electrons in low-energy electron diffraction (LEED) experiments probing a crystalline surface. An ideal electron gun emits a monochromatic electron beam. Using Eq. (9.46), the momentum of such a perfectly monochromatic electron

Fig. 9.8 Probability density function $w(x) = |\psi(x)|^2$ of a particle with *boxcar* momentum distribution. The blue line marks the half width $2\Delta x$



wave would be:

$$\begin{aligned} p_0 &= \sqrt{2m_e E_{\text{kin}}} = \sqrt{2 \times 9.1094 \times 10^{-31} \text{ kg} \times 100 \times 1.6022 \times 10^{-19} \text{ J}} \\ &= 5.4 \times 10^{-24} \text{ kg m s}^{-1}. \end{aligned} \quad (9.66)$$

A real electron gun, however, emits electrons with a certain energy spread and thus the momentum scatters around the average momentum. In our case, $\Delta p = 2.5 \times 10^{-3} = 1.35 \times 10^{-26} \text{ kg m s}^{-1}$. Using this information, we can plot $w(x)$. The result is shown in Fig. 9.8. The function has a central principle maximum around $x = 0$ and several weak side maxima. Repeated measurements of the electron's position would localize it statistically within a range of several nanometers from the center. In **subproblem (b)**, we quantify this resulting uncertainty in position, defining Δx as the distance from the center where the probability density drops to 50% of the maximum value. The condition for the uncertainty Δx is thus

$$w(\Delta x) \stackrel{!}{=} \frac{1}{2}w(0) = \frac{1}{2} \frac{\Delta p}{\pi \hbar} \quad (9.67)$$

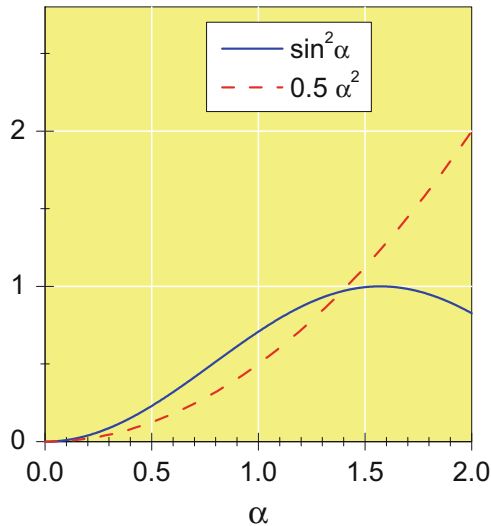
and

$$\frac{\hbar}{\pi \Delta p} \frac{\sin^2 \left(\frac{\Delta p \Delta x}{\hbar} \right)}{\Delta x^2} = \frac{\Delta p}{2\pi \hbar} \quad (9.68)$$

which can be written in the following way:

$$\sin^2 \left(\frac{\Delta p \Delta x}{\hbar} \right) = \frac{1}{2} \left(\frac{\Delta p \Delta x}{\hbar} \right)^2 \quad (9.69)$$

Fig. 9.9 Graphical solution of the nonlinear equation $\sin^2 \alpha = \frac{1}{2}\alpha^2$



If we define $\alpha = \frac{\Delta p \Delta x}{\hbar}$ we must solve the transcendental equation

$$\sin^2 \alpha = \frac{1}{2}\alpha^2 \quad (9.70)$$

This can be done graphically by seeking the intersection point, which is at $\alpha \approx 1.39$ (see Fig. 9.9). We therefore find the following relation between the uncertainties in momentum and position:

$$\Delta p \Delta x = 1.39\hbar \quad (9.71)$$

Note that our result is consistent with Heisenberg's uncertainty principle [4]:

$$\Delta p \Delta x \geq \hbar \quad (9.72)$$

The uncertainties in position and momentum are mutually related. An increase in Δp leads to a decrease in Δx and vice versa. Applied to the concrete example of diffraction experiments, this has concrete implications: a highly monochromatic gun with small Δp guarantees a large Δx , which is advantageous in diffraction experiments where constructive and destructive interference of large wave trains is needed. An electron gun with a large energy spread and thus large Δp , in contrast, would result in small values of Δx and interference between atomic layers at a crystal surface would be hampered. Note that typical atomic layer distances in a crystal are within the range of a few tenths of a nanometer.

Problem 9.8 (Gaussian Wave Packet Propagation)

- a. Prove that the Gaussian wave packet

$$\psi(x, t) = N \left(\frac{1}{\alpha + i\beta t} \right)^{\frac{1}{2}} e^{i(k_0 x - \omega_0 t)} e^{-\frac{(x - v_g t)^2}{4(\alpha + i\beta t)}} \quad (9.73)$$

is a solution of the time-dependent Schrödinger-equation of a free particle of mass m . N is a normalization constant, the parameter α is the initial variance σ_x^2 of the wave packet, $\omega_0 = \frac{\hbar k_0^2}{2m}$, $\beta = \frac{\hbar}{2m}$, the group velocity $v_g = \frac{\hbar k_0}{m}$.

- b. Determine the normalization constant N in Eq. (9.73).
c. Give an interpretation of Eq. (9.73) by plotting the probability density $\psi^* \psi$ for $t = 0$ s, $t = 2 \times 10^{-14}$ s, and $t = 5 \times 10^{-14}$ s for a ballistic electron with a group velocity of 10^6 m s $^{-1}$. The electron is initially located within 10^{-9} m at $x(t = 0) = 0$.

Solution 9.8 Few textbooks deal with explicit solutions of the *time-dependent* Schrödinger equation. Here, we consider the ballistic movement of a free particle in one spatial dimension with time. The probability of locating the particle within a certain interval between x and $x + dx$ is determined by the absolute square of the wave function, $|\psi(x, t)|^2$.

In **subproblem (a)**, we prove that Eq. (9.73) is a solution of the time-dependent Schrödinger equation. The straightforward, but somewhat tedious way is to calculate the derivatives of $\psi(x, t)$ in x and t and to show that $i\hbar \frac{\partial}{\partial t} \psi(x, t)$ equals $-\frac{\hbar^2}{2m} \frac{\partial^2}{\partial x^2} \psi(x, t)$. Making use of the chain rule, the first derivative in x is

$$\begin{aligned} \frac{\partial \psi}{\partial x} &= N \sqrt{\frac{1}{\alpha + i\beta t}} (ik_0) e^{i(k_0 x - \omega_0 t)} e^{-\frac{(x - v_g t)^2}{4(\alpha + i\beta t)}} \\ &\quad + N \sqrt{\frac{1}{\alpha + i\beta t}} e^{i(k_0 x - \omega_0 t)} e^{-\frac{(x - v_g t)^2}{4(\alpha + i\beta t)}} \left(-\frac{2(x - v_g t)}{4(\alpha + i\beta t)} \right) \end{aligned}$$

and thus

$$\frac{\partial \psi}{\partial x} = \psi(x, t) \left(ik_0 - \frac{2(x - v_g t)}{4(\alpha + i\beta t)} \right).$$

To form the second derivative, we use the chain rule on the last equation again and obtain

$$\begin{aligned}\frac{\partial^2 \psi}{\partial x^2} &= \psi(x, t) \left(\left(ik_0 - \frac{2(x - v_g t)}{4(\alpha + i\beta t)} \right)^2 - \frac{2}{4(\alpha + i\beta t)} \right) \\ &= \psi(x, t) \left(-k_0^2 - \frac{4ik_0(x - v_g t) + 2}{4(\alpha + i\beta t)} + \frac{4(x - v_g t)^2}{16(\alpha + i\beta t)^2} \right)\end{aligned}\quad (9.74)$$

The time derivative is:

$$\begin{aligned}\frac{\partial \psi}{\partial t} &= \left(-\frac{i\beta}{2(\alpha + i\beta t)} \right) N \sqrt{\frac{1}{\alpha + i\beta t}} e^{i(k_0 x - \omega_0 t)} e^{-\frac{(x - v_g t)^2}{4(\alpha + i\beta t)}} \\ &\quad + N \sqrt{\frac{1}{\alpha + i\beta t}} (-i\omega_0) e^{i(k_0 x - \omega_0 t)} e^{-\frac{(x - v_g t)^2}{4(\alpha + i\beta t)}} \\ &\quad + \left(\frac{2(x - v_g t)v_g}{4(\alpha + i\beta t)} + \frac{(x - v_g t)^2 4i\beta}{16(\alpha + i\beta t)^2} \right) N \sqrt{\frac{1}{\alpha + i\beta t}} e^{i(k_0 x - \omega_0 t)} e^{-\frac{(x - v_g t)^2}{4(\alpha + i\beta t)}}\end{aligned}$$

After sorting and multiplication with $i\hbar$ we obtain:

$$i\hbar \frac{\partial \psi}{\partial t} = \psi(x, t) \left(\hbar\omega_0 + \frac{2\hbar\beta}{4(\alpha + i\beta t)} + \frac{2i\hbar v_g(x - v_g t)}{4(\alpha + i\beta t)} - \frac{4\hbar\beta(x - v_g t)^2}{16(\alpha + i\beta t)^2} \right).$$

If we take into account that $\hbar\beta = \frac{\hbar^2}{2m}$, $\hbar v_g = \frac{\hbar^2 k_0}{2m}$, and $\hbar\omega_0 = \frac{\hbar^2 k_0^2}{2m}$, we obtain:

$$\begin{aligned}i\hbar \frac{\partial \psi}{\partial t} &= -\frac{\hbar^2}{2m} \psi(x, t) \left(-k_0^2 - \frac{2}{4(\alpha + i\beta t)} - \frac{4ik_0(x - v_g t)}{4(\alpha + i\beta t)} + \frac{4(x - v_g t)^2}{16(\alpha + i\beta t)^2} \right) \\ &\stackrel{\text{Eq. (9.74)}}{=} -\frac{\hbar^2}{2m} \frac{\partial^2 \psi}{\partial x^2}\end{aligned}$$

Thus, the wave packet satisfies the time-dependent Schrödinger equation. In **subproblem (b)**, we determine the normalization constant N . We also check if the total probability integrated over the whole one-dimensional space remains constant with time. If this were not the case, Eq. (9.73) would not describe a physically meaningful situation. Normalization requires the unit probability of finding the particle of between $x = -\infty$ and $x = +\infty$. Hence,

$$1 \stackrel{!}{=} \int_{-\infty}^{+\infty} \psi^*(x, t)\psi(x, t) dx = N^2 \sqrt{\frac{1}{\alpha - i\beta t}} \sqrt{\frac{1}{\alpha + i\beta t}} \int_{-\infty}^{+\infty} e^{-\frac{(x - v_g t)^2}{4(\alpha - i\beta t)}} e^{-\frac{(x - v_g t)^2}{4(\alpha + i\beta t)}} dx$$

As

$$\frac{1}{\alpha + i\beta t} \frac{1}{\alpha - i\beta t} = \frac{1}{\alpha^2 + \beta^2 t^2}$$

and

$$\frac{1}{\alpha + i\beta t} + \frac{1}{\alpha - i\beta t} = \frac{2\alpha}{\alpha^2 + \beta^2 t^2}$$

both the prefactors and the integral can be simplified:

$$1 \stackrel{!}{=} N^2 \sqrt{\frac{1}{\alpha^2 + \beta^2 t^2}} \int_{-\infty}^{+\infty} e^{-\frac{2\alpha(x-v_g t)^2}{4(\alpha^2 + \beta^2 t^2)}} dx$$

The integral can be evaluated using a definite integral from the integral table (see Eq. (A.46)):

$$\int_{-\infty}^{+\infty} e^{-a^2 u^2} du = \frac{\sqrt{\pi}}{a}.$$

After the substitution $u = x - v_g t$ and $a = \left(\frac{\alpha}{2(\alpha^2 + \beta^2 t^2)} \right)^{\frac{1}{2}}$ we obtain

$$1 \stackrel{!}{=} N^2 \sqrt{\frac{1}{\alpha^2 + \beta^2 t^2}} \sqrt{\frac{2\pi(\alpha^2 + \beta^2 t^2)}{\alpha}}$$

and thus the normalization constant is independent of time: $N = \left(\frac{\alpha}{2\pi} \right)^{\frac{1}{4}}$. According to our calculations, the probability density of the particle is

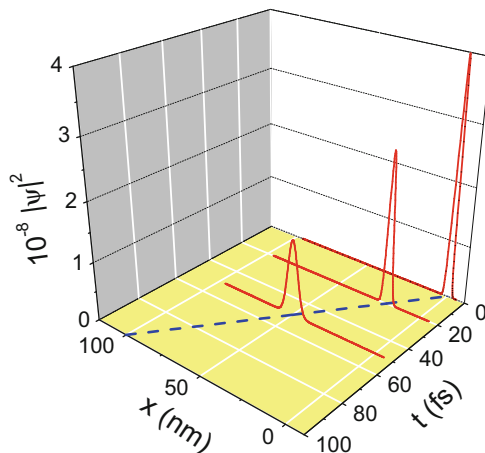
$$w(x, t) = \psi^*(x, t)\psi(x, t) = \left(\frac{\alpha}{2\pi} \right)^{\frac{1}{2}} \left(\frac{1}{\alpha^2 + \beta^2 t^2} \right)^{\frac{1}{2}} e^{-\frac{\alpha(x-v_g t)^2}{2(\alpha^2 + \beta^2 t^2)}} \quad (9.75)$$

It is a Gaussian distribution centered around $x(t) = v_g t$, i.e., the wave packet moves with the group velocity v_g as time proceeds. At the same time, however, the wave packet also spreads over time. By comparison with Eq. (A.64), defining the normal distribution, we identify the time-dependent variance of the wave packet:

$$\sigma^2(t) = \alpha \left(1 + \frac{\beta^2 t^2}{\alpha^2} \right). \quad (9.76)$$

This spreading of the wave packet is illustrated in **subproblem (c)**. We consider an electron with velocity $v_g = 10^6 \text{ m s}^{-1}$. This corresponds to a wave vector $k_0 =$

Fig. 9.10 Movement and spreading of the Gaussian wave packet with time. The blue dashed line marks the classical trajectory of the particle according to Eq. (9.52) moving with the group velocity v_g . The center of the Gaussian wave packet follows the classical trajectory



$\frac{mv_g}{\hbar} = 8.6 \times 10^9 \text{ m}^{-1}$, and to a kinetic energy of $E = \frac{\hbar^2 k_0^2}{2m} = 4.55 \times 10^{-19} \text{ J}$, or 2.8 eV. The electron could, for example, have been emitted after an interaction of a photon with an atom. We assume that the electron is initially confined to a spatial dimension of 1 nm. Therefore, $\alpha = 10^{-18} \text{ m}$. The parameter β has the dimension of a velocity and has a value of $5.7884 \times 10^{-5} \text{ m s}^{-1}$. This determines the density of the electron's wave packet according to Eq. (9.75). In Fig. 9.10, the wave packet is plotted for the time $t = 0, 20 \text{ fs}, \text{ and } 50 \text{ fs}$ ($1 \text{ fs} = 10^{-15} \text{ s}$). Within this time, the electron classically travels 20 nm and 50 nm respectively. The classical trajectory (blue dashed line) is calculated according to Eq. (9.52). Although the center of the wave packet follows this classical trajectory, the spreading of the wave packet over time is evident. After 50 fs, the width of the wave packet is about three times the initial width.

Problem 9.9 (Conservation of the Norm of the Wave Function)

If $|\psi(t_0)\rangle$ is the initial state of a quantum system at time t_0 and \hat{H} its time-independent Hamiltonian, the state of the system at time $t_0 + \tau$ is:

$$|\psi(t_0 + \tau)\rangle = \exp\left(-\frac{i}{\hbar}\hat{H}\tau\right)|\psi(t_0)\rangle \quad (9.77)$$

- Prove Eq. (9.77). Hint: Use a Taylor series expansions of the exponential function and $|\psi(t)\rangle$.
- Using Eq. (9.77), prove that if $\psi(t)$ is normalized at $t = t_0$, then it is normalized at arbitrary t .

Solution 9.9 The probability interpretation of quantum mechanics is frequently doubted by students, perhaps as often as the validity of the second law of thermodynamics. The interpretation of $|\psi|^2$ as a probability density in fact requires the total probability, i.e., the norm, to be conserved. It is our task in this problem to rigorously show this on the basis of the postulates of quantum mechanics (Sect. 9.1.2). Apart from the Hamiltonian \hat{H} and the wave function at $t = t_0$, no further specifications are made about the system. The problem is an occasion to deal with the numerous postulates of quantum mechanics found in Sect. 9.1.2.1.

In **subproblem (a)**, we consider a special operator acting on the wave function, namely the *propagator*

$$\hat{U}(\tau) = \exp\left(-\frac{i}{\hbar}\hat{H}\tau\right). \quad (9.78)$$

We show that \hat{U} applied to wave function at t_0 yields the wave function at a later time $t > t_0$. As a hint, it was recommended to expand \hat{U} and $|\psi(t)\rangle$. We thus start with a Taylor series expansion of the wave function (see Eq. (A.54) in the Appendix):

$$|\psi(t_0 + \tau)\rangle \stackrel{\text{Eq. (A.54)}}{=} \sum_{n=0}^{\infty} \frac{\tau^n}{n!} \frac{\partial^n}{\partial t^n} |\psi(t = t_0)\rangle \quad (9.79)$$

The sum on the right-hand side, however, can be written in a compact form using an exponential operator acting on the state $|\psi(t)\rangle$ at time $t = t_0$:

$$\sum_{n=0}^{\infty} \frac{\tau^n}{n!} \frac{\partial^n}{\partial t^n} |\psi(t = t_0)\rangle \stackrel{\text{Eq. (A.55)}}{=} \exp\left(\tau \frac{\partial}{\partial t}\right) |\psi(t = t_0)\rangle \quad (9.80)$$

This exponential operator thus *shifts* the wave function forward in time by a value τ , which justifies the terminus propagator:

$$|\psi(t_0 + \tau)\rangle = \exp\left(\tau \frac{\partial}{\partial t}\right) |\psi(t_0)\rangle \quad (9.81)$$

What is left is to replace the time derivative with the Hamiltonian. Using $\hat{H} = i\hbar \frac{\partial}{\partial t}$ (see Eq. (9.16)), we find

$$|\psi(t_0 + \tau)\rangle = \exp\left(\tau \frac{\hat{H}}{i\hbar}\right) |\psi(t_0)\rangle = \hat{U}(\tau) |\psi(t_0)\rangle \quad (9.82)$$

which proves Eq. (9.77).

As an application of the postulates of quantum mechanics in Sect. 9.1.2.1, it is worth looking at the special properties of \hat{U} : Because of

$$|\psi(t_0)\rangle = \underbrace{\hat{U}(-\tau) \hat{U}(\tau)}_{=1} |\psi(t_0)\rangle = \hat{U}^{-1}(\tau) \hat{U}(\tau) |\psi(t_0)\rangle$$

the *inverse* of $\hat{U}(\tau)$ is $\hat{U}(-\tau)$. The inverse of \hat{U} , however, is also the adjoint operator of \hat{U} , and thus:

$$\hat{U}(-\tau) = \exp\left(+\frac{i}{\hbar}\hat{H}\tau\right) = \exp\left(-\frac{i}{\hbar}\hat{H}\tau\right)^* = \hat{U}^+(\tau).$$

As a consequence,

$$\hat{U}^+ = \hat{U}^{-1} \Leftrightarrow \hat{U}^+ \hat{U} = 1. \quad (9.83)$$

An operator satisfying Eq. (9.83) is called **unitary operator**, and the transformation Eq. (9.82) is thus called a **unitary transformation**. This leads us to **subproblem (b)**, where we prove that the wave function, if normalized at $t = t_0$, is also normalized at $t > t_0$, e.g., at $t = t_0 + \tau$. The norm is the *scalar product*

$$\langle \psi(t_0) | \psi(t_0) \rangle = \langle \psi(t_0) | \underbrace{\hat{U}^+(\tau) \hat{U}(\tau)}_1 \psi(t_0) \rangle = \langle (\hat{U}^+(\tau))^+ \psi(t_0) | \hat{U}(\tau) \psi(t_0) \rangle \quad (9.84)$$

Because of $(\hat{U}^+)^+ = \hat{U}$, we can thus write:

$$\langle \psi(t_0) | \psi(t_0) \rangle = \langle \hat{U}(\tau) \psi(t_0) | \hat{U}(\tau) \psi(t_0) \rangle = \langle \psi(t_0 + \tau) | \psi(t_0 + \tau) \rangle \quad (9.85)$$

which was to be proven. The conservation of the norm of the wave function is thus the consequence of the unitary transformation of the wave function using the propagator \hat{U} . In Problem 9.8 the conservation of the probability was shown for the special case of a wave packet. The wave packet depicted in Fig. 9.10 broadens over time, but the total probability density remains constant. In this exercise, we have seen that this property of the wave function is general. The conservation of the norm would hold even in a more complex situation, e.g., if a wave packet would be partially reflected at a wall.

Problem 9.10 (Operators I)

Hint: It is recommended that you have already dealt with Problem 9.6. For the treatment of the harmonic oscillator problem the creation and annihilation operators

$$\mathbf{a}^+ = \sqrt{\frac{m\omega}{2\hbar}} \left(\hat{x} - \frac{i}{m\omega} \hat{p} \right) \quad (9.86)$$

$$\mathbf{a} = \sqrt{\frac{m\omega}{2\hbar}} \left(\hat{x} + \frac{i}{m\omega} \hat{p} \right) \quad (9.87)$$

are introduced, where \hat{x} and \hat{p} are the operators of position and momentum of the particle of mass m . The particle moves in a harmonic potential $V(x) = \frac{m\omega^2 x^2}{2}$ at an angular frequency ω .

- a. Prove the commutation relations

$$[\hat{x}, \hat{p}] = -\frac{\hbar}{i} \quad (9.88)$$

$$[\mathbf{a}, \mathbf{a}^+] = 1 \quad (9.89)$$

$$[\mathbf{N}, \mathbf{a}^+] = \mathbf{a}^+ \quad (9.90)$$

$$[\mathbf{N}, \mathbf{a}] = -\mathbf{a} \quad (9.91)$$

where the number operator is defined by means of $\mathbf{N} = \mathbf{a}^+ \mathbf{a}$.

- b. Show that the Hamiltonian of the harmonic oscillator problem can be written:

$$\hat{H} = \hbar\omega \left(\mathbf{N} + \frac{1}{2} \right). \quad (9.92)$$

- c. If $|n\rangle$ is the state function of the harmonic oscillator in its n th excited state, prove and interpret the following relations:

$$\mathbf{N} \mathbf{a} |n\rangle = (n - 1) \mathbf{a} |n\rangle \quad (9.93)$$

$$\mathbf{N} \mathbf{a}^+ |n\rangle = (n + 1) \mathbf{a}^+ |n\rangle \quad (9.94)$$

Solution 9.10 In this exercise, we become more familiarized with operator calculus in quantum mechanics. We acquire an insight into how this can be advantageously used for the description of the harmonic oscillator model, which is of key importance, e.g., in vibrational spectroscopy.

The momentum operator of a particle moving in one dimension has already been introduced in Problem 9.6:

$$\hat{p} = \frac{\hbar}{i} \frac{\partial}{\partial x} \quad (9.95)$$

We use \hat{p} together with the position operator \hat{x} to formulate the operators \mathbf{a}^+ and \mathbf{a} according to Eqs. (9.86) and (9.87). These are called creation and annihilation operator and it is our goal to clarify their significance. In **subproblem (a)**, we prove commutation relations for \mathbf{a} , \mathbf{a}^+ , and a third operator called the number operator:

$$\mathbf{N} = \mathbf{a}^+ \mathbf{a} \quad (9.96)$$

The commutator of two operators has been defined in Eq. (9.17). The significance of the commutator becomes clear if we realize that two mathematical objects do not necessarily obey the commutative law. If the order of two operators acting on a wave function does influence the result, then they have a non-zero commutator. An example is the operators of position of momentum, where the order does in fact matter: if we consider the expressions

$$\hat{x}\hat{p}\psi(x) = \hat{x}\frac{\hbar}{i}\frac{\partial}{\partial x}\psi(x) = \frac{\hbar}{i}x\frac{\partial\psi(x)}{\partial x}$$

and

$$\hat{p}\hat{x}\psi(x) = \frac{\hbar}{i}\frac{\partial}{\partial x}(\hat{x}\psi(x)) = \frac{\hbar}{i}\psi(x) + \frac{\hbar}{i}x\frac{\partial\psi(x)}{\partial x}$$

we notice that

$$[\hat{x}, \hat{p}] = \hat{x}\hat{p} - \hat{p}\hat{x} = -\frac{\hbar}{i} \quad (9.97)$$

which is the first of the commutator expressions that was meant to be shown.

It is straightforward to apply Eq. (9.17) to \mathbf{a}^+ and \mathbf{a} :

$$\begin{aligned} [\mathbf{a}, \mathbf{a}^+] &= \mathbf{a}\mathbf{a}^+ - \mathbf{a}^+\mathbf{a} \\ &= \frac{m\omega}{2\hbar} \left[\left(\hat{x} + \frac{i}{m\omega}\hat{p} \right) \left(\hat{x} - \frac{i}{m\omega}\hat{p} \right) - \left(\hat{x} - \frac{i}{m\omega}\hat{p} \right) \left(\hat{x} + \frac{i}{m\omega}\hat{p} \right) \right] \\ &= \frac{m\omega}{2\hbar} \left[-\frac{2i}{m\omega} (\hat{x}\hat{p} - \hat{p}\hat{x}) \right] \\ &= -\frac{i}{\hbar} [\hat{x}, \hat{p}] \stackrel{\text{Eq. (9.97)}}{=} 1 \end{aligned} \quad (9.98)$$

This was shown. Note that after expansion of the terms in the first line of Eq. (9.98), the terms containing \hat{x}^2 and \hat{p}^2 cancel each other out. To prove Eq. (9.90), we can use Eq. (9.89):

$$[\mathbf{N}, \mathbf{a}^+] \stackrel{\text{Eq. (9.96)}}{=} \mathbf{a}^+ \mathbf{a} \mathbf{a}^+ - \mathbf{a}^+ \mathbf{a}^+ \mathbf{a} = \mathbf{a}^+ [\mathbf{a}, \mathbf{a}^+] \stackrel{\text{Eq. (9.89)}}{=} \mathbf{a}^+ \quad (9.99)$$

In the same fashion, Eq. (9.91) is shown:

$$[\mathbf{N}, \mathbf{a}] \stackrel{\text{Eq. (9.96)}}{=} \mathbf{a}^+ \mathbf{a} \mathbf{a} - \mathbf{a} \mathbf{a}^+ \mathbf{a} = -[\mathbf{a}, \mathbf{a}^+] \mathbf{a} \stackrel{\text{Eq. (9.89)}}{=} -\mathbf{a} \quad (9.100)$$

To understand the meaning of these operators we move on to **subproblem (b)**, where we show that the Hamiltonian of the harmonic oscillator problem can be rewritten in a simpler form containing the number operator. From the Schrödinger equation of the harmonic oscillator Eqs. (9.18) and (9.20) we may extract the Hamiltonian in the form:

$$\hat{H} = \frac{\hat{p}^2}{2m} + \frac{m\omega^2}{2}\hat{x}^2 \quad (9.101)$$

where we have considered Eq. (9.95). In this form, the relation to the classic Hamiltonian $H = E_{\text{kin}} + V$ is obvious. To prove Eq. (9.92) it is best to show that the right-hand side of this equation is equivalent to Eq. (9.101):

$$\begin{aligned} \hbar\omega \left(\mathbf{N} + \frac{1}{2} \right) &= \hbar\omega \left(\mathbf{a}^+ \mathbf{a} + \frac{1}{2} \right) \\ &= \hbar\omega \left(\frac{m\omega}{2\hbar} \left(\hat{x} - \frac{i}{m\omega} \hat{p} \right) \left(\hat{x} + \frac{i}{m\omega} \hat{p} \right) + \frac{1}{2} \right) \\ &= \frac{m\omega^2}{2} \left(\hat{x}^2 - \frac{i}{m\omega} \underbrace{(\hat{p}\hat{x} - \hat{x}\hat{p})}_{-[\hat{x}, \hat{p}]} + \frac{1}{m^2\omega^2} \hat{p}^2 \right) + \frac{\hbar\omega}{2} \\ &\stackrel{\text{Eq. (9.97)}}{=} \frac{m\omega^2}{2} \hat{x}^2 - \frac{m\omega^2}{2} \frac{i}{m\omega} \frac{\hbar}{i} + \frac{\hat{p}^2}{2m} + \frac{\hbar\omega}{2} \\ &= \frac{\hat{p}^2}{2m} + \frac{m\omega^2}{2} \hat{x}^2 \stackrel{\text{Eq. (9.101)}}{=} \hat{H} \end{aligned} \quad (9.102)$$

Here, it is worth comparing this special form of the Hamiltonian with the expression for the energies of the harmonic oscillator, Eq. (9.19). It is obvious that $[\hat{H}, \mathbf{N}] = 0$ and thus the number operator and the Hamiltonian operator are commuting operators, meaning that they share the same spectrum of eigenfunctions. In the form

$$\hbar\omega \left(\mathbf{N} + \frac{1}{2} \right) \psi_n = \hbar\omega \left(\mathbf{n} + \frac{1}{2} \right) \psi_n \quad (9.103)$$

the significance of \mathbf{N} now becomes very clear: it yields the number of quanta, n , by which the oscillator is excited. In a notation with ket vectors,

$$\mathbf{N}|n\rangle = n|n\rangle. \quad (9.104)$$

Moving on to **subproblem (c)**, we show further relations revealing the significance of the operators \mathbf{a} and \mathbf{a}^+ . Employing the commutator relations Eqs. (9.90) and (9.91) we first consider the expression:

$$\mathbf{N}\mathbf{a}|n\rangle \stackrel{\text{Eq. (9.91)}}{=} (\mathbf{a}\mathbf{N} - \mathbf{a})|n\rangle = \mathbf{a}(\mathbf{N} - 1)|n\rangle \stackrel{\text{Eq. (9.104)}}{=} \mathbf{a}(n - 1)|n\rangle = (n - 1)\mathbf{a}|n\rangle. \quad (9.105)$$

which proves Eq. (9.93)

Using the same trick with the commutator relation Eq. (9.90) we obtain:

$$\mathbf{N}\mathbf{a}^+|n\rangle \stackrel{\text{Eq. (9.90)}}{=} \mathbf{a}^+(\mathbf{N} + 1)|n\rangle \stackrel{\text{Eq. (9.104)}}{=} \mathbf{a}^+(n + 1)|n\rangle = (n + 1)\mathbf{a}^+|n\rangle. \quad (9.106)$$

Our interpretation of these expressions is based on the number operator: If it is applied to the state $\mathbf{a}^+|n\rangle$, it yields $n + 1$ quanta. Moreover, a state $\mathbf{a}|n\rangle$ contains $n - 1$ quanta. That is, \mathbf{a}^+ increases n by 1; it creates a quantum, whereas \mathbf{a} decreases n by 1, it annihilates a quantum. Further analysis would in fact show that

$$\mathbf{a}^+|n\rangle = \sqrt{n + 1}|n + 1\rangle \quad (9.107)$$

and

$$\mathbf{a}|n\rangle = \sqrt{n}|n - 1\rangle \quad (9.108)$$

At the end of this exercise, we reflect on the use of this concept, for example, in conjunction with spectroscopy. A very important application is the derivation of **selection rules** for the harmonic oscillator,¹¹ as these operators describe transitions between harmonic oscillator states. In addition, if the harmonic oscillator model is applied to the case of electromagnetic waves and the photon picture of light, the raising and lowering operators describe the creation and annihilation of photons in elementary interaction processes with matter. Moreover, we use these operators in Problem 9.17 to solve the quantum double well.

¹¹See Eq. (10.18) in Chap. 10.

Problem 9.11 (Operators II)

For the description of two-level systems the **Pauli spin matrices**

$$\sigma_x = \begin{pmatrix} 0 & 1 \\ 1 & 0 \end{pmatrix}; \quad \sigma_y = \begin{pmatrix} 0 & -i \\ i & 0 \end{pmatrix}; \quad \sigma_z = \begin{pmatrix} 1 & 0 \\ 0 & -1 \end{pmatrix} \quad (9.109)$$

are introduced.

- Verify that the Pauli spin matrices satisfy the commutation rules for the angular momentum apart from a constant factor.
- Consider a two-level system with a ground state $|g\rangle$ and an excited state $|e\rangle$. A general state of the system is:

$$\alpha|e\rangle + \beta|g\rangle = \begin{pmatrix} \alpha \\ \beta \end{pmatrix} \quad (9.110)$$

Use the Pauli spin matrices to construct *ladder* operators σ_+ and σ_- with the following properties:

$$\sigma_+|g\rangle = |e\rangle; \quad \sigma_-|e\rangle = |g\rangle; \quad \sigma_+|e\rangle = 0; \quad \sigma_-|g\rangle = 0 \quad (9.111)$$

- What is the effect of σ_z acting on ground and excited states?

Solution 9.11 This second exercise on operator calculus focuses on Pauli spin matrices and their use in conjunction with the description of spin and two-level systems in general. In **subproblem (a)**, we verify that the Pauli spin matrices defined in Eq. (9.109) satisfy the angular momentum commutation rules apart from a constant factor. Here, we must recapitulate at first these rules for examinations in spectroscopy or advanced physical chemistry with which we should be very familiar. Given a system with angular momentum vector $\mathbf{J} = (J_x, J_y, J_z)$ and the related angular momentum operators \hat{J}_x , \hat{J}_y , and \hat{J}_z , the three components of the angular momentum cannot be measured at the same time with arbitrary precision, because they do not commute:

$$[\hat{J}_x, \hat{J}_y] = i\hbar\hat{J}_z \quad (9.112)$$

$$[\hat{J}_y, \hat{J}_z] = i\hbar\hat{J}_x \quad (9.113)$$

$$[\hat{J}_z, \hat{J}_x] = i\hbar\hat{J}_y \quad (9.114)$$

The square of the angular momentum, $J^2 = J_x^2 + J_y^2 + J_z^2$ and the z -component is usually chosen to define the state of angular momentum. The respective operators commute with each other:

$$[\hat{J}^2, \hat{J}_z] = 0 \quad (9.115)$$

Matrices (see Sect. A.3.16 in the Appendix) are mathematical objects that do not necessarily follow the commutative law. It is straightforward to check this for the Pauli spin matrices:

$$\begin{aligned} [\sigma_x, \sigma_y] &= \sigma_x \sigma_y - \sigma_y \sigma_x = \begin{pmatrix} 0 & 1 \\ 1 & 0 \end{pmatrix} \begin{pmatrix} 0 & -i \\ i & 0 \end{pmatrix} - \begin{pmatrix} 0 & -i \\ i & 0 \end{pmatrix} \begin{pmatrix} 0 & 1 \\ 1 & 0 \end{pmatrix} \\ &= \begin{pmatrix} i & 0 \\ 0 & -i \end{pmatrix} - \begin{pmatrix} -i & 0 \\ 0 & i \end{pmatrix} = 2i \begin{pmatrix} 1 & 0 \\ 0 & -1 \end{pmatrix} = 2i\sigma_z \end{aligned} \quad (9.116)$$

In the same way, we obtain:

$$\begin{aligned} [\sigma_y, \sigma_z] &= \sigma_y \sigma_z - \sigma_z \sigma_y = \begin{pmatrix} 0 & -i \\ i & 0 \end{pmatrix} \begin{pmatrix} 1 & 0 \\ 0 & -1 \end{pmatrix} - \begin{pmatrix} 1 & 0 \\ 0 & -1 \end{pmatrix} \begin{pmatrix} 0 & -i \\ i & 0 \end{pmatrix} \\ &= \begin{pmatrix} 0 & i \\ i & 0 \end{pmatrix} - \begin{pmatrix} 0 & -i \\ -i & 0 \end{pmatrix} = 2i \begin{pmatrix} 0 & 1 \\ 1 & 0 \end{pmatrix} = 2i\sigma_x \end{aligned} \quad (9.117)$$

and

$$\begin{aligned} [\sigma_z, \sigma_x] &= \sigma_z \sigma_x - \sigma_x \sigma_z = \begin{pmatrix} 1 & 0 \\ 0 & -1 \end{pmatrix} \begin{pmatrix} 0 & 1 \\ 1 & 0 \end{pmatrix} - \begin{pmatrix} 0 & 1 \\ 1 & 0 \end{pmatrix} \begin{pmatrix} 1 & 0 \\ 0 & -1 \end{pmatrix} \\ &= \begin{pmatrix} 0 & 1 \\ -1 & 0 \end{pmatrix} - \begin{pmatrix} 0 & -1 \\ 1 & 0 \end{pmatrix} = 2i \begin{pmatrix} 0 & -i \\ i & 0 \end{pmatrix} = 2i\sigma_y \end{aligned} \quad (9.118)$$

In summary, the Pauli spin matrices follow the commutation rules

$$[\sigma_x, \sigma_y] = 2i\sigma_z \quad [\sigma_y, \sigma_z] = 2i\sigma_x \quad [\sigma_z, \sigma_x] = 2i\sigma_y. \quad (9.119)$$

A comparison with Eq. (9.114) shows that, apart from a factor $\frac{\hbar}{2}$, the Pauli spin matrices σ_x , σ_y , and σ_z follow the same commutation rules as the operators of the three angular momentum components J_x , J_y , and J_z . For completeness, we may also construct the matrix:

$$\begin{aligned} \sigma^2 &= \sigma_x^2 + \sigma_y^2 + \sigma_z^2 \\ &= \begin{pmatrix} 0 & 1 \\ 1 & 0 \end{pmatrix} \begin{pmatrix} 0 & 1 \\ 1 & 0 \end{pmatrix} + \begin{pmatrix} 0 & -i \\ i & 0 \end{pmatrix} \begin{pmatrix} 0 & -i \\ i & 0 \end{pmatrix} + \begin{pmatrix} 1 & 0 \\ 0 & -1 \end{pmatrix} \begin{pmatrix} 1 & 0 \\ 0 & -1 \end{pmatrix} \\ &= \begin{pmatrix} 1 & 0 \\ 0 & 1 \end{pmatrix} + \begin{pmatrix} 1 & 0 \\ 0 & 1 \end{pmatrix} + \begin{pmatrix} 1 & 0 \\ 0 & 1 \end{pmatrix} = 3\mathbf{I}_2 \end{aligned} \quad (9.120)$$

with \mathbf{I}_2 the (2,2) unit matrix. It is obvious that each of the Pauli spin matrices commutes with the unit matrix. Thus, the commutation rule Eq. (9.115) also finds

its analogy in:

$$[\sigma^2, \sigma_z] = 0. \quad (9.121)$$

In **subproblem (b)**, we focus on the use of the Pauli spin matrices for the description of a quantum mechanical two-level system. This may describe, for example, a proton or an electron with spin $\frac{1}{2}$ in an external magnetic field. Depending on the orientation, the spin with regard to the magnetic field, the energy of the particle splits into two states (Zeeman effect). Two-level systems, however, are also important in spectroscopy for the treatment of the fundamental interaction between light and matter: absorption, emission, and induced emission (see Chap. 10). Here, the two-level system represents an atom or molecule with an initial state $|i\rangle$ and a final state $|f\rangle$, whereas the electromagnetic field is described in the model of a harmonic oscillator with quantum energy $\hbar\omega$ matching the energy difference between the states $|i\rangle$ and $|f\rangle$. In the literature, such a model is known as a Jaynes Cummings model. The latter makes use of Pauli spin matrices to describe the transitions of the two-level system. In the present problem, we consider the ground state denoted $|g\rangle$ and an excited state $|e\rangle$, as illustrated in Fig. 9.11. A general *mixed* state of the system is given according to Eq. (9.110) where the absolute values of the two complex numbers α and β give the probability of finding the system in the pure states $|e\rangle$ and $|g\rangle$ respectively. This two-level system can be represented mathematically by vectors where the ground and the excited state are given as:

$$|g\rangle = \begin{pmatrix} 0 \\ 1 \end{pmatrix}; \quad |e\rangle = \begin{pmatrix} 1 \\ 0 \end{pmatrix}. \quad (9.122)$$

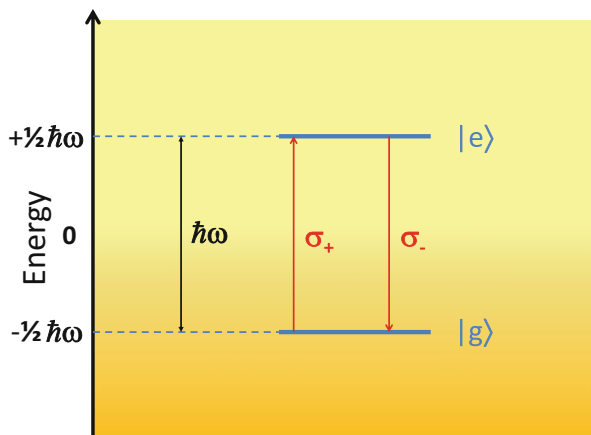


Fig. 9.11 A quantum mechanical two-level system of a ground and an excited state with an energy difference $\hbar\omega$. Ladder operators σ_+ and σ_- mediate transitions between the two states

Our task is to find ladder operators describing the transitions between these two states. According to the problem text, these ladder operators can be constructed from the Pauli spin matrices. There are two possibilities of finding these operators: guessing is of course possible for the student, with mathematical intuition. We follow the second, systematic way. Starting with σ_+ , we assume that this operator can be written as a linear combination of the Pauli spin matrices:

$$\sigma_+ = a\sigma_x + b\sigma_y + c\sigma_z = \begin{pmatrix} c & a - ib \\ a + ib & -c \end{pmatrix} \quad (9.123)$$

According to Eq. (9.111), we can set up two equations to determine the coefficients a , b , and c :

$$\begin{pmatrix} c & a - ib \\ a + ib & -c \end{pmatrix} \begin{pmatrix} 0 \\ 1 \end{pmatrix} = \begin{pmatrix} a - ib \\ -c \end{pmatrix} \stackrel{!}{=} \begin{pmatrix} 1 \\ 0 \end{pmatrix} \quad (9.124)$$

and

$$\begin{pmatrix} c & a - ib \\ a + ib & -c \end{pmatrix} \begin{pmatrix} 1 \\ 0 \end{pmatrix} = \begin{pmatrix} c \\ a + ib \end{pmatrix} \stackrel{!}{=} \begin{pmatrix} 0 \\ 0 \end{pmatrix} \quad (9.125)$$

From these equations, it is immediately clear that $c = 0$. For a and b we have two equations:

$$a - ib = 1 \quad (9.126)$$

and

$$a + ib = 0 \quad (9.127)$$

The addition of Eqs. (9.126) and (9.127) yields the result $a = \frac{1}{2}$, whereas subtraction gives $b = \frac{i}{2}$. We reinsert these values in Eq. (9.123) and obtain the result:

$$\sigma_+ = \frac{1}{2} (\sigma_x + i\sigma_y) = \begin{pmatrix} 0 & 1 \\ 0 & 0 \end{pmatrix} \quad (9.128)$$

For the second ladder operator σ_- we can proceed in exactly the same way. The result is:

$$\sigma_- = \frac{1}{2} (\sigma_x - i\sigma_y) = \begin{pmatrix} 0 & 0 \\ 1 & 0 \end{pmatrix} \quad (9.129)$$

In **subproblem (c)**, we examine the effect of σ_z on the states of the two-level system. We have:

$$\sigma_z|g\rangle = \begin{pmatrix} 1 & 0 \\ 0 & -1 \end{pmatrix} \begin{pmatrix} 0 \\ 1 \end{pmatrix} = -\begin{pmatrix} 0 \\ 1 \end{pmatrix} = -1|g\rangle \quad (9.130)$$

and

$$\sigma_z|e\rangle = \begin{pmatrix} 1 & 0 \\ 0 & -1 \end{pmatrix} \begin{pmatrix} 1 \\ 0 \end{pmatrix} = \begin{pmatrix} 1 \\ 0 \end{pmatrix} = +1|e\rangle \quad (9.131)$$

We can interpret this in the following way: in a two-level system with spin, σ_z projects out the spin orientation. In subproblem (a), we have seen that the Pauli matrices need to be multiplied by a factor of $\frac{\hbar}{2}$ to obtain the spin operators. Thus,

$$\hat{S}_z|-\frac{1}{2}\rangle = \frac{\hbar}{2}\sigma_z|-\frac{1}{2}\rangle = -\frac{\hbar}{2}|-\frac{1}{2}\rangle \quad (9.132)$$

and

$$\hat{S}_z|+\frac{1}{2}\rangle = \frac{\hbar}{2}\sigma_z|+\frac{1}{2}\rangle = \frac{\hbar}{2}|+\frac{1}{2}\rangle \quad (9.133)$$

In a general two-level system, σ_z can be used to determine the energy of the state. If the energy of the ground state is $-\frac{\hbar\omega}{2}$ and that of the excited state $+\frac{\hbar\omega}{2}$ (see Fig. 9.11), then the Hamiltonian of this system is apparently:

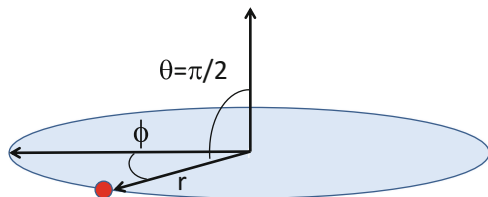
$$\hat{H} = \frac{\hbar\omega}{2}\sigma_z, \quad (9.134)$$

and

$$\hat{H}|g\rangle = -\frac{\hbar\omega}{2}|g\rangle; \quad \hat{H}|e\rangle = +\frac{\hbar\omega}{2}|e\rangle \quad (9.135)$$

In summary, we have seen how a special type of matrix as a concrete representation of operators can be used to describe transitions in a two-level system. We were able to formulate the Hamiltonian of such a system, which, as mentioned above, is the basis for the Jaynes Cummings model used in optics and spectroscopy.

Fig. 9.12 The model of an electron, which is free to move on a ring with a radius of r



Problem 9.12 (Quantization: The Electron on a Ring)

An electron may freely move on a ring with a radius r (see Fig. 9.12). The Schrödinger equation for this problem is:

$$-\frac{\hbar^2}{2mr^2} \frac{\partial^2}{\partial\phi^2} \psi(\phi) = E\psi(\phi) \quad (9.136)$$

where the azimuthal angle ϕ characterizes the position of the electron.

- a. Can you motivate Eq. (9.136)?
- b. A general form of the wave function is

$$\psi(\phi) = A e^{iM\phi}. \quad (9.137)$$

Show that Eq. (9.137) is a solution of Eq. (9.136).

- c. Determine the constants A and M from the assumption that the wave function is normalized and unique, i.e., $\psi(\phi + 2\pi) = \psi(\phi)$. What is the relationship between the energy and M ?

Solution 9.12 The electron on the ring is an instructive example of how quantization results as a consequence of boundary conditions. An application of this simple model to electronic excitations in the benzene molecule is shown below in Problem 9.13. In **subproblem (a)**, we derive the Schrödinger equation Eq. (9.136) for the wave function $\psi(\phi)$. As stated in the problem text, the electron moves freely, i.e., it moves in a constant potential that can be set to zero. The general form of the Schrödinger equation is thus:

$$-\frac{\hbar^2}{2m} \Delta \psi = E\psi. \quad (9.138)$$

As can be seen in Fig. 9.12, the azimuthal angle ϕ is the only degree of freedom left to the electron forced onto the ring. The movement of the electron is best described in spherical coordinates in which the Laplace operator in the general Schrödinger equation reads (see Eq. (A.68)):

$$\Delta = \frac{1}{r^2} \frac{\partial}{\partial r} \left(r^2 \frac{\partial}{\partial r} \right) + \frac{1}{r^2 \sin \theta} \frac{\partial}{\partial \theta} \left(\sin \theta \frac{\partial}{\partial \theta} \right) + \frac{1}{r^2 \sin^2 \theta} \frac{\partial^2}{\partial \phi^2} \quad (9.139)$$

We choose the origin of the coordinate system in the center of the ring, and we can assume that the ring plane is aligned to the equator $\theta = \frac{\pi}{2}$. Hence, $\sin \theta = 1$. Because θ and the radial coordinate r are constant, the first two terms in Eq. (9.139) are zero and the Laplacian reduces to:

$$\Delta = \frac{1}{r^2} \frac{\partial^2}{\partial \phi^2}.$$

Therefore, the Schrödinger equation for the electron on the ring is given by Eq. (9.136).

In **subproblem (b)**, we seek general solutions by inserting the ansatz $\psi(\phi) = Ae^{iM\phi}$ in Eq. (9.136). As

$$\frac{\partial \psi}{\partial \phi} = iMAe^{iM\phi} = iM\psi(\phi)$$

and therefore

$$\frac{\partial^2 \psi}{\partial \phi^2} = -M^2 Ae^{iM\phi} = -M^2 \psi(\phi),$$

we see that Eq. (9.137) satisfies Eq. (9.136):

$$\frac{\hbar^2 M^2}{2mr^2} \psi(\phi) = E\psi(\phi)$$

As a consequence, the energy of the electron is related to the parameter M via $E = \frac{\hbar^2 M^2}{2mr^2}$.

In **subproblem (c)**, we further narrow the wave function by applying suitable boundary conditions. The uniqueness of the wave function requires $\psi(\phi + 2\pi) = \psi(\phi)$, i.e., like the angle ϕ also the wave function must be periodic in multiples of 2π . Thus, $A \exp(iM\phi) \stackrel{!}{=} A \exp(iM\phi + 2\pi i)$ which is satisfied if M is integral. Therefore,

$$E = \frac{\hbar^2 M^2}{2mr^2}; \quad M = 0, \pm 1, \pm 2, \dots \quad (9.140)$$

A discrete spectrum of energy levels is a consequence of the special boundary conditions. Finally, we exploit the normalization condition. The total probability of finding the electron on the ring is 1. Therefore,

$$\int_0^{2\pi} \psi^* \psi d\phi = \int_0^{2\pi} Ae^{-iM\phi} Ae^{iM\phi} d\phi = A^2 \int_0^{2\pi} d\phi = 2\pi A^2 \stackrel{!}{=} 1$$

$$\psi(\phi) = \frac{1}{\sqrt{2\pi}} e^{iM\phi}; \quad M = 0, \pm 1, \pm 2, \dots \quad (9.141)$$

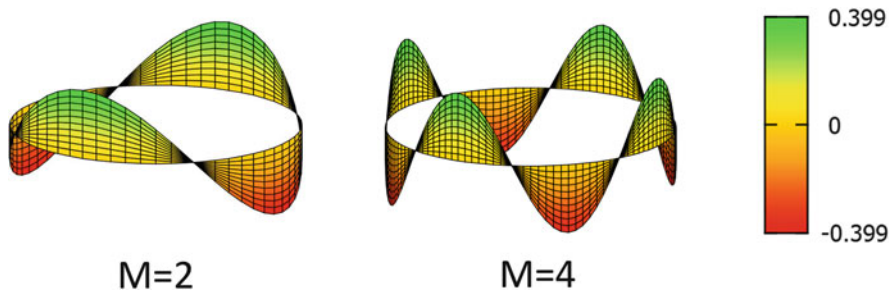


Fig. 9.13 Illustration of the solutions for the electron on the ring in a quantum mechanical treatment. The real part of the complex wave functions is shown for the quantum numbers $M = 2$ and $M = 4$

The real part of the complex wave function is illustrated in Fig. 9.13 for $M = 2$ and $M = 4$. Note that according to Eq. (9.141) the ground state wave function ($M = 0$) has a constant value across the ring, whereas excited states exhibit a harmonic behavior, where the number of full oscillations across the ring is an integer.

Problem 9.13 (Electronic Excitation of the Benzene Molecule)

Hint: This problem assumes that you have dealt with Problem 9.12.

The electron on the ring (Problem 9.12) is a simple model system for the six delocalized π electrons in the benzene molecule C_6H_6 . Assume a ring radius of 140 pm.

- Calculate the energies of the states $M = 0, \pm 1, \pm 2$ and make a term diagram.
- Distribute the six π electrons for the collective ground state. Assume that empty states with the lowest energy are occupied and the maximum occupation of a state with quantum number M is 2.
- What is the configuration for the first collective excited state? Calculate the excitation energy from the ground state. Compare your results with the spectroscopic result, according to which the transition from the electronic ground state to the first excited state of benzene is observed at a wavelength of 253 nm.

Solution 9.13 Electronic excitations involving delocalized π -electrons, so-called $\pi \rightarrow \pi^*$ transitions, are highly important in relation to **chromophores**, i.e., groups of atoms within a material responsible for its color. Benzene (Fig. 9.14) is one of the prime examples of a molecule with delocalized π electrons. In this problem, we apply the simple model of the electron on the ring (Problem 9.12) to the electronic properties of this molecule. We assume that the six π electrons of benzene move independently from each other across the ring. Moreover, any interaction with

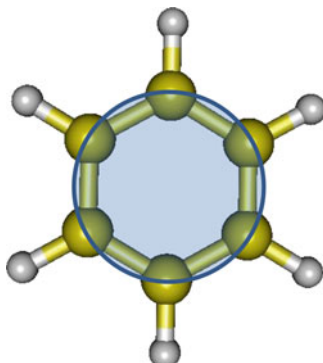


Fig. 9.14 The benzene molecule C_6H_6 with its cyclic structure. The six π electrons are delocalized over the hexagonal ring (blue). The radius of the ring (blue) is approximately identical to the carbon-carbon distance of 140 pm

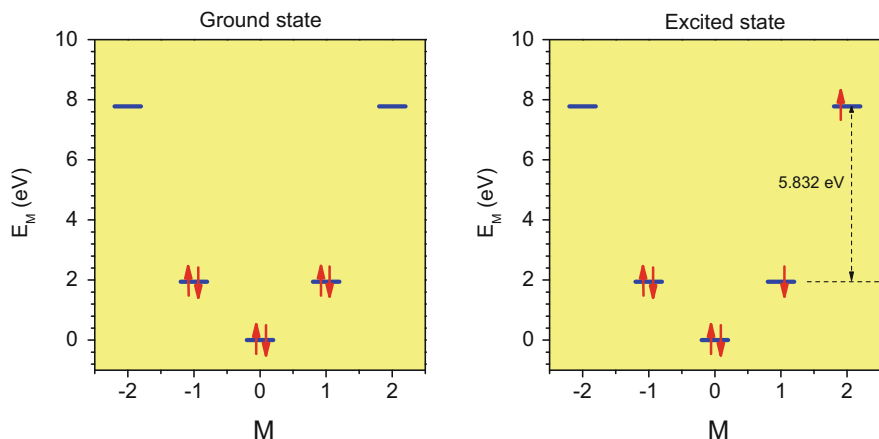


Fig. 9.15 Term scheme characterizing the electronic states of benzene. The arrows pointing upward and downward represent π -electrons with opposite spin

atomic cores is neglected altogether. The crudeness of this approximation has the advantage of simplicity.

In **subproblem (a)**, we model the electronic ground state by distributing the six π electrons on the one electron state resulting from Eq. (9.140). With the mass of the electron $m = 9.10939 \times 10^{-31}$ kg, $r = 1.4 \times 10^{-10}$ m and $\hbar = 1.054572 \times 10^{-34}$ J s we obtain:

$$E_M = M^2 \times 1.944 \text{ eV}$$

The resulting energy for $M = 0$ is thus 0 eV, for $M = \pm 1$ it is $E_{\pm 1} = 1.944$ eV, and for $M = \pm 2$ it is $E_{\pm 2} = 7.776$ eV. These energy levels are outlined in Fig. 9.15.

Based on the one-electron states characterized by the quantum number M , we now construct the configuration for the electronic ground state in **subproblem (b)**. As the ground state has the lowest total energy, we occupy the lowest levels first. Taking account of the Pauli principle, only two electrons with opposite spin orientation can occupy one state of quantum number M . Therefore, as illustrated in the left diagram in Fig. 9.15, the ground state configuration is characterized by filled levels of $M = 0$ and $M = \pm 1$.

In **subproblem (c)**, we consider the first excited state. The latter is reached if one electron from a state $M = \pm 1$ is removed and brought into a state with $M = \pm 2$, as shown in the right-hand diagram of Fig. 9.15. In our approximation of non-interacting electrons, we can assume that the energy difference between the excited state and the ground state is simply the difference between the levels $M = \pm 1$ and $M = \pm 2$, which is the excitation energy

$$E_{\text{ex}} = \frac{\hbar^2}{2mr^2} (2^2 - 1^2) = \frac{3\hbar^2}{2mr^2} = 5.832 \text{ eV}.$$

The transition can be mediated by a photon of wave length $\lambda = \frac{hc}{E_{\text{ex}}} = 213 \text{ nm}$. This result is quite close to the experimental value of 253 nm within the ultraviolet spectral range. We conclude that, despite its simplicity, the model of the electron on the ring predicts the correct order of magnitude for the electronic excitation of the benzene molecule. Analogous models exist for chain-like molecules containing delocalized π -electrons, such as the butadiene molecule. In this case, the simple quantum mechanical model is the particle in a one-dimensional box. A practical application of ultraviolet spectroscopy is discussed in Problem 10.3.

Problem 9.14 (Hydrogen 1s Wave Function)

- a. Show that the ground state wave function of the hydrogen atom,

$$\psi_{n=1,l=0}(r, \theta, \phi) = \left(\frac{1}{\pi a_0^3} \right)^{\frac{1}{2}} \exp\left(-\frac{r}{a_0}\right), \quad (9.142)$$

is normalized.

- b. Calculate the expectation value of the radial coordinate r of the electron in its ground state.
 c. Calculate the probability that the electron is located within a sphere of radius 10^{-15} m ; in other words, the probability of finding the electron in the hydrogen nucleus.

Solution 9.14 This problem is a straightforward application of quantum mechanical rules and integration. We deal with the ground state solution of the hydrogen problem and prove in **subproblem (a)** that the 1s wave function is normalized, i.e.,

we must show that:

$$\int |\psi_{n=1,l=0}(r, \theta, \phi)|^2 dV = 1 \quad (9.143)$$

In spherical coordinates (see Sect. A.3.11 in the Appendix), the integral is:

$$\begin{aligned} & \int_{r=0}^{\infty} \int_{\phi=0}^{2\pi} \int_{\theta=0}^{\pi} \frac{1}{\pi a_0^3} \exp\left(-\frac{2r}{a_0}\right) r^2 \sin \theta dr d\theta d\phi \\ &= \frac{1}{\pi a_0^3} \underbrace{\int_{r=0}^{\infty} r^2 \exp\left(-\frac{2r}{a_0}\right) dr}_{\frac{a_0^3}{4}, \text{ see Eq. (A.45)}} \underbrace{\int_0^{2\pi} d\phi}_{2\pi} \underbrace{\int_0^{\pi} \sin \theta d\theta}_{2} = 1 \end{aligned}$$

Thus, the 1s wave function is indeed normalized.

In **subproblem (b)**, we calculate the expectation value for the radial coordinate in this state (see postulate 6 in Sect. 9.1.2.1),

$$\langle r \rangle = \int \psi_{1s}^* r \psi_{1s} dV. \quad (9.144)$$

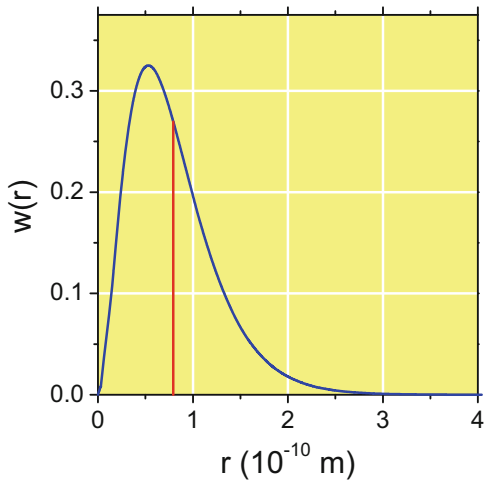
The definite integral Eq. (A.45), $\int_0^{\infty} x^n e^{-ax} = \frac{n!}{a^{n+1}}$ can be used for the calculation of integrals with arbitrary powers of the radial coordinate. The integration over the angles yields the same result as in subproblem (a). Hence,

$$\langle r \rangle = \frac{4\pi}{\pi a_0^3} \int_0^{\infty} r^3 \exp\left(-\frac{2r}{a_0}\right) = \frac{4}{a_0^3} \frac{3!}{\left(\frac{2}{a_0}\right)^4} = \frac{3}{2} a_0 \quad (9.145)$$

This result may look astonishing at first sight. We must not confuse it with the *most probable* radius of the electron, which is given by the maximum of the probability density function $w(r) = |\psi_{1s}|^2 r^2$ shown in Fig. 9.16. Its maximum is at $r = a_0$, i.e., the most probable distance of the electron in the ground state is identical to the Bohr radius. The expectation value for r we have just computed is at $1.5a_0$. As can be seen in Fig. 9.16, the probability density decreases steeply for large distances, and also for small distances of the electron from the nucleus. In **subproblem (c)**, we calculate the probability of finding the electron within the nucleus. The notion of finding the electron in the nucleus may seem strange at first. However, such a calculation is of importance for the estimation of the probability of a certain type of elementary particle reaction predicted in the year 1935 by Hideki Yukawa:



Fig. 9.16 Probability density function of the radial coordinate in the 1s ground state of the hydrogen atom. The maximum and thus the most probable distance of the electron is at $r = a_0 \approx 0.529 \times 10^{-10}$ m. The red line marks the expectation value calculated in subproblem (b)



The so-called K-capture of some isotopes such as $^{37}_{18}\text{Ar}$ is the reaction of an electron of the electron shell (most likely the K-shell) with a proton of the nucleus, converting the latter into a neutron and an electron neutrino ν_e . Therefore, what is the probability of finding the electron within the hydrogen nucleus? We assume a radius of the nucleus of $r_N = 10^{-15}$ m. Obviously, this probability is:

$$p = \int_{r=0}^{r_N} \int_{\phi=0}^{2\pi} \int_{\theta=0}^{\pi} \frac{1}{\pi a_0^3} \exp\left(-\frac{2r}{a_0}\right) r^2 \sin \theta \, dr \, d\theta \, d\phi \quad (9.147)$$

The difference from our calculation in subproblem (a) is that we have to integrate from $r = 0$ to $r = r_N$. From the integral table in the Appendix we use Eq. (A.44) and obtain:

$$\begin{aligned} p &= \frac{4\pi}{\pi a_0^3} \int_0^{r_N} r^2 \exp\left(-\frac{2r}{a_0}\right) dr \\ &= \frac{4}{a_0^3} \left[\exp\left(-\frac{2r}{a_0}\right) \left(-\frac{a_0 r^2}{2} - \frac{2ra_0^2}{4} - \frac{2a_0^3}{8} \right) \right]_0^{r_N} \\ &= \exp\left(-\frac{2r_N}{a_0}\right) \left(-\frac{2r_N^2}{a_0^2} - \frac{2r_N}{a_0} - 1 \right) - (-1) \\ &= 1 - e^{-2\left(\frac{r_N}{a_0}\right)} \left(1 + 2\left(\frac{r_N}{a_0}\right) + 2\left(\frac{r_N}{a_0}\right)^2 \right) = 9 \times 10^{-15} \end{aligned} \quad (9.148)$$

Hence, the probability of finding the electron within the nucleus is only about 10^{-14} . Given one mole of hydrogen atoms, there are, nevertheless, about 6 billion atoms in which the electron is located within the nucleus.

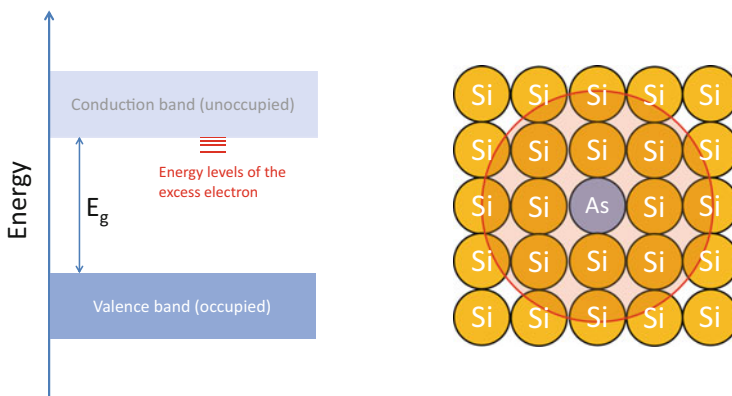


Fig. 9.17 *Left:* Band model of n-doped silicon. *Right:* Incorporation of arsenic into a silicon crystal lattice (schematic)

Problem 9.15 (Hydrogen Problem Applied to Semiconductor Technology)

The properties of pure and doped silicon are of high importance in semiconductor technology. Silicon is a semiconductor with a *band gap* of 1.12 eV between the valence band and the conduction band. At room temperature, the electric conductivity of silicon is weak. Why? To increase its conductivity, arsenic (n-doping) or boron (p-doping) is incorporated into the silicon crystal (see Fig. 9.17). Arsenic has an excess valence electron that can be approximately treated using a modified hydrogen problem.

- Calculate the three lowest energies of the excess electron. Assume an *effective mass* $m^* = 0.3 m_e$ of this electron and a dielectric constant of $\epsilon = 11.7$ for the surrounding medium silicon. Calculate the ionization energy of this excess electron. Explain why n-doped silicon has considerably increased room-temperature conductivity.
- What is the distance to the excess electron from the arsenic core? How many Si atoms are within the sphere, defined by the Bohr radius of the excess electron? The density of silicon is 2.34 g cm^{-3} .
- The above description can only be realistic for small concentrations of As, i.e., if a mutual interaction between defects can be neglected. Estimate a critical As concentration above which the electron orbits of neighboring As defects penetrate each other. Using the band structure of silicon, can you explain the consequences for the defect states?

Solution 9.15 This exercise includes an adaption of Bohr's atom model to a special problem in semiconductor physics. We characterize the spectrum of energy levels of

an n-doped Si crystal. Such a simple treatment already provides essential features without becoming too involved in the details of solid state physics. Silicon is a semiconductor, i.e., under ambient conditions it is neither an electric insulator nor is it a real conductor. The reason for this can be explained using a simplified band model as shown in Fig. 9.17 (left-hand diagram). Electric conduction requires free charge carriers in the conduction band. To excite an electron from the filled valence band to the conduction band, however, the energy of the *band gap* $E_g = 1.12 \text{ eV}$ is needed at least. At room temperature, the thermal energy $k_B T$ is only 26 meV. Hence, a thermal excitation is unlikely and free charge carriers are not available under room temperature conditions.

In **subproblem (a)** we consider an isolated arsenic atom embedded in the silicon crystal lattice. The latter is described as a continuum with a dielectric constant of $\epsilon = 11.7$. Compared with silicon with electron configuration $[\text{Ne}]3s^23p^2$, arsenic with electron configuration $[\text{Ar}]4s^24p^3$ has an excess valence electron. We treat this excess electron using the hydrogen problem (Eq. (9.21)) with the following modifications: (1) we assume an effective charge of the ion core¹² of $Z_{\text{eff}}e = 1e$. (2) we assume an *effective mass*¹³ of the excess electron $m^* = 0.3$. Taken together, the modified Rydberg formula for the energy levels of the excess electron is:

$$E_n = -\frac{m^*e^4}{8\epsilon^2\epsilon_0^2h^2} \frac{1}{n^2} = -\frac{0.3 \text{ Ry}}{\epsilon^2} \frac{1}{n^2}; \quad n = 1, 2, \dots \quad (9.149)$$

with Ry being 13.606 eV (see Eq. (9.22)). The first three energy levels are thus $E_1 = -29.8 \text{ meV}$, $E_2 = -7.5 \text{ meV}$, $E_3 = -3.3 \text{ meV}$ relative to the lower edge of the conduction band. Note that ionization of the arsenic atom ($n \rightarrow \infty$) causes the generation of one free charge carrier. The ionization energy for this process is just thus 29.8 meV, which is close to the thermal energy at room temperature. As a consequence, according to this simple model, doping of silicon crystals with arsenic increases its room temperature conductivity.

In **subproblem (b)**, we scrutinize the plausibility of the model. Bohr's formula for the radius of the electron orbit according to the above modifications is:

$$r_n = \frac{4\pi\epsilon\epsilon_0\hbar^2}{m^*e^2} n^2 = \frac{\epsilon}{0.3} \frac{4\pi\epsilon_0\hbar^2}{e^2} n^2 = \frac{\epsilon}{0.3} a_0 n^2 \quad n = 1, 2, \dots \quad (9.150)$$

with $a_0 = 0.5292 \times 10^{-10} \text{ m}$. The radius r_1 of the excess electron in its ground state is thus $21 \times 10^{-8} \text{ cm}$. A sphere with this radius has a volume of $V = \frac{4\pi}{3} r_1^3 =$

¹²See also Problem 9.5, where, for the lithium atom, we estimated an effective charge of 1.26 based on the experimental value of the ionization energy.

¹³The justification of an effective mass in solid state physics is based on the fact that the motion of an electron in the crystal is not free. While maintaining the expression for the kinetic energy, $E_{\text{kin}} = \frac{\hbar^2 k^2}{2m}$, the effective mass can be derived from the curvature of electron bands at special points in the crystal's reciprocal k-space.

$3.9 \times 10^{-20} \text{ cm}^3$. Using the given density of $\rho = 2.34 \text{ g cm}^{-3}$ and the molar mass of silicon $M_{\text{Si}} = 28.09 \text{ g mol}^{-1}$, the number of silicon atoms within this sphere is $\frac{N_A \rho V}{M_{\text{Si}}} \approx 2000$. Hence, the continuum treatment of the silicon crystal as a dielectricum seems plausible.

Finally, in **subproblem (c)**, we consider the case in which the arsenic defects are no longer isolated. In our simple model, we estimate the critical concentration of arsenic atoms where the orbits of the excess electrons penetrate each other. If we consider a cube with an edge length $2r_1 = 42 \times 10^{-8} \text{ cm}$, the orbits of neighboring arsenic defects would touch each other. This cube has a volume of $(2r_1)^3 = 7.4 \times 10^{-20} \text{ cm}^3$ with one arsenic defect at each of its corners, contributing $\frac{1}{8}$ of its sphere. Hence, within such a cube, there is $8 \times \frac{1}{8} = 1$ arsenic defect and the critical defect density is thus:

$$\mathcal{N}_{\text{crit.}} = \frac{1}{(2r_1)^3} = 1.3 \times 10^{19} \text{ cm}^{-3}. \quad (9.151)$$

The consequences for the band structure are shown in Fig. 9.18. Although the energy levels of isolated excess electrons are sharply defined, the mutual perturbation of neighboring defects leads to a splitting of these levels into a quasi-continuum of possible defect states and thus the formation of a *band tail* located beneath the lower edge of the conduction band.

Problem 9.16 (Variational Method)

According to the variational principle, an estimation E_0 of the ground state energy of a system characterized by its Hamiltonian \hat{H} can be obtained by a minimization of the energy functional

(continued)

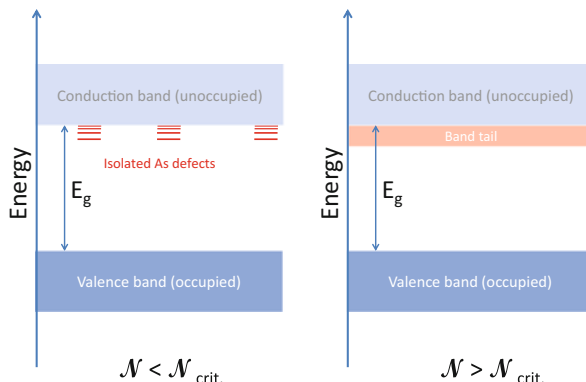


Fig. 9.18 Effect of defect concentration on the band structure (schematic)

Problem 9.16 (continued)

$$\bar{H} = \frac{\langle \psi | \hat{H} | \psi \rangle}{\langle \psi | \psi \rangle} \stackrel{!}{=} \min. \quad (9.152)$$

$|\psi\rangle$ is an appropriate test function depending on one or more optimization parameters that are varied during the minimization process. With this test function $E_0 = \bar{H}$ is the best approximation of the ground state energy that can be obtained.

- a. Consider the Hamiltonian of the hydrogen atom and use the Gaussian function

$$\psi(r) = N e^{-\alpha r^2} \quad (9.153)$$

with the normalization constant N and the variational parameter α as a test function to determine E_0 as an estimation of the ground state energy. Compare your result with the exact ground state energy. *Hint: It is convenient to introduce atomic units.*

- b. Repeat the calculation with the two-parameter function

$$\psi(r) = c_1 e^{-\alpha_1 r^2} + c_2 e^{-\alpha_2 r^2} \quad (9.154)$$

where $\alpha_1 = 2.87$ and $\alpha_2 = 0.28$ are fixed exponents and c_1 and c_2 are the variational parameters. *Hints: Write the energy functional in the form*

$$\bar{H} = \frac{c_1^2 H_{11} + 2c_1 c_2 H_{12} + c_2^2 H_{22}}{c_1^2 S_{11} + 2c_1 c_2 S_{12} + c_2^2 S_{22}} = \frac{N}{D}, \quad (9.155)$$

Transform the equations for the minimum condition in a system of equations for the coefficients c_1 and c_2 . Exploit the condition that the denominator D is 1 if ψ is normalized.

Solution 9.16 In this exercise, we deal with approximative methods for the solution of the time-independent Schrödinger equation. The variational principle is the basis of many methods in quantum chemistry. Concepts such as the effective charge we have dealt with in Problem 9.5 may be quite useful. However, there is no systematic way of improving the results. Of high value in atomic and molecular structure theory are concepts that may be systematically improved – even if the improvement leads to an increase in computational costs. Starting from a suitable test function with one or more adjustable parameters, the energy functional \bar{H} is calculated and minimized by variation of the parameter set. The minimum provides the best estimation for the ground state energy with the chosen test function. Here, we apply a method to the hydrogen atom, a system for which we know the exact result of the ground

state energy, the negative Rydberg constant (see Eq. (9.22)), or $E_{\text{exact}} = -0.5 E_h$ in atomic units.

In **subproblem (a)**, we consider a single Gaussian to be a test function given in Eq. (9.153). At first sight, it may seem artificial to treat the hydrogen problem using a Gaussian function. However, because of their properties, Gaussian functions are widely used in quantum chemistry to construct wave functions. Hence, our problem is instructive. We start by writing down the Hamiltonian of the hydrogen problem. In the ground state (1s state, $l = 0$), the effective Hamiltonian in atomic units (Sect. 9.1.4) is:

$$\hat{H} = \underbrace{-\frac{1}{2} \left(\frac{\partial^2}{\partial r^2} + \frac{2}{r} \frac{\partial}{\partial r} \right)}_{\hat{T}} \underbrace{-\frac{1}{r}}_V \quad (9.156)$$

where \hat{T} is the operator of the kinetic energy of the electron. V is its potential energy, i.e., the attractive Coulomb potential with the core. Our goal is to calculate Eq. (9.152). We start with the denominator, where we assume that our test function is normalized (see Problem 9.14), i.e.

$$\langle \psi | \psi \rangle = 4\pi \int_0^\infty N e^{-\alpha r^2} N e^{-\alpha r^2} r^2 dr \stackrel{!}{=} 1 \quad (9.157)$$

Thus,

$$\langle \psi | \psi \rangle = 4\pi N^2 \int_0^\infty e^{-2\alpha r^2} r^2 dr \stackrel{\text{Eq. (A.49)}}{=} 4\pi N^2 \frac{1}{4} \sqrt{\frac{\pi}{(2\alpha)^3}} = 1 \quad (9.158)$$

and the normalization constant is therefore:

$$N^2 = \left(\frac{2\alpha}{\pi} \right)^{\frac{3}{2}}. \quad (9.159)$$

The numerator splits into two parts, one with the kinetic energy, and one with the potential energy:

$$\bar{H} = \langle \psi | \hat{T} | \psi \rangle + \langle \psi | V | \psi \rangle \quad (9.160)$$

The second term is:

$$\begin{aligned} \langle \psi | V | \psi \rangle &= -4\pi \int_0^\infty N e^{-\alpha r^2} \frac{1}{r} N e^{-\alpha r^2} r^2 dr \\ &= -\left(\frac{2\alpha}{\pi} \right)^{\frac{3}{2}} 4\pi \int_0^\infty e^{-2\alpha r^2} r dr \\ &\stackrel{\text{Eq. (A.48)}}{=} -\left(\frac{8\alpha}{\pi} \right)^{\frac{1}{2}}. \end{aligned} \quad (9.161)$$

Because

$$\frac{\partial}{\partial r} e^{-\alpha r^2} = -2\alpha r e^{-\alpha r^2} \quad (9.162)$$

and

$$\frac{\partial^2}{\partial r^2} e^{-\alpha r^2} = \frac{\partial}{\partial r} \left(-2\alpha e^{-\alpha r^2} \right) = (4\alpha^2 r^2 - 2\alpha) e^{-\alpha r^2} \quad (9.163)$$

the kinetic energy term is:

$$\begin{aligned} \langle \psi | \hat{T} | \psi \rangle &= 4\pi \int_0^\infty N e^{-\alpha r^2} (-2\alpha^2 r^2 + \alpha + 2\alpha) N e^{-\alpha r^2} r^2 dr \\ &= \left(\frac{2\alpha}{\pi} \right)^{\frac{3}{2}} 4\pi \left[\underbrace{-2\alpha \int_0^\infty e^{-2\alpha r^2} r^4 dr}_{\frac{3}{8} \sqrt{\frac{\pi}{(2\alpha)^5}}} + \underbrace{3\alpha \int_0^\infty e^{-2\alpha r^2} r^2 dr}_{=\frac{1}{4} \sqrt{\frac{\pi}{(2\alpha)^3}}} \right] \end{aligned} \quad (9.164)$$

where we have again used the integral table in the Appendix (Eq. (A.49)). This expression reduces to:

$$\langle \psi | \hat{T} | \psi \rangle = -\frac{3\alpha}{2} + 3\alpha = \frac{3\alpha}{2} \quad (9.165)$$

Using Eqs. (9.160), (9.161), and (9.165), we obtain the expression for the energy functional:

$$\bar{H} = \frac{3}{2}\alpha - \left(\frac{8\alpha}{\pi} \right)^{\frac{1}{2}} \quad (9.166)$$

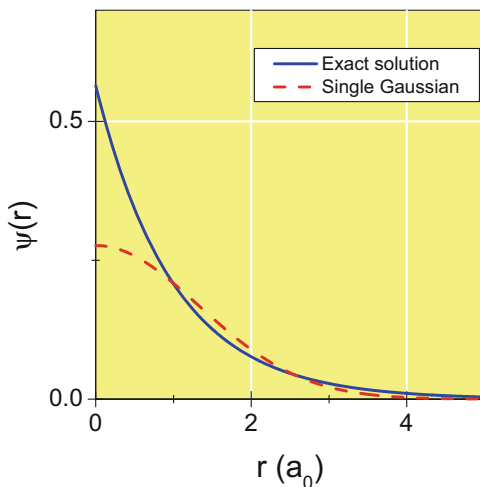
Now, we can minimize the functional by setting the first derivative to zero:

$$\frac{\partial \bar{H}}{\partial \alpha} = \frac{3}{2} - \frac{1}{2} \left(\frac{8}{\pi} \right)^{\frac{1}{2}} \alpha_{\min}^{-\frac{1}{2}} \stackrel{!}{=} 0 \quad (9.167)$$

Solving for α_{\min} , we obtain:

$$\alpha_{\min} = \frac{8}{9\pi} = 0.2829 \quad (9.168)$$

Fig. 9.19 Comparison between the exact 1s wave function of the hydrogen atom (solid line) and a Gaussian test function with exponent $\alpha = 0.2829$ (dashed line)



Reinserting the optimal exponent into Eq. (9.166), we obtain an estimation of the ground state energy:

$$E_0 = -\frac{4}{3\pi} = -0.4244 E_h = -11.51 \text{ eV}. \quad (9.169)$$

The use of a single Gaussian as a test function reaches about 85% of the true ground state energy E_{exact} . The optimized test function is shown in Fig. 9.19 together with the exact ground state wave function.¹⁴ Both functions are quite different, both in the core region and at larger distances from the core, where the exact wave function decays more rapidly than the Gaussian function. As mentioned above, the variational principle offers the possibility of arriving at an improved result if we use a more flexible test function. This is examined in **subproblem (b)**, which, however, is quite tedious. Our test function has now two fixed primitive Gaussian functions. The exponent $\alpha_2 = 0.28$ is essentially the optimal value obtained in subproblem (a), whereas the Gaussian function with $\alpha_1 = 2.87$ is more pronounced in the near-core region. We begin by constructing the energy functional, which should be written in

¹⁴We have dealt with the exact solution in Problem 9.14 on page 257. In the literature, atomic orbital functions with exponential decay in the region far from the core are also called Slater functions.

the form given in Eq. (9.155). Using Eq. (9.154) the denominator is:

$$\begin{aligned}
 \langle \psi | \psi \rangle &= 4\pi \int_0^\infty (c_1 e^{-\alpha_1 r^2} + c_2 e^{-\alpha_2 r^2}) (c_1 e^{-\alpha_1 r^2} + c_2 e^{-\alpha_2 r^2}) r^2 dr \\
 &= 4\pi \left[c_1^2 \int_0^\infty e^{-2\alpha_1 r^2} r^2 dr + 2c_1 c_2 \int_0^\infty e^{-(\alpha_1 + \alpha_2)r^2} r^2 dr \right. \\
 &\quad \left. + c_2^2 \int_0^\infty e^{-2\alpha_2 r^2} r^2 dr \right] \\
 &\stackrel{\text{Eq. (A.49)}}{=} 4\pi \left[c_1^2 \frac{1}{4} \sqrt{\frac{\pi}{(2\alpha_1)^3}} + 2c_1 c_2 \frac{1}{4} \sqrt{\frac{\pi}{(\alpha_1 + \alpha_2)^3}} + c_2^2 \frac{1}{4} \sqrt{\frac{\pi}{(2\alpha_2)^3}} \right] \\
 &= c_1^2 \left(\frac{\pi}{2\alpha_1} \right)^{\frac{3}{2}} + 2c_1 c_2 \left(\frac{\pi}{\alpha_1 + \alpha_2} \right)^{\frac{3}{2}} + c_2^2 \left(\frac{\pi}{2\alpha_2} \right)^{\frac{3}{2}} \\
 &= c_1^2 S_{11} + 2c_1 c_2 S_{12} + c_2^2 S_{22}
 \end{aligned} \tag{9.170}$$

The coefficients S_{11} , S_{12} , and S_{22} depend only on the given exponents $\alpha_1 = 2.87$ and $\alpha_2 = 0.28$. Their values are $S_{11} = 0.40491$, $S_{12} = 0.99600$, and $S_{22} = 13.28749$. Later, we exploit the fact that the expression Eq. (9.170), which is the norm of the test wave function, is unity. The numerator of the energy functional $\langle \psi | \hat{H} | \psi \rangle$ consists of two terms, the kinetic energy and the potential energy. For the latter, we have:

$$\begin{aligned}
 \langle \psi | V | \psi \rangle &= 4\pi \int_0^\infty (c_1 e^{-\alpha_1 r^2} + c_2 e^{-\alpha_2 r^2}) \left(-\frac{1}{r} \right) (c_1 e^{-\alpha_1 r^2} + c_2 e^{-\alpha_2 r^2}) r^2 dr \\
 &= -4\pi \left[c_1^2 \int_0^\infty e^{-2\alpha_1 r^2} r dr + 2c_1 c_2 \int_0^\infty e^{-(\alpha_1 + \alpha_2)r^2} r dr \right. \\
 &\quad \left. + c_2^2 \int_0^\infty e^{-2\alpha_2 r^2} r dr \right] \\
 &\stackrel{\text{Eq. (A.48)}}{=} -4\pi \left[c_1^2 \frac{1}{4\alpha_1} + 2c_1 c_2 \frac{1}{2(\alpha_1 + \alpha_2)} + c_2^2 \frac{1}{4\alpha_2} \right] \\
 &= - \left[c_1^2 \frac{\pi}{\alpha_1} + 2c_1 c_2 \frac{2\pi}{(\alpha_1 + \alpha_2)} + c_2^2 \frac{\pi}{\alpha_2} \right] \\
 &= c_1^2 V_{11} + 2c_1 c_2 V_{12} + c_2^2 V_{22}
 \end{aligned} \tag{9.171}$$

where $V_{11} = -1.09463$, $V_{12} = -1.99466$, and $V_{22} = -11.21997$ respectively. The kinetic energy term is:

$$\begin{aligned}\langle \psi | \hat{T} | \psi \rangle &= 4\pi \int_0^\infty (c_1 e^{-\alpha_1 r^2} + c_2 e^{-\alpha_2 r^2}) \left(-\frac{1}{2} \frac{\partial^2}{\partial r^2} - \frac{1}{r} \frac{\partial}{\partial r} \right) (c_1 e^{-\alpha_1 r^2} + c_2 e^{-\alpha_2 r^2}) r^2 dr \\ &= 4\pi \int_0^\infty (c_1 e^{-\alpha_1 r^2} + c_2 e^{-\alpha_2 r^2}) (-2\alpha_1^2 r^2 + 3\alpha_1) c_1 e^{-\alpha_1 r^2} r^2 dr \\ &\quad + 4\pi \int_0^\infty (c_1 e^{-\alpha_1 r^2} + c_2 e^{-\alpha_2 r^2}) (-2\alpha_2^2 r^2 + 3\alpha_2) c_2 e^{-\alpha_2 r^2} r^2 dr\end{aligned}\quad (9.172)$$

Here, we have made use of Eqs. (9.162) and (9.163). Further evaluation yields:

$$\begin{aligned}\langle \psi | \hat{T} | \psi \rangle &= 4\pi c_1^2 \left[-2\alpha_1^2 \int_0^\infty e^{-2\alpha_1 r^2} r^4 dr + 3\alpha_1 \int_0^\infty e^{-2\alpha_1 r^2} r^2 dr \right] \\ &\quad + 4\pi c_1 c_2 \left[-2(\alpha_1^2 + \alpha_2^2) \int_0^\infty e^{-(\alpha_1 + \alpha_2)r^2} r^4 dr \right. \\ &\quad \left. + 3(\alpha_1 + \alpha_2) \int_0^\infty e^{-(\alpha_1 + \alpha_2)r^2} r^2 dr \right] \\ &\quad + 4\pi c_2^2 \left[-2\alpha_2^2 \int_0^\infty e^{-2\alpha_2 r^2} r^4 dr + 3\alpha_2 \int_0^\infty e^{-2\alpha_2 r^2} r^2 dr \right]\end{aligned}\quad (9.173)$$

The integrals are again evaluated using Eq. (A.49) in the Appendix:

$$\begin{aligned}\langle \psi | \hat{T} | \psi \rangle &= 4\pi c_1^2 \left[-2\alpha_1^2 \frac{3}{8} \sqrt{\frac{\pi}{(2\alpha_1)^5}} + 3\alpha_1 \frac{1}{4} \sqrt{\frac{\pi}{(2\alpha_1)^3}} \right] \\ &\quad + 4\pi c_1 c_2 \left[-2(\alpha_1^2 + \alpha_2^2) \frac{3}{8} \sqrt{\frac{\pi}{(\alpha_1 + \alpha_2)^5}} + 3(\alpha_1 + \alpha_2) \frac{1}{4} \sqrt{\frac{\pi}{(\alpha_1 + \alpha_2)^3}} \right] \\ &\quad + 4\pi c_2^2 \left[-2\alpha_2^2 \frac{3}{8} \sqrt{\frac{\pi}{(2\alpha_2)^5}} + 3\alpha_2 \frac{1}{4} \sqrt{\frac{\pi}{(2\alpha_2)^3}} \right]\end{aligned}\quad (9.174)$$

If we introduce

$$\langle \psi | \hat{T} | \psi \rangle = c_1^2 T_{11} + 2c_1 c_2 T_{12} + c_2^2 T_{22}\quad (9.175)$$

then the coefficients are

$$T_{11} = \frac{3}{2} \left(\frac{\pi^3}{8\alpha_1} \right)^{\frac{1}{2}} = 1.74313 \quad (9.176)$$

$$T_{12} = \frac{3\pi}{2} \left(\sqrt{\frac{\pi}{\alpha_1 + \alpha_2}} - (\alpha_1^2 + \alpha_2^2) \sqrt{\frac{\pi}{(\alpha_1 + \alpha_2)^5}} \right) = 0.76227 \quad (9.177)$$

$$T_{22} = \frac{3}{2} \left(\frac{\pi^3}{8\alpha_2} \right)^{\frac{1}{2}} = 5.58074 \quad (9.178)$$

The numerator of the energy functional is thus:

$$\begin{aligned} \langle \psi | \hat{H} | \psi \rangle &= \langle \psi | \hat{T} | \psi \rangle + \langle \psi | V | \psi \rangle \\ &= c_1^2 H_{11} + 2c_1 c_2 H_{12} + c_2^2 H_{22} \end{aligned} \quad (9.179)$$

where $H_{11} = 0.64850$, $H_{12} = -1.23239$, and $H_{22} = -5.63923$. We have now constructed the energy functional in the form Eq. (9.155). In the next step, \bar{H} must be minimized by variation of the coefficients c_1 and c_2 , i.e., by taking the derivatives with regard to c_1 and c_2 :

$$\frac{\partial \bar{H}}{\partial c_1} \stackrel{!}{=} 0; \quad \frac{\partial \bar{H}}{\partial c_2} \stackrel{!}{=} 0 \quad (9.180)$$

A direct evaluation of the resulting equations is tedious, because they can barely be solved for these coefficients. If we consider N as the numerator of the energy functional and D as its denominator, we use the product rule:

$$\frac{\partial \bar{H}}{\partial c_1} = \frac{\partial}{\partial c_1} \frac{N}{D} = \frac{D \frac{\partial N}{\partial c_1} - N \frac{\partial D}{\partial c_1}}{D^2} \quad (9.181)$$

The denominator is nonzero. Thus,

$$\frac{\partial \bar{H}}{\partial c_1} \stackrel{!}{=} 0 \Leftrightarrow D \frac{\partial N}{\partial c_1} - N \frac{\partial D}{\partial c_1} = 0 \Leftrightarrow \frac{\partial N}{\partial c_1} - \bar{H} \frac{\partial D}{\partial c_1} = 0 \quad (9.182)$$

With

$$\frac{\partial N}{\partial c_1} = 2c_1 H_{11} + 2c_2 H_{12}; \quad \frac{\partial D}{\partial c_1} = 2c_1 S_{11} + 2c_2 S_{12}$$

we obtain the equation

$$(H_{11} - \bar{H} S_{11}) c_1 + (H_{12} - \bar{H} S_{12}) c_2 = 0 \quad (9.183)$$

By taking the derivative with regard to c_2 , we obtain:

$$(H_{22} - \bar{H}S_{22}) c_2 + (H_{12} - \bar{H}S_{12}) c_1 = 0. \quad (9.184)$$

These equations constitute a system of equations for the coefficients c_1 and c_2 :

$$\begin{pmatrix} H_{11} - \bar{H}S_{11} & H_{12} - \bar{H}S_{12} \\ H_{12} - \bar{H}S_{12} & H_{22} - \bar{H}S_{22} \end{pmatrix} \begin{pmatrix} c_1 \\ c_2 \end{pmatrix} = 0 \quad (9.185)$$

Nontrivial solutions are obtained if the secular determinant is zero:

$$\begin{vmatrix} H_{11} - \bar{H}S_{11} & H_{12} - \bar{H}S_{12} \\ H_{12} - \bar{H}S_{12} & H_{22} - \bar{H}S_{22} \end{vmatrix} = (H_{11} - \bar{H}S_{11})(H_{22} - \bar{H}S_{22}) - (H_{12} - \bar{H}S_{12})^2 = 0 \quad (9.186)$$

This is a quadratic equation for the energy functional \bar{H} with the two roots:

$$\bar{H}_{1,2} = \frac{-B \pm \sqrt{B^2 - 4AC}}{2A} \quad (9.187)$$

where $A = S_{11}S_{22} - S_{12}^2$, $B = 2H_{12}S_{12} - H_{11}S_{22} - H_{22}S_{11}$, and $C = H_{11}H_{22} - H_{12}^2$. The two roots are $\bar{H}_1 = 2.47862 E_h$, and $\bar{H}_2 = -0.47586 E_h$. The first root apparently corresponds to a maximum energy, the second to the minimum energy sought. If we compare it with the result from subproblem (a), $-0.4244 E_h$, we conclude that the addition of a second Gaussian improves the estimate for the ground state energy to about 95% of the exact result, $-0.5 E_h$. The results are summarized in Table 9.2.

Having obtained the optimal value for \bar{H} , our next goal is the determination of the variational parameters c_1 and c_2 for the negative solution. We insert \bar{H}_2 in Eq. (9.183). This yields:

$$c_2 = -\frac{H_{11} - \bar{H}_2 S_{11}}{H_{12} - \bar{H}_2 S_{12}} c_1 \quad (9.188)$$

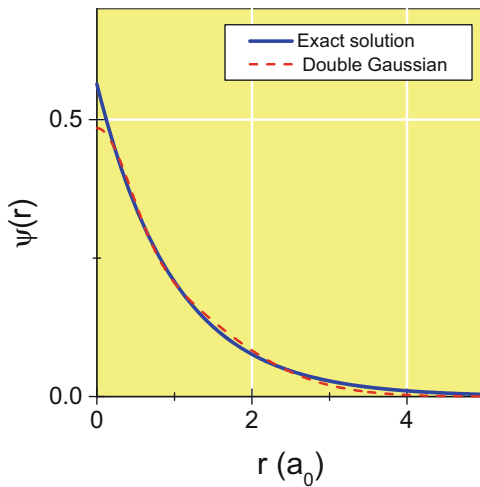
The second condition is the normalization of the test wave function:

$$c_1^2 S_{11} + 2c_1 c_2 S_{12} + c_2^2 S_{22} \stackrel{!}{=} 1 \quad (9.189)$$

Table 9.2 Estimated ground state energies of the hydrogen problem based on the variational principle in comparison with the exact result

Wave function	1 Gaussian	2 Gaussians	Exact (Slater function)
E_0 (Hartree units)	-0.4244	-0.4759	-0.50

Fig. 9.20 Comparison of the exact 1s wave function of the hydrogen atom (*solid line*) with the optimized test functions with two Gaussian functions (*dashed line*)



Substituting c_2 and solving for c_1 we obtain:

$$c_1 = \left(S_{11} + \left(\frac{H_{11} - \bar{H}_2 S_{11}}{H_{12} - \bar{H}_2 S_{12}} \right)^2 S_{22} - 2 \frac{H_{11} - \bar{H}_2 S_{11}}{H_{12} - \bar{H}_2 S_{12}} S_{12} \right)^{-\frac{1}{2}} = 0.22963 \quad (9.190)$$

and for the second coefficient $c_2 = 0.25472$. The resulting optimized test function is shown in Fig. 9.20 in comparison with the exact wave function (solid line). The optimized double Gaussian test function is quite close to the exact function, with deviations in the near-core and in the far-core region, where the test function takes a steeper course. We conclude that the use of a more flexible double Gaussian test function not only improves the result for the ground state energy, it better resembles the shape of the exact wave function compared with the single Gaussian test function shown in Fig. 9.19. It is worth looking at the remaining deviations in more detail by plotting the radial probability density $w(r) = 4\pi|\psi(r)|^2 r^2$, i.e., the probability of finding the electron between r and $r + dr$. This is done in Fig. 9.21. In this representation, the remaining deviations in the far core region appear more pronounced. Note that the accurate description of electronic structure in the far core region is crucial in chemistry. The method we have applied in this problem can be extended to even more flexible test functions. Contemporary quantum chemistry uses **Gaussian basis sets** with a higher number of primitive Gaussian functions. These give a much more accurate description both in the near core region and – important for chemical bonding – in the region far from the core. Of course, these methods rely on the numerical computation of the integrals and the solution of large systems of equations. Looking back on our solution, we have seen how the variational principle is used to obtain an approximative solution to the well-known hydrogen problem. Even a test function that only approximately compares with the

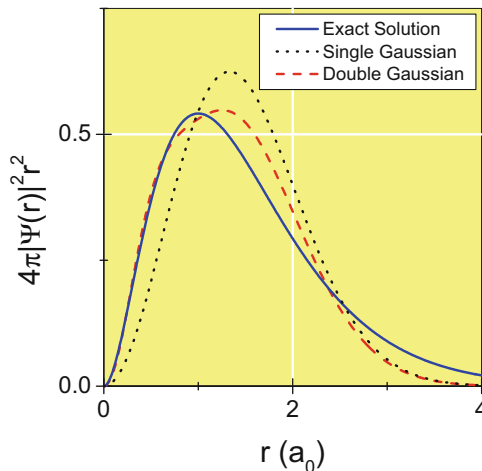


Fig. 9.21 Radial probability density of the exact hydrogen 1s wave function (solid line), the optimized double Gaussian function (dashed line), and the optimized single Gaussian function (dotted line)

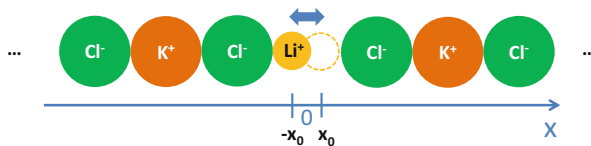


Fig. 9.22 Linear chain of K^+ and Cl^- ions with a vacancy as a model of a lithium doped KCl crystal. Due to the quantum mechanical tunnel effect, the Li^+ ion can switch between the two stable positions

exact solution yields an estimation of the ground state energy that is remarkably close to the exact result.

Problem 9.17 (The Quantum Double Well)

Consider a lithium ion that is free to move in x -direction within a K^+ vacancy in an atomic chain of KCl (see Fig. 9.22). Using atomic units, the potential can be approximated by a double-well potential

$$V(x) = \frac{\eta}{x_0^4} (x^2 - x_0^2)^2 \quad (9.191)$$

(continued)

Problem 9.17 (continued)

with the two minima at $x = \pm x_0$ ($x_0 = 1.38 a_0$) and a local maximum $V(0) = \eta = 5 \times 10^{-4} E_h$ ($1 E_h = 27.12 \text{ eV}$, $a_0 = 0.5292 \text{ \AA}$).

- Write down the time-independent Schrödinger equation for the lithium ion.
- To solve the Schrödinger equation, expand the wave function of the problem in a series of harmonic oscillator functions $\phi_n(x)$:

$$\psi(x) = \sum_{n=0} c_n \phi_n(x) \quad (9.192)$$

Write the Hamiltonian in the form:

$$\hat{H} = \hat{H}_0 + U(x) \quad (9.193)$$

where \hat{H}_0 is the Hamiltonian of the harmonic oscillator, and $U(x)$ is an effective potential of the particle.

- Show that the solution of the Schrödinger equation is equivalent to the solution of the eigenvalue problem

$$H_{mn} c_n = E c_n \quad n, m = 0, 1, 2, \dots \quad (9.194)$$

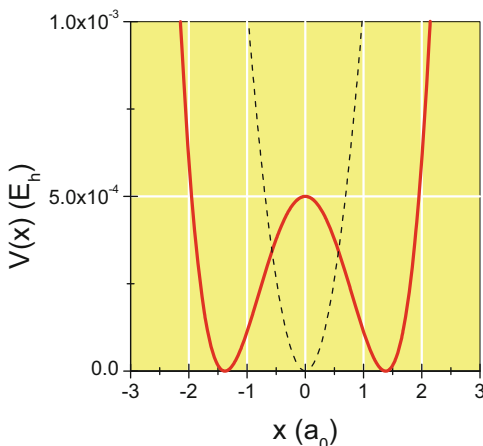
where

$$H_{m,n} = \hbar\omega \left(m + \frac{1}{2} \right) \delta_{mn} + \int_{-\infty}^{+\infty} \phi_m^*(x) U(x) \phi_n(x) dx \quad (9.195)$$

- Use the bra-ket notation and harmonic oscillator algebra introduced in Problem 9.10 and express the matrix elements $H_{m,n}$ in terms of the parameters given.
- Make a suitable choice for the harmonic oscillator angular frequency ω and use numerical methods to determine at least the energies of the ground state and the first excited state and their wave functions.

Solution 9.17 The context of this quantum mechanical problem is related to solid-state chemistry and physics. More precisely, we deal with a simplified model of lithium-doped potassium chloride (Li:KCl). We have already considered the latter as an example of a system that exhibits a Schottky anomaly (see Problem 8.8). Figure 9.22 shows a linear chain of K^+ and Cl^- ions. Near $x = 0$ one potassium is replaced by a Li^+ cation. As the latter has a smaller ionic radius, it has two stable equivalent positions and the ion can switch between these two positions, either by thermal motion or by means of the quantum mechanical *tunnel effect*. In the latter case, the lithium ion tunnels through the potential barrier between the two positions.

Fig. 9.23 Double-well model potential of the lithium ion in the vacancy (solid line). Also shown (dashed line) is the reference harmonic oscillator potential used for the solution of the quantum double well problem



The potential of the lithium in the vacancy, Eq. (9.191), is a symmetric double-well with minima at $\pm x_0$. It is plotted in Fig. 9.23 using the parameters η and x_0 given in the problem text. The use of atomic units simplifies the calculations in the following. Distances are thus defined in multiples of the Bohr radius a_0 , energies in multiples of hartree energy E_h . The form of the potential can be explained by strong repulsive interaction between Li^+ and Cl^- for $|x| > 2 a_0$, and electrostatic interaction between Li^+ and all ions in the chain, which, compared with the interaction at $x = 0$, is slightly more attractive if the Li^+ moves closer to the neighboring Cl^- . Our goal is to investigate this system using quantum mechanics. This is highly instructive, not only because double-well potentials have promising applications such as quantum dots or quantum antennas. From a mathematical point of view, we learn how to use a complete orthogonal system of functions to solve the time-independent Schrödinger equation exactly. Of course, in the end, we must use numerical methods, such as linear algebra, to obtain solutions. Starting with **subproblem (a)**, we write down the Schrödinger equation of the time-independent problem characterized by the double-well potential Eq. (9.191). In atomic units, the Schrödinger equation is:

$$\left[-\frac{1}{2m_{\text{Li}}} \frac{\partial^2}{\partial x^2} + \frac{\eta}{x_0^4} (x^2 - x_0^2)^2 \right] \psi(x) = E\psi(x) \quad (9.196)$$

Note that the mass of the lithium ion needs to be provided in multiples of the electron mass (see Sect. A.1): $m_{\text{Li}} = 6.94 m_u = 12650.8 m_e$ where the electron mass m_e is set to unity in atomic units. There are several possibilities for solving the Schrödinger equation. One possibility is to define a discrete grid of points along the x -axis and to discretize the second derivative in addition to the potential and the wave function. The other possibility is to expand the unknown wave function in a series of functions that constitute a complete orthogonal set. In this case, we use the harmonic oscillator functions $\phi_n(x)$ ($n = 0, 1, 2, \dots$) as such a complete set. These

functions¹⁵ are solutions of:

$$\left[-\frac{1}{2m_{\text{Li}}} \frac{\partial^2}{\partial x^2} + \frac{m_{\text{Li}}\omega^2}{2}x^2 \right] \phi_n(x) = E_n \phi_n(x) \quad (9.197)$$

where $E_n = \omega(n + \frac{1}{2})$ are the known energy eigenvalues of the harmonic oscillator with an angular frequency ω . The term in brackets in Eq. (9.196) is the Hamiltonian \hat{H} of the quantum double-well.

Following the instruction given in **subproblem (b)**, we rewrite the Hamiltonian as a sum of the harmonic oscillator Hamiltonian \hat{H}_0 plus an effective potential $U(x)$:

$$\begin{aligned} \hat{H} &= -\frac{1}{2m_{\text{Li}}} \frac{\partial^2}{\partial x^2} + \frac{m_{\text{Li}}\omega^2}{2}x^2 + \underbrace{\frac{\eta}{x_0^4} (x^2 - x_0^2)^2 - \frac{m_{\text{Li}}\omega^2}{2}x^2}_{U(x)} \\ &= \hat{H}_0 + U(x) \end{aligned} \quad (9.198)$$

The new potential function $U(x)$ is simply the difference between the double-well potential and the harmonic oscillator potential, where we are free to choose a suitable value for ω .

In **subproblem (c)**, we use this special form to show that it leads to an eigenvalue problem. Switching to bra-ket notation, the expansion of the unknown wave function in harmonic oscillator states $|n\rangle$ is

$$|\psi\rangle = \sum_{n=0} c_n |n\rangle. \quad (9.199)$$

The Schrödinger equation can thus be written

$$(\hat{H}_0 + U) \sum_{n=0} c_n |n\rangle = E \sum_{n=0} c_n |n\rangle \quad (9.200)$$

The trick is to multiply from the left with $\langle\psi| = \sum_m c_m^* \langle m|$:

$$\sum_{n,m} c_m^* c_n \underbrace{\langle m | \hat{H}_0 + U | n \rangle}_{H_{mn}} = E \sum_{n,m} c_m^* c_n \underbrace{\langle m | n \rangle}_{\delta_{nm}} \quad (9.201)$$

¹⁵Harmonic oscillator wave functions are illustrated in Fig. 9.1. Explicit formulas are provided in the Appendix, Sect. A.3.13.

We thus obtain the eigenvalue equation Eq.(9.194), and because $\hat{H}_0|n\rangle = \omega(n + \frac{1}{2})|n\rangle$, the matrix elements H_{mn} are given by:

$$H_{mn} = \omega \left(m + \frac{1}{2} \right) \delta_{mn} + \langle m | U | n \rangle \quad (9.202)$$

which is simply Eq.(9.195) in bra-ket notation. The determination of the matrix elements H_{mn} is our next task in **subproblem (d)**. We could solve the integrals in Eq.(9.195) numerically using explicit forms of the harmonic oscillator wave functions in the Appendix Eq.(A.76) in combination with the recurrence relation Eq.(A.77). Here, however, we can benefit from Dirac's abstract bra-ket notation. We solve the integrals without explicit usage of the harmonic oscillator wave functions, merely by using harmonic oscillator algebra based on creation and annihilation operators introduced in Problem 9.10, Eqs.(9.86) and (9.87). Using these equations, it can be shown that the position operator can be written

$$\hat{x} = \frac{1}{\sqrt{2m_{\text{Li}}\omega}} (\mathbf{a}^+ + \mathbf{a}) \quad (9.203)$$

The position operator can be inserted into the expression containing the effective potential:

$$\begin{aligned} U(x) &= \frac{\eta}{x_0^4} (x^2 - x_0^2)^2 - \frac{m_{\text{Li}}\omega^2}{2} x^2 \\ &= \frac{\eta}{x_0^4} (x^4 - 2x^2x_0^2 + x_0^4) - \frac{m_{\text{Li}}\omega^2}{2} x^2 \end{aligned} \quad (9.204)$$

The matrix elements of the effective potential are:

$$\langle m | U(x) | n \rangle = \frac{\eta}{x_0^4} \langle m | x^4 | n \rangle - \left(\frac{2\eta}{x_0^2} + \frac{m_{\text{Li}}\omega^2}{2} \right) \langle m | x^2 | n \rangle + \underbrace{\eta \langle m | n \rangle}_{\delta_{mn}}. \quad (9.205)$$

Using Eq.(9.203), we obtain:

$$x^2 = \frac{1}{2m_{\text{Li}}\omega} (\mathbf{a}^+ \mathbf{a}^+ + \mathbf{a} \mathbf{a}^+ + \mathbf{a}^+ \mathbf{a} + \mathbf{a} \mathbf{a}) \quad (9.206)$$

and

$$\begin{aligned} x^4 &= \frac{1}{4m_{\text{Li}}^2\omega^2} (\mathbf{a}^+ \mathbf{a}^+ \mathbf{a}^+ \mathbf{a}^+ + \mathbf{a}^+ \mathbf{a}^+ \mathbf{a} \mathbf{a}^+ + \mathbf{a}^+ \mathbf{a}^+ \mathbf{a}^+ \mathbf{a} + \mathbf{a}^+ \mathbf{a}^+ \mathbf{a} \mathbf{a} \\ &\quad + \mathbf{a} \mathbf{a}^+ \mathbf{a}^+ \mathbf{a}^+ + \mathbf{a} \mathbf{a}^+ \mathbf{a} \mathbf{a}^+ + \mathbf{a} \mathbf{a}^+ \mathbf{a}^+ \mathbf{a} + \mathbf{a} \mathbf{a}^+ \mathbf{a} \mathbf{a} \\ &\quad + \mathbf{a}^+ \mathbf{a} \mathbf{a}^+ \mathbf{a}^+ + \mathbf{a}^+ \mathbf{a} \mathbf{a} \mathbf{a}^+ + \mathbf{a}^+ \mathbf{a} \mathbf{a}^+ \mathbf{a} + \mathbf{a}^+ \mathbf{a} \mathbf{a} \mathbf{a} \\ &\quad + \mathbf{a} \mathbf{a} \mathbf{a}^+ \mathbf{a}^+ + \mathbf{a} \mathbf{a} \mathbf{a} \mathbf{a}^+ + \mathbf{a} \mathbf{a} \mathbf{a}^+ \mathbf{a} + \mathbf{a} \mathbf{a} \mathbf{a} \mathbf{a}). \end{aligned} \quad (9.207)$$

For the evaluation of the matrix elements $\langle m|x^2|n\rangle$ and $\langle m|x^4|n\rangle$ we insert these operator expressions and consider the relations:

$$\mathbf{a}^+|n\rangle = \sqrt{n+1}|n+1\rangle; \quad \mathbf{a}|n\rangle = \sqrt{n}|n-1\rangle \quad (9.208)$$

which appeared in Problem 9.10. Using the orthogonality of the harmonic oscillator states, $\langle m|n\rangle = \delta_{m,n}$, we obtain, for example:

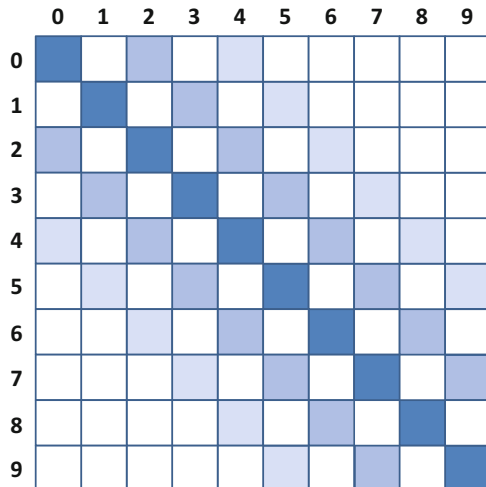
$$\begin{aligned}\langle m|\mathbf{a}^+\mathbf{a}^+|n\rangle &= \sqrt{(n+1)(n+2)}\delta_{m,n+2} \\ \langle m|\mathbf{a}^+\mathbf{a}|n\rangle &= \sqrt{n}\delta_{m,n} \\ \langle m|\mathbf{a}^+\mathbf{a}^+\mathbf{a}\mathbf{a}|n\rangle &= \sqrt{n(n-1)(n-1)n}\delta_{m,n} \\ \langle m|\mathbf{a}^+\mathbf{a}^+\mathbf{a}^+\mathbf{a}|n\rangle &= \sqrt{n n(n+1)(n+2)}\delta_{m,n+2}\end{aligned}$$

Note that the order of the operators in the various terms matters. If we analyze all 20 operator terms in this way, we obtain:

$$\begin{aligned}H_{mn} = \omega \left(m + \frac{1}{2} \right) \delta_{m,n} + \eta \delta_{m,n} \\ + \frac{\eta}{x_0^4} \sqrt{(n+1)(n+2)(n+3)(n+4)}\delta_{m,n+4} \\ + \frac{\eta}{x_0^4} \left(\sqrt{(n+1)^3(n+2)} + n\sqrt{(n+1)(n+2)} + (n+3)\sqrt{(n+1)(n+2)} \right. \\ \left. + \sqrt{(n+1)(n+2)^3} \right) \delta_{m,n+2} \\ + \frac{\eta}{x_0^4} \left(n(n-1) + (n+1)^2 + 2n(n+1) + n^2 + (n+1)(n+2) \right) \delta_{m,n} \\ + \frac{\eta}{x_0^4} \left(\sqrt{n(n-1)^3} + (n-2)\sqrt{n(n-1)} \right. \\ \left. + (n+1)\sqrt{n(n-1)} + \sqrt{n^3(n-1)} \right) \delta_{m,n-2} \\ + \frac{\eta}{x_0^4} \sqrt{n(n-1)(n-2)(n-3)}\delta_{m,n-4} \\ - \left(\frac{2\eta}{x_0^2} + \frac{m_{\text{Li}}\omega^2}{2} \right) \left(\sqrt{(n+1)(n+2)}\delta_{m,n+2} + (n+(n+1))\delta_{m,n} \right. \\ \left. + \sqrt{n(n-1)}\delta_{m,n-2} \right). \quad (9.209)\end{aligned}$$

The appearance of the Kronecker deltas $\delta_{m,n}$, $\delta_{m,n\pm 2}$, and $\delta_{m,n\pm 4}$ indicates that most of the matrix elements H_{mn} are zero. Nonzero matrix elements in the

Fig. 9.24 Sparse occupation of the Hamiltonian matrix H_{mn} for the quantum double-well problem for a 10×10 matrix (schematic). White fields represent matrix elements with zero value, shaded fields represent elements that are nonzero



Hamiltonian matrix appear in a band near the diagonal, as illustrated schematically in Fig. 9.24.

We are now ready to solve the problem numerically in **subproblem (e)**. At first, we choose the angular frequency ω . In principle, the solution will not depend on this choice. However, if ω is too large or too small, convergence of the result with regard to the number of harmonic oscillator states in the calculation may be an issue. The harmonic oscillator potential should thus approximately fit the double-well potential and should thus be adapted to the parameters η , the mass m , and x_0 . A possible choice could be:

$$\omega = \sqrt{\frac{8\eta}{m_{\text{Li}}x_0^2}} = 4.07466 \times 10^{-4} \text{ a.u.} \quad (9.210)$$

The resulting potential of the reference harmonic oscillator is shown in Fig. 9.23 (blue dotted line). A numerical procedure to diagonalize the Hamiltonian matrix (Eq. (9.209)) can be implemented in various ways, for example, by using mathematical software or a programming language. In the latter case, powerful linear algebra libraries are available.¹⁶

With the above choice for ω it is sufficient to use 20 harmonic oscillator functions. The resulting eigenvalue spectrum, obtained by diagonalization of the resulting 20×20 matrix, is shown for the first six states in Fig. 9.25, together with the double-well potential. Numerical values are also given in Table 9.3. The ground state and the first excited state are separated by a small splitting of only $\Delta = 3.32 \times 10^{-6} E_h$ or 0.1 meV. As can be seen in Fig. 9.25, there is also a grouping

¹⁶The most common one is LAPACK, <http://www.netlib.org/lapack/>.

Fig. 9.25 The first six energy levels of the quantum double-well, as obtained from the solution of Eq. (9.194). The splitting between the ground state ($n = 0$) and the first excited state ($n = 1$) is very small ($\Delta = 3.4 \times 10^{-6} E_h$)

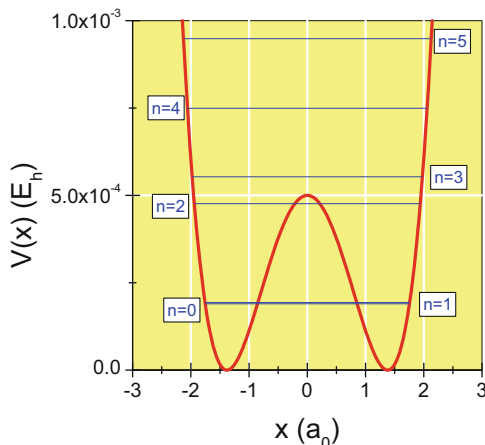


Table 9.3 The first six energy states of the quantum double-well obtained from the solution of Eq. (9.194)

n	$E_n (10^{-4} E_h)$
0	1.8996
1	1.9339
2	4.7630
3	5.5326
4	7.4947
5	9.4820

of states $n = 2$ and $n = 3$ with a larger splitting of $77 \times 10^{-6} E_h$ discernible. The energies of these states are close to the potential barrier at $x = 0$.

For the visualization of the wave functions, we use Eq. (9.192) and the eigenvectors of the various states. We need the general form of the harmonic oscillator wave functions Eq. (A.76) and the recurrence relation Eq. (A.77) for the Hermite polynomials to construct the double-well wave functions. The first six solutions are shown in Fig. 9.26.

It is striking that states with even n are also even functions, i.e. $\psi_n(x) = \psi(-x)$ for $n = 0, 2, 4$, whereas the states with odd n are asymmetrical: $\psi_n(-x) = -\psi(x)_n$ for $n = 1, 3, 5$. The ground state wave function and the solution for $n = 1$ have a high amplitude and thus high probability¹⁷ near the stable sites of the Li^+ at $x = \pm x_0$. However, for the ground state in particular, there is also a nonzero probability of finding the Li^+ within the potential barrier, and this causes the possibility of tunneling through the barrier. In contrast, the states $n \geq 2$ with energies comparable with the energy barrier or higher have a considerable probability in the region of the barrier, although, by symmetry, odd states have $|\psi_n(0)|^2 = 0$.

¹⁷The probability of finding the Li^+ between x and $x + dx$ is $|\psi_n(x)|^2$.

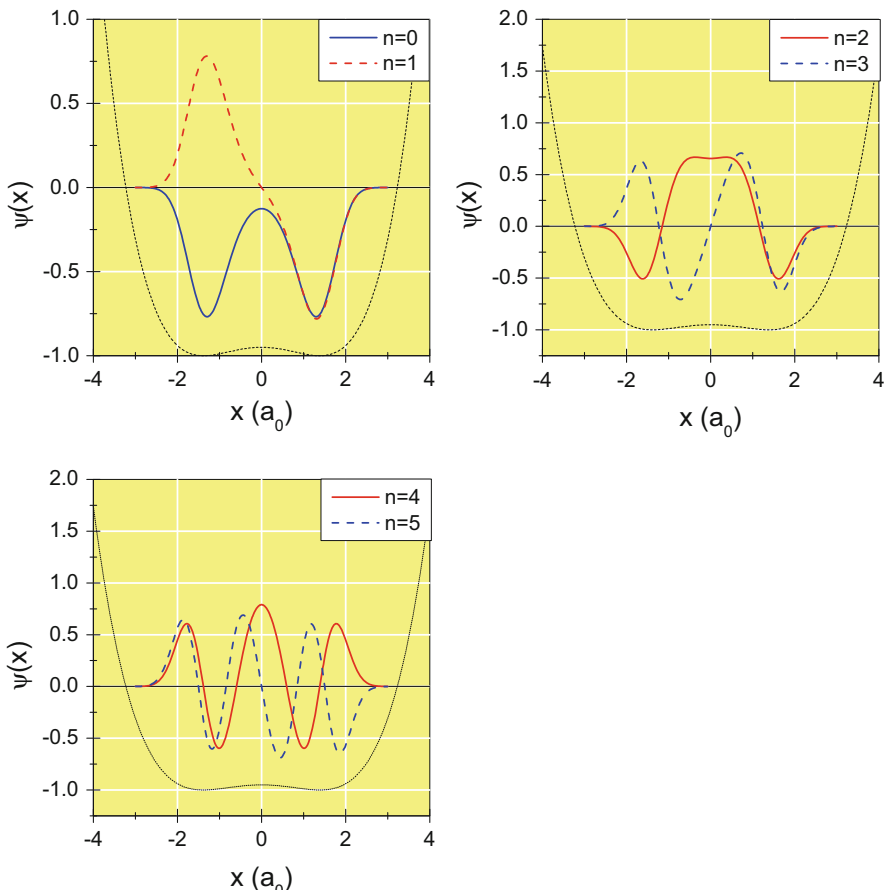


Fig. 9.26 Wave functions in the double-well potential (*short dashed*) of the ground state ($n = 0$) and the first excited states. The wave functions are alternately either symmetrical ($n = 0, 2, 4$) or asymmetrical ($n = 1, 3, 5$)

It is worth mentioning that the model of the one-dimensional atomic chain in Fig. 9.22 can only yield qualitative results for the description of the Li:KCl system. A K^+ vacancy in a KCl crystal has a three-dimensional structure and the potential of a Li^+ ion has not two, but eight local minima. The simple one-dimensional model, however, contains the essential physics to understand the behavior of such multiwell systems. In summary, we have learned how harmonic oscillator wave functions can be used as a complete orthogonal set of functions to solve the Schrödinger equation for the special case of a quantum double-well potential. The method is general and can be used for other potentials, e.g., the asymmetric quantum double-well.

Problem 9.18 (The Chemical Bond)

Hint: It is recommended that the reader has dealt with Problem 9.16.

The simplest chemical system that exhibits a chemical bond between two nuclei is the H_2^+ molecule ion. Use the variational principle (Problem 9.16) to derive approximate analytical solutions for the potential between the two nuclei at rest at positions $\mathbf{R}_1 = (0, 0, -\frac{R}{2})$ and $\mathbf{R}_2 = (0, 0, +\frac{R}{2})$. As a suitable trial wave function use a linear combination of hydrogen 1s wave functions located at the sites of the nuclei 1 and 2 respectively:

$$\psi(\mathbf{r}) = c_1 \psi_1(r_1) + c_2 \psi_2(r_2) \quad (9.211)$$

where $r_1 = |\mathbf{r} - \mathbf{R}_1|$, $r_2 = |\mathbf{r} - \mathbf{R}_2|$, and ψ_1 and ψ_2 have the form

$$\psi_{1s}(r) = \frac{1}{\sqrt{\pi a_0^3}} e^{-\frac{r}{a_0}}. \quad (9.212)$$

- Write down the Hamiltonian \hat{H} for the electron, using atomic units.
- Calculate the *overlap integral*

$$S = \int \psi_1(\mathbf{r}) \psi_2(\mathbf{r}) dV = \langle \psi_1 | \psi_2 \rangle \quad (9.213)$$

as a function of the internuclear distance R . *Hint:* Introduce the confocal elliptical coordinates

$$\mu = \frac{r_1 + r_2}{R}; \quad \mu \in [1, \infty] \quad (9.214)$$

$$\nu = \frac{r_1 - r_2}{R}; \quad \nu \in [-1, 1] \quad (9.215)$$

- and the angle $\phi \in [0, 2\pi]$ defined in Fig. 9.27. The volume element expressed in these coordinates is $dV = \frac{R^3}{8} (\mu^2 - \nu^2) d\mu d\nu d\phi$.
- Use the same integration technique to evaluate the Coulomb integral

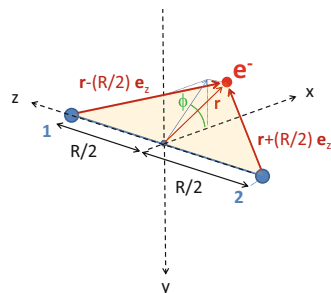
$$C = \int \psi_1(\mathbf{r}) \frac{1}{r_2} \psi_1(\mathbf{r}) dV = \langle \psi_1 | \frac{1}{r_2} | \psi_1 \rangle \quad (9.216)$$

and the exchange integral

$$A = \int \psi_1(\mathbf{r}) \frac{1}{r_1} \psi_2(\mathbf{r}) dV = \langle \psi_1 | \frac{1}{r_1} | \psi_2 \rangle \quad (9.217)$$

(continued)

Fig. 9.27 Geometry of the H_2^+ molecular ion. The origin of the molecule-fixed coordinate system is in the middle of the connecting line; nuclei 1 and 2 are at positions $(0, 0, \pm \frac{R}{2})$. The electron at position \mathbf{r} and the two nuclei define a plane that is tilted by an angle ϕ with regard to the x -axis



Problem 9.18 (continued)

as a function of R .

- d. Insert the trial function Eq. (9.212) into the equation

$$\bar{H} = \frac{\langle \psi | \hat{H} | \psi \rangle}{\langle \psi | \psi \rangle} \stackrel{!}{=} \min. \quad (9.218)$$

for the variational principle and derive an eigenvalue equation for the electron energy. Show that one of the two solutions yields to a bonding of the two nuclei. Determine c_1 and c_2 .

Solution 9.18 Perhaps the most important application of quantum mechanics in chemistry is the explanation of chemical bonds from first principles. Contemporary methods in quantum chemistry provide accurate descriptions of the electronic structure of molecules and solids. However, these methods typically require great numerical effort. Paper and pencil approaches are possible for only the simplest systems, and, moreover, in an approximate manner. Nevertheless, they allow a qualitative understanding of the nature of the chemical bond. Here, we deal with the simplest possible molecular system, the H_2^+ molecular ion. The geometry is shown schematically in Fig. 9.27. The goal of the exercise is to determine the potential between the two nuclei as a function of the internuclear distance R . In the electronic ground state, we expect the potential energy curve

$$V(R) = V_{\text{rep}}(R) + E_{\text{el}}(R) \quad (9.219)$$

to exhibit a minimum. In atomic units¹⁸, which we use in the following, $V_{\text{rep}} = \frac{+1}{R}$ is the electrostatic repulsion of the two positively charged nuclei. E_{el} is the electronic energy acting as an effective potential, calculated at a given bond distance R . The

¹⁸See Sect. 9.1.4. Note that in atomic units the unit length is $1a_0$, and the unit energy is $1 E_h$.

Schrödinger equation of the electron moving in the Coulomb potential of the two nuclei is:

$$\left[-\frac{1}{2} \Delta - \frac{1}{r_1} - \frac{1}{r_2} \right] \psi(\mathbf{r}) = E_{\text{el}} \psi(\mathbf{r}) \quad (9.220)$$

where $r_1 = |\mathbf{r} - \frac{R}{2} \mathbf{e}_z|$ is the distance of the electron from nucleus 1, and $r_2 = |\mathbf{r} + \frac{R}{2} \mathbf{e}_z|$ is the distance of the electron from nucleus 2 respectively, and \mathbf{e}_z is the unit vector in the z -direction.

The Hamiltonian sought in **subproblem (a)** is thus:

$$\hat{H} = -\frac{1}{2} \Delta - \frac{1}{r_1} - \frac{1}{r_2}. \quad (9.221)$$

It is worth noting that this quantum mechanical problem can be solved precisely by introducing confocal elliptical coordinates [5]. The approximate solution based on the variational principle, however, shows much of the spirit of a quantum chemical treatment. The variational principle was already used in Problem 9.16. The strategy is to use a suitable test function containing a number of adjustable parameters and to minimize the total energy. Improvement of the test function, for example, by increasing the number of parameters, is a systematic approach to the exact solution. In this problem, the test function is a linear combination of hydrogen 1s wave functions centered at the sites of the two nuclei:

$$\psi(\mathbf{r}) = c_1 \psi_1(r_1) + c_2 \psi_2(r_2) = \frac{1}{\sqrt{\pi}} [c_1 e^{-r_1} + c_2 e^{-r_2}] \quad (9.222)$$

Apparently, the coefficients c_1 and c_2 are the two adjustable parameters. Note that in the limiting case $R = 0$ where the two nuclei constitute a helium core with a nuclear charge $Ze = 2e$, this test wave function does not coincide with the exact ground state solution of the He^+ problem, $\psi_{\text{He}^+} \sim e^{-2r}$.

In **subproblem (b)** and **subproblem (c)**, we deal with three different integrals involved in the treatment of the H_2^+ ion. The first integral is the **overlap integral**

$$S(R) = \int \psi_1(\mathbf{r}) \psi_2(\mathbf{r}) dV = \frac{1}{\pi} \int e^{-|\mathbf{r} - \frac{R}{2} \mathbf{e}_z|} e^{-|\mathbf{r} + \frac{R}{2} \mathbf{e}_z|} dV = \frac{1}{\pi} \int e^{-(r_1 + r_2)} dV. \quad (9.223)$$

For the solution we switch to a representation using the confocal elliptical coordinates μ and ν introduced in Eqs. (9.214) and (9.215), in addition to the angle ϕ . It is the angle of the plane defined by the sites of the nuclei and the electron relative to the xz -plane. The significance of the coordinate μ becomes clearer if we imagine that the electron resides on an ellipse, whose two focal points are the sites of the nuclei. As each point on an ellipse leaves constant the sum of distances to the focal points, and because $R\mu = r_1 + r_2$, the coordinate μ has an analog in the radial distance of the electron in the hydrogen problem formulated with spherical coordinates: the

curve of constant μ is an ellipse, as the sphere is an area of constant radial distance. The other coordinate, ν , is related to the difference in the distances between the electron and the nuclear sites. If ν is varied at constant μ , the electron moves on the ellipse. An analogy to the quantity $\cos \theta$ in spherical coordinates is thus established. With the volume element given in the problem text, the overlap integral is thus:

$$S(R) = \frac{1}{\pi} \int_1^\infty d\mu \int_{-1}^{+1} d\nu \int_0^{2\pi} d\phi \frac{R^3}{8} (\mu^2 - \nu^2) e^{-R\mu}. \quad (9.224)$$

Integration over ϕ is trivial and yields a factor 2π . The separation with regard to the other coordinates yields:

$$S(R) = \frac{R^3}{4} \int_1^\infty \mu^2 e^{-R\mu} d\mu \underbrace{\int_{-1}^{+1} d\nu}_{=2} - \frac{R^3}{4} \int_1^\infty e^{-R\mu} d\mu \underbrace{\int_{-1}^{+1} \nu^2 d\nu}_{=\frac{2}{3}}. \quad (9.225)$$

Because

$$\int_1^\infty \mu^2 e^{-R\mu} d\mu \stackrel{\text{Eq. (A.44)}}{=} e^{-R\mu} \left(-\frac{\mu^2}{R} - \frac{2\mu}{R^2} - \frac{2}{R^3} \right) \Big|_1^\infty = 0 + e^{-R} \left(\frac{1}{R} + \frac{2}{R^2} + \frac{2}{R^3} \right) \quad (9.226)$$

and

$$\int_1^\infty e^{-R\mu} d\mu = -\frac{e^{-R\mu}}{R} \Big|_1^\infty = 0 + \frac{e^{-R}}{R} \quad (9.227)$$

the result for the overlap integral is

$$S(R) = e^{-R} \left(\frac{R^2}{3} + R + 1 \right). \quad (9.228)$$

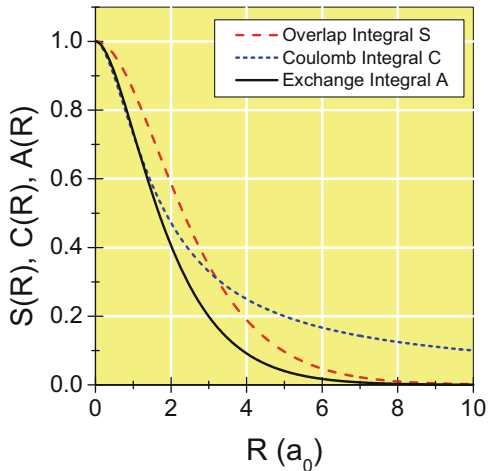
$S(R)$ is plotted in Fig. 9.28. The overlap integral diminishes rapidly for increasing R . The second integral is the Coulomb integral Eq. (9.216),

$$C(R) = \int \frac{\psi_1^2(r_1)}{r_2} dV = \frac{1}{\pi} \int \frac{e^{-2r_1}}{r_2} dV. \quad (9.229)$$

Because $r_1 = \frac{R}{2}(\mu + \nu)$ and $r_2 = \frac{R}{2}(\mu - \nu)$, the introduction of elliptical coordinates yields:

$$C(R) = \frac{1}{\pi} \int_0^{2\pi} d\phi \int_1^\infty d\mu \int_{-1}^{+1} d\nu e^{-R(\mu+\nu)} \frac{2}{R} \frac{1}{\mu - \nu} \frac{R^3}{8} (\mu^2 - \nu^2). \quad (9.230)$$

Fig. 9.28 Overlap integral S , Coulomb integral C , and exchange integral A as a function of the distance between the two hydrogen nuclei



Integration over ϕ is again trivial and further simplification is possible by means of the third binomial formula:

$$C(R) = \frac{R^2}{2} \int_{\mu=1}^{\infty} \int_{\nu=-1}^{+1} e^{-R(\mu+\nu)} (\mu + \nu) d\mu d\nu. \quad (9.231)$$

Separation of the integrals yields:

$$C(R) = \frac{R^2}{2} \int_1^{\infty} e^{-R\mu} \mu d\mu \int_{-1}^{+1} e^{-R\nu} d\nu + \frac{R^2}{2} \int_1^{\infty} e^{-R\mu} d\mu \int_{-1}^{+1} e^{-R\nu} \nu d\nu \quad (9.232)$$

where

$$\int_1^{\infty} e^{-R\mu} \mu d\mu \stackrel{\text{Eq. (A.43)}}{=} -\frac{e^{-R\mu}}{R^2} (R\mu + 1) \Big|_1^{\infty} = \frac{e^{-R}}{R^2} (R + 1) \quad (9.233)$$

$$\int_{-1}^{+1} e^{-R\nu} \nu d\nu \stackrel{\text{Eq. (A.43)}}{=} -\frac{e^{-R\nu}}{R^2} (R\nu + 1) \Big|_{-1}^{+1} = -\frac{e^{-R}}{R^2} (R + 1) + \frac{e^{-R}}{R^2} (1 - R) \quad (9.234)$$

$$\int_{-1}^{+1} e^{-R\nu} d\nu = \frac{1}{R} (e^R - e^{-R}). \quad (9.235)$$

With these results, the Coulomb integral is:

$$C(R) = \frac{1}{R} - e^{-2R} \left(1 + \frac{1}{R} \right) \quad (9.236)$$

This function is shown in Fig. 9.28 (short dashed line). At large R , the integral diminishes as R^{-1} and thus has a long range. The calculation of the third integral, called the exchange integral, uses the same methods:

$$A(R) = \int \frac{\psi_1 \psi_2}{r_1} dV = \frac{1}{\pi} \int \frac{e^{-(r_1+r_2)}}{r_1} dV \quad (9.237)$$

Introduction of elliptical coordinates and integration over the angle ϕ yields

$$\begin{aligned} A(R) &= \frac{R^2}{2} \int_1^\infty \int_{-1}^{+1} e^{-R\mu} (\mu - v) d\mu dv \\ &= \frac{R^2}{2} \int_1^\infty e^{-R\mu} \mu d\mu \underbrace{\int_{-1}^{+1} dv}_{=2} - \frac{R^2}{2} \int_1^\infty e^{-R\mu} d\mu \underbrace{\int_{-1}^{+1} v dv}_{=1} \end{aligned} \quad (9.238)$$

After insertion of Eqs. (9.227) and (9.233), the result for the exchange integral is:

$$A(R) = e^{-R} (1 + R). \quad (9.239)$$

It is also plotted in Fig. 9.28. In **subproblem (d)**, we apply the variational principle. From now on, it is convenient to switch to Dirac's bra-ket notation. We exploit the fact that the hydrogen 1s wave function is normalized, as we have shown in Problem 9.14. Moreover, we assume that the mixing parameters c_1 and c_2 are real. The denominator of the energy functional Eq. (9.218) is thus:

$$\begin{aligned} D &= \langle \psi | \psi \rangle = (c_1 \langle \psi_1 | + c_2 \langle \psi_2 |) (c_1 | \psi_1 \rangle + c_2 | \psi_2 \rangle) \\ &= c_1^2 \underbrace{\langle \psi_1 | \psi_1 \rangle}_{=1} + 2c_1 c_2 \underbrace{\langle \psi_1 | \psi_2 \rangle}_{=S} + c_2^2 \underbrace{\langle \psi_2 | \psi_2 \rangle}_{=1} \\ &= c_1^2 + 2c_1 c_2 S + c_2^2. \end{aligned} \quad (9.240)$$

For the calculation of the nominator of the energy functional we take into account that the Hamiltonian Eq. (9.221) acting on either of the two wave functions yields:

$$\left(-\Delta - \frac{1}{r_1} - \frac{1}{r_2} \right) | \psi_1 \rangle = E_0 | \psi_1 \rangle - \frac{1}{r_2} | \psi_1 \rangle \quad (9.241)$$

and

$$\left(-\Delta - \frac{1}{r_1} - \frac{1}{r_2} \right) | \psi_2 \rangle = E_0 | \psi_2 \rangle - \frac{1}{r_1} | \psi_2 \rangle \quad (9.242)$$

where $E_0 = -0.5 E_h = -13.605693 \text{ eV}$ is the ground state energy of the hydrogen atom. Thus, the nominator of the energy functional is¹⁹

$$\begin{aligned}
 N &= \langle \psi | \hat{H} | \psi \rangle = (c_1 \langle \psi_1 | + c_2 \langle \psi_2 |) \left(-\Delta - \frac{1}{r_1} - \frac{1}{r_2} \right) (c_1 | \psi_1 \rangle + c_2 | \psi_2 \rangle) \\
 &= c_1^2 E_0 \underbrace{\langle \psi_1 | \psi_1 \rangle}_{=1} - c_1^2 \underbrace{\langle \psi_1 | \frac{1}{r_2} | \psi_1 \rangle}_{=C} + c_1 c_2 E_0 \underbrace{\langle \psi_1 | \psi_2 \rangle}_{=S} - c_1 c_2 \underbrace{\langle \psi_1 | \frac{1}{r_1} | \psi_2 \rangle}_{=A} \\
 &\quad + c_1 c_2 E_0 \underbrace{\langle \psi_2 | \psi_1 \rangle}_{=S} - c_1 c_2 \underbrace{\langle \psi_2 | \frac{1}{r_2} | \psi_1 \rangle}_{=A} + c_2^2 E_0 \underbrace{\langle \psi_2 | \psi_2 \rangle}_{=1} - c_2^2 \underbrace{\langle \psi_2 | \frac{1}{r_1} | \psi_2 \rangle}_{=C} \\
 &= c_1^2 (E_0 - C) + 2c_1 c_2 (E_0 S - A) + c_2^2 (E_0 - C)
 \end{aligned} \tag{9.243}$$

The necessary conditions for a minimum as required in Eq. (9.218) is:

$$\frac{\partial \bar{H}}{\partial c_1} = 0; \quad \frac{\partial \bar{H}}{\partial c_2} = 0. \tag{9.244}$$

As shown in Problem 9.16 (Eq. (9.182) on page 269), these conditions are equivalent to:

$$\frac{\partial N}{\partial c_1} - \bar{H} \frac{\partial D}{\partial c_1} = 0 \tag{9.245}$$

and

$$\frac{\partial N}{\partial c_2} - \bar{H} \frac{\partial D}{\partial c_2} = 0. \tag{9.246}$$

As a consequence, we arrive at the following system of equations:

$$(E_0 - C - \bar{H}) c_1 + (E_0 S - A - \bar{H} S) c_2 = 0 \tag{9.247}$$

$$(E_0 S - A - \bar{H} S) c_1 + (E_0 - C - \bar{H}) c_2 = 0 \tag{9.248}$$

With the abbreviations $H_{11} = E_0 - C$ and $H_{12} = E_0 S - A$, the system is:

$$\begin{pmatrix} H_{11} - \bar{H} & H_{12} - \bar{H} S \\ H_{12} - \bar{H} S & H_{11} - \bar{H} \end{pmatrix} \begin{pmatrix} c_1 \\ c_2 \end{pmatrix} = 0 \tag{9.249}$$

¹⁹Note that because of the mathematical form of ψ_1 and ψ_2 , $\langle \psi_1 | \psi_2 \rangle = \langle \psi_2 | \psi_1 \rangle$.

A nontrivial solution requires the secular determinant to be zero:

$$(H_{11} - \bar{H})^2 - (H_{12} - \bar{H}S)^2 = 0 \quad (9.250)$$

This is a quadratic equation:

$$(1 - S^2) \bar{H}^2 + 2(H_{12}S - H_{11})\bar{H} + H_{11}^2 - H_{12}^2 = 0 \quad (9.251)$$

with two solutions (see Eq. (A.4))

$$\bar{H}_{1/2} = \frac{2(H_{11} - H_{12}S) \pm \sqrt{4(H_{11} - H_{12}S)^2 - 4(1 - S^2)(H_{11}^2 - H_{12}^2)}}{2(1 - S^2)} \quad (9.252)$$

which can be written in compact form

$$\bar{H}_{1/2} = \frac{H_{11} - H_{12}S \pm (H_{11}S - H_{12})}{1 - S^2} \quad (9.253)$$

and simplified even further to yield the two solutions:

$$\bar{H}_1 = E_u = \frac{H_{11} - H_{12}}{1 - S} = \frac{E_0 - C - E_0S + A}{1 - S} = E_0 - \frac{C - A}{1 - S} \quad (9.254)$$

and

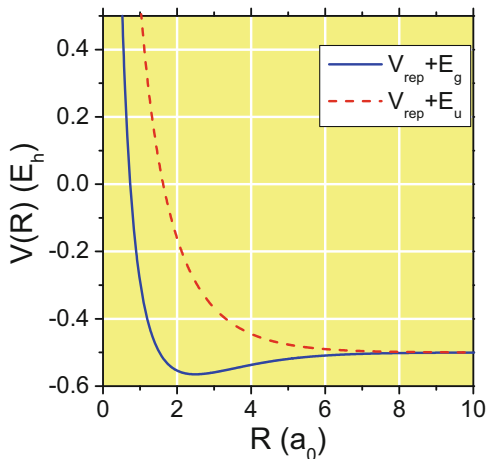
$$\bar{H}_2 = E_g = \frac{H_{11} + H_{12}}{1 + S} = \frac{E_0 - C + E_0S - A}{1 + S} = E_0 - \frac{C + A}{1 + S}. \quad (9.255)$$

The two energy eigenvalues E_g and E_u of the electron can thus be expressed by the integrals, $S(R)$, $C(R)$, $A(R)$, and the ground state energy of the hydrogen atom, E_0 . Focusing on the entire system of the H_2^+ ion, we identify these solutions as the electronic contribution E_{el} to the total potential energy according to Eq. (9.219). The resulting potential curves are shown in Fig. 9.29. It is striking that the blue curve related to the energy eigenvalue E_g has a minimum at $R_{\min} = 2.5a_0$, whereas the red curve has a monotonic behavior that is thus repulsive at all distances. We have therefore shown that one of the two solutions leads to bonding of the two nuclei. Furthermore, both potential curves have the same long-range behavior:

$$V(R) = \underbrace{\frac{1}{R}}_{V_{\text{rep}}} + E_0 - \frac{C \pm A}{1 \pm S} \xrightarrow{R \rightarrow \infty} E_0 = -0.5 \quad (9.256)$$

This is because the last term compensates for the electrostatic repulsion of the nuclei at long distances due to the long-range behavior of the Coulomb integral (see Eq. (9.236)) whereas the overlap and exchange integrals are negligible at large

Fig. 9.29 Potential between the hydrogen nuclei in the H_2^+ molecular ion, obtained from an approximate solution of the one electron Schrödinger equation using the variational method



distances. The value $V(R) = -0.5$ at large distances is the total energy of a neutral hydrogen atom and a hydrogen cation. If we neglect the zero-point energy, the formation of a stable H_2^+ molecular ion according to



involves an energy change $V(R_{\min}) - E_0 = -0.065 E_h = -1.76 \text{ eV}$. To determine the two coefficients, c_1 and c_2 , we insert the two solutions for \bar{H} (Eqs. (9.254) and (9.255)) into Eq. (9.249). For the solution with energy E_u , this yields:

$$c_2 = \frac{H_{11} - \bar{H}}{\bar{H}S - H_{12}} c_1 = \frac{H_{11} - \frac{H_{11}-H_{12}}{1-S}}{\frac{H_{11}-H_{12}}{1-S}S - H_{12}} c_1 = -\frac{H_{11}S - H_{12}}{H_{11}S - H_{12}} c_1 = -c_1. \quad (9.258)$$

Moreover, normalization of the total wave function requires:

$$\langle \psi | \psi \rangle = c_1^2 + 2c_1c_2S + c_2^2 = 1. \quad (9.259)$$

Therefore, we obtain:

$$2c_1^2 - 2c_1^2S = 1 \quad (9.260)$$

and thus

$$c_1 = -c_2 = \frac{1}{\sqrt{2(1-S)}}. \quad (9.261)$$

The wave function is thus:

$$\psi_u(r) = \frac{1}{\sqrt{2\pi(1-S)}} \left(e^{-|r-\mathbf{R}_1|} - e^{-|r-\mathbf{R}_2|} \right). \quad (9.262)$$

In a completely analogous way, we treat the solution with the eigenvalue E_g . Here, we find

$$c_1 = c_2 = \frac{1}{\sqrt{2(1+S)}} \quad (9.263)$$

and, as a consequence, the ground state wave function is:

$$\psi_g(r) = \frac{1}{\sqrt{2\pi(1+S)}} \left(e^{-|r-\mathbf{R}_1|} + e^{-|r-\mathbf{R}_2|} \right). \quad (9.264)$$

In the terminology of quantum chemistry, ψ_g and ψ_u are molecular orbitals, constructed by a linear combination of the two atomic orbitals ψ_1 and ψ_2 centered at the sites of the nuclei. Both wave functions are plotted for $R = R_{\min} = 2.5a_0$ in Fig. 9.30. Apparently, the ground state ψ_g is symmetrical with regard to an inversion of the molecule, whereas the excited state ψ_u is antisymmetric with regard to inversion. It is worth comparing ψ_g and ψ_u with the ground state ($n = 0$) and the first excited state ($n = 1$) in the quantum double-well problem (Problem 9.17, Fig. 9.26 on page 280). In both problems, the symmetrical solution is energetically favorable compared with the asymmetrical solution. An argument for the bonding nature of the symmetrical solution in the H_2^+ ion is the nonzero electronic charge density among the hydrogen nuclei. In the asymmetrical solution ψ_u , in contrast, the electronic density is repelled from the center of the molecule by symmetry.

In summary, we have applied the variational principle to the simplest molecular system, the H_2^+ ion, containing only one electron. We have shown that ground state electronic energy overcompensates for the electrostatic repulsion of the two hydrogen nuclei at a distance of $R = 2.5a_0$. It is worth noting that the construction of molecular orbitals from atomic orbitals using linear combination is not restricted to 1s orbitals. Extended test wave functions with additional p orbitals, for example, allow polarization effects to be included in the model. The method thus allows a systematic improvement of the solution.

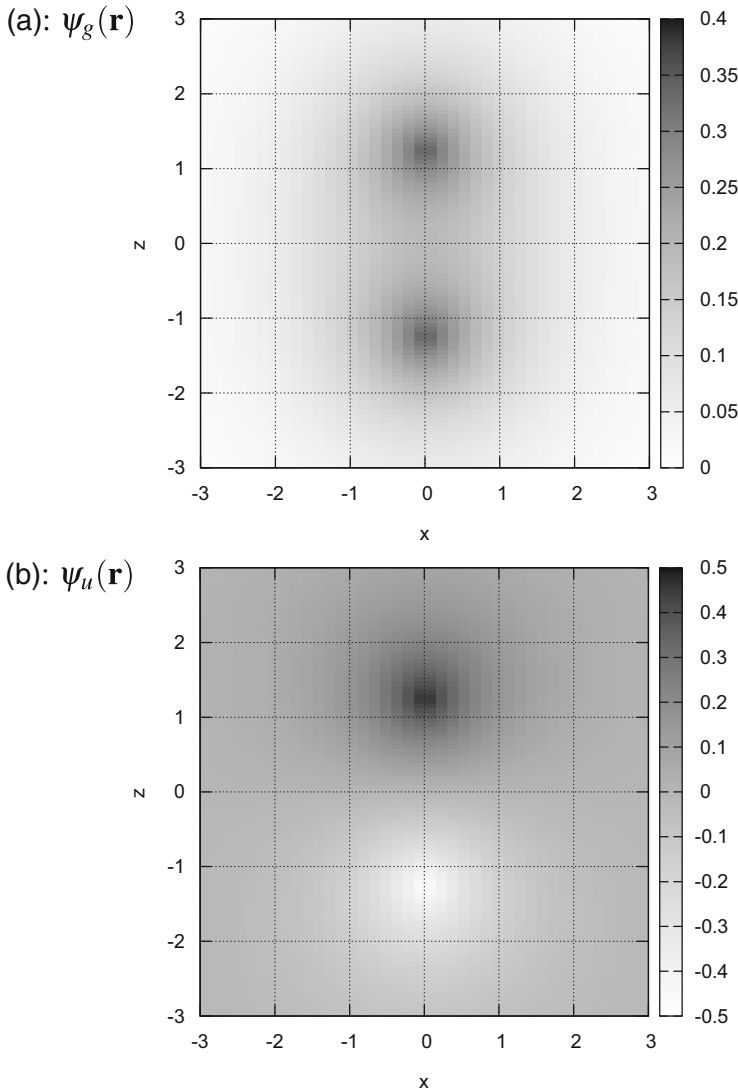


Fig. 9.30 Approximate solutions for the electronic wave functions of the H_2^+ ion based on the variational principle: (a) ground state ψ_g according to Eq. (9.264). (b) excited state ψ_u according to Eq. (9.262). Using inversion symmetry, ψ_u is characterized by zero electronic density in the center of mass

References

1. Gearhart CA (2002) Planck, the quantum, and the historians. *Phys Perspect* 4:170
2. Rud Nielsen J (1976) Niels Bohr collected works, vol 3. The correspondence principle. North-Holland, Amsterdam
3. Schrödinger E (1921) Versuch zur modellmäßigen Deutung des Terms der scharfen Nebenserien. *Z Phys* 4:347
4. Bohm D (1951) Quantum theory. Prentice Hall, New York
5. Grivet JP (2002) The hydrogen molecular ion revisited. *J Chem Educ* 79:127

Chapter 10

Spectroscopy

Abstract Spectroscopy is an important experimental technique for determining properties of atoms and molecules, predominantly by means of their interaction with electromagnetic waves. The foundations of spectroscopy are closely related to the quantum states of matter; thus, the basic concepts in part recapitulate the contents of quantum mechanics (Chap. 9). The presented set of problems deals with different kinds of spectroscopy in the various regions of the electromagnetic spectrum. One focus is on problems that demonstrate how quantitative analysis of spectra provides detailed information on molecular structure and bonding. Other problems deal with the principle and dynamics of the laser, which is the most important laboratory light source in contemporary spectroscopy.

10.1 Basic Concepts

10.1.1 Fundamental Interaction Process Between Light and Matter

There are three basic types of interaction between an electromagnetic wave (frequency ν , wave vector \mathbf{k}) or a photon (energy $E = h\nu$, momentum $\mathbf{p} = \hbar\mathbf{k}$) and matter, i.e., an atom or molecule. The latter are represented by a two-level system.¹ These three types are illustrated in Fig. 10.1.

Induced absorption of a photon causes an excitation of the atom or molecule from a state of lower energy to a state of higher energy. **Spontaneous emission**, in contrast, is the transition of the atom or molecule from a state of higher energy to a state of lower energy under emission of a photon. A third process, called **induced emission**, is the transition from an excited state to a state of lower energy induced by a photon under emission of a second photon. Conservation of energy and momentum are guaranteed by the basic rules of quantum mechanics.² A transition is possible if the appropriate **selection rules** are fulfilled. The photon frequency involved with the transition is then related to the difference in energy between the two states E_{final}

¹We have dealt with a quantum mechanical description of a two-level system in Problem 9.11.

²Energy conservation in absorption and emission processes is guaranteed in the limit $t \rightarrow \infty$.

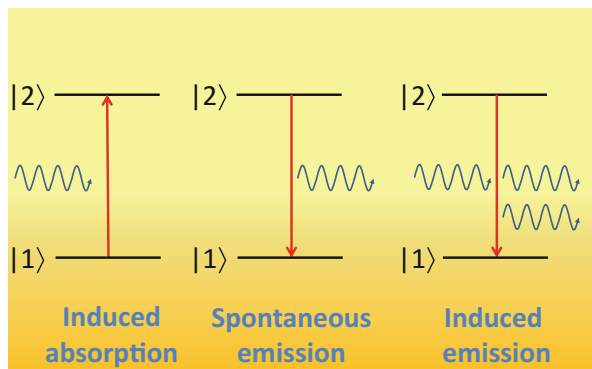


Fig. 10.1 The fundamental processes of interaction of matter with light. Matter is represented by an atomic or molecular two-level system that absorbs or emits photons

and E_{initial} of the atom or molecule. For the absorption, the photon frequency is:

$$h\nu = E_{\text{final}} - E_{\text{initial}}; \quad E_{\text{final}} > E_{\text{initial}}. \quad (10.1)$$

For emission processes,

$$h\nu = E_{\text{initial}} - E_{\text{final}}; \quad E_{\text{initial}} > E_{\text{final}}. \quad (10.2)$$

Experimentally, the absorption of light is measured by the attenuated spectral intensity $I(\nu)$ of an electromagnetic wave traveling through a medium of **optical depth** τ :

$$I(\nu) = I_0(\nu) \exp(-\tau) \quad (10.3)$$

$I_0(\nu)$ is the spectral intensity of the light source measured without an absorbing medium. Ideally, the optical depth τ depends on the length of the optical path L , the number density \mathcal{N} of the absorbing species, and its **attenuation cross section** $\sigma(\nu)$:

$$\tau(\nu) = \mathcal{N} \sigma(\nu) L. \quad (10.4)$$

Equation (10.3) is called **Lambert Beer law**. Other related quantities common in absorption spectroscopy are the **transmittance**

$$T(\nu) = \frac{I(\nu)}{I_0(\nu)} \quad (10.5)$$

and the spectral **absorbance**

$$A_{10}(\nu) = -\log_{10} T(\nu). \quad (10.6)$$

Note that in the literature the absorbance is sometimes based on the natural logarithm, $A_e(\nu) = -\ln T(\nu)$. Moreover, in the presence of light beam attenuation due to scattering losses, the terminus **extinction** or **attenuance** is used instead of the absorbance.

Moreover, a quantitative description of absorption and emission processes sketched in Fig. 10.1 can be based on rate equations involving the spectral energy density of the electromagnetic field, $u(\nu)$, and the Einstein coefficients. The probability per second that an atom or molecule absorbs a photon of frequency ν is given by:

$$\frac{dP_{12}}{dt} = B_{12}u(\nu) \quad (10.7)$$

where B_{12} is the Einstein coefficient for induced absorption. Accordingly, the probability per second for induced emission of an excited atom or molecule is:

$$\frac{dP_{21}}{dt} = B_{21}u(\nu) \quad (10.8)$$

where B_{21} is the Einstein coefficient for induced emission. The probability per second of spontaneous emission does not depend on the energy density of the electromagnetic field:

$$\frac{dP_{21}}{dt} = A_{21} \quad (10.9)$$

A_{21} is the respective Einstein coefficient for spontaneous emission. The **lifetime** τ of the excited state with regard to spontaneous emission is:

$$\tau = \frac{1}{A_{21}}. \quad (10.10)$$

Higher order processes involve the absorption and emission of more than one photon. Light scattering processes, for example, are based on the absorption of a photon under excitation of the scattering atom or molecule on a **virtual intermediate state**, followed by the emission of a second photon and the subsequent transition back to the initial state (Rayleigh scattering), or to another final state (Raman scattering). Raman scattering is illustrated in Fig. 10.2 for the case of Stokes scattering and anti-Stokes scattering.

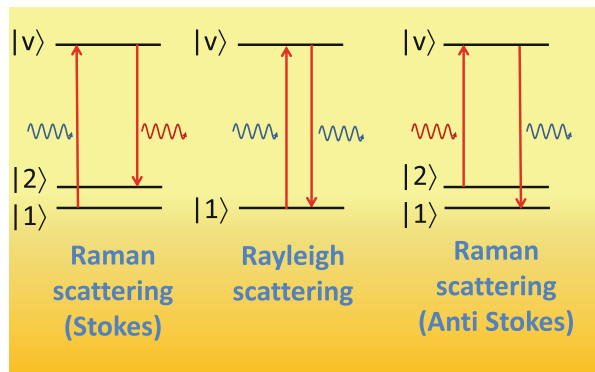


Fig. 10.2 Light scattering processes. Stokes scattering (*left*) starts from a low-lying initial state, and the emitted photon has a lower frequency than the absorbed one (red shift). Rayleigh scattering (*middle*) involves the same level as the final and initial state. Anti-Stokes scattering (*right*) starting from a state of higher energy results in a blue shift of the emitted photon

10.1.2 Rotational Spectroscopy: The Rigid Rotator

The simplest quantum mechanical model associated with molecular rotation is the diatomic rigid rotator outlined in Fig. 10.3. Its energy levels are given by:

$$E_J = \hbar BJ(J + 1) \quad J = 0, 1, 2, \dots \quad (10.11)$$

where J is the rotational quantum number, and B is the rotational constant in frequency units:

$$B = \frac{\hbar}{8\pi^2 I} \quad (10.12)$$

B is related to the rotator's moment of inertia

$$I = \mu r^2 \quad (10.13)$$

with the effective mass μ depending on the masses of the two centers:

$$\mu = \frac{m_1 m_2}{m_1 + m_2} \quad (10.14)$$

As textbooks show, the solutions of the Schrödinger equation for the dumbbell-shaped rigid rotator are the spherical harmonics $Y_{JM}(\theta, \phi)$ (see Sect. A.3.14 in

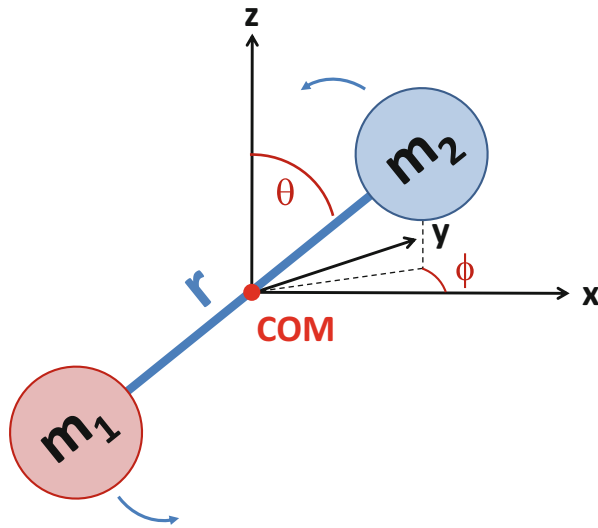


Fig. 10.3 The diatomic dumbbell-shaped rotator. The center of mass (COM) is the origin of the molecule-fixed coordinate system. The orientation of the molecule is fully described by the tilt angle θ and the azimuthal angle ϕ

the appendix). The two angles θ and ϕ completely define the orientation of the molecule. Because the energy levels Eq. (10.11) do not depend on the orientational quantum number M , they are degenerated. The degeneracy corresponds to the number $(2J + 1)$ of possible M values for a given J . Rotational transitions mediated by the absorption or emission of light are bound to selection rules. Pure rotational transitions require a permanent electric dipole moment and, moreover

$$\Delta J = \pm 1; \quad \Delta M = 0, \pm 1. \quad (10.15)$$

As a consequence of the energy levels Eq. (10.11) and these selection rules, the pure rotation spectrum exhibits equidistant transitions, as shown in Fig. 10.4.

10.1.3 Vibrational Spectroscopy of Molecules

Key to the description of the vibrational spectroscopy of molecules is the model of the **harmonic oscillator** (see Sect. 9.1.2.3). Given a force constant k and an effective

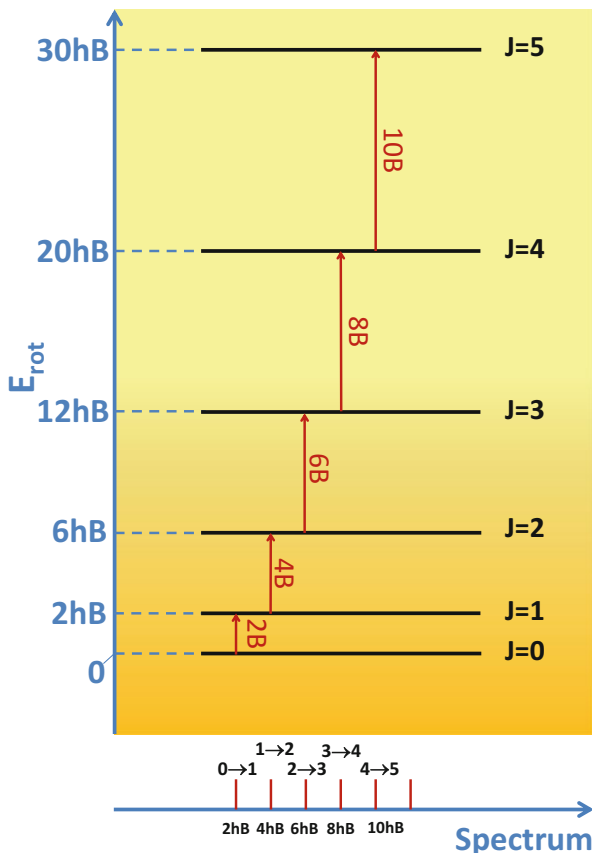


Fig. 10.4 The energy levels of the rigid diatomic rotator and the resulting spectrum of equidistant lines

mass μ , the harmonic oscillation frequency is

$$\nu_e = \frac{1}{2\pi} \sqrt{\frac{k}{\mu}}. \quad (10.16)$$

The quantum energy of the oscillator is $h\nu_e$ and the energy levels are

$$E_n = h\nu_e \left(n + \frac{1}{2} \right) \quad n = 0, 1, 2, \dots \quad (10.17)$$

where n is the vibrational quantum number. The selection rules for transitions of an harmonic oscillator between two states n and n' are:

$$\Delta n = n - n' = \pm 1. \quad (10.18)$$

Moreover, an *induced* electric dipole moment must be involved with the vibrational transition. **Anharmonicity** of the potentials between atomic cores lowers the energy of a vibrational transition. The generally observed relation (see Problem 10.6) is

$$E_n = h\nu_e \left(n + \frac{1}{2} \right) - x_e h\nu_e \left(n + \frac{1}{2} \right)^2 \quad (10.19)$$

where x_e is an anharmonicity constant.

10.2 Problems

Additional problems related to spectroscopy can be found in Chap. 9.

Problem 10.1 (Units of Measurement in Spectroscopy)

Different units of measurement are used in spectroscopy.

- Clarify the relationship between energy (E), frequency (ν), wavelength (λ), and wave number ($\tilde{\nu}$).
- For the following data, provide the missing values of E , ν , λ , and $\tilde{\nu}$. Assign the data to the respective range within the electromagnetic spectrum.
 - $E = 1 \text{ eV}$.
 - $\lambda = 21 \text{ cm}$ (hyperfine splitting of hydrogen)
 - Room temperature thermal energy ($k_B T$, $T = 298.15 \text{ K}$).
 - $\tilde{\nu} = 2170 \text{ cm}^{-1}$ (CO stretch vibration).
 - $E = 13.6 \text{ eV}$ (ionization energy of the hydrogen atom).
 - $E = 511 \text{ keV}$ (positron annihilation radiation).

Solution 10.1 In this exercise, we familiarize ourselves with the basic units used in spectroscopy. The use of different units in the various spectroscopic disciplines may seem confusing at first sight. However, depending on the range of the electromagnetic spectrum (Table 10.1), where transitions of atoms and molecules occur, some units are indeed more appropriate than others. In **subproblem (a)**, we give the relationships among energy, frequency, wavelength, and wave number. The

Table 10.1 The ranges of the electromagnetic spectrum

Range	Wavelength	Energy
Gamma rays	0–0.01 nm	124 keV–∞
X-rays	0.01–10 nm	124 eV–124 keV
Ultraviolet (UV)	10–380 nm	3.26–124 eV
Visible (Vis)	380–780 nm	1.59–3.26 eV
Infrared (IR)	780 nm–1 mm	1.24 meV–1.59 eV
Microwaves	1 mm–100 cm	1.24 μeV–1.24 meV
Radiowaves	100 cm–∞	0–1.24 μeV

relation between energy and frequency is established by:

$$E = h\nu \quad (10.20)$$

where $h = 6.62606957(29) \times 10^{-34}$ J s is the Planck constant (see Sect. A.1 in the appendix). The relation between frequency and wavelength is:

$$\lambda\nu = c \quad (10.21)$$

where $c = 299,792,458$ m s⁻¹ is the vacuum speed of light.³ Finally, the wave number is the reciprocal wavelength:

$$\tilde{\nu} = \frac{1}{\lambda}. \quad (10.22)$$

In **subproblem (b)**, we look at some instructive examples. The first example is the energy $E = 1$ eV, i.e., the kinetic energy, that a particle with charge e gains if it passes a potential difference of 1 V. This is the unit electron volt that is common in many spectroscopic disciplines. In SI units, this energy is $E = 1.60218 \times 10^{-19}$ J, and the frequency is:

$$\nu = \frac{E}{h} = 2.41799 \times 10^{14} \text{ Hz} \approx 242 \text{ THz.}$$

The wavelength is:

$$\lambda = \frac{c}{\nu} = 1.23984 \times 10^{-6} \text{ m} \approx 1.24 \mu\text{m} = 1240 \text{ nm.}$$

³In a dielectric medium with dielectric constant ϵ and permeability μ the speed of light is $\frac{c}{\sqrt{\epsilon\mu}}$.

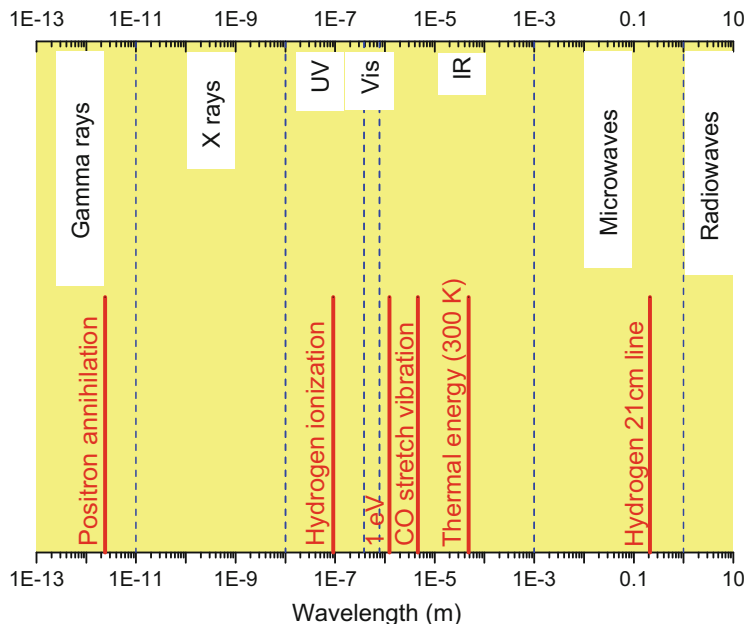


Fig. 10.5 Survey over the electromagnetic spectrum, classified according to the spectral ranges given in Table 10.1. Also indicated are the positions of characteristic spectroscopic transitions of Problem 10.1b

and the wave number is:

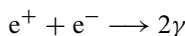
$$\tilde{\nu} = \frac{1}{\lambda} = 806,556 \text{ m}^{-1} = 8065.56 \text{ cm}^{-1}. \quad (10.23)$$

Note that it is more common to express the wave number in \$\text{cm}^{-1}\$ than in \$\text{m}^{-1}\$.

We assign these values to the infrared range (IR); more precisely, the near infrared (NIR) range, as also indicated in Fig. 10.5 along with the other examples of this subproblem. The second example is the hyperfine splitting of hydrogen with its characteristic transition at \$\lambda = 21 \text{ cm}\$, resulting from the *flipping* of the electron spin relative to the orientation of the nuclear spin. It is within the microwave spectral range of the electromagnetic spectrum. In radio astronomy the 21 cm line is key for the measurement of hydrogen in space. Conversion to wave number yields \$\tilde{\nu} = 0.0476 \text{ cm}^{-1}\$, an energy of \$E = 5.9 \mu\text{eV}\$, and a frequency of \$\nu = 1.4 \text{ GHz}\$. The third example is not related to a special transition, it is the thermal energy at room temperature,

$$E = k_B T = 1.38065 \times 10^{-23} \text{ J K}^{-1} \times 298.15 \text{ K} = 4.11641 \times 10^{-21} \text{ J} = 25.69 \text{ meV}.$$

To estimate if energy levels of atoms, molecules, or solids are populated at room temperature, comparison with this energy value is crucial (see Problem 9.15 at page 260). Room temperature thermal energy corresponds to a frequency of $\nu = 6.2 \times 10^{12} \text{ Hz}$, $\lambda = 48 \mu\text{m}$, and $\tilde{\nu} = 207 \text{ cm}^{-1}$. It is thus located in the IR spectral range, more precisely, the mid infrared (MIR). The fourth example is related to the excitation of the stretch vibration of the carbon monoxide molecule at $\tilde{\nu} = 2170 \text{ cm}^{-1}$. It is related to a wavelength $\lambda = 4.61 \mu\text{m}$, frequency $\nu = 6.51 \times 10^{13} \text{ Hz}$, and energy $E = 0.269 \text{ eV}$. This transition is thus also located in the mid infrared spectral range. In fact, IR spectroscopy is the key method for measuring vibrational transitions of molecules. The fifth example is the well-known ionization energy of atomic hydrogen, $E = 13.6 \text{ eV}$. Also known as Rydberg energy (see Eq. (9.22)), this energy is important in quantum chemistry. The corresponding frequency is $\nu = 3.29 \times 10^{15} \text{ Hz}$, the wavelength is $\lambda = 91.2 \text{ nm}$, and the wave number is⁴ $\tilde{\nu} = 109,691 \text{ cm}^{-1}$. The ionization energy of hydrogen is thus assigned to the ultraviolet spectral range. The last example is positron annihilation radiation, corresponding to the characteristic energy $E = 511 \text{ keV}$ in the gamma ray spectral range. The radiation is the result of the reaction:



producing two γ photons.⁵ The frequency of the photons is $\nu = 1.2 \times 10^{20} \text{ Hz}$, the wavelength is $\lambda = 0.0024 \text{ nm}$, and the wave number is $\tilde{\nu} = 4.12 \times 10^9 \text{ cm}^{-1}$. These are quite extreme values. Nevertheless, gamma spectroscopy has important applications: in medicine, positron emission tomography (PET) is used as an imaging technique for metabolic processes in the body. Möbbauer spectroscopy has important applications in geology and metrology.

Problem 10.2 (Doppler Broadening of Spectral Lines)

Apart from a natural line width, a significant source of the broadening of spectral lines of atoms and molecules in the gas phase is caused by the Doppler effect. Compared with the frequency ν_0 of an external electromagnetic wave seen by a molecule or atom at rest, the frequency changes to:

$$\nu = \nu_0 \left(1 + \frac{v_x}{c}\right) \quad (10.24)$$

where v_x is the velocity component of the atom or molecule in line with the wave field, and $v_x \ll c$ (see Fig. 10.6).

(continued)

⁴The exact result, determined using $E = 13.605693 \text{ eV}$ would be $109,737 \text{ cm}^{-1}$.

⁵Conservation of energy and momentum requires the generation of two photons. Each photon has the energy $E = m_e c^2 = 9.10938 \times 10^{-31} \text{ kg} \times (299,792,458 \text{ m s}^{-1})^2 \approx 511 \text{ keV}$.

Problem 10.2 (continued)

- a. Assume a Maxwell-Boltzmann velocity distribution of the gas particles and show that the Doppler effect causes a Gaussian line profile with half width

$$\Delta\nu = \frac{v_0}{c} \sqrt{\frac{8k_B T \ln 2}{m}} \quad (10.25)$$

where T is the temperature, and m the mass of the gas particles.

- b. Calculate the Doppler line width of the rovibrational transition ($J = 1, n = 0 \rightarrow J = 0, n = 1$) of carbon monoxide $^{12}\text{C}^{16}\text{O}$ found at $2,139.427\text{ cm}^{-1}$ at a temperature of 300 K.
 c. For a temperature of 300 and 430 K, calculate the Doppler line widths of the sodium D₁ and D₂ lines found at 508.332466 and 508.848717 THz respectively.

Solution 10.2 This problem deals with the broadening of spectral lines of gaseous particles. The problem is also related to the kinetic theory of gases in Chap. 7. Although every spectral line has a natural line width owing to the finite lifetime of an excited state (see Eq. (10.10)), there are other mechanisms that lead to a further broadening of a spectral line. Significant broadening may be caused by the Doppler effect due to the thermal movement of the gas particles.

In **subproblem (a)**, we investigate the effect on the line profile in detail and find a proof of Eq. (10.25). We consider the simplified arrangement shown in Fig. 10.6, which is typical for absorption spectroscopy of atoms or molecules in the gas phase. We assume a number density \mathcal{N}_{tot} and a transition of the molecules at a frequency ν_0 of arbitrary sharpness with an absorption cross section σ_0 . If we consider the fictive case in which all molecules in the gas cell were at rest, then, according to Eq. (10.4),

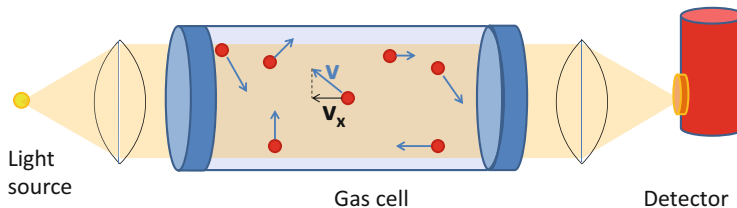


Fig. 10.6 Absorption spectroscopy probing atoms or molecules in a gas cell (schematic)

the optical depth would be a delta function centered around ν_0 :

$$\tau(\nu - \nu_0) = \mathcal{N}_{\text{tot}} \delta(\nu - \nu_0) \sigma_0 L. \quad (10.26)$$

L is the length of the gas cell and $\delta(\nu - \nu_0)$ is Dirac's delta function centered at the frequency ν_0 . The optical depth integrated over the whole frequency range, is:

$$\int_{-\infty}^{+\infty} \tau(\nu - \nu_0) d\nu = \mathcal{N}_{\text{tot}} \sigma_0 L \int_{-\infty}^{+\infty} \delta(\nu - \nu_0) d(\nu - \nu_0) \stackrel{\text{Eq. (A.52)}}{=} \mathcal{N}_{\text{tot}} \sigma_0 L. \quad (10.27)$$

Next, we take the motion of the molecules, which causes the Doppler effect, into account. If an emitter of a wave is in motion, the frequency of the wave is higher if the emitter moves toward the observer, and it is lower if the emitter goes in the opposite direction. Usually, textbooks show that this Doppler effect is a consequence of wave theory, but Eq. (10.24) can also be shown in a rigorous way in the photon picture of light, if we take into account the recoil of a photon emitting atom or molecule [1]. In absorption spectroscopy, however, the light source can be considered at rest, whereas the gas particle takes the role of the "observer". In this case, the same relation, Eq. (10.24) holds:

$$\nu = \nu_0 \left(1 + \frac{v_x}{c}\right) \quad (10.28)$$

Note that v_x is the velocity component of a certain molecule in line with the wave vector of the electromagnetic field. The fact that the field probes many molecules, each moving with a different velocity, is taken into account by assuming a Maxwell–Boltzmann distribution of the particle velocity. In Problem 7.1, we have seen that the velocity distribution for the velocity component in the x -direction is a normalized Gaussian distribution. Thus, the number density of particles with the velocity v_x is:

$$\mathcal{N}(v_x) = \mathcal{N}_{\text{tot}} \left(\frac{m}{2\pi k_B T} \right)^{\frac{1}{2}} \exp \left(-\frac{m}{2k_B T} v_x^2 \right) dv_x = \frac{\mathcal{N}_{\text{tot}}}{\sqrt{\pi} v_m} \exp \left(-\frac{v_x^2}{v_m^2} \right) dv_x \quad (10.29)$$

Here, we have introduced the *most probable* velocity v_m derived in Eq. (7.19). We annotate that:

$$\int_{-\infty}^{+\infty} \mathcal{N}(v_x) dv_x = \frac{\mathcal{N}_{\text{tot}}}{v_m \sqrt{\pi}} \int_{-\infty}^{+\infty} e^{-\frac{v_x^2}{v_m^2}} dv_x \stackrel{\text{Eq. (A.46)}}{=} \frac{\mathcal{N}_{\text{tot}}}{v_m \sqrt{\pi}} v_m \sqrt{\pi} = \mathcal{N}_{\text{tot}}. \quad (10.30)$$

The decisive step now is the transformation of this velocity distribution into a distribution of the number density as a function of resonance frequency. Dependent on v_x , the atom or molecule absorbs radiation at a slightly different frequency.

Solving Eq. (10.24) for v_x , we can make the following substitutions:

$$v_x = c \frac{v - v_0}{v_0} \quad (10.31)$$

and

$$dv_x = \frac{c}{v_0} d(v - v_0). \quad (10.32)$$

Equation (10.30) may be written as:

$$\int_{-\infty}^{+\infty} \mathcal{N}(v_x) dv_x = \int_{-\infty}^{+\infty} \underbrace{\mathcal{N}_{\text{tot}} \frac{c}{v_0 v_m \sqrt{\pi}} e^{-\left(\frac{c}{v_0 v_m}\right)^2 (v - v_0)^2} d(v - v_0)}_{\mathcal{N}(v - v_0)} \stackrel{\text{Eq. (A.46)}}{=} \mathcal{N}_{\text{tot}} \quad (10.33)$$

With the identified distribution function $\mathcal{N}(v - v_0)$ the optical depth analogous to Eq. (10.26) can be written:

$$\tau(v - v_0) = \mathcal{N}_{\text{tot}} \sigma_0 L \frac{c}{v_0 v_m \sqrt{\pi}} e^{-\left(\frac{c}{v_0 v_m}\right)^2 (v - v_0)^2} \quad (10.34)$$

In comparison with the last equation with the *normal distribution* Eq. (A.64) found in the appendix, we can identify its *standard deviation*

$$\sigma = \frac{v_m - v_0}{\sqrt{2}} \frac{c}{v_0 v_m}. \quad (10.35)$$

The half-width of the Doppler-broadened spectral line is thus obtained using Eq. (A.65), which relates the half-width to the standard deviation:

$$\delta v = 2\sigma \sqrt{2 \ln 2} = 2 \frac{v_0}{c} v_m \sqrt{\ln 2} \quad (10.36)$$

If we replace v_m using Eq. (7.19), we finally obtain Eq. (10.25), which was shown.

In **subproblem (b)**, we calculate the expected Doppler width for a special rovibrational transition of the CO molecule at room temperature at $\tilde{v}_0 = 2139.427 \text{ cm}^{-1}$. Using the relation between wave number and frequency, $\tilde{\nu} = \frac{v}{c}$, we obtain the expression for the Doppler width in wave numbers, which is:

$$\Delta \tilde{\nu} = \frac{\tilde{v}_0}{c} \sqrt{\frac{8k_B T \ln 2}{m}}. \quad (10.37)$$

Hence,

$$\sqrt{\frac{8k_B T \ln 2}{m}} = \sqrt{\frac{8 \times 1.38065 \times 10^{-23} \text{ J K}^{-1} \times 300 \text{ K} \times 0.69315}{28 \times 1.66059 \times 10^{-27} \text{ kg}}} = 70,284 \text{ cm s}^{-1}. \quad (10.38)$$

Therefore, the line width sought is:

$$\Delta\tilde{\nu} = \frac{2139.427 \text{ cm}^{-1}}{29,979,245,800 \text{ cm s}^{-1}} \times 70,284 \text{ cm s}^{-1} = 0.005 \text{ cm}^{-1}, \quad (10.39)$$

corresponding to $\Delta\nu = 48 \text{ MHz}$. This result is in fact close to the observed line width at a low pressure in the gas cell. Note that in typical undergraduate spectroscopy laboratories the resolution is usually not sufficient to determine this line width. In these cases, the observed line width is mostly determined by the spectrometer itself.

In **subproblem (c)**, we deal with another example, the well-known sodium D-line doublet in the visible part of the electromagnetic spectrum. From the periodic table in the appendix, we take the atomic mass of sodium, $22.99 m_u$. Thus,

$$\sqrt{\frac{8k_B T \ln 2}{m_{\text{Na}}}} = \begin{cases} 775.6 \text{ m s}^{-1}; T = 300 \text{ K} \\ 928.6 \text{ m s}^{-1}; T = 430 \text{ K} \end{cases} \quad (10.40)$$

Using Eq. (10.25) and the given transition frequencies 508.332466 THz (D₁ line) and 598.848717 THz (D₂ line) respectively we obtain the values for the Doppler width shown in Table 10.2. The values are within the GHz range and are thus much smaller than for the splitting of this doublet. Experimentally, both line profiles would have a shoulder because the *hyperfine structure splitting* of the Na 3^2S ground state of 1.772 GHz is close to the experimental line width. The hyperfine structure of the excited state, in contrast, is usually not resolved with simple absorption spectroscopy. Measuring line widths has interesting technical applications: for example, the temperature dependence of the Doppler width (Eq. (10.25)) opens up the possibility of determining the temperature of flames from a spectroscopic measurement.

Table 10.2 Doppler line width of sodium D lines

	300 K	430 K
$\Delta\nu(\text{D}_1)$	1.315 GHz	1.575 GHz
$\Delta\nu(\text{D}_2)$	1.316 GHz	1.576 GHz

Problem 10.3 (UV Absorption of Proteins)

In biochemical analytics, the concentration of polypeptides can be determined by measuring their ultraviolet absorption at a wave length of 280 nm. At this wave length, the extinction coefficients of the amino acids tryptophan (Trp), tyrosine (Tyr), and cysteine (Cys) are: $\epsilon_{\text{Trp}} = 5690 \text{ M}^{-1} \text{ cm}^{-1}$, $\epsilon_{\text{Tyr}} = 1280 \text{ M}^{-1} \text{ cm}^{-1}$, $\epsilon_{\text{Cys}} = 120 \text{ M}^{-1} \text{ cm}^{-1}$, respectively (S.C. Gill, P.H. von Hippel, Anal. Biochem. **182** (1989), 319; 1 M = 1 mol l^{-1}). According to the Lambert–Beer law, the absorbances A_i of these species are then given by:

$$A_i = \epsilon_i c_i L \quad (10.41)$$

where c_i is their concentration (unit: mol l^{-1}) and L the optical path length. Assume a path length of 1 cm.

- A sample containing the enzyme glutamate dehydrogenase containing 4 units of Trp, 18 units of Tyr, and 6 units of Cys absorbs 30% of the incoming radiation. Calculate the concentration of the enzyme.
- Oxytocin ($\text{C}_{43}\text{H}_{66}\text{N}_{12}\text{O}_{12}\text{S}_2$) contains 2 units of Cys and 1 unit of Tyr. What is the absorbance of a sample of 1 l solution containing 1 g oxytocin?

Solution 10.3 This exercise deals with a concrete application of optical absorption spectroscopy in chemical analytics. In Problem 9.13, we have dealt with the UV absorption of benzene due to electronic excitation of its system of π electrons. Amino acids with rings such as Trp and Tyr (see Fig. 10.7) absorb light within the ultraviolet spectral range at a wave length of 280 nm. Cysteine also weakly absorbs light at this wave length. As these molecules are found in the amino acid sequences of larger protein structures, their UV absorption can be used for a quantitative analysis. In **subproblem (a)**, we determine the concentration of glutamate dehydrogenase in a sample that absorbs 30% of the incoming light at a wave length of 280 nm. According to Eqs. (10.5) and (10.6), the absorbance is:

$$A = -\log_{10} \frac{I}{I_0} = -\log_{10} \frac{1 - 0.3}{1} = 0.155 \quad (10.42)$$

At least at low concentrations⁶, this total absorbance can be taken as the sum of the absorbances of the three active subunits Cys, Trp, and Tyr:

$$A = \sum_i A_i = L \sum_i \epsilon_i c_i \quad (10.43)$$

⁶At high concentrations the effects of scattering including multiple scattering events need to be taken into account.

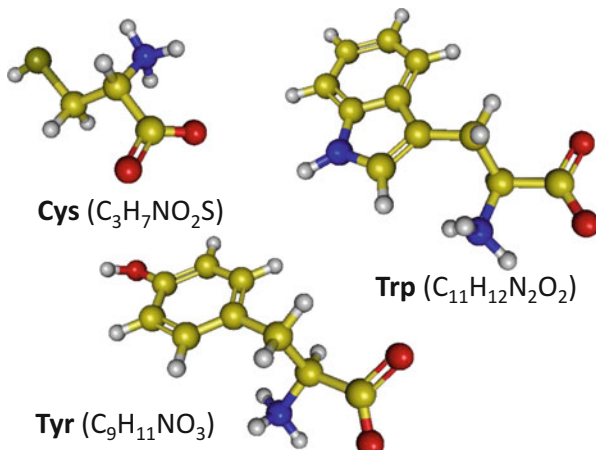


Fig. 10.7 Molecular structure of the three amino acids cysteine (Cys), tyrosine (Tyr), and tryptophan (Trp)

If $z_{\text{Cys}} = 6$, $z_{\text{Tyr}} = 18$, and $z_{\text{Trp}} = 4$ are the numbers of Cys, Tyr, and Trp units in glutamate dehydrogenase and c is the sought concentration of this enzyme, we have

$$A = Lc \sum_i \epsilon_i z_i \quad (10.44)$$

and thus

$$\begin{aligned} c &= \frac{A}{L \sum_i \epsilon_i z_i} = \frac{0.155}{1 \text{ cm} (4 \times 5690 + 18 \times 1280 + 6 \times 120) \text{ M}^{-1} \text{ cm}^{-1}} \\ &= 3.33 \times 10^{-6} \text{ M}. \end{aligned} \quad (10.45)$$

In **subproblem (b)**, the absorbance of a sample of 1 g oxytocin in 11 solution is calculated. Thus, we must determine the molar mass of this molecule. From the formula $C_{43}H_{66}N_{12}O_{12}S_2$, we obtain the molar mass $M = 1007 \text{ g mol}^{-1}$. Thus, the concentration of the sample is $c = 9.9 \times 10^{-4} \text{ M}$. As the molecule contains 2 units of Cys and 1 unit of Tyr, the sought absorbance of a sample is:

$$\begin{aligned} A &= Lc (2\epsilon_{\text{Cys}} + \epsilon_{\text{Tyr}}) = 1 \text{ cm} \times 9.9 \times 10^{-4} \text{ M} (2 \times 120 + 1280) \text{ M}^{-1} \text{ cm}^{-1} \\ &= 1.5, \end{aligned} \quad (10.46)$$

which is a large value. The transmitted intensity would be only $I = I_0 10^{-1.5} = 0.03 I_0$.

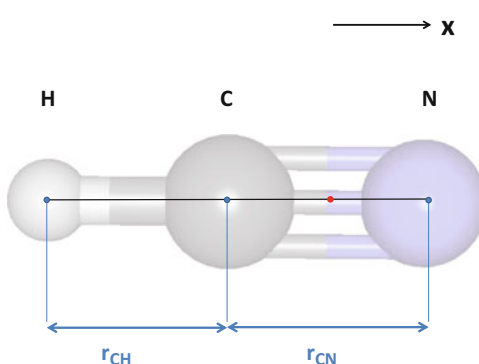
Problem 10.4 (HCN Molecular Structure)

By means of microwave spectroscopy, the following rotational constants for various isotopomers of the linear HCN molecule were determined (E.F. Pearson et al., Z. Naturforsch. **31a** (1976), 1394): $\text{H}^{13}\text{C}^{14}\text{N}$: $B_0 = 43170.140\text{ MHz}$; $\text{H}^{12}\text{C}^{14}\text{N}$: $B_0 = 44315.9757\text{ MHz}$.

- Find expressions for the positions of the atomic cores with regard to the molecule's center of mass.
- Find an expression for the moment of inertia in the center of mass frame of reference that depends only on the nuclear masses and the bond length r_{CN} and r_{CH} .
- Provided that the Born-Oppenheimer approximation is valid for the ground state of HCN, the bond lengths are not affected by different isotopic masses. Determine the bond lengths in the HCN ground state. *Hint: use an iterative procedure or mathematical software to solve the system of equations.*

Solution 10.4 In this problem, we deal with the structure determination of a linear triatomic molecule: HCN (Fig. 10.8). The goal is to determine the bond lengths of the C-H and the C-N bond by the measurement of the rotational constants from at least two different isotopomers. These have different nuclear masses, but it can be expected that the bond lengths, which are only determined by electronic structure,⁷ are the same. This is a consequence of the Born-Oppenheimer approximation, according to which the total wave function of a molecule (electronic and nuclear degrees of freedom) can be separated into a nuclear part and an electronic part.

Fig. 10.8 The linear structure of the HCN molecule. The center of mass, indicated by the red dot, is along the C-N bond



⁷See Problem 9.18 dealing with chemical bonding in the simplest possible molecular system, the H_2^+ molecule ion.

In **subproblem (a)** we begin by searching expressions for the positions of the three nuclei in the center of mass frame of reference. Note that for different isotopomers the center of mass is at different positions on the molecular axis of symmetry. We need them to form the moments of inertia, which in turn are related to the rotational constants (see Eq. (10.12)). The center of mass, indicated as a dot in Fig. 10.8, lies between the heavier carbon and nitrogen cores. It is thus reasonable to tentatively set the origin at the carbon site. This choice sets $\tilde{x}_C = 0$, $\tilde{x}_N = r_{CN}$, $\tilde{x}_H = -r_{CH}$. The position of the center of mass in this system is:

$$\tilde{x}_{COM} = \frac{m_H \tilde{x}_H + m_C \tilde{x}_C + m_N \tilde{x}_N}{M} = \frac{m_N r_{CN} - m_H r_{CH}}{M}$$

where $M = m_H + m_C + m_N$ is the total mass of the molecule. In the new frame of reference centered at the molecular center of mass, the positions of the atoms are thus:

$$x_H = -\frac{m_N r_{CN} - m_H r_{CH}}{M} - r_{CH} = x_C - r_{CH} \quad (10.47)$$

$$x_C = -\frac{m_N r_{CN} - m_H r_{CH}}{M} \quad (10.48)$$

$$x_N = -\frac{m_N r_{CN} - m_H r_{CH}}{M} + r_{CN} = x_C + r_{CN} \quad (10.49)$$

In **subproblem (b)**, we write down the moment of inertia in the center of mass frame of reference. The moments of inertia of the molecule are $I_{xx} = 0$, $I_{yy} = I_{zz} = I$ where

$$I = m_N (r_{CN} + x_C)^2 + m_C x_C^2 + m_H (x_C - r_{CH})^2 \quad (10.50)$$

The goal is to write this as an expression that contains only the known masses of the nuclei and the bond lengths r_{CH} and r_{CN} . Using Eq. (10.48), we substitute the position of the carbon, x_C . After some algebra, we obtain:

$$I = \left(m_N - \frac{m_N^2}{M} \right) r_{CN}^2 + \left(m_H - \frac{m_H^2}{M} \right) r_{CH}^2 + \frac{2m_N m_H}{M} r_{CN} r_{CH} \quad (10.51)$$

This equation gives the relation of the moment of inertia with the bond lengths and the masses. On the other hand, I is related to the rotational constant:

$$I = \frac{\hbar}{8\pi^2 B_0} \quad (10.52)$$

With two different rotational constants for two different sets of nuclear masses, we have two equations for the two unknown bond lengths:

$$I_1 = A_1 r_{\text{CN}}^2 + B_1 r_{\text{CH}}^2 + C_1 r_{\text{CN}} r_{\text{CH}} \quad (10.53)$$

$$I_2 = A_2 r_{\text{CN}}^2 + B_2 r_{\text{CH}}^2 + C_2 r_{\text{CN}} r_{\text{CH}} \quad (10.54)$$

where $A_i = \left(m_{\text{N},i} - \frac{m_{\text{N},i}^2}{M_i}\right)$, $B_i = \left(m_{\text{H},i} - \frac{m_{\text{H},i}^2}{M_i}\right)$, and $C_i = \frac{2m_{\text{N},i}m_{\text{H},i}}{M_i}$, $i = 1, 2$ are *effective masses*.

Unfortunately, these equations are not linear in the bond lengths. Thus, we have to seek the solutions numerically. This is tackled in **subproblem (c)**. In the appendix, Sect. A.3.19, Newton's method for the solution of a nonlinear system of equations is described. A computer code is easily set up that implements Newton's method for this problem. The output from such a computer code is shown below. Starting from a reasonable initial guess of the bond lengths of 1 Å for both bonds, Newton's method converges within about 10 iterations toward $r_{\text{CN}} = 1.1569$ Å and $r_{\text{CH}} = 1.0689$ Å. As can be seen in the output, the exchange of ^{12}C with ^{13}C changes the nuclei's positions relative to the center of mass by about 0.02 Å. The calculation is for a perfectly rigid rotator. Even in the vibrational ground state, however, a slight correction of the rotational constants originating from rotation vibration coupling is present. Such corrections are considered in Problem 10.7. As shown there, these corrections change the bond lengths obtained to the order of 10^{-3} Å.

Newton's iterative method output

```

HCN molecule bond length fit from rotational constants
-----
Set 1 of parameters
Mass hydrogen (AMU) = 1
Mass carbon (AMU) = 12
Mass nitrogen (AMU) = 14
Rotational constant CONSTANT (MHz): 44,315.975700000003

Set 2 OF parameters
Mass hydrogen (AMU) = 1
Mass carbon (AMU) = 13
Mass nitrogen (AMU) = 14
Rotational constant (MHz): 43,170.139999999999

First guess for C-H bond length: 1.0000000000000000
First guess for C-N bond length: 1.0000000000000000

-----  

Iteration   RCN           RCH           change  

  1  1.0000000000000000  1.0000000000000000  0.70619656180318990  

  2  1.1693171526360502  1.6855984872546519  0.45107329962153475  

  3  1.1619308212493202  1.2345856673258784  0.13531172982914874  

  4  1.1572904709386174  1.0993535284743816  2.35462763144434587E-002  

  5  1.1568804427643493  1.0758108224877616  5.0490108282347035E-003  

  6  1.1568658506399643  1.0707618327458888  1.3471014543344922E-003  

  7  1.1568650954812927  1.0694147315032179  3.7060871846898122E-004  

  8  1.1568650406800285  1.0690441227888006  1.0248400700867961E-004  

  9  1.1568650365173896  1.0689416387818764  2.8377157568438860E-005  

  10 1.1568650361987829  1.0689132616243098  7.8602836566623653E-006  

  11 1.1568650361743491  1.0689054013406531  2.1774629146439651E-006  

  17 1.1568650361723185  1.0689023908752948  3.5529568176428938E-009

-----  

RESULT:  

-----  

Bond length C-H (angstrom): 1.0689023908752948  

Bond length C-N (angstrom): 1.1568650361723185

-----  

Positions of nuclei (center of mass frame of reference)
-----  

Set      Hydrogen          Carbon          Nitrogen  

  1  -1.6291693581174120  -0.56026696724211722  0.59659806893020129  

  2  -1.6091598235730507  -0.54025743269775583  0.61660760347456267

-----  

Moments of inertia
-----  

Set 1: I= 11.403991274338289    AMU angstrom**2  

Set 2: I= 11.706679667685872    AMU angstrom**2

-----  

Derived rotational constants
-----  

Set 1: I= 44315.975682761506    MHz, deviation: -1.7238496027971451E-005 MHz  

Set 2: I= 43170.139983842339    MHz, deviation: -1.6157661917759469E-005 MHz

```

Looking back on our solution, we have gained an insight into the structure determination of a rigid linear polyatomic molecule based on rotational constants of isotopomers. Owing to different nuclear masses, these isotopomers have different moments of inertia, but identical bond lengths. In fact, isotopic substitution is an often applied method in spectroscopy (see also Problem 10.6). To obtain results we had to resort to a numerical solution. It is worth drawing attention to the problems arising if more complex molecules are investigated: (1) the more complex case of nonlinear molecules is dealt with in Problem 10.5. (2) The case of polyatomic molecules with more than just three nuclear sites can indeed be tackled by systematic isotopic substitution to increase experimental data sets. This case, however, involves another problem: such molecules are more flexible, i.e., they appear in different conformations. In addition, nonrigid or *floppy* molecules

change their structure depending on their rotational state, which makes the correct interpretation of rotation or rotation-vibration spectra very puzzling.

Problem 10.5 (Asymmetric Top Rotation Spectra)

The water molecule (H_2^{16}O) is an asymmetric top molecule. Its bond length is $r_{\text{OH}} = 0.9584 \text{ \AA}$, the angle enclosed by the OH bonds is 104.45° .

- Determine the center of mass of the molecule, its moments of inertia, and its rotational constants A , B , and C . By convention, the rotational constants are named according to $A \geq B \geq C$.
- Consider the asymmetry parameter

$$\kappa = \frac{2B - A - C}{A - C} \quad (10.55)$$

ranging from -1 to $+1$. A value of $\kappa = -1$ would indicate the limiting case of prolate symmetric top molecule; a value of $+1$, in contrast, would indicate the case of an oblate symmetric top. Calculate the asymmetry parameter for water.

- Energy levels of the rotational states of asymmetric tops can be written in the form:

$$E(J\tau) = \frac{1}{2}(A + C)J(J + 1) + \frac{1}{2}(A - C)E_{J\tau}(\kappa) \quad (10.56)$$

where J is the rotational quantum number and $\tau = -J, \dots, +J$ is an index. Note that in this notation energy levels are expressed in frequency units of Hertz. The function $E_{J\tau}(\kappa)$ is found in Table 10.3. Calculate the energy levels of the H_2O molecule for $J = 1, 2$. Also, calculate the energy levels of water by treating the molecule formally as an prolate or an oblate symmetric top molecule. Plot the energy levels in a term diagram. Can you explain the special labeling of asymmetric top rotator states $J_{K_a K_c}$ in Table 10.3?

- With which axis of inertia does the permanent electric dipole moment of the H_2O molecule coincide? For transitions between pure rotational energy levels the following selection rules hold for the H_2O molecule: $\Delta J = 0, \pm 1$, $\Delta K_a = \pm 1, \pm 3$, $\Delta K_c = \mp 1, \mp 3$. Based on your results from subproblem (c), determine the possible allowed transitions and the frequency at which they occur.

Solution 10.5 This exercise deals with the rotational energy levels of symmetric and asymmetric top molecules. We familiarize ourselves with the quantum numbers involved in the description of their rotational states, and the special treatment of

Table 10.3 Algebraic relations for asymmetric rotor energy levels according to H.W. Kroto, *Molecular Rotation Spectra*, Wiley, London, 1975

$J_{K_a K_c}$	τ	$E_{J\tau}(\kappa)$
0 ₀₀	0	0
1 ₁₀	-1	$\kappa + 1$
1 ₁₁	0	0
1 ₀₁	+1	$\kappa - 1$
2 ₂₀	-2	$2(\kappa + \sqrt{\kappa^2 + 3})$
2 ₂₁	-1	$\kappa + 3$
2 ₁₁	0	4κ
2 ₁₂	+1	$\kappa - 3$
2 ₀₂	+2	$2(\kappa - \sqrt{\kappa^2 + 3})$

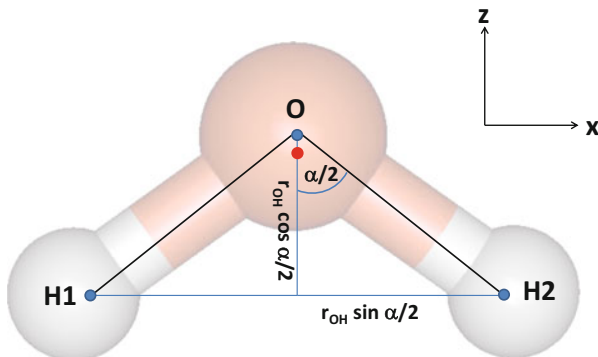


Fig. 10.9 The water molecule

asymmetric top rigid rotators. Although the rotation spectra of diatomics are quite regular, it is complicated to interpret the asymmetric top rotational spectra. The water molecule is perhaps the most prominent example of an asymmetric rotor with a well-known geometry.

In subproblem (a), we determine the moments of inertia and the three rotational constants of the molecule. Given the OH bond length r_{OH} and the angle between the OH bonds α , we must first seek the center of mass. The situation is shown in Fig. 10.9. We are free to select the orientation of the molecule and tentatively place the oxygen atom in the origin at (0,0,0). Then, the coordinates of the hydrogen atoms H₁ and H₂ be $\mathbf{r}_{\text{H}_1} = (-r_{\text{OH}} \sin \frac{\alpha}{2}, 0, -r_{\text{OH}} \cos \frac{\alpha}{2})$ and $\mathbf{r}_{\text{H}_2} = (+r_{\text{OH}} \sin \frac{\alpha}{2}, 0, -r_{\text{OH}} \cos \frac{\alpha}{2})$ respectively. The center of mass is generally defined

$$\mathbf{r}_{\text{COM}} = \frac{\sum_i m_i \mathbf{r}_i}{\sum_i m_i} \quad (10.57)$$

where m_i are the masses of the atoms at position \mathbf{r}_i . The oxygen has an atomic weight of $m_O = 16$ amu; both hydrogens have a mass of 1 amu. Thus,

$$\mathbf{r}_{\text{COM}} = \frac{1}{18} \begin{pmatrix} 0 \\ 0 \\ -2r_{\text{OH}} \cos \frac{\alpha}{2} \end{pmatrix} = \frac{1}{9} \begin{pmatrix} 0 \\ 0 \\ -r_{\text{OH}} \cos \frac{\alpha}{2} \end{pmatrix} \quad (10.58)$$

The center of mass is thus 0.065 \AA displaced from the oxygen center in a negative z -direction toward the hydrogens (red point in Fig. 10.9). Relative to the center of mass, the oxygen is at position $\mathbf{r}_O = (0, 0, \frac{1}{9}r_{\text{OH}} \cos \frac{\alpha}{2})$, whereas the hydrogens take the positions $\mathbf{r}_{H1} = (-r_{\text{OH}} \sin \frac{\alpha}{2}, 0, -\frac{8}{9}r_{\text{OH}} \cos \frac{\alpha}{2})$ and $\mathbf{r}_{H2} = (+r_{\text{OH}} \sin \frac{\alpha}{2}, 0, -\frac{8}{9}r_{\text{OH}} \cos \frac{\alpha}{2})$ respectively. With these coordinates, we are ready to write down the moment of inertia tensor. The general definition is

$$\mathbf{I} = \sum_i m_i \begin{pmatrix} y_i^2 + z_i^2 & -x_i y_i & -x_i z_i \\ -y_i x_i & x_i^2 + z_i^2 & -y_i z_i \\ -z_i x_i & -z_i y_i & x_i^2 + y_i^2 \end{pmatrix} \quad (10.59)$$

As our choice of coordinates was such that the coordinate axes already coincide with the principal axes of inertia, the off-diagonal elements are all zero. The diagonal elements need to be calculated. For I_{xx} we obtain:

$$I_{xx} = 16 \text{ amu} \left(\frac{r_{\text{OH}}}{9} \cos \frac{\alpha}{2} \right)^2 + 2 \text{ amu} \left(\frac{8r_{\text{OH}}}{9} \cos \frac{\alpha}{2} \right)^2 = \left(\frac{4r_{\text{OH}}}{3} \cos \frac{\alpha}{2} \right)^2 \text{ amu} \quad (10.60)$$

and thus⁸ $I_{xx} = 1.0175 \times 10^{-47} \text{ kg m}^2$. The second principal moment is:

$$I_{yy} = 16 \text{ amu} \left(\frac{r_{\text{OH}}}{9} \cos \frac{\alpha}{2} \right)^2 + 2 \text{ amu} \left[\left(r_{\text{OH}} \sin \frac{\alpha}{2} \right)^2 + \left(\frac{8r_{\text{OH}}}{9} \cos \frac{\alpha}{2} \right)^2 \right] \quad (10.61)$$

or $I_{yy} = 2.9232 \times 10^{-47} \text{ kg m}^2$. The third principal moment is:

$$I_{zz} = 2 \text{ amu} \left(r_{\text{OH}} \sin \frac{\alpha}{2} \right)^2 = 1.9059 \times 10^{-47} \text{ kg m}^2. \quad (10.62)$$

With these results, we can calculate the three rotational constants:

$$A = \frac{h}{8\pi^2 I_{xx}} = 824,768 \text{ MHz} \quad (10.63)$$

⁸1 amu = $1.66054 \times 10^{-27} \text{ kg}$.

$$B = \frac{\hbar}{8\pi^2 I_{zz}} = 440,318 \text{ MHz} \quad (10.64)$$

$$C = \frac{\hbar}{8\pi^2 I_{yy}} = 287,083 \text{ MHz} \quad (10.65)$$

The constants are ordered according to $A \geq B \geq C$. In **subproblem (b)** we determine the asymmetry parameter κ defined in Eq. (10.55). This parameter is highly useful for the interpretation of asymmetric top rotation spectra. By insertion of the values for A , B , and C we obtain a value of $\kappa = -0.4300$. In the limiting case in which two of the three moments of inertia are identical, the molecule becomes a **symmetric top** molecule. One distinguishes between more cigar-shaped *prolate* symmetric tops with $A > B = C$ and more disk-shaped *oblate* symmetric tops with $A = B > C$ respectively. The energy levels of symmetric top rigid rotators are found in the textbooks:

$$E_{JK} = \frac{\hbar^2}{2I_b} J(J+1) + K^2 \hbar^2 \left(\frac{1}{2I_a} - \frac{1}{2I_b} \right) \quad \text{prolate} \quad (10.66)$$

$$E_{JK} = \frac{\hbar^2}{2I_b} J(J+1) + K^2 \hbar^2 \left(\frac{1}{2I_c} - \frac{1}{2I_b} \right) \quad \text{oblate} \quad (10.67)$$

If the energy levels are expressed as a frequency in Hertz, these expressions simply read:

$$E_{JK} = BJ(J+1) + K^2(A - B) \quad \text{prolate, } B = C \quad (10.68)$$

and

$$E_{JK} = BJ(J+1) + K^2(C - B) \quad \text{prolate, } A = B \quad (10.69)$$

Compared with the treatment of the diatomic rigid rotator, a new quantum number, $K = 0, \pm 1, \dots, \pm J$ occurs. The energy levels are degenerated because of the K^2 dependence. The wave functions for the symmetric top rotator are the *Wigner rotation functions* $D_{MK}^J(\theta, \phi, \psi)$. They are generalized spherical harmonics depending on the three *Euler angles* describing the orientation of a molecule in space [2]. Although the symmetric top rigid rotator problem can be treated exactly in a straightforward fashion, the asymmetric rotor problem is tedious, although analytic expressions for the energy levels exist. They can be found if for a given quantum number J the wave function is written as a series over all possible Wigner functions:

$$\Psi_{JM} = \sum_{K=-J}^J c_K D_{MK}^J \quad (10.70)$$

The resulting expressions for $J = 0, 1, 2$ are given in the text of **subproblem (c)** (Eq. (10.56) and Table 10.3). It is our task to calculate these first rotational levels for the water molecule. Like the quantum number K in the symmetric top case, there

is an index $\tau = -J, \dots, +J$ for the $(2J + 1)$ energy levels. The case $J = 0$ is trivial; we find $E(0, 0) = 0$. Starting with $J = 1$, we take Eq. (10.56) and pick the appropriate function $E_{1,-1}(\kappa)$ from Table 10.3. Looking at the definition of the asymmetry parameter κ we notice that simplifications are possible:

$$E(1, -1) = \frac{1}{2}(A+C)2 + \frac{1}{2}(A-C) \left(\frac{2B-A-C}{(A-C)} + 1 \right) = A+B = 1265,086 \text{ MHz} \quad (10.71)$$

In a similar fashion, we obtain:

$$E(1, 0) = \frac{1}{2}(A+C)2 = A+C = 1111,851 \text{ MHz} \quad (10.72)$$

and

$$E(1, +1) = \frac{1}{2}(A+C)2 + \frac{1}{2}(A-C) \left(\frac{2B-A-C}{(A-C)} - 1 \right) = A+B = 727,401 \text{ MHz} \quad (10.73)$$

For $J = 2$, we can simplify the expressions for $\tau = -1, 0, 2$ in an analogous way and obtain:

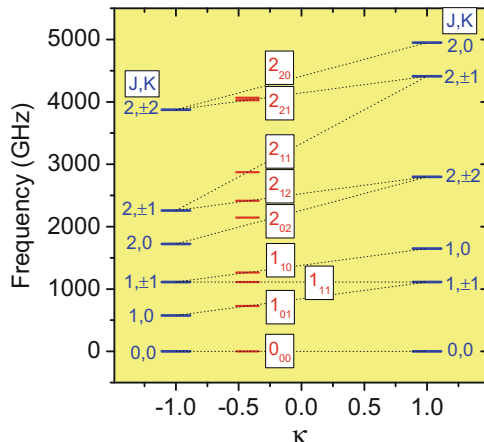
$$E(2, -1) = 4A + B + C = 4,026,473 \text{ MHz} \quad (10.74)$$

$$E(2, 0) = A + 4B + C = 2,873,123 \text{ MHz} \quad (10.75)$$

$$E(2, +1) = A + B + 4C = 2,413,418 \text{ MHz} \quad (10.76)$$

The cases $J = 2, \tau = \pm 2$ are more complicated. The expression from Table 10.3 is $E_{2,\pm 2}(\kappa) = 2 \left(\kappa \pm \sqrt{\kappa^2 + 3} \right)$ and by insertion of the proper value of κ the results are $E(2, -2) = 4,063,909 \text{ MHz}$ and $E(2, +2) = 2,144,767 \text{ MHz}$. As requested, we plot all these values in a term diagram, which is depicted in Fig. 10.10 (red levels). The labeling of the various levels is in accordance with the first column of Table 10.3, in the form J_{K_a, K_c} . At first sight, this notation seems to be quite opaque. In the rest of this exercise we try to obtain a deeper understanding of this notation, which is common in the literature. Therefore, we formally treat the water molecule as a symmetric top rigid rotator and determine the energy levels. We start with the prolate case ($\kappa = -1$), in which the rotational constants B and C are identical. We use Eq. (10.68) to calculate the energy levels for $J = 0, 1, 2$ and the possible values for the quantum number K . The results are depicted in Fig. 10.10 on the left-hand side at $\kappa = -1$. Next, we consider the oblate case ($\kappa = +1, B = A$) and proceed in an analogous way. In the term diagram, these energy levels are shown on the right-hand side at $\kappa = +1$. A close look at the dashed lines connecting certain prolate and oblate energy levels reveals the meaning of the special labeling of asymmetric top rotator states plotted at the appropriate $\kappa = -0.43$. Consider, for example, the asymmetric top level 2_{12} . It is exactly on the intersection line between the prolate $2, \pm 1$ state and the oblate $2, \pm 2$ state. Most

Fig. 10.10 Correlation diagram of the first H_2^{16}O rotational levels (red lines). The special labeling of the levels is in accordance with Table 10.3. Also shown are the energy levels for water treated formally as a prolate symmetric top ($\kappa = -1$, rotational constant $B = C$), and as an oblate symmetric top ($\kappa = +1$, rotational constant $B = A$)



of the levels match with an appropriate intersection line.⁹ Figure 10.10 is called a **correlation diagram**. It reveals the location of energy levels of the water molecule if the asymmetry parameter κ changes between the limiting cases -1 (prolate) to $+1$ (oblate). Although the numbers K are only quantum numbers for these limiting cases of symmetric top rotors, they are also used as projection quantum numbers in the case of an asymmetric top rotator.

The irregularity in the asymmetric top energy levels clearly complicates the rotation spectra. In **subproblem (d)**, we focus on possible transitions between the energy levels. The selection rules for asymmetric top molecules are generally complicated. They depend on the direction of the dipole moment. In our case of the H_2O molecule, the direction of the permanent dipole moment coincides with the symmetry axis of the molecule, i.e., the z -axis in Fig. 10.9. This is because the neutral molecule has a negative partial charge at the oxygen end, and a positive partial charge at the hydrogen end. As the z -axis is also the b -axis of inertia, the selection rules for so-called *b-type transitions* hold. These are:

$$\Delta J = 0, \pm 1, \quad \Delta K_a = \pm 1, \pm 3, \quad \Delta K_c = \mp 1, \mp 3 \quad (10.77)$$

where K_a is the projection quantum number on the limiting case of a prolate symmetric top, and K_b the projection quantum number on the oblate symmetric top. Transitions between $J = 0$ and $J = 1$ are apparently forbidden. Only two transitions are possible:

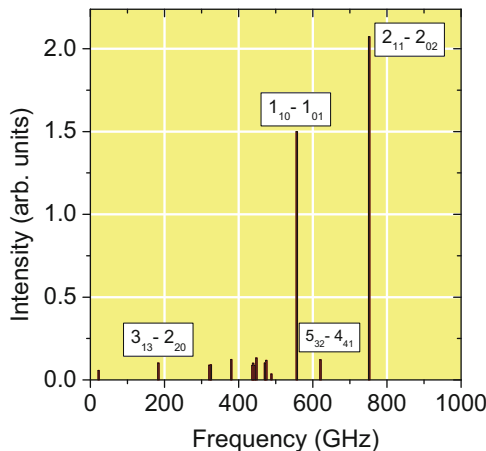
$$1_{10} \leftrightarrow 1_{01} : \Delta E = (12,365,086 - 727,401) \text{ MHz} = 537,685 \text{ MHz}$$

and

$$2_{11} \leftrightarrow 2_{02} : \Delta E = (2,873,123 - 2,144,767) \text{ MHz} = 728,356 \text{ MHz}$$

⁹The deviations are due to the fact that the intersection lines have a curvature.

Fig. 10.11 Microwave pure rotational stick spectrum of H_2^{16}O according to data taken from F.C. de Lucia, P. Helminger, W.H. Kirchhoff, *Microwave spectra of molecules of astrophysical interest V: water vapor, J. Phys. Chem. Ref. Data, 2 (1974), 211*



Note that because of the irregular spacing between the rotational transitions; transitions from higher excited molecules ($J > 2$) certainly agglomerate in the vicinity of these two transitions. This complicates the interpretation of microwave spectra. Useful for the assignment of transitions is the fact that states with higher J have a lower occupation probability because of the Boltzmann statistics. Therefore, transitions from these states have a lower intensity in the microwave spectrum. Such a spectrum is shown in Fig. 10.11. Note the transition with the lowest frequency at 22.2 GHz. It is the $6_{16} \leftrightarrow 5_{23}$ transition. The frequency of many kitchen microwave ovens is aligned with this transition.

Problem 10.6 (IR Spectra of Diatomics I)

- ${}^1\text{H}^{35}\text{Cl}$ has an infrared transition at $2,991 \text{ cm}^{-1}$ assigned to the stretching vibration of this diatomic molecule. For the homonuclear diatomics such as H_2 or Cl_2 no infrared active transition is observed. Why?
- Calculate the force constant k of ${}^1\text{H}^{35}\text{Cl}$ in the approximation of the harmonic oscillator.
- Calculate the wave number of the infrared transition if hydrogen is replaced by deuterium.
- The potential between H and Cl is essentially anharmonic. A frequently used model for the anharmonic oscillator is the Morse potential

$$V(r) = D_e \left[1 - e^{-a(r-R_e)} \right]^2 \quad (10.78)$$

and the energy states of the Morse oscillator are given by:

(continued)

Problem 10.6 (continued)

$$E_n = h\nu \left(n + \frac{1}{2} \right) - \frac{(h\nu)^2}{4D_e} \left(n + \frac{1}{2} \right)^2 \quad (10.79)$$

where ν is the frequency of the stretch mode, $D_e = 7.41 \times 10^{-19}$ J is the depth of the potential, and $R_e = 1.275$ Å is its minimum. For the parameter a describing the steepness of the potential the following relation holds:

$$a = \sqrt{\frac{k}{2D_e}} \quad (10.80)$$

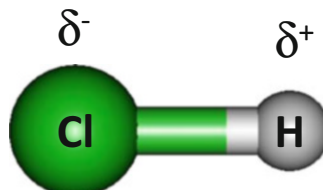
How many vibrational states has the HCl molecule?

- e. An anharmonic oscillator allows overtone transitions. Calculate the wave number of the transition $n = 0 \rightarrow 2$. At which wave number would the *hot band* $n = 1 \rightarrow 2$ be observed? On the basis of occupation probabilities, judge if the hot band is observed at $T = 300$ K.

Solution 10.6 Hydrogen chloride (Fig. 10.12) is a heteronuclear diatomic molecule. Chlorine is more electronegative and causes an accumulation of electronic charge density δ^- at its atomic site, and a depletion of charge density at the hydrogen site. This causes a static electric dipole moment of the molecule and, in addition, a **polar bond**. For this reason, a harmonic variation of the bond length causes an **induced electric dipole moment** which may couple to the oscillating electric field of an electromagnetic wave. As a consequence, the H-Cl stretch mode is infrared active and the transition is observed at $\tilde{\nu} = 2991$ cm $^{-1}$.

In **subproblem (a)**, we explain why analogous transitions are not observed for the homonuclear diatomics H₂ and Cl₂. For symmetry reasons, it is obvious that these molecules do not carry partial charges at their atomic sites and their atomic bonds are not polar. Therefore, no induced dipole moment is involved with the harmonic variation of their bond lengths. Hence, their stretch modes do not couple to the external electrical field of an electromagnetic wave and these modes are infrared inactive.

Fig. 10.12 The heteronuclear diatomic HCl



In **subproblem (b)**, we treat the stretching mode of the HCl molecule within the approximation of the harmonic oscillator and calculate the force constant k associated with the bond. Using Eq. (10.16), the force constant is:

$$k = \mu (2\pi\nu)^2 = \mu (2\pi\tilde{\nu}c)^2 \quad (10.81)$$

For the HCl molecule, the effective mass is thus:

$$\mu_{\text{HCl}} = \frac{\mu_{\text{H}}\mu_{\text{Cl}}}{\mu_{\text{H}} + \mu_{\text{Cl}}} = \frac{35}{36} \times 1.66054 \times 10^{-27} \text{ kg} = 1.61441 \times 10^{-27} \text{ kg}. \quad (10.82)$$

Hence, the force constant sought is

$$\begin{aligned} k &= 1.61441 \times 10^{-27} \text{ kg} (2\pi \times 2991 \text{ cm}^{-1} \times 2.997925 \times 10^{10} \text{ cm s}^{-1})^2 \\ &= 512.4424 \text{ kg s}^{-2} \approx 512 \text{ N m}^{-1}. \end{aligned}$$

The wave number of a vibrational transition depends on the effective mass. It is common practice in vibrational spectroscopy to change the isotopes of certain atomic species to obtain additional information about the molecular structure and dynamics.

In **subproblem (c)**, we determine the wave number of the stretch vibration if hydrogen is replaced by deuterium. Note that this does not notably change the electronic structure of the molecule. Thus, the value of the force constant k is not affected by this replacement. Again using Eq. (10.16), we can write:

$$\frac{\nu_{\text{DCI}}}{\nu_{\text{HCl}}} = \sqrt{\frac{\mu_{\text{HCl}}}{\mu_{\text{DCI}}}} \quad (10.83)$$

The effective mass for DCl is (Eq. (10.82)) $\mu_{\text{DCI}} = \frac{2 \times 35}{37} m_u$. Taking the effective masses for both isotopomers and the relation between frequency and wave number ($\tilde{\nu} = \frac{\nu}{c}$), we obtain:

$$\frac{\tilde{\nu}_{\text{DCI}}}{\tilde{\nu}_{\text{HCl}}} = 0.717 \quad (10.84)$$

Thus, the stretch mode of DCl is expected at:

$$\tilde{\nu}_{\text{DCI}} = 0.717 \times 2991 \text{ cm}^{-1} = 2145 \text{ cm}^{-1}.$$

In **subproblem (d)**, we take anharmonicity into account and deal with the number of vibrational states in the HCl molecule. When reading the problem text for the first time we get stuck and ask ourselves what this means: the *number* of vibrational states. We must be aware that, depending on the shape of the potential, a quantum system may have a finite number of discrete bound states. Although for example

the particle in a box with infinite walls and also the harmonic oscillator have an infinite number of discrete states, a particle in a finite potential well is an example of a system that has only a finite number of discrete states. For energies exceeding the potential well depth, the energy spectrum becomes continuous and the particle may leave the box. Extrapolated to the case of a vibrating diatomic molecule with an interatomic potential allowing for dissociation, the number of bound states should be finite. A simple and frequently used model for the anharmonic potential between two atomic sites is the Morse potential Eq. (10.78). It has only three parameters a , D_e , and R_e , and it has the advantage that the energy levels are well-defined (Eq. (10.79)):

$$E_n = h\nu \left(n + \frac{1}{2} \right) - \frac{(h\nu)^2}{4D_e} \left(n + \frac{1}{2} \right)^2$$

The first term is identical to the harmonic oscillator expression for the energy in state n . The second term can be interpreted as a correction resulting from anharmonicity. The minus sign is important, i.e., the correction leads to shrinking of the energy differences between adjacent states. The situation is illustrated in Fig. 10.13, where the potential is plotted with the given values for the potential depth D_e , the potential minimum R_e , and the parameter a describing the steepness of the potential,

$$a = \sqrt{\frac{k}{2D_e}} = 1.85951 \times 10^{10} \text{ m}^{-1}. \quad (10.85)$$

Also shown are the energy levels resulting from Eq. (10.79) and the quantum energy $h\nu = h\tilde{v}c = 5.9414 \times 10^{-20} \text{ J} = 0.37 \text{ eV}$. In Fig. 10.14, the energies E_n are plotted against the quantum number n . As the dissociation energy is gradually reached, the energy levels are expected to approach one another, which is indeed the

Fig. 10.13 The anharmonic potential in the HCl molecule, based on the Morse oscillator model. Also shown are the resulting energy levels of the Morse oscillator

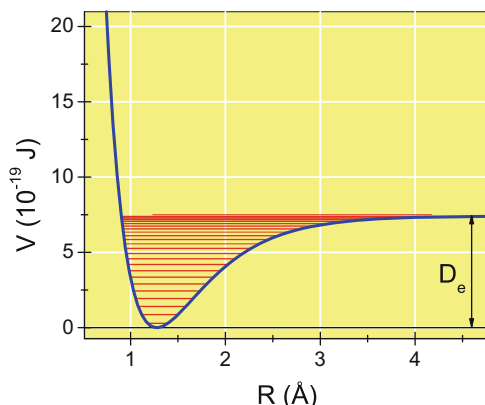
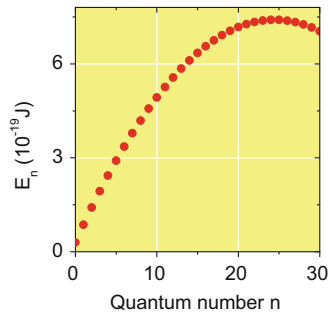


Fig. 10.14 Vibrational energies of the HCl molecule as a function of quantum number n , calculated with Eq. (10.79). Realistic energy levels are those between $n = 0$ and 24



case for quantum numbers up to $n = 24$. For $n > 24$, however, Eq. (10.79) predicts that E_n become smaller with increasing n . This is unphysical. Therefore, the number of vibrational states of the HCl molecule is 25 ($n = 0$ –24).

As we have seen, one consequence of anharmonicity is the shift in the energy levels. The energies of the first levels are

$$E_0 = \frac{h\nu}{2} - \frac{(h\nu)^2}{4D_e} \frac{1}{4} = 0.29410 \times 10^{-20} \text{ J} \quad (10.86)$$

$$E_1 = \frac{h\nu}{2} 3 - \frac{(h\nu)^2}{4D_e} \frac{9}{4} = 8.64420 \times 10^{-20} \text{ J} \quad (10.87)$$

$$E_2 = \frac{h\nu}{2} 5 - \frac{(h\nu)^2}{4D_e} \frac{25}{4} = 1.41092 \times 10^{-19} \text{ J} \quad (10.88)$$

Therefore, the fundamental $n = 0 \rightarrow 1$ transition is observed at:

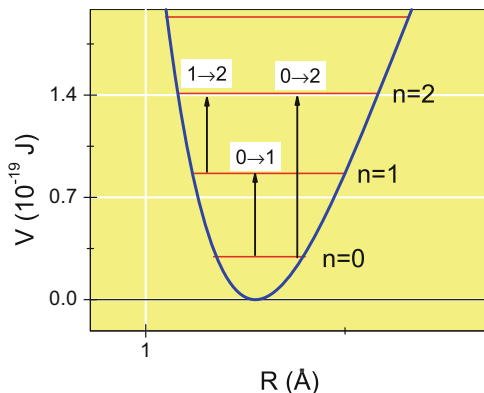
$$\tilde{\nu}_{0 \rightarrow 1} = \frac{\Delta E_{0 \rightarrow 1}}{hc} = 2871 \text{ cm}^{-1} \quad (10.89)$$

which means a red-shift of 120 cm^{-1} , in comparison with the pure harmonic wave number. The transition is shown in Fig. 10.15 in another term scheme of the first few vibrational levels. Also shown in this figure are additional transitions that we deal with in **subproblem (e)**. A consequence of anharmonicity is the breaking of selection rules of the harmonic oscillator. Therefore, the overtone transition $n = 0 \rightarrow 2$ is no longer forbidden. Taking the energy difference between the levels $n = 2$ and the ground state we find:

$$\tilde{\nu}_{0 \rightarrow 2} = \frac{\Delta E_{0 \rightarrow 2}}{hc} = 5623 \text{ cm}^{-1}. \quad (10.90)$$

Note that overtone transitions and combination bands are always much less intense than the corresponding fundamentals. **Hot bands** are another type of IR transitions. In absorption spectroscopy, they result from the excitation of a molecule

Fig. 10.15 Term scheme and vibrational excitations in the region of the first excited states of the HCl molecule



in an excited vibrational state. In our case, we consider the transition $n = 1 \rightarrow 2$. By taking the difference in energy between these two states we obtain:

$$\tilde{v}_{1 \rightarrow 2} = \frac{\Delta E_{1 \rightarrow 2}}{hc} = 2752 \text{ cm}^{-1}. \quad (10.91)$$

We further investigate whether this transition should be observable under room temperature conditions using occupation probabilities. What is behind it? The transition $n = 1 \rightarrow 2$ is only observable if the state $n = 1$ is notably occupied. The occupation probability p_n for a state n follows the Boltzmann statistics:

$$p_n = \frac{\exp\left(-\frac{E_n}{k_B T}\right)}{\sum_n \exp\left(-\frac{E_n}{k_B T}\right)} \quad (10.92)$$

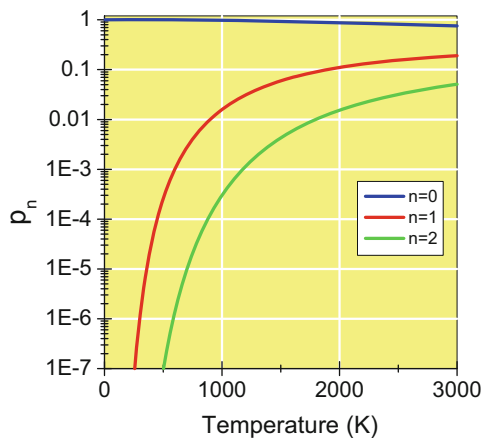
At room temperature, the thermal energy ($k_B T \approx 4 \times 10^{-21} \text{ J}$) is considerably lower than the vibrational quantum energy.¹⁰ It is therefore justified to consider only the first few vibrational levels. At room temperature ($T = 300 \text{ K}$), we obtain the following occupation probability for $n = 1$:

$$p_1 \approx \frac{\exp\left(-\frac{E_1}{k_B T}\right)}{\exp\left(-\frac{E_0}{k_B T}\right) + \exp\left(-\frac{E_1}{k_B T}\right) + \exp\left(-\frac{E_2}{k_B T}\right)} = 1.05 \times 10^{-6}.$$

A similar calculation for the ground state would show $p_0 \approx 0.999999$. Thus, the level $n = 1$ has negligible occupation probability. At room temperature, therefore, the hot band transition $n = 1 \rightarrow 2$ is not detectable using usual laboratory spectrometer hardware. The variation of occupation probabilities with temperature

¹⁰See also Problem 10.1b.

Fig. 10.16 Occupation probabilities of the ground state and the first two excited vibrational states of the HCl molecule according to Boltzmann statistics



is shown in Fig. 10.16 for the ground state and the first two excited states. At 1,000 K the probability of the first excited state reaches a value of about 1%. Are hot bands thus relevant at all for room temperature experiments? An inspection of the IR spectrum of the greenhouse gas CO₂, for example, reveals a hot band in the region of its asymmetric bending mode ($\tilde{\nu} \approx 673 \text{ cm}^{-1}$). The spectra of other polyatomic molecules such as SF₆, another greenhouse gas, are also complicated by hot bands.

Problem 10.7 (IR Spectra of Diatomics II)

In high resolution IR spectroscopy experiments, the fundamental stretch mode and the first overtone of the diatomic CO was investigated. The measured IR transitions are given in Table 10.4.

- a. The energy levels of the perturbed rotation-vibration energy are:

$$\begin{aligned} E_{nJ} = & V(R_e) + h\nu_e \left(n + \frac{1}{2} \right) + hB_e J(J+1) \\ & - h\nu_e x_e \left(n + \frac{1}{2} \right)^2 - h\alpha_e \left(n + \frac{1}{2} \right) J(J+1) - h\bar{D}_e J^2(J+1)^2 \end{aligned} \quad (10.93)$$

where $V(R_e)$ is the potential at the equilibrium bond length R_e , ν_e is the harmonic frequency of the stretch vibration, x_e the anharmonicity constant, α_e is the rotation vibration coupling constant, \bar{D}_e is the centrifugal distortion constant. Determine B_e , α_e , R_e , x_e , \bar{D}_e from a suitable polynomial fit of the spectroscopic data. Hint: Write down relations for the transition

(continued)

Problem 10.7 (continued)

frequencies of the fundamental and first overtone. Introduce new parameters $J' = J + 1$ and $m = -J'$ (P -branch), $m = J'$ (R -branch).

- b. The centrifugal distortion constant is related to the rotational constant B_e via

$$\bar{D}_e = \frac{4B_e^3}{\nu_e^2}. \quad (10.94)$$

Does the fitted result for \bar{D}_e satisfy this condition?

- c. Use relations provided in Problem 10.6 to set up a Morse potential model for the CO molecule. Determine the bond dissociation energy for the CO molecule.
d. The vibrational Hamiltonian of a diatomic including anharmonic corrections can be written:

$$H_{\text{vib}} = H_{\text{harmonic}} + \frac{1}{3!} \left(\frac{\partial^3 V}{\partial q^3} \right)_e q^3 + \frac{1}{4!} \left(\frac{\partial^4 V}{\partial q^4} \right)_e q^4 + \dots \quad (10.95)$$

where q is the elongation $r - R_e$ and $\left(\frac{\partial^3 V}{\partial q^3} \right)_e$ and $\left(\frac{\partial^4 V}{\partial q^4} \right)_e$ are the cubic and quartic force constants respectively. The latter are related to experimentally accessible quantities by means of:

$$\alpha_e = \frac{-2B_e^2}{\nu_e} \left[\frac{2B_e R_e^3 \left(\frac{\partial^3 V}{\partial q^3} \right)_e}{h\nu_e^2} + 3 \right] \quad (10.96)$$

and

$$x_e \nu_e = \frac{B_e^2 R_e^4}{4h\nu_e^2} \left[\frac{10B_e R_e^2 \left(\frac{\partial^3 V}{\partial q^3} \right)_e^2}{3h\nu_e^2} - \left(\frac{\partial^4 V}{\partial q^4} \right)_e \right] \quad (10.97)$$

Determine the cubic and quartic force constants and compare the resulting anharmonic potential model with the Morse potential model from subproblem (c).

Solution 10.7 With this challenging exercise, we explore the foundations of molecular spectroscopy beyond the rigid rotator-harmonic oscillator (RRHO) approximation. In Problem 10.4 we have determined bond lengths of a molecule from the rotational constants obtained from pure rotation spectra. In the discussion of the

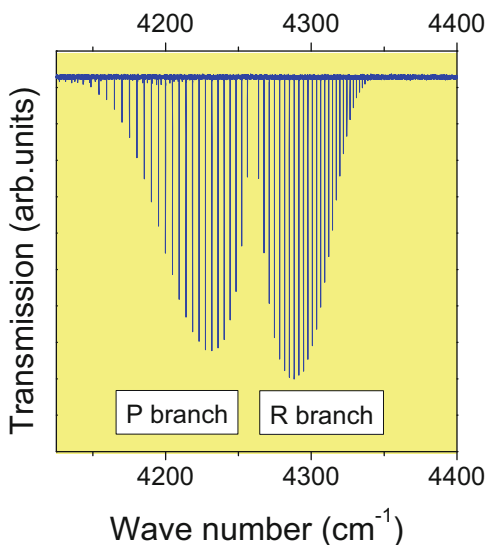
Table 10.4 Measured wave numbers of gas-phase rovibrational transitions of carbon monoxide

J	$n = 0 \rightarrow 1$		$n = 0 \rightarrow 2$	
	P	R	P	R
0	2, 139.427	2, 147.082	4, 256.216	4, 263.837
1	2, 135.547	2, 150.856	4, 252.301	4, 267.542
2	2, 131.632	2, 154.596	4, 248.317	4, 271.177
3	2, 127.683	2, 158.300	4, 244.262	4, 274.740
4	2, 123.700	2, 161.969	4, 240.138	4, 278.234
5	2, 119.681	2, 165.601	4, 235.947	4, 281.656
6	2, 115.629	2, 169.198	4, 231.685	4, 285.009
7	2, 111.544	2, 172.759	4, 227.354	4, 288.289
8	2, 107.423	2, 176.284	4, 222.954	4, 291.499
9	2, 103.270	2, 179.772	4, 218.486	4, 294.638
10	2, 099.083	2, 183.224	4, 213.949	4, 297.704
11	2, 094.863	2, 186.639	4, 209.343	4, 300.700
12	2, 090.609	2, 190.018	4, 204.668	4, 303.623
13	2, 086.322	2, 193.360	4, 199.929	4, 306.475
14	2, 082.003	2, 196.664	4, 195.117	4, 309.254
15	2, 077.650	2, 199.931	4, 190.239	4, 311.961
16	2, 073.265	2, 203.161	4, 185.295	4, 314.596
17	2, 068.847	2, 206.354	4, 180.282	4, 317.159
18	2, 064.397	2, 209.509	4, 175.203	4, 319.649
19	2, 059.915	2, 212.626	4, 170.055	4, 322.064
20	2, 055.401	2, 215.705	4, 164.839	4, 324.409
21	2, 050.855	2, 218.746	4, 159.560	4, 326.681
22	2, 046.276	2, 221.749	4, 154.212	4, 328.878
23	2, 041.667	2, 224.713	4, 148.797	4, 331.004
24	2, 037.026	2, 227.639		4, 333.053
25		2, 230.526		4, 335.030
26		2, 233.375		
27		2, 236.185		

All values in cm^{-1} . J is the rotational quantum number of the final state for the P-branch ($J+1 \rightarrow J$), and of the initial state for the R-branch ($J \rightarrow J+1$) respectively

results it was mentioned that even in the vibrational ground state, the rotational constants are slightly influenced by vibration rotation coupling. Neglect of such effects involves a slight systematic error in the determination of bond lengths. In this problem, we focus on such effects in detail and treat vibration and rotation all together. In gas-phase infrared absorption spectra, vibrational transitions go along with changes in the rotational state. The selection rules for a diatomic rotor, $\Delta J = \pm 1$ (see Eq. (10.15)), lead to a regular wing-like arrangement of the vibration rotation transitions as shown in Fig. 10.17 for the first overtone vibration. The experimental line positions are given in Table 10.4. The P-branch results from transitions $n, J+1 \rightarrow n+1, J$, the R-branch from the transitions $n, J \rightarrow n+1, J+1$

Fig. 10.17 Rotationally resolved IR spectrum in the region of the first overtone ($0 \rightarrow 2$) of the $^{12}\text{C}^{16}\text{O}$ stretch vibration



respectively. J is the usual rotational quantum number. The Q-branch $n, J \rightarrow n+1, J$ is left out.¹¹ In **subproblem (a)**, we use these data to determine spectroscopic constants included in Eq. (10.93). It is useful to analyze this equation, which is the result of a tedious perturbation treatment of the rigid-rotator harmonic-oscillator (RRHO) model, in detail. The first three terms are the vibration-rotation energy of the unperturbed RRHO model. The following three terms are the first corrections from the perturbation treatment, which typically lead to a decrease in the energy levels. Anharmonicity—the first correction term—has already been introduced in Problem 10.6. The second correction is the rotation vibration coupling, whereas the last correction stems from the centrifugal distortion of the molecule depending on its rotational state. For the comparison with the experimental data we must set up expressions for the transition frequencies in the fundamental and overtone region. We start with writing down the energies for the ground and the first vibrationally excited state. Following the hints given, we introduce the new parameter $J' = J + 1$:

$$E_{0,J} = \frac{\hbar\nu_e}{2} - \frac{\hbar\nu_e x_e}{4} + hB_0(J' - 1)J' - h\bar{D}_e(J' - 1)^2J'^2 \quad (10.98)$$

$$E_{0,J+1} = \frac{\hbar\nu_e}{2} - \frac{\hbar\nu_e x_e}{4} + hB_0J'(J' + 1) - h\bar{D}_eJ'^2(J' + 1)^2 \quad (10.99)$$

¹¹The Q-branch would require $\Delta J = 0$ which is forbidden. Infrared active modes of polyatomic molecules, however, have a Q-branch if the induced electric dipole moment is oriented perpendicular to the symmetry axis of a molecule. A Q-branch is also observed in the vibration rotation spectrum of the paramagnetic NO molecule.

$$E_{1,J} = \frac{3h\nu_e}{2} - \frac{9h\nu_e x_e}{4} + hB_1(J' - 1)J' - h\bar{D}_e(J' - 1)^2 J'^2 \quad (10.100)$$

$$E_{1,J+1} = \frac{3h\nu_e}{2} - \frac{9h\nu_e x_e}{4} + hB_1 J'(J' + 1) - h\bar{D}_e J'^2 (J' + 1)^2 \quad (10.101)$$

Moreover, we have introduced the vibrationally corrected rotational constants

$$\begin{aligned} B_0 &= B_e - \frac{\alpha_e}{2} \\ B_1 &= B_e - \frac{3\alpha_e}{2}. \end{aligned} \quad (10.102)$$

Before we consider energy differences, this auxiliary calculation is useful:

$$\begin{aligned} J'^2(J' + 1)^2 &= J'^2(J'^2 + 2J' + 1) = J'^4 + 2J'^3 + J'^2 \\ (J' - 1)^2 J'^2 &= (J'^2 - 2J' + 1)J'^2 = J'^4 - 2J'^3 + J'^2 \end{aligned}$$

If we consider the difference between these two expressions, all terms but the cubic ones cancel each other out. As a consequence, we can form the transition frequencies for the P-branch of the fundamental lines:

$$P:\Delta\nu_{0,J+1 \rightarrow 1,J} = \frac{E_{1,J} - E_{0,J+1}}{h} = \nu_e - 2\nu_e x_e - (B_1 + B_0)J' + (B_1 - B_0)J'^2 + 4\bar{D}_e J'^3 \quad (10.103)$$

$$R:\Delta\nu_{0,J \rightarrow 1,J+1} = \frac{E_{1,J+1} - E_{0,J}}{h} = \nu_e - 2\nu_e x_e + (B_1 + B_0)J' + (B_1 - B_0)J'^2 - 4\bar{D}_e J'^3 \quad (10.104)$$

Inspection of these expressions reveals that they can be combined if we introduce the new parameter $m = -J'$ for the P-branch and $m = J'$ for the R-branch. Then, the transition frequencies for the region $n = 0 \rightarrow 1$ are:

$$\Delta\nu_m = \nu_e - 2\nu_e x_e + (B_1 + B_0)m + (B_1 - B_0)m^2 - 4\bar{D}_e m^3 \quad (10.105)$$

The corresponding wave numbers are obtained after division by the speed of light, $c = 2.99792458 \times 10^{10} \text{ cm s}^{-1}$. If we plot the transition wave numbers against m , we obtain a curved line. Such a plot is shown in Fig. 10.18. A cubic fit of the form:

$$\Delta\tilde{\nu}(m) = a_0 + a_1 m + a_2 m^2 + a_3 m^3 \quad (10.106)$$

with these data provide the values of $\nu_e(1 - 2x_e)$, $B_1 + B_0$, $B_1 - B_0$, and \bar{D}_e . The result of the cubic fit is shown in Table 10.5. Before we further evaluate these results, we must first consider the transitions of the first overtone.

Fig. 10.18 Polynomial plot of the experimental data of rovibrational transitions in the region $n = 0 \rightarrow 1$. For the definition of the parameter m , see the text of subproblem (a)

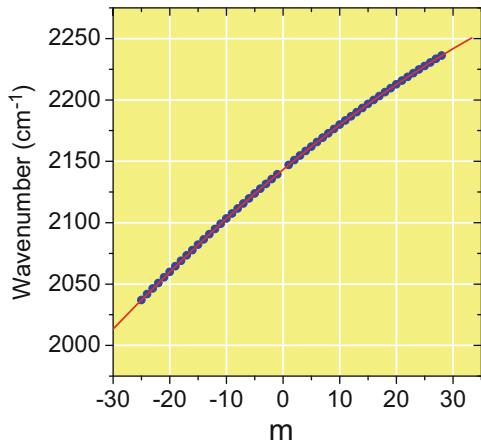


Table 10.5 Results of the polynomial fit of the experimental data put into graphs in Fig. 10.18 and in Fig. 10.19

Vib. transition	a_0	a_1	a_2	a_3
$0 \rightarrow 1$	2143.27144(7)	3.82754(1)	-0.0175	$-2.443(2) \times 10^{-5}$
$0 \rightarrow 2$	4260.0617(2)	3.81006(2)	-0.035	$-2.449(4) \times 10^{-5}$

The coefficients a_i , $i = 0, \dots, 4$ are defined in Eq. (10.106). Numbers in parentheses give the statistical uncertainty in units of the last significant digit. All values are in units of cm^{-1}

The treatment is very similar. After introduction of a vibrationally corrected rotational constant $B_2 = B_e - \frac{5\alpha_e}{2}$ we obtain the expressions

$$\text{P: } \Delta\nu_{0,J+1 \rightarrow 2,J} = \frac{E_{2,J} - E_{0,J+1}}{\hbar} = 2\nu_e - 6\nu_ex_e - (B_2 + B_0)J' + (B_2 - B_0)J'^2 + 4\bar{D}_eJ'^3 \quad (10.107)$$

$$\text{R: } \Delta\nu_{0,J \rightarrow 2,J+1} = \frac{E_{2,J+1} - E_{0,J}}{\hbar} = 2\nu_e - 6\nu_ex_e + (B_2 + B_0)J' + (B_2 - B_0)J'^2 - 4\bar{D}_eJ'^3 \quad (10.108)$$

which can be combined to form:

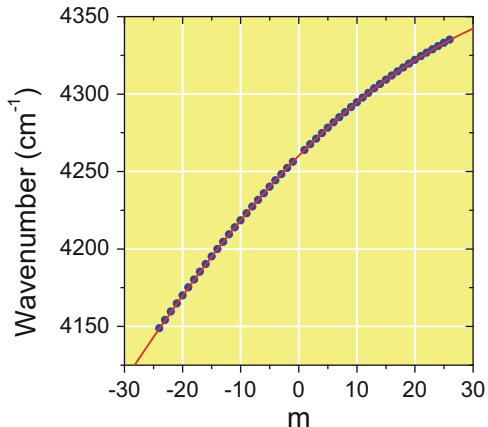
$$\Delta\nu_m = 2\nu_e - 6\nu_ex_e + (B_2 + B_0)m + (B_2 - B_0)m^2 - 4\bar{D}_em^3. \quad (10.109)$$

A plot of the data of the overtone region against m is shown in Fig. 10.19. The results of the polynomial fit are shown in Table 10.5.

We are now ready to exploit the data in Table 10.5 to obtain the quantities sought. First, we focus on the coefficients a_0 containing the harmonic wave number and the anharmonicity constant. From

$$a_0^{0 \rightarrow 1} = \tilde{\nu}_e - 2\tilde{\nu}_ex_e$$

Fig. 10.19 Polynomial plot of the experimental data of rovibrational transitions in the region $n = 0 \rightarrow 2$. For the definition of the parameter m , see the text of subproblem (a):



$$a_0^{0 \rightarrow 2} = 2\tilde{v}_e - 6\tilde{v}_e x_e$$

we obtain

$$\tilde{v}_e = 3a_0^{0 \rightarrow 1} - a_0^{0 \rightarrow 2} = 2169.7526(1) \text{ cm}^{-1} \quad (10.110)$$

and

$$x_e = \frac{2a_0^{0 \rightarrow 1} - a_0^{0 \rightarrow 2}}{2\tilde{v}_e} = 6.1024 \times 10^{-3}. \quad (10.111)$$

Focusing on the coefficients a_1 and a_2 , we can determine the rotational constants. Because

$$a_1^{0 \rightarrow 1} = \frac{1}{c} (B_1 + B_0)$$

$$a_2^{0 \rightarrow 1} = \frac{1}{c} (B_1 - B_0),$$

we obtain¹²

$$\frac{B_1}{c} = \frac{a_1^{0 \rightarrow 1} + a_2^{0 \rightarrow 1}}{2} = 1.90502(1) \text{ cm}^{-1}. \quad (10.112)$$

¹²Values of rotational constants obtained from infrared spectroscopy are often presented in units of cm^{-1} . The numbers in brackets indicate the error of the fit in units of the last significant digit.

and

$$\frac{B_0}{c} = \frac{a_1^{0 \rightarrow 1} - a_2^{0 \rightarrow 1}}{2} = 1.92252(1) \text{ cm}^{-1}. \quad (10.113)$$

In frequency units, we thus obtain $B_1 = 57,111.1(3)$ MHz and $B_0 = 57,635.7(3)$ MHz. The difference in the rotational constants is the vibration-rotation constant α_e :

$$\alpha_e = B_0 - B_1 = 524.6(6) \text{ MHz}. \quad (10.114)$$

The equilibrium rotational constant B_e follows from (Eq. (10.102))

$$\frac{B_e}{c} = \frac{B_0}{c} + \frac{\alpha_e}{2c} = 1.93127(2) \text{ cm}^{-1}. \quad (10.115)$$

or $B_e = 57898.0(6)$ MHz. Having obtained the rotational constants, we can determine the C-O bond length. The effective mass for the CO rotor is:

$$\mu = \frac{m_C m_O}{m_C + m_O} = 6.8571 \text{ amu} = 1.138655 \times 10^{-26} \text{ kg}. \quad (10.116)$$

The relation between the rotational constant and the moment of inertia I or the bond length R_e is

$$B_e = \frac{h}{8\pi^2 I} = \frac{h}{8\pi^2 \mu R_e^2} \quad (10.117)$$

and thus

$$R_e = \sqrt{\frac{h}{8\pi^2 \mu B_e}} = 1.1282 \times 10^{-10} \text{ m} \quad (10.118)$$

or 1.1282 Å. For comparison, the bond length R_0 evaluated with the rotational constant in the vibrational ground state, B_0 , is 1.131 Å. Finally, we determine the centrifugal distortion constant contained in the parameter a_3 . The results from the two data sets are similar. From the data set of the $0 \rightarrow 1$ transitions, we obtain $\bar{D}_e = -\frac{a_3^{0 \rightarrow 1}}{4} = 0.183098$ MHz. From the overtone transitions, $\bar{D}_e = -\frac{a_3^{0 \rightarrow 2}}{4} = 0.183548$ MHz results. Hence, a value of 0.1833(2) MHz for \bar{D}_e is consistent with the data. The value for the centrifugal distortion constant is further scrutinized in **subproblem (b)**. According to Eq. (10.94) it can be related to B_e . This alternative way of computing \bar{D}_e is another test of the integrity of the data sets. With $\nu_e = c\tilde{\nu}_e = 65.04755 \times 10^6$ MHz the centrifugal distortion constant is

$$\bar{D}_e = \frac{4B_e^3}{\nu_e^2} = 0.18348 \text{ MHz}.$$

This value is in good agreement with the result from subproblem (a) and the condition Eq. (10.94) is reflected by the data.

Starting with **subproblem (c)** we focus on the anharmonic potential between the carbon and the oxygen core. The Morse potential model was introduced in Problem 10.6 and we apply it here once more. Comparison of Eq. (10.79) with Eq. (10.93) reveals the relationship between the anharmonicity constant x_e and the depth of the Morse potential, D_e :

$$\begin{aligned} D_e &= \frac{h\nu_e}{4x_e} = \frac{6.62606957 \times 10^{-34} \text{ Js} \times 6.504755 \times 10^{13} \text{ s}^{-1}}{4 \times 6.1024 \times 10^{-3}} \\ &= 1.7657 \times 10^{-18} \text{ J} = 11.02 \text{ eV} \end{aligned} \quad (10.119)$$

In the Morse oscillator model, the bond dissociation energy D_0 of CO is the difference between D_e and the zero point vibration energy, $E_{n=0,J=0}$, which can be calculated according to Eq. (10.93):

$$E_{n=0,J=0} = h\nu_e \left(\frac{1}{2} - \frac{x_e}{4} \right) = 0.13 \text{ eV}.$$

Hence,

$$D_0 = D_e - E_{n=0,J=0} = 10.89 \text{ eV}. \quad (10.120)$$

The force constant k is calculated using Eq. (10.16):

$$\begin{aligned} k &= \mu(2\pi\nu_e)^2 = 1.138655 \times 10^{-26} \text{ kg} (2\pi \times 6.504755 \times 10^{13} \text{ s}^{-1})^2 \\ &= 1902.014 \text{ N m}^{-1}. \end{aligned} \quad (10.121)$$

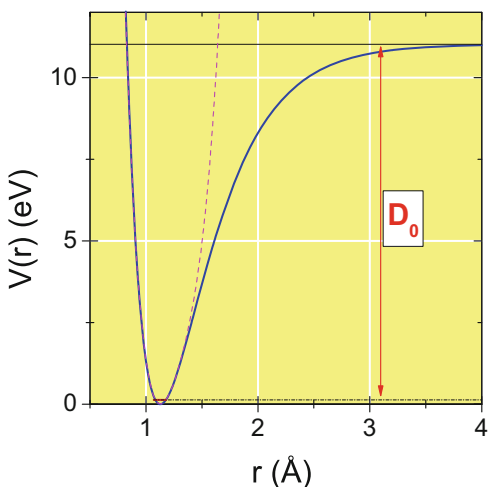
The Morse parameter a follows from Eq. (10.80):

$$a = \sqrt{\frac{k}{2D_e}} = 2.321 \times 10^{10} \text{ m}^{-1} = 2.321 \text{ \AA}^{-1} \quad (10.122)$$

The third parameter is simply the equilibrium distance $R_e = 1.1282 \text{ \AA}$. A plot of the Morse potential for CO is depicted in Fig. 10.20. A second way of analyzing the anharmonic potential in the CO molecule is to consider cubic and quartic force constants. They are related to the spectroscopic parameters that we have already determined in subproblem (a). We rearrange Eqs. (10.96) and (10.97) in **subproblem (d)**:

$$V^{(3)} = \left(\frac{\partial^3 V}{\partial q^3} \right)_e = -\frac{h\nu_e^2}{2B_e R_e^3} \left[3 + \frac{\nu_e \alpha_e}{2B_e^2} \right] = -1.36397 \times 10^{14} \text{ J m}^{-3} \quad (10.123)$$

Fig. 10.20 Modeling of the potential between carbon and oxygen. The *solid line* is the Morse potential derived from spectroscopic constants. The *dashed line* is the anharmonic potential derived from the cubic and quartic force constants



The quartic force constant is:

$$V^{(4)} = \left(\frac{\partial^4 V}{\partial q^4} \right)_e = \frac{10B_e R_e^2}{3h\nu_e^2} \left(\frac{\partial^3 V}{\partial q^3} \right)_e^2 - \frac{4h\nu_e^2}{B_e^2 R_e^4} x_e \nu_e = 8.1040 \times 10^{24} \text{ J m}^{-4} \quad (10.124)$$

With these anharmonic force constants the carbon-oxygen potential

$$V(r) = -\frac{1}{2}k(r - R_e)^2 + \frac{1}{3!}V^{(3)}(r - R_e)^3 + \frac{1}{24!}V^{(4)}(r - R_e)^4 \quad (10.125)$$

takes the form shown as the dashed line in Fig. 10.20. For $r < R_e$, the potential is very close to the Morse potential. For $r > R_e$, however, the potentials are in line only up to about a bond length of 1.5 Å. Larger elongations are not adequately described by the cubic and quartic force constants. Higher order force constants would be needed to describe such situations. Looking back on the exercise, we have learned how to cope with larger sets of spectroscopic data and how the fundamental molecular properties such as the bond length and the bond dissociation energy can be extracted from these data. Doing so we went beyond the models of the rigid rotator and the harmonic oscillator.

Problem 10.8 (Vibrational Modes of Polyatomic Molecules)

Consider the formaldehyde molecule H₂CO shown in Fig. 10.21.

- Write down the point symmetry elements of the molecule. To which point group does this molecule belong?

(continued)

Problem 10.8 (continued)

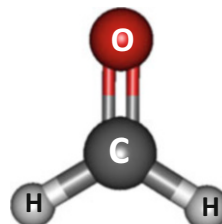
- How many vibrational degrees of freedom does the molecule possess?
- Use group theory to find the symmetry types of the normal modes.
- Which of the normal modes are infrared active, which are Raman active?

Solution 10.8 In this problem, we deal with normal modes of polyatomic molecules. The concrete example is the formaldehyde molecule H_2CO . Many problems in molecular spectroscopy are significantly simplified if symmetry considerations and group theory are used to describe molecular properties. Here, we use formaldehyde as a simple and instructive case that may be a topic in both written and oral examinations.

Starting with **subproblem (a)**, we enumerate the point symmetry elements of the molecule. A point symmetry operation transforms a molecule in such a way that the result of the transformation cannot be distinguished from the initial state. First, every molecule has at least one point symmetry element, the **identity**, which is often forgotten; therefore, we mention it first. The symmetry operation involved with the identity is the operator \hat{E} . Then, the molecule has a twofold **rotation axis**; the operation is \hat{C}_2 . Further point symmetry elements are **vertical mirror planes**, the xz -plane and the yz -plane. The operators are $\hat{\sigma}_v(xz)$ and $\hat{\sigma}'_v(yz)$. The point symmetry elements (except for the identity) are shown in Fig. 10.22. Almost certainly, when molecular symmetry was introduced in your chemistry lectures, it was done using the water molecule as an instructive example. If we compare formaldehyde with water, we see that they share the same point symmetry elements.¹³ Like the H_2O molecule, formaldehyde has the point group C_{2v} .

In **subproblem (b)** we determine the number of vibrational degrees of freedom. The molecule has $N = 4$ nuclei, and each of the nuclei has three translational degrees of freedom. Hence, the molecule has $3N = 12$ degrees of freedom. To obtain the number of vibrational degrees of freedom, we subtract the three pure translational degrees of freedom of the molecule's center of mass. Moreover,

Fig. 10.21 The structure of the H_2CO molecule



¹³Apart from the point symmetry elements mentioned, the inversion center, horizontal mirror planes and improper axes are possible point symmetry elements.

Fig. 10.22 Point symmetry properties of the H₂CO molecule

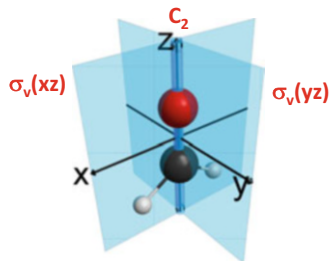


Table 10.6 Character table of the point group C_{2v}

C_{2v}	\hat{E}	\hat{C}_2	$\hat{\sigma}_v(xz)$	$\hat{\sigma}'_v(yz)$		
A_1	1	1	1	1	z	x^2, y^2, z^2
A_2	1	1	-1	-1	R_z	xy
B_1	1	-1	1	-1	x, R_y	xz
B_2	1	-1	-1	1	y, R_x	yz

formaldehyde possesses three rotational degrees of freedom. Therefore, the number of vibrational degrees of freedom is $3N - 6 = 6$.

In **subproblem (c)**, we determine the various **symmetry types** of these normal modes. Why symmetry types? Scientists have realized that certain molecular quantities behave differently under application of the molecule's point symmetry operations. The electronic density and the molecular Hamiltonian of H₂CO, for example, are invariant under all four symmetry operations that we have identified. However, quantities such as molecular orbitals may change their sign under rotation or mirror operations. In the point group C_{2v} , there are four different ways for a physical quantity to transform under the possible point symmetry operations. They can thus be classified according to the four symmetry types A_1 , A_2 , B_1 , and B_2 . In terms of group theory the latter are the *irreducible representations* of the point group.

The **character table** of the point group breaks down the different transformation behavior of the various symmetry types. It is shown in Table 10.6. Without a detailed harmonic analysis, for example, based on a quantum chemical method, it is possible to evaluate the symmetry types of the six vibrational degrees of freedom. Therefore, we seek the *reducible representation* Γ_{red} of the nuclei's movement and we must decompose it into irreducible representations Γ_i according to:

$$\Gamma_{\text{red}} = \sum_{i=1}^4 a_i \Gamma_i \quad (10.126)$$

The coefficients a_i are obtained from the reduction formula

$$a_i = \frac{1}{h} \sum \chi_{\text{red}}(\hat{R}) \chi_i(\hat{R}) \quad (10.127)$$

Here, $\chi_i(\hat{R})$ is the character of one of the symmetry operations \hat{R} taken from the character table and χ_{red} is the respective character of the reducible representation for this symmetry operation, and h is the order of the group, which is 4 in this case.

For each symmetry operation \hat{R} , we consider the transformation

$$\mathbf{T}(\hat{R})\mathbf{X} = \mathbf{X}' \quad (10.128)$$

where \mathbf{T} is the transformation matrix of the symmetry operation acting on the "vector" \mathbf{X} containing the positions of all nuclei. The character of the symmetry operation sought is simply the trace¹⁴ $\text{Tr}(\mathbf{T}(\hat{R}))$.

The identity operation is represented by a (12×12) unit matrix:

$$\begin{pmatrix} 1 & 0 & 0 & 0 & 0 & 0 & 0 & 0 & 0 & 0 & 0 & 0 \\ 0 & 1 & 0 & 0 & 0 & 0 & 0 & 0 & 0 & 0 & 0 & 0 \\ 0 & 0 & 1 & 0 & 0 & 0 & 0 & 0 & 0 & 0 & 0 & 0 \\ 0 & 0 & 0 & 1 & 0 & 0 & 0 & 0 & 0 & 0 & 0 & 0 \\ 0 & 0 & 0 & 0 & 1 & 0 & 0 & 0 & 0 & 0 & 0 & 0 \\ 0 & 0 & 0 & 0 & 0 & 1 & 0 & 0 & 0 & 0 & 0 & 0 \\ 0 & 0 & 0 & 0 & 0 & 0 & 1 & 0 & 0 & 0 & 0 & 0 \\ 0 & 0 & 0 & 0 & 0 & 0 & 0 & 1 & 0 & 0 & 0 & 0 \\ 0 & 0 & 0 & 0 & 0 & 0 & 0 & 0 & 1 & 0 & 0 & 0 \\ 0 & 0 & 0 & 0 & 0 & 0 & 0 & 0 & 0 & 1 & 0 & 0 \\ 0 & 0 & 0 & 0 & 0 & 0 & 0 & 0 & 0 & 0 & 1 & 0 \\ 0 & 0 & 0 & 0 & 0 & 0 & 0 & 0 & 0 & 0 & 0 & 1 \end{pmatrix} \begin{pmatrix} x_O \\ y_O \\ z_O \\ x_C \\ y_C \\ z_C \\ x_{H1} \\ y_{H1} \\ z_{H1} \\ x_{H2} \\ y_{H2} \\ z_{H3} \end{pmatrix} = \begin{pmatrix} x_O \\ y_O \\ z_O \\ x_C \\ y_C \\ z_C \\ x_{H1} \\ y_{H1} \\ z_{H1} \\ x_{H2} \\ y_{H2} \\ z_{H3} \end{pmatrix} \quad (10.129)$$

and it is immediately obvious that the trace is $\text{Tr}(\mathbf{T}(\hat{E})) = 12$ and thus $\chi_{\text{red}}(\hat{E}) = 12$. For the other symmetry operations, considerable simplifications are possible. The trace of the transformation matrix is only determined by its diagonal elements, whereas the off-diagonal elements are not important. Only those nuclei that are not displaced during the symmetry operation thus contribute to the trace and we can confine the analysis to these nuclei. For example, a rotation by 180° displaces the hydrogens H1 and H2, whereas the oxygen and carbon are not displaced. The x and y coordinates of the latter change their sign. The effective transformation is thus:

$$\begin{pmatrix} -1 & 0 & 0 & 0 & 0 & 0 \\ 0 & -1 & 0 & 0 & 0 & 0 \\ 0 & 0 & 1 & 0 & 0 & 0 \\ 0 & 0 & 0 & -1 & 0 & 0 \\ 0 & 0 & 0 & 0 & -1 & 0 \\ 0 & 0 & 0 & 0 & 0 & 1 \end{pmatrix} \begin{pmatrix} x_O \\ y_O \\ z_O \\ x_C \\ y_C \\ z_C \end{pmatrix} = \begin{pmatrix} -x_O \\ -y_O \\ z_O \\ -x_C \\ -y_C \\ z_C \end{pmatrix} \quad (10.130)$$

¹⁴See Sect.A.3.16 in the Appendix.

and the trace of the transformation matrix is -2 . Thus, $\chi_{\text{red}}(\hat{C}_2) = -2$. The two vertical mirror planes are similarly evaluated. For $\hat{\sigma}_v(xz)$ the sign of the y -coordinate changes (see Fig. 10.22) for carbon and oxygen, and the hydrogens.

$$\begin{pmatrix} 1 & 0 & 0 & 0 & 0 & 0 & 0 & 0 & 0 & 0 & 0 \\ 0 & -1 & 0 & 0 & 0 & 0 & 0 & 0 & 0 & 0 & 0 \\ 0 & 0 & 1 & 0 & 0 & 0 & 0 & 0 & 0 & 0 & 0 \\ 0 & 0 & 0 & 1 & 0 & 0 & 0 & 0 & 0 & 0 & 0 \\ 0 & 0 & 0 & 0 & -1 & 0 & 0 & 0 & 0 & 0 & 0 \\ 0 & 0 & 0 & 0 & 0 & 1 & 0 & 0 & 0 & 0 & 0 \\ 0 & 0 & 0 & 0 & 0 & 0 & 1 & 0 & 0 & 0 & 0 \\ 0 & 0 & 0 & 0 & 0 & 0 & 0 & -1 & 0 & 0 & 0 \\ 0 & 0 & 0 & 0 & 0 & 0 & 0 & 0 & 1 & 0 & 0 \\ 0 & 0 & 0 & 0 & 0 & 0 & 0 & 0 & 0 & 1 & 0 \\ 0 & 0 & 0 & 0 & 0 & 0 & 0 & 0 & 0 & 0 & 1 \end{pmatrix} \begin{pmatrix} x_O \\ y_O \\ z_O \\ x_C \\ y_C \\ z_C \\ x_{H1} \\ y_{H1} \\ z_{H1} \\ x_{H2} \\ y_{H2} \\ z_{H3} \end{pmatrix} = \begin{pmatrix} x_O \\ -y_O \\ z_O \\ x_C \\ -y_C \\ z_C \\ x_{H1} \\ -y_{H1} \\ z_{H1} \\ x_{H2} \\ -y_{H2} \\ z_{H3} \end{pmatrix} \quad (10.131)$$

The trace of the transformation matrix is 4 , and thus $\chi_{\text{red}}(\hat{\sigma}_v(xz)) = 4$. The second vertical mirror plane again displaces the hydrogens, we can leave them aside. The transformation changes the sign of the x -coordinates of carbon and oxygen:

$$\begin{pmatrix} -1 & 0 & 0 & 0 & 0 & 0 \\ 0 & 1 & 0 & 0 & 0 & 0 \\ 0 & 0 & 1 & 0 & 0 & 0 \\ 0 & 0 & 0 & -1 & 0 & 0 \\ 0 & 0 & 0 & 0 & 1 & 0 \\ 0 & 0 & 0 & 0 & 0 & 1 \end{pmatrix} \begin{pmatrix} x_O \\ y_O \\ z_O \\ x_C \\ y_C \\ z_C \end{pmatrix} = \begin{pmatrix} -x_O \\ y_O \\ z_O \\ -x_C \\ y_C \\ z_C \end{pmatrix} \quad (10.132)$$

We therefore obtain $\chi_{\text{red}}(\hat{\sigma}'_v(yz)) = 2$. It is useful to summarize these results in an additional line in the character table, as shown in Table 10.7. With the help of Eq. (10.127), we can determine the coefficients a_i :

$$a_{A_1} = \frac{1}{4} [12 \cdot 1 + (-2) \cdot 1 + 4 \cdot 1 + 2 \cdot 1] = 4 \quad (10.133)$$

Table 10.7 Character table of the point group C_{2v}

C_{2v}	\hat{E}	\hat{C}_2	$\hat{\sigma}_v(xz)$	$\hat{\sigma}'_v(yz)$		
A_1	1	1	1	1	z	x^2, y^2, z^2
A_2	1	1	-1	-1	R_z	xy
B_1	1	-1	1	-1	x, R_y	xz
B_2	1	-1	-1	1	y, R_x	yz
I_{red}	12	-2	4	2		

$$a_{A_2} = \frac{1}{4} [12 \cdot 1 + (-2) \cdot 1 + 4 \cdot (-1) + 2 \cdot (-1)] = 1 \quad (10.134)$$

$$a_{B_1} = \frac{1}{4} [12 \cdot 1 + (-2) \cdot (-1) + 4 \cdot 1 + 2 \cdot (-1)] = 4 \quad (10.135)$$

$$a_{B_2} = \frac{1}{4} [12 \cdot 1 + (-2) \cdot (-1) + 4 \cdot (-1) + 2 \cdot 1] = 3 \quad (10.136)$$

As a consequence, the reducible representation is reduced into irreducible representations according to:

$$\Gamma_{\text{red}} = 4A_1 + A_2 + 4B_1 + 3B_2. \quad (10.137)$$

However, the movements we have analyzed also contain translations and rotations of the molecule as a whole. The character table reveals the symmetry types of the translations x, y, z , in addition to rotations R_x, R_y, R_z in the last column. The representation of the translations and rotations are

$$\Gamma_{\text{trans}} = A_1 + B_1 + B_2 \quad (10.138)$$

$$\Gamma_{\text{rot}} = A_2 + B_1 + B_2 \quad (10.139)$$

By subtraction of the latter we obtain the result for the vibrations:

$$\Gamma_{\text{vib}} = \Gamma_{\text{red}} - \Gamma_{\text{trans}} - \Gamma_{\text{rot}} = 3A_1 + 2B_1 + B_2. \quad (10.140)$$

We come to the conclusion that three normal modes have the symmetry type A_1 , two modes are of type B_1 , and one mode has symmetry type B_2 . In fact, an elaborate harmonic analysis of the molecule based on quantum chemical methods would confirm this result. Why might this information be useful? Just one application of this result is the prediction of infrared activity in **subproblem (d)**. Infrared active modes and the translations x, y , and z share the same symmetry type. The information is found in the character tables. All six of the normal modes are infrared active. Moreover, a vibrational mode is Raman active if its symmetry type corresponds to one of the products x^2, y^2, z^2, xy, xz , or yz . The latter information can also be taken from the character table. We conclude that all modes of formaldehyde are also Raman active.

The six normal modes of H_2CO , as they are obtained from a quantum chemical vibrational analysis, are shown in Fig. 10.23. The modes are ordered according to increasing vibrational frequencies. The mode with the lowest frequency ν_1 is a bending mode of symmetry type B_2 . The two B_1 modes are a rocking mode ν_2 and the mode ν_6 at highest frequency, which is an asymmetric C-H stretch mode. The three modes of symmetry type A_1 are C-O stretch movements combined with in-phase and out-of-phase scissoring motion of the C-H bonds (ν_3 and ν_4), and the symmetric C-H stretch mode ν_5 .

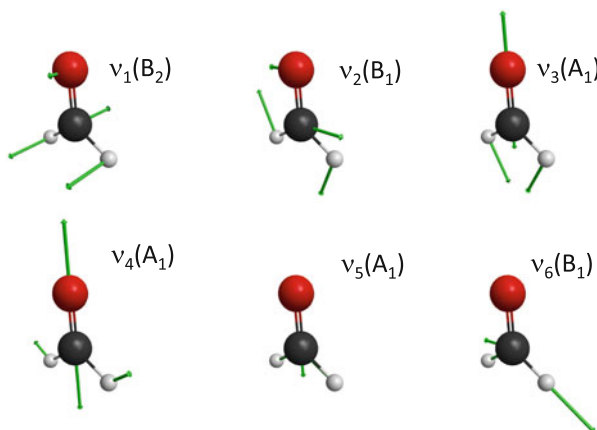


Fig. 10.23 The six normal modes of the H_2CO molecule

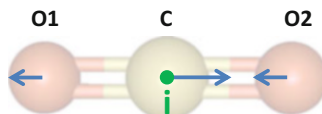


Fig. 10.24 The CO_2 molecule and its asymmetric stretch mode v_3 . If the oxygens O1 and O2 belong to the same isotopic species, then additional selection rules from nuclear spin statistics take effect. One point symmetry element of the molecule is its inversion center i . Arrows indicate schematically the motion of the v_3 vibrational mode

Problem 10.9 (Influence of Nuclear Spin Statistics)

The IR absorption of the linear molecule $^{12}\text{C}^{16}\text{O}_2$ is investigated in the region of the asymmetric stretch mode v_3 (Fig. 10.24). Near the band center, the first observable rovibrational transition of the P branch is found at $2,347.576 \text{ cm}^{-1}$. The first observable transition of the R branch is found at $2,349.918 \text{ cm}^{-1}$. ^{16}O has zero nuclear spin. The linear molecule with inversion center belongs to the point group $D_{\infty h}$. A character table is given in Table 10.8. The symmetry type of the asymmetric stretch mode is Σ_u^+ .

- Which subsets of rovibrational transitions are forbidden because of nuclear spin statistics?
- Determine the C-O bond length in CO_2 in its vibrational ground state. Ignore the centrifugal distortion.

Solution 10.9 In this exercise, our attention is drawn to nuclear spin statistics and its influence on the spectra of molecules with symmetric structure. The prominent

Table 10.8 Character table of the point group $D_{\infty h}$, according to [3]

$D_{\infty h}$	\hat{E}	$2\hat{C}(\phi)$	$\hat{\sigma}_v$	\hat{i}	$2\hat{S}(\phi)$	\hat{C}_2		
Σ_g^+	1	1	1	1	1	1		$x^2 + y^2, z^2$
Σ_g^-	1	1	-1	1	1	-1	R_z	
Π_g	2	$2 \cos \phi$	0	2	$-2 \cos \phi$	0	(R_x, R_y)	(xz, yz)
Δ_g	2	$2 \cos 2\phi$	0	2	$2 \cos 2\phi$	0		$(x^2 - y^2, xy)$
Σ_u^+	1	1	1	-1	-1	-1	z	
Σ_u^-	1	1	-1	-1	-1	1		
Π_u	2	$2 \cos \phi$	0	-2	$2 \cos \phi$	0	(x, y)	
Δ_u	2	$2 \cos 2\phi$	0	-2	$-2 \cos 2\phi$	0		

example is $^{12}\text{C}^{16}\text{O}_2$ where, as it turns out, every second rovibrational transition is forbidden in the region of the asymmetric stretch band $v_3 = 0 \rightarrow 1$.

In **subproblem (a)**, we identify the subset of transitions that are forbidden owing to nuclear spin statistics. For this, we need to bring together the given facts and consider the consequences for the symmetry of the molecule's wave function. Nuclei of the same isotopic species are indistinguishable quantum mechanical objects. In $^{12}\text{C}^{16}\text{O}_2$, we have a two-particle system of ^{16}O nuclei, which we could label 1 and 2. Now, consider an exchange operator \hat{T} acting on the nuclei's wave function with the result that the particles are exchanged:

$$\hat{T}\psi(1, 2) = \tau\psi(2, 1); \quad \tau \in \mathbb{C} \quad (10.141)$$

If the operator acts twice, then the original situation is re-established. This requires a condition for the eigenvalue τ :

$$\hat{T}\hat{T}\psi(1, 2) = \hat{T}\tau\psi(2, 1) = \tau^2\psi(1, 2) = \psi(1, 2) \quad (10.142)$$

$$\tau = \begin{cases} +1; & \text{Bosons} \\ -1; & \text{Fermions} \end{cases} \quad (10.143)$$

According to the *spin-statistics theorem*, the case $\tau = +1$ applies to particles with integer spin, whereas the asymmetric case, in which the sign of the wave function changes, applies to particles with half-integral spin. As ^{16}O nuclei have zero nuclear spin and are thus bosons; the sign of their total wave function does not change upon exchange of the particles. For spin 0 particles the nuclear spin wave function is symmetrical. Moreover, the electronic part of the molecule's wave function in the electronic ground state is symmetrical. However, the rotational and the vibrational parts require attention. The rotational wave functions of a linear molecule are the spherical harmonics $Y_{JM}(\theta, \phi)$ with the property of alternating

parity¹⁵ with the rotational quantum number J :

$$\hat{P}Y_{JM}(\theta, \phi) = (-1)^J Y_{JM}(\pi - \theta, \phi + \pi) \quad (10.144)$$

This can easily be checked for low-order spherical harmonics listed in the appendix (Sect. A.3.14). Thus, for even $J = 0, 2, 4, \dots$, the sign of the rotational part of the total wave function does not change upon inversion, whereas for odd values ($J = 1, 3, \dots$) it does. The behavior of the vibrational part of the wave function depends on the symmetry of the normal mode and the number of quanta by which it is excited. If we inspect the behavior of the asymmetric stretch mode v_3 under inversion (see Fig. 10.24) we see that the movement of the nuclei is just reversed under the inversion operation. The latter is a point symmetry element of the molecule. The point group of the molecule is $D_{\infty h}$. In terms of group theory, the symmetry type of the asymmetric stretch mode is Σ_u^+ and the character for the inversion operation is -1 , as can be seen from the character table of this point group, Table 10.8. If the number of quanta in this mode is odd ($n = 1, 3, 5, \dots$), then the symmetry type of the vibrational wave function corresponds to the symmetry type of the normal mode. If, however, the number of quanta in the mode is even—the ground state $n = 0$ included—then the wave function is totally symmetrical and its sign does not change under the inversion operation.¹⁶ Now, we combine this information and consider the relevant parts of the total wave function as a product of vibrational and rotational parts:

$$\hat{P}\psi_{nJ} = \hat{P}\psi_{\text{vib},n}\psi_{\text{rot},J} \stackrel{!}{=} +1\psi_{\text{vib},n}\psi_{\text{rot},J} \quad (10.145)$$

This condition is satisfied if even values of J are combined with even values of n , and, moreover, if odd values of J are combined with odd values of n .

Thus, to answer the question of subproblem (a), nuclear spin statistics forbids rotational states with an odd quantum number J in the vibrational ground state $n_3 = 0$. In the singly excited state $n_3 = 1$, rotational states with even J are forbidden. A term scheme with the first allowed and the forbidden rovibrational transitions of the $^{12}\text{C}^{16}\text{O}_2$ molecule is shown in Fig. 10.25. Apparently, every second transition is forbidden in the P- and in the R-branches.

With this information we can solve **subproblem (b)**, in which we determine the bond lengths of the two C-O bonds in the vibrational ground state. It turns out that we can fall back on many of the formulas we have used in Problem 10.7. But first we have to consider the differences in the term scheme between diatomics such as CO and linear polyatomic molecules such as CO_2 . Clearly, a molecule with more than

¹⁵The parity operation \hat{P} is an inversion with the result $(x, y, z) \rightarrow (-x, -y, -z)$ or $(r, \theta, \phi) \rightarrow (r, \pi - \theta, \phi + \pi)$.

¹⁶This follows from the fact that harmonic oscillator wave functions (Eq. (A.76), see also Fig. 9.1), have even parity for even quantum numbers $n = 0, 2, 4, \dots$, and odd parity for odd quantum numbers $n = 1, 3, 5, \dots$

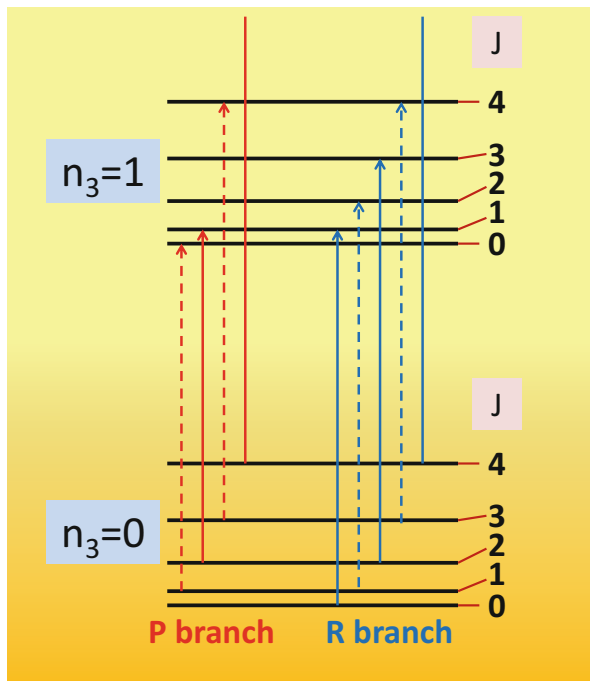


Fig. 10.25 Term scheme (schematic) of the first allowed (solid lines) and forbidden rovibrational transitions (dashed lines) of the asymmetric stretch vibration for the $^{12}\text{C}^{16}\text{O}_2$ molecule

two nuclei has more than one single vibrational degrees of freedom. The triatomic carbon dioxide ($N = 3$) has $3N - 5 = 4$ vibrational degrees of freedom. Two of them, the bending modes ν_{2a} and ν_{2b} , are twofold degenerate. The mode ν_1 is the symmetrical stretch mode. In the adaption of Eq. (10.93) to the triatomic case, variable degeneracies d_i of different vibrational modes should thus be considered. Anharmonicity not only implies overtones, but also combinations and their mutual interaction. There are anharmonicity constants x_{ij} for each pair of normal modes. In addition, for each of the normal modes there is a rotation-vibration coupling constant $\alpha_{e,i}$. The adapted expression for the energy levels of the triatomic is thus:

$$\begin{aligned}
 E_{n_1 n_2 n_3 J} &= V(R_e) + \sum_{i=1}^3 h\nu_{e,i} \left(n_i + \frac{d_i}{2} \right) + hB_e J(J+1) \\
 &\quad - \frac{1}{2} \sum_{i=1}^3 \sum_{j=1}^3 h x_{i,j} \left(n_i + \frac{d_i}{2} \right) \left(n_j + \frac{d_j}{2} \right) - \sum_{i=1}^3 h \alpha_{e,i} \left(n_i + \frac{d_i}{2} \right) J(J+1) \\
 &\quad - h \bar{D}_e J^2 (J+1)^2.
 \end{aligned} \tag{10.146}$$

Note the factor $\frac{1}{2}$ in front of the double sum preventing double counting. It is common practice to introduce a rotational constant

$$B_{n_1 n_2 n_3} = B_e - \sum_{i=1}^3 \alpha_{e,i} \left(n_i + \frac{d_i}{2} \right) \quad (10.147)$$

for the vibrational state, which is the generalization of the constants B_i ($i = 0, 1, 2$) we have used in the diatomic case in Problem 10.7. It is clear that with the sparse information given in this problem, we are not able to determine the equilibrium rotational constant B_e and thus the equilibrium C-O bond distance. This would require determination of the rotation vibration constants $\alpha_{e,i}$ for all normal modes. Here we concentrate on the determination of B_{000} , the ground state rotational constant from which the bond length in the ground state can be determined. We must figure out how this is possible with the information of only two line positions in the P- and the R-branches of the transition¹⁷ $000 \rightarrow 001$. At first, the notion is important that for the calculation of a transition frequency between the ground state and the singly excited asymmetric stretch mode many of the terms are unchanged in these two states and thus cancel each other out. With $d_1 = d_3 = 1$ and $d_2 = 2$, we obtain for the P-branch ($J' = J + 1 \rightarrow J$, see the introduction of the number J' in Problem 10.7)

$$\begin{aligned} \Delta\nu &= \frac{E_{001,J} - E_{000,J+1}}{h} \\ &= \nu_{e,3} - 2x_{33} - \frac{1}{2}x_{13} - x_{23} - (B_{001} + B_{000})J' + (B_{001} - B_{000})J'^2 \end{aligned} \quad (10.148)$$

and for the R-branch ($J \rightarrow J' = J + 1$)

$$\begin{aligned} \Delta\nu &= \frac{E_{001,J+1} - E_{000,J}}{h} \\ &= \nu_{e,3} - 2x_{33} - \frac{1}{2}x_{13} - x_{23} + (B_{001} + B_{000})J' + (B_{001} - B_{000})J'^2. \end{aligned} \quad (10.149)$$

In the problem text, the wave numbers of the first observable transitions of these branches are given. According to Fig. 10.25 the first observable transition for the P-branch has $J' = 2$, whereas the R-branch starts with $J' = 1$. We therefore obtain two equations

$$\Delta\nu_P = \nu_{e,3} - 2x_{33} - \frac{1}{2}x_{13} - x_{23} + 2B_{001} - 6B_{000} \quad (10.150)$$

¹⁷Note that there are at least three different methods for the notation of vibrational states of the CO₂ molecule in use in textbooks and in the scientific literature. The notation used in this problem is sufficient here, but it is not the most general one.

and

$$\Delta\nu_R = \nu_{e,3} - 2x_{33} - \frac{1}{2}x_{13} - x_{23} + 2B_{001} \quad (10.151)$$

for the frequencies of these two transitions. By taking the difference between these frequencies and multiplying with the speed of light, we arrive at:

$$c(\Delta\tilde{\nu}_R - \Delta\tilde{\nu}_P) = 6B_{000}. \quad (10.152)$$

With $\Delta\tilde{\nu}_R = 2349.918 \text{ cm}^{-1}$ and $\Delta\tilde{\nu}_P = 2347.576 \text{ cm}^{-1}$, the ground state rotational constant is:

$$B_{000} = \frac{1}{6} \times 2.99792458 \times 10^{-10} \text{ cm s}^{-1} \times 2.342 \text{ cm}^{-1} = 11701.9 \text{ MHz}. \quad (10.153)$$

It is related via Eq. (10.12) to the moment of inertia of the molecule,

$$I = m_{^{16}\text{O}}(-r_{\text{CO}})^2 + m_{^{16}\text{O}}(+r_{\text{CO}})^2 = 2m_{^{16}\text{O}}r_{\text{CO}}^2, \quad (10.154)$$

and thus to the ground state bond length sought r_{CO} :

$$r_{\text{CO}} = \sqrt{\frac{h}{8\pi^2 2m_{^{16}\text{O}} B_{000}}} = 1.162 \times 10^{-10} \text{ m} \quad (10.155)$$

Our result for the C-O bond lengths within the CO₂ molecule in its vibrational ground state is thus 1.162 Å.

Problem 10.10 (LASER-I)

Consider an optical resonator containing an active material represented by a four-level system, as shown in Fig. 10.26. The laser transition is between the states |2⟩ and |1⟩. Population inversion between these two states is achieved by pumping from the ground level |0⟩ into the state |3⟩ with a pump rate of R_{03} , followed by relaxation into the state |2⟩ within the decay time T_{32} . The transition |2⟩ → |1⟩ is possible either by spontaneous emission (decay time T_{21}) or by stimulated emission with a cross section σ .

- For efficient laser operation, is it better to choose a system with T_{10} much shorter than T_{21} , or a system with $T_{10} > T_{21}$?
- An ideal four-level laser can be described by the following rate equations for the population N_2 of the upper state |2⟩ and the photon density Φ :

(continued)

Problem 10.10 (continued)

$$\frac{dN_2}{dt} = -\frac{N_2}{\tau} - \sigma c N_2 \Phi + R \quad (10.156)$$

$$\frac{d\Phi}{dt} = -\frac{\Phi}{\tau_r} + \sigma c N_2 \Phi \quad (10.157)$$

- R is the pump rate, i.e., the number of particles per volume and time being excited into the upper level, τ is the lifetime of $|2\rangle$ in the zero field including nonradiative relaxation. The relaxation time τ_r of the photon density accounts for radiative losses in the cavity, including transmission through one of the mirrors where the laser radiation is emitted, and c is the speed of light. Determine the steady-state population of the upper level $|2\rangle$ in addition to the minimum pump rate R_{crit} necessary for operation with a He-Ne laser ($\tau = 1 \times 10^{-8}$ s, $\tau_r = 3 \times 10^{-8}$ s, $\sigma = 3 \times 10^{-13}$ cm 2) and for a Nd:YAG laser ($\tau = 2.5 \times 10^{-4}$ s, $\tau_r = 7 \times 10^{-10}$ s, $\sigma = 8 \times 10^{-19}$ cm 2)
- c. Consider small distortions from the steady-state values N_{2s} and Φ_s , $N_2(t) = N_{2s} + n$, and $\Phi(t) = \Phi_s + \phi$. Show that the population distortions can be described by a damped oscillator

$$\frac{d^2n}{dt^2} + 2\delta \frac{dn}{dt} + \omega^2 n = 0 \quad (10.158)$$

where δ is a damping parameter and ω is the angular frequency of the relaxation oscillations. Compare the relaxation behavior of the He-Ne laser and the Nd:YAG laser using the parameters given above and a pumping rate of $R = 2R_{\text{crit}}$. Which laser shows relaxation oscillations?

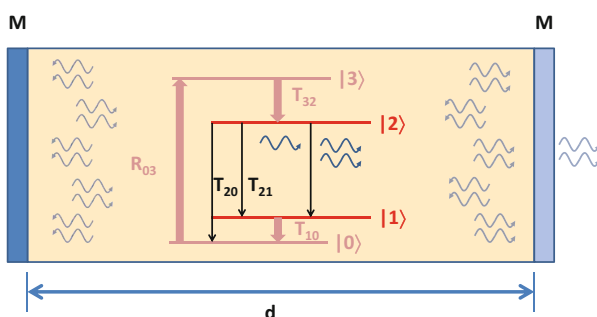


Fig. 10.26 Principle of laser operation (schematic). The active medium is represented by a four-level quantum system within a resonator of d in length. The laser transition is between levels $|2\rangle$ and $|1\rangle$. At least one of the mirrors (M) has nonzero transmission

Solution 10.10 Lasers¹⁸ are an indispensable tool of spectroscopy, as they provide monochromatic coherent light of high intensity. Here, we deal with the principles of laser operation using the model sketched in Fig. 10.26. Within an optical resonator, there is an active medium that is represented by a four-level quantum system. Under operating conditions, the level $|2\rangle$ has a higher population than the lower level $|1\rangle$. This inversion is crucial, as it allows stimulated emission of quanta with the energy $h\nu = E_2 - E_1$ and thus a build-up of radiation within the resonator of this frequency. In the zero field the population inversion would decay owing to spontaneous emission (decay time T_{21}) or because of other nonradiative processes, and reach the population given by the Boltzmann distribution at a certain temperature. An effective mechanism of inversion is achieved by a suitable pump mechanism involving the transition from the ground state $|0\rangle$ to a higher state $|3\rangle$ with the rate R_{03} . Owing to rapid relaxation, the upper laser level $|2\rangle$ is then substantially populated. In **subproblem (a)**, we assess the efficiency of an active medium regarding the decay time of the lower laser level $|1\rangle$. If N_1 and N_2 are the densities of the lower and the upper levels respectively, the degree of inversion is simply the difference $N_2 - N_1$. Now, if the decay time T_{10} were long compared with T_{21} , the lower level $|1\rangle$ would already be populated because of spontaneous emission processes. Thus, the inversion would decrease owing to a flooding of the lower level $|1\rangle$. Therefore, for good laser operation, we need the opposite situation, i.e., a very short lifetime of the level $|1\rangle$, so that ideally, $N_1 = 0$ holds. The answer is thus that $T_{10} \ll T_{21}$ is needed for laser operation. Moreover, simple models like ours assume that the pumping mechanism yields a constant rate by which the upper level $|2\rangle$ is populated. This requires a constant population of the ground state, N_0 . Under these conditions, the four-level laser system can be described by the two rate equations Eqs. (10.156) and (10.157). The equation for the time-dependent population density of the upper laser level $|2\rangle$, $N_2(t)$ can be motivated primarily by the rate equations for induced and spontaneous emission (Eqs. (10.8) and (10.9)). The photon density Φ can be related to the spectral energy density $u(\nu)$ introduced in Sect. 10.1.1 via $u(\nu) = h\nu\Phi$. One relevant parameter is the lifetime τ of the level $|2\rangle$, which includes spontaneous decay in addition to nonradiative processes that depopulate this level. Moreover, the time τ_r describes the decay of the photon density caused by imperfect reflectivity of the mirrors, dissipation, and, of course, losses due to coupling out of the radiation because of transmission through at least one of the mirrors. The first terms on the right-hand side of Eqs. (10.156) and (10.157) describe these loss mechanisms of N_2 and Φ respectively. However, the photon density is fed by means of stimulated emission with the cross section σ , represented by the second term in Eq. (10.157). This gain is proportional to N_2 , which in turn decreases by the same amount (second term in Eq. (10.156)). The constant pumping rate R increases N_2 (third term in Eq. (10.156)). Apparently, we do not account for details such as an index of refraction that is different from unity. We assume that electromagnetic waves propagate through the resonator at the vacuum speed of light c . Here, it

¹⁸The word *laser* is the abbreviation for light amplification by stimulated emission of radiation.

is worth mentioning that these laser equations are similar to those describing the Lotka-Volterra kinetic model of oscillating chemical reactions that we have dealt with in Problems 6.6 and 6.7. Hence, in the following, we benefit from what we have worked out in chemical kinetics. It is not easy to solve these coupled equations without numerical methods.

The first point we examine in **subproblem (b)** are the stationary solutions. These are characterized by a constant population N_{2s} of the upper laser level, and a constant photon density Φ_s . The first derivatives of these quantities are thus zero. Taking Eq. (10.157), we obtain:

$$0 = -\frac{\Phi_s}{\tau_r} + \sigma c N_{2s} \Phi_s \quad (10.159)$$

which yields the stationary state population

$$N_{2s} = \frac{1}{\sigma c \tau_r}. \quad (10.160)$$

Interestingly, within this simple model N_{2s} does not depend on the pump rate R ; it depends only on the cross section for stimulated emission and the decay time of Φ . For a He-Ne gas laser with $\tau_r = 3 \times 10^{-8}$ s and $\sigma = 3 \times 10^{-13}$ cm² we obtain:

$$N_{2s}^{\text{He-Ne}} = 4 \times 10^9 \text{ cm}^{-3}. \quad (10.161)$$

For a Nd:YAG solid-state laser the steady-state density is:

$$N_{2s}^{\text{Nd:YAG}} = \frac{1}{8 \times 10^{-19} \text{ cm}^2 \times 3 \times 10^{10} \text{ cm s}^{-1} \times 7 \times 10^{-10} \text{ s}} = 6 \times 10^{16} \text{ cm}^{-3}. \quad (10.162)$$

Note that τ_r does not depend on the active material, but on the quality of the resonator. Next, we determine the critical pump rate above which laser operation is observed. The latter requires $\Phi_s > 0$. Insertion of Eq. (10.160) in Eq. (10.156) yields an expression for the photon density as a function of the pump rate:

$$\Phi_s = \tau_r R - \frac{1}{\sigma c \tau} \quad (10.163)$$

From the condition $\Phi_s \stackrel{!}{=} 0$, we obtain the critical pump rate

$$R_{\text{crit}} = \frac{1}{\sigma c \tau \tau_r} = \frac{N_{2s}}{\tau} \quad (10.164)$$

For the He-Ne gas laser, we obtain:

$$R_{\text{crit}}^{\text{He-Ne}} = 4 \times 10^{17} \text{ cm}^{-3} \text{ s}^{-1}. \quad (10.165)$$

For the Nd:YAG laser, the critical pump rate is orders of magnitude higher:

$$R_{\text{crit}}^{\text{Nd:YAG}} = 2 \times 10^{20} \text{ cm}^{-3} \text{ s}^{-1}. \quad (10.166)$$

On the one hand, the Nd:YAG laser has a much longer lifetime of the upper laser level, which reduces R_{crit} , but this is overcompensated for by the much smaller cross section for stimulated emission. Different types of lasers may also differ in their dynamic behavior, which we investigate in **subproblem (c)**. We examine how the system behaves if the steady-state values of N_2 and Φ_s are distorted by small deviations n and ϕ respectively. We show that the systems behave like a damped oscillator. If we insert $N_2(t) = N_{2s} + n(t)$ in Eq. (10.156) we obtain

$$\frac{dN_2(t)}{dt} = \frac{dn(t)}{dt} = -\frac{N_{2s}}{\tau} - \frac{n(t)}{\tau} - \sigma c (N_{2s} + n(t)) (\Phi_s + \phi(t)) + R \quad (10.167)$$

and thus

$$\begin{aligned} \frac{dn(t)}{dt} &= \underbrace{-\frac{N_{2s}}{\tau} - \sigma c N_{2s} \Phi_s + R}_{=0} - \frac{n(t)}{\tau} - \sigma c \Phi_s n(t) - \sigma c N_{2s} \phi(t) - \underbrace{\sigma c n(t) \phi(t)}_{\text{neglected}} \\ &= -\frac{n(t)}{\tau} - \sigma c \Phi_s n(t) - \sigma c N_{2s} \phi(t). \end{aligned} \quad (10.168)$$

The nonlinear term containing the product $n(t)\phi(t)$ is ignored, as n and ϕ are considered to be small distortions. In the same way, we treat Eq. (10.157) and obtain

$$\begin{aligned} \frac{d\phi(t)}{dt} &= -\frac{\Phi_s}{\tau_r} - \frac{\phi(t)}{\tau_r} + \sigma c (N_{2s} + n(t)) (\Phi_s + \phi(t)) \\ &= \underbrace{-\frac{\Phi_s}{\tau_r} + \sigma c N_{2s} \Phi_s}_{=0} - \frac{\phi(t)}{\tau_r} + \sigma c \Phi_s n(t) + \sigma c N_{2s} \phi(t) + \underbrace{\sigma c n(t) \phi(t)}_{\text{neglected}} \\ &= -\frac{\phi(t)}{\tau_r} + \sigma c \underbrace{N_{2s}}_{=\frac{1}{\sigma c \tau_r}} \phi(t) + \sigma c \Phi_s n(t) \\ &= \sigma c \Phi_s n(t) \end{aligned} \quad (10.169)$$

Now, by taking the derivative of Eq. (10.168), we obtain

$$\frac{d^2 n(t)}{dt^2} = -\left(\frac{1}{\tau} + \sigma c \Phi_s\right) \frac{dn(t)}{dt} - \sigma c \frac{1}{\sigma c \tau_r} \frac{d\phi(t)}{dt} \quad (10.170)$$

and by substitution of the derivative of $\phi(t)$ using Eq. (10.169), we arrive at

$$\frac{d^2 n(t)}{dt^2} + \left(\frac{1}{\tau} + \sigma c \Phi_s \right) \frac{dn(t)}{dt} + \frac{\sigma c}{\tau_r} \Phi_s n(t) = 0 \quad (10.171)$$

This differential equation has the form Eq. (10.158). It describes damped oscillations with angular frequency

$$\omega = \sqrt{\frac{\sigma c}{\tau_r} \Phi_s} \quad (10.172)$$

and damping parameter

$$\delta = \frac{1}{2} \left(\frac{1}{\tau} + \sigma c \Phi_s \right) \quad (10.173)$$

For the analysis of the dynamic behavior we assume a pump rate that is twice the critical pump rate for laser operation. With $R = 2R_{\text{crit}}$ the angular relaxation, frequency is

$$\omega = \sqrt{\frac{1}{\tau \tau_r}} \quad (10.174)$$

and the damping parameter is

$$\delta = \frac{1}{\tau} \quad (10.175)$$

Now we solve Eq. (10.158), which is a homogeneous differential equation with constant coefficients. The general solution is:

$$n(t) = c_1 e^{\lambda_1 t} + c_2 e^{\lambda_2 t} \quad (10.176)$$

where the constants c_1 and c_2 follow from the initial conditions. The parameters λ_1 and λ_2 are the roots of the characteristic polynomial

$$\lambda^2 + 2\delta\lambda + \omega^2 = 0 \quad (10.177)$$

which we obtain using Eq. (A.4):

$$\lambda_{1,2} = -\delta \pm \sqrt{\delta^2 - \omega^2} \quad (10.178)$$

Now we need to consider two cases regarding the sign of the discriminant $\delta^2 - \omega^2$. If it is positive then λ_1 and λ_2 are real and the solution for the initial condition

$n(t = 0) = n_0$ is¹⁹

$$n(t) = n_0 e^{-\delta t} \cosh \left(\sqrt{\delta^2 - \omega^2} t \right). \quad (10.179)$$

If, however, $\delta^2 - \omega^2$ is negative, then λ_1 and λ_2 are complex conjugate numbers, $\lambda_1 = -\delta + i\sqrt{\omega^2 - \delta^2}$ and $\lambda_2 = -\delta - i\sqrt{\omega^2 - \delta^2}$. Insertion in Eq. (10.176) reveals the damped oscillatory behavior of $n(t)$ in this case²⁰:

$$n(t) = n_0 e^{-\delta t} \cos \left(\sqrt{\omega^2 - \delta^2} t \right) \quad (10.180)$$

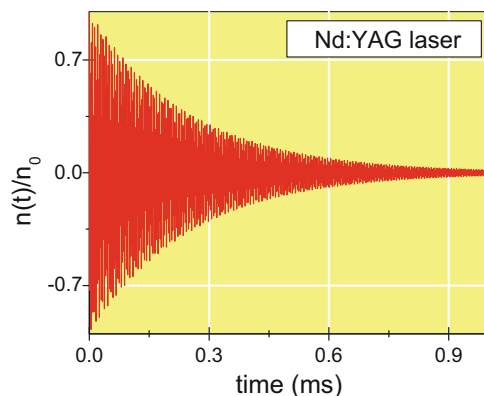
With the parameters τ and τ_r given for the He-Ne laser and the Nd:YAG laser we can calculate ω and δ according to Eqs. (10.174) and (10.175). The results are given in Table 10.9. For the Nd:YAG laser ω largely exceeds the damping parameter δ for the assumed pump rate. This laser type thus exhibits relaxation oscillations, as shown in Fig. 10.27. The oscillations have a frequency of:

$$\frac{1}{2\pi} \sqrt{\omega^2 - \delta^2} \approx 380 \text{ kHz} \quad (10.181)$$

Table 10.9 Parameters influencing the dynamic behavior of lasers concerning small deviations from the stationary state

Laser type	τ (s)	τ_r (s)	ω (rad s ⁻¹)	δ (s ⁻¹)	Relaxation oscillations
He-Ne	1×10^{-8}	3×10^{-8}	5.7×10^7	10^8	No
Nd:YAG	2.5×10^{-4}	7×10^{-10}	2.4×10^6	4×10^3	Yes

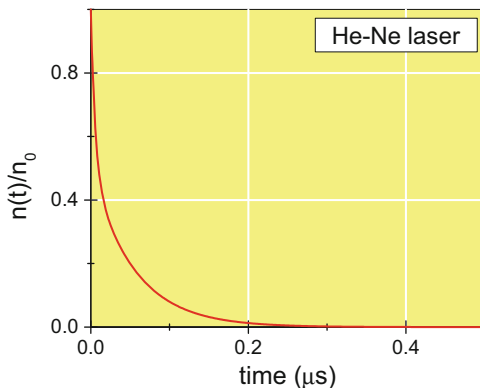
Fig. 10.27 Relaxation dynamics for the Nd:YAG laser, calculated with Eq. (10.180) and the parameters given in the text. Small distortions decay in a damped oscillation within the time scale of 1 ms



¹⁹Note that the hyperbolic cosine function is defined $\cosh x = \frac{1}{2} (e^x + e^{-x})$.

²⁰Note that $\cos x = \frac{1}{2} (e^{ix} + e^{-ix})$ (see Eq. (A.11) in the appendix).

Fig. 10.28 Relaxation dynamics for the He-Ne laser, calculated using Eq. (10.179) and the parameters given in the text. Small distortions $n(t)$ are damped out within the time range of $1 \mu\text{s}$



and decay within 1 ms. In contrast, in the case of the He-Ne laser, small distortions from the stationary state are damped out within $1 \mu\text{s}$ without oscillating behavior, as illustrated in Fig. 10.28.

In the next problem, a numerical solution of the laser equations is examined that confirm the oscillatory behavior around the stationary state seen in the case of the Nd:YAG laser.

Problem 10.11 (LASER-II)

This problems assumes that you have dealt with Problem 10.10. Consider the four-level laser model introduced in Problem 10.10 (Fig. 10.26). Solve the laser equations

$$\frac{dN_2}{dt} = -\frac{N_2}{\tau} - \sigma c N_2 \Phi + R \quad (10.182)$$

$$\frac{d\Phi}{dt} = -\frac{\Phi}{\tau_r} + \sigma c N_2 \Phi \quad (10.183)$$

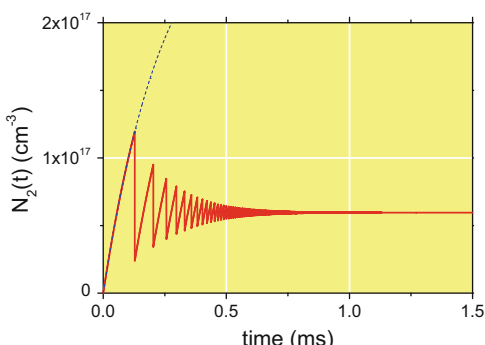
for the population of the upper laser level N_2 and the photon density in the oscillator Φ numerically either by using mathematical software or by writing a computer code based, for example, on the Runge-Kutta scheme of integration (see appendix Sect. A.3.18). Examine the switch-on behavior of the Nd:YAG laser by selecting the initial conditions $N_2 = 0$ and $\Phi(t = 0) = \epsilon$ where ϵ is a small positive number. Use parameters given in Problem 10.10, simulate on a time scale that covers a few milliseconds, and assume a pump rate $R = 5R_{\text{crit}}$. Why do you need $\epsilon > 0$? Can you explain the complex switch-on behavior?

Solution 10.11 This exercise assumes that you have already dealt with Problem 10.10, where the principle of laser light sources was investigated and a stationary solution for the rate equations Eqs. (10.182) and (10.183) was determined. In addition, small deviations from the stationary state values N_{2s} and Φ_s could be treated by neglecting the nonlinearity in these equations. A full solution of these equations requires, however, numerical methods. As for the Lotka-Volterra model for oscillating chemical reactions in Problem 6.7 we can use the Runge-Kutta method (Sect. A.3.18) to integrate Eqs. (10.182) and (10.183) into a discrete grid with a time step interval $h = t_{n+1} - t_n$ ($n = 1, 2, \dots$). Starting from the initial values $N_2(0) = 0$ and $\Phi(0) = 0$, we investigate the switch-on behavior of the Nd:YAG laser. In Problem 10.10 we have seen that this type of laser shows the tendency toward relaxation oscillations. If the pumping is switched on at $t = 0$, the laser is far from its stationary state and it is interesting to examine how the stationary state is established. There is a hint given that we assume a small initial value of the photon density $\Phi(0) = \epsilon$. The reason becomes clear if we inspect Eq. (10.183): the gain of the photon density described by the second term is proportional to Φ . Hence, if $\Phi = 0$ then the photon density stays exactly zero for $t > 0$. We have thus to start from a small photon density ϵ , say $\Phi(0) = 0.1$, resulting, for example, from noise in the resonator. An analogous problem does not occur for N_2 because the gain term of N_2 is the constant pump rate R . For the simulation, we assume a pump rate of $R = 5R_{\text{crit}}$. Let us calculate the expected stationary state values N_{2s} and Φ_s . The stationary population density N_{2s} is independent of R and takes the value $5.96 \times 10^{16} \text{ cm}^{-3}$ (see Eq. (10.162)). By means of Eq. (10.163) we obtain:

$$\Phi_s = \tau_r R - \frac{1}{\sigma c \tau} = \tau_r 5R_{\text{crit}} - \frac{1}{\sigma c \tau} \stackrel{\text{Eq. (10.164)}}{=} \frac{4}{\sigma c \tau} = 6.7 \times 10^{11} \text{ cm}^{-3}, \quad (10.184)$$

where we have used the parameters $\sigma = 8 \times 10^{-19} \text{ cm}^2$ and $\tau = 2.5 \times 10^{-4} \text{ s}^{-1}$. For the simulation, it is crucial that the integration of Eqs. (10.182) and (10.183) is performed on a fine grid, e.g., $h = 10^{-11} \text{ s}$. Results of the simulation are shown in Figs. 10.29 and 10.30. N_2 starts from zero and continuously grows to reach a value of $1.2 \times 10^{17} \text{ cm}^{-3}$. During this time period, the photon density in the resonator is

Fig. 10.29 Switch-on behavior of an Nd:YAG laser obtained from a numerical simulation based on Eqs. (10.182) and (10.183). The population of the upper laser level as a function of time is shown. The dashed line is the behavior according to Eq. (10.186)



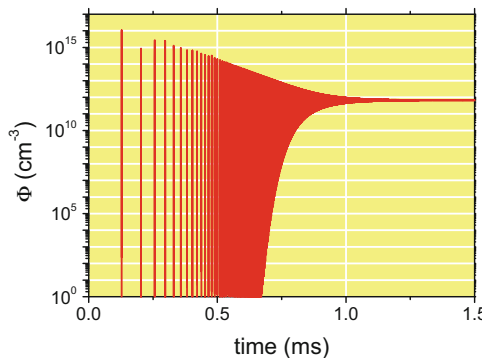


Fig. 10.30 Switch-on behavior of an Nd:YAG laser obtained from a numerical simulation based on Eqs. (10.182) and (10.183). The photon density within the resonator is shown to be a function of time. Note the logarithmic scale for Φ

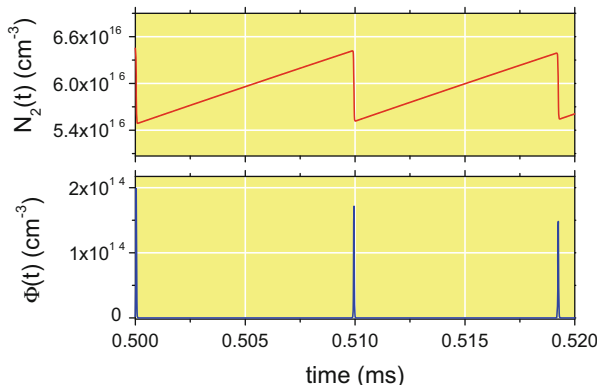


Fig. 10.31 Population of the upper laser level N_2 and photon density Φ as a function of time. Snapshot of the simulation between 0.5 and 0.52 ms.

close to zero. At $t \approx 0.13$ ms, however, Φ exhibits a sharp *spike* and N_2 is suddenly reduced to about $2.5 \times 10^{16} \text{ cm}^{-3}$, increases again until at 0.21 ms, the population of the upper laser level is again suddenly reduced, accompanied by another spike in the photon density. This pattern is repeated in the following, with the tendency that the time between consecutive spikes of Φ and setbacks of N_2 respectively, becomes shorter and shorter. In Fig. 10.31, a snapshot of the simulation between 0.50 and 0.52 ms is shown where the sawtooth-like variation of N_2 and the spikes of the photon density are seen in more detail.

Next, we examine the dynamic behavior in detail. The appearance of spikes is related to the coupling between the population density N_2 and the photon density Φ , which is initially negligibly small for a long period. During this period the coupling term in Eq. (10.182) can be omitted:

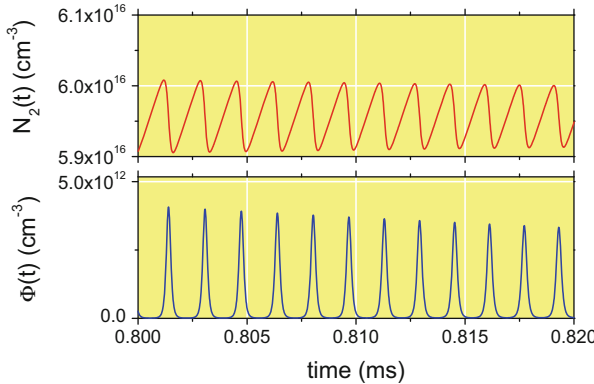


Fig. 10.32 Population of the upper laser level N_2 and photon density Φ as a function of time. Snapshot of the simulation between 0.8 and 0.82 ms

$$\frac{dN_2}{dt} + \frac{N_2}{\tau} \approx R \quad (10.185)$$

The solution of this inhomogeneous differential equation is given by (see also appendix Sect. A.3.18)

$$N_2(t) \approx R\tau \left(1 - e^{-\frac{t}{\tau}}\right) = 5N_{2s} \left(1 - e^{-\frac{t}{\tau}}\right) \quad (10.186)$$

where we have made use of Eq. (10.164). The limiting behavior according to Eq. (10.186) is also shown in Fig. 10.29 as a dashed line. It is in line with the simulation result, until after about 0.13 ms, the coupling with the photon density comes into effect and causes the immediate depopulation of the upper level and a momentary increase in Φ . Then, however, the photon density decays rapidly with a time constant of $\tau_r = 7 \times 10^{-10}$ s, and Φ reaches a value of nearly zero within this time scale. As the upper laser level was not completely depopulated, the recovery of N_2 starts from a higher value until the next spike appears.

Figure 10.32 shows the behavior between 0.80 and 0.82 ms. The repetition rate of spikes has become higher, and they are wider. In Fig. 10.33, where a snapshot of the simulation between 1.20 and 1.22 ms is shown, N_2 and Φ exhibit a nearly harmonic oscillatory behavior around the stationary state values calculated above.

Looking back on our results we were able to numerically solve the laser equations and to simulate the switch-on behavior of the Nd:YAG laser including the appearance of spikes and the relaxation from a highly nonlinear behavior into the stationary state. Oscillations around the stationary state treated in Problem 10.11 are confirmed by the simulation.

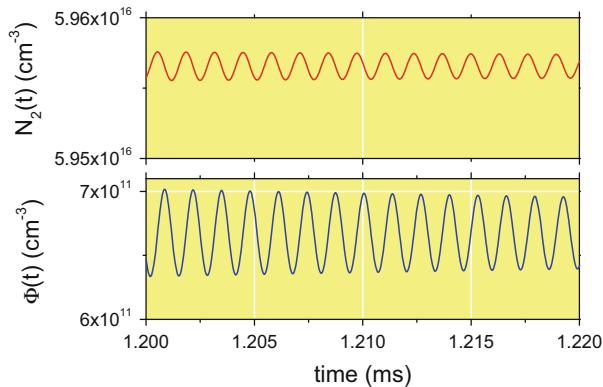


Fig. 10.33 Population of the upper laser level N_2 and photon density Φ as a function of time. Snapshot of the simulation between 1.2 and 1.22 ms

References

1. Louisell WH (1973) Quantum statistical properties of radiation. Wiley, New York
2. Edmonds AR (1957) Angular momentum in quantum mechanics. Princeton University Press, Princeton
3. McHale JL (1999) Molecular spectroscopy. Prentice Hall, Upper Saddle River

Appendix A

A.1 Physical Constants

In the following table the values of the fundamental physical constants are collected (Tables A.1).

Table A.1 Derived constants contain experimental uncertainties in brackets in units of the last digit

Constant	Symbol	Value
Avogadro constant	N_A	$6.02214129(27) \times 10^{23} \text{ mol}^{-1}$
Speed of light in vacuum	c	$299,792,458 \text{ m s}^{-1}$
Electric constant	ϵ_0	$8.854187817 \dots \times 10^{-12} \text{ A}^2 \text{ s}^4 \text{ kg}^{-1} \text{ m}^{-2}$
Elementary charge	e	$1.602176565(35) \times 10^{-19} \text{ A s}$
Planck constant	h	$6.62606957(29) \times 10^{-34} \text{ J s}$
Atomic mass unit	m_u	$1.660538921(73) \times 10^{-27} \text{ kg}$
Electron mass	m_e	$9.10938291(40) \times 10^{-31} \text{ kg}$
Boltzmann constant	k_B	$1.3806488(13) \times 10^{-23} \text{ J K}^{-1}$
Molar gas constant	R	$8.314462(75) \text{ J K}^{-1} \text{ mol}^{-1}$
Faraday constant	F	$96485.3365(21) \text{ A s mol}^{-1}$
Bohr radius	a_0	$0.52917721092(17) \times 10^{-10} \text{ m}$

Source: P.J. Mohr, B.N. Taylor, D.B. Newell, *CODATA recommended values of the fundamental physical constants: 2010*, Rev. Mod. Phys. **84** (2012), 1527

Table A.2 Some common physical units and their relation to the respective SI unit

Name	Symbol	Relation to SI
<i>Length, l</i>		
Meter (SI unit)	m	
Centimeter	cm	10^{-2} m
Nanometer	nm	10^{-9} m
Bohr	a_0	5.29177×10^{-11} m
Ångström	Å	10^{-10} m
<i>Energy, E</i>		
Joule (SI unit)	J	
Erg (cgs unit)	erg	10^{-7} J
Hartree (au)	E_h	$\frac{\hbar^2}{m_e a_0^2} \approx 4.35975 \times 10^{-18}$ J
Rydberg	Ry	$\frac{E_h}{2} \approx 2.17987 \times 10^{-18}$ J
Electronvolt	eV	$e V \approx 1.60218 \times 10^{-19}$ J
Calorie, thermochemical	cal	4.184 J
<i>Pressure, p</i>		
Pascal (SI unit)	Pa	
Bar	bar	10^5 Pa
Torr	Torr	133.322 Pa

Source: IUPAC, I. Mills et al., *Quantities, units and symbols in physical chemistry*, Blackwell Science, 1993

A.2 Physical Units and Their Conversion

The correct use of physical quantities frequently involves a conversion between different units (Table A.2). The recommended system is the International system of units (SI) defining the meter, the kilogram, the second, and ampere as the physical units of length, mass, time, and electric current respectively. For reasons of practicality, atomic units (au) are common in quantum chemistry (see Sect. 9.1.4).

A.3 Compilation of Mathematical Formulas

A.3.1 Binomial Formulas

First binomial formula:

$$(a + b)^2 = a^2 + 2ab + b^2 \quad (\text{A.1})$$

Second binomial formula:

$$(a - b)^2 = a^2 - 2ab + b^2 \quad (\text{A.2})$$

Third binomial formula:

$$(a + b)(a - b) = a^2 - b^2 \quad (\text{A.3})$$

A.3.2 Quadratic Equation

The roots of the quadratic equation $ax^2 + bx + c = 0$ are

$$x_{1,2} = \frac{-b \pm \sqrt{b^2 - 4ac}}{2a}; \quad b^2 - 4ac > 0 \quad (\text{A.4})$$

where $\Delta = b^2 - 4ac$ is called discriminant. If $\Delta = 0$, then the quadratic equation has only one root; if $\Delta > 0$, it has two real solutions, if $\Delta < 0$ the solutions are complex.

A.3.3 Logarithms

$$\ln(a) + \ln(b) = \ln(ab) \quad (\text{A.5})$$

$$\ln(a) - \ln(b) = \ln\left(\frac{a}{b}\right) \quad (\text{A.6})$$

$$\ln(a^x) = x \ln(a) \quad (\text{A.7})$$

A.3.4 Complex Numbers

A complex number

$$z = u + iv \quad (\text{A.8})$$

can be represented by a vector in a two-dimensional complex plane, spanned by the number line of the real part (horizontal axis), and the number line of the imaginary part (vertical axis), see Fig. A.1. The real part of z is $\text{Re}(z) = u$, the imaginary part is $\text{Im}(z) = v$. The **imaginary unit** is defined by

$$i^2 = -1. \quad (\text{A.9})$$

The same number can be represented by:

$$z = |z|e^{i\phi} \quad (\text{A.10})$$

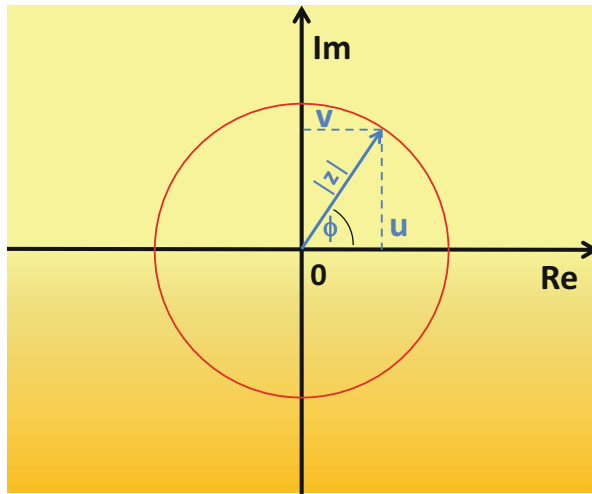


Fig. A.1 A complex number $z = u + iv$ in the two-dimensional complex plane

where $|z|$ is the absolute value of z and $e^{i\phi}$ is a phase factor depending on the angle ϕ defined in Fig. A.1. Particularly useful is **Euler's formula**

$$e^{i\phi} = \cos \phi + i \sin \phi. \quad (\text{A.11})$$

Moreover, an important operation is **complex conjugation**:

$$z^* = (u + iv)^* = (u - iv) = |z|e^{-i\phi}. \quad (\text{A.12})$$

As a consequence, the absolute square of complex number z is:

$$|z|^2 = z^* z. \quad (\text{A.13})$$

A.3.5 Derivatives

A.3.5.1 Basic Differentiation Rules

The sum rule

$$\frac{d}{dx} (af(x) + bg(x)) = a \frac{df(x)}{dx} + b \frac{dg(x)}{dx} \quad (\text{A.14})$$

The product rule

$$\frac{d}{dx} (f(x)g(x)) = \frac{df(x)}{dx}g(x) + f(x)\frac{dg(x)}{dx} \quad (\text{A.15})$$

The quotient rule

$$\frac{d}{dx} \frac{f(x)}{g(x)} = \frac{\frac{df(x)}{dx}g(x) - f(x)\frac{dg(x)}{dx}}{g^2(x)} \quad (\text{A.16})$$

The chain rule

$$\frac{d}{dx} f(g(x)) = \frac{df(g)}{dg(x)} \frac{dg(x)}{dx} \quad (\text{A.17})$$

A.3.5.2 Basic Derivatives

$$\frac{d}{dx} C = 0 \quad (\text{A.18})$$

$$\frac{d}{dx} x = 1 \quad (\text{A.19})$$

$$\frac{d}{dx} x^n = nx^{n-1} \quad (\text{A.20})$$

$$\frac{d}{dx} e^x = e^x \quad (\text{A.21})$$

$$\frac{d}{dx} a^x = a^x \ln a \quad (\text{A.22})$$

$$\frac{d}{dx} \ln x = \frac{1}{x} \quad (\text{A.23})$$

$$\frac{d}{dx} \log_a x = \frac{1}{x \ln a} \quad (\text{A.24})$$

$$\frac{d}{dx} \sin x = \cos x \quad (\text{A.25})$$

$$\frac{d}{dx} \cos x = -\sin x \quad (\text{A.26})$$

A.3.5.3 Partial Derivatives and Total Derivatives

Consider a function $f(t, x, y)$ depending on several variables x , y , and t . As in the case of a function with one variable, the *partial* derivative with regard to x is defined by the difference quotient in the limit $h \rightarrow 0$:

$$\frac{\partial f(t, x, y)}{\partial x} = \lim_{h \rightarrow 0} \frac{f(t, x + h, y) - f(t, x, y)}{h}. \quad (\text{A.27})$$

The rules for partial differentiation follow the above rules for the differentiation of a function with only one variable; the other variables are held constant. Example: consider $f(t, x, y) = 3x^2y - t$. The partial derivative with regard to x is:

$$\frac{\partial f}{\partial x} = 6xy. \quad (\text{A.28})$$

Consider a case in which the variables $x(t)$ and $y(t)$ themselves depend on t . In this case, the *total* derivative of a function $f(t, x, y)$ with regard to time is:

$$\frac{df(x, y, t)}{dt} = \frac{\partial f}{\partial t} + \frac{\partial f}{\partial x} \frac{dx}{dt} + \frac{\partial f}{\partial y} \frac{dy}{dt}. \quad (\text{A.29})$$

A.3.6 Basic Integration Rules

Multiplication by constant

$$\int af(x) dx = a \int f(x) dx \quad (\text{A.30})$$

Sum rule

$$\int (f(x) + g(x)) dx = \int f(x) dx + \int g(x) dx \quad (\text{A.31})$$

Integration by parts

$$\int f(x) \frac{d g(x)}{dx} dx = f(x)g(x) - \int g(x) \frac{d f(x)}{dx} dx \quad (\text{A.32})$$

A.3.6.1 Multiple Integrals and Change of Variables

Consider a multiple integral of the form $\iint f(x, y) dx dy$. Frequently, a transformation of the variables x and y to a set of new variables u v is considered via

$$x = x(u, v) \quad y = y(u, v).$$

Then, the double integral can be written

$$\iint f(x, y) dx dy = \iint f(x(u, v), y(u, v)) \frac{\partial(u, v)}{\partial(x, y)} du dv \quad (\text{A.33})$$

with the **Jacobian**

$$\frac{\partial(u, v)}{\partial(x, y)} = \begin{vmatrix} \frac{\partial u}{\partial x} & \frac{\partial v}{\partial x} \\ \frac{\partial u}{\partial y} & \frac{\partial v}{\partial y} \end{vmatrix} \quad (\text{A.34})$$

The method can be generalized to functions with more than two variables.

A.3.7 Integral Table

Improper integrals (C is a constant):

$$\int x^n dx = \frac{1}{n+1} x^{n+1} + C; \quad n \neq -1 \quad (\text{A.35})$$

$$\int \frac{dx}{x} = \ln x + C \quad (\text{A.36})$$

$$\int \frac{dx}{ax+b} = \frac{1}{a} \ln(ax+b) + C \quad (\text{A.37})$$

$$\int \frac{dx}{(ax+b)(fx+g)} = \frac{1}{bf-ag} \ln \frac{fx+g}{ax+b} \quad (\text{A.38})$$

$$\int \sin(ax) dx = -\frac{1}{a} \cos(ax) \quad (\text{A.39})$$

$$\int \cos(ax) dx = \frac{1}{a} \sin(ax) \quad (\text{A.40})$$

$$\int \sin(ax) \cos(ax) dx = \frac{1}{2a} \sin^2(ax) \quad (\text{A.41})$$

$$\int e^{ax} dx = \frac{e^{ax}}{a} \quad (\text{A.42})$$

$$\int x e^{ax} dx = \frac{e^{ax}}{a^2} (ax - 1) \quad (\text{A.43})$$

$$\int x^2 e^{ax} dx = e^{ax} \left(\frac{x^2}{a} - \frac{2x}{a^2} + \frac{2}{a^3} \right) \quad (\text{A.44})$$

Some definite integrals:

$$\int_0^\infty x^n e^{-ax} = \frac{n!}{a^{n+1}} \quad (\text{A.45})$$

$$\int_0^\infty e^{-a^2 x^2} dx = \frac{\sqrt{\pi}}{2a}, \quad a > 0 \quad (\text{A.46})$$

$$\int_0^\infty x^2 e^{-a^2 x^2} dx = \frac{\sqrt{\pi}}{4a^3}, \quad a > 0 \quad (\text{A.47})$$

$$\int_0^\infty x^n e^{-ax^2} dx = \frac{k!}{2a^{k+1}}, \quad a > 0, \text{ for every odd positive integer } n = 2k + 1 \quad (\text{A.48})$$

$$\int_0^\infty x^n e^{-ax^2} dx = \frac{1 \cdot 3 \cdot \dots \cdot (2k-1)}{2^{k+1}} \sqrt{\frac{\pi}{a^{2k+1}}}, \\ a > 0, \text{ for every even positive integer } n = 2k \quad (\text{A.49})$$

$$\int_0^u e^{-x^2} dx = \frac{\sqrt{\pi}}{2} \operatorname{erf}(u), \quad \text{see Eq. (A.60)} \quad (\text{A.50})$$

$$\int_{-\infty}^{+\infty} \frac{\sin^2(ax)}{x^2} dx = \pi |a| \quad (\text{A.51})$$

Dirac's delta function:

$$\int_{-\infty}^{+\infty} \delta(x) dx = 1 \quad \text{where } \delta(x) = \begin{cases} +\infty, & x = 0 \\ 0, & x \neq 0 \end{cases} \quad (\text{A.52})$$

For an arbitrary function $f(x)$, the following equation holds:

$$\int_{-\infty}^{+\infty} f(x) \delta(x) dx = f(0) \quad (\text{A.53})$$

A.3.8 Power Series Expansions

Taylor series for a function $f(x)$ around its value at x_0 :

$$f(x) = \sum_n \frac{f^{(n)}(x_0)}{n!} (x - x_0)^n \quad (\text{A.54})$$

Further power series expansions:

$$e^x = \sum_{n=0}^{\infty} \frac{x^n}{n!} = 1 + x + \frac{x^2}{2!} + \frac{x^3}{3!} + \dots \quad (\text{A.55})$$

$$\ln(1+x) = \sum_{n=1}^{\infty} (-1)^{n+1} \frac{x^n}{n} = x - \frac{x^2}{2} + \frac{x^3}{3} + \dots \quad (\text{A.56})$$

$$\frac{1}{1-x} = \sum_{n=0}^{\infty} x^n = 1 + x + x^2 + x^3 + \dots \quad (\text{A.57})$$

$$\frac{x}{e^x - 1} = 1 - \frac{x}{2} + B_1 \frac{x^2}{2!} - B_2 \frac{x^4}{4!} + \dots \quad (\text{A.58})$$

where B_n are the Bernoulli numbers; $B_1 = \frac{1}{6}$, $B_2 = \frac{1}{30}$.

$$(1 \pm x)^{\frac{1}{2}} = 1 \pm \frac{1}{2}x - \frac{1 \cdot 1}{2 \cdot 4}x^2 \pm \frac{1 \cdot 1 \cdot 3}{2 \cdot 4 \cdot 6}x^3 - \frac{1 \cdot 1 \cdot 3 \cdot 5}{2 \cdot 4 \cdot 6 \cdot 8}x^4 \dots \quad (\text{A.59})$$

$$\operatorname{erf}(x) = \frac{2}{\sqrt{\pi}} \sum_{n=0}^{\infty} \frac{(-1)^n x^{2n+1}}{n!(2n+1)} = \frac{2}{\sqrt{\pi}} \left(x - \frac{x^3}{3} + \frac{x^5}{10} - \frac{x^7}{42} + \dots \right) \quad (\text{A.60})$$

A.3.9 Factorials and the Stirling Formula

The factorial $n!$ is defined as the product

$$n! = n(n-1)(n-2)\dots(2)(1) \quad (\text{A.61})$$

Stirling's approximation for $n!$ is:

$$\ln n! = n \ln n - n. \quad (\text{A.62})$$

A more accurate Stirling formula is:

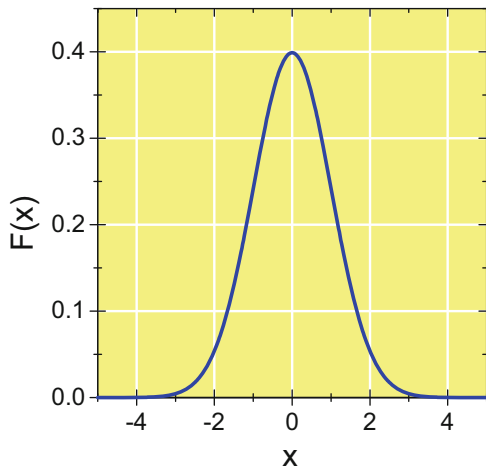
$$\ln n! = \left(n + \frac{1}{2} \right) \ln n - n + \ln \sqrt{2\pi} \quad (\text{A.63})$$

A.3.10 Normal Distribution

The normal distribution is a continuous distribution used in probability theory and statistics:

$$F(x) = \frac{1}{\sqrt{2\pi}\sigma^2} \exp \left[-\frac{1}{2} \left(\frac{x-\mu}{\sigma} \right)^2 \right] \quad (\text{A.64})$$

Fig. A.2 Plot of a normal distribution around an average value $\mu = 0$ and a standard deviation $\sigma = 1$



μ is the average of the random variable x , σ^2 its variance, and σ its standard deviation (Fig. A.2). The half width or *full width at half maximum FWHM* is

$$\text{FWHM} = 2\sigma\sqrt{2 \ln 2}. \quad (\text{A.65})$$

A.3.11 Spherical Coordinates

For problems with spherical symmetry, the use of spherical coordinates $r = \sqrt{x^2 + y^2 + z^2}$ (radial coordinate, interval $[0, \infty]$), $\theta = \arccos\left(\frac{z}{\sqrt{x^2+y^2+z^2}}\right)$ (inclination, interval $[0, \pi]$), and $\phi = \arctan\left(\frac{y}{x}\right)$ (azimuth, interval $[0, 2\pi]$) are often used instead of Cartesian coordinates x , y , and z :

$$\begin{pmatrix} x \\ y \\ z \end{pmatrix} = \begin{pmatrix} r \sin \theta \cos \phi \\ r \sin \theta \sin \phi \\ r \cos \theta \end{pmatrix} \quad (\text{A.66})$$

The volume element in spherical coordinates is:

$$dV = r^2 \sin \theta \, dr \, d\theta \, d\phi. \quad (\text{A.67})$$

In spherical coordinates, the Laplace operator has the following form:

$$\Delta = \frac{1}{r^2} \frac{\partial}{\partial r} \left(r^2 \frac{\partial}{\partial r} \right) + \frac{1}{r^2 \sin \theta} \frac{\partial}{\partial \theta} \left(\sin \theta \frac{\partial}{\partial \theta} \right) + \frac{1}{r^2 \sin \theta} \frac{\partial^2}{\partial \phi^2} \quad (\text{A.68})$$

A.3.12 Cylindrical Coordinates

For problems with cylindrical symmetry, the use of cylindrical coordinates $r = \sqrt{x^2 + y^2}$ (radial distance, interval $[0, \infty]$), z (height, interval $[-\infty, \infty]$), and ϕ (azimuth, interval $[0, 2\pi]$) is appropriate:

$$\begin{pmatrix} x \\ y \\ z \end{pmatrix} = \begin{pmatrix} r \cos \phi \\ r \sin \phi \\ z \end{pmatrix}. \quad (\text{A.69})$$

The volume element is:

$$dV = r dr d\phi dz. \quad (\text{A.70})$$

In cylindrical coordinates, the Laplace operator has the following form:

$$\Delta = \frac{1}{r} \frac{\partial}{\partial r} \left(r \frac{\partial}{\partial r} \right) + \frac{1}{r^2} \frac{\partial^2}{\partial \phi^2} + \frac{\partial^2}{\partial z^2} \quad (\text{A.71})$$

A.3.13 Harmonic Oscillator Wave Functions

Explicit expressions for the harmonic oscillator wave functions are ($\alpha = \frac{m\omega}{\hbar}$, $y = \sqrt{\alpha}x$)

$$\psi_0(x) = \left(\frac{\alpha}{\pi} \right)^{\frac{1}{4}} e^{-\frac{y^2}{2}} \quad (\text{A.72})$$

$$\psi_1(x) = \left(\frac{\alpha}{\pi} \right)^{\frac{1}{4}} \sqrt{2}y e^{-\frac{y^2}{2}} \quad (\text{A.73})$$

$$\psi_2(x) = \left(\frac{\alpha}{\pi} \right)^{\frac{1}{4}} \frac{1}{\sqrt{2}} (2y^2 - 1) e^{-\frac{y^2}{2}} \quad (\text{A.74})$$

$$\psi_3(x) = \left(\frac{\alpha}{\pi} \right)^{\frac{1}{4}} \frac{1}{\sqrt{3}} (2y^3 - 3y) e^{-\frac{y^2}{2}} \quad (\text{A.75})$$

The formula for general n is:

$$\psi_n(x) = \left(\frac{\alpha}{\pi} \right)^{\frac{1}{4}} \frac{1}{\sqrt{2^n n!}} H_n(y) e^{-\frac{y^2}{2}} \quad (\text{A.76})$$

where $H_n(y)$ is a Hermite polynomial. To obtain wave functions with higher n , the recurrence relation

$$H_{n+1}(y) = 2yH_n(y) - 2nH_{n-1}(y) \quad (\text{A.77})$$

can be used starting from $H_0(y) = 1$ and $H_1(y) = 2y$.

A.3.14 Spherical Harmonics

Explicit expressions for spherical harmonics $Y_{lm}(\theta, \phi)$ for $l = 0, 1, 2, \dots$ and $m = -l, -l+1, \dots, -1, 0, +1, \dots, l-1, l$:

$$Y_{00} = \frac{1}{\sqrt{4\pi}} \quad (\text{A.78})$$

$$Y_{10} = \sqrt{\frac{3}{4\pi}} \cos \theta \quad (\text{A.79})$$

$$Y_{1\pm 1} = \mp \sqrt{\frac{3}{8\pi}} \sin \theta e^{\pm i\phi} \quad (\text{A.80})$$

$$Y_{20} = \sqrt{\frac{5}{16\pi}} (3 \cos^2 \theta - 1) \quad (\text{A.81})$$

$$Y_{2\pm 1} = \mp \sqrt{\frac{15}{8\pi}} \sin \theta \cos \theta e^{\pm i\phi} \quad (\text{A.82})$$

$$Y_{2\pm 2} = \sqrt{\frac{15}{32\pi}} \sin^2 \theta e^{\pm 2i\phi} \quad (\text{A.83})$$

For general l, m :

$$Y_{lm}(\theta, \phi) = \sqrt{\frac{2l+1}{4\pi} \frac{(l-m)!}{(l+m)!}} P_{lm}(\cos \theta) e^{im\phi} \quad (\text{A.84})$$

with the associated Legendre polynomial

$$P_{lm}(x) = \frac{(-1)^m}{2^l l!} (1-x^2)^{\frac{m}{2}} \frac{d^{l+m}}{dx^{l+m}} (x^2 - 1)^l \quad (\text{A.85})$$

A.3.15 Radial Wave Functions of the Hydrogen Problem

Explicit radial wave functions $R_{nl}(r)$ for the $n = 1, 2, 3, l = 0, \dots, n-1$ (Bohr radius $a_0 = \frac{4\pi\epsilon_0\hbar^2}{m_e e^2}$):

$$R_{10}(r) = 2a_0^{-\frac{3}{2}} e^{-\frac{r}{a_0}} \quad (\text{A.86})$$

$$R_{20}(r) = \frac{1}{\sqrt{2}} a_0^{-\frac{3}{2}} \left(1 - \frac{r}{2a_0}\right) e^{-\frac{r}{2a_0}} \quad (\text{A.87})$$

$$R_{21}(r) = \frac{1}{\sqrt{24}} a_0^{-\frac{3}{2}} \frac{r}{a_0} e^{-\frac{r}{2a_0}} \quad (\text{A.88})$$

$$R_{30}(r) = \frac{2}{\sqrt{27}} a_0^{-\frac{3}{2}} \left(1 - \frac{2r}{3a_0} + \frac{2r^2}{27a_0^2}\right) e^{-\frac{r}{3a_0}} \quad (\text{A.89})$$

$$R_{31}(r) = \frac{8}{27\sqrt{6}} a_0^{-\frac{3}{2}} \left(1 - \frac{r}{6a_0}\right) \frac{r}{a_0} e^{-\frac{r}{3a_0}} \quad (\text{A.90})$$

$$R_{32}(r) = \frac{4}{81\sqrt{30}} a_0^{-\frac{3}{2}} \frac{r^2}{a_0^2} e^{-\frac{r}{3a_0}} \quad (\text{A.91})$$

For general n, l , the radial wave function is:

$$R_{nl}(r) = \sqrt{\left(\frac{2}{na_0}\right)^3 \frac{(n-l-1)!}{2n[(n+l)!]^3}} e^{-\frac{r}{na_0}} \left(\frac{2r}{na_0}\right)^l L_{n-l-1}^{2l+1} \left(\frac{2r}{na_0}\right) \quad (\text{A.92})$$

where $L_j^k(\rho)$ is an associated Laguerre polynomial. The functions are normalized according to $\int_0^\infty R_{nl}(r)R_{nl}(r)r^2 dr = 1$.

A.3.16 Matrices

A (n,m) matrix \mathbf{A} is an arrangement of numbers in n rows and m columns:

$$\mathbf{A} = \begin{pmatrix} a_{11} & a_{12} & \cdots & a_{1m} \\ a_{21} & a_{22} & \cdots & a_{2m} \\ \vdots & \vdots & \ddots & \vdots \\ a_{n1} & a_{n2} & \cdots & a_{nm} \end{pmatrix} \quad (\text{A.93})$$

The **trace** of a (n,n) square matrix \mathbf{A} is the sum over its diagonal elements:

$$\text{Tr } \mathbf{A} = \sum_i^n a_{ii} \quad (\text{A.94})$$

The sum of two (n,m) matrices \mathbf{A} and \mathbf{B} is a (n,m) matrix \mathbf{C} . Its matrix elements are obtained by simple summation:

$$c_{ij} = a_{ij} + b_{ij}; \quad i = 1, \dots, n; \quad j = 1, \dots, m \quad (\text{A.95})$$

Multiplication of a matrix \mathbf{A} with a scalar number c is calculated by multiplying each matrix element with this number. The matrix elements of the result \mathbf{B} are thus:

$$b_{ij} = c a_{ij}. \quad (\text{A.96})$$

The multiplication of a (n,p) matrix \mathbf{A} with a (p,m) matrix \mathbf{B} yields a (n,m) matrix \mathbf{C} . Its matrix elements are obtained by summation over products of matrix elements:

$$c_{ij} = \sum_k^p a_{ik} b_{kj} \quad (\text{A.97})$$

The inverse \mathbf{A}^{-1} of a (n,n) square matrix \mathbf{A} is defined by

$$\mathbf{A}^{-1} \mathbf{A} = \mathbf{I}_n \quad (\text{A.98})$$

where is \mathbf{I}_n is a (n,n) unit matrix.

A.3.17 Cramer's Rule for the Solution of a System of Linear Equations

Although there are numerically more efficient methods of solving a system of linear equations available, Cramer's rule is often used in *paper and pencil* problems. If \mathbf{A} is a square $n \times n$ coefficient matrix and \mathbf{y} is a column vector with n elements, then the system of equations $\mathbf{Ax} = \mathbf{y}$ with the solution vector \mathbf{x} containing the n solutions can be solved by forming the determinant of the coefficient matrix,

$$\det \mathbf{A} = \begin{vmatrix} a_{11} & a_{12} & \cdots & a_{1n} \\ a_{21} & a_{22} & \cdots & a_{2n} \\ \vdots & \vdots & \ddots & \vdots \\ a_{n1} & a_{n2} & \cdots & a_{nn} \end{vmatrix}, \quad (\text{A.99})$$

in addition to the n determinants

$$\det \mathbf{A}_i = \begin{vmatrix} a_{11} & a_{12} & \cdots & y_1 & \cdots & a_{1n} \\ a_{21} & a_{22} & \cdots & y_2 & \cdots & a_{2n} \\ \vdots & \vdots & \cdots & \vdots & \cdots & \vdots \\ a_{j1} & a_{j2} & \cdots & y_j & \cdots & a_{jn} \\ \vdots & \vdots & \cdots & \vdots & \cdots & \vdots \\ a_{n1} & a_{n2} & \cdots & y_n & \cdots & a_{nn} \end{vmatrix}; \quad i = 1, \dots, n \quad (\text{A.100})$$

in which the i -th column is replaced by the elements of the vector \mathbf{y} . Then, the solution vector \mathbf{x} is given by the n elements

$$x_i = \frac{\det \mathbf{A}_i}{\det \mathbf{A}}; \quad i = 1, \dots, n. \quad (\text{A.101})$$

A.3.18 Analytic Solution for a First-Order Inhomogeneous Differential Equation

A first-order inhomogeneous differential equation

$$\frac{dy(x)}{dx} + f(x)y = g(x) \quad (\text{A.102})$$

has the analytic solution

$$y(x) = \frac{1}{M(x)} \left(\int g(x)M(x) dx + C \right). \quad (\text{A.103})$$

C is an integration constant defined by the boundary conditions, and M is the *integrating factor*:

$$M(x) = e^{\int f(x) dx}. \quad (\text{A.104})$$

A.3.19 Newton's Method of Solving a Nonlinear System of Equations

Consider a general system of equations

$$\mathbf{f}(\mathbf{x}) = \begin{bmatrix} f_1(x_1, \dots, x_n) \\ f_2(x_1, \dots, x_n) \\ \vdots \\ f_n(x_1, \dots, x_n) \end{bmatrix} = 0 \quad (\text{A.105})$$

for which the solution vector $\mathbf{x} = \boldsymbol{\xi} = (\xi_1 \dots \xi_n)^T$ is to be determined. If the solution exists and if \mathbf{x}^0 is a first guess that is reasonably close to the solution $\boldsymbol{\xi}$, an iterative method can be set up such that the updated approximations \mathbf{x}^{i+1} converge toward $\boldsymbol{\xi}$. Starting from the first guess ($i = 0$), the next improved vector is:

$$\mathbf{x}^{i+1} = \mathbf{x}^i - \mathbf{J}^{-1}\mathbf{f}(\mathbf{x}^i) \quad (\text{A.106})$$

where

$$\mathbf{J} = \begin{pmatrix} \frac{\partial f_1}{\partial x_1} & \cdots & \frac{\partial f_1}{\partial x_n} \\ \vdots & & \vdots \\ \frac{\partial f_n}{\partial x_1} & \cdots & \frac{\partial f_n}{\partial x_n} \end{pmatrix} \quad (\text{A.107})$$

is the derivative matrix (**Jacobian** matrix) whose determinant must be nonzero. For simple problems (e.g., $n = 2$) the formation of the inverse \mathbf{J}^{-1} is straightforward. For larger systems, however, the numerically expensive formation of the inverse can be avoided. If $\mathbf{v}^i = \mathbf{x}^{i+1} - \mathbf{x}^i$ is the difference vector between successive iterations, Eq. (A.107) is equivalent to the linear system of equations

$$\mathbf{J}\mathbf{v}^i = \mathbf{f}(\mathbf{x}^i). \quad (\text{A.108})$$

A.3.20 Bernoulli Differential Equation

A differential equation of the form

$$\frac{dy}{dx} = f(x)y + g(x)y^n \quad n \neq 0, 1 \quad (\text{A.109})$$

is called a Bernoulli equation. A Bernoulli equation can be transformed into a linear differential equation, if we introduce:

$$\tilde{y} = y^{1-n}. \quad (\text{A.110})$$

Then, we obtain:

$$\frac{d\tilde{y}}{dx} = (1-n)f(x)\tilde{y} + (1-n)g(x), \quad (\text{A.111})$$

which can be treated as described in Sect. A.3.18.

A.3.21 Numerical Integration Schemes for the Initial Value Problem $\dot{y}(t) = f(t, y)$

Consider the initial value problem

$$\frac{dy(t)}{dt} = f(t, y(t)) \quad (\text{A.112})$$

with the initial condition $y(t_0 = 0) = y_0$. Numerical approximations on a grid of equidistant points t_n ($n = 1, 2, 3, \dots$) with the step interval $h = t_{n+1} - t_n$ are available with different error orders¹:

- The Euler method (error $O(h^2)$):

$$y_{n+1} = y_n + hf(t_n, y_n) \quad (\text{A.113})$$

- Second-order Runge-Kutta method (error $O(h^3)$)

$$k_1 = hf(t_n, y_n) \quad (\text{A.114})$$

$$k_2 = hf\left(t_n + \frac{h}{2}, y_n + \frac{k_1}{2}\right) \quad (\text{A.115})$$

$$y_{n+1} = y_n + k_2 \quad (\text{A.116})$$

- Fourth-order Runge-Kutta method (error $O(h^5)$)

$$k_1 = hf(t_n, y_n) \quad (\text{A.117})$$

$$k_2 = hf\left(t_n + \frac{h}{2}, y_n + \frac{k_1}{2}\right) \quad (\text{A.118})$$

$$k_3 = hf\left(t_n + \frac{h}{2}, y_n + \frac{k_2}{2}\right) \quad (\text{A.119})$$

$$k_4 = hf(t_n + h, y_n + k_3) \quad (\text{A.120})$$

$$y_{n+1} = y_n + \frac{k_1}{6} + \frac{k_2}{3} + \frac{k_3}{3} + \frac{k_4}{6} \quad (\text{A.121})$$

¹Source: W.H. Press, S. Teukolsky, W.T. Vetterling, B.P. Flannery *Numerical recipes in C: the art of scientific computing*, Cambridge University Press, Cambridge, 1988

A.4 Periodic Table of Elements

1	2	3	4	5	6	7	8	9	10	11	12	13	14	15	16	17	18																																																																																																																																																																																																																																																																																																																																																																																																																																																																																																																																																																																																																																																																																																																																					
1 H Hydrogen	2 He Helium	3 Li Lithium	4 Be Boron	5 B Boron	6 Vb VIIb	7 Vlb VIIlb	8 — —	9 — —	10 — —	11 — —	12 — —	13 — —	14 — —	15 — —	16 — —	17 — —	18 — —																																																																																																																																																																																																																																																																																																																																																																																																																																																																																																																																																																																																																																																																																																																																					
11 Na Sodium	12 Mg Magnesium	13 Al Aluminum	14 Si Silicon	15 P Phosphorus	16 O Oxygen	17 F Fluorine	18 Ne Neon	19 K Potassium	20 Ca Calcium	21 Sc Scandium	22 Ti Titanium	23 V Vanadium	24 Cr Chromium	25 Mn Manganese	26 Fe Iron	27 Co Cobalt	28 Ni Nickel	29 Cu Copper	30 Zn Zinc	31 Ga Gallium	32 Ge Germanium	33 As Arsenic	34 Se Selenium	35 Br Bromine	36 Kr Krypton	37 Rb Rubidium	38 Sr Strontium	39 Y Yttrium	40 Zr Zirconium	41 Nb Niobium	42 Mo Molybdenum	43 Ru Rhodium	44 Tc* Technetium	45 Ru Ruthenium	46 Rh Rhodium	47 Pd Palladium	48 Ag Silver	49 Cd Cadmium	50 In Indium	51 Sn Antimony	52 Te Tellurium	53 I Iodine	54 Xe Xenon	55 Cs Cesium	56 Ba Barium	57 Fr* Francium	58 La Lanthanum	59 Ce Cerium	60 Pr Praseodymium	61 Nd Neodymium	62 Sm Samarium	63 Eu Europium	64 Gd Gadolinium	65 Tb Terbium	66 Dy Dysprosium	67 Ho Holmium	68 Er Erbium	69 Tm Thulium	70 Yb Ytterbium	71 Lu Lutetium	72 Hf Hafnium	73 Ta Tantalum	74 W Tungsten	75 Os Osmium	76 Ir Iridium	77 Pt Platinum	78 Au Gold	79 Hg Mercury	80 Tl Thallium	81 Bi Bismuth	82 Po Polonium	83 At Astatine	84 Rn* Radium	85 (222)	86 (223)	87 (223)	88 (224)	89 (227)	90 Ac* Actinium	91 Th* Thorium	92 Pa* Protactinium	93 U* Uranium	94 Np* Neptunium	95 Pu* Plutonium	96 (244)	97 (247)	98 (243)	99 (251)	100 (257)	101 (258)	102 (259)	103 (263)	104 Lr* Lawrencium	105 No* Nobelium	106 Md* Meitnerium	107 Es* Einsteinium	108 Fm* Fermium	109 Cm* Curium	110 Bk* Berkelium	111 Cf Californium	112 Nh Nhastium	113 Nh Nhastium	114 Nh Nhastium	115 Nh Nhastium	116 Nh Nhastium	117 Nh Nhastium	118 Nh Nhastium	119 Nh Nhastium	120 Nh Nhastium	121 Nh Nhastium	122 Nh Nhastium	123 Nh Nhastium	124 Nh Nhastium	125 Nh Nhastium	126 Nh Nhastium	127 Nh Nhastium	128 Nh Nhastium	129 Nh Nhastium	130 Nh Nhastium	131 Nh Nhastium	132 Nh Nhastium	133 Nh Nhastium	134 Nh Nhastium	135 Nh Nhastium	136 Nh Nhastium	137 Nh Nhastium	138 Nh Nhastium	139 Nh Nhastium	140 Nh Nhastium	141 Nh Nhastium	142 Nh Nhastium	143 Nh Nhastium	144 Nh Nhastium	145 Nh Nhastium	146 Nh Nhastium	147 Nh Nhastium	148 Nh Nhastium	149 Nh Nhastium	150 Nh Nhastium	151 Nh Nhastium	152 Nh Nhastium	153 Nh Nhastium	154 Nh Nhastium	155 Nh Nhastium	156 Nh Nhastium	157 Nh Nhastium	158 Nh Nhastium	159 Nh Nhastium	160 Nh Nhastium	161 Nh Nhastium	162 Nh Nhastium	163 Nh Nhastium	164 Nh Nhastium	165 Nh Nhastium	166 Nh Nhastium	167 Nh Nhastium	168 Nh Nhastium	169 Nh Nhastium	170 Nh Nhastium	171 Nh Nhastium	172 Nh Nhastium	173 Nh Nhastium	174 Nh Nhastium	175 Nh Nhastium	176 Nh Nhastium	177 Nh Nhastium	178 Nh Nhastium	179 Nh Nhastium	180 Nh Nhastium	181 Nh Nhastium	182 Nh Nhastium	183 Nh Nhastium	184 Nh Nhastium	185 Nh Nhastium	186 Nh Nhastium	187 Nh Nhastium	188 Nh Nhastium	189 Nh Nhastium	190 Nh Nhastium	191 Nh Nhastium	192 Nh Nhastium	193 Nh Nhastium	194 Nh Nhastium	195 Nh Nhastium	196 Nh Nhastium	197 Nh Nhastium	198 Nh Nhastium	199 Nh Nhastium	200 Nh Nhastium	201 Nh Nhastium	202 Nh Nhastium	203 Nh Nhastium	204 Nh Nhastium	205 Nh Nhastium	206 Nh Nhastium	207 Nh Nhastium	208 Nh Nhastium	209 Nh Nhastium	210 Nh Nhastium	211 Nh Nhastium	212 Nh Nhastium	213 Nh Nhastium	214 Nh Nhastium	215 Nh Nhastium	216 Nh Nhastium	217 Nh Nhastium	218 Nh Nhastium	219 Nh Nhastium	220 Nh Nhastium	221 Nh Nhastium	222 Nh Nhastium	223 Nh Nhastium	224 Nh Nhastium	225 Nh Nhastium	226 Nh Nhastium	227 Nh Nhastium	228 Nh Nhastium	229 Nh Nhastium	230 Nh Nhastium	231 Nh Nhastium	232 Nh Nhastium	233 Nh Nhastium	234 Nh Nhastium	235 Nh Nhastium	236 Nh Nhastium	237 Nh Nhastium	238 Nh Nhastium	239 Nh Nhastium	240 Nh Nhastium	241 Nh Nhastium	242 Nh Nhastium	243 Nh Nhastium	244 Nh Nhastium	245 Nh Nhastium	246 Nh Nhastium	247 Nh Nhastium	248 Nh Nhastium	249 Nh Nhastium	250 Nh Nhastium	251 Nh Nhastium	252 Nh Nhastium	253 Nh Nhastium	254 Nh Nhastium	255 Nh Nhastium	256 Nh Nhastium	257 Nh Nhastium	258 Nh Nhastium	259 Nh Nhastium	260 Nh Nhastium	261 Nh Nhastium	262 Nh Nhastium	263 Nh Nhastium	264 Nh Nhastium	265 Nh Nhastium	266 Nh Nhastium	267 Nh Nhastium	268 Nh Nhastium	269 Nh Nhastium	270 Nh Nhastium	271 Nh Nhastium	272 Nh Nhastium	273 Nh Nhastium	274 Nh Nhastium	275 Nh Nhastium	276 Nh Nhastium	277 Nh Nhastium	278 Nh Nhastium	279 Nh Nhastium	280 Nh Nhastium	281 Nh Nhastium	282 Nh Nhastium	283 Nh Nhastium	284 Nh Nhastium	285 Nh Nhastium	286 Nh Nhastium	287 Nh Nhastium	288 Nh Nhastium	289 Nh Nhastium	290 Nh Nhastium	291 Nh Nhastium	292 Nh Nhastium	293 Nh Nhastium	294 Nh Nhastium	295 Nh Nhastium	296 Nh Nhastium	297 Nh Nhastium	298 Nh Nhastium	299 Nh Nhastium	300 Nh Nhastium	301 Nh Nhastium	302 Nh Nhastium	303 Nh Nhastium	304 Nh Nhastium	305 Nh Nhastium	306 Nh Nhastium	307 Nh Nhastium	308 Nh Nhastium	309 Nh Nhastium	310 Nh Nhastium	311 Nh Nhastium	312 Nh Nhastium	313 Nh Nhastium	314 Nh Nhastium	315 Nh Nhastium	316 Nh Nhastium	317 Nh Nhastium	318 Nh Nhastium	319 Nh Nhastium	320 Nh Nhastium	321 Nh Nhastium	322 Nh Nhastium	323 Nh Nhastium	324 Nh Nhastium	325 Nh Nhastium	326 Nh Nhastium	327 Nh Nhastium	328 Nh Nhastium	329 Nh Nhastium	330 Nh Nhastium	331 Nh Nhastium	332 Nh Nhastium	333 Nh Nhastium	334 Nh Nhastium	335 Nh Nhastium	336 Nh Nhastium	337 Nh Nhastium	338 Nh Nhastium	339 Nh Nhastium	340 Nh Nhastium	341 Nh Nhastium	342 Nh Nhastium	343 Nh Nhastium	344 Nh Nhastium	345 Nh Nhastium	346 Nh Nhastium	347 Nh Nhastium	348 Nh Nhastium	349 Nh Nhastium	350 Nh Nhastium	351 Nh Nhastium	352 Nh Nhastium	353 Nh Nhastium	354 Nh Nhastium	355 Nh Nhastium	356 Nh Nhastium	357 Nh Nhastium	358 Nh Nhastium	359 Nh Nhastium	360 Nh Nhastium	361 Nh Nhastium	362 Nh Nhastium	363 Nh Nhastium	364 Nh Nhastium	365 Nh Nhastium	366 Nh Nhastium	367 Nh Nhastium	368 Nh Nhastium	369 Nh Nhastium	370 Nh Nhastium	371 Nh Nhastium	372 Nh Nhastium	373 Nh Nhastium	374 Nh Nhastium	375 Nh Nhastium	376 Nh Nhastium	377 Nh Nhastium	378 Nh Nhastium	379 Nh Nhastium	380 Nh Nhastium	381 Nh Nhastium	382 Nh Nhastium	383 Nh Nhastium	384 Nh Nhastium	385 Nh Nhastium	386 Nh Nhastium	387 Nh Nhastium	388 Nh Nhastium	389 Nh Nhastium	390 Nh Nhastium	391 Nh Nhastium	392 Nh Nhastium	393 Nh Nhastium	394 Nh Nhastium	395 Nh Nhastium	396 Nh Nhastium	397 Nh Nhastium	398 Nh Nhastium	399 Nh Nhastium	400 Nh Nhastium	401 Nh Nhastium	402 Nh Nhastium	403 Nh Nhastium	404 Nh Nhastium	405 Nh Nhastium	406 Nh Nhastium	407 Nh Nhastium	408 Nh Nhastium	409 Nh Nhastium	410 Nh Nhastium	411 Nh Nhastium	412 Nh Nhastium	413 Nh Nhastium	414 Nh Nhastium	415 Nh Nhastium	416 Nh Nhastium	417 Nh Nhastium	418 Nh Nhastium	419 Nh Nhastium	420 Nh Nhastium	421 Nh Nhastium	422 Nh Nhastium	423 Nh Nhastium	424 Nh Nhastium	425 Nh Nhastium	426 Nh Nhastium	427 Nh Nhastium	428 Nh Nhastium	429 Nh Nhastium	430 Nh Nhastium	431 Nh Nhastium	432 Nh Nhastium	433 Nh Nhastium	434 Nh Nhastium	435 Nh Nhastium	436 Nh Nhastium	437 Nh Nhastium	438 Nh Nhastium	439 Nh Nhastium	440 Nh Nhastium	441 Nh Nhastium	442 Nh Nhastium	443 Nh Nhastium	444 Nh Nhastium	445 Nh Nhastium	446 Nh Nhastium	447 Nh Nhastium	448 Nh Nhastium	449 Nh Nhastium	450 Nh Nhastium	451 Nh Nhastium	452 Nh Nhastium	453 Nh Nhastium	454 Nh Nhastium	455 Nh Nhastium	456 Nh Nhastium	457 Nh Nhastium	458 Nh Nhastium	459 Nh Nhastium	460 Nh Nhastium	461 Nh Nhastium	462 Nh Nhastium	463 Nh Nhastium	464 Nh Nhastium	465 Nh Nhastium	466 Nh Nhastium	467 Nh Nhastium	468 Nh Nhastium	469 Nh Nhastium	470 Nh Nhastium	471 Nh Nhastium	472 Nh Nhastium	473 Nh Nhastium	474 Nh Nhastium	475 Nh Nhastium	476 Nh Nhastium	477 Nh Nhastium	478 Nh Nhastium	479 Nh Nhastium	480 Nh Nhastium	481 Nh Nhastium	482 Nh Nhastium	483 Nh Nhastium	484 Nh Nhastium	485 Nh Nhastium	486 Nh Nhastium	487 Nh Nhastium	488 Nh Nhastium	489 Nh Nhastium	490 Nh Nhastium	491 Nh Nhastium	492 Nh Nhastium	493 Nh Nhastium	494 Nh Nhastium	495 Nh Nhastium	496 Nh Nhastium	497 Nh Nhastium	498 Nh Nhastium	499 Nh Nhastium	500 Nh Nhastium	501 Nh Nhastium	502 Nh Nhastium	503 Nh Nhastium	504 Nh Nhastium	505 Nh Nhastium	506 Nh Nhastium	507 Nh Nhastium	508 Nh Nhastium	509 Nh Nhastium	510 Nh Nhastium	511 Nh Nhastium	512 Nh Nhastium	513 Nh Nhastium	514 Nh Nhastium	515 Nh Nhastium	516 Nh Nhastium	517 Nh Nhastium	518 Nh Nhastium	519 Nh Nhastium	520 Nh Nhastium	521 Nh Nhastium	522 Nh Nhastium	523 Nh Nhastium	524 Nh Nhastium	525 Nh Nhastium	526 Nh Nhastium	527 Nh Nhastium	528 Nh Nhastium	529 Nh Nhastium	530 Nh Nhastium	531 Nh Nhastium	532 Nh Nhastium	533 Nh Nhastium	534 Nh Nhastium	535 Nh Nhastium	536 Nh Nhastium	537 Nh Nhastium	538 Nh Nhastium	539 Nh Nhastium	540 Nh Nhastium	541 Nh Nhastium	542 Nh Nhastium	543 Nh Nhastium	544 Nh Nhastium	545 Nh Nhastium	546 Nh Nhastium	547 Nh Nhastium	548 Nh Nhastium	549 Nh Nhastium	550 Nh Nhastium	551 Nh Nhastium	552 Nh Nhastium	553 Nh Nhastium	554 Nh Nhastium	555 Nh Nhastium	556 Nh Nhastium	557 Nh Nhastium	558 Nh Nhastium	559 Nh Nhastium	560 Nh Nhastium	561 Nh Nhastium	562 Nh Nhastium	563 Nh Nhastium	564 Nh Nhastium	565 Nh Nhastium	566 Nh Nhastium	567 Nh Nhastium	568 Nh Nhastium	569 Nh Nhastium	570 Nh Nhastium	571 Nh Nhastium	572 Nh Nhastium	573 Nh Nhastium	574 Nh Nhastium	575 Nh Nhastium	576 Nh Nhastium	577 Nh Nhastium	578 Nh Nhastium	579 Nh Nhastium	580 Nh Nhastium	581 Nh Nhastium	582 Nh Nhastium	583 Nh Nhastium	584 Nh Nhastium	585 Nh Nhastium	586 Nh Nhastium	587 Nh Nhastium	588 Nh Nhastium	589 Nh Nhastium	590 Nh Nhastium	591 Nh Nhastium	592 Nh Nhastium	593 Nh Nhastium	594 Nh Nhastium	595 Nh Nhastium	596 Nh Nhastium	597 Nh Nhastium	598 Nh Nhastium	599 Nh Nhastium	600 Nh Nhastium	601 Nh Nhastium	602 Nh Nhastium	603 Nh Nhastium	604 Nh Nhastium	605 Nh Nhastium	606 Nh Nhastium	607 Nh Nhastium	608 Nh Nhastium	609 Nh Nhastium	610 Nh Nhastium	611 Nh Nhastium	612 Nh Nhastium	613 Nh Nhastium	614 Nh Nhastium	615 Nh Nhastium	616 Nh Nhastium	617 Nh Nhastium	618 Nh Nhastium	619 Nh Nhastium	620 Nh Nhastium	621 Nh Nhastium	622 Nh Nhastium	623 Nh Nhastium	624 Nh Nhastium	625 Nh Nhastium	626 Nh Nhastium	627 Nh Nhastium	628 Nh Nhastium	629 Nh Nhastium	630 Nh Nhastium	631 Nh Nhastium	632 Nh Nhastium	633 Nh Nhastium	634 Nh Nhastium	635 Nh Nhastium	636 Nh Nhastium	637 Nh Nhastium	638 Nh Nhastium	639 Nh Nhastium	640 Nh Nhastium	641 Nh Nhastium	642 Nh Nhastium	643 Nh Nhastium	644 Nh Nhastium	645 Nh Nhastium	646 Nh Nhastium	647 Nh Nhastium	648 Nh Nhastium	649 Nh Nhastium	650 Nh Nhastium	651 Nh Nhastium	652 Nh Nhastium	653 Nh Nhastium	654 Nh Nhastium	655 Nh Nhastium	656 Nh Nhastium	657 Nh Nhastium	658 Nh Nhastium	659 Nh Nhastium	660 Nh Nhastium	661 Nh Nhastium	662 Nh Nhastium	663 Nh Nhastium	664 Nh Nhastium	665 Nh Nhastium	666 Nh Nhastium	667 Nh Nhastium	668 Nh Nhastium	669 Nh Nhastium	670 Nh Nhastium	671 Nh Nhastium	672 Nh Nhastium	673 Nh Nhastium	674 Nh Nhastium	675 Nh Nhastium	676 Nh Nhastium	677 Nh Nhastium	678 Nh Nhastium	679 Nh Nhastium	680 Nh Nhastium	681 Nh Nhastium	682 Nh Nhastium	683 Nh Nhastium	684 Nh Nhastium	685 Nh Nhastium	686 Nh Nhastium	687 Nh Nhastium	688 Nh Nhastium	689 Nh Nhastium	690 Nh Nhastium	691 Nh Nhastium	692 Nh Nhastium	693 Nh Nhastium	694 Nh Nhastium	695 Nh Nhastium	696 Nh Nhastium	697 Nh Nhastium	698 Nh Nhastium	699 Nh Nhastium	700 Nh Nhastium	701 Nh Nhastium	702 Nh Nhastium	703 Nh Nhastium	704 Nh Nhastium	705 Nh Nhastium	706 Nh Nhastium	707 Nh Nhastium	708 Nh Nhastium	709 Nh Nhastium	710 Nh Nhastium	711 Nh Nhastium	712 Nh Nhastium	713 Nh Nhastium	714 Nh Nhastium	715 Nh Nhastium	716 Nh Nhastium	717 Nh Nhastium	718 Nh Nhastium	719 Nh Nhastium	720 Nh Nhastium	721 Nh Nhastium	722 Nh Nhastium	723 Nh Nhastium	724 Nh Nhastium	725 Nh Nhastium	726 Nh Nhastium	727 Nh Nhastium	728 Nh Nhastium	729 Nh Nhastium	730 Nh Nhastium	731 Nh Nhastium	732 Nh Nhastium	733 Nh Nhastium	734 Nh Nhastium	735 Nh Nhastium	736 Nh Nhastium	737 Nh Nhastium</

A.5 List of Symbols

Latin symbols:

A	(1) Helmholtz free energy (1 J); (2) Absorbance; (3) Area (1 m^2); (4) Pre-exponential factor in reaction kinetics (unit depends on reaction order)
A_{nm}	Einstein coefficient of spontaneous emission ($1 \text{ Hz} = 1 \text{ s}^{-1}$)
a	(1) First van der Waals parameter ($1 \text{ kg m}^5 \text{ mol}^{-2} \text{ s}^{-2}$); (2) Activity of a substance
a_0	Bohr radius (see Sect. A.1)
B	(1) Rotational constant ($1 \text{ Hz} = 1 \text{ s}^{-1}$); (2) Second virial coefficient ($1 \text{ m}^3 \text{ mol}^{-1}$); (3) Bernoulli number
B_{nm}	Einstein coefficient of induced emission or induced absorption ($1 \text{ J}^{-1} \text{ m}^3 \text{ s}^{-2}$)
b	Second van der Waals parameter ($1 \text{ m}^3 \text{ mol}^{-1}$)
C	(1) Heat capacity (1 J K^{-1}); (2) Third virial coefficient ($1 \text{ m}^6 \text{ mol}^{-2}$)
C_p	Constant pressure heat capacity (1 J K^{-1})
C_V	Constant volume heat capacity (1 J K^{-1})
\hat{C}_n	Rotation operation related to an n -fold rotation axis
c	(1) Concentration (1 mol m^{-3}); (2) Speed of light (physical constant, see Sect. A.1)
c_p	Constant pressure heat capacity ($1 \text{ J K}^{-1} \text{ mol}^{-1}$)
c_v	Constant volume molar heat capacity ($1 \text{ J K}^{-1} \text{ mol}^{-1}$)
D	Diffusion constant ($1 \text{ m}^2 \text{ s}^{-1}$)
D_e	Well depth of Morse potential (1 J)
\tilde{D}_e	Centrifugal distortion constant ($1 \text{ Hz} = 1 \text{ s}^{-1}$)
D_{MK}^J	Wigner rotation function, generalized spherical harmonic
E	Energy (1 J)
\hat{E}	Identity operation
E_a	Energy of activation (1 J mol^{-1})
F	Force ($1 \text{ N} = 1 \text{ kg m s}^{-2}$)
G	Gibbs free energy (1 J)
g_i	(1) Molar Gibbs free energy (1 J mol^{-1}); (2) Degree of degeneracy of the i th energy level
H	(1) Enthalpy (1 J); (2) Hamiltonian, i.e., total kinetic and potential energy of a system (1 J)
\bar{H}	Energy functional (1 J)
h	(1) Planck constant (physical constant, see Sect. A.1); (2) Molar enthalpy ($1 \text{ J K}^{-1} \text{ mol}^{-1}$)
$\hbar = \frac{h}{2\pi}$	Planck constant divided by 2π
I	(1) Impingement rate ($1 \text{ m}^{-2} \text{ s}^{-1}$); (2) Moment of inertia (1 kg m^2); (3) Nuclear spin
i	Imaginary unit

J	Rotational quantum number
\mathbf{J}	Angular momentum vector ($1 \text{ kg m}^2 \text{ s}^{-1}$)
K	Equilibrium constant of a chemical reaction
K_a	Dissociation constant
Kn	Knudsen number
k	(1) Rate constant of a chemical reaction (unit depends on reaction order); (2) Force constant (1 N m^{-1})
k_B	Boltzmann constant (physical constant, see Sect. A.1)
L	Optical path length (1 m)
\hat{L}	Operator of the orbital angular momentum
l	Quantum number of the orbital angular momentum in the hydrogen problem
M	(1) Molar mass (1 kg mol^{-1}); (2) Magnetic or orientational quantum number
m	(1) Mass (1 kg); (2) Magnetic quantum number in the hydrogen problem
m_u	Atomic mass unit (physical constant, see Sect. A.1)
m_e	Electron mass (physical constant, see Sect. A.1)
N	Number of particles
\mathcal{N}	Number density of particles (1 m^{-3})
\mathcal{N}	Number of identical copies in a statistical ensemble
n	(1) Amount of substance (1 mol); (2) Vibrational quantum number; (3) Principal quantum number in the hydrogen problem
N_A	Avogadro constant (physical constant, see Sect. A.1)
P	Power ($1 \text{ W} = 1 \text{ J s}^{-1}$)
\hat{P}	Parity operator
P_{lm}	Associated Legendre polynomial
p	(1) Pressure ($1 \text{ Pa} = 1 \text{ kg m}^{-1} \text{ s}^{-2}$); (2) Momentum (1 kg m s^{-1}); (3) Probability
p^\ominus	Standard pressure (100,000 Pa)
Q	(1) Heat (1 J); (2) Partition function of a system
q	Partition function
R	(1) Molar gas constant (physical constant, see Sect. A.1); (2) Radial wave function in the hydrogen problem
r	(1) Reaction rate ($1 \text{ mol m}^{-3} \text{ s}^{-1}$); (2) Radial coordinate (1 m)
S	Entropy (1 J K^{-1})
s	(1) Distance (1 m); (2) Molar entropy ($1 \text{ J K}^{-1} \text{ mol}^{-1}$)
T	(1) Temperature (1 K); (2) Transmittance
\hat{T}	Exchange operator
t	Time (1 s)
$t_{\frac{1}{2}}$	Half life (1 s)
U	Internal energy (1 J)
u	(1) Molar internal energy (1 J mol^{-1}); (2) Spectral energy density of the electromagnetic radiation field (1 J s m^{-3})

V	(1) Volume (1 m^3); (2) Potential energy (1 J)
v	(1) Velocity (1 m s^{-1}); (2) Molar volume ($1 \text{ m}^3 \text{ mol}^{-1}$)
W	(1) Work (1 J); (2) Statistical weight
x	(1) Mole fraction; (2) Cartesian coordinate, position (1 m)
x_e	Anharmonicity constant of diatomic molecule
x_{ij}	Anharmonicity constant of the i th and the j th vibrational mode of a polyatomic molecule ($1 \text{ Hz} = 1 \text{ s}^{-1}$)
Y_{lm}, Y_{JM}	Spherical harmonic function
y	Cartesian coordinate (1 m)
Z	Atomic number of an element
z	(1) Cartesian coordinate (1 m); (2) Collision frequency ($1 \text{ Hz} = 1 \text{ s}^{-1}$)

Greek symbols:

α	Isobaric thermal expansion coefficient (1 K^{-1})
α_e	Vibration-rotation coupling constant ($1 \text{ Hz} = 1 \text{ s}^{-1}$)
β	Parameter $(k_B T)^{-1}$ in statistical thermodynamics
Γ	Representation in group theory
γ	(1) Heat capacity ratio; (2) Surface energy density or surface tension (1 J m^{-2}); (3) Activity coefficient
Δ	(1) Delta operator, partial derivative with regard to the extent of the reaction; (2) Laplace operator; (3) Difference between energy levels
δ_{nm}	Kronecker delta, $\delta_{nm} = 1$ if $n = m$ and zero otherwise
δ_l	Quantum defect
ϵ_0	Electric constant (physical constant, see Sect. A.1)
θ	Inclination or polar angle (1 rad)
κ	(1) Isothermal compressibility ($1 \text{ Pa}^{-1} = 1 \text{ kg}^{-1} \text{ m s}^2$); (2) Asymmetry parameter in molecular rotation spectroscopy
Λ	Thermal wavelength (1 m)
λ	(1) Mean free path (1 m); (2) Wave length (1 m)
μ	(1) Chemical potential (J mol^{-1}); (2) Effective mass (1 kg)
ν	(1) Stoichiometric number of substance; (2) Frequency ($1 \text{ Hz} = 1 \text{ s}^{-1}$)
$\tilde{\nu}$	Wave number (1 m^{-1})
ξ	Extent of reaction (1 mol)
ξ^{eq}	Equilibrium extent of reaction (1 mol)
Π	Internal pressure ($1 \text{ Pa} = 1 \text{ kg m}^{-1} \text{ s}^{-2}$)
ρ	Mass density (1 kg m^{-3})
σ	(1) Stefan-Boltzmann constant (see Eq. (9.8) at page 215); (2) Attenuation cross section in spectroscopy (1 m^2); (3) Variance of a distribution function
$\sigma_x, \sigma_y, \sigma_z$	Pauli spin matrices
$\hat{\sigma}_h$	Mirror operation related to a horizontal mirror plane
$\hat{\sigma}_v$	Mirror operation related to a vertical mirror plane

τ	(1) Optical depth; (2) Lifetime (1 s)
Φ	Photon density (1 m^{-3})
ϕ	Azimuthal angle (1 rad)
χ_i	Character of representation i
ψ	Quantum mechanical wave function
ω	Angular frequency (1 rad s^{-1})

A.6 List of Acronyms

AFM	Atomic force microscopy
COM	Center of mass
ESCA	Electron spectroscopy for chemical analysis
IR	Infrared spectral range
LASER	Light amplification by stimulated emission of radiation
LCAO	Linear combination of atomic orbitals
LEED	Low-energy electron diffraction
MIR	Mid infrared spectral range
Nd:YAG	Neodymium-doped yttrium aluminum garnet ($\text{Nd}: \text{Y}_3\text{Al}_5\text{O}_{12}$)
NIR	Near infrared spectral range
PET	Positron emission tomography
PSE	Periodic system of elements
RRHO	Rigid rotor harmonic oscillator approximation in molecular spectroscopy
STM	Scanning tunneling microscopy
SI	International system of units (Système international d'unités)
TCA	Trichloroacetic acid
TOF	Time of flight
UHV	Ultrahigh vacuum
UV	Ultraviolet spectral range
UPS	Ultraviolet photoelectron spectroscopy
XPS	X-ray photoelectron spectroscopy

Index

- Absorbance, 295
Absorption process, 293
Activity, 53
Activity coefficient, 54
Anharmonicity constant, 299, 343
Annihilation operator, 245
Anti-Stokes scattering, 295
Arrhenius equation, 121
Associated Legendre Polynomial, 368
Asymmetric top molecule, 313
Asymmetry parameter, 313
Atomic units, 220
Attenuance, 295
Autocatalytic reaction, 138
Avogadro constant, 10, 357
Avogadro, Amedeo, 147
- Band model
 metal, 227
 semi-conductor, 260
Basis set, 271
Bernoulli numbers, 224, 365
Bimolecular reaction, 120
Black body, 224
Black body radiation, 215
Bohr radius, 357
Boltzmann constant, 357
Boltzmann, Ludwig, 147
Bond dissociation energy, 333
Born Haber cycle, 76
Born, Max, 147, 216
Born-Oppenheimer approximation, 309
Bra-vector, 216
- Calorimetry, 71, 77
Catalyst, 98
Cathode rays, 213, 224
Center of mass, 314
Character table, 336, 341
Characteristic polynomial, 350
Chemical accuracy, 76
Chemical potential, 85
Chemical reaction, 9
 oscillating, 7, 138, 142
Chemisorption, 193
Chromophor, 255
Clapeyron equation, 52, 56
Clausius-Clapeyron equation, 53
Colligative properties, 52, 64
Collisional broadening, 166
Commutator, 245
Complex number, 359
Complimentary error function, 155
Compressibility, 20
Compression factor, 25
Concentration, 11
Correlation diagram, 318
Correspondence principle, 223, 231
Creation operator, 245
Critical point, 26
Cubic force constant, 326
Cumulative probability, 157, 194
Cylindrical coordinates, 367
Cysteine, 307
- Dalton, John, 9, 147, 213
de Broglie wavelength, 214
de Broglie, Louis-Victor, 214

- Degeneracy, 178
 Delta function, 304, 364
 Derivative
 partial, 362
 total, 362
 Diffusion, 186, 192
 Diffusion constant, 191
 Discriminant, 350, 359
 Dissociation constant, 87
 Dissociation reaction, 10
 Doppler effect, 303
 Double well problem, 272
- Educt, 10
 Effective mass, 149, 296
 Effusion, 91, 166
 Einstein coefficients, 295
 Einstein, Albert, 214
 Electron impact heating, 224
 Elementary reaction, 120
 Ellingham diagram, 80
 Emission process
 induced, 293
 spontaneous, 293
 Endergonic process, 73
 Endothermic process, 72
 Energy, 1, 30
 Energy of activation, 121
 Ensemble, 176
 Enthalpy, 31
 Enthalpy of formation, 71
 Enthalpy of reaction, 72
 Entropy, 33, 175, 176
 conformational, 179
 monatomic gas, 199
 Entropy of reaction, 72
 Equation of state
 perfect gas, 19, 154
 van der Waals gas, 19
 virial, 19, 24
 Equilibrium
 chemical, 130
 mechanical, 37, 39
 thermodynamic, 39
 Equilibrium constant, 85
 Equipartition theorem, 215
 Error function, 195
 Euler angles, 316
 Euler equation, 52
 Euler's formula, 360
 Exchange operator, 341
 Exergonic process, 73
 Exergonic reaction, 80
- Exothermic process, 72
 Extensive quantity, 18
 Extent of reaction, 7, 10, 72, 83, 128, 130
 Extinction, 295
- Factorial, 365
 Fick's second law, 191
 First law of thermodynamics, 30
 Fraunhofer, Joseph, 213
 Free expansion, 32, 33, 184
 perfect gas, 43
 van der Waals gas, 44
 FWHM, 366
- Gamma spectroscopy, 302
 Gaussian, 218
 Gibbs free energy, 34
 Gibbs paradox, 177
 Glutamate dehydrogenase, 307
 Group theory, 335
- Haken, Hermann, 7
 Half width, 366
 Half-life, 123
 Hamilton function, 231
 Hard sphere model, 149
 Harmonic oscillator, 218, 244, 297
 Hartree, 220
 Heat, 30
 Heat capacity
 isobaric, 32
 isochoric, 30, 202
 Heat capacity ratio, 34
 Heat conduction, 166
 Helmholtz free energy, 34
 Henderson-Hasselbalch equation, 87
 Hermite polynomial, 368
 Hess's law, 73
 Hot band, 320
 Hyperfine structure splitting
 hydrogen, 301
 sodium, 306
- Ice, 68, 173
 Ideal mixture, 62
 Imaginary unit, 359
 Impingement rate, 150, 167
 Intensive quantity, 18
 Internal energy, 30
 Internal pressure, 31

- Inversion, 347
Irreducible representation, 336
Irreversibility, 192
Irreversible process, 32, 43
Isotopic substitution, 312
- Jacobian, 372
Jaynes Cummings model, 250
- K-capture, 259
Ket-vector, 216
Kirchoff's law, 73
Knudsen number, 165
Kronecker delta, 377
- Lambert Beer law, 294
LASER, 7, 347
Law of mass action, 85
Levinthal paradox, 180
Limiting reactant, 10
Liquid petroleum gas, 62
Lotka-Volterra model, 139, 143, 348
- Mößbauer spectroscopy, 302
Macrostate, 175
Matrix, 369
Maxwell construction, 26
Maxwell relations, 35
Maxwell-Boltzmann velocity distribution, 147, 304
Microstate, 175
Molar gas constant, 12
Molar mass, 11
Molar volume, 11
Mole fraction, 11
Molecular orbital, 290
Molecularity, 120
Moment of inertia, 296
Moment of inertia tensor, 315
Morse potential, 319, 333
Multiplicity, 201
- Normal distribution, 188, 191, 305
Nuclear spin statistics, 340
Number operator, 244, 245
- Operator
adjoint, 216
- annihilation, 245
creation, 245
exchange, 341
Hermitian, 216
Laplace, 366, 367
momentum, 233, 245
number, 245
parity, 342
self adjoint, 216
unitary, 243
- Optical depth, 294, 304
Ortho hydrogen, 202
Oscillator
damped, 349
Lorentz, 222
Ostwald solubility coefficient, 109
Overtone transition, 320
- P-branch, 327
Para hydrogen, 202
Parity operation, 342
Partial derivative, 362
Partition function, 176
canonical, 177
molecular, 178
Pauli principle, 257
Pauli spin matrices, 248
Perfect gas, 19, 31, 35, 43
Permutation, 184
Phase diagram, 18
Photoelectron spectroscopy, 226
Physical constants, 357
Physisorption, 193
Planck constant, 200, 357
Planck, Max, 215
Point group, 334
Point symmetry, 334
Positron emission tomography, 302
Pre-exponential factor, 121
Pressure, 148
Probability, 147
Propagator, 242
- Q-branch, 328
Quantum chemistry, 271, 282, 358
Quantum defect, 230
Quantum double-well
asymmetric, 280
symmetric, 272
Quantum number
magnetic, 219
orbital angular momentum, 219

- orientational, 297
- principal, 219
- rotational, 296
- vibrational, 299
- Quartic force constant, 326
- R-branch, 327
- Radio astronomy, 301
- Raman scattering, 295
- Random walk, 192
- Raoult's law, 3, 54
- Rate constant, 120
- Reactant, 10
- Reaction rate, 119
- Representation
 - irreducible, 336
 - reducible, 336
- Rigid rotator, 178, 296
- Rotational constant, 296, 311, 313, 329, 344
- Runge-Kutta method, 144, 373
- Rutherford, Ernest, 213
- Rydberg atoms, 230
- Sackur-Tetrode equation, 199
- Scanning force microscopy, 192
- Scanning tunneling spectroscopy, 192
- Schottky anomaly, 206, 273
- Schrödinger equation, 217
- Second law of thermodynamics, 33
- Semiconductor, 261
- Sodium D-line, 306
- Spectroscopy
 - rotational, 296
 - vibrational, 297
- Spherical harmonics, 368
- Spin-statistics theorem, 341
- Standard deviation, 366
- Standard state, 53, 60, 71
- Statistical weight, 176
- Stefan-Boltzmann law, 215
- Stirling approximation, 188
- Stirling formula, 365
- Stoichiometric number, 10
- Stokes scattering, 295
- Supercritical phase, 18, 27
- Superposition principle, 216, 232, 234
- Surface science, 193
- Surface tension, 68
- Symmetric top molecule, 316
- Symmetry operation, 335
- Symmetry type, 335, 336
- Syngas, 97
- Synthesis reaction, 9
- System, 17
 - closed, 18
 - heterogeneous, 51
 - isolated, 17
 - nonconservative, 232
 - open, 18
- Tempering, 225
- Term symbol, 201
- Termolecular reaction, 120
- Thermal expansion coefficient, 20
- Thermal wavelength, 179
- Thomson, Joseph John, 213
- Time invariance, 48
- Total derivative, 362
- Transition state, 96, 122
- Transmittance, 294
- Tryptophan, 307
- Tunnel effect, 273
- Two-level system, 206, 248, 250
- Tyrosine, 307
- Uncertainty principle, 237
- Unimolecular reaction, 120
- Unitary transformation, 243
- van der Waals equation, 19
- van der Waals model, 26, 31, 35, 43
- Van't Hoff reaction isobar, 86, 89
- Variance, 366
- Virial coefficient
 - second, 19, 24
 - third, 19, 25
- Virial equation, 19
- Water gas shift reaction, 9, 97, 104
- Wave packet, 234
- Wave-particle duality, 214
- Wigner rotation functions, 316
- X-rays, 13, 226
- Yukawa, Hideki, 258
- Zeeman effect, 250
- Zeeman, Pieter, 213